AD702512

HYDRONAUTICS, incorporated
research in hydrodynamics

Research, consulting, and advanced engineering in the fields of NAVAL and INDUSTRIAL HYDRODYNAMICS. Offices and Laboratory in the Washington, D. C. area: Pindell School Road, Howard County, Laurel, Md.

267

AD 702 512

ANALYSIS AND MODEL TESTS TO DETERMINE FORCES AND MOTIONS OF AN OIL RETENTION BOOM

W. T. Lindenmuth, et al

Hydronautics, Incorporated
Laurel, Maryland

January 1970

HYDRONAUTICS, Incorporated

TECHNICAL REPORT 948-1(I)

ANALYSIS AND MODEL TESTS TO DETERMINE FORCES AND MOTIONS OF AN OIL RETENTION BOOM

By

W. T. Lindenmuth, J. O. Scherer
and P. Van Dyke

January 1970

DISTRIBUTION OF THIS DOCUMENT IS UNLIMITED

Prepared Under
Department of Transportation Contract No.
DOT-CG-93907-A
for the
U. S. Coast Guard

UNCLASSIFIED
Security Classification

DOCUMENT CONTROL DATA - R&D	
(Security classification of title, body of abstract and indexing annotation must be entered when the overall report is classified)	
1. ORIGINATING ACTIVITY (Corporate author) HYDRONAUTICS, Incorporated Pindell School Road, Howard County, Laurel, Maryland 20810	2a. REPORT SECURITY CLASSIFICATION Unclassified
	2b. GROUP
3. REPORT TITLE ANALYSIS AND MODEL TESTS TO DETERMINE FORCES AND MOTIONS OF AN OIL RETENTION BOOM	
4. DESCRIPTIVE NOTES (Type of report and inclusive dates) Technical Report - January 1970	
5. AUTHOR(S) (Last name, first name, initial) Lindenmuth, W. T., Scherer, J. O., and Van Dyke, P.	

6. REPORT DATE	7a. TOTAL NO. OF PAGES	7b. NO. OF REFS
January 1970	263	5

8a. CONTRACT OR GRANT NO. DOT-CG-93907-A	9a. ORIGINATOR'S REPORT NUMBER(S) Technical Report 948(I)-1
b. PROJECT NO.	
c.	9b. OTHER REPORT NO(S) (Any other numbers that may be assigned this report)
d.	
10. AVAILABILITY/LIMITATION NOTICES DISTRIBUTION OF THIS DOCUMENT IS UNLIMITED	
11. SUPPLEMENTARY NOTES	12. SPONSORING MILITARY ACTIVITY Dept. of Transportation for the U. S. Coast Guard

13. ABSTRACT

A theoretical analysis of the loads and motions of a continuous, elastic, oil retention boom of arbitrary configuration is presented. The boom is subjected to loads of wind, current, and an irregular sea. The analytical method was programmed for an IBM 1130 computer and used to generate data for a variety of oil booms. Towing tank test were conducted on selected boom configurations and serve to check the theoretical analysis.

DD FORM 1 JAN 64 1473

UNCLASSIFIED
Security Classification

UNCLASSIFIED

Security Classification

14. KEY WORDS	LINK A ROLE	LINK A WT	LINK B ROLE	LINK B WT	LINK C ROLE	LINK C WT
Pollution						
Oil Spills						
Oil Boom						

INSTRUCTIONS

1. **ORIGINATING ACTIVITY:** Enter the name and address of the contractor, subcontractor, grantee, Department of Defense activity or other organization (*corporate author*) issuing the report.

2a. **REPORT SECURITY CLASSIFICATION:** Enter the overall security classification of the report. Indicate whether "Restricted Data" is included. Marking is to be in accordance with appropriate security regulations.

2b. **GROUP:** Automatic downgrading is specified in DoD Directive 5200.10 and Armed Forces Industrial Manual. Enter the group number. Also, when applicable, show that optional markings have been used for Group 3 and Group 4 as authorized.

3. **REPORT TITLE:** Enter the complete report title in all capital letters. Titles in all cases should be unclassified. If a meaningful title cannot be selected without classification, show title classification in all capitals in parenthesis immediately following the title.

4. **DESCRIPTIVE NOTES:** If appropriate, enter the type of report, e.g., interim, progress, summary, annual, or final. Give the inclusive dates when a specific reporting period is covered.

5. **AUTHOR(S):** Enter the name(s) of author(s) as shown on or in the report. Enter last name, first name, middle initial. If military, show rank and branch of service. The name of the principal author is an absolute minimum requirement.

6. **REPORT DATE:** Enter the date of the report as day, month, year; or month, year. If more than one date appears on the report, use date of publication.

7a. **TOTAL NUMBER OF PAGES:** The total page count should follow normal pagination procedures, i.e., enter the number of pages containing information.

7b. **NUMBER OF REFERENCES:** Enter the total number of references cited in the report.

8a. **CONTRACT OR GRANT NUMBER:** If appropriate, enter the applicable number of the contract or grant under which the report was written.

8b, 8c, & 8d. **PROJECT NUMBER:** Enter the appropriate military department identification, such as project number, subproject number, system numbers, task number, etc.

9a. **ORIGINATOR'S REPORT NUMBER(S):** Enter the official report number by which the document will be identified and controlled by the originating activity. This number must be unique to this report.

9b. **OTHER REPORT NUMBER(S):** If the report has been assigned any other report numbers (*either by the originator or by the sponsor*), also enter this number(s).

10. **AVAILABILITY/LIMITATION NOTICES:** Enter any limitations on further dissemination of the report, other than those imposed by security classification, using standard statements such as:

(1) "Qualified requesters may obtain copies of this report from DDC."

(2) "Foreign announcement and dissemination of this report by DDC is not authorized."

(3) "U. S. Government agencies may obtain copies of this report directly from DDC. Other qualified DDC users shall request through ______________________."

(4) "U. S. military agencies may obtain copies of this report directly from DDC. Other qualified users shall request through ______________________."

(5) "All distribution of this report is controlled. Qualified DDC users shall request through ______________________."

If the report has been furnished to the Office of Technical Services, Department of Commerce, for sale to the public, indicate this fact and enter the price, if known.

11. **SUPPLEMENTARY NOTES:** Use for additional explanatory notes.

12. **SPONSORING MILITARY ACTIVITY:** Enter the name of the departmental project office or laboratory sponsoring (*paying for*) the research and development. Include address.

13. **ABSTRACT:** Enter an abstract giving a brief and factual summary of the document indicative of the report, even though it may also appear elsewhere in the body of the technical report. If additional space is required, a continuation sheet shall be attached.

It is highly desirable that the abstract of classified reports be unclassified. Each paragraph of the abstract shall end with an indication of the military security classification of the information in the paragraph, represented as *(TS)*, *(S)*, *(C)*, or *(U)*.

There is no limitation on the length of the abstract. However, the suggested length is from 150 to 225 words.

14. **KEY WORDS:** Key words are technically meaningful terms or short phrases that characterize a report and may be used as index entries for cataloging the report. Key words must be selected so that no security classification is required. Identifiers, such as equipment model designation, trade name, military project code name, geographic location, may be used as key words but will be followed by an indication of technical context. The assignment of links, roles, and weights is optional.

DD FORM 1 JAN 64 1473 (BACK)

UNCLASSIFIED

Security Classification

TABLE OF CONTENTS

(Volume I)

		Page
1.	INTRODUCTION	1
2.	THEORETICAL ANALYSIS	3
	2.1 Dimensional Analysis	5
	2.2 Static Analysis	9
	2.3 Dynamic Analysis	14
3.	OIL BOOM MODEL TESTS	17
	3.1 The Model	17
	3.2 Test Procedures	22
	3.3 Discussion of Test Results	24
	3.3.1 Tests in Calm Water	24
	3.3.2 Tests in Waves	28
4.	COMPARISON OF ANALYTICAL RESULTS WITH MODEL TESTS	30
	4.1 Static Tests	30
	4.2 Dynamic Tests	31
5.	SUGGESTED METHOD OF USING COMPUTED DATA IN APPENDICES A AND B	34
6.	CONCLUSIONS AND RECOMMENDATIONS	39
	REFERENCES	42
	APPENDIX A - STATIC OUTPUT	A-1
	(Volume II)	
	APPENDIX B - DYNAMIC OUTPUT	B-1
	APPENDIX C - STATIC EQUATIONS	C-1
	APPENDIX D - DYNAMIC EQUATIONS	D-1

1. INTRODUCTION

Oil well leaks and spills from damaged tankers are sources of pollution that can contaminate beaches and destroy marine life. The recent leaks in the Santa Barbara Channel and the breaking up of the Torrey Canyon have led to increased emphasis on the urgent need to develop systems to contain spilled oil and to remove it from the ocean surface. Obviously, it is most desirable to prevent similar occurrences in the future. Unfortunately, experience shows that even our best efforts cannot prevent the occasional occurrences of major maritime disasters by human error, mechanical failure and environmental stress. Thus, the potential for incidents involving massive oil spills will remain with us and special techniques and equipment to facilitate their removal from both coastal and inland waters will be required.

Oil naturally tends to spread rapidly to form a thin film over the water surface. Environmental conditions of wind, current and waves only serve to augment this tendency. In order to efficiently recover oil from the water surface it must first be collected and/or contained in a small area with a relatively thick film. Many candidate collection and retention systems have been proposed and, undoubtedly, many more will be inverted in the near future. In particular, many forms of floating oil retention booms have been proposed to prevent the spread of oil slicks.

There are currently several oil boom designs on the market. These booms have been used successfully to retain oil and other debris in relatively sheltered waters. However, attempts to use existing hardware off-shore at Santa Barbara were severely hampered due to mechanical failure of the oil booms.

HYDRONAUTICS, Incorporated, under the sponsorship of the U. S. Coast Guard, has undertaken a study to provide basic quantitative engineering data on the performance of oil retention booms in a seaway. The aim of this resulting report is to provide designers and evaluators of oil retention booms with information and data to aid in the prediction of boom loads, shapes, and motions. In particular, the research is intended to provide information which will aid in answering the following questions:

1. What are the local loads in an oil retention boom and what are the end or mooring loads in the presence of wind, currents, and seas?

2. What will be the overall configuration assumed by an oil boom under the loads imposed by the sea?

3. What are the motions of the boom in a seaway? In particular, will the boom ever be completely immersed by a wave crest or lift clear of a wave trough permitting oil to escape?

4. What are the maximum local stresses in an oil retention boom and where along its length will these occur?

The study is primarily a theoretical analysis of the oil retention boom to provide information on a large variety of boom configurations and sea conditions. This theoretical analysis is backed up by the results of an experimental program. Towing tank tests conducted on selected boom configurations have provided information which serves to check the accuracy of the theoretical analysis.

The analytical method that was developed was programmed for an IBM 1130 computer and this program used to generate data for oil booms varying several controlling parameters.

2. THEORETICAL ANALYSIS

The complete analytical solution for the motions and loads on an oil retention boom of arbitrary configuration subjected to the loads of wind, current, and an irregular sea is a formidable task. The problem is difficult because of its highly nonlinear nature and the large number of parameters involved.

The important parameters in determining the performance of an oil retention boom can be divided into four groups. These are physical properties, hydrodynamic properties, mooring conditions and environmental conditions. Twenty-seven variables are included in the four groups. These are listed in Table 1.

TABLE 1.- PARAMETERS AFFECTING BOOM PERFORMANCE

Physical Properties

Cross sectional shape
Specific gravity
Center of gravity location
Shear center location
Tensile modulus of elasticity, E
Shear modulus of elasticity, G
Vertical section moment of inertia, I_v
Horizontal section moment of inertia, I_h
Polar section moment of inertia, J
Effective structural cross-sectional area, A
Absolute size
Length

Hydrodynamic Properties

Skin friction coefficient
Drag coefficient for flow normal to boom axis
(same as horizontal damping coefficient)
Vertical damping coefficient
Horizontal added mass coefficient
Vertical added mass coefficient

(Note: These must be defined for both that portion of the boom in the air as well as the portion in the water, and, in general, these are all non-linear functions of the local boom positions).

Mooring Conditions

Mooring configuration (spacing and orientation to the sea)
Mooring spring constants
Mooring damping coefficients
Mooring effective masses

Environmental Conditions

Wind strength
Wind direction
Current strength
Current direction
Wave spectrum
Dominant wave direction

2.1 Dimensional Analysis

The effective number of variables involving boom properties can be reduced by non-dimensionalizing. In order to do this, non-dimensional parameters must be found that relate the stiffness of the boom to the buoyant and dynamic forces acting on it in such a way that the correct relation between them is maintained. The deflection of the boom can be non-dimensionalized by expressing the deflection in terms of a characteristic length. Thus:

$$\frac{\delta}{L} = K \frac{FL^2}{EI} \tag{1}$$

where

- δ = deflection, ft
- L = a characteristic length, ft
- K = a function of the load distribution and boundary conditions of the boom,
- F = applied load, lb
- E = modulus of elasticity, lb/ft^2, and
- I = section moment of inertia, ft^4.

Since both buoyant and dynamic forces are involved, they must be non-dimensionalized in such a way that their relative magnitude compared to the elastic stiffness (EI) of the boom is maintained. The buoyant and dynamic forces must, of course, be kept in proper proportion relative to each other. For example, a wave passing the boom will change the immersion of the boom

and thus change the buoyant force on the boom. The wave also has orbital velocities associated with it and will thus induce dynamic forces proportional to the Froude number squared.

$$(\text{Froude number})^2 = \frac{V^2}{gL} \qquad (2)$$

where

V = a characteristic velocity (wind or current), ft-sec^{-1}

g = gravitational acceleration, ft-sec^{-2}

Thus, to maintain the proper relation between dynamic and buoyant forces, the Froude number must be constant. Since the acceleration of gravity (g) is fixed:

$$V^2 \propto L \qquad (3)$$

The Reynolds number, a measure of the relative magnitude of the dynamic forces compared to the viscous forces, must also be considered. Reynolds number is expressed as:

$$(\text{Reynolds number}) = \frac{\rho VL}{\mu} \qquad (4)$$

where

ρ = fluid density (air or water), lb-sec^2-ft^{-4}

μ = fluid viscosity (air or water), lb-sec-ft^{-2}

For a given sea condition ρ and μ are fixed; thus, for a constant Reynolds number:

$$V \propto \frac{1}{L} \tag{5}$$

This result is, of course, incompatible with Equation (3). Fortunately, the major influence of viscosity is only to modify the dynamic coefficients. The magnitude of this effect is usually small compared to the influence of the buoyant forces. In fact, within the range of practical boom sizes (say 2 to 10 feet in height) the influence of a change in Reynolds number will be negligible.

Non-dimensionalizing can therefore be accomplished using the Froude number to provide the required relation between dynamic and buoyant forces, i.e., between V and L.

The buoyant forces F_B are proportional to L^3. The dynamic forces of wind F_a and current F_w are proportional to V^2L^2. Therefore, boom deflections due to buoyancy δ_B, wind δ_a and current δ_w can be expressed non-dimensionally with the aid of Equations (1) and (3):

$$\frac{\delta_B}{L} = K_B \frac{F_B L^2}{EI} \propto \frac{L^5}{EI}$$

$$\frac{\delta_a}{L} = K_a \frac{F_a L^2}{EI} \propto \frac{L^5}{EI}$$

$$\frac{\delta_w}{L} = K_w \frac{F_w L^2}{EI} \propto \frac{L^5}{EI} \tag{6}$$

Thus, geometrically similar booms of different absolute size will behave the same if the ratio L^5/EI is maintained and wind and current velocities are adjusted proportional to $\sqrt{L}$.

Absolute size can now be eliminated as a parameter if we define non-dimensional parameters:

$$\text{Stiffness, } S' = \frac{EI}{\rho_w g L^5}$$

$$\text{Wind speed, } V_a' = \sqrt{\frac{\frac{1}{2}\rho_A V_a{}^2 L^4}{EI}}$$

$$\text{Current, } V_w' = \sqrt{\frac{\frac{1}{2}\rho_w V_w{}^2 L^4}{EI}}$$

$$\text{Wave height, } h' = \frac{h}{L} \tag{7}$$

where

ρ_w = density of water,

ρ_A = density of air, and

h = wave height.

To apply this scaling to the real sea one further assumption is made. That is, that the scaled energy distribution of the waves in one sea state is the same as in another sea state. (e.g. sea state 3 is a scale model of, say, sea state 4).

While this non-dimensionalizing is, of course, not necessary, it does provide a useful framework for comparing the performance of booms of slightly differing sizes.

It was originally planned to carry out both a static analysis (constant wind and current with no waves) and a dynamic analysis with a single numerical solution technique programmed for a digital computer. This technique would provide a three-dimensional solution and would include the most important non-linearities. While such a program is feasible, difficulties encountered in developing a satisfactory computational procedure precluded development beyond the static solution. A linearized analysis was therefore developed to predict the dynamic performance. A description of both the static and the dynamic analysis follows. An explanation of the equations involved is presented in Appendix C for the static solution and in Appendix D for the dynamic solution.

2.2 Static Analysis

The type of oil retention boom treated is a continuous elastic beam floating on the water surface. The water surface is assumed flat (no waves) so that the only environmental loads imposed on the boom are from wind and current. The boom is divided into a large number of imaginary elements, each of which is assumed sufficiently short so that angular deflections within its length are small, and so that classical linear beam theory will, therefore, be valid in computing the deflections of each

element. It has also been assumed that torsional deflections of the boom are sufficiently small so that they produce negligible changes in the horizontal and vertical sectional properties of the boom.

Some important non-linearities are included in the static analysis and should be noted. First, the classical beam deflection and equilibrium equations have been modified to include the influence of the tension on deflection. The non-linear coupling of tension and deflection is necessary to permit the solution for booms of small or negligible stiffness.

In general, large deflections are required of the entire boom configuration. Therefore, in order to correctly resolve the loads and map the complete boom configurations, it is necessary to include all trigometric relations in the equations. These trigometric relations not only make the equations non-linear but produce additional coupling between the force variables and the position variables.

A third type of non-linearity is encountered in computing the hydrodynamic and hydrostatic loads acting on the boom. These loads are based on the position and orientation of the middle of each individual element of the boom. Hydrostatic loads are determined by computing the actual displaced volume of each element and take full account of its cross-sectional shape. Hydrodynamic and aerodynamic loads are computed separately in a direction tangential to the boom axis and normal to the boom axis. To do this, the flow velocity (air and water) is resolved into components tangential to and normal to the boom axis. Tangential

loads are based on the wetted surface of the element and a skin friction coefficient (C_f). Normal loads are based on the frontal area of the element and a drag coefficient (C_D). In computing the data presented in Appendix A, C_f and C_D were taken as 0.04 and 1.00 respectively for the portion of the boom in air as well as the immersed portion.

Roll torques are based on the assumption that the hydrodynamic and aerodynamic centers of pressure are located at the midpoint of the projected area (in water and in air) of each element. The torque is then taken to be the hydrodynamic or aerodynamic normal load times the distance between their respective centers of pressure and the boom shear center. Of course, hydrostatic roll stability and torsional stiffness of the boom are also included in the calculations.

The numerical solution for the loads and shape of an oil retention boom requires the simultaneous solution of four types of equations. These equations, along with a complete description, are presented in Appendix A. However, a brief description of the function of each type of equation is presented in the following paragraphs.

The first type of equations are the six "equilibrium" equations. These equations relate the forces and moments on one end of an element to the forces and moments on the other end of the element in terms of the deflections and applied loads. They insure that each element of the boom, and thus the entire boom, is in equilibrium such that all the externally applied loads are balanced by internal structural loads.

The second type of equations are the six "deflection" equations. These express the deflection of each element in terms of the applied loads and the structural forces and moments on the ends of the element which are transferred from the neighboring elements.

The third type are the six "shape" equations. These relate the position of one end of each element to the position of the other end in terms of its angular position and the deflections within the element. They insure that the end of each element has the same position and orientation in space as the end of the mating element. That is, the boom forms a smooth continuous curve.

These 18 equations are applied to each element and are sufficient to solve for all the internal loads, deflections, and overall shape once the applied loads and mooring conditions are known. The mooring conditions are specified in the fourth type of equations, the "boundary condition" equations. There are 12 of these equations, 6 for each end of the boom. These equations form explicit relations between the forces and moments on the ends of the boom and their location and orientation in space. The boundary conditions applied to all data in Appendix A are: (1) the ends of the boom must be located at specified positions (the vertical position is specified to be at the equilibrium waterline), and (2) that there be no bending moments or torque at the ends (i.e., a flexible connection between the boom and its mooring).

A boom represented by N elements will have 18 N + 12 simultaneous equations to be solved. Since 10 elements were used in obtaining the results presented in Appendix A, it was necessary to solve a set of 192 simultaneous equations for each case.

The numerical solution of these equations is carried out on an IBM 1130 digital computer. The computational technique must, of course, possess mathematical stability if the solution is to converge. This stability depends on how the non-linear terms are treated, how the equations are normalized, and the order in which the computations are carried out. Considerable difficulty was encountered in obtaining a stable solution for all boom configurations. This was particularly true for solutions involving booms of low but finite stiffness. It was found necessary to express the equations in the form of a linear, small amplitude perturbation about an assumed solution, and to include derivatives of all applied load functions with respect to boom position. The result is a set of linear simultaneous equations which are presented in Appendix C.

These equations have been arranged in matrix form and are solved using Gauss' reduction method (Reference 1). Because of the necessity of expanding non-linear terms, an iterative calculation procedure is required. In each iteration the previously computed configuration is used as the assumed configuration in the expanded terms. The calculations for the hydrodynamic loads on the boom, which are a function of the boom position, are based on the boom position in the previous iteration. Initial

conditions are provided by assuming the boom floats at its equilibrium waterline and lies in a specified curve between its moorings. In the cases where the boom was relatively stiff compared to the applied loads,a circular arc curve was used as the initial curve. In cases where the boom was relatively limber, the curve assumed by a boom of zero stiffness was used to reduce the number of iterations required for convergence. These zero stiffness curves were obtained from Reference 2.

Typically, four iterations were required to obtain satisfactory convergence. With the boom divided into 10 elements this required about 15 minutes of computer time; an additional 15 minutes were required to automatically plot the results. Thus, a total of about one half hour of computer time was required to produce the results for each case presented in Appendix A.

2.3 Dynamic Analysis

A continuously elastic oil boom floating on the water surface is again treated. However, the non-linearities which were included in the static analysis are not included in the dynamic analysis. It is assumed that the basic boom geometry (planform) is the result of the steady wind and current loads as computed in the static analysis. The waves are assumed to be long crested and to cause only small oscillatory perturbations about this basic shape. It is further assumed that the radius of curvature of the boom under steady loads is large

compared to the radius of curvature from wave induced motion so that, at any point on the boom, the wave induced motions and loads will be statistically the same as those on an infinitely long straight boom with the same mean tension and orientation to the sea. The latter assumption requires fluctuations in tension from waves to be small compared to the mean tension imposed by wind and current. These assumptions permit a dynamic solution to be linearized about the steady-state solution.

The problem is formulated separately in the vertical and horizontal planes. The governing equations in both planes are linear, fourth order differential equations. These are presented as Equations [D-4] and [D-21] in Appendix D for the vertical and horizontal planes respectively. These equations are solved to obtain the unit response operator of the boom as a function of wave frequency.

To obtain statistical information it is necessary to have a representation of the spectral energy density as a function of wave frequency in the desired sea conditions. We have selected the Pierson-Moskowitz spectrum which is given by Equation [13]. The spectral density of any desired quantity at any wave frequency is obtained from the product of the square of its unit response amplitude and the amplitude squared spectral density of the wave spectrum. The root-mean-square amplitude is then found by integrating to find the square root of the area under the curve of spectral density. Finally, the statistical properties of the Rayleigh distribution formula are used to find

the average, average of one-third highest, average of one-tenth highest, and maximum expected value for each desired quantity. The complete formulation for these is presented in Appendix D.

The output of the dynamic analysis gives the above statistical values for the following quantities as a function of the boom properties, boom tension, sea state, and orientation to the sea.

Vertical Plane:

Resonant Frequencies
Absolute Vertical motion of boom (Displacement)
Bending Moment
Shear
Relative Vertical motion between the boom and the Water Surface (Immersion)
Slope
Curvature

Horizontal Plane:

Resonant Frequencies
Absolute Horizontal motion of boom (Displacement)
Bending Moment
Shear
Slope
Curvature

Maximum loads on the boom are obtained by adding the static and dynamic loads (bending moment and shear) separately in both the vertical and horizontal planes. These are then combined by taking the vector sum of both components (i.e. the square root of the sum of the squares).

A limitation of this linearized approach is that statistical information on fluctuations in tension cannot be obtained. However, an empirical relation has been developed to estimate the average tension at the ends of the boom. This relation is given in Equation (14) and reflects the increase in boom drag due to the orbital velocity of the waves.

Results of the dynamic calculations are presented in Appendix D.

3. OIL BOOM MODEL TESTS

To verify the results of the analytical study of Phase I, a model test program was conducted in the HYDRONAUTICS Ship Model Basin. A description of the model, test procedures, and results follows:

3.1 The Model

A scale model of an oil boom must be dynamically as well as geometrically similar to the prototype. To satisfy dynamic (Froude) scaling, the "bending stiffness" EI and "torsional rigidity" GJ of the model must be scaled to the fifth power of the scale ratio λ:

$$\lambda = \frac{D_p}{D_m} = \frac{L_p}{L_m} \tag{8}$$

where

D = diameter, ft

L = Length, ft

p = subscript denoting "prototype", and

m = subscript denoting "model".

A non-dimensional stiffness S' may be defined that must be constant for both model and prototype:

$$S' = \left(\frac{EI}{\rho g D^5}\right)_m = \left(\frac{EI}{\rho g D^5}\right)_p \tag{9}$$

where

ρ = mass density of water, slug-ft^{-3}

g = acceleration of gravity, ft-sec^{-2}

Thus,

$$(EI)_m = \frac{(EI)_p}{\lambda^5} \frac{\rho_m}{\rho_p} \tag{10}$$

Similarly,

$$R' = \left(\frac{GJ}{\rho g D^5}\right)_m = \left(\frac{GJ}{\rho g D^5}\right)_p \tag{11}$$

The ratio ρ_m/ρ_p in Equation (10) is a correction for the difference in density of fresh water (model) and salt water (prototype) ≈ 0.97.

The bending stiffness and torsional rigidity of a realistic oil retention boom model are quite small due to the dynamic scaling criterion. The model boom must be extremely flexible to simulate a full-size boom. To achieve this flexibility with materials that were readily available, the model boom was fabricated of wooden 15-inch long cylindrical segments connected by 1-inch joints of polyvinyl chloride (PVC) tubing. All flexing of the model occurs in the 5/8-inch diameter joints. The model consists of 19 segments and 18 joints, giving a total model length, L = 25.25 ft.

The segment diameter = 3.60 inches. However, the ends of the segments are tapered with 45° cones to permit the joints to bend to 90°.

Each segment has four slots evenly spaced around its perimeter to hold inserts. The inserts are of steel or wood and are exchanged to effect changes in model density and center of gravity.

Figure 1 is a photograph of the model showing the details of construction.

The model was built to simulate a continuous oil boom constructed with a thin elastic skin inflated to a 6-foot diameter and ballasted with water. Of course, the model more closely simulates a segmented oil boom in which the flexibility is concentrated at the joints.

The model parameters were chosen to be representative of a realistic oil boom configuration. However, the corresponding prototype is not necessarily a viable design.

The bending stiffness, EI, and torsional rigidity, GJ, of the oil boom prototype and model (where $\lambda = 20$) are tabulated below.

TABLE 2. - OIL BOOM CHARACTERISTICS

	Model	Prototype
L, ft.	25.25	505.0
D, ft	0.30	6.0
EI, lb-in^2	29.0*	95.6×10^6
GJ, lb-in^2	27.4*	90.5×10^6

*Note: Effective value.

The values of EI and GJ are given as effective values for the model, i.e., the stiffness of the joint is adjusted by the relative lengths of the joint and the model segment to obtain the stiffness equivalent to a model boom having continuous flexibility.

The effective bending stiffness and torsional rigidity of the model may be expressed as dimensionless quantities to eliminate absolute size as a parameter (see Equation (9)):

$$L' = L/D = 84.1$$

$$S' = \frac{EI}{\rho g D^5} = 1.33$$

$$R' = \frac{GJ}{\rho g D^5} = 1.26$$

The model was tested in four conditions of ballast. These conditions are given as dimensionless quantities in Table 3.

TABLE 3. - MODEL BALLAST CONDITIONS

Model Designation	A	B	C	D
$4W/\rho g \pi L D^2$	0.700	0.700	0.625	0.625
CG/D	0.096	0.049	0.055	0.107
H/D	0.742	0.742	0.672	0.672
A_F/LD	0.683	0.683	0.608	0.608

where

W = model weignt, lb

CG = distance from boom axis to center of gravity, ft

H = draft, ft

A_F = frontal area, ft^2 (see Figure 2).

3.2 Test Procedures

The oil boom model was tested in the HYDRONAUTICS Ship Model Basin in both calm water (steady state) and irregular long-crested waves. The model was towed, to simulate ocean currents (relative to the oil boom mooring system), at nominal speeds of 0.25, 0.50, and 0.75 fps. Corresponding full scale currents are 0.66, 1.33, and 1.99 knots, respectively.

The model was towed with elastic mooring lines 5.42 ft.long attached to the ends of the model. These were used in order to transmit a nearly constant (due to the very low spring constant) towing force to the model. In this manner, the effects of carriage surge were damped out and the model speed (current) was held more nearly constant.

The boom mooring was symmetric in all tests, i.e., the line intersecting the two mooring points is at right angles to the current. The spacing between the mooring points on the towing bar was adjustable from 0 to 15 feet. A spacing of 8 feet was chosen to represent a "fixed" mooring. This represents a condition where the full scale oil boom is moored to buoys or other fixed moorings which are spaced 160 ft. apart and symmetric to the flow. In other tests the mooring spacing was adjusted to simulate "drogue" mooring i.e., where the oil boom is attached to drogue anchors that have no transverse resistance so that the mooring lines are parallel to the flow. Thus, in these tests, the spacings between the mooring points and between the boom ends are equal.

Drag (towing force) of the oil boom was measured by a variable reluctance type modular force gage upon which the towing bar was mounted. The gage capacity is 10 lb, but the forces involved in these tests ranged from only 0.1 to 1.0 lb. A low signal to noise ratio was a result of carriage-induced vibrations in the towing bar and the low drag forces involved. However, by integrating the gage output over long time periods (50 sec), the dc component of the signal was effectively separated from the noise. These average (integrated) drag readings were repeated several times during each test and showed to be reliable to within ±0.02 lb.

The shape of the oil boom in the horizontal plane was recorded photographically. The still camera was located about 11 ft above the water surface. Typical photos of the boom in calm water and in waves are shown in Figure 3. The grid in these photos was made of cords spaced at 2 ft. intervals in a plane 1.79 ft above the water level.

Irregular long-crested waves are generated by a wedge-shaped plunger at one end of the towing tank. Significant wave height and the spectrum of wave energy are controlled by a mechanically driven set of several sine-cosine potentiometers rotating at different frequencies and in random phase. The irregular signal generated by the system can be repeated by recycling to the same initial phases between potentiometers. The signal would ordinarily repeat only after about an hour in operation.

The tests in waves were conducted so that individual runs (in the same sea state) were made over a similar irregular wave profile. The wave profile, with respect to a point on the towing carriage, was measured by a sonic probe and recorded on a visicorder. The profile was recorded for about two minutes during the first run in each of the three significant wave heights $\bar{H}_{\frac{1}{3}}$ (sea states). Records were not produced during succeeding runs.

Two movie cameras were used to record the motions of the oil boom when towed in head seas (all tests in waves were conducted with current and waves running in the same direction). One movie camera was mounted overhead next to the still camera and the other was located about 5 ft. above the water and angled to give an oblique view of the water surface. The cameras were run simultaneously at a rate of 12 frames per second for about 55 seconds during each test.

3.3 Discussion of Test Results

3.3.1 Tests in Calm Water - The model was well-behaved in the calm water tests. After some initial oscillations, due to the acceleration to the desired towing speed, the boom quickly assumed a steady shape. To simulate drogue mooring, the mooring spacing was adjusted while underway until an equilibrium (steady) shape was found in which the towing lines were parallel, i.e., the boom end spacing, S_B, equal to the mooring spacing, S_M.

After the boom had reached equilibrium,a photograph was made to record the shape in the horizontal plane (see Figure 3). The profile seen in a photograph is not the true boom shape because of parallax errors.

Offsets were taken from the photographs and corrected for parallax to obtain the profiles in Figures 4 to 9. These are profiles of the oil boom centerline. The coordinate system for each profile was shifted so that the x-axis passed halfway between the boom ends and the y-axis passed through the point of one end. The oil boom profiles were not exactly symmetrical due to non-uniformities in the model construction and towing lines.

The measured towing conditions for each test in Figures 4 to 9 are given in Table 4 in non-dimensional form.

There do not appear to be any significant changes in the model profiles with respect to the four geometries (A, B, C and D). Change in the vertical center of gravity (see Table 3) would not be expected to affect the towing behavior in calm water. A change in model density might be expected to have an effect due to the increase in drag with greater submergence. However, this effect is not readily apparent in the figures. Note that the change in draft between model configurations is about 10 percent. A 5 percent increase in Froude number can be expected to change the drag by the same amount as a 10 percent increase in draft.

TABLE 4. - CALM WATER TOWING CONDITIONS

Figure Number	Mooring Condition	Model	Test Number	F_D	S_M/L	S_B/L	T/L	C_D
4	Fixed	A	1	0.2360	0.3168	0.2966	0.2976	0.215
		B	18	0.2360	0.3168	0.2991	0.3007	0.215
		C	29	0.2410	0.3168	0.3070	0.2950	0.205
		D	41	0.2400	0.3168	0.2951	0.3054	0.219
5	Fixed	A	2	0.1570	0.3168	0.3106	0.2662	0.240
		B	15	0.1530	0.3168	0.3020	0.3155	0.280
		C	27	0.1670	0.3168	0.3166	0.2645	0.225
		D	39	0.1700	0.3168	0.3109	0.3036	0.215
6	Fixed	A	3	0.0750	0.3168	0.3739	0.2551	0.275
		B	14	0.0700	0.3168	0.4364	0.2506	0.137
		C	26	0.0800	0.3168	0.4125	0.2579	0.236
		D	37	0.0860	0.3168	0.3634	0.2593	0.149
7	Drogue	A	6	0.2280	0.1782	0.1874	0.2891	0.164
		B	17	0.2370	0.2110	0.2145	0.2887	0.170
		C	30	0.2400	0.2178	0.2239	0.2854	0.172
		D	42	0.2460	0.2110	0.2089	0.3010	0.185
8	Drogue	A	5	0.1480	0.3037	0.3066	0.2949	0.218
		B	16	0.1510	0.3037	0.2634	0.2888	0.228
		C	28	0.1650	0.3037	0.3110	0.2941	0.210
		D	40	0.1640	0.2839	0.2878	0.2867	0.175
9	Drogue	A	4	0.0700	0.5279	0.6308	0.2872	0.260
		B	13	0.0720	0.4356	0.4781	0.2705	0.115
		C	25	0.0810	0.4784	0.5159	0.2629	0.315
		D	38	0.0830	0.4819	0.5188	0.2615	0.097

S_M = Mooring spacing (towline spacing as fixed to towing carriage)

S_B = Boom and spacing(towline spacing as fixed to the boom ends)

L = Boom length

T = Towline length

F_D = Froude number = $V/\sqrt{gL}$

C_D = Drag coefficient (see Equation 12)

Significant changes in the boom profile arise from the towing speed (Froude number) and the lateral spacing between the mooring points. These changes are obvious in the figures and follow trends that would normally be expected.

Calm water drag data are presented in Table 4 and Figure 10. The drag coefficient is defined by

$$C_D = \frac{D}{\frac{1}{2}\rho V^2 HL} \qquad (12)$$

where

D = drag, lb.,

V = current velocity, fps.,

H = draft, ft.,

L = boom length, ft.

The drag data are shown as a function of mooring spacing, S_M. The mooring conditions, fixed or drogue, and Froude numbers are indicated by the data point symbols. No significant effects due to Froude number or mooring conditions are apparent from these data. The model configurations are not indicated in this figure; however, they also show no effect. A dashed line is shown to indicate the tendency of the drag coefficient to increase as mooring spacing increases, as should be expected.

3.3.2 Tests in Waves - Irregular waves were generated in the towing tank in such a way that their (amplitude squared) spectral density $S(\omega)$ would simulate the spectrum given by Pierson-Moskowitz (Ref. 3). This spectrum may be expressed as

$$S(\omega) = 16.8\ (\omega)^{-5}\ e^{-\left[\frac{33.56}{(\bar{H}_{\frac{1}{3}})^2(\omega)^4}\right]},\ \text{ft}^2\text{-sec} \qquad (13)$$

where

ω = frequency, rad/sec

$\bar{H}_{\frac{1}{3}}$ = significant wave height, ft., and 16.8 and 33.56 are empirical constants.

The "significant" value is defined as the average of the highest one-third values of the parameter in question. The parameters in this report are generally given as amplitudes. Wave height is the exception and is a "double" amplitude measured from crest to succeeding trough.

The wave records from the model tests were treated statistically to find the spectral density as a function of wave frequency ω and the significant wave height. Three different "seas" were generated and correspond, nominally,to Sea States 3, 4 and 5. Each different sea was used for tests at a different current as given in Table 5. The spectral densities are shown in Figures 11, 12 and 13 along with the Pierson-Moskowitz spectrum having the same significant wave height. The wave data

show good agreement with the desired spectrum. However, it should be noted that the data points represent the wave energy contained in the frequency band between the data points. If data points are calculated for more narrow frequency bands they will show that the wave energy is actually concentrated at the discrete frequencies at which energy is supplied to the wavemaker.

TABLE 5. - CURRENT AND WAVES USED IN MODEL TESTS

Sea State	3	4	5
Significant wave height $\overline{H}_{\frac{1}{3}}$, ft.	4.91	6.80	13.33
Current V_k, knots*	0.67	1.33	1.99

* Given to prototype scale.

The model behavior in waves was similar to behavior in calm water. A mean profile similar to those in calm water tests was assumed after starting the carriage, but the segments oscillated about this mean profile in response to the action of the waves.

In Sea State 3 the boom segments did not submerge. Water occasionally washed over segments of the boom in Sea State 4 and did so frequently in Sea State 5. The middle segment was totally submerged about half of the time during tests in the highest Sea State. At no time was a segment seen to lift out of the water.

The drag data for tests in waves are presented in Figure 10, along with the data from calm water tests. These data show that the drag is significantly increased by the presence of waves. In all other respects the drag in waves is similar to the drag in calm water.

Data were taken from a frame-by-frame analysis of motion pictures to determine the boom motions in terms of angles of roll γ, pitch β, and yaw α between adjoining segments. The significant values of the angular motion amplitudes were found and are presented in Figures 14, 15 and 16. It should be noted that these angles represent the average angles for a complete segment length and should be divided by the segment length to get an angle per unit length or curvature.

Model configuration, i.e., center of gravity and weight, and mooring spacing had no discernable effect on the motions that were measured. The effect of wave height, however, is evident and follows expected trends, e.g., higher waves cause greater motions.

4. COMPARISON OF ANALYTICAL RESULTS WITH MODEL TESTS

4.1 Static Tests

The "static" program was used to generate data for an oil boom with all input parameters corresponding to those in (calm water) model tests numbers 1, 2 and 3. (See Tables 2, 3, and 4). The computed and the experimental values of drag coefficient are compared in Table 6 and the steady-state boom geometries in the horizontal plane are presented for comparison in Figures 17, 18 and 19.

TABLE 6. - COMPARISON OF MEASURED AND COMPUTED DRAG COEFFICIENTS

Model Test Number	Froude Number, F_D	Drag Coefficients, C_D		Difference, percent
		Measured	Computed	
1	0.236	0.215	0.214	0.5
2	0.157	0.240	0.221	7.9
3	0.075	0.275	0.250	9.1

The computed results show, in general, good agreement with the model experiments. The computed drag coefficients agree within the accuracy of the model measurements (see Figure 10). The computed boom geometries compare favorably with the model measurements, again considering the accuracy shown in the model tests (Figures 4 to 9).

4.2 Dynamic Tests

The "dynamic" gram was applied to give statistical values of pitch angle β and yaw angle α between two points on a continuous boom. The longitudinal separation between these two points is just ΔL, (Δx in Equation (D-19)) the link length of the model boom. The input parameters corresponded to those of model boom "A" in all other respects.

The calculated significant values of pitch and yaw are presented in Figures 20 and 21, respectively, as functions of significant wave height with contours for relative heading angles of 0, 30, 45, 60, and 90 degrees. It is interesting to

note the implications of these curves. First, the pitch amplitude is zero at the 90 degree heading and maximum at 0 degrees while yaw amplitude is zero at both 0 and 90 degrees and maximum around 45 degrees. At 90 degree heading (beam seas) the boom moves in heave and sway but does not bend in either plane. At 0 degrees (head seas) the boom contours the waves with heave and pitch but has no motion in the horizontal plane. Second, yaw and pitch increase with increasing wave height up to some limiting value. The limiting value, a function of boom heading, is related to the maximum slope that can occur (discounting breaking waves) in the sea.

Unfortunately, model test data do not represent any particular heading angle. Nominal values of heading angle were found to be 60, 45 and 15 degrees corresponding to model test data at significant wave heights of 4.91, 6.80 and 13.33 feet, respectively. Calculated values of significant pitch amplitude and yaw amplitude for these parameters are shown along with the model test data in Figures 22 and 23, respectively.

The agreement between calculated and observed boom motions in the vertical plane (pitch amplitude) is quite good. However, observed yaw amplitudes are roughly twice as large as those calculated for the horizontal plane. Two important factors help to explain the apparant disparity in the relative agreement between measurements and calculations in these two planes. First, waterplane area has a large effect on motions in the vertical plane but virtually no effect in the horizontal plane. The

waterplane acts like a spring in the vertical direction and tends to force the boom to follow the contour of the passing wavetrain. In fact, the waterplane can dominate all other factors in the vertical plane. Hence, "limber" booms, regardless of other design details, tend to identically contour the sea. In the horizontal plane, on the other hand, factors such as virtual mass, damping and tension tend to have a relatively larger bearing on boom response to waves. Second, and perhaps more important, the assumption that the behavior of a section of an oil boom can be approximated with an element in a straight and infinitely long (one-dimensional) boom loses validity in the horizontal plane. The oil boom model, under tow, exhibited a characteristic U-shaped geometry in the horizontal plane whereas in the vertical plane the boom is, indeed, a straight-line (in calm water). In light of these two factors, it is not surprising that agreement between the model tests and calculations was better in the vertical plane than in the horizontal plane.

Statistical values of boom height relative to the wave height (immersion) were also calculated for a boom with parameters corresponding to those of model "A". These results indicate that this design would never become immersed. Model observations, on the other hand, showed some immersion in Sea State 4 and frequent cases in Sea State 5 where a wave crest would pass over sections of the boom. This analytical method does not account for the effects of boom curvature and "choppy" or breaking waves on boom immersion which may be important considerations for oil containment.

5. SUGGESTED METHOD OF USING COMPUTED DATA IN APPENDICES A AND B

The data in Appendices A and B are in dimensional form. The input parameters were chosen with the U. S. Coast Guard to have a range that would be useful in assessing boom designs that are currently under development. Thus, booms with dimensional parameters similar to those used to generate the data may be treated directly. However, booms having grossly different sizes may also be treated if their non-dimensional characteristics compare with the corresponding non-dimensional input parameters (see Equations (7) through (11) and Table 3). In this case, the computer output data must also be treated non-dimensionally to obtain the proper scale factors.

To illustrate a method of using the computed data, an example problem is presented in the following paragraphs.

GIVEN: A boom with the same characteristics as configuration X (see Table A-1) in a 40-knot wind, 1-knot current and 10-foot waves; total length = 100 feet between two moorings spaced 80 feet apart and oriented 90-degrees to the wind, current and waves; Young's modulus of boom cylinder material, E = 1000 psi.

FIND: Average mooring loads, average stress due to bending at the middle of the boom, average roll angle of the skirt at the middle, maximum expected stresses induced by waves, significant sway amplitude, and maximum relative submergence.

ANALYSIS:

(1) The results of the model test drag data suggest that the drag in waves can be estimated from the calm water drag augmented by a factor which accounts for the effect of orbital velocities:

$$D_w = D_o \left(1 + c\,\frac{\overline{H}_{\frac{1}{3}}\,\omega_{max}}{V_w}\right)^2 \qquad (14)$$

where

D_w = drag in waves, lb

D_o = drag in calm water, lb

c = empirical constant = 0.42

ω_{max} = frequency of maximum wave energy, rad-sec^{-1},

V_w = current, ft-sec^{-1}

Another way of looking at Equation (14) is that the term $V_w + c\overline{H}_{\frac{1}{3}}\,\omega_{max}$ is an effective current = V_e so that

$$D_w = D_o \left(\frac{V_e}{V_w}\right)^2 \qquad (15)$$

In this problem, $\overline{H}_{\frac{1}{3}}$ = 10 ft and:

$$\omega_{max} \text{ (from Sea State tables)} = \frac{2\pi}{\text{Period}_{max}}$$

$$= \frac{2\pi}{8.9} = 0.71$$

Thus,

$$V_e = (1)1.689 + 0.42\ (10.)0.71$$

$$= 1.689 + 2.96 = 4.65 \text{ ft-sec}^{-1}$$

$$= 2.75 \text{ knots}$$

No data are available at 2.75 knot current; however, the values at 2 knots may be extrapolated using the ratio $(2.75/2)^2 = 1.89$. The tension at the ends of the boom for 2 knots (from Test No. X-0-2-90 Appendix A) is 3420 lb. Thus, tension due to a 2.75 knot current in 10-ft. waves is:

$$1.89\ (3420) = 6450 \text{ lb.}$$

Now, add to this the tension due to 40 knot wind (Test No. X-40-0-90) = 170 lb. to get: average mooring load = 6620 lbs.

(2) The steady state bending moment for this mooring condition is seen to be independent of wind and current. M = 20 ft-lb at the middle of the boom. The fiber stress due to bending in the 2-ft. diameter cylinder is given by

$$\sigma = \frac{M}{Z} = \frac{EMc}{EI}\text{, psi} \qquad (16)$$

where

c = distance from neutral axis to the outermost fiber, in.

Z = section modulus, in^3.

Thus,

$$\sigma = \frac{10^3 (20 \cdot 12) 12}{10^5}$$
$$= 29 \text{ psi}$$

Note that in this boom design, tensile loads are supported by a cable at the bottom of the skirt.

(3) If we assume that roll angle varies linearly with drag, the average roll angle at the middle of the boom can be found using a method analogous to part 1., i.e.,

$$\theta = 1.89\ (27.5) + 3.2$$
$$= 55 \text{ degrees}$$

(At the ends, the average roll angle decreases to about 22 degrees).

(4) From the planview of the boom in Appendix A we might assume that the most severe bending due to waves will occur near the ends of the boom. Hence, choose 45 degrees as the heading angle for dynamic data in Appendix B. The average tension (6600 lb) is outside the range given in the tables, so extrapolation must be used. The following table lists the parameters of interest taken from Appendix B.

Page	Heading Angle, deg.	Tension, lb.	Max. Bending Mom. ft-lb Vertical	Max. Bending Mom. ft-lb Horizontal	Max. Immersion ft.	Sway $\bar{v}_{\frac{1}{3}}$ ft.
B-176	30	0	80.5	72.5	0.28	2.49
B-177	30	2000	28.7	53.3	0.91	2.50
B-178	30	4000	19.0	43.0	1.25	2.51
B-179	60	0	38.7	62.3	0.26	4.31
B-180	60	2000	20.6	45.5	0.49	4.32
B-181	60	4000	13.1	37.3	0.74	4.33
Extrap-olated	45	6600	11.0	23.0	1.25	3.41

Note: The extrapolated values in this table were obtained by first interpolating between 30 and 60 degrees.

A conservative estimate of the maximum bending moment is obtained by taking the vector sum of bending in the vertical and horizontal planes:

$$M_{max} = \sqrt{(11)^2 + (23)^2} = 26 \text{ ft-lb}$$

Using Equation (16), obtain the maximum fiber stress induced by waves σ = 37 psi. Add this to the maximum steady state bending stress to find the maximum expected fiber stress σ_{max} = 66 psi.

The significant sway amplitude is 3.4 feet near the ends of the boom and 5.0 feet (page B-183) at the middle.

The maximum immersion is estimated to be 1.25 feet. This is greater than the available freeboard (0.87). The corresponding root-mean-square immersion amplitude is 0.38 feet. Probability theory (assuming Gaussian distribution, Ref. 4) predicts that a boom with this immersion amplitude and freeboard will be submerged at any given point less than 0.01 percent of the time. However, the model test data indicates that the dynamic program underestimates immersion in real waves.

6. CONCLUSIONS AND RECOMMENDATIONS

The work done in this study shows the feasibility of developing a realistic mathematical model to determine loads and motions of an oil retention boom in a seaway. This model should provide useful data to aid in the design of oil retention booms. However, both the static and dynamic models are limited in their range of application because of the nature of assumptions made in developing the models.

The static model is the most general and includes the important non-linearities. It is, however, limited to booms which can be modeled by a continuous elastic beam. Since many proposed boom designs are composed of a number of relatively rigid segments connected by limber joints, it is recommended that the static model be extended to cover this type of boom.

The linearized dynamic analysis is the most severely limited because of the restrictive nature of the assumptions that were made. In particular, it was assumed that at any point on the boom, the wave induced motions and loads on the boom would be statistically the same as those on an infinitely long, straight boom with the same mean tension and orientation to the sea. It was also assumed that fluctuations in tension from waves are small compared to the mean tension. The experiments in this study indicate that neither of these assumptions is well justified and, in fact, under conditions of large seas and little current, these assumptions may lead to considerable error.

The linearized dynamic analysis also does not permit changes in hydrodynamic and hydrostatic coefficients which result from a local change in boom immersion. These changes are important in determining the performance of the boom in large seas where the response is highly non-linear and they are vital under conditions where the boom might be completely immersed in a wave crest or lift clear of a wave trough - important factors to establish, since either will permit the escape of oil. Probably the greatest limitation of the dynamic analysis is that it provides no information on fluctuations in tension.

These limitations can be removed by conducting a dynamic analysis in the same manner as the static analysis is now done. This can be accomplished within the framework of the current static program. With this method, each iteration would represent a small increment in time. Sufficient iterations would be

carried out to provide an adequate statistical sample. It is recommended that such an analysis be carried out if more detailed results are desired.

The model tests conducted in this study show that oil boom behavior in a seaway can be realistically simulated in a towing tank. The greatest difficulty with model tests is perhaps connected with the ability to construct a model with the proper bending characteristics. Analysis of motion data from tests in irregular waves is straightforward but very tedious. However, tests may be conducted in regular waves to obtain the motion response amplitude operators, RAO's. The RAO's may then be used to predict the statistical motions in any desired wave spectrum. Bending moments can be predicted from the motions (curvature). Tension at the ends of the boom can be measured directly. Stereo photography might be proposed to obtain the heave response of the model. It is suggested that model testing be considered for further development and selection of the "optimum" oil boom.

REFERENCES

1. Sokolnikoff and Redheffer, "Chapter 9, Numerical Analysis," Mathematics of Physics and Modern Engineering, page 687, McGraw-Hill Book Co., New York, 1958.

2. Pode, L., and Rosenthal, L., "Cable Function Tables For Small Critical Angles," Supplement to David Taylor Model Basin Report 687, September 1955.

3. Michel, W. H., "Sea Spectra Simplified," Marine Technology, 5, No. 1 (1968).

4. Wong, K. K., "Coupled Response of a Float-Supported Aircraft in a Seaway," HYDRONAUTICS, Incorporated Technical Report 513-2, May 1966.

5. Hsieh, T., et. al., "Rough Water Mating of Roll-On/Roll-Off Ships with Beach Discharge Lighters," HYDRONAUTICS, Inc., Technical Report 636-1, July 1967.

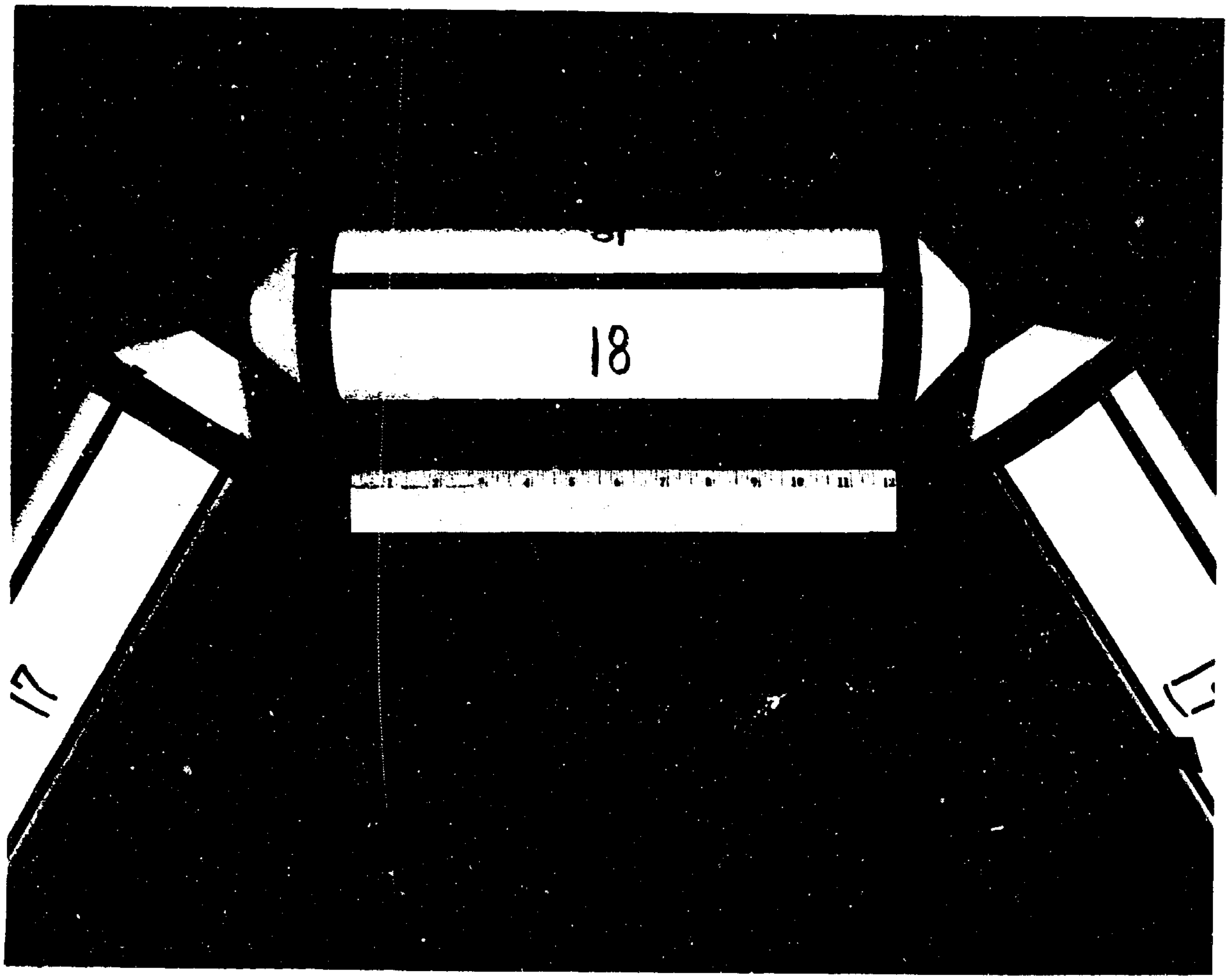

FIGURE 1 - VIEW OF MODEL SHOWING DETAILS OF CONSTRUCTION

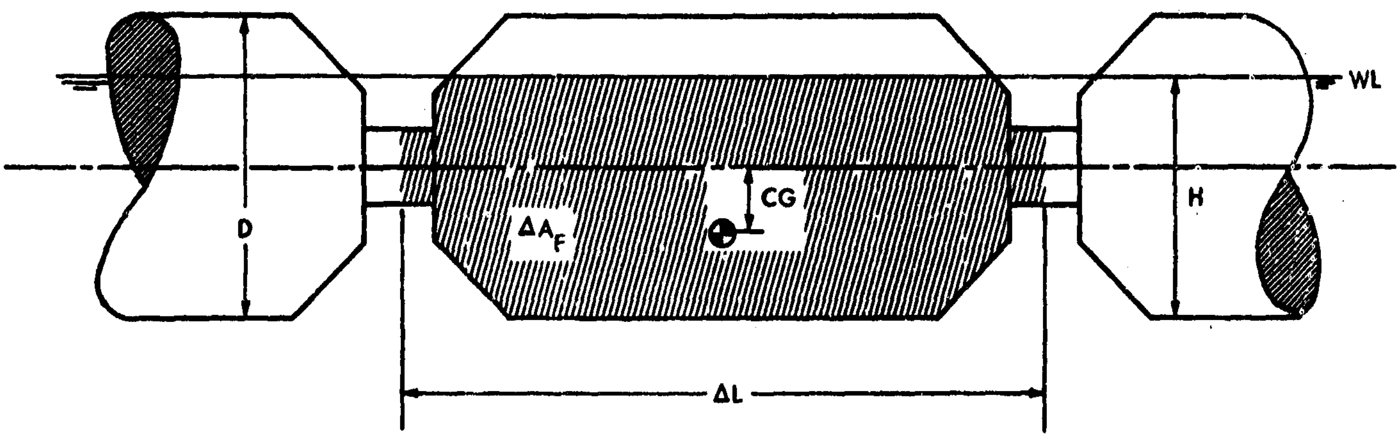

(DRAWING IS NOT TO SCALE)

FIGURE 2 - MODEL DEFINITION SKETCH

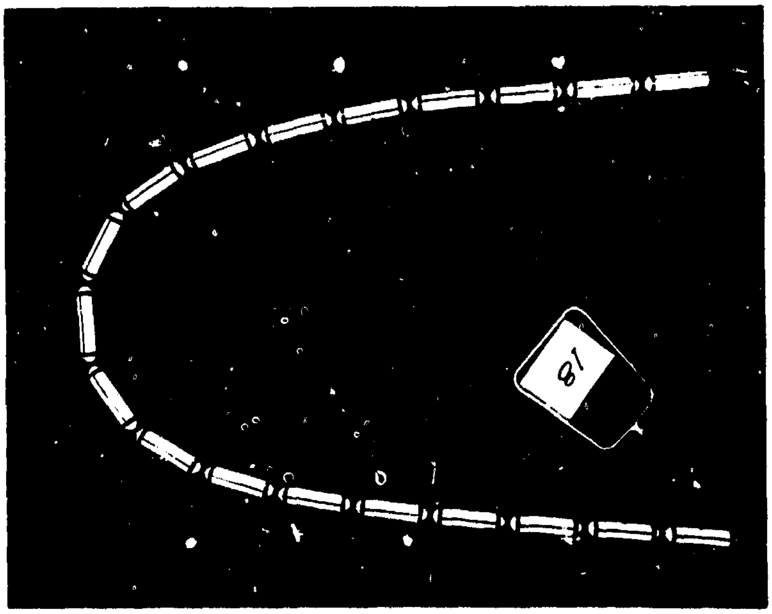

a. CALM WATER

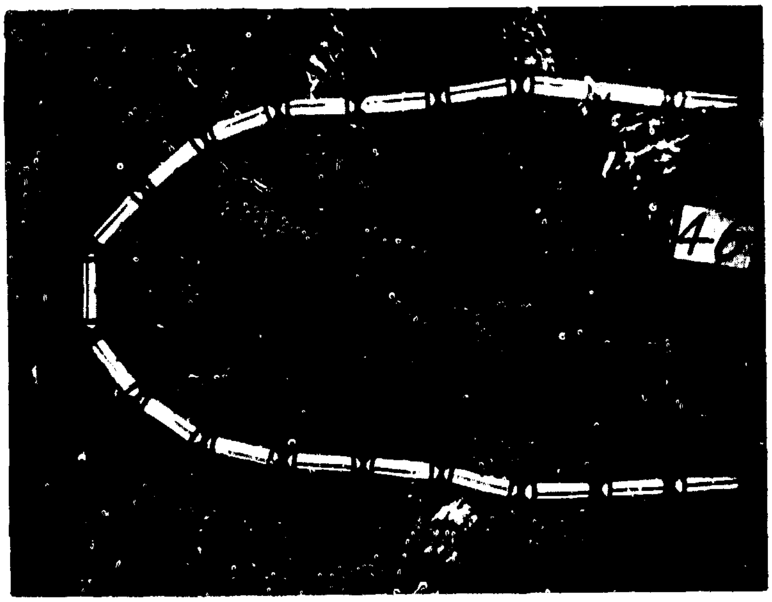

b. WAVES

FIGURE 3 - TYPICAL PHOTOS OF OIL BOOM

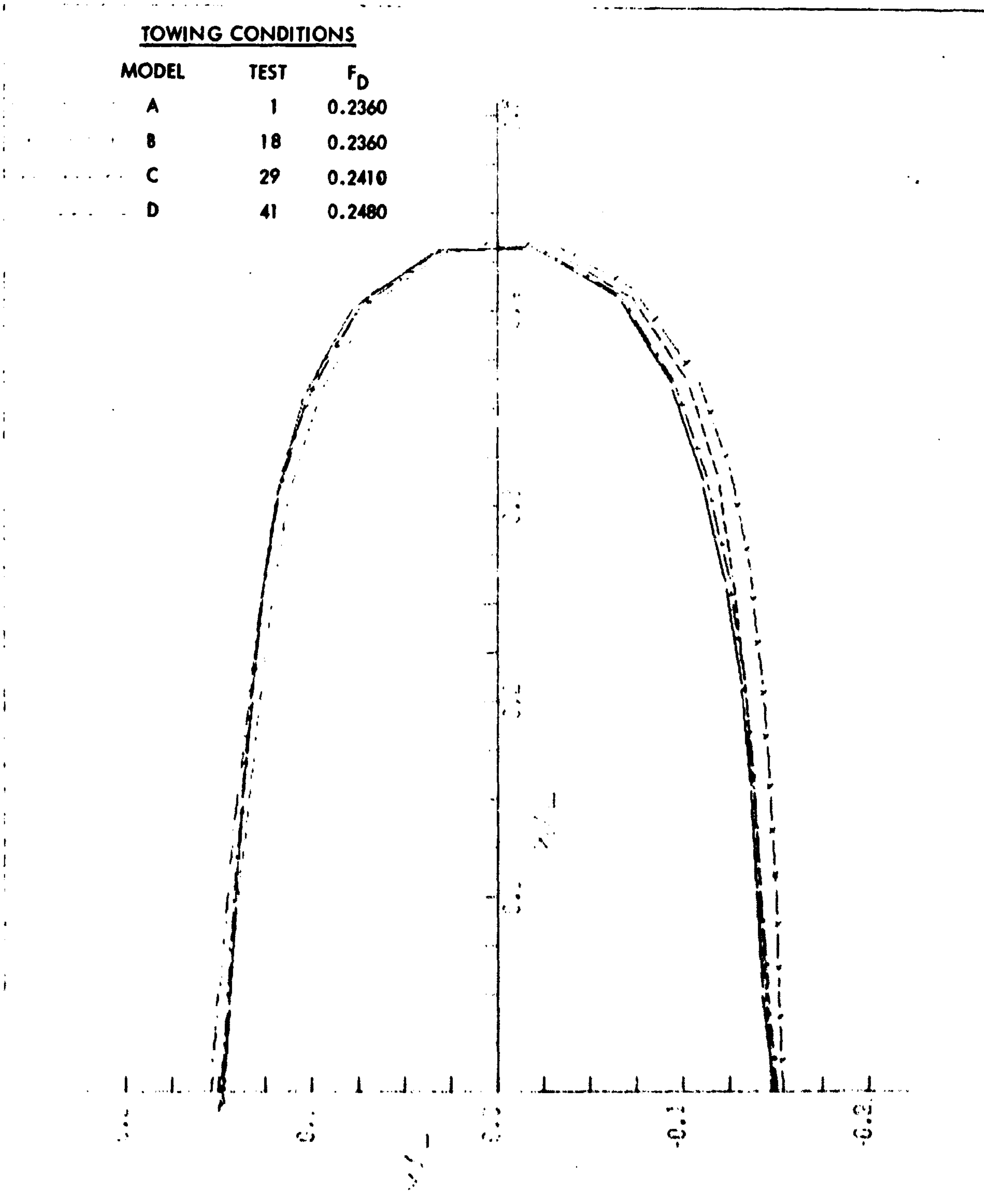

FIGURE 4 - STEADY STATE (CALM WATER) OIL BOOM GEOMETRY FROM MODEL TESTS; MOORING = FIXED, NOMINAL CURRENT = 1.99 KNOTS

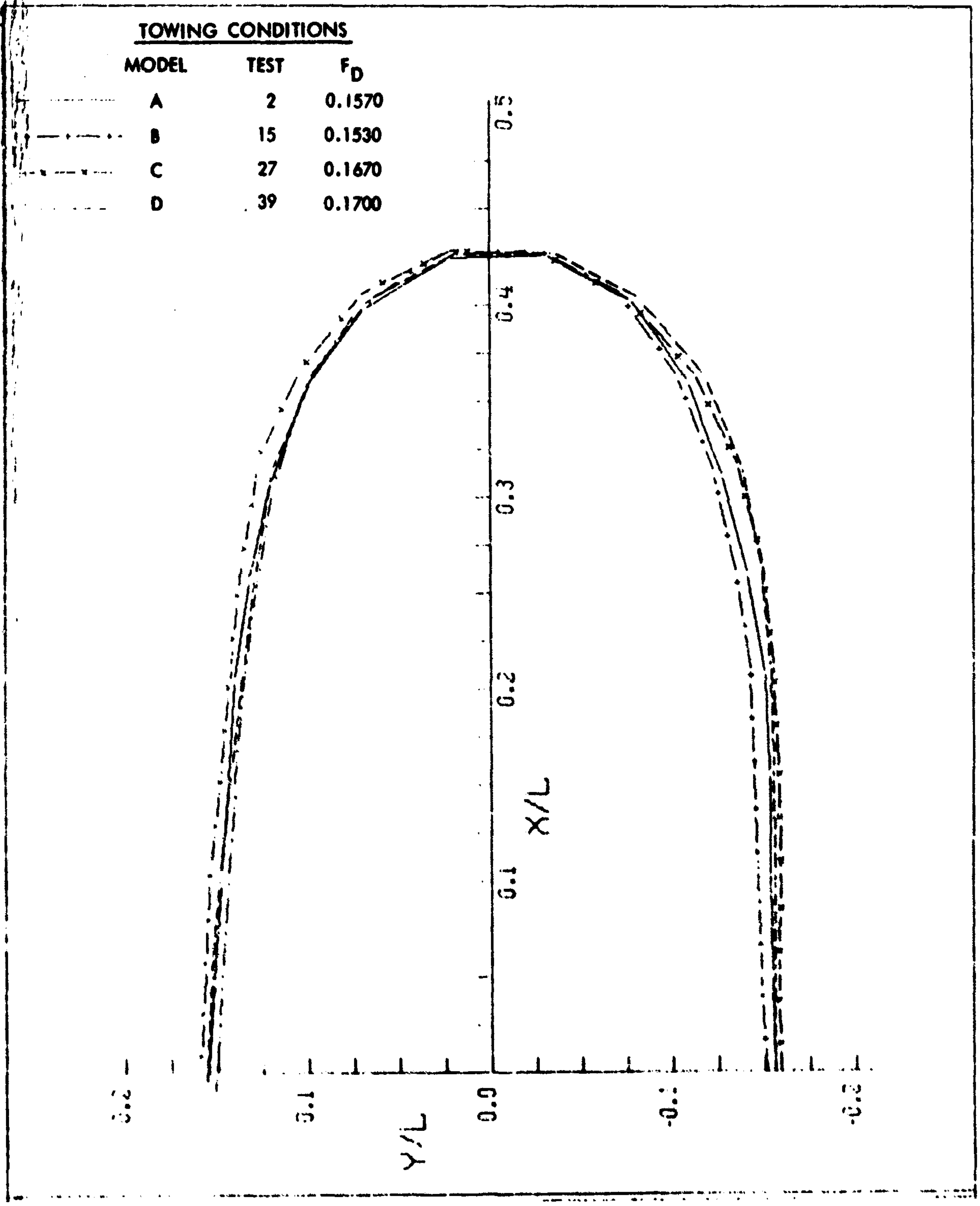

FIGURE 5 - STEADY STATE (CALM WATER) OIL BOOM GEOMETRY FROM MODEL TESTS; MOORING = FIXED, NOMINAL CURRENT = 1.33 KNOTS

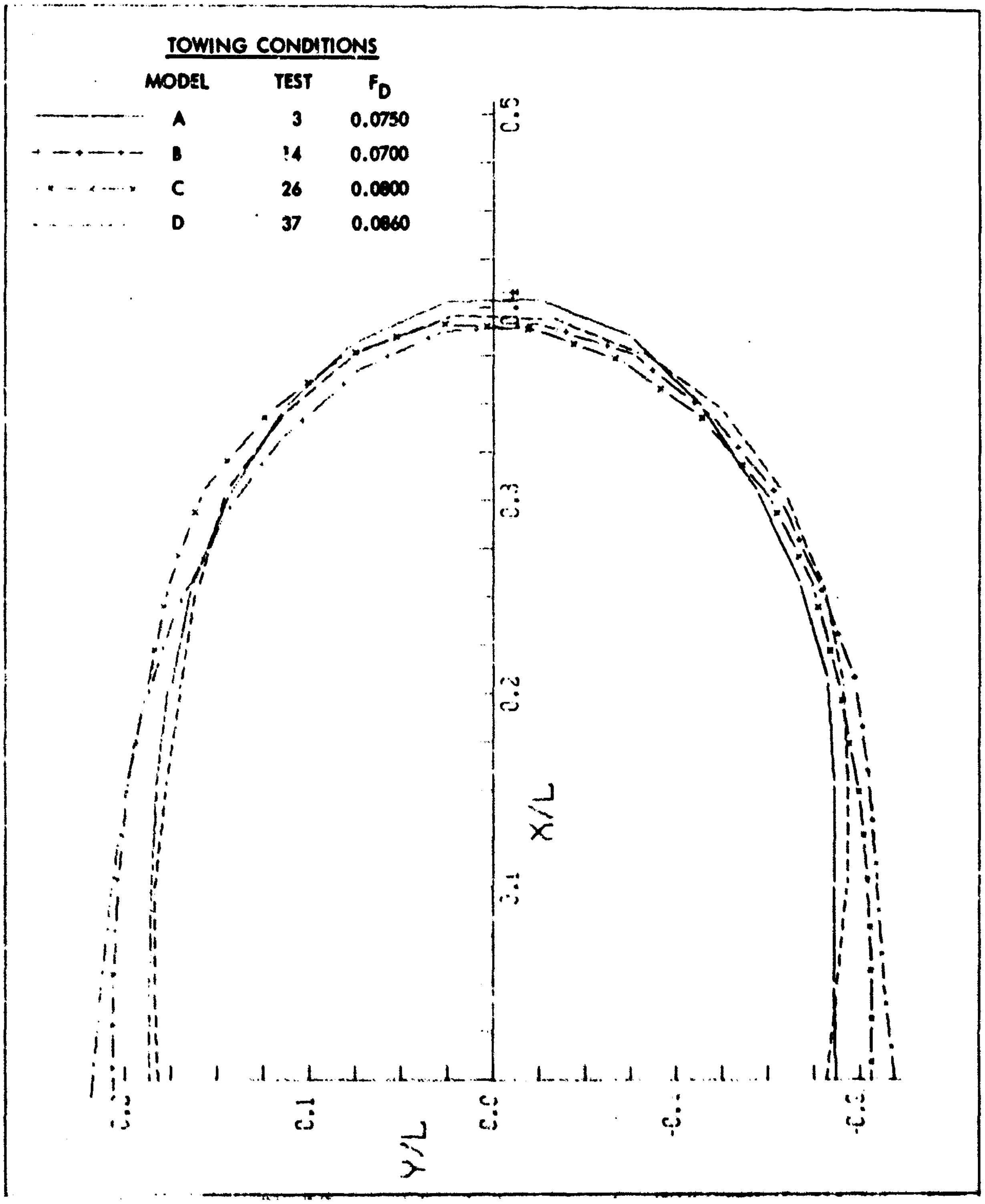

FIGURE 6 - STEADY STATE (CALM WATER) OIL BOOM GEOMETRY FROM MODEL TESTS; MOORING = FIXED, NOMINAL CURRENT = 0.66 KNOTS

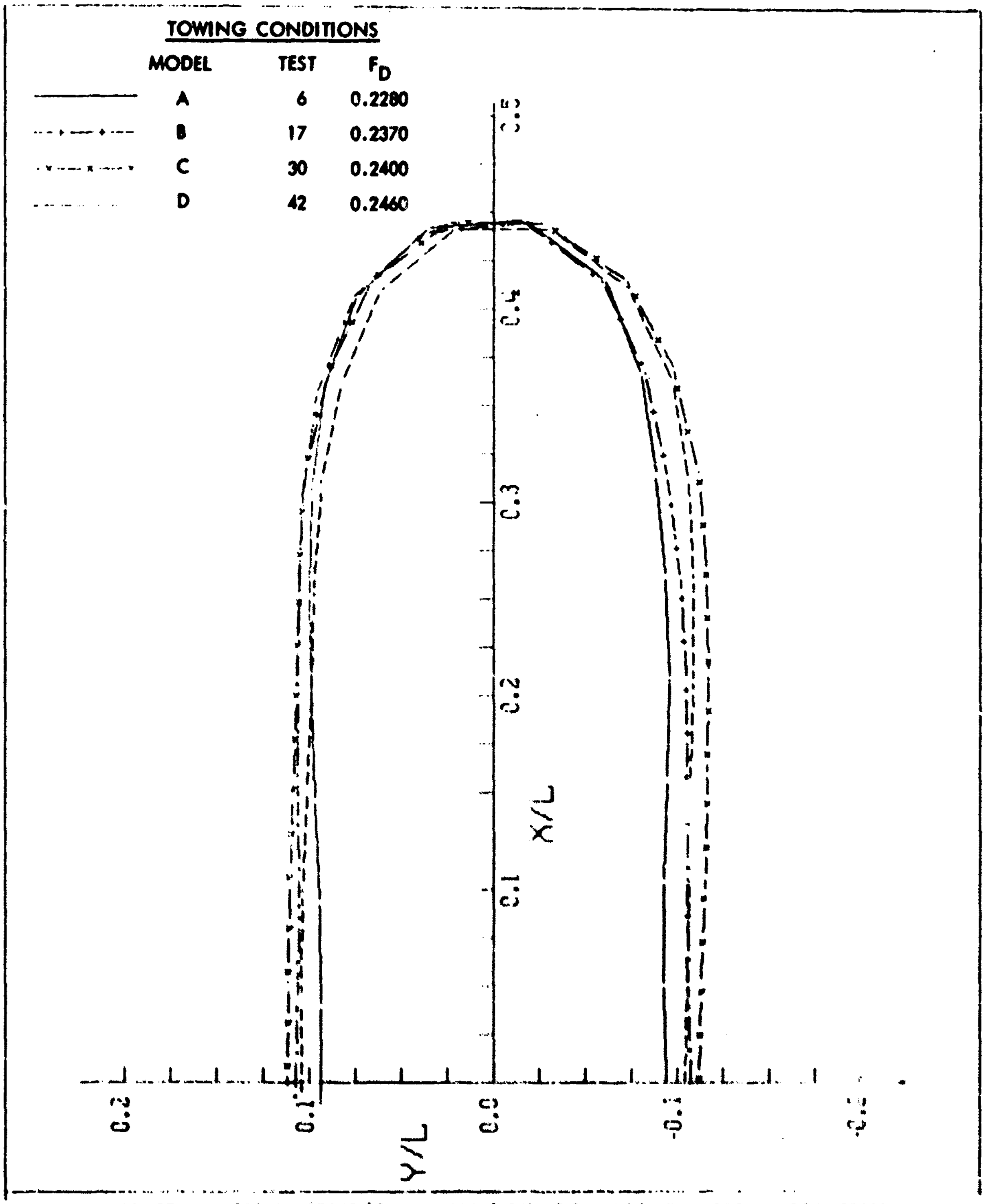

FIGURE 7 - STEADY STATE (CALM WATER) OIL BOOM GEOMETRY FROM MODEL TESTS; MOORING = DROGUE, NOMINAL CURRENT = 1.99 KNOTS

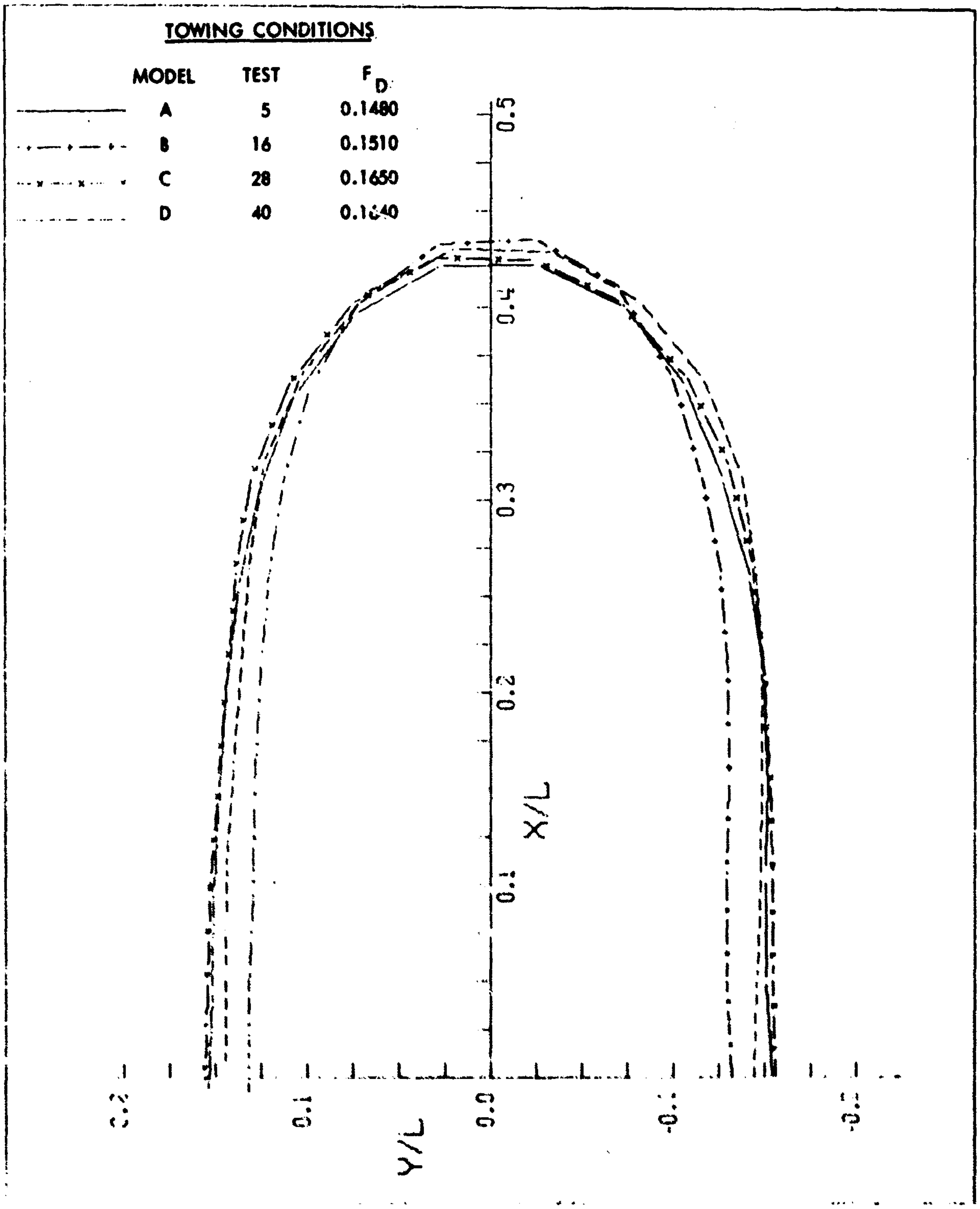

FIGURE 8 - STEADY STATE (CALM WATER) OIL BOOM GEOMETRY FROM MODEL TESTS; MOORING = DROGUE, NOMINAL CURRENT = 1.33 KNOTS

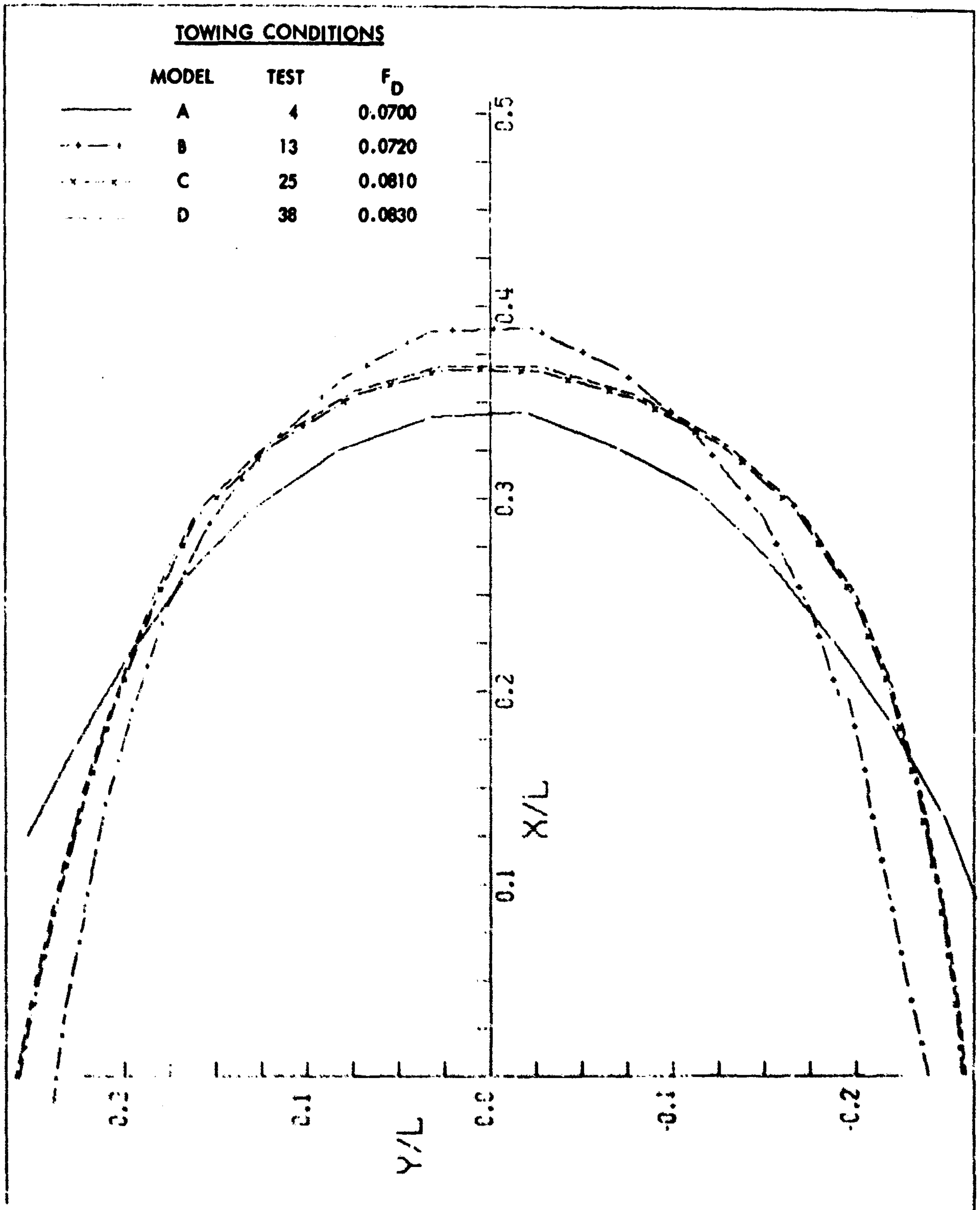

FIGURE 9 - STEADY STATE (CALM WATER) OIL BOOM GEOMETRY FROM MODEL TESTS; MOORING = DROGUE, NOMINAL CURRENT = 0.66 KNOTS

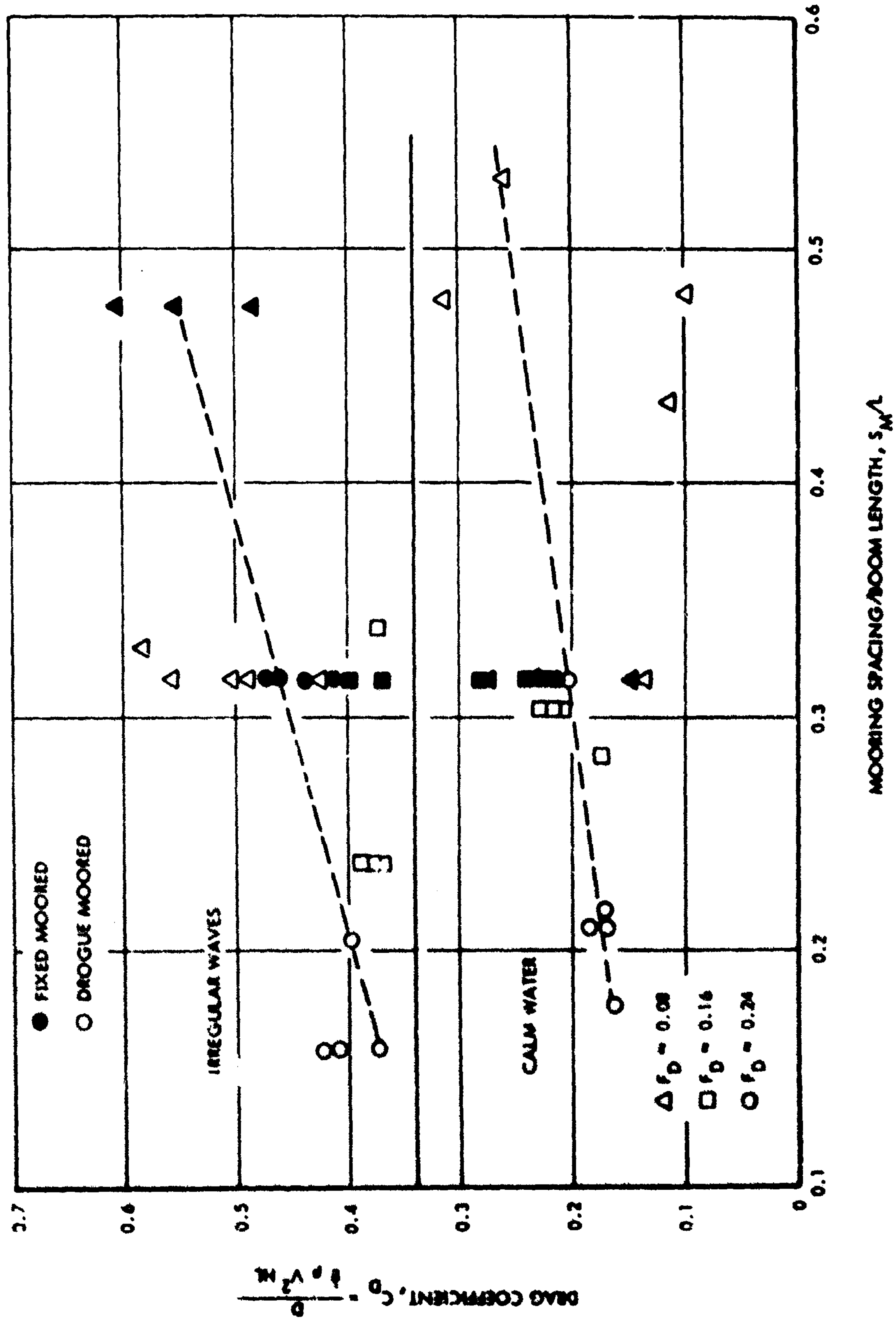

FIGURE 10 - OIL BOOM MODEL TEST DRAG DATA

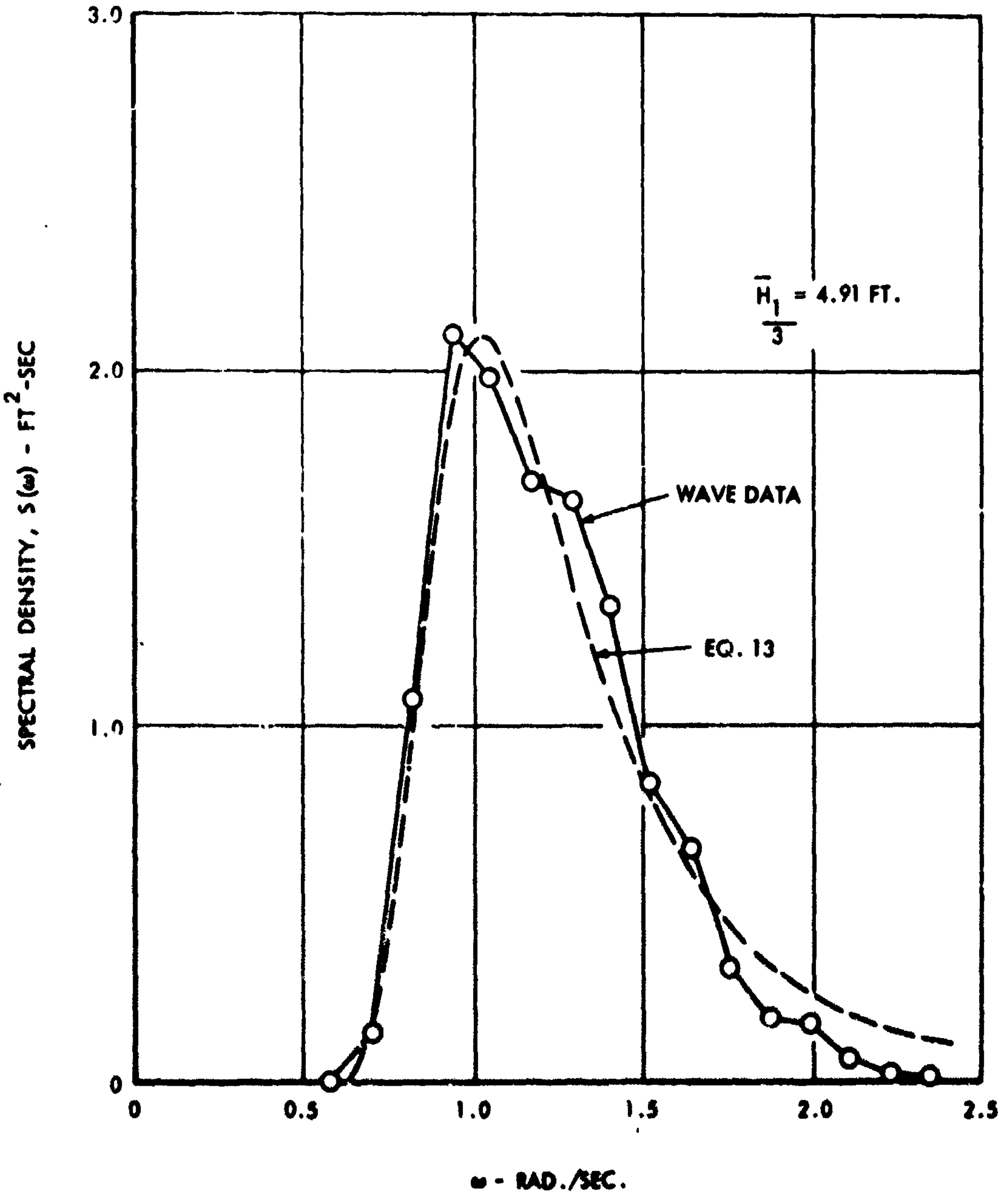

FIGURE 11 - SEA STATE 3 MODEL TEST WAVE SPECTRUM

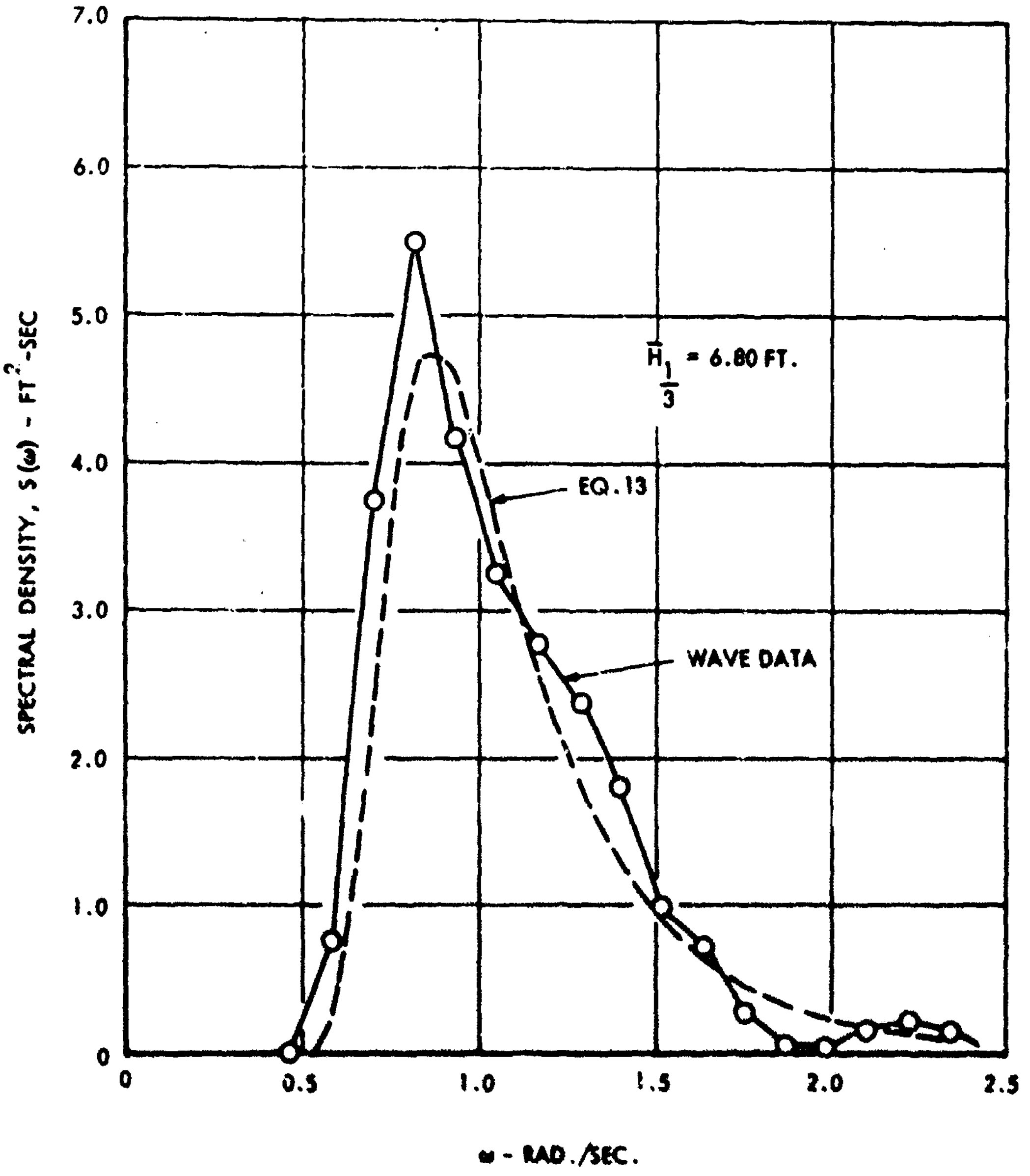

FIGURE 12 - SEA STATE 4 MODEL TEST WAVE SPECTRUM

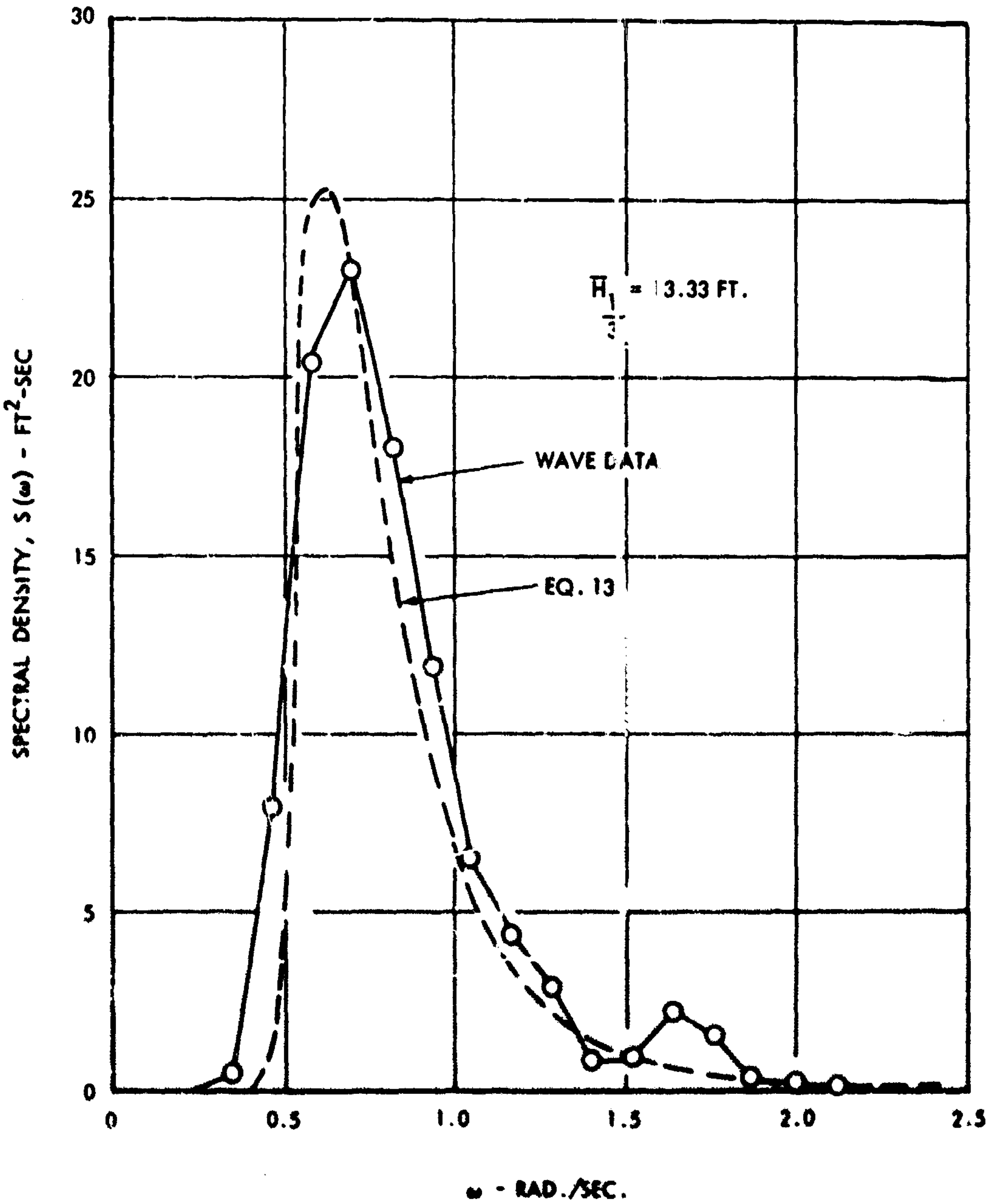

FIGURE 13 - SEA STATE 5 MODEL TEST WAVE SPECTRUM

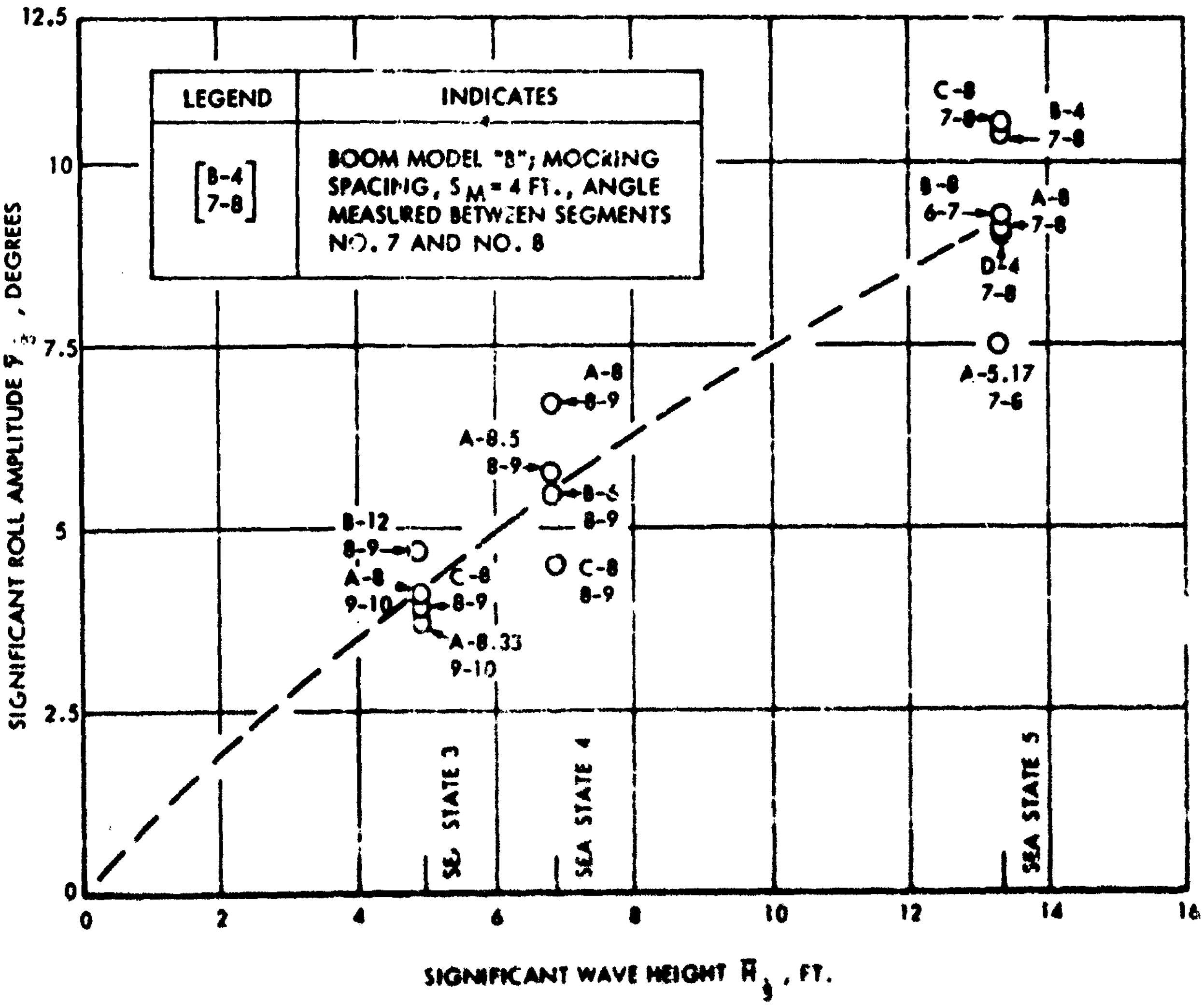

FIGURE 14 - SIGNIFICANT ROLL MOTION IN IRREGULAR WAVES

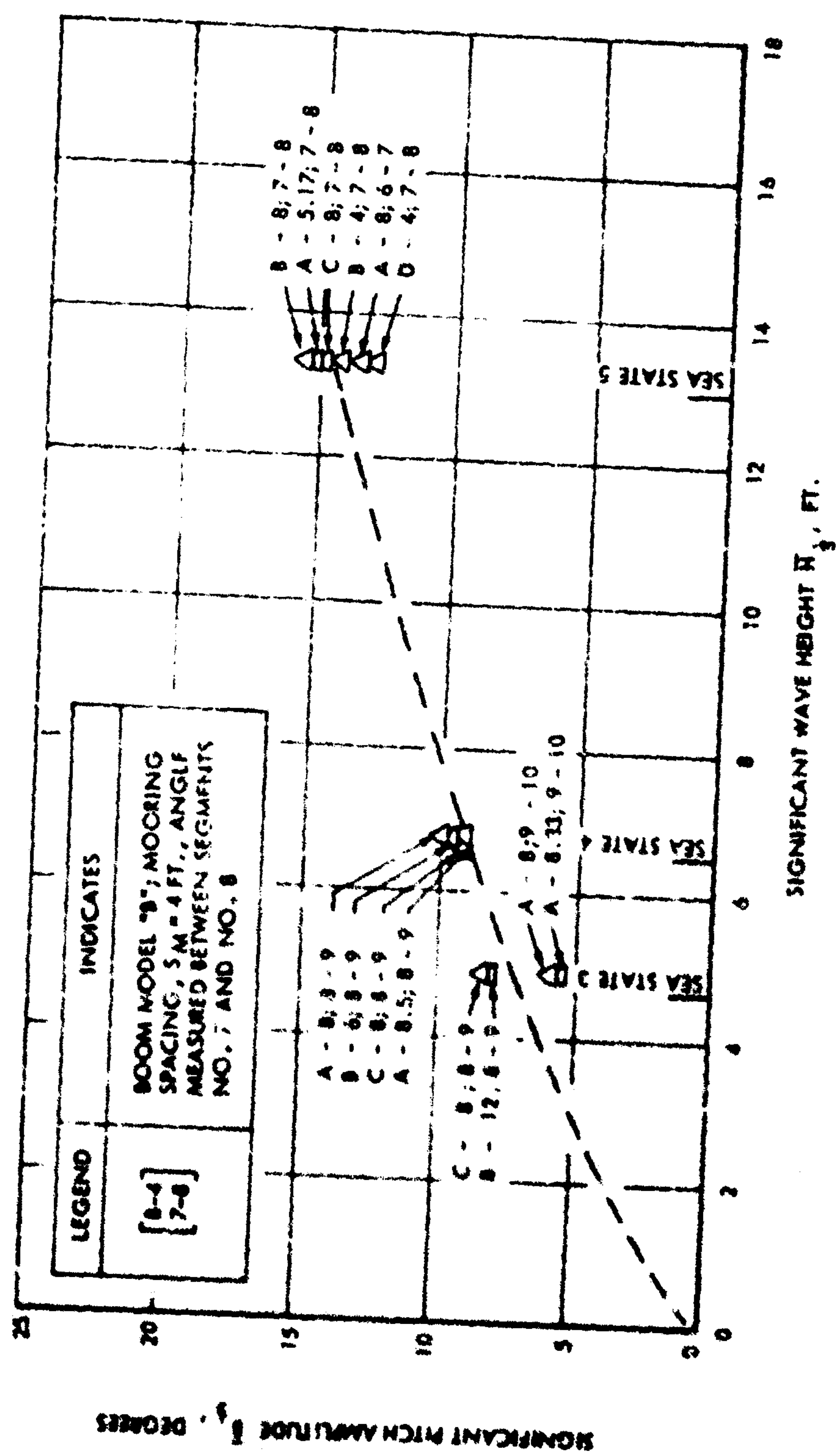

FIGURE 15 - SIGNIFICANT PITCH MOTION IN IRREGULAR WAVES

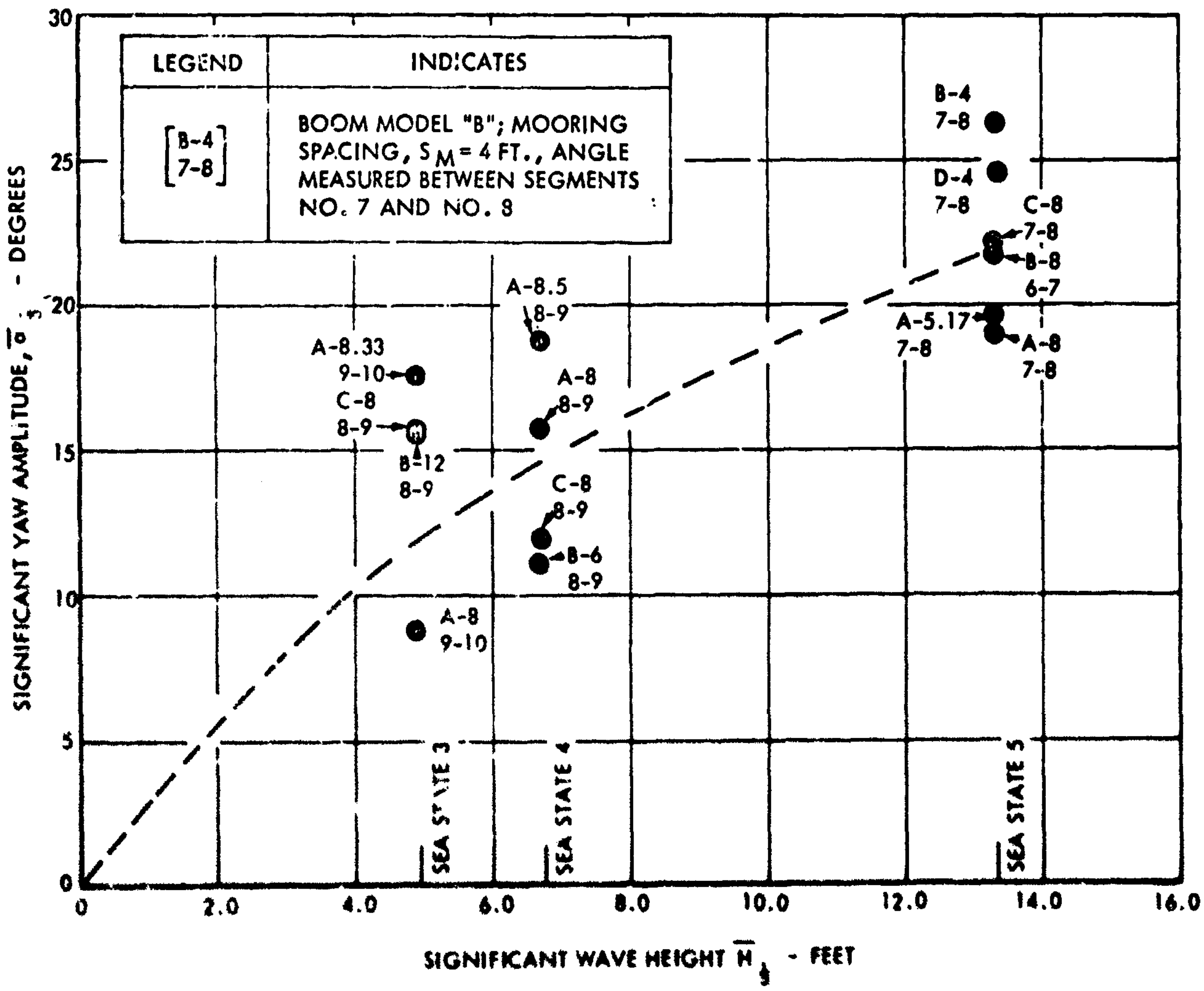

FIGURE 16 - SIGNIFICANT YAW MOTION IN IRREGULAR WAVES

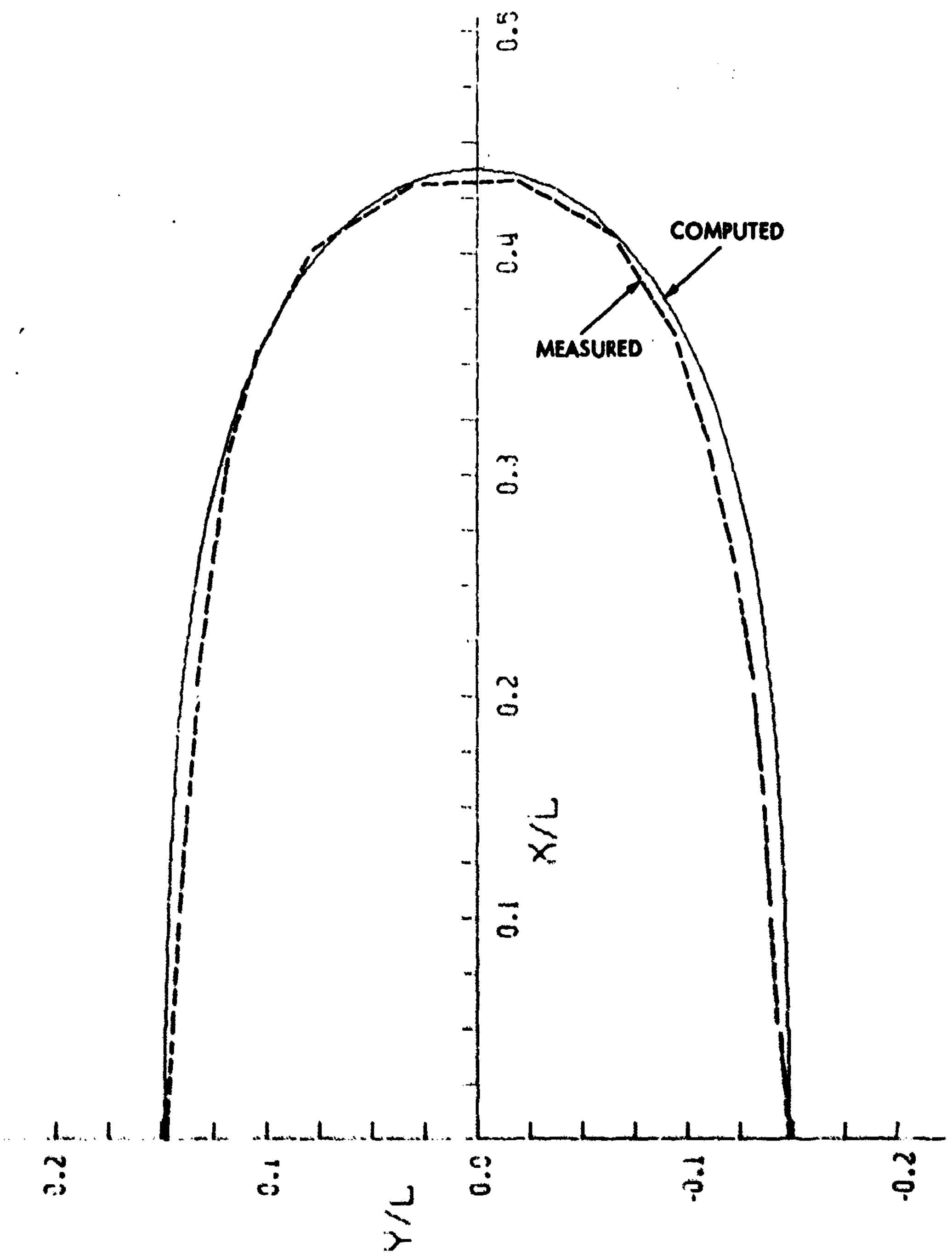

FIGURE 17 - COMPARISON OF COMPUTED AND MEASURED BOOM GEOMETRY, TEST NO. 1; FIXED MOORING, MODEL A, F_D = 0.236, CURRENT = 1.99 KNOTS

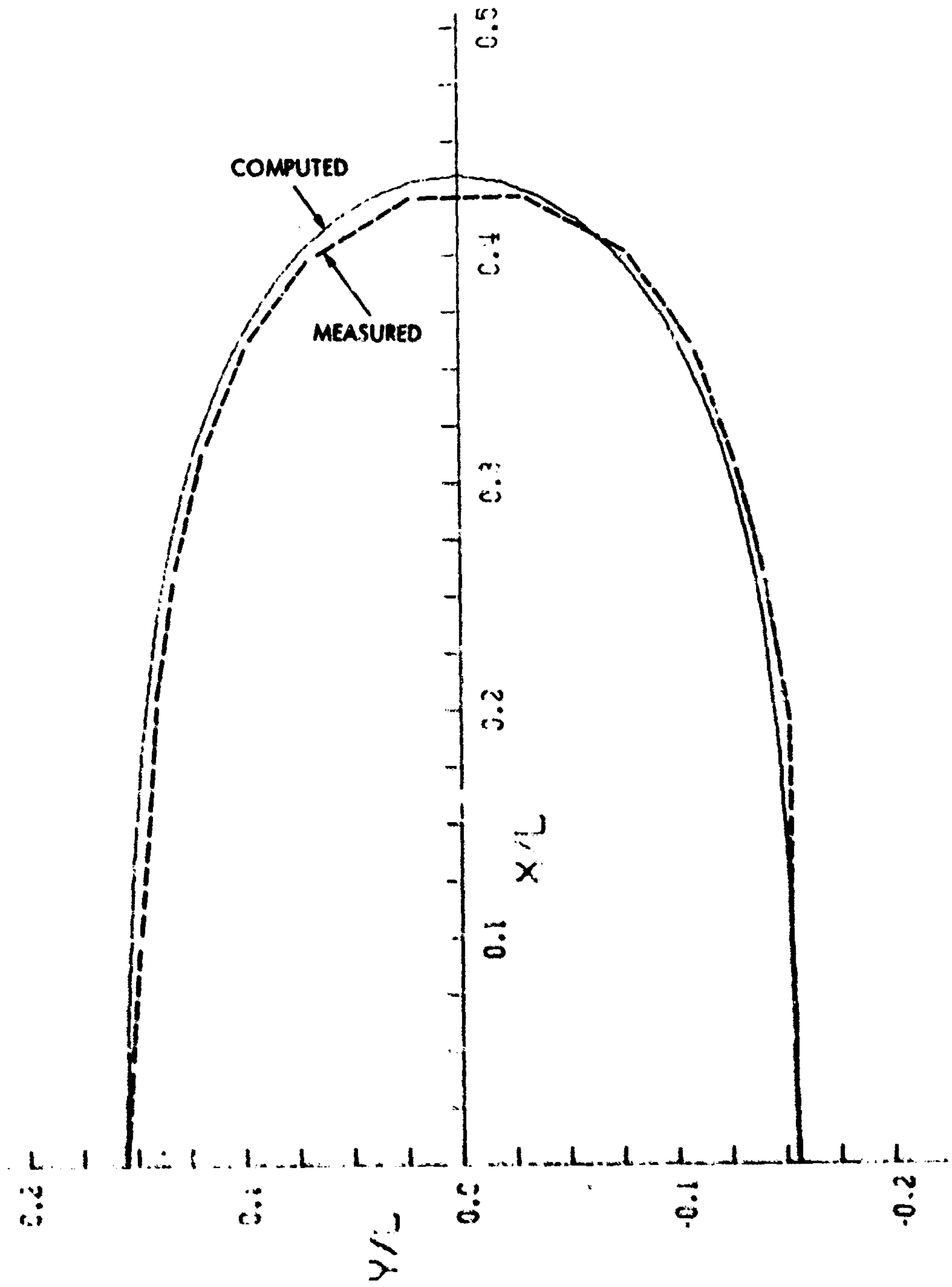

FIGURE 18 - COMPARISON OF COMPUTED AND MEASURED BOOM GEOMETRY, TEST NO. 2; FIXED MOORING, MODEL A, F_D = 0.157, CURRENT = 1.33 KNOTS

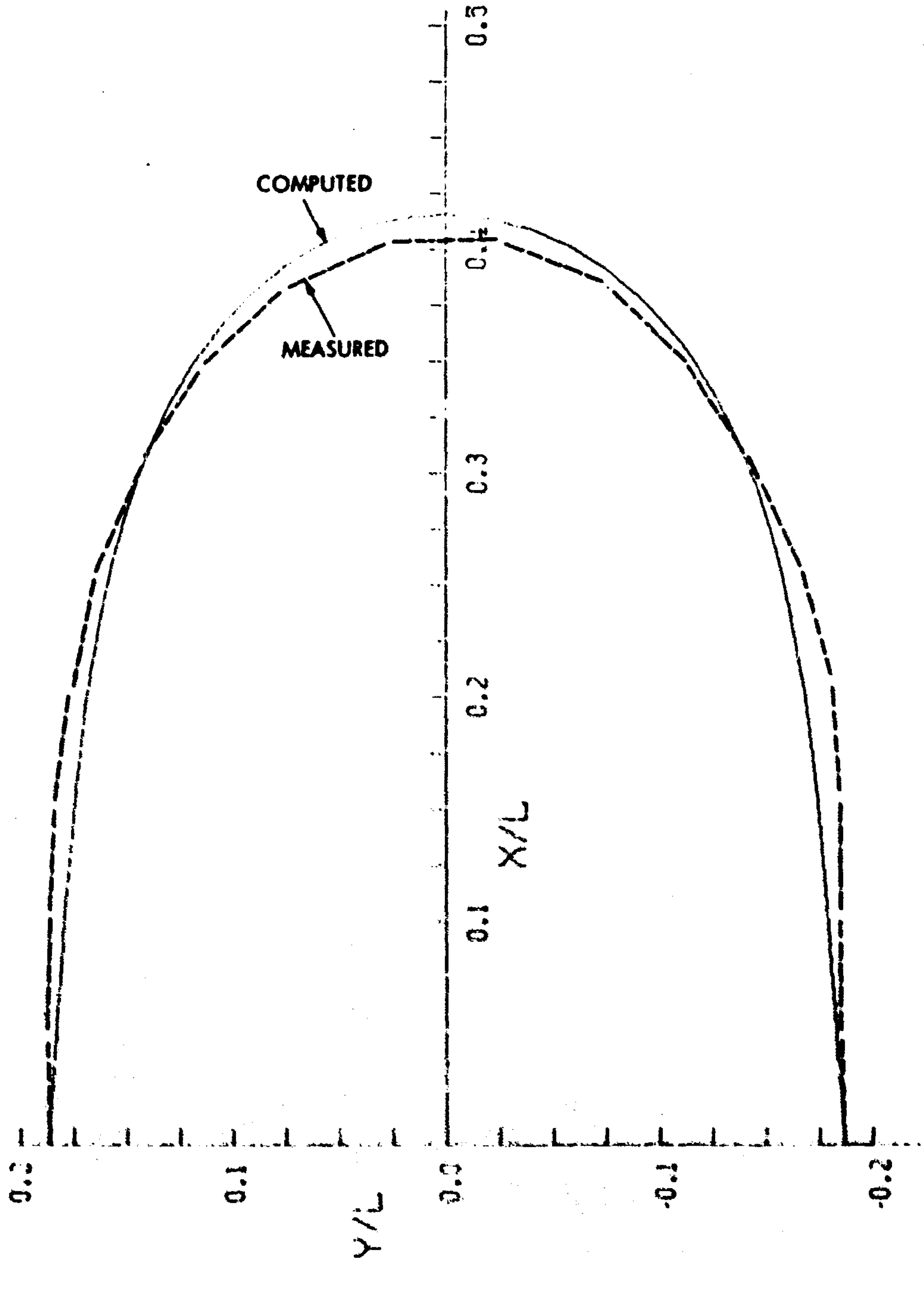

FIGURE 19 - COMPARISON OF COMPUTED AND MEASURED BOOM GEOMETRY, TEST NO. 3; FIXED MOORING, MODEL A, F_D = 0.075, CURRENT = 0.66 KNOTS

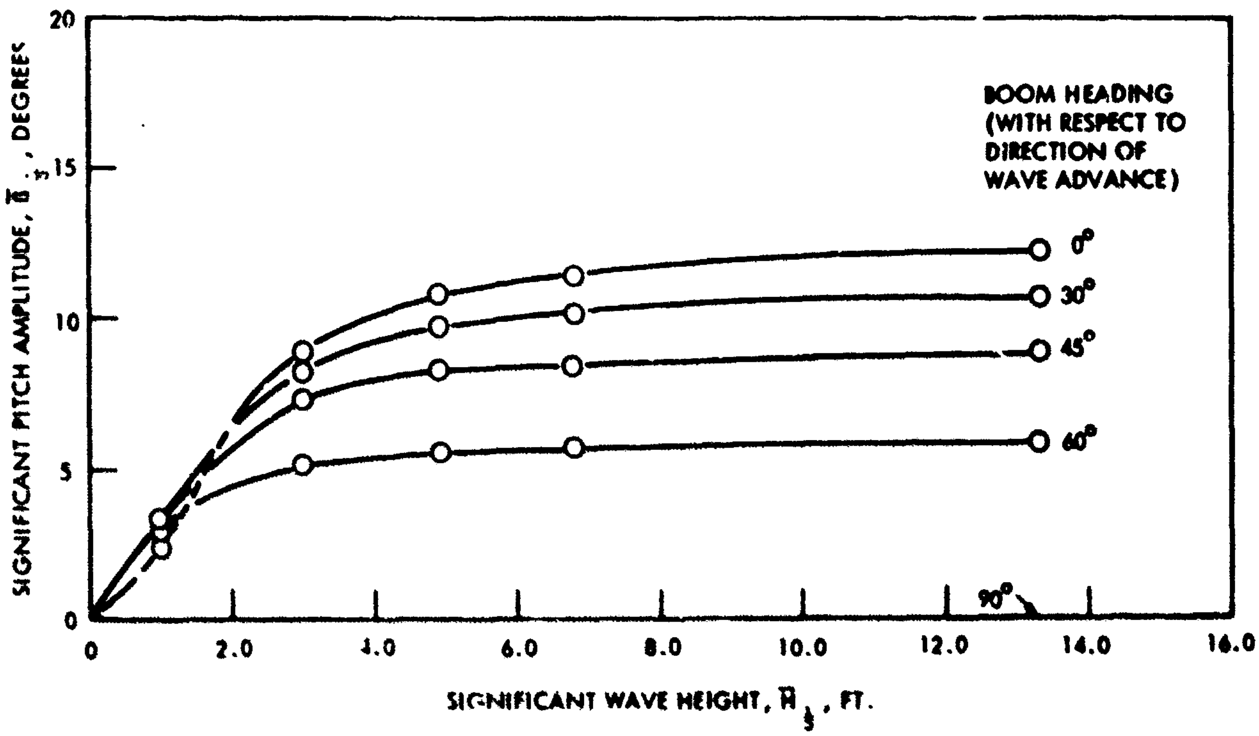

FIGURE 20 - CALCULATED MOTIONS IN THE VERTICAL PLANE

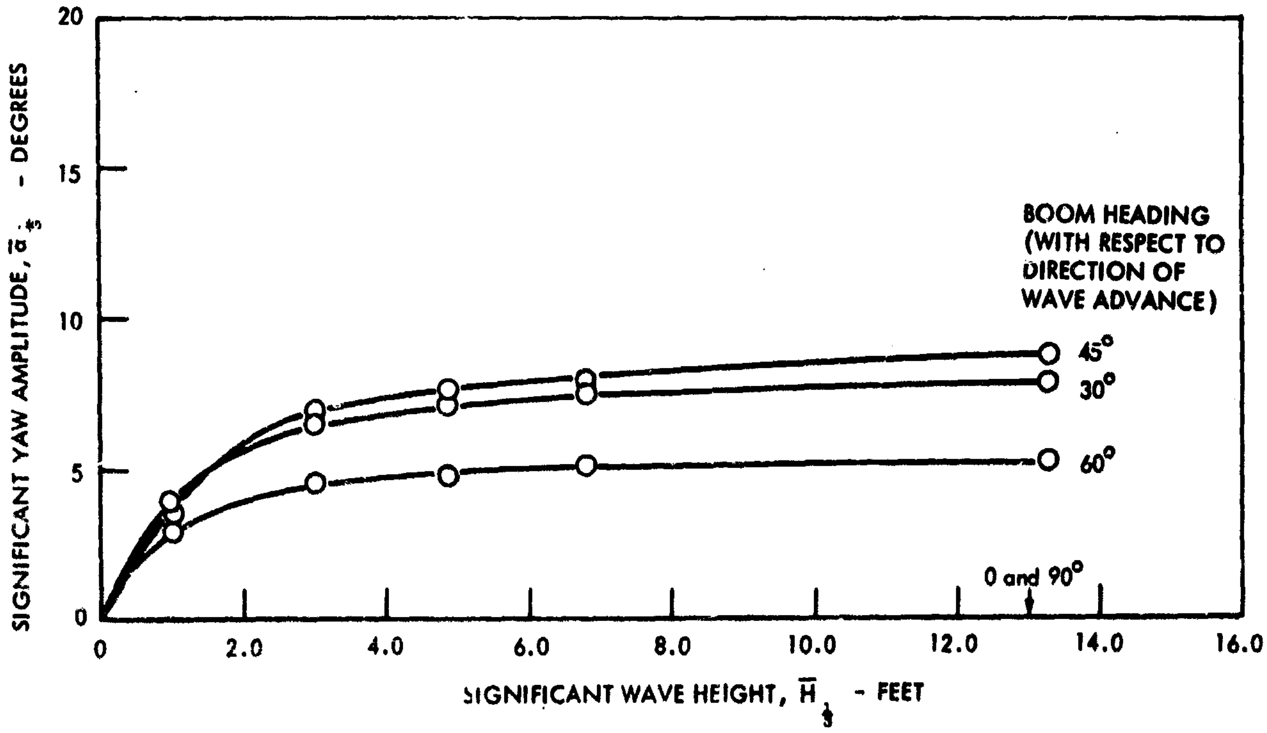

FIGURE 21 - CALCULATED MOTIONS IN THE HORIZONTAL PLANE

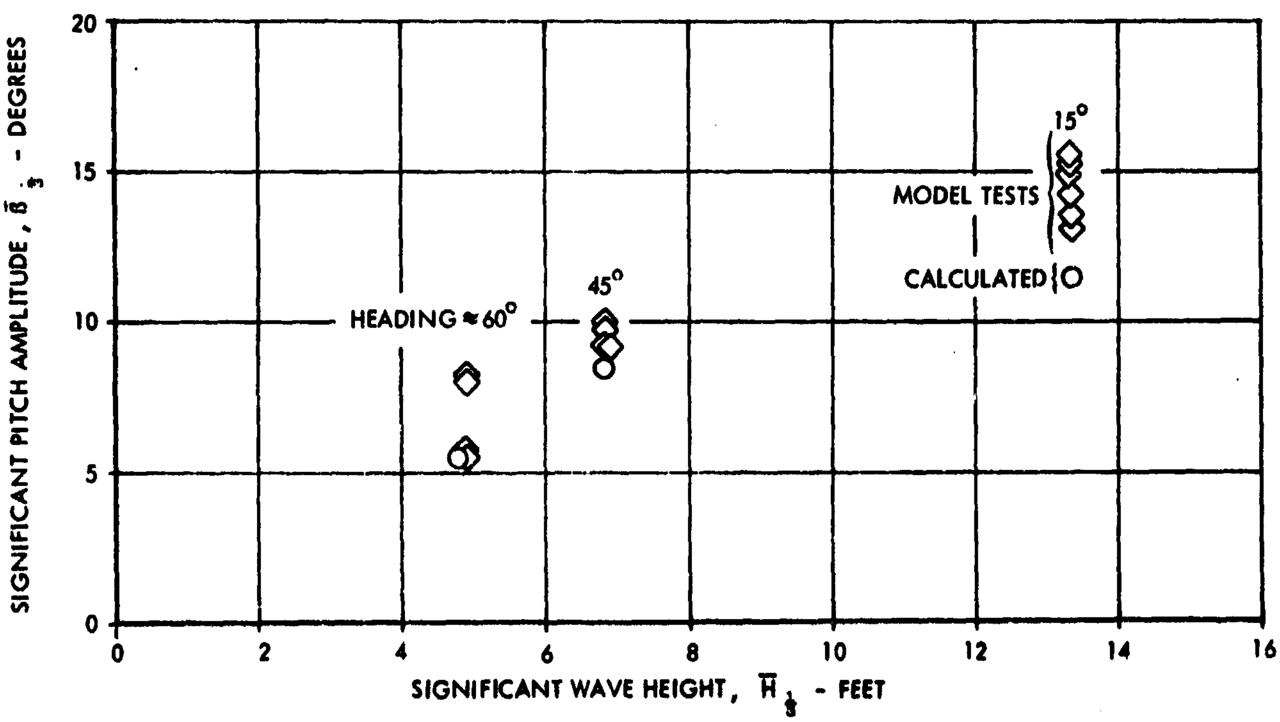

FIGURE 22 - COMPARISON OF CALCULATED AND OBSERVED PITCH MOTION IN IRREGULAR WAVES

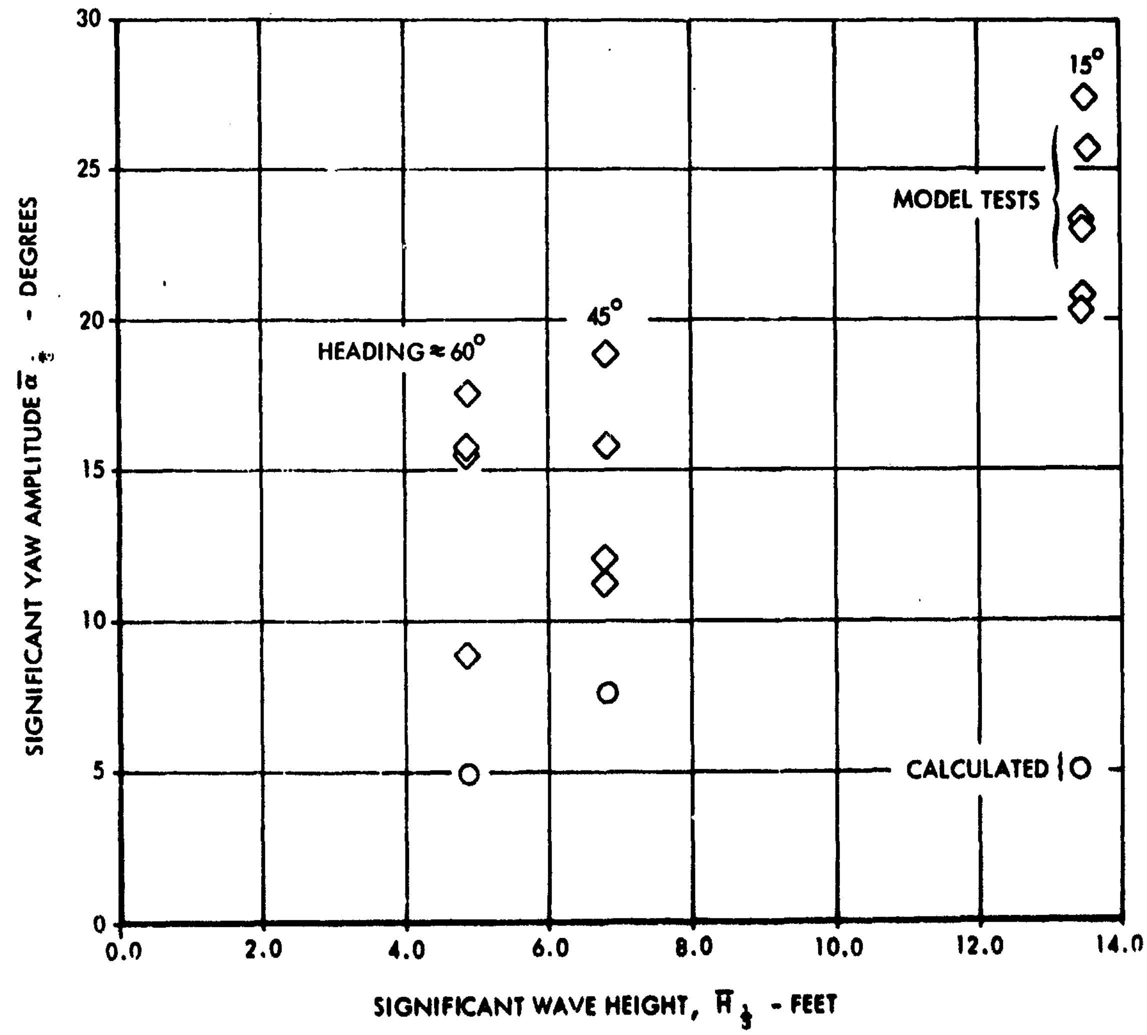

FIGURE 23 - COMPARISON OF CALCULATED AND OBSERVED YAW MOTIONS IN IRREGULAR WAVES

APPENDIX A
STATIC OUTPUT

Oil boom configuration parameters for input to the static program were selected with representatives of the U. S. Coast Guard. Twelve sets of oil boom physical characteristics were chosen and are summarized in Table A-1.

Four mooring conditions were investigated for each configuration. In each, a 100-foot (L = 100) length of boom is fix-moored between moorings spaced 80 feet apart. The moorings are oriented at 0, 30, 60 and 90 degrees to the direction of wind and current. The mooring angle is defined as that between the wind and current axis and a straight-line between the two mooring points.

Eight combinations of wind and current were investigated for each configuration and mooring orientation. These are summarized in Table A-2.

The computed calm water data is presented in graphic form in figures which follow. Each figure has a coded title which identifies the input parameters. For example, "TEST NO. IV-29-2-60" corresponds to Configuration IV, Wind = 29 knots, Current = 2 knots, and Mooring Orientation = 60 degrees, respectively.

TABLE A-1. PHYSICAL CHARACTERISTICS OF OIL BOOM CONFIGURATIONS

Configuration	I	II	III	IV	V	VI	VII	VIII	IX	X	XI	XII
Cylinder Dia., Ft.	8.0	8.0	10.0	10.0	1.6	1.6	1.6	1.6	2.0	2.0	2.0	2.0
Skirt Depth, ft.	-	-	-	-	6.4	6.4	6.4	6.4	8.0	8.0	8.0	8.0
Shear Center, Ft.*	0	0	0	0	0	7.2	0	7.2	0	9.0	0	9.0
Center of Gravity, ft*	0.67	0.67	0.83	0.83	5.6	5.6	5.6	5.6	7.0	7.0	7.0	7.0
Cylinder Draft, ft.	4.8	6.4	6.0	8.0	0.90	0.90	0.28	0.28	1.13	1.13	0.35	0.35
Weight, lb/ft.	2015.0	2760.0	3150.0	4312.0	75.0	75.0	15.0	15.0	117.2	117.2	23.4	23.4
Stiffness (EI), lb-in²	4.1×10^9	4.1×10^9	10^{10}	10^{10}	4.1×10^4	4.1×10^4	4.1×10^4	4.1×10^4	10^5	10^5	10^5	10^5
lb-ft²	2.85×10^7		6.95×10^7			2.85×10^2			6.95×10^2			

* Note: Measured down from centerline of cylinder.

TABLE A-2. STEADY STATE SEA CONDITIONS

Configurations	Wind V_w, knots	Current V_c, knots
I, II, V, VI, VII and VIII	0	2
	15	0
	17	0 and 2
	20	2
	22	0 and 2
	40	0
III, IV, IX, X, XI and XII	0	2
	20	2
	22	0 and 2
	26	2
	29	0 and 2
	40	0

The steady state boom geometry is shown in plan view (labelled profile). The X axis is parallel and the Y axis is normal to the wind and current direction. X and Y are non-dimensionalized by the boom length, L.

The force, moment and curvature are plotted as a function of X, the length measured along the boom axis (not the same X as in the plan view). The length is non-dimensionalized by the total boom length, L. The points X/L = 0.0 and 1.0 are at the ends of the boom where the former is the end which corresponds to the mooring at the origin in the plan view.

Three different lines are used to delineate forces, moments and curvatures along the boom in three directions:

TABLE A-3

Direction / Variable	Axial	Normal	Tangential
Force	Tension (T)	N-shear (SN)	T-shear (ST)
Moment	Torque (Q)	T-moment (MT)	N-moment (MN)
Curvature	Theta* (θ)	D-beta ($\Delta\beta$)	D-phi ($\Delta\Phi$)
Note: Theta is roll angle and not a curvature.			

These directions and variables are shown in Figures C-1 through C-3.

Each variable has been divided by its absolute maximum value (along the boom) so that the ordinates of the plots vary only from -1.0 to +1.0. For example, in Test No. I-0-2-0 tension is divided by 0.3140 E 05. This corresponds to the ordinate of -1.0 at $X/L \approx 0.5$. Thus, the (absolute) maximum tension is -0.314×10^5 near the middle of the boom, i.e., 31,400 pounds in compression.

Each figure does not include all of the variables listed in Table A-3. Those variables which have zero or inconsequential values are generally not included.

In all cases the boom was represented by 10 elements and the loads and positions were calculated at the junction between each element and at the boom ends. In cases where the mooring angle is small the computer plots appear kinked at the down-stream end. This is because the computer drawn plots are generated by simply drawing straight-lines between the computer points. To obtain intermediate values in these cases it is justified to fair a smooth curve through the computed points.

Some difficulty was encountered in obtaining a convergent solution for the most limber booms at a mooring angle of zero. The resulting data for these cases is somewhat less accurate than for the other mooring angles. However, these data still provide the correct level of loading and should be satisfactory for structural estimates.

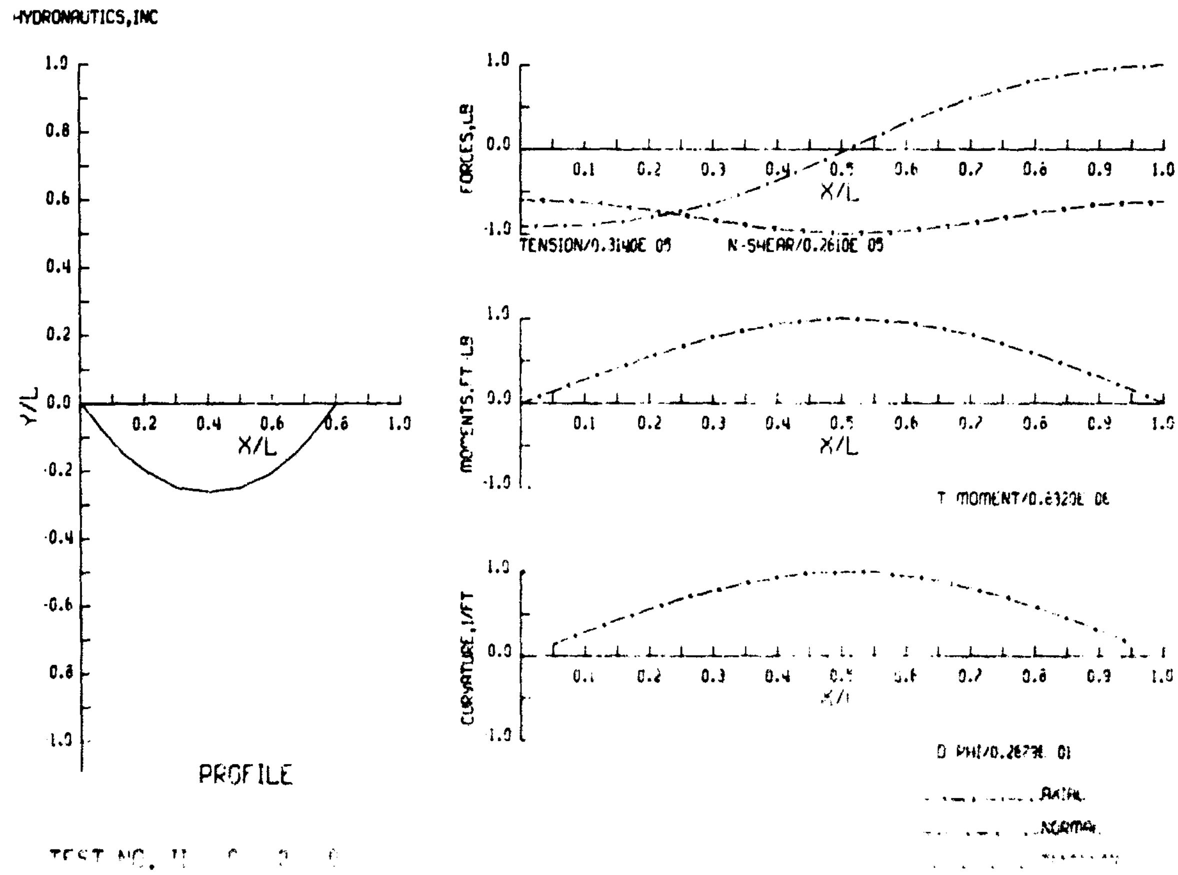
HYDRONAUTICS,INC
PROFILE
Y/L
X/L
FORCES,LB
TENSION/0.3140E 05
N-SHEAR/0.2610E 05
MOMENTS,FT-LB
T MOMENT/0.6320E 06
CURVATURE,1/FT
D PHI/0.2673E 01
AXIAL
NORMAL

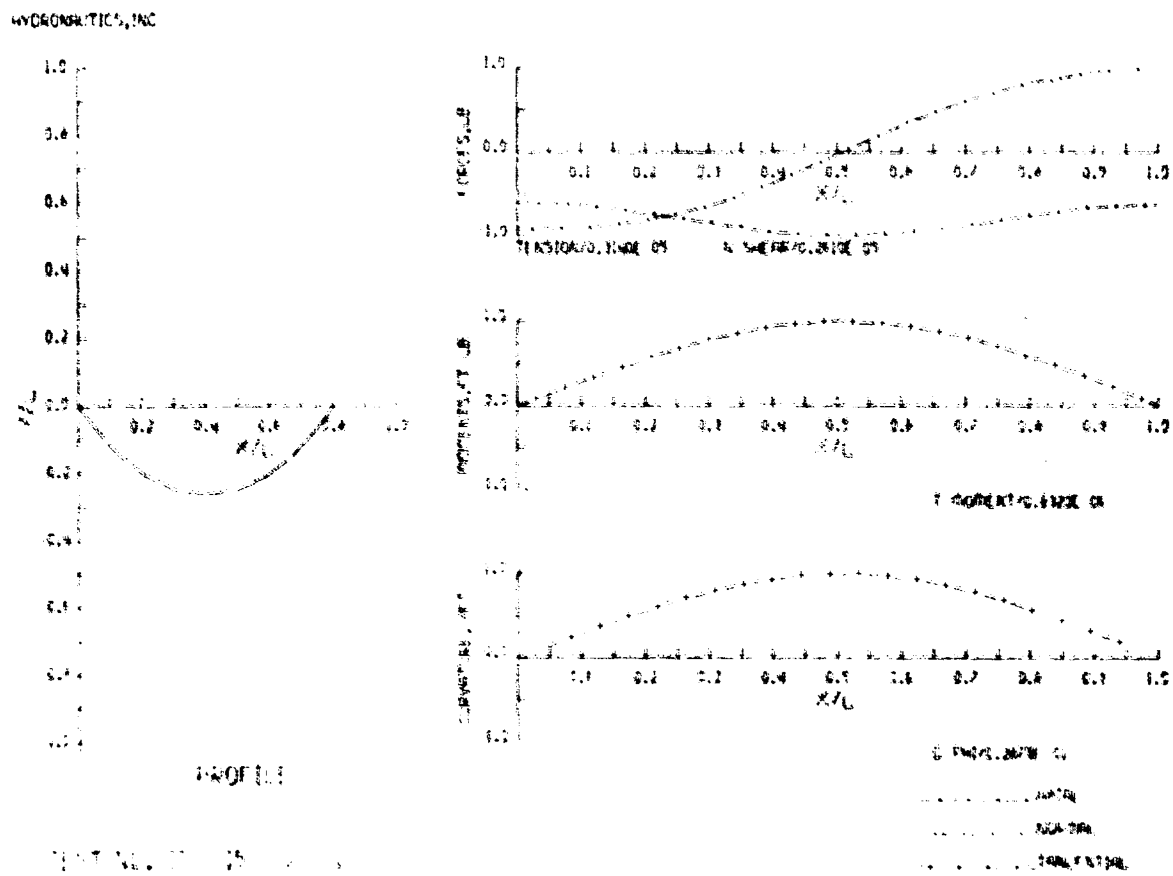
HYDRONAUTICS,INC
T MOMENT/0.6320E 06

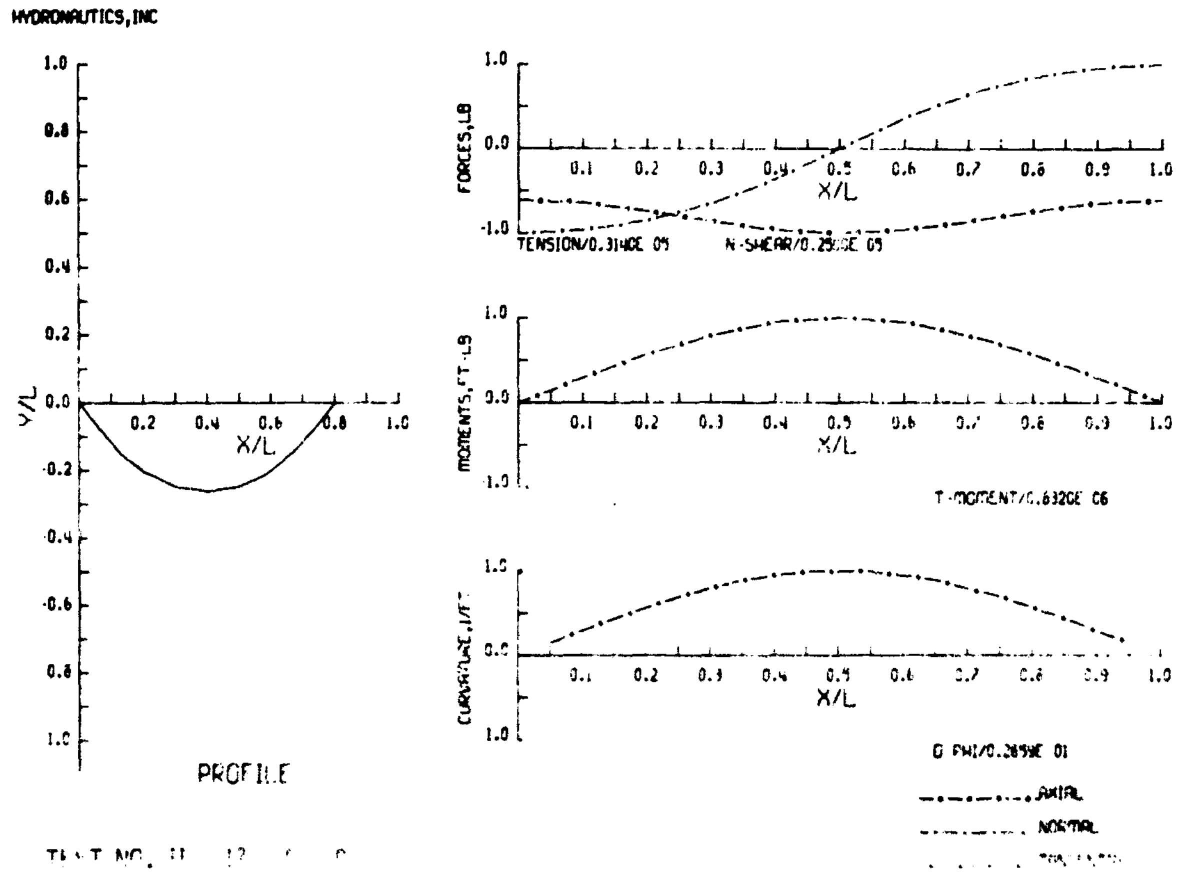

HYDRONAUTICS,INC
FORCES,LB
X/L
TENSION/0.314E 05
MOMENTS,FT-LB
T-MOMENT/0.632E 06
CURVATURE,1/FT
Y/L
PROFILE
AXIAL
NORMAL

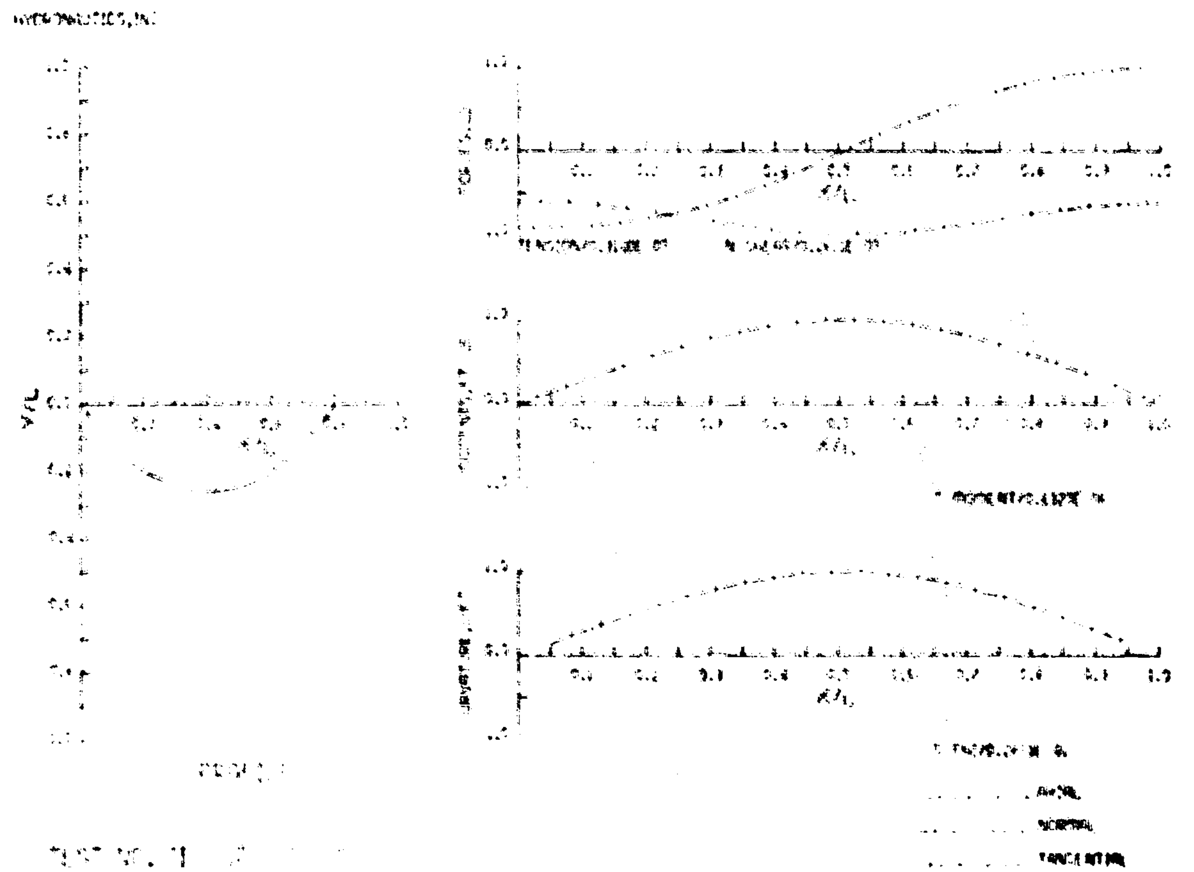

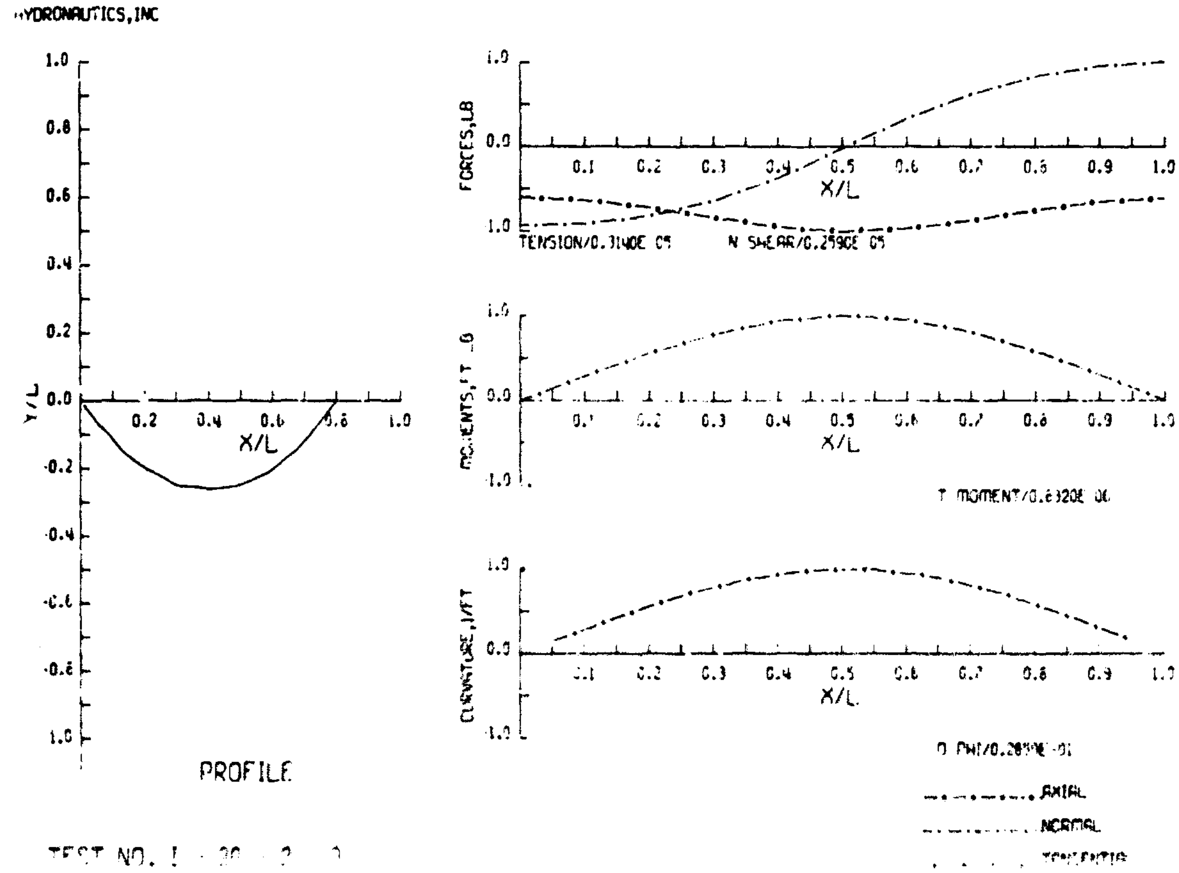
HYDRONAUTICS, INC
PROFILE
Y/L
X/L
FORCES, LB
TENSION/0.3140E 05
N SHEAR/0.2590E 05
T MOMENT/0.6320E 06
CURVATURE, 1/FT
AXIAL
NORMAL

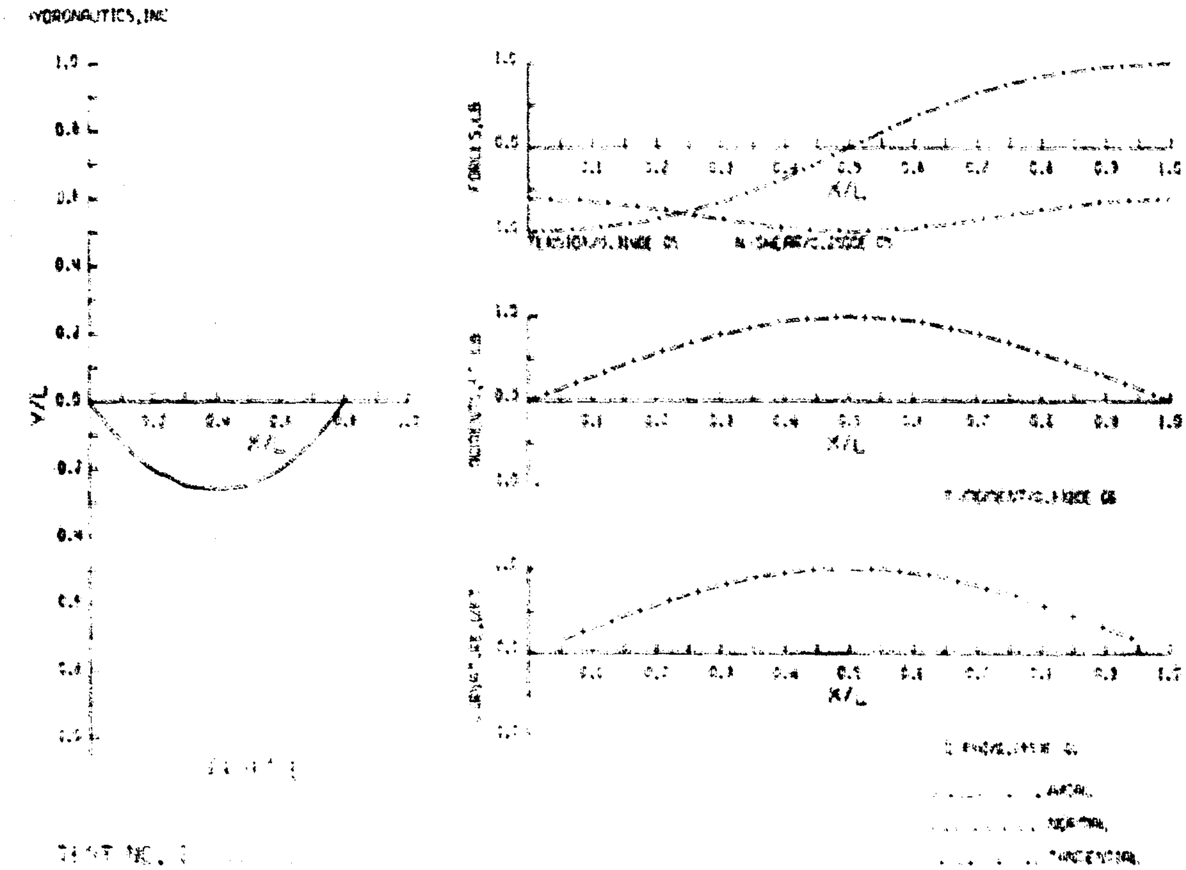
HYDRONAUTICS, INC
Y/L
X/L
FORCES, LB
NORMAL
TANGENTIAL

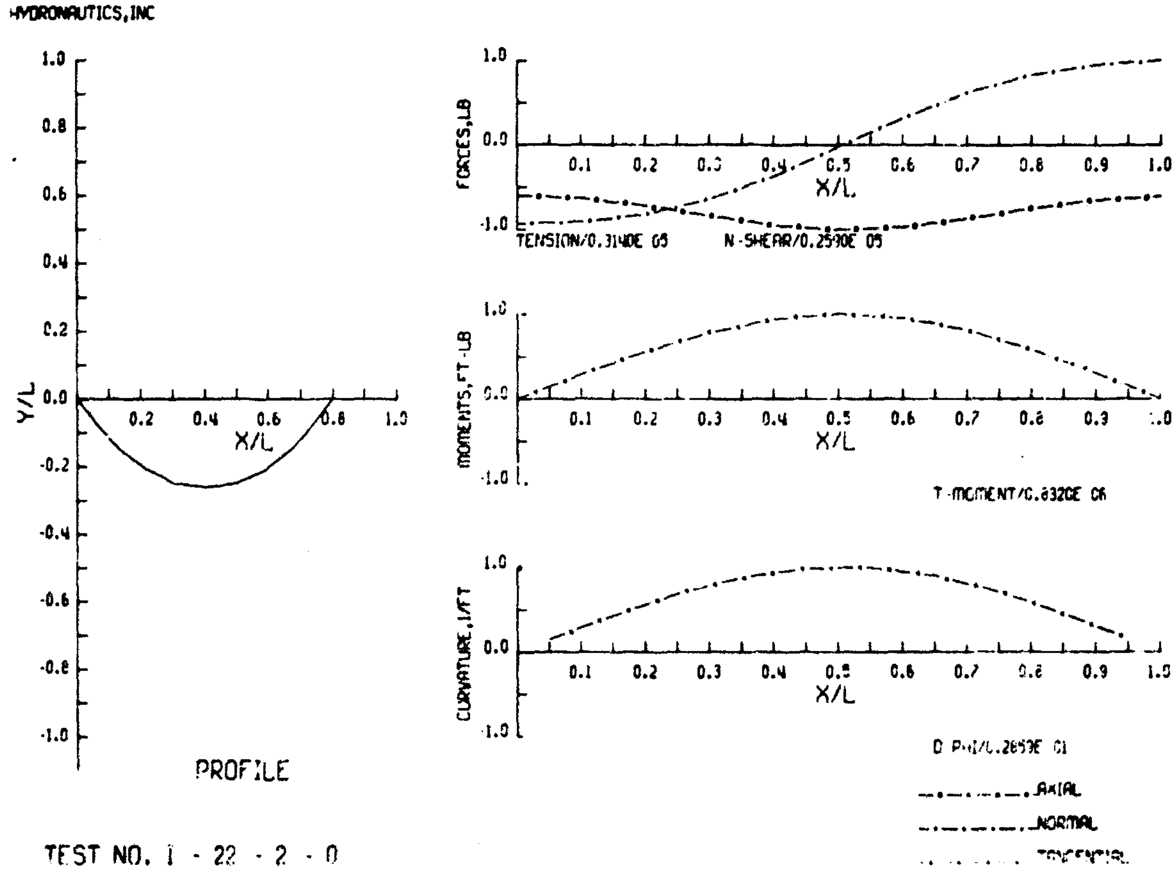
HYDRONAUTICS, INC
PROFILE
Y/L
X/L
FORCES, LB
TENSION/0.3140E 05
N-SHEAR/0.2590E 05
MOMENTS, FT-LB
T-MOMENT/0.832OE 06
CURVATURE, 1/FT
D PHI/L.2653E 01
AXIAL
NORMAL
TANGENTIAL
TEST NO. 1 - 22 - 2 - 0

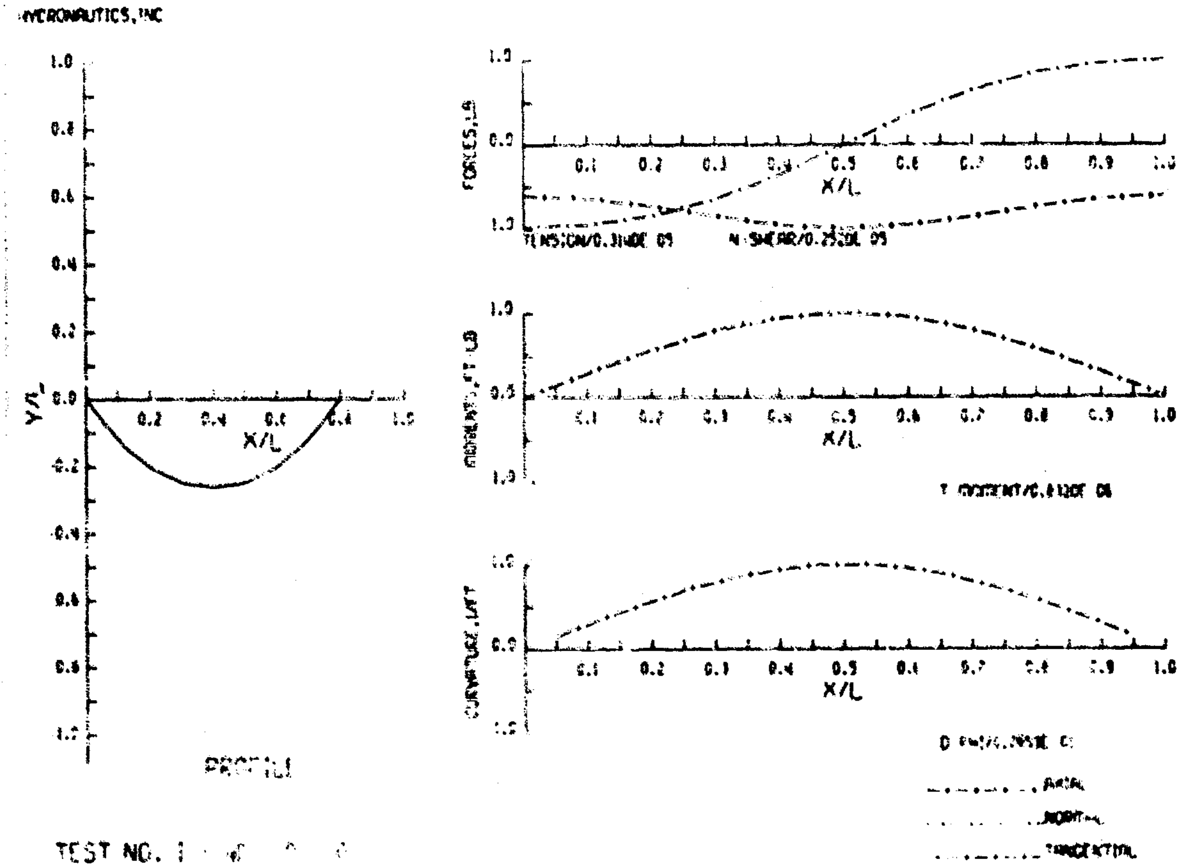
HYDRONAUTICS, INC
Y/L
X/L
FORCES, LB
TENSION/0.3140E 05
N-SHEAR/0.2520E 05
MOMENTS, FT-LB
CURVATURE, 1/FT
AXIAL
TANGENTIAL
TEST NO.

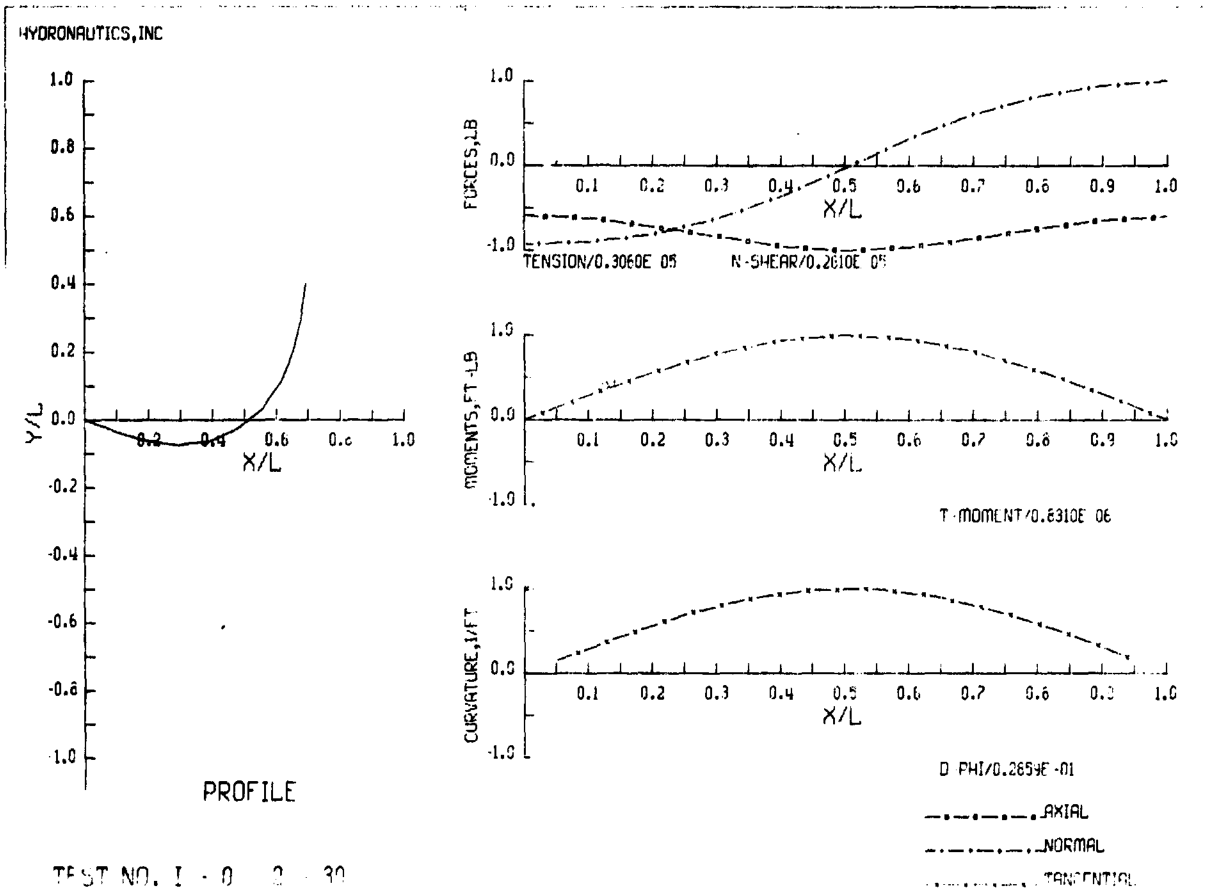
HYDRONAUTICS,INC
Y/L
X/L
PROFILE
FORCES,LB
TENSION/0.3060E 05
N-SHEAR/0.2610E 05
MOMENTS,FT-LB
T-MOMENT/0.8310E 06
CURVATURE,1/FT
D PHI/0.2659E-01
AXIAL
NORMAL

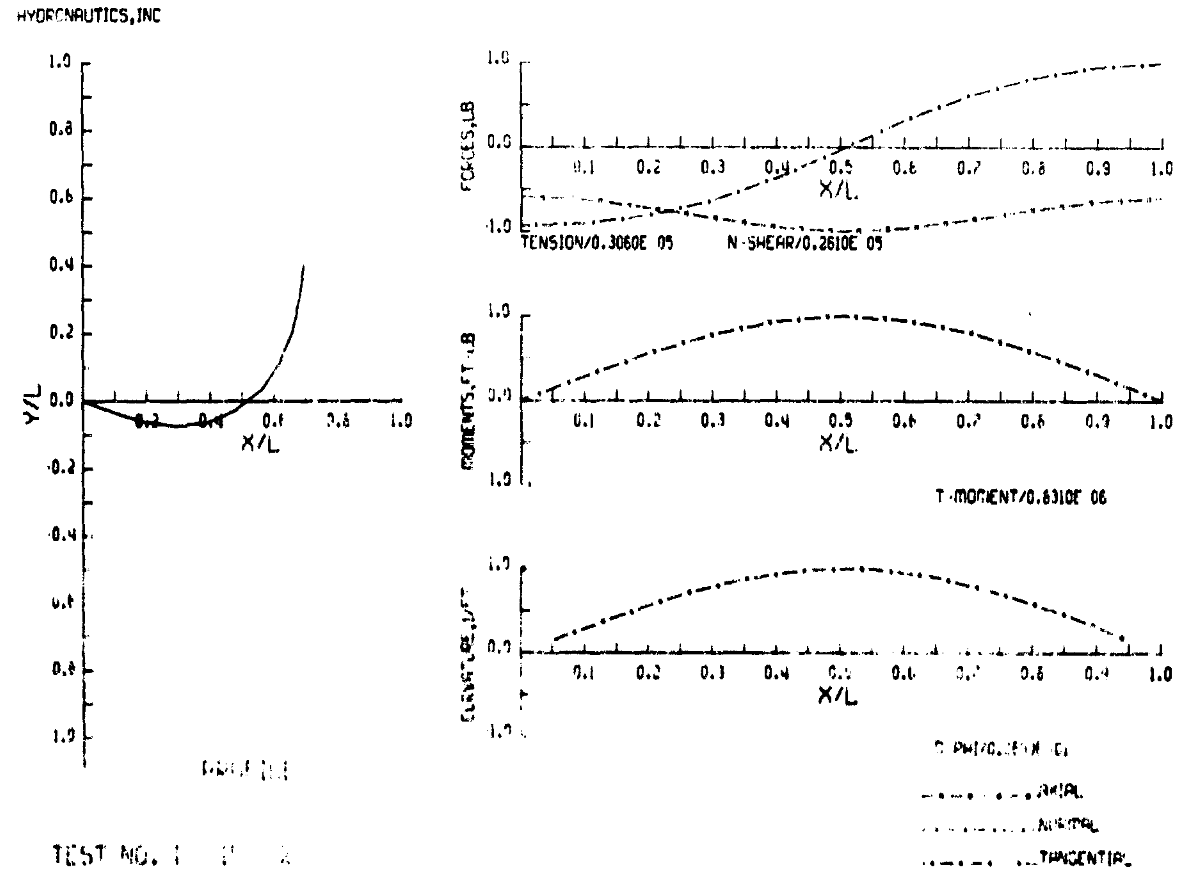
HYDRONAUTICS,INC
Y/L
X/L
FORCES,LB
TENSION/0.3060E 05
N-SHEAR/0.2610E 05
T-MOMENT/0.8310E 06
AXIAL
TANGENTIAL

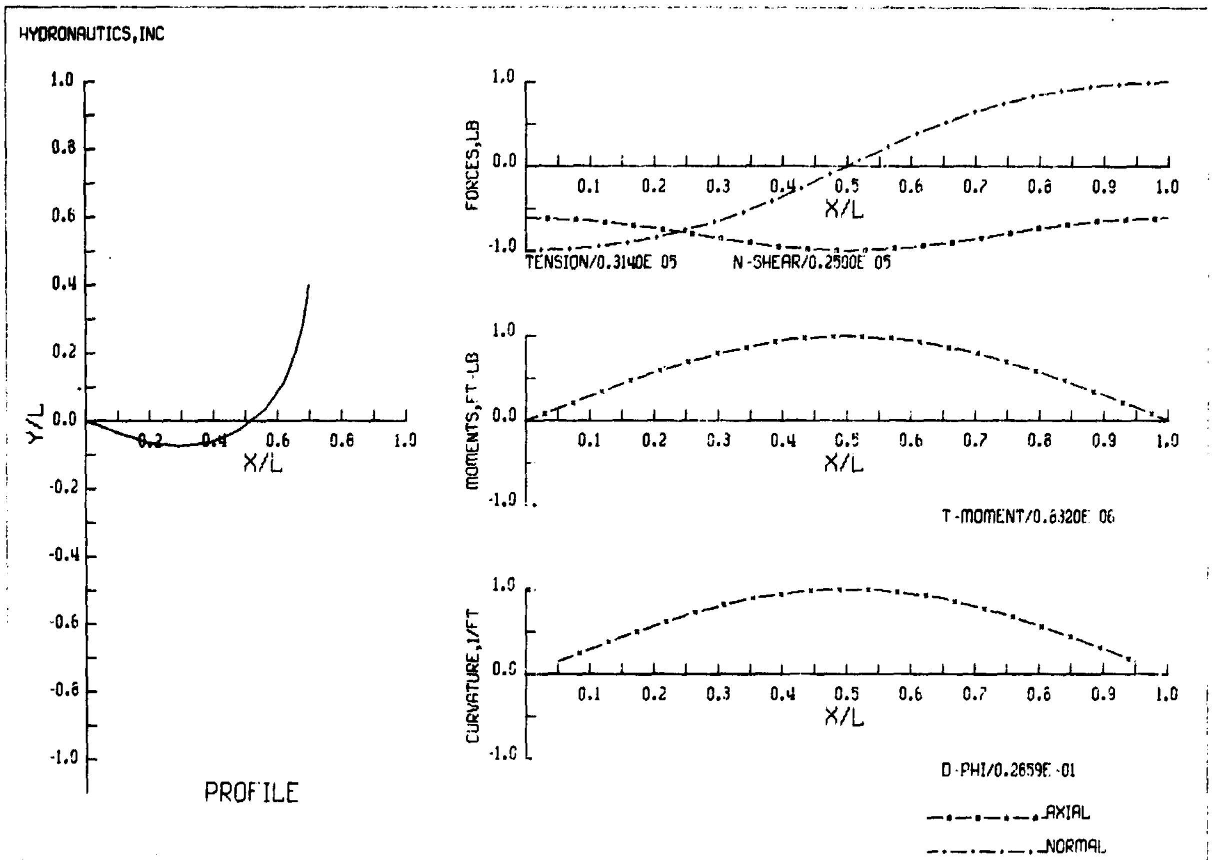

TEST NO. I - 12 0 - 30

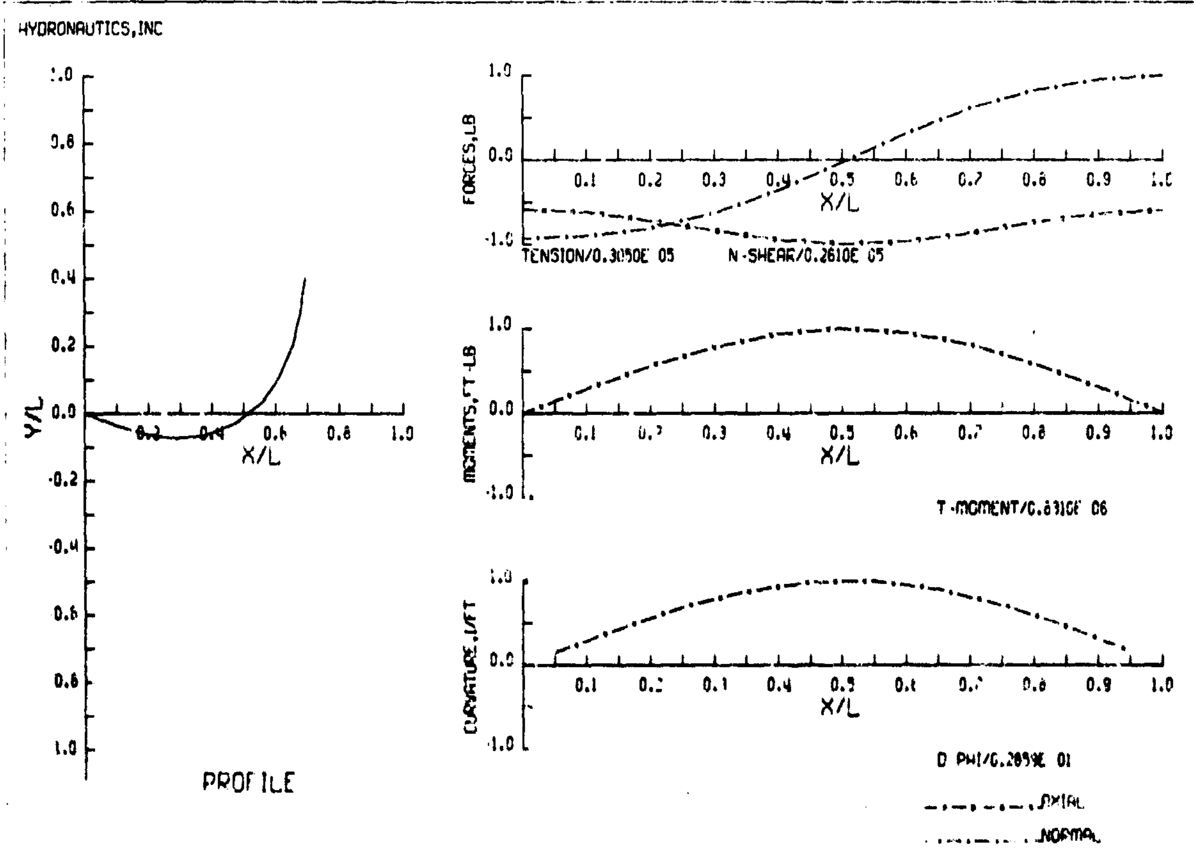

TEST NO. I - 12 - 2 - 30

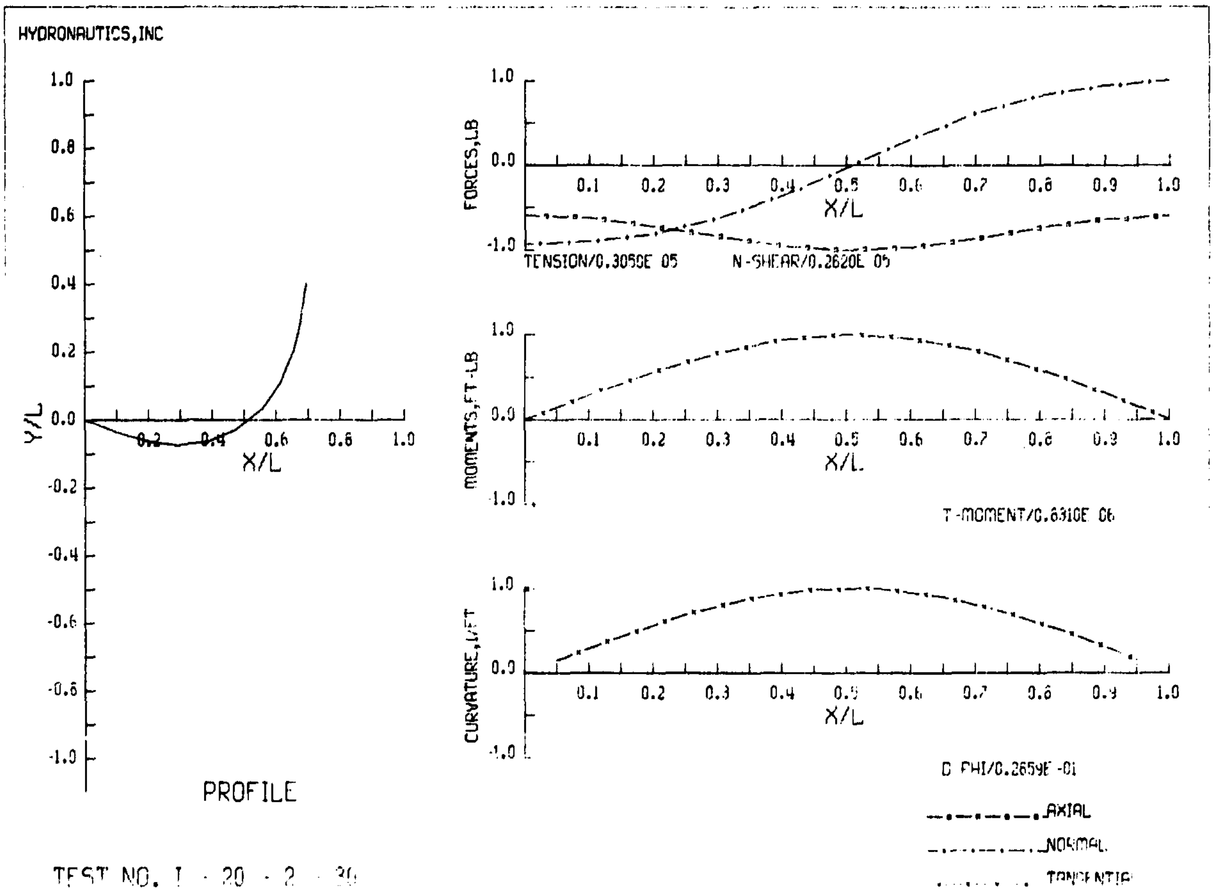
HYDRONAUTICS, INC
PROFILE
Y/L
X/L
FORCES, LB
TENSION/0.3050E 05
N-SHEAR/0.2620E 05
MOMENTS, FT-LB
T-MOMENT/0.6310E 06
CURVATURE, 1/FT
D PHI/0.2659E -01
AXIAL
NORMAL
TANGENTIAL
TEST NO. I - 20 - 2 - 30

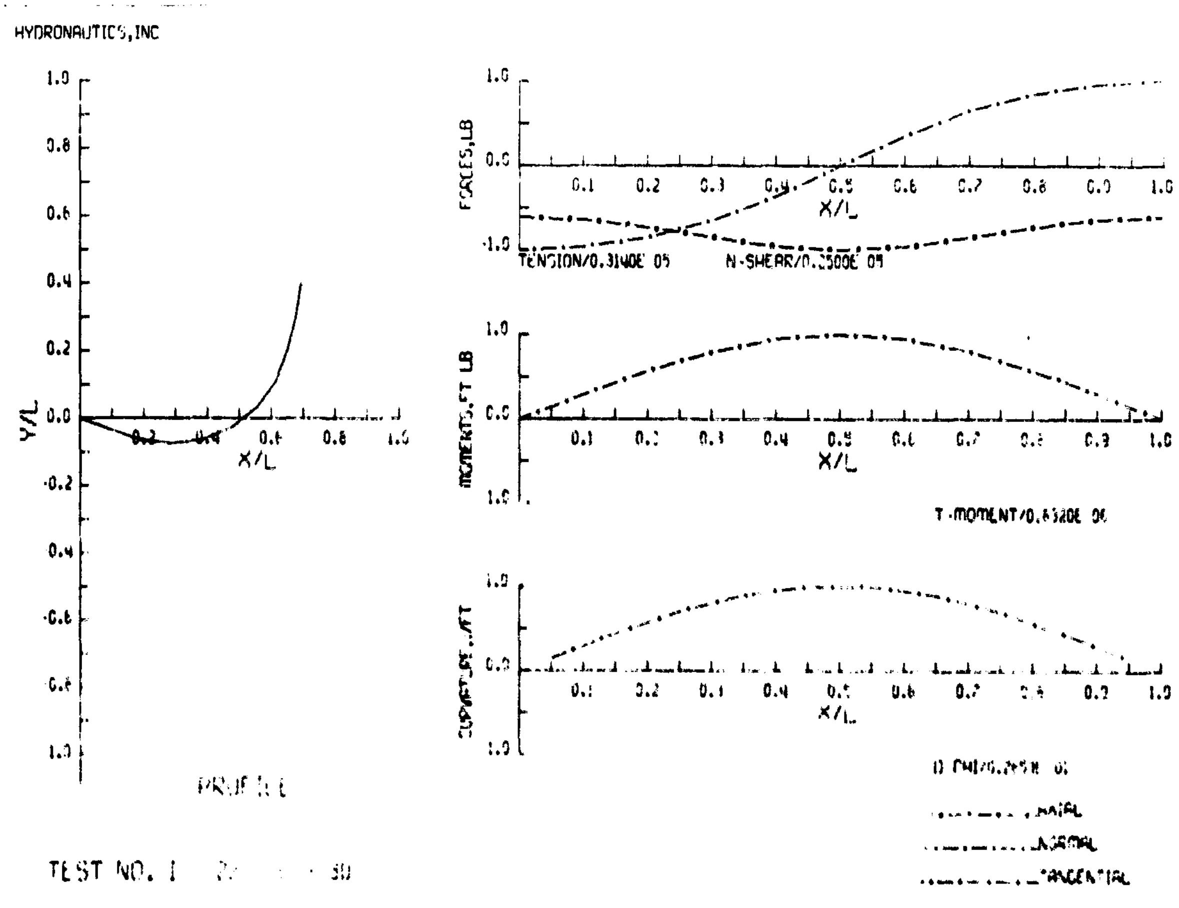
HYDRONAUTICS, INC
Y/L
X/L
FORCES, LB
TENSION/0.3140E 05
MOMENTS, FT LB
T-MOMENT
AXIAL
NORMAL
TANGENTIAL
TEST NO. I

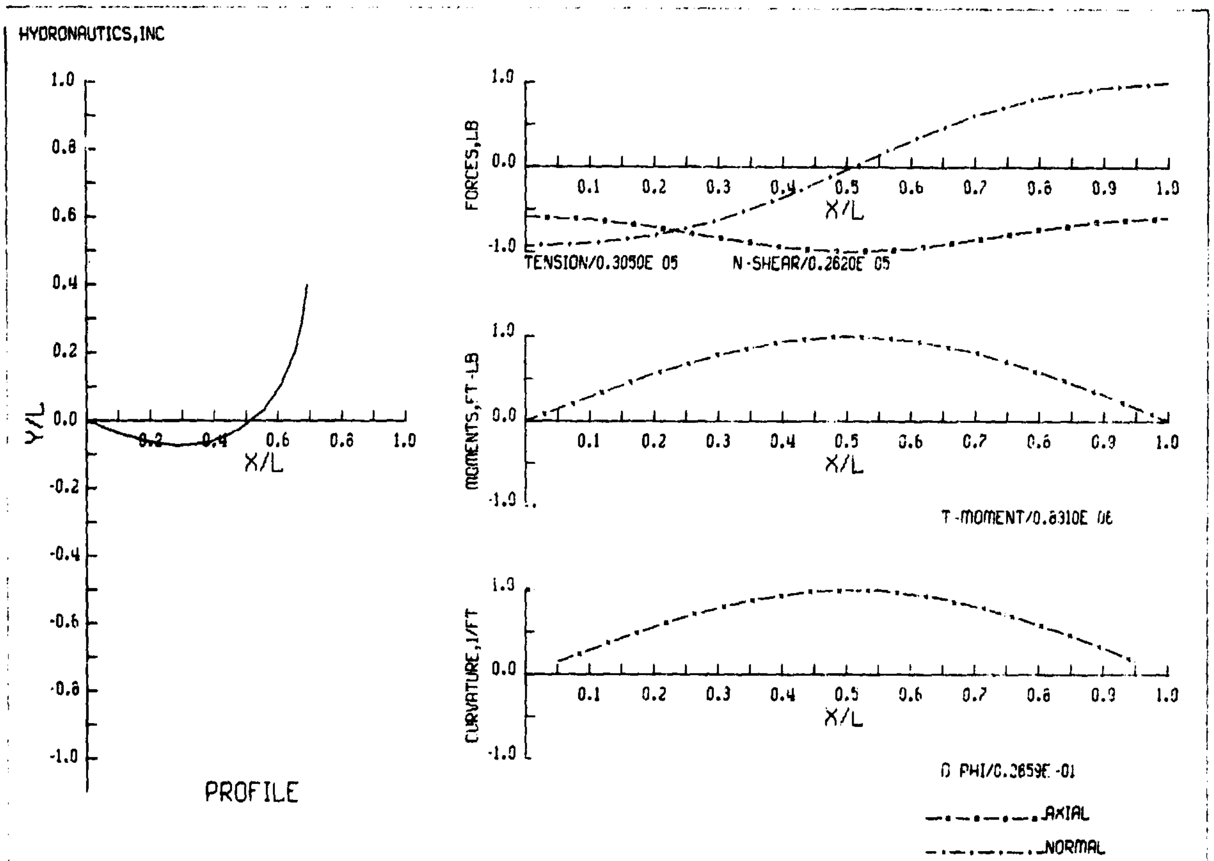

TEST NO. I - 22 - 2 - 30

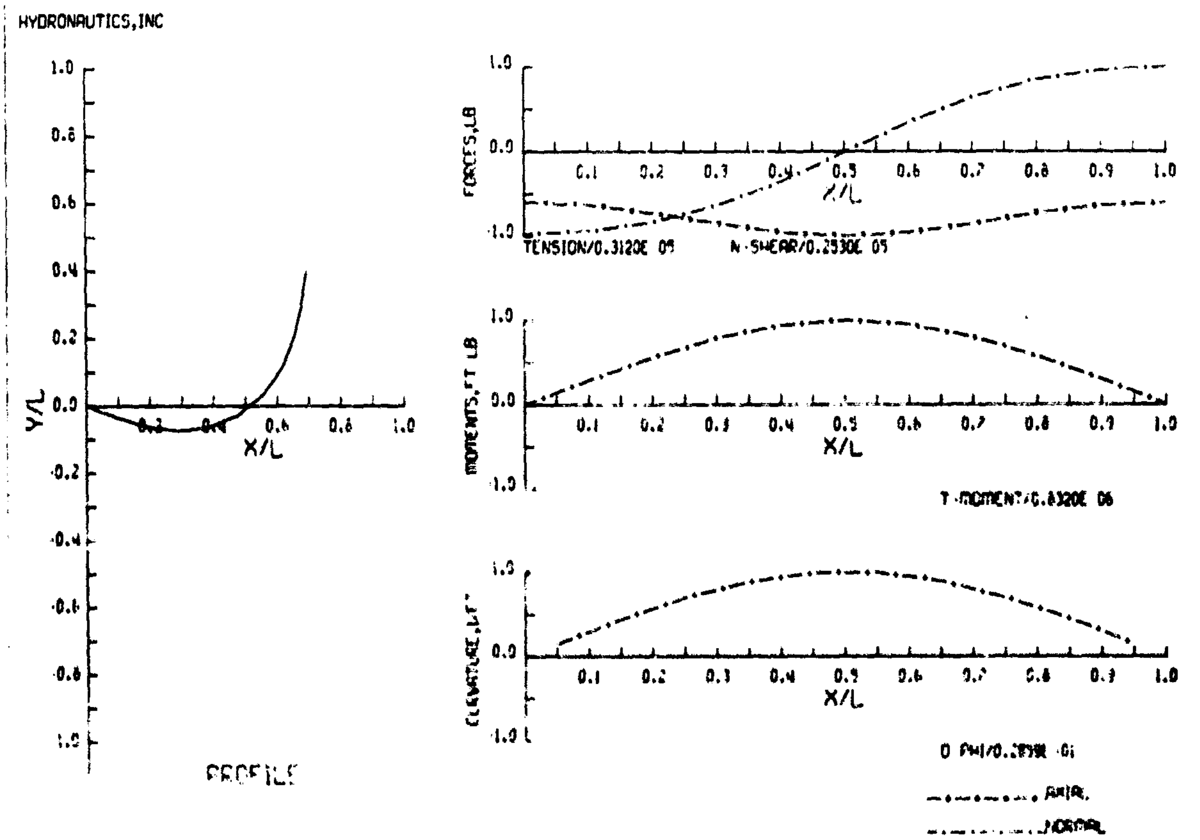

TEST NO. I - 40 - [illegible] - 30

HYDRONAUTICS,INC

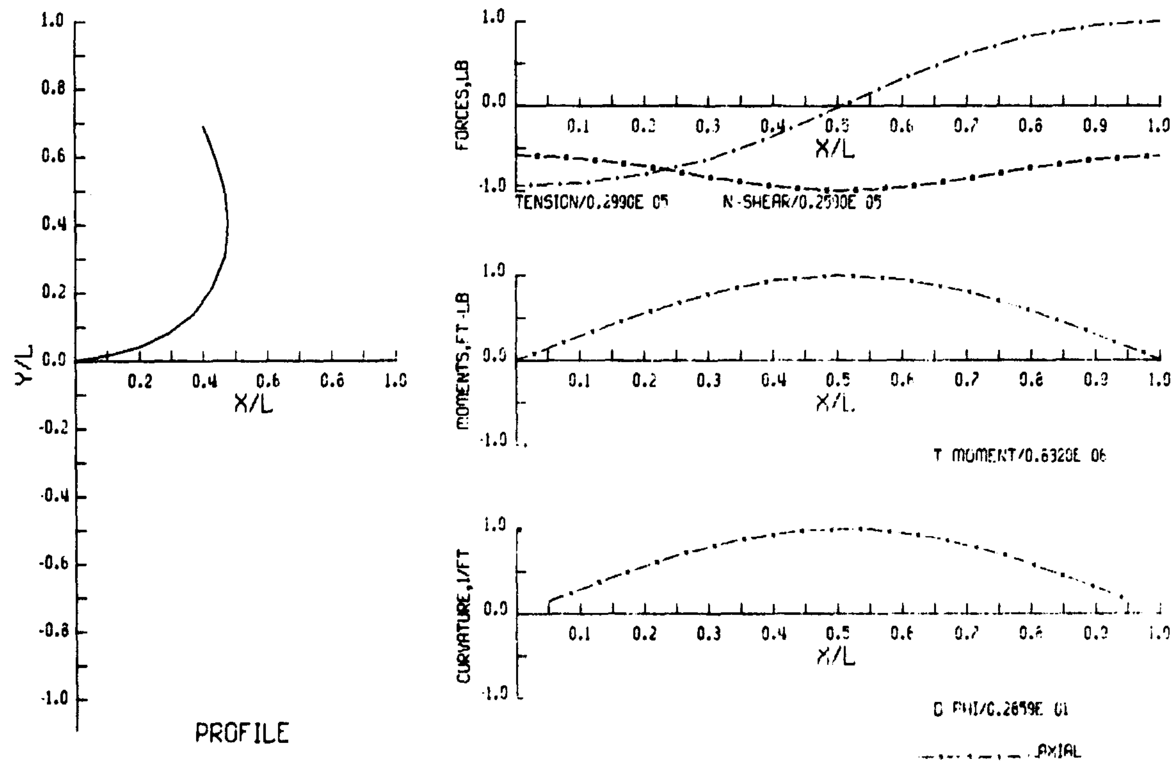

TEST NO. I - 0 - 2 - 60

HYDRONAUTICS,INC

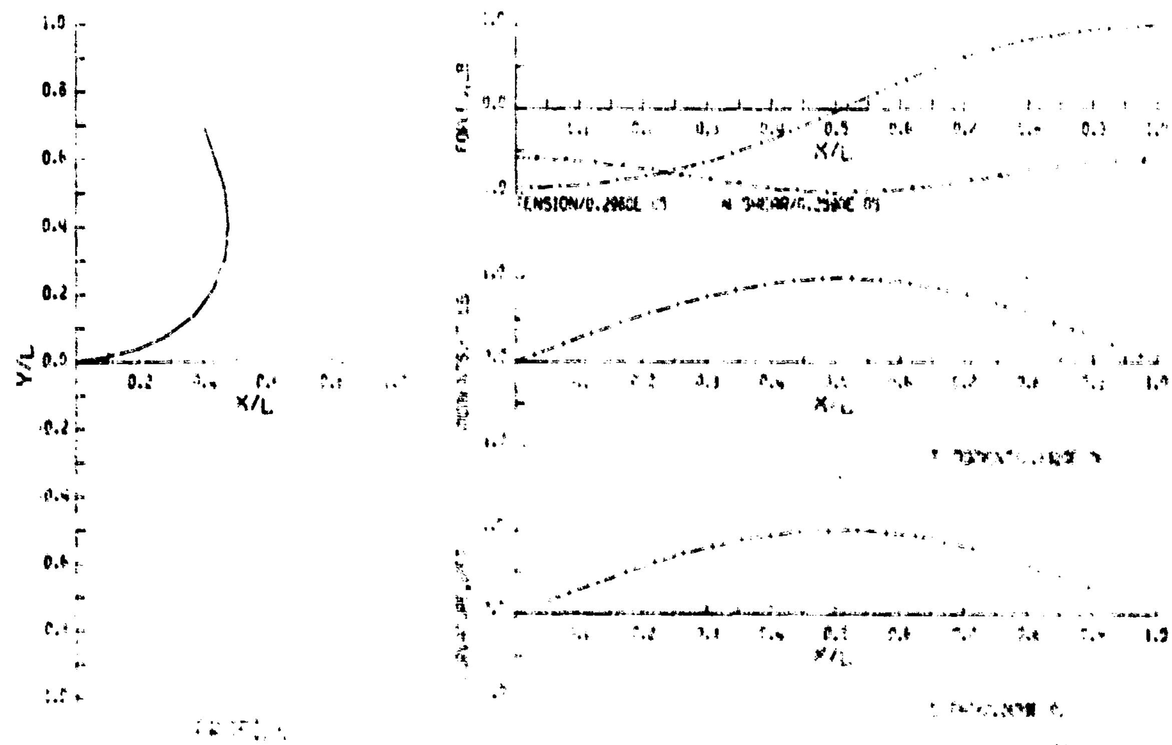

TEST NO.

HYDRONAUTICS,INC

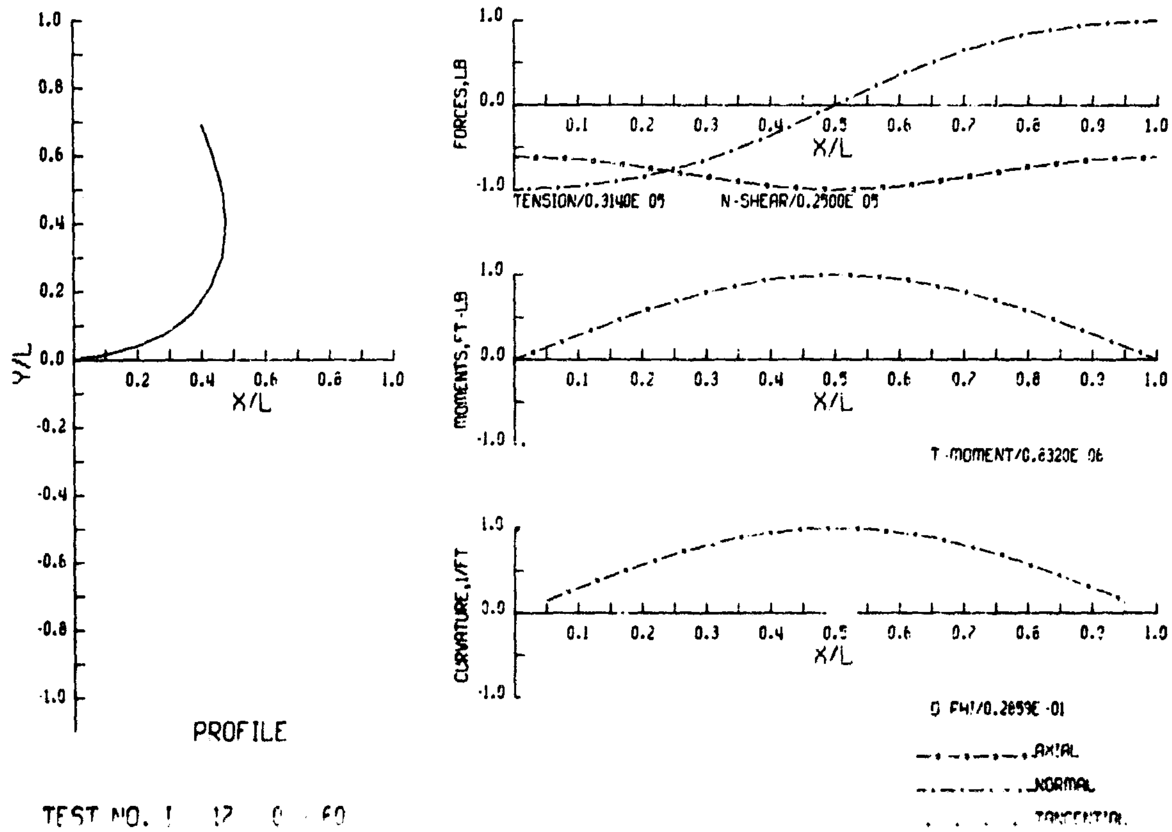

TEST NO. 1 17 0 60

HYDRONAUTICS,INC

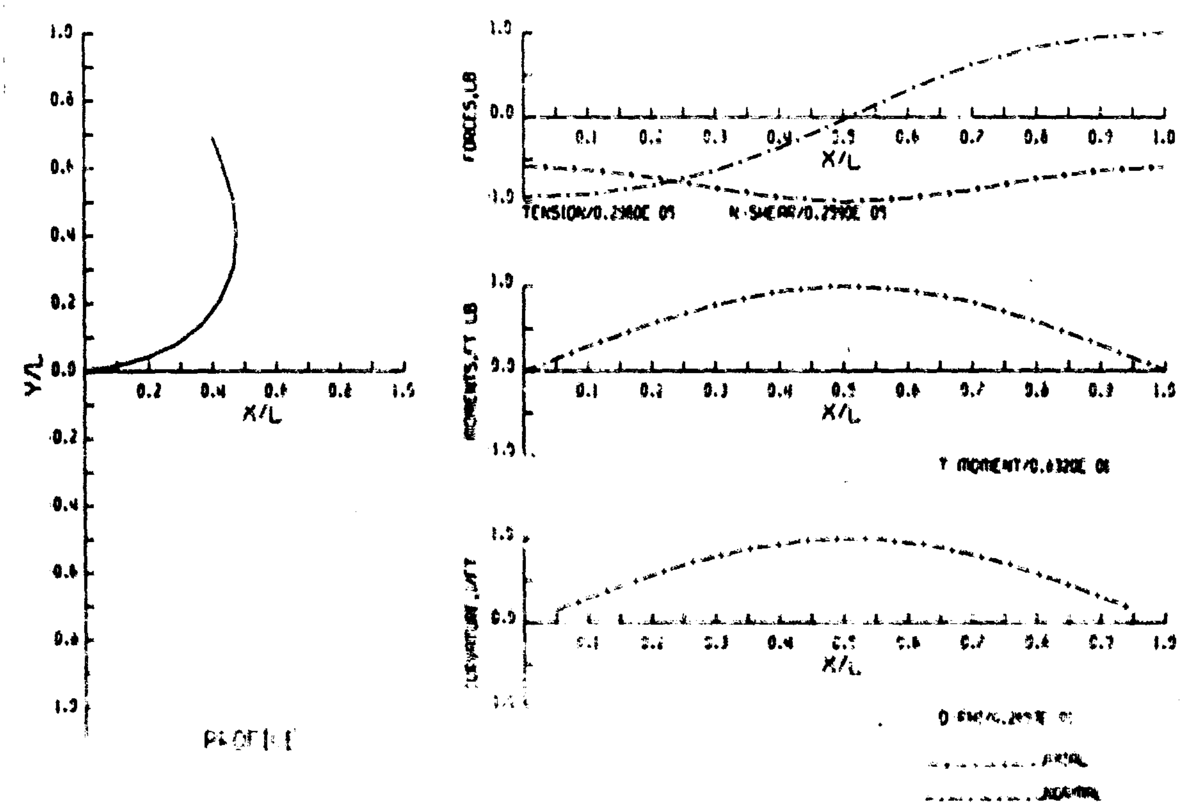

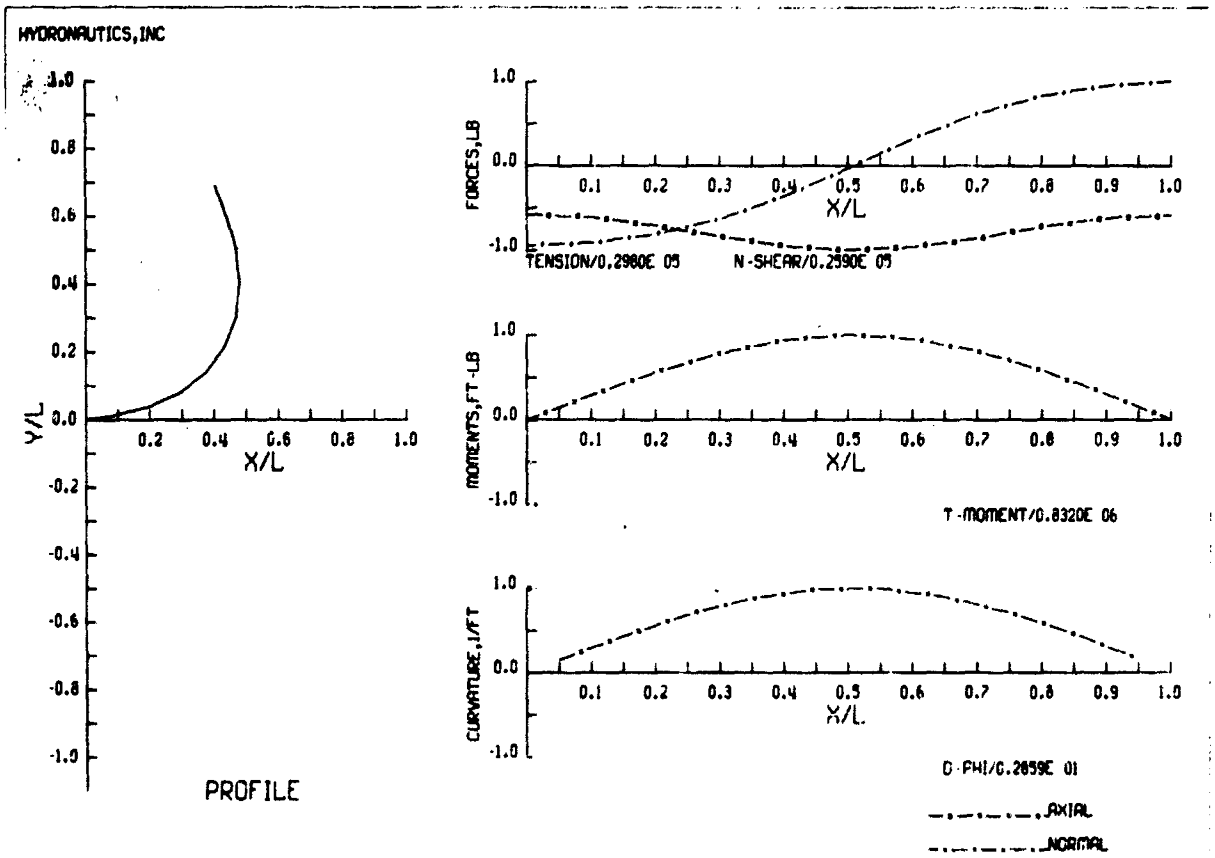

TEST NO. I - 20 - 2 - 60

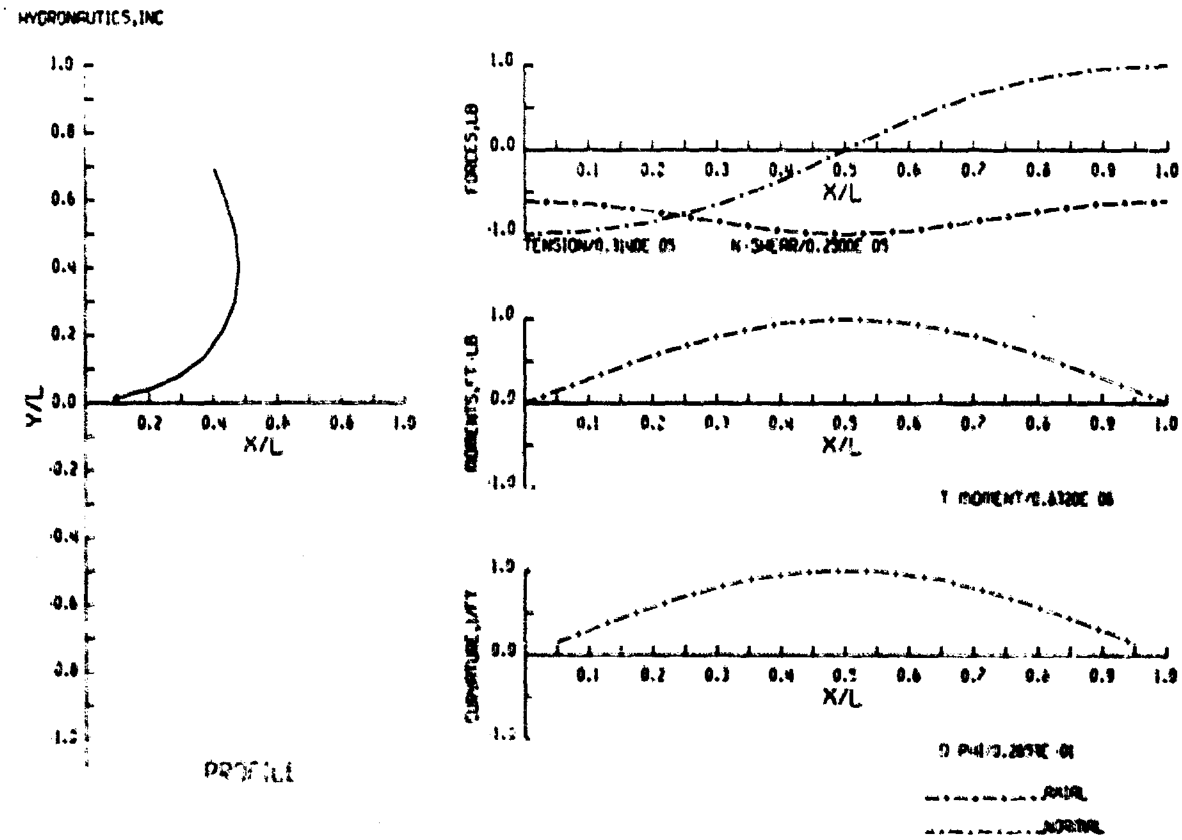

TEST NO. [illegible] - 60

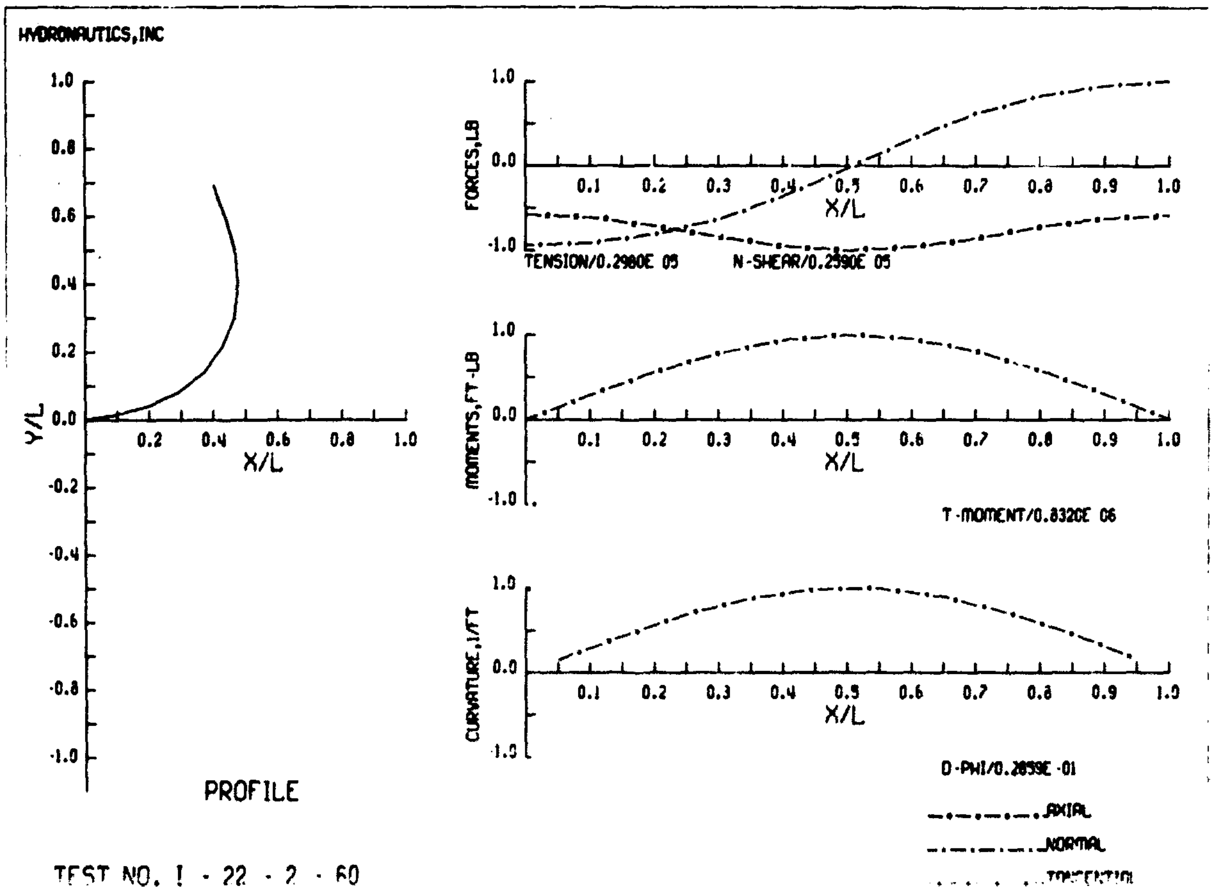
HYDRONAUTICS,INC
Y/L
X/L
PROFILE
FORCES,LB
TENSION/0.2980E 05
N-SHEAR/0.2590E 05
MOMENTS,FT-LB
T-MOMENT/0.8320E 06
CURVATURE,1/FT
D-PHI/0.2859E-01
AXIAL
NORMAL
TEST NO. I - 22 - 2 - 60

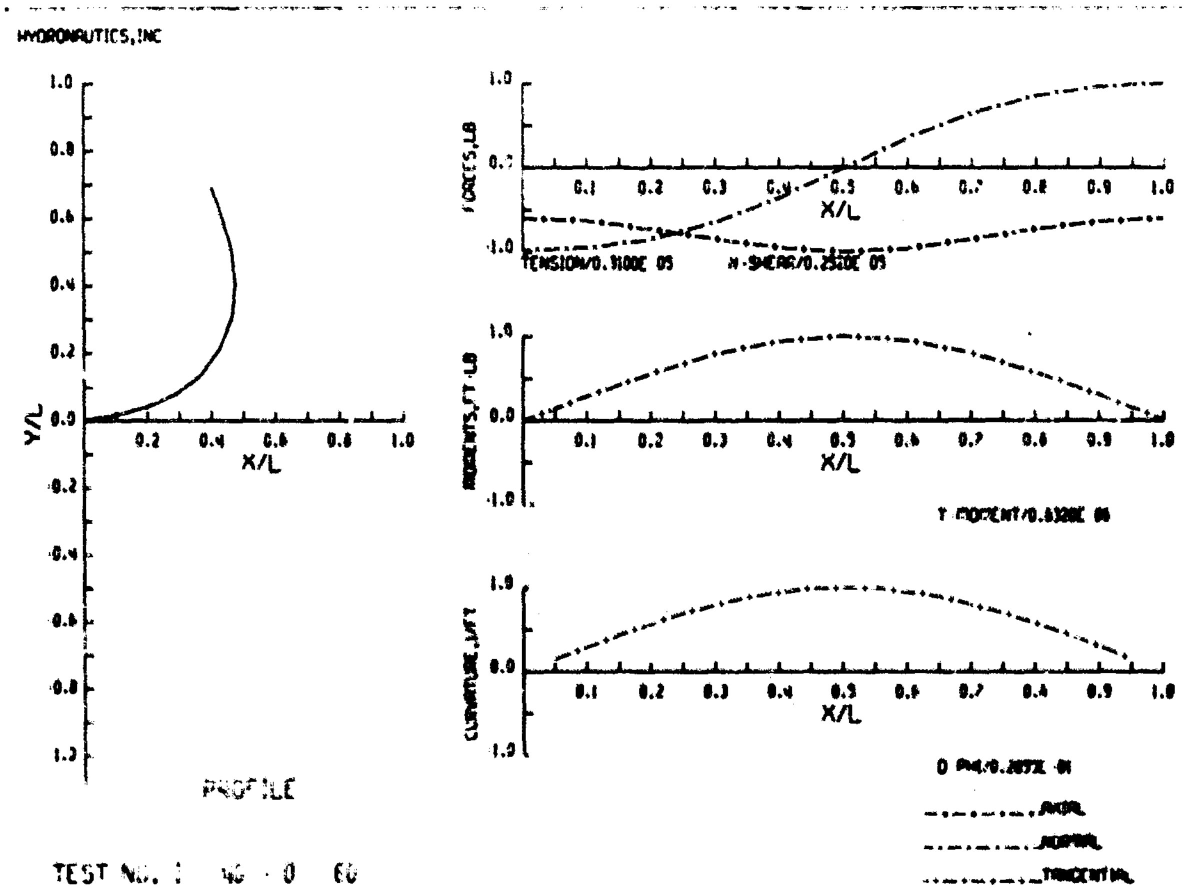
HYDRONAUTICS,INC
Y/L
X/L
TENSION/0.3100E 05
X/L
X/L
AXIAL
NORMAL
TANGENTIAL

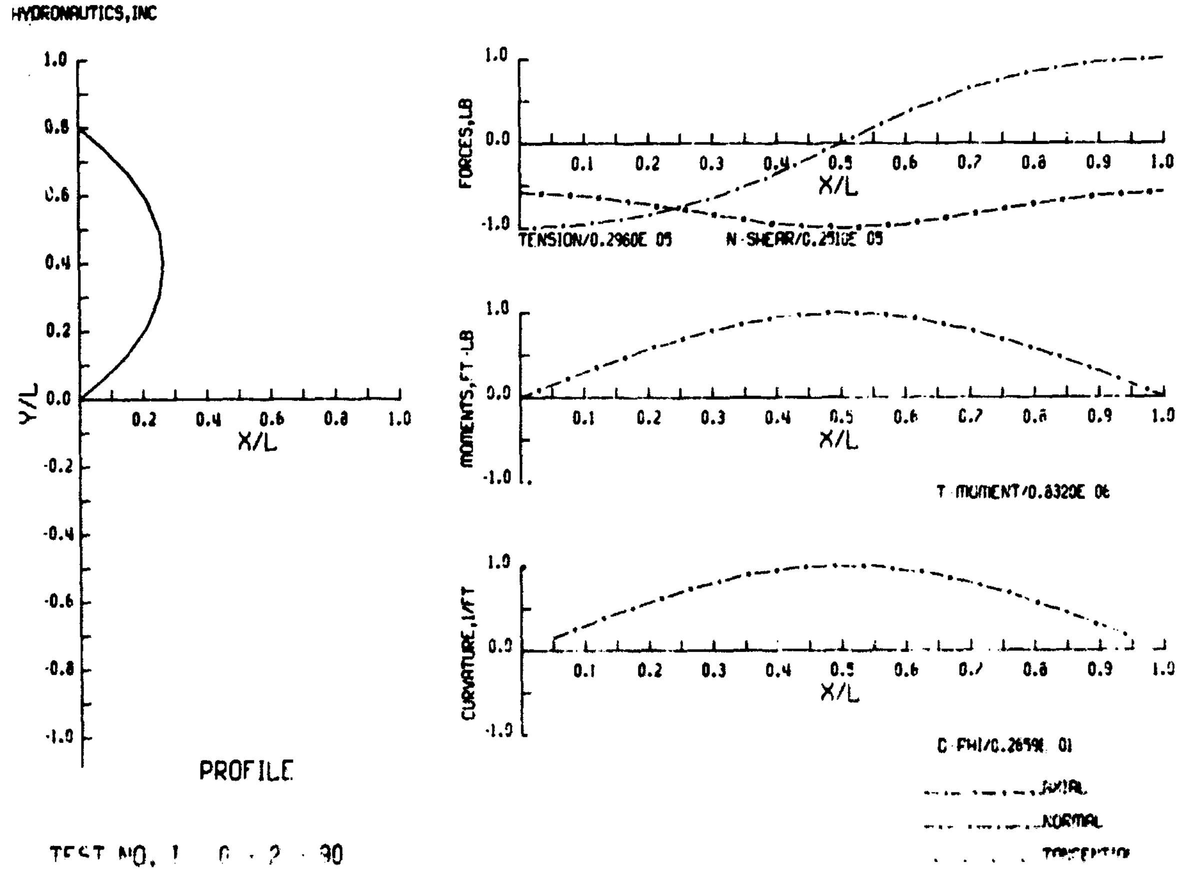
HYDRONAUTICS,INC
Y/L
X/L
PROFILE
FORCES,LB
TENSION/0.2960E 05
MOMENTS,FT-LB
T-MOMENT/0.8320E 06
CURVATURE,1/FT
AXIAL
NORMAL

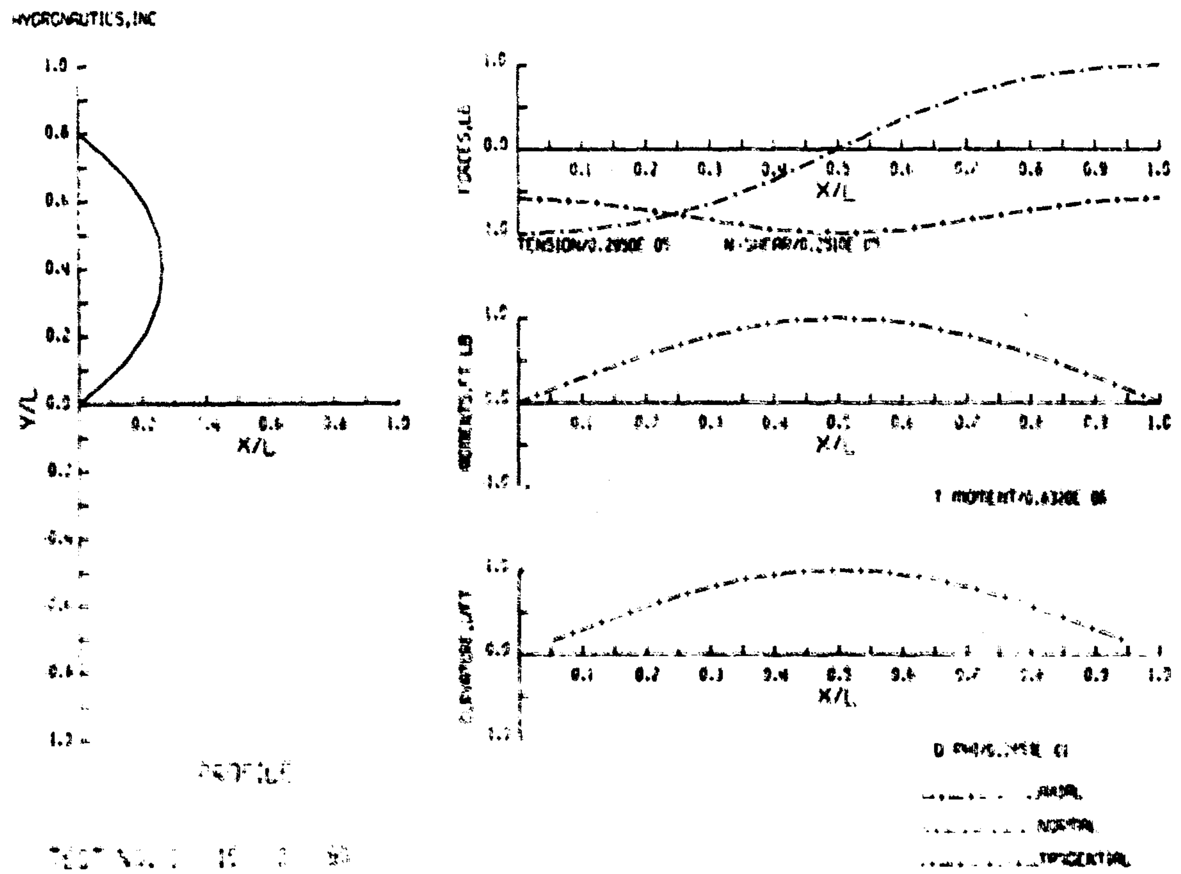
HYDRONAUTICS,INC
Y/L
X/L
AXIAL
NORMAL
TANGENTIAL

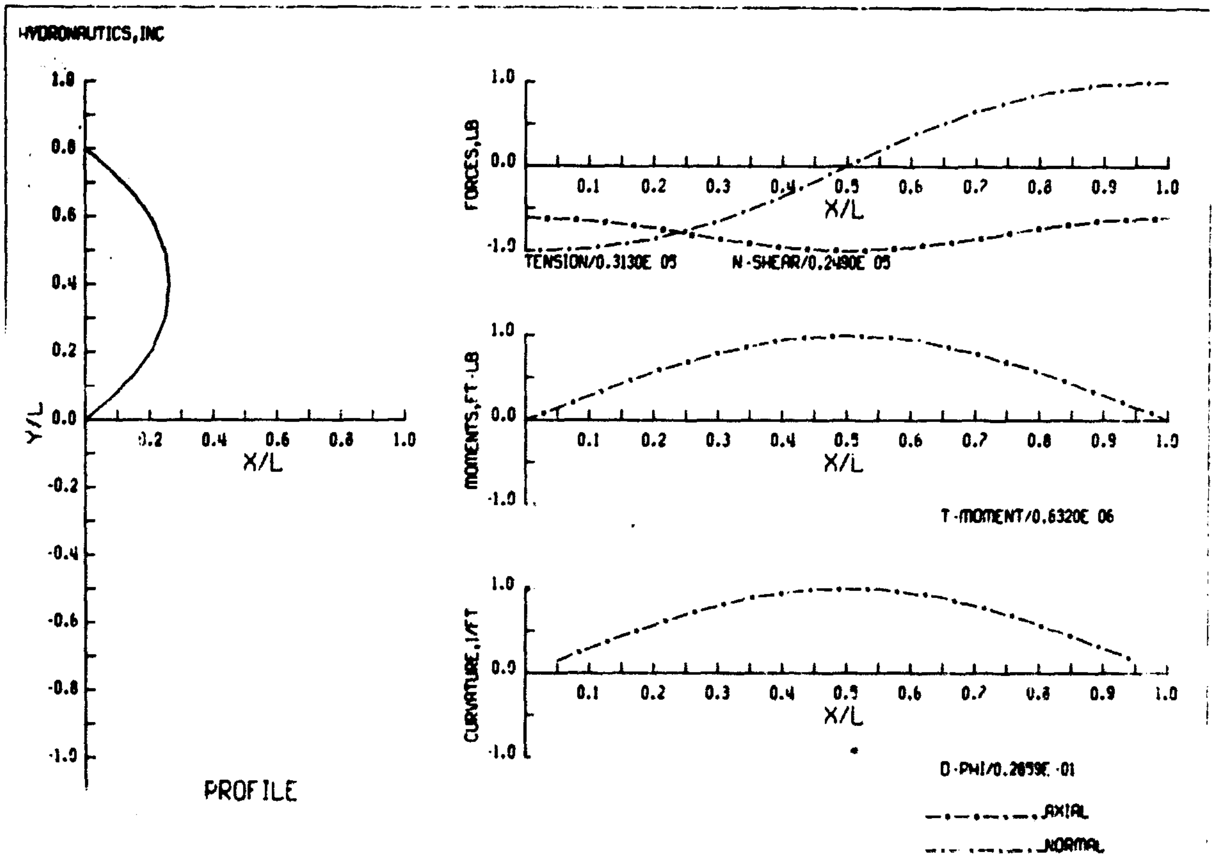

TEST NO. I - 12 - 0 - 90

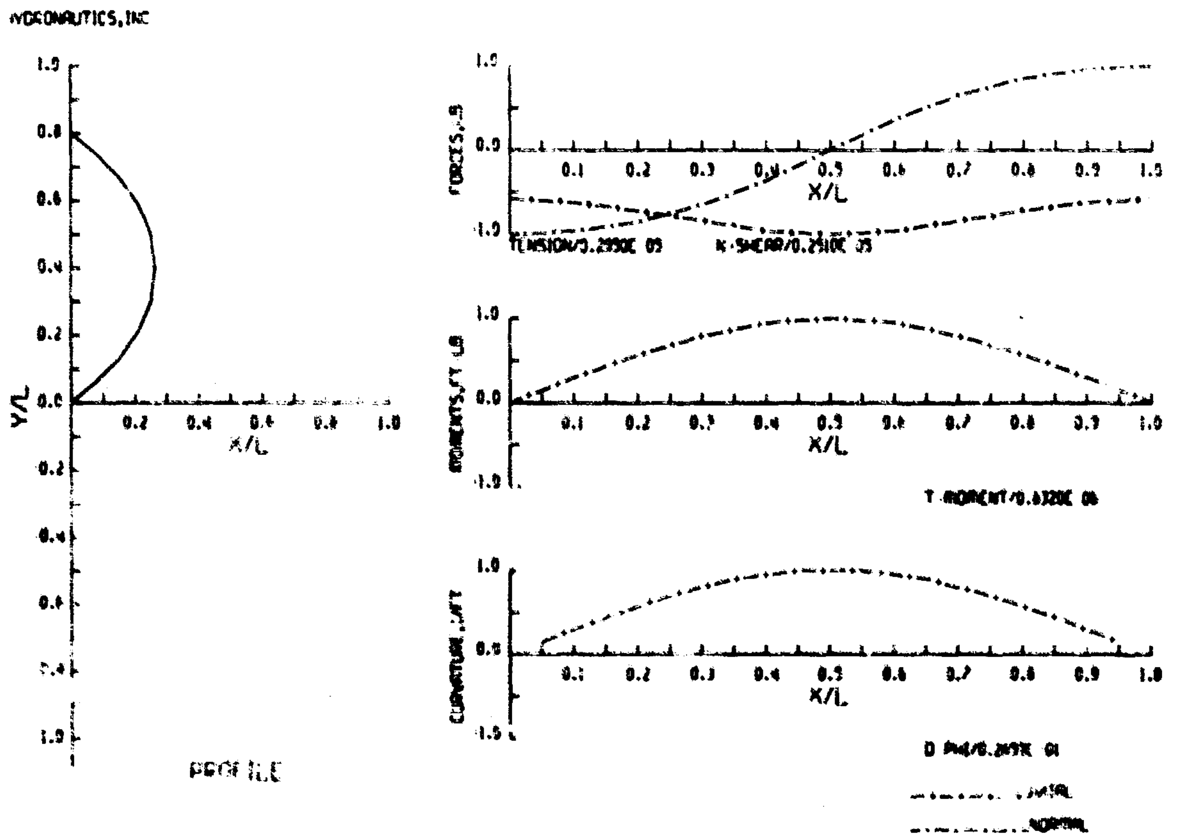

TEST NO. I - 12 - 2 - 90

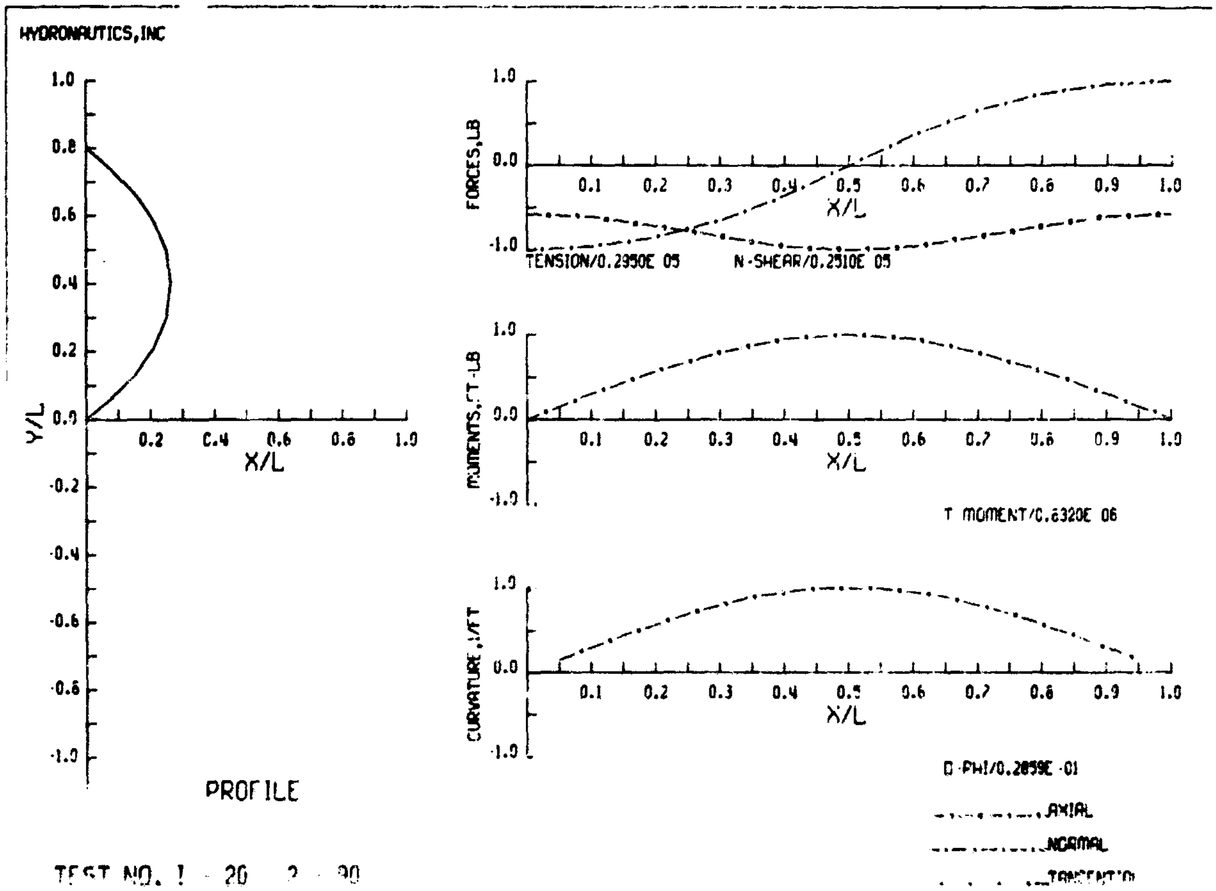
HYDRONAUTICS, INC
Y/L
X/L
PROFILE
FORCES, LB
TENSION/0.2950E 05
N-SHEAR/0.2510E 05
MOMENTS, FT-LB
T MOMENT/0.6320E 06
CURVATURE, 1/FT
D-PHI/0.2859E -01
AXIAL
NORMAL

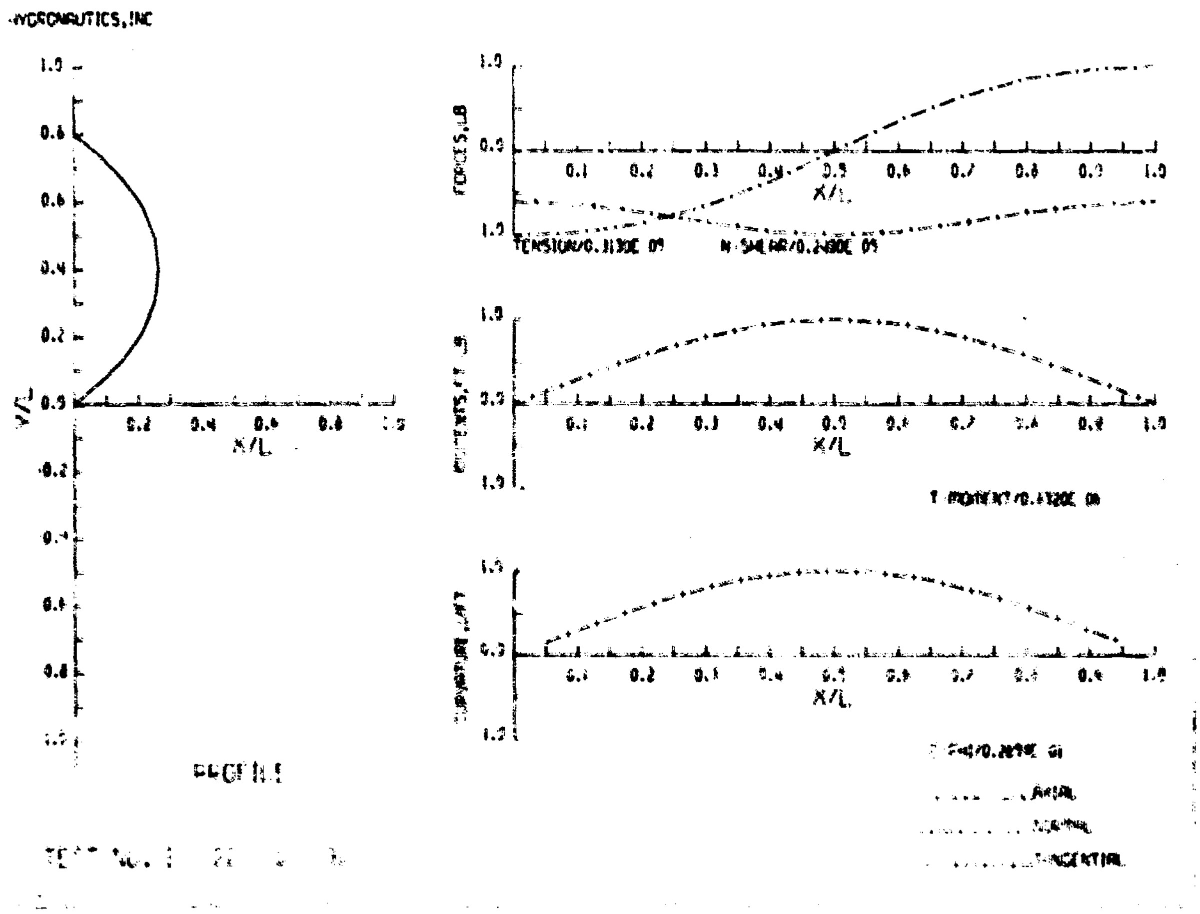
HYDRONAUTICS, INC
X/L
AXIAL
TANGENTIAL

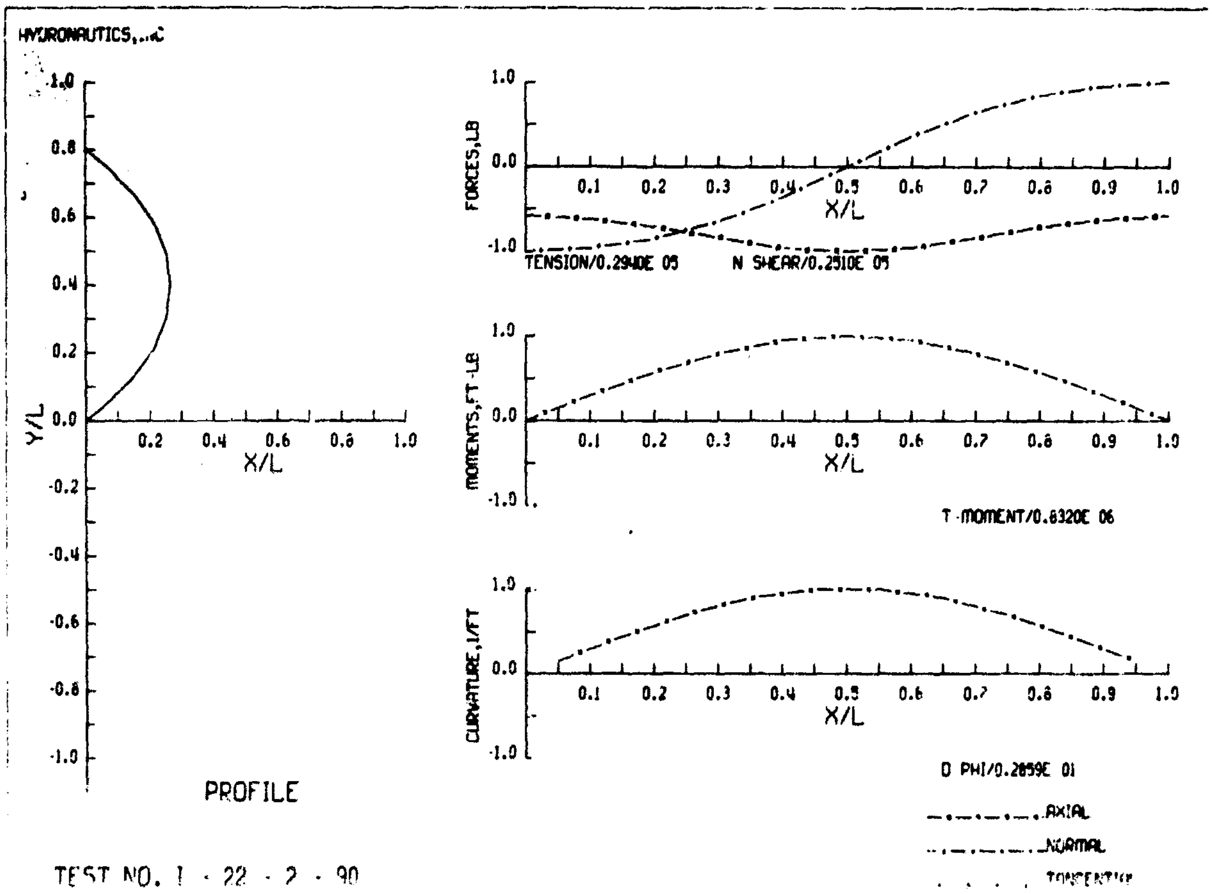
HYDRONAUTICS,..C
PROFILE
Y/L
X/L
FORCES,LB
TENSION/0.2940E 05
N SHEAR/0.2510E 05
MOMENTS,FT-LB
T-MOMENT/0.8320E 06
CURVATURE,1/FT
D PHI/0.2859E 01
AXIAL
NORMAL
TEST NO. 1 - 22 - 2 - 90

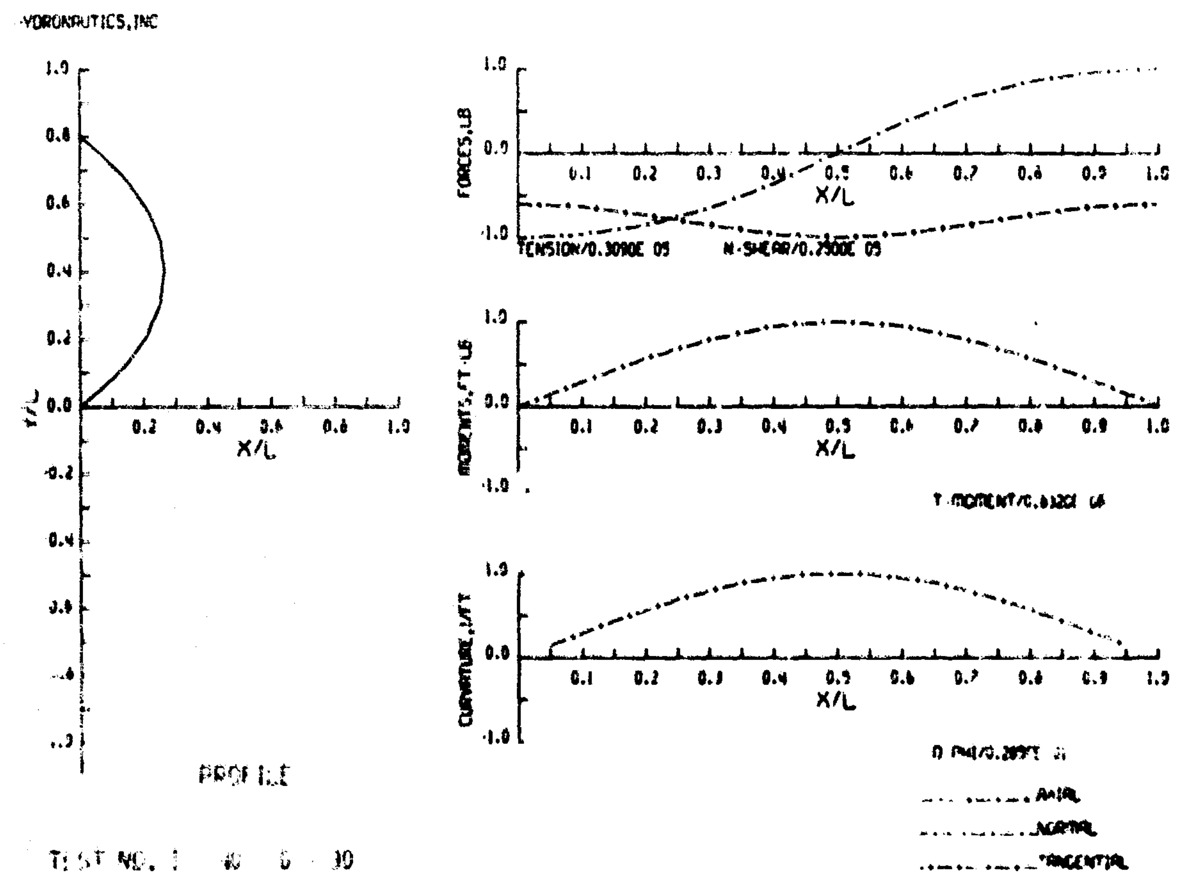
YDRONAUTICS,INC
Y/L
X/L
FORCES,LB
TENSION/0.3090E 05
N-SHEAR/0.2500E 05
MOMENTS,FT-LB
CURVATURE,1/FT
AXIAL
NORMAL
TANGENTIAL

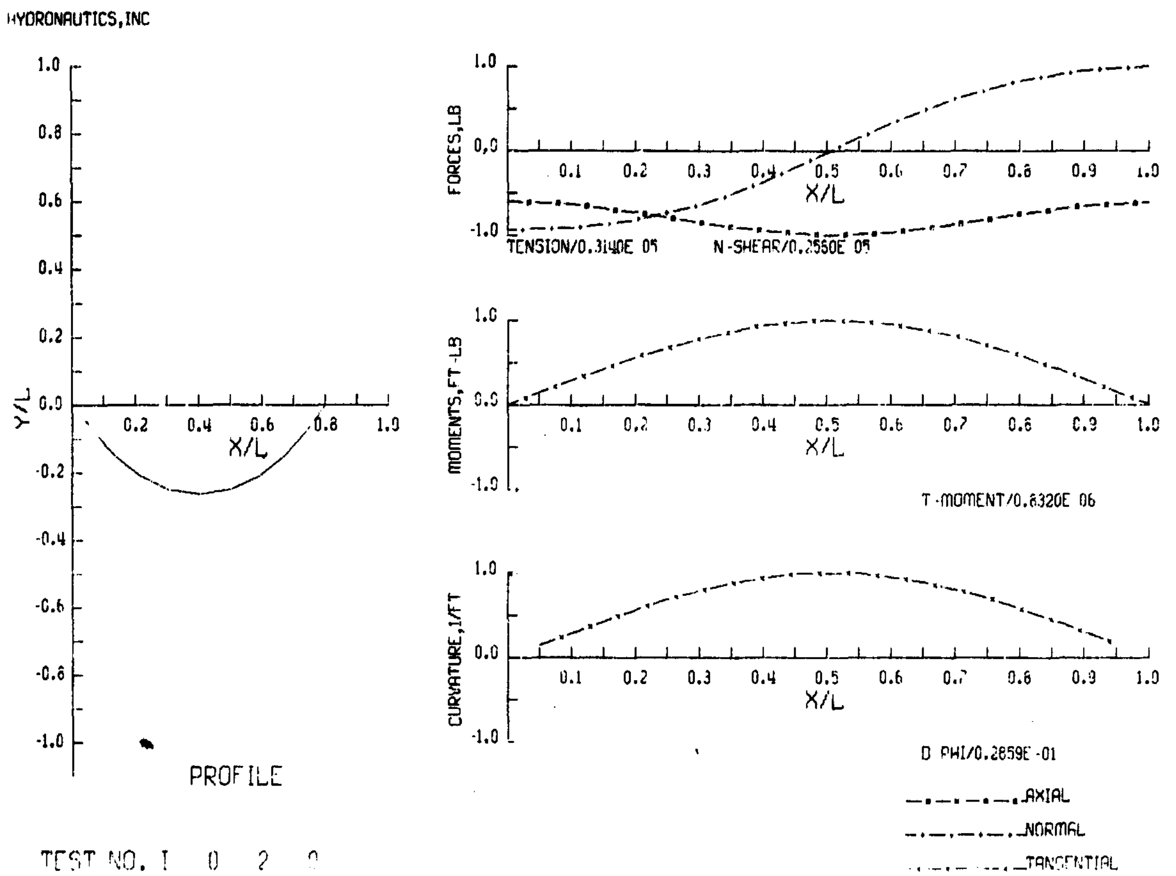
HYDRONAUTICS,INC
Y/L
X/L
PROFILE
FORCES,LB
TENSION/0.3140E 05
N-SHEAR/0.2560E 05
MOMENTS,FT-LB
T-MOMENT/0.8320E 06
CURVATURE,1/FT
D PHI/0.2859E-01
AXIAL
NORMAL
TANGENTIAL
TEST NO. I 0 2 0

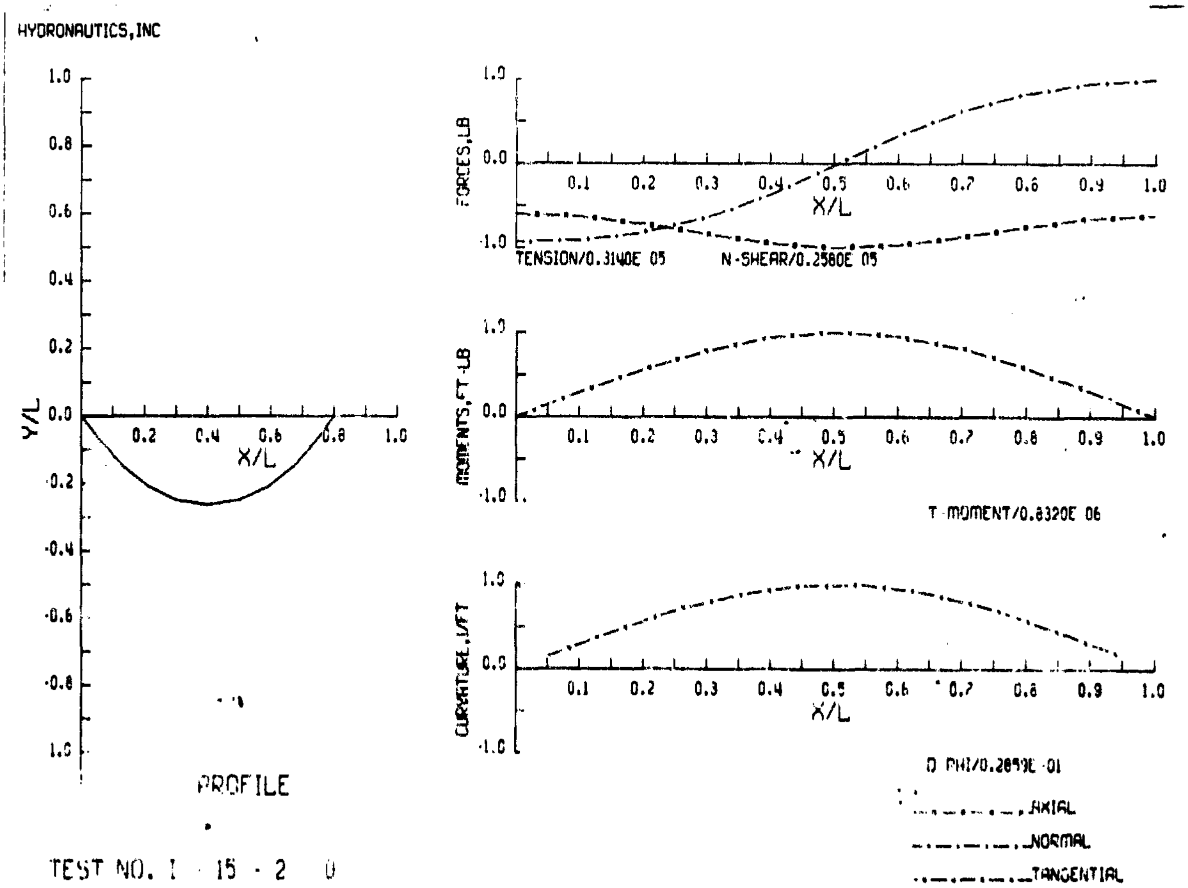
HYDRONAUTICS,INC
Y/L
X/L
PROFILE
FORCES,LB
TENSION/0.3140E 05
N-SHEAR/0.2580E 05
MOMENTS,FT-LB
T-MOMENT/0.8320E 06
CURVATURE,1/FT
D PHI/0.2859E-01
AXIAL
NORMAL
TANGENTIAL
TEST NO. I 15 2 0

HYDRONAUTICS,INC

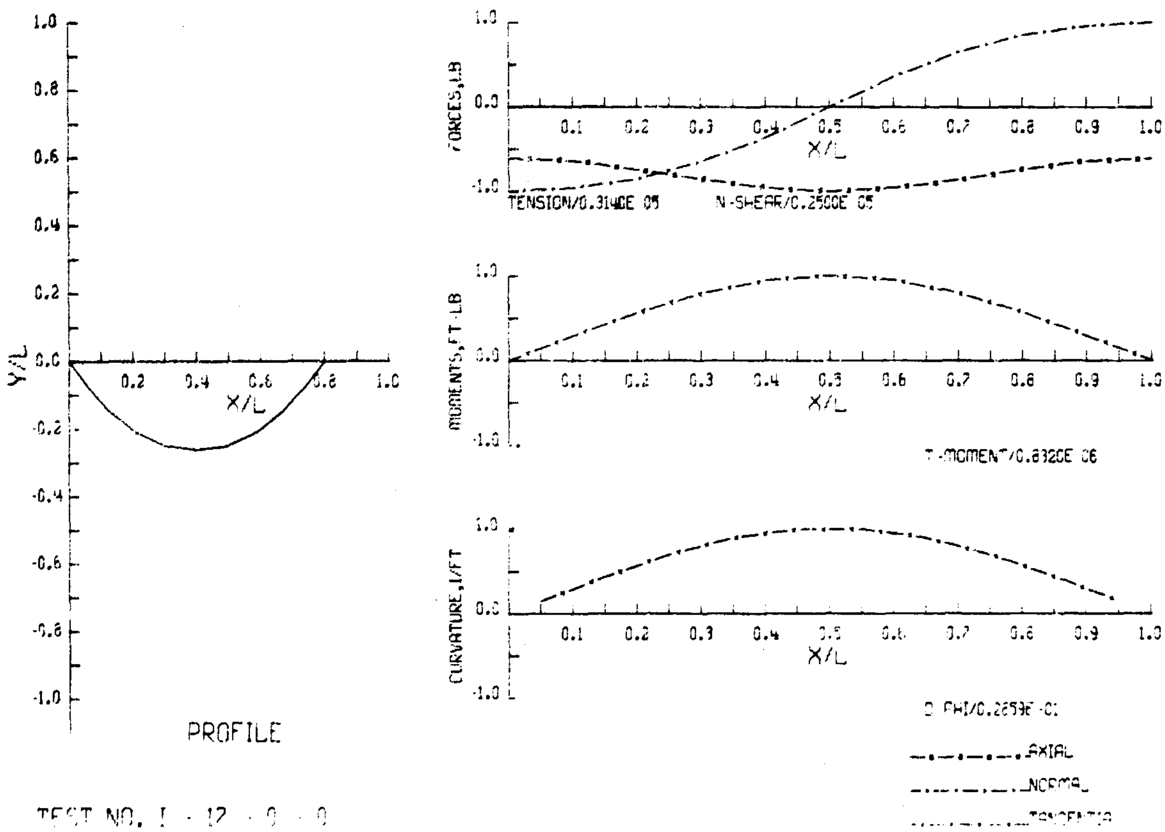

TEST NO. I - 12 - 0 - 0

HYDRONAUTICS,INC

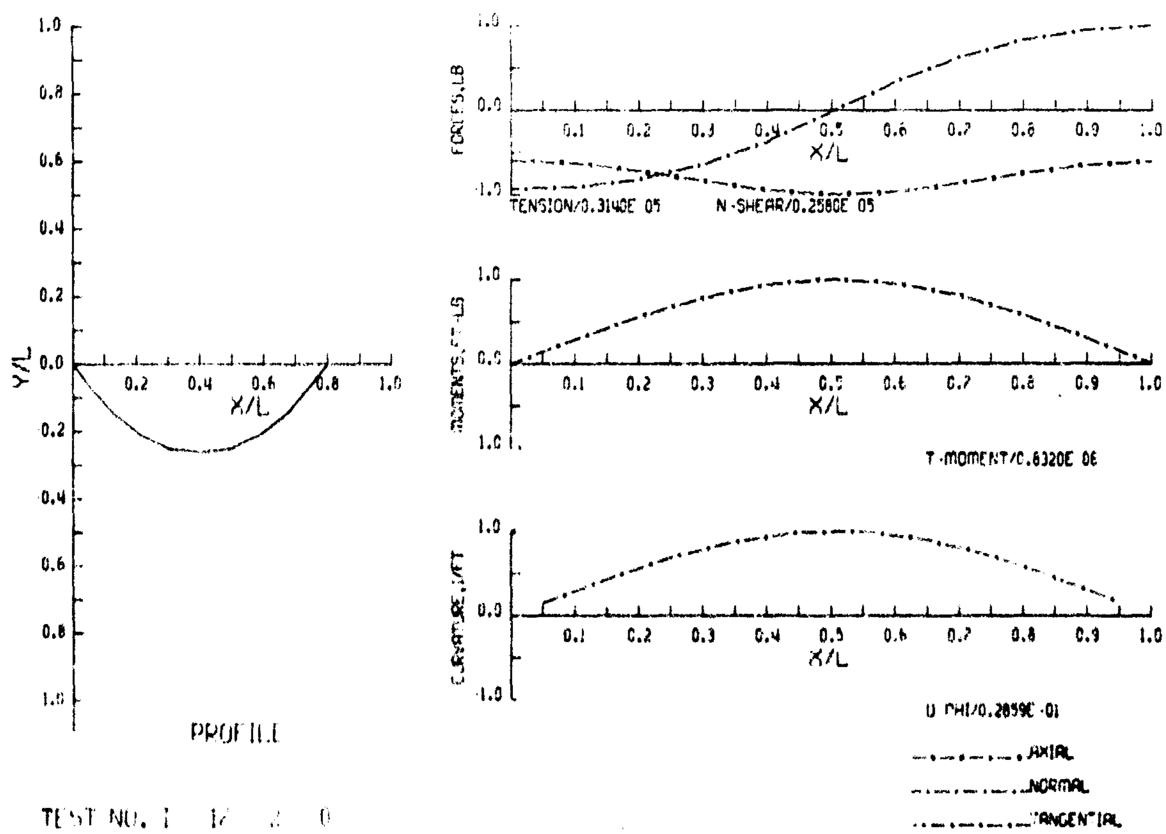

TEST NO. I - 12 - 2 - 0

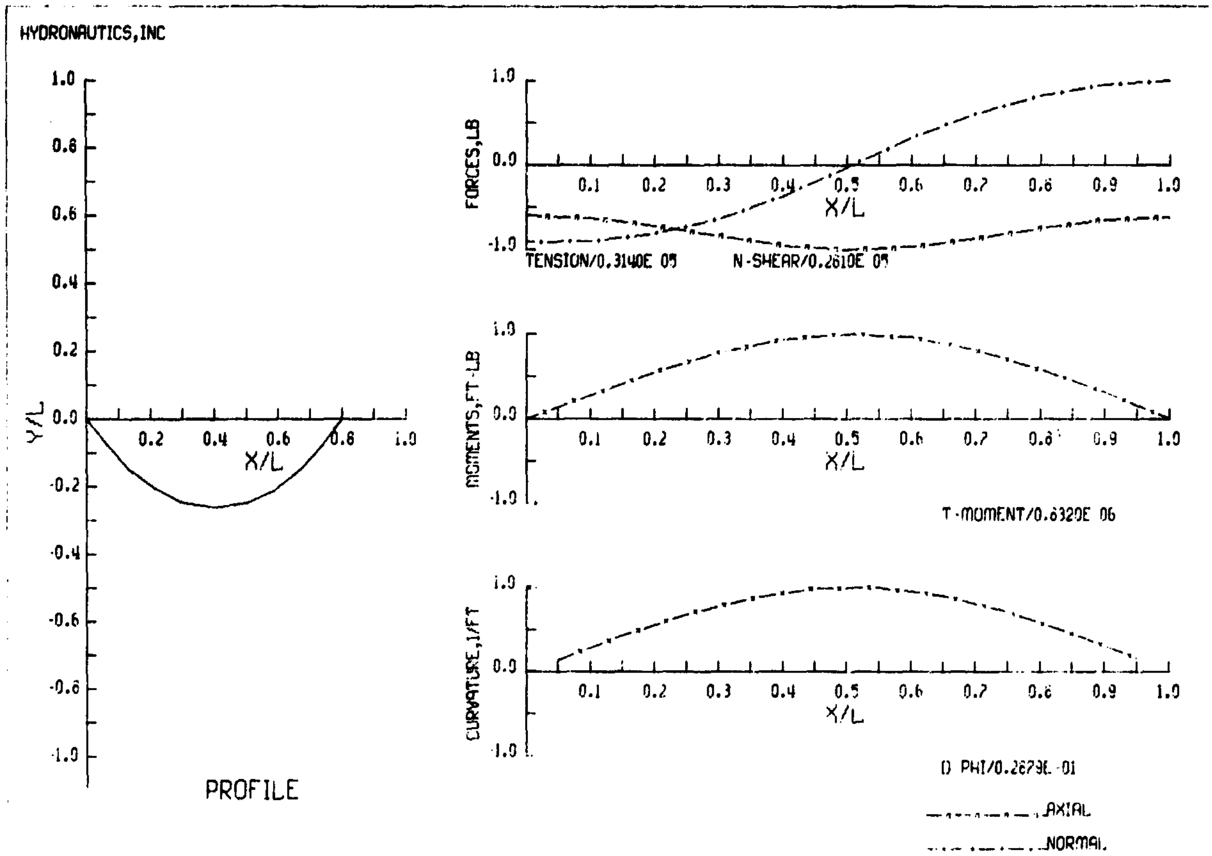

TEST NO. II 20 - 2 - 0

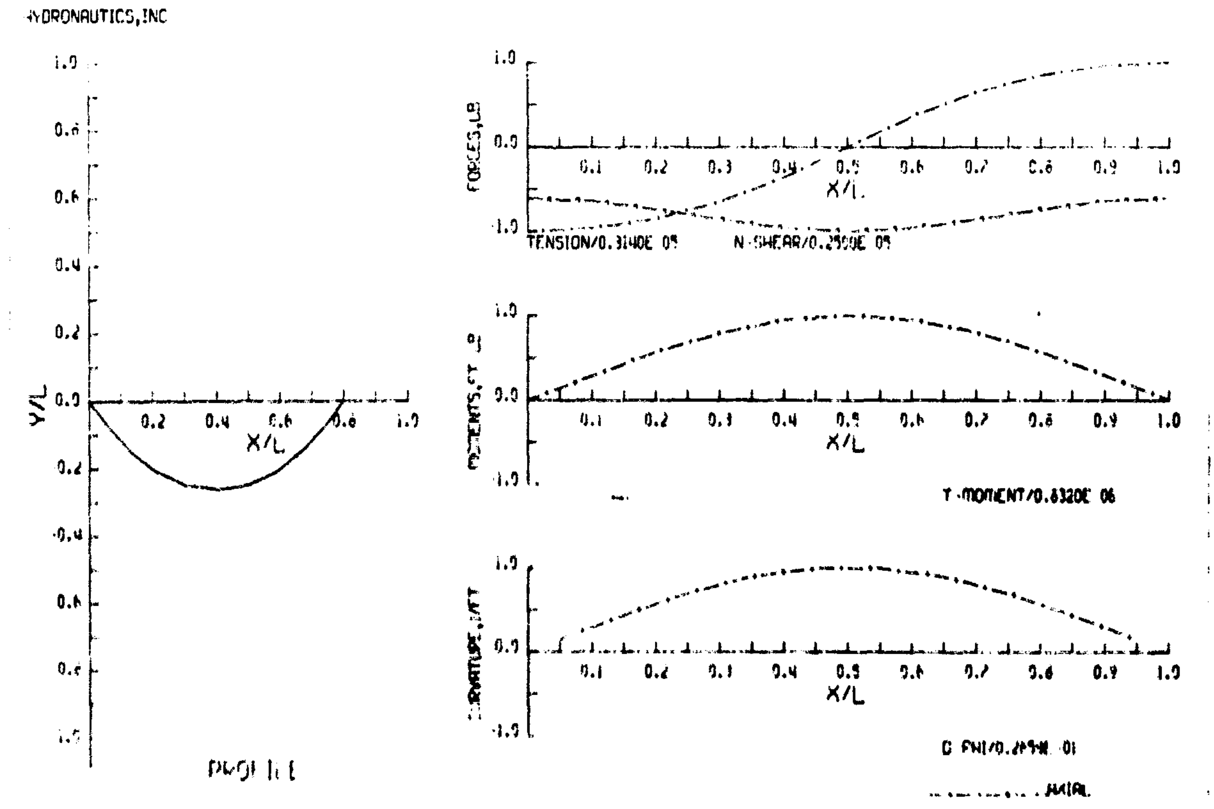

TEST NO. II 22 0 9

HYDRONAUTICS, INC

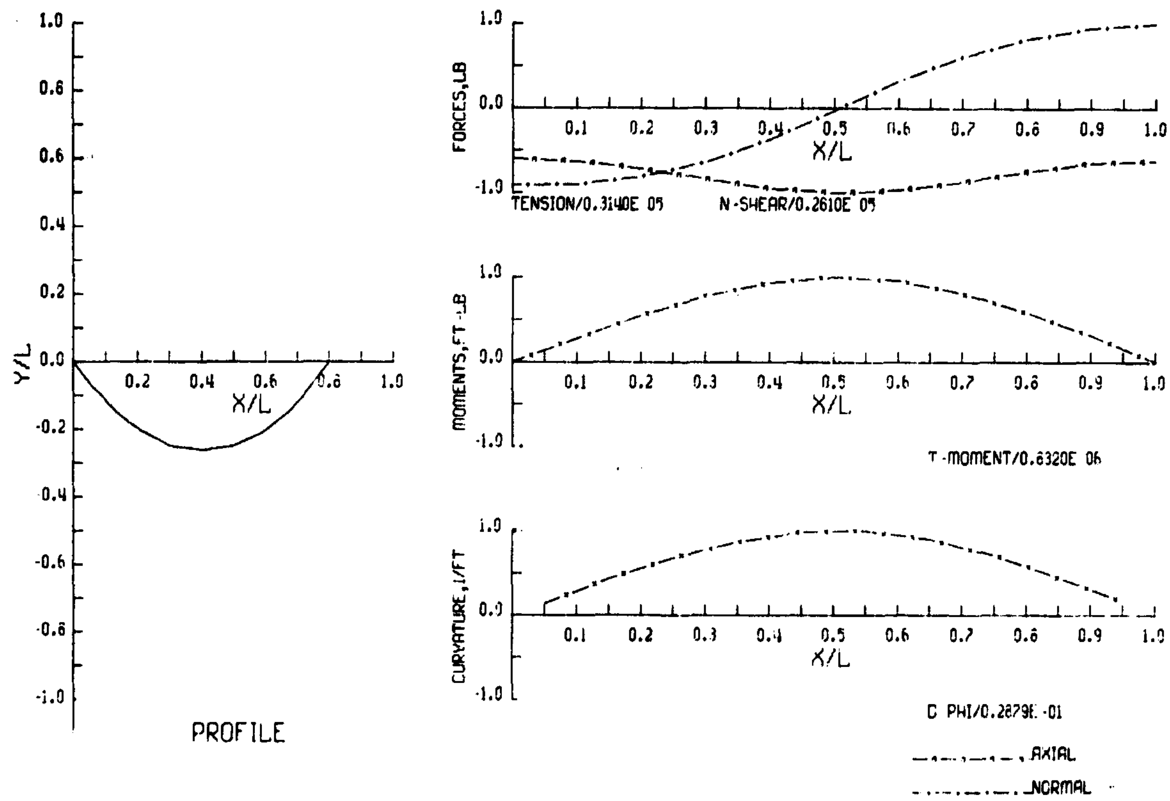

TEST NO. II - 22 - 2 - 0

HYDRONAUTICS, INC

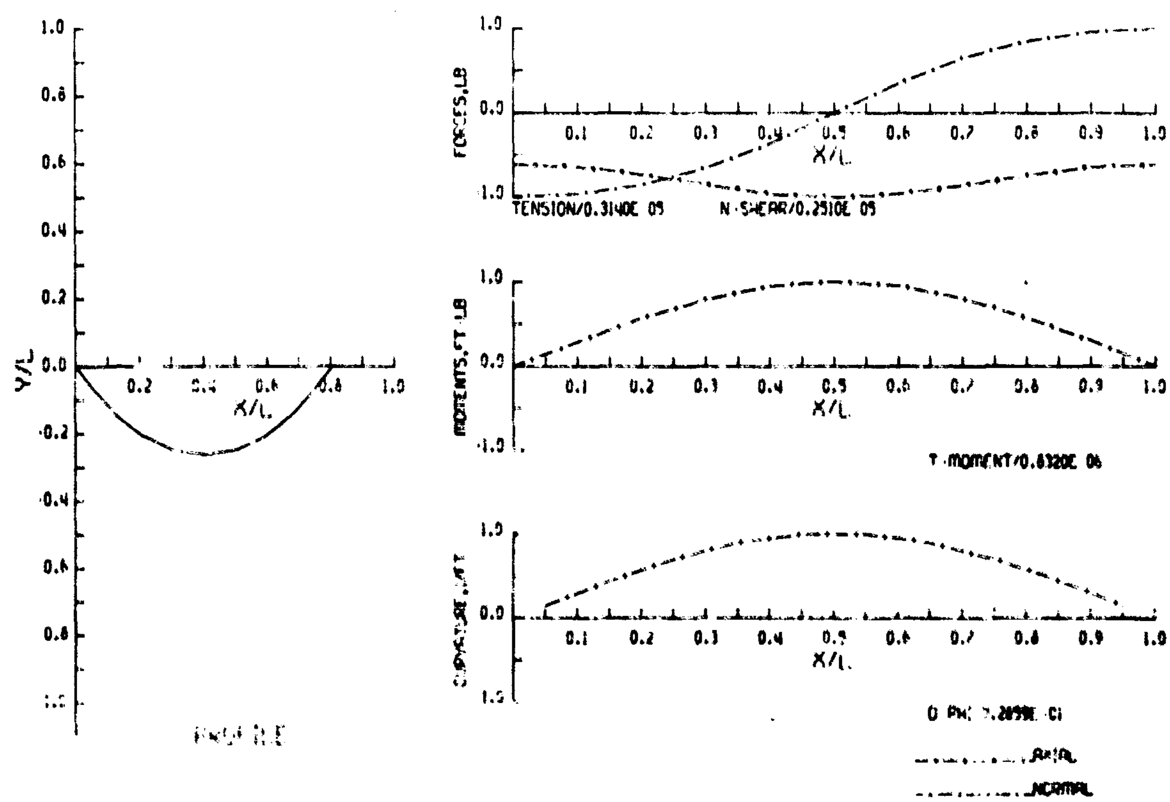

TEST NO. [illegible]

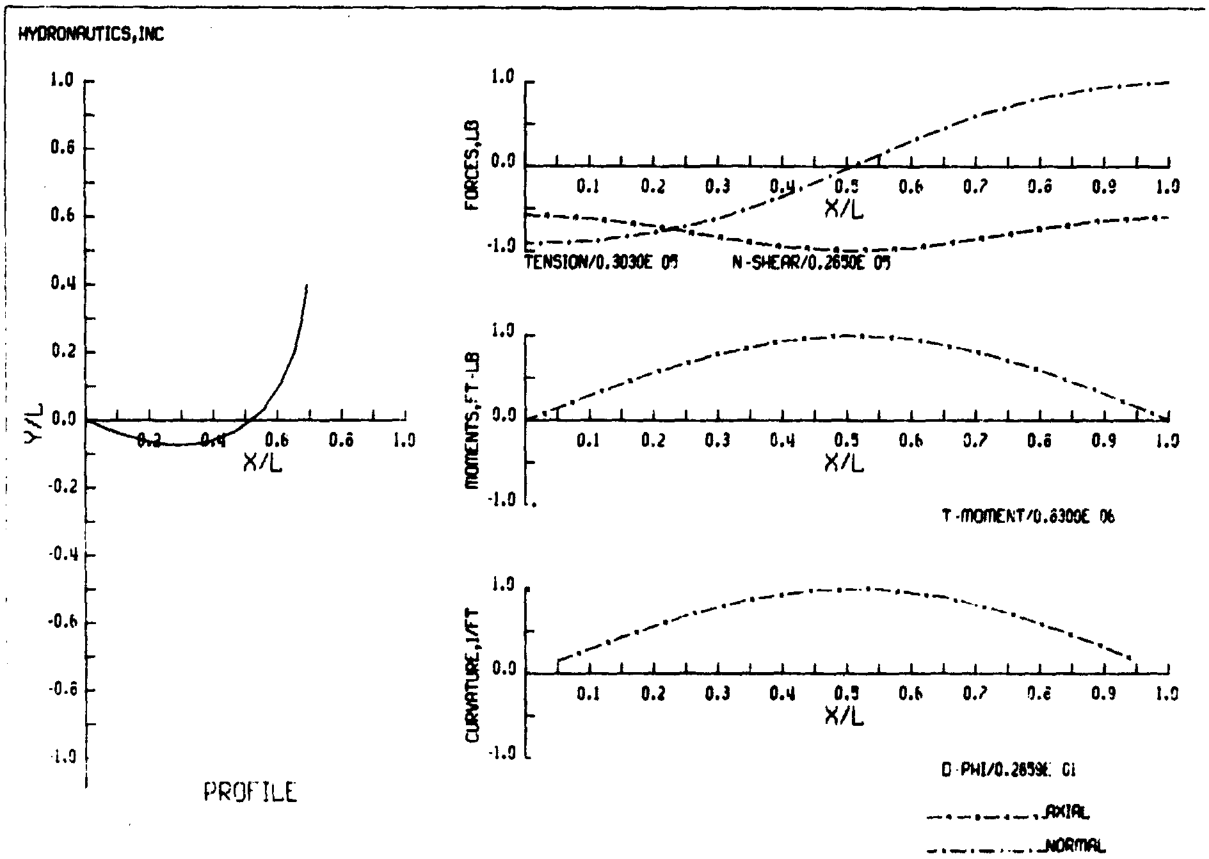

TEST NO. II 0 2 30

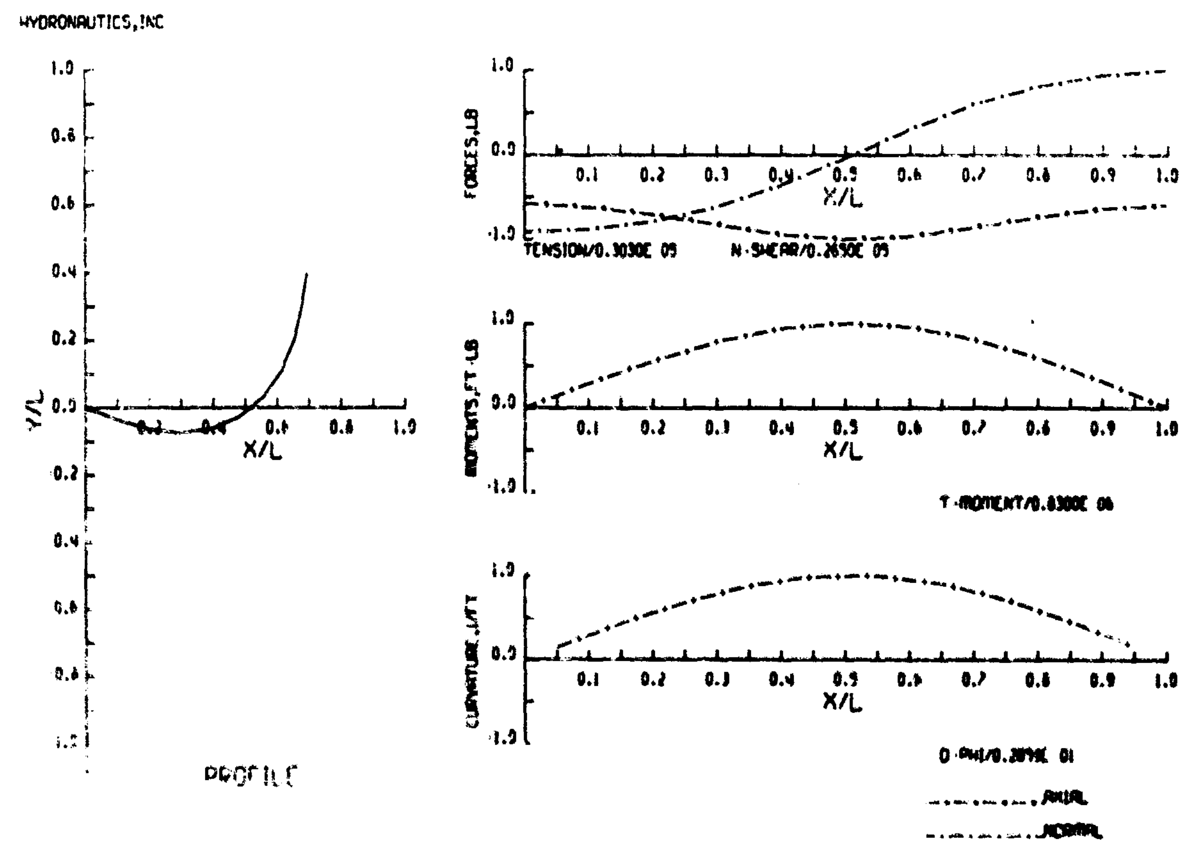

TEST NO. II 15 2 30

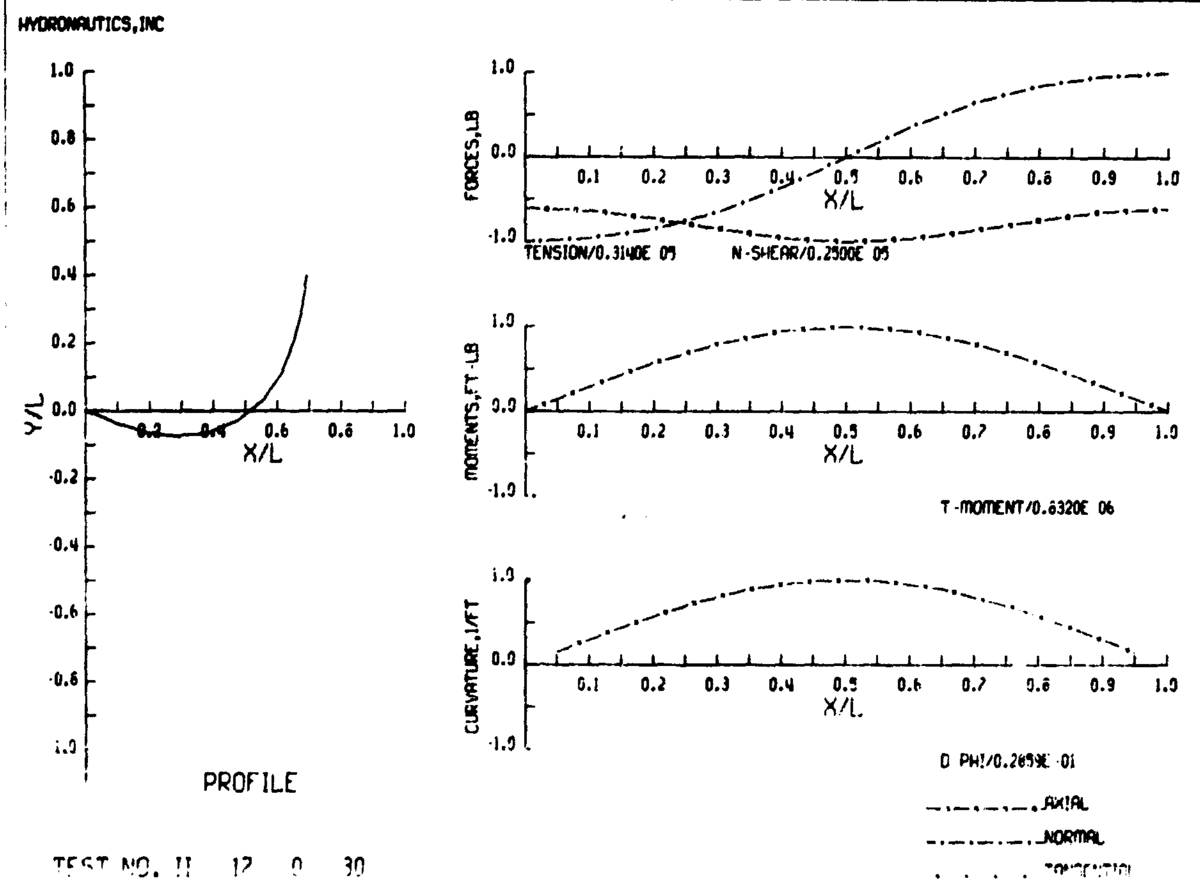

TEST NO. II 12 0 30

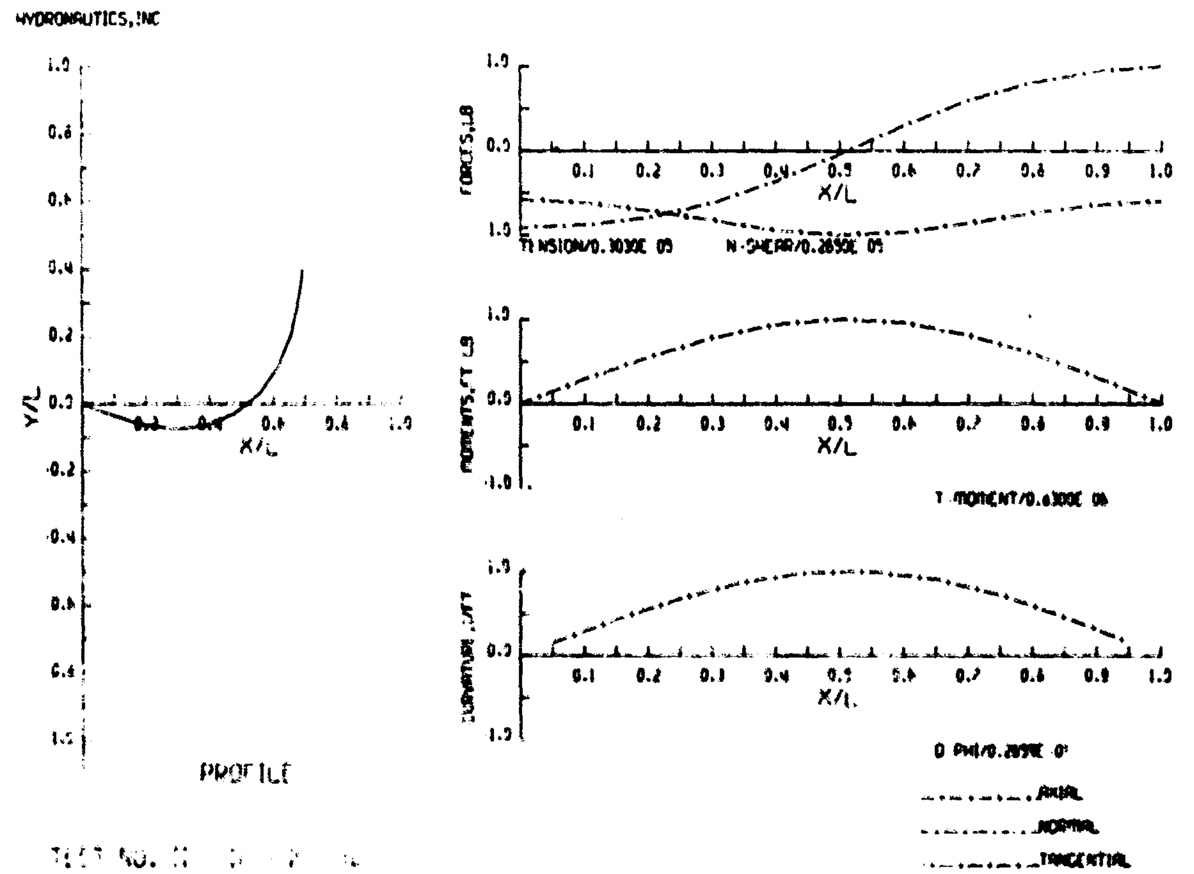

TEST NO. II

HYDRONAUTICS,INC

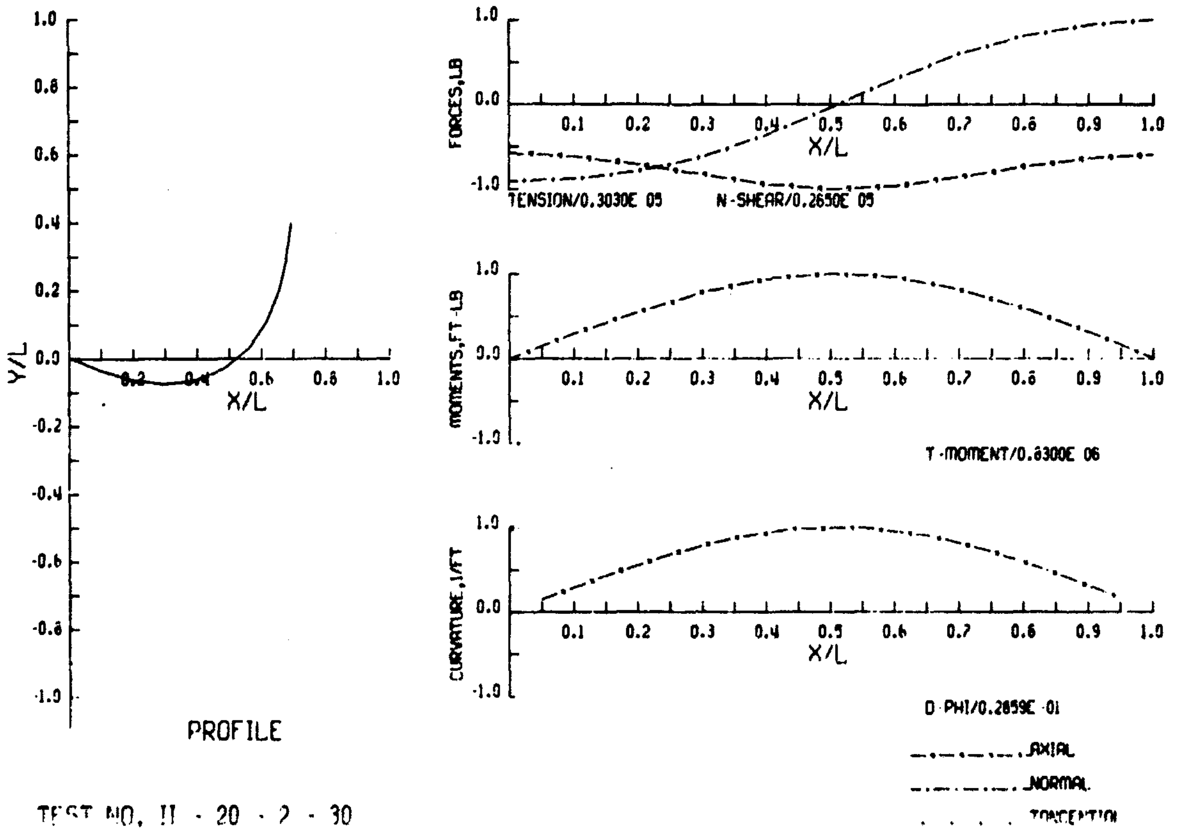

TEST NO. II - 20 - 2 - 30

HYDRONAUTICS,INC

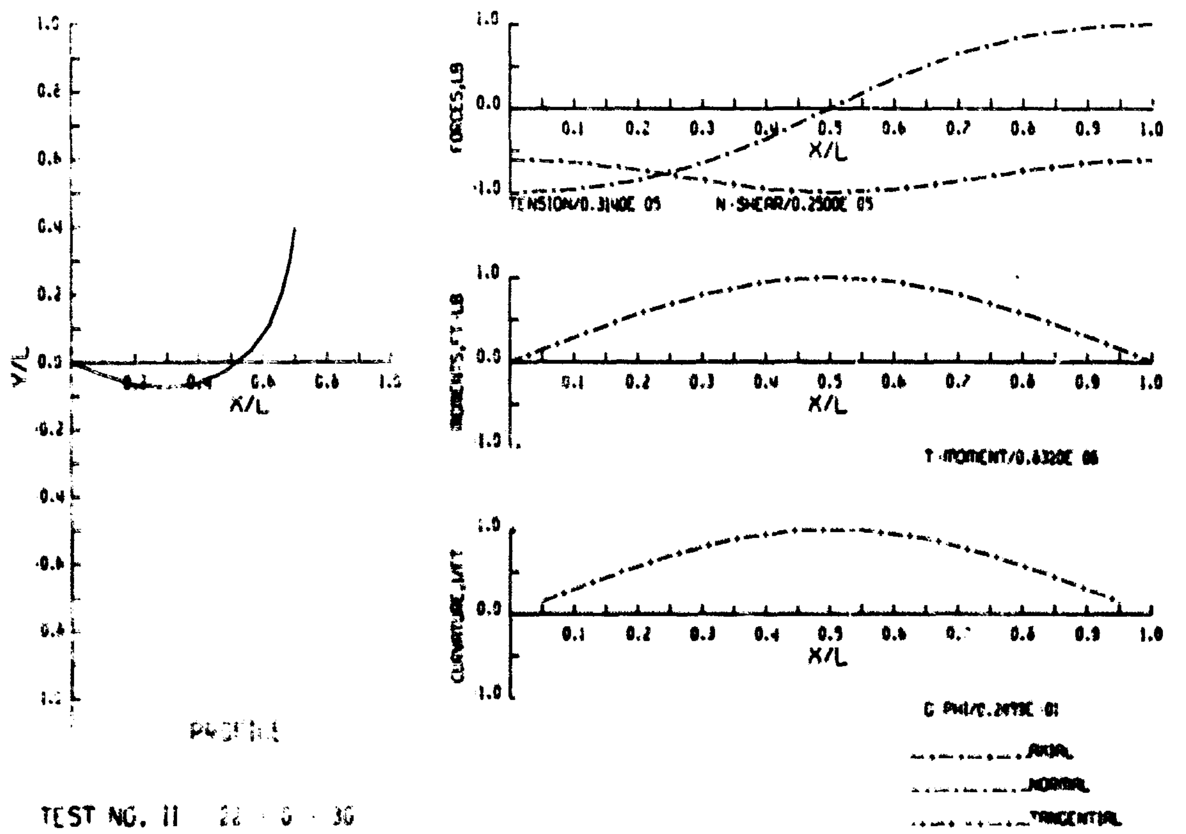

TEST NO. II

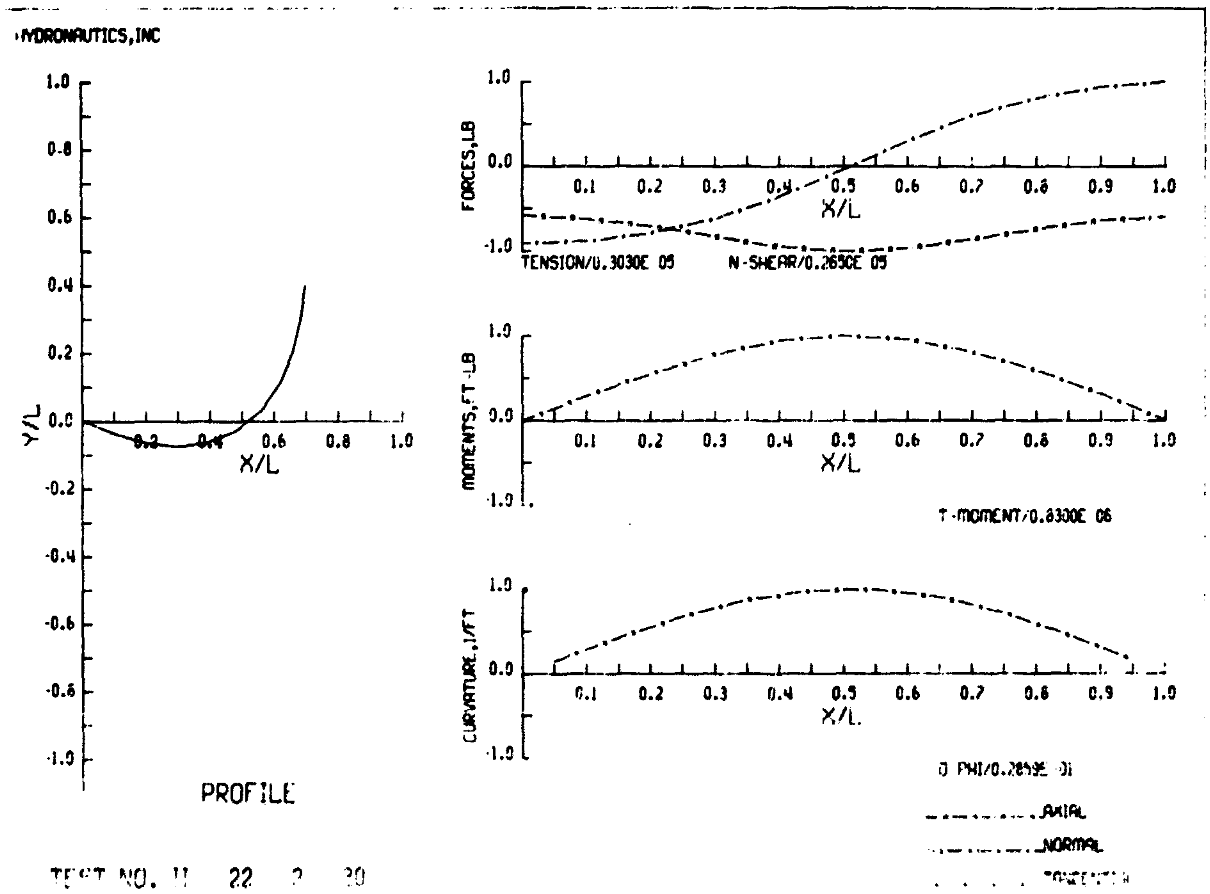
HYDRONAUTICS,INC
PROFILE
Y/L
X/L
FORCES,LB
TENSION/0.3030E 05
N-SHEAR/0.2650E 05
MOMENTS,FT-LB
T-MOMENT/0.8300E 06
CURVATURE,1/FT
AXIAL
NORMAL

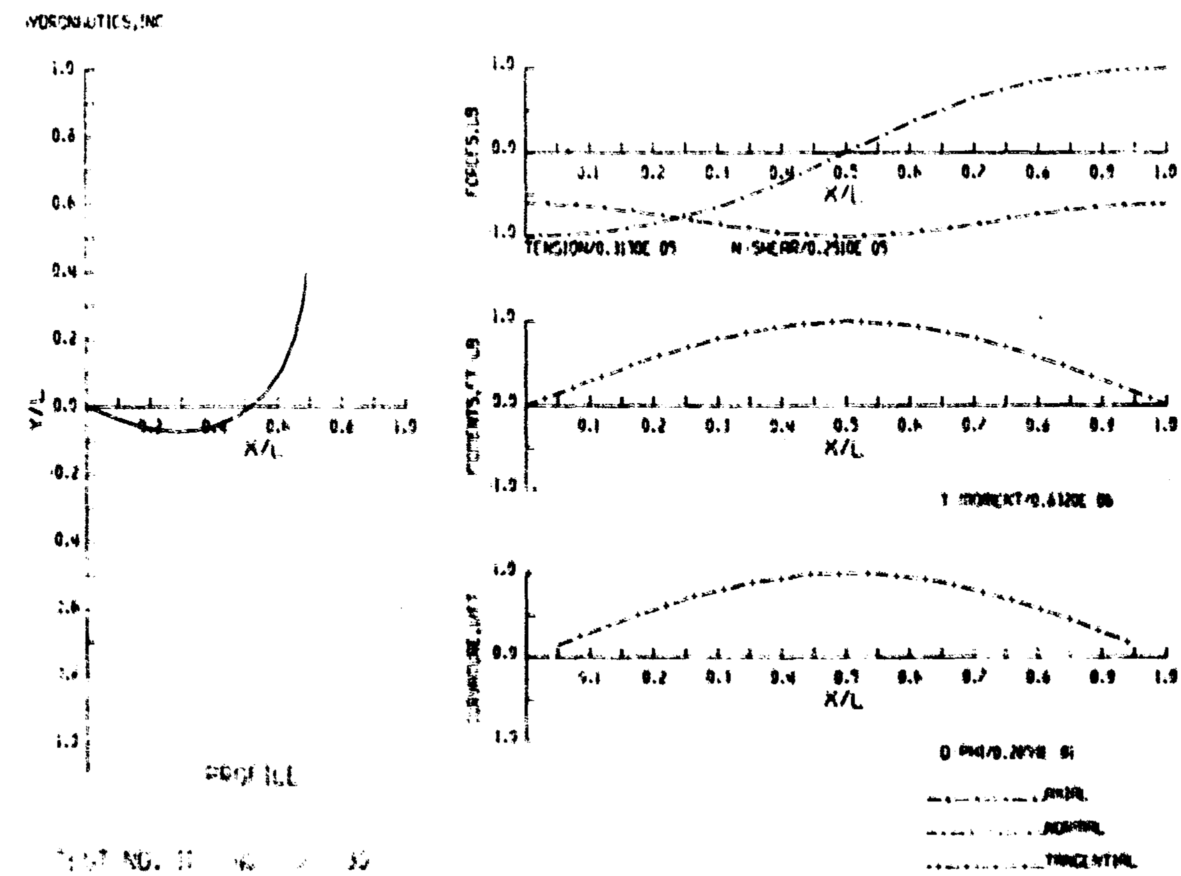
PROFILE
X/L
MOMENTS,FT-LB
AXIAL
NORMAL
TANGENTIAL

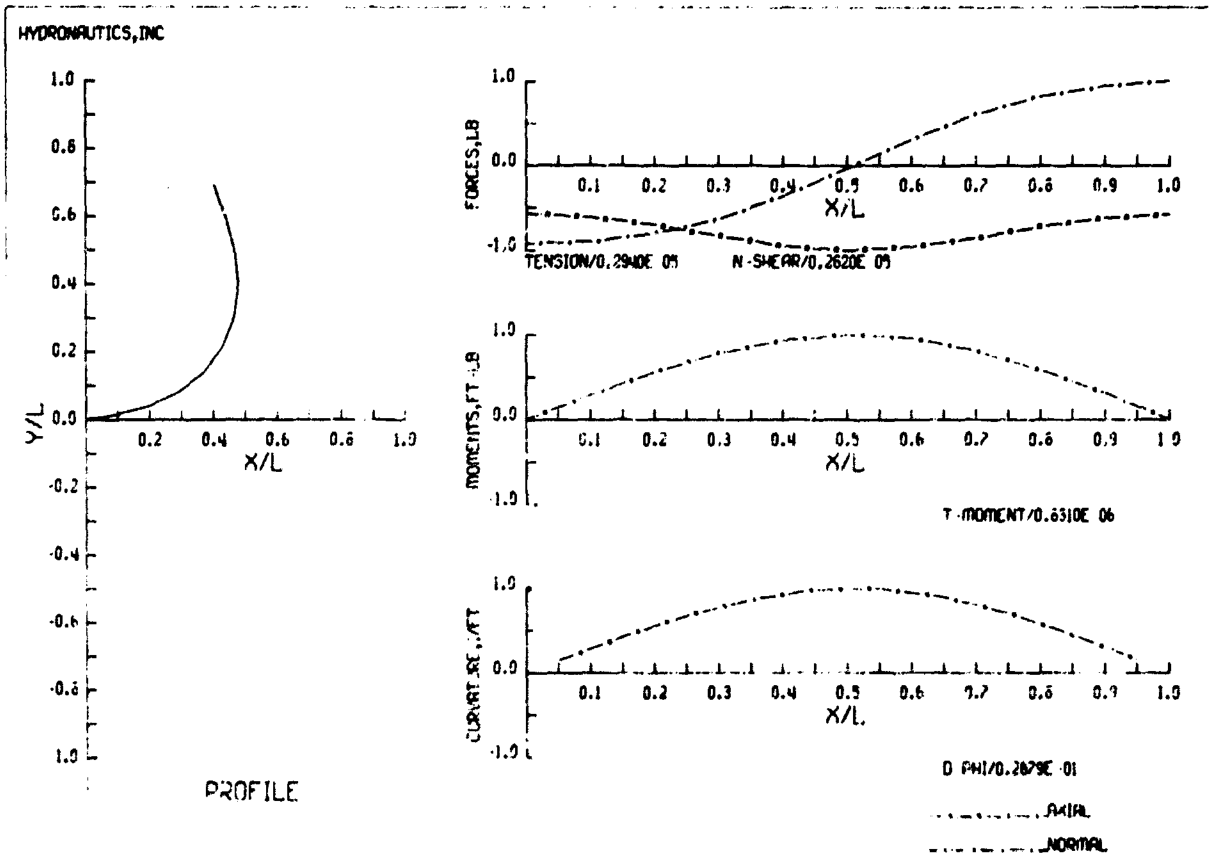

TEST NO. II - 0 - 2 - FC

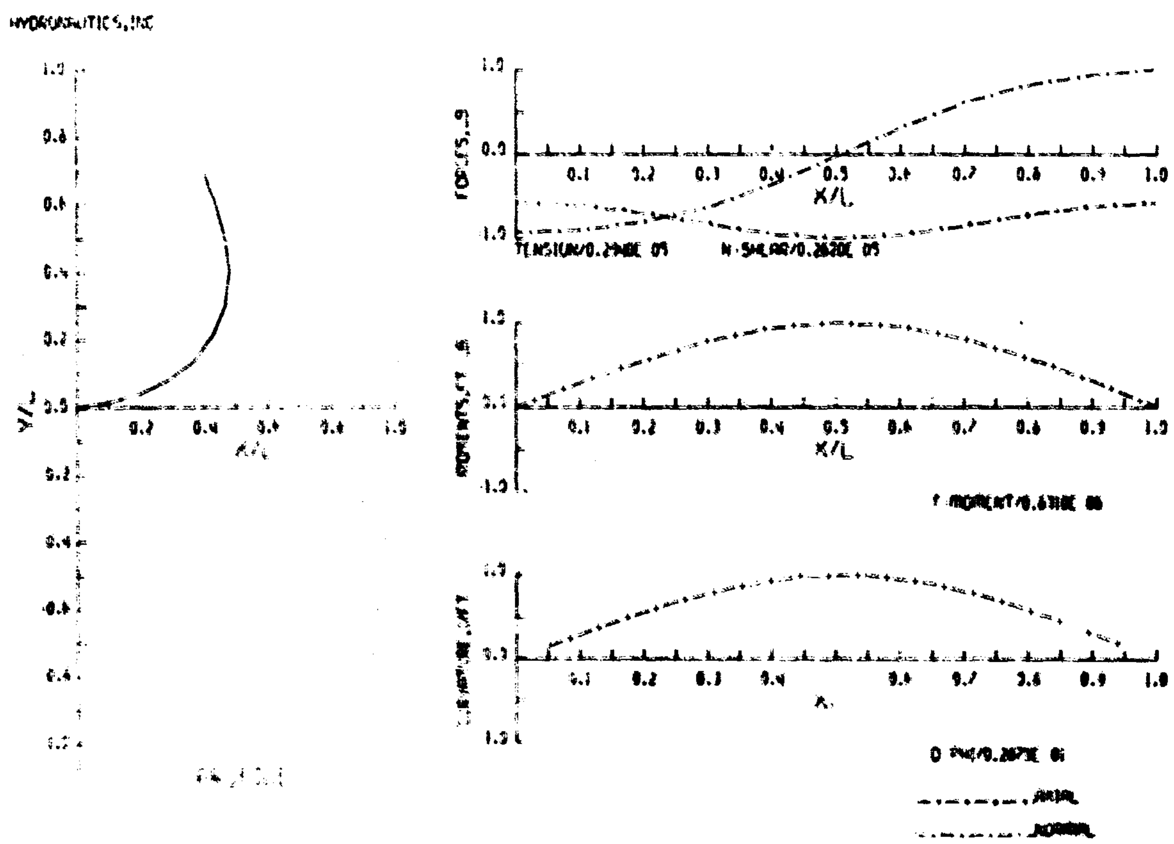

TEST NO. II

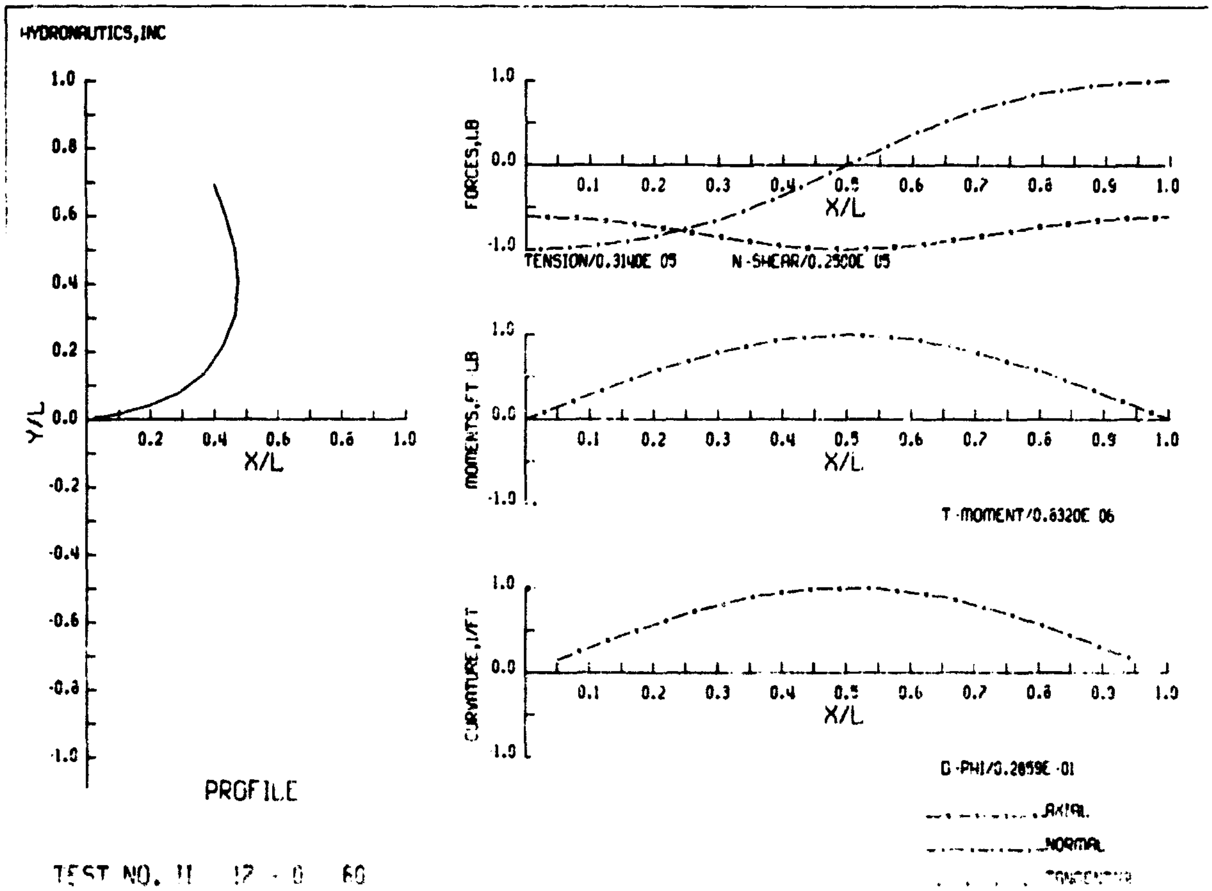
HYDRONAUTICS, INC
Y/L
X/L
PROFILE
FORCES,LB
TENSION/0.3140E 05
N-SHEAR/0.2500E 05
MOMENTS,FT LB
T-MOMENT/0.6320E 06
CURVATURE,1/FT
G-PHI/0.2859E-01
AXIAL
NORMAL

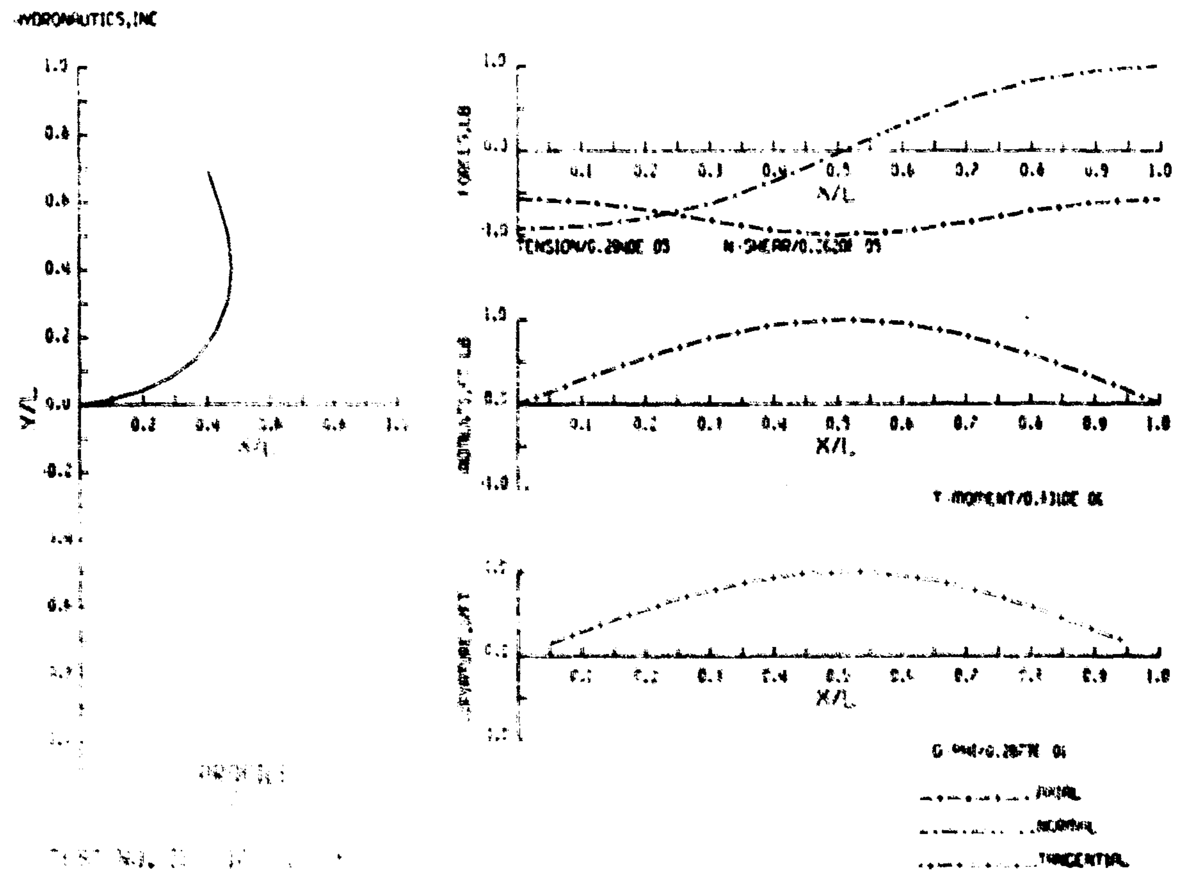
HYDRONAUTICS, INC
Y/L
X/L
T-MOMENT
AXIAL
NORMAL
TANGENTIAL

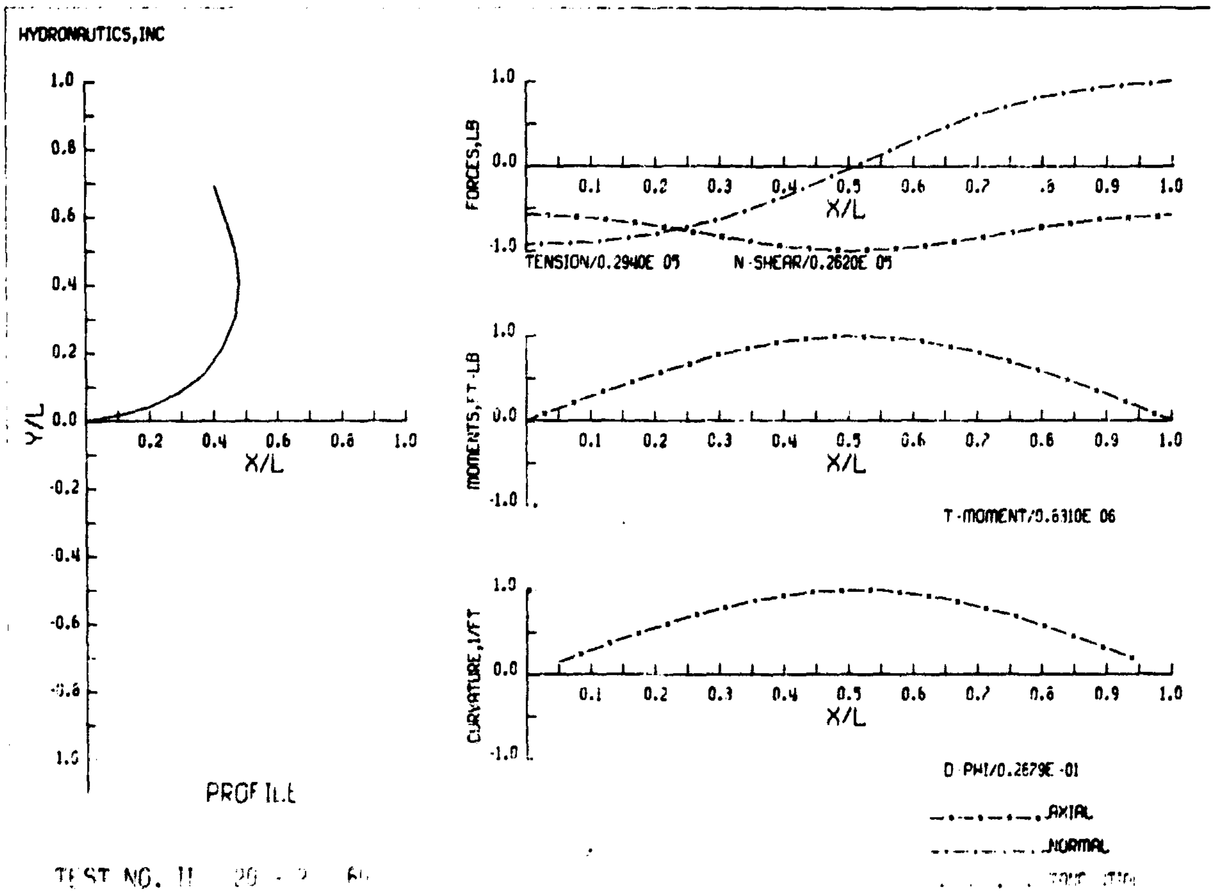

TEST NO. II 20 - 2 60

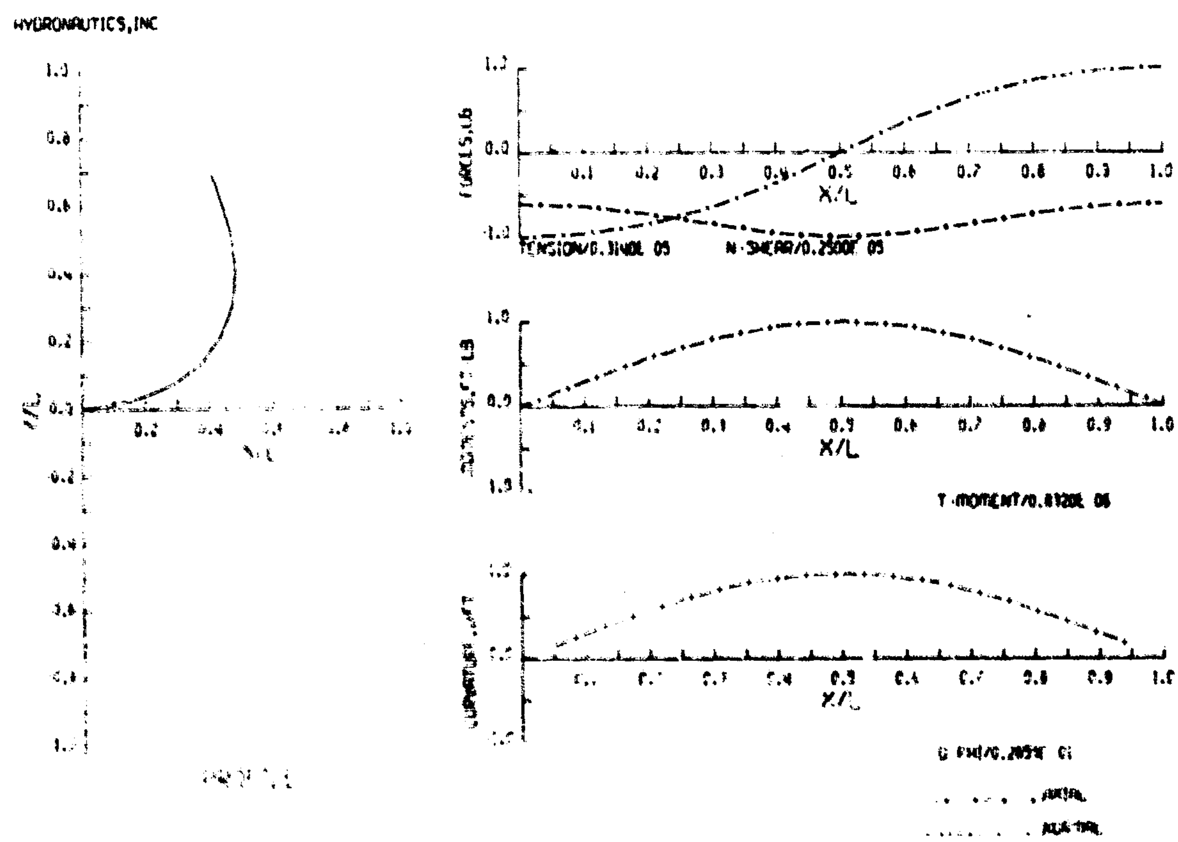

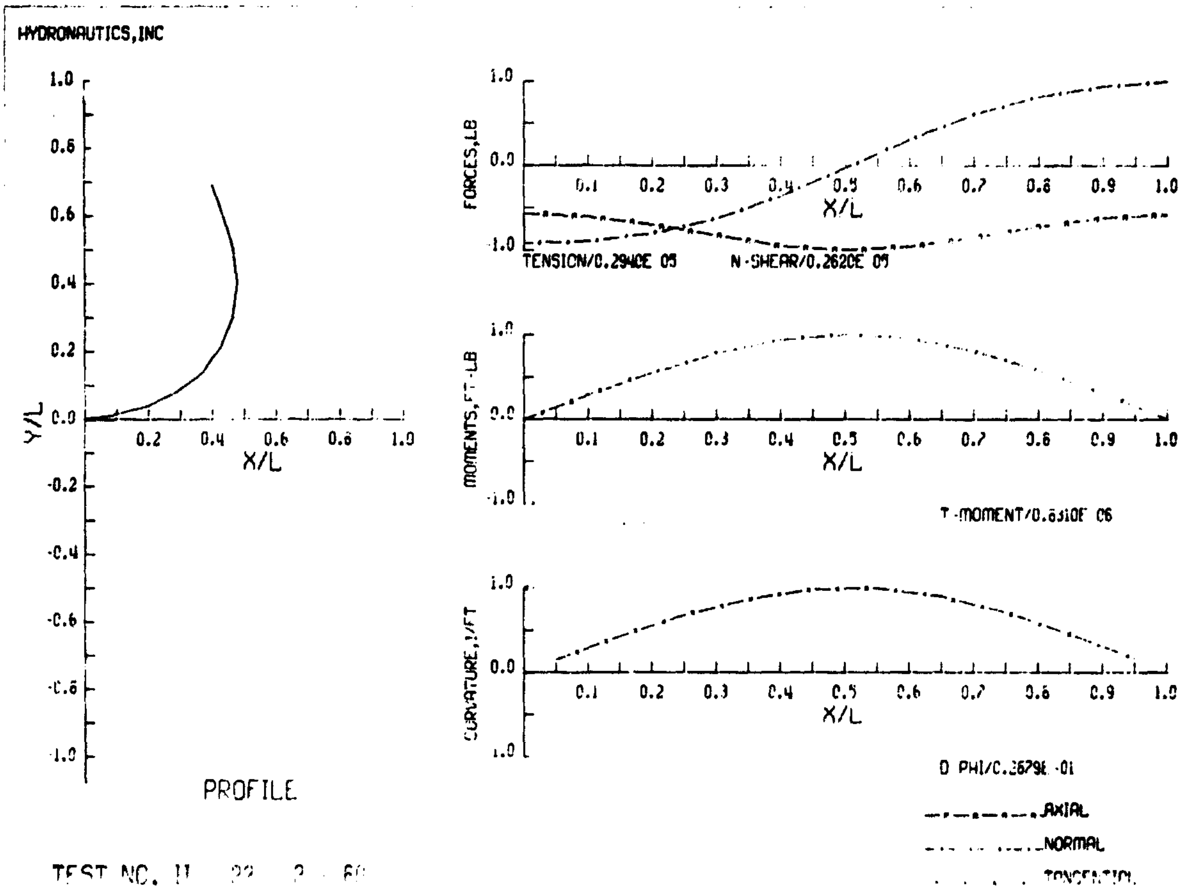
HYDRONAUTICS,INC
Y/L
X/L
PROFILE
FORCES,LB
TENSION/0.2940E 05
N-SHEAR/0.2620E 05
T-MOMENT/0.6310E 06
CURVATURE,1/FT
D PHI/0.2679E-01
AXIAL
NORMAL

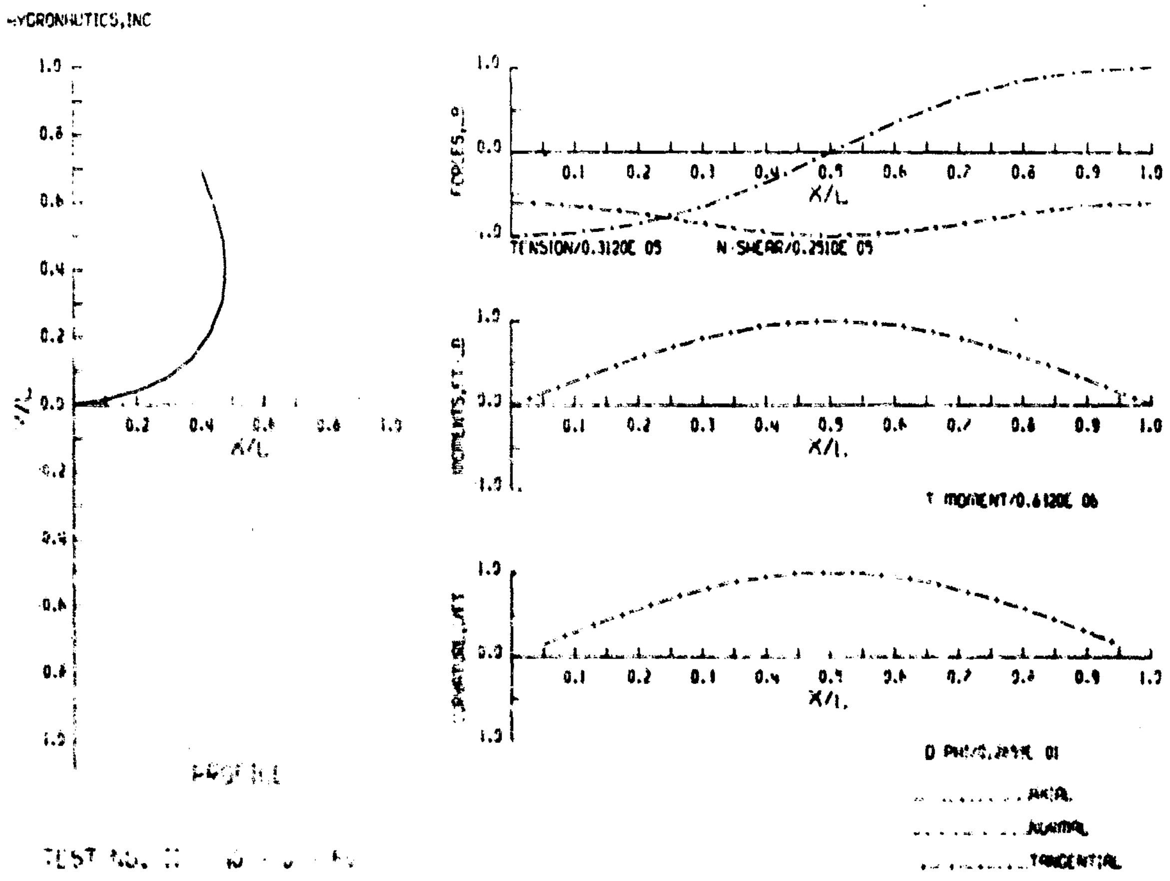
TENSION/0.3120E 05
N-SHEAR/0.2510E 05
X/L
T MOMENT/0.6120E 06
AXIAL
NORMAL
TANGENTIAL

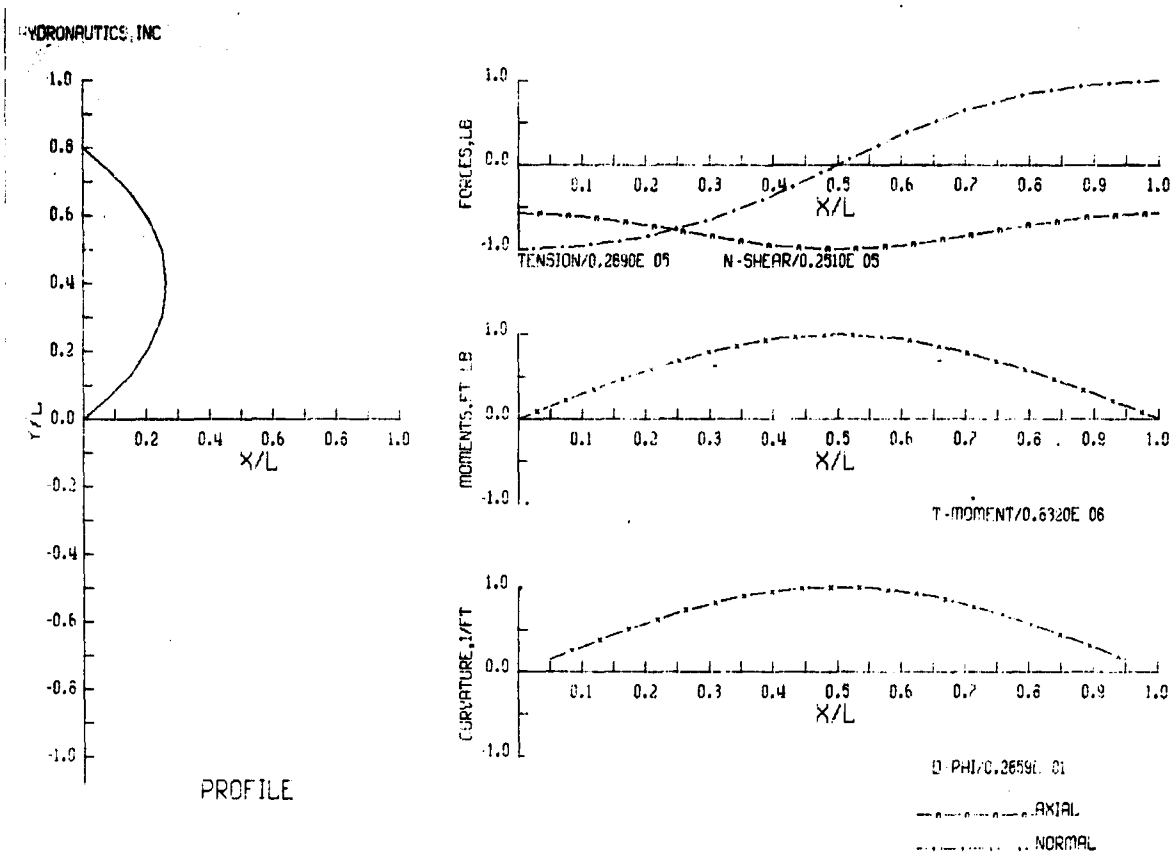

TEST NO. II - 0 - 2 - 90

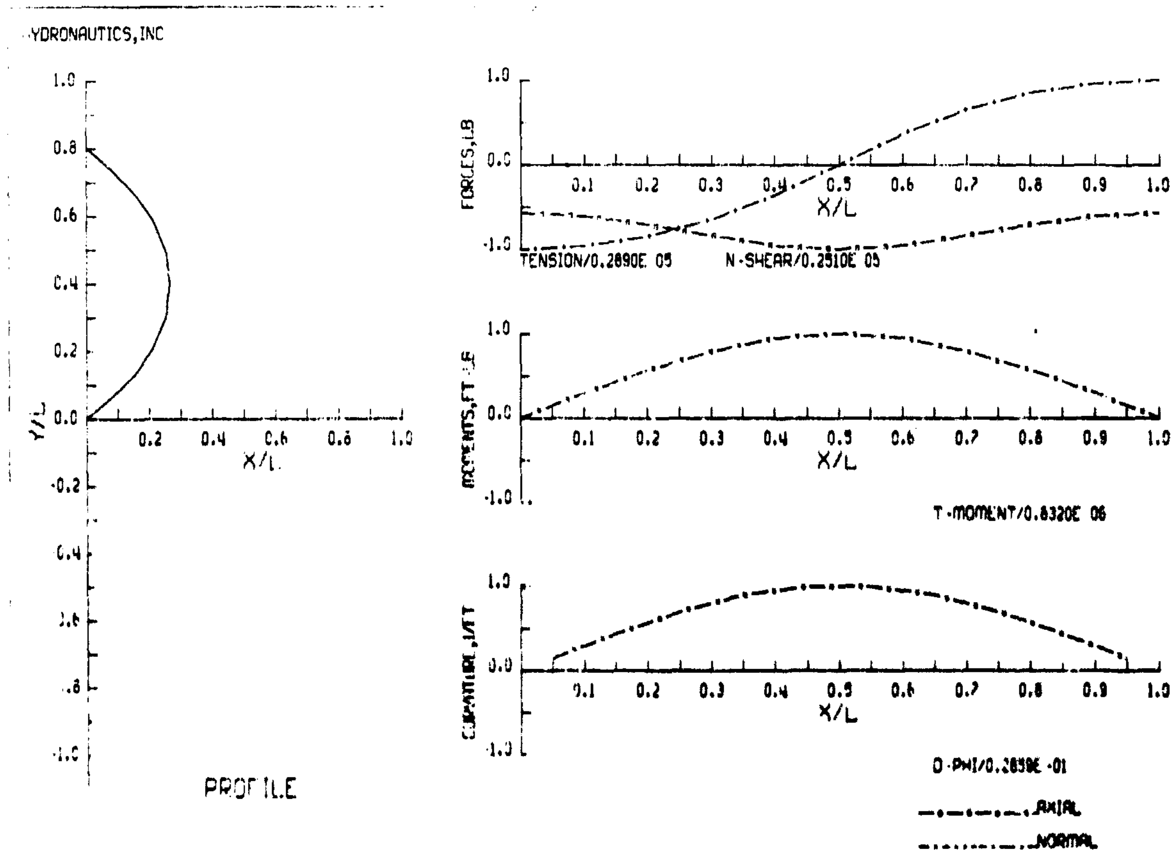

TEST NO. II 15 - 2 - 90

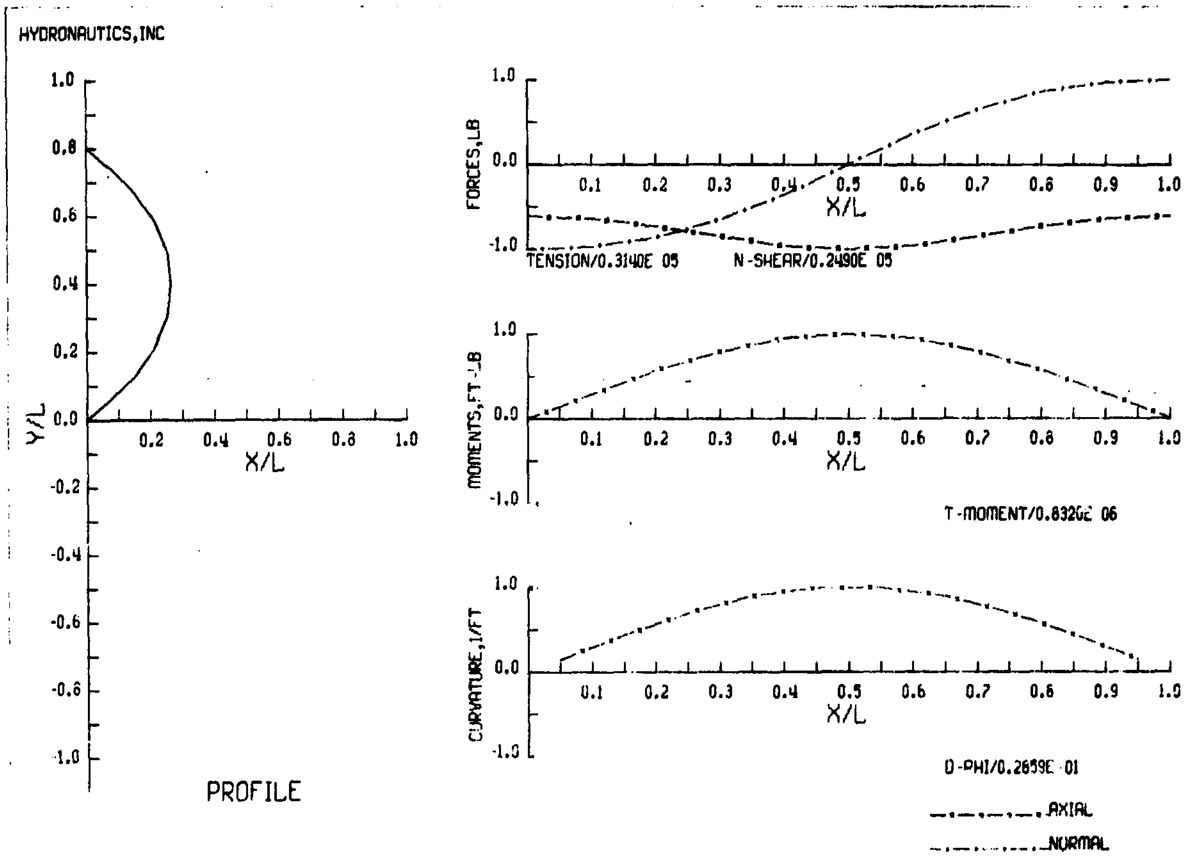

TEST NO. II - 12 - 0 - 90

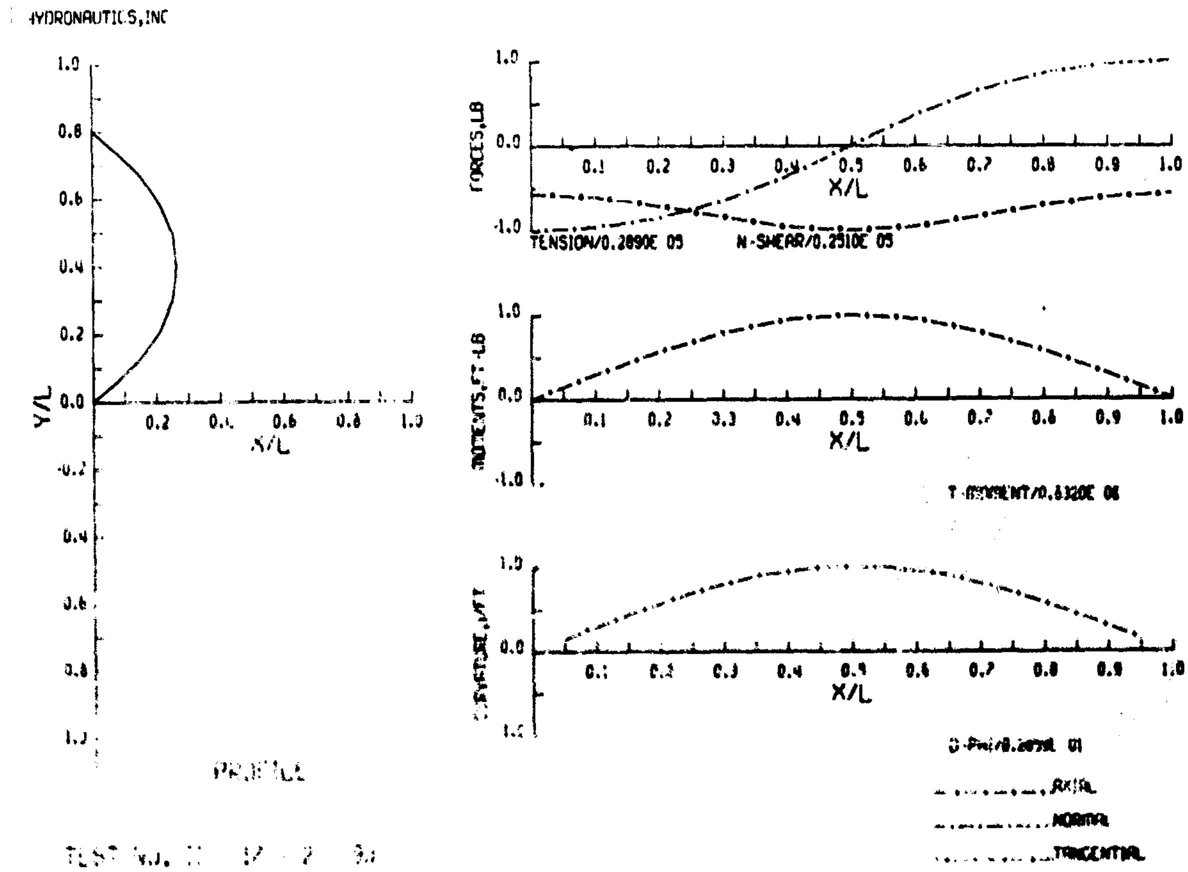

TEST NO. II - 12 - 2 - 90

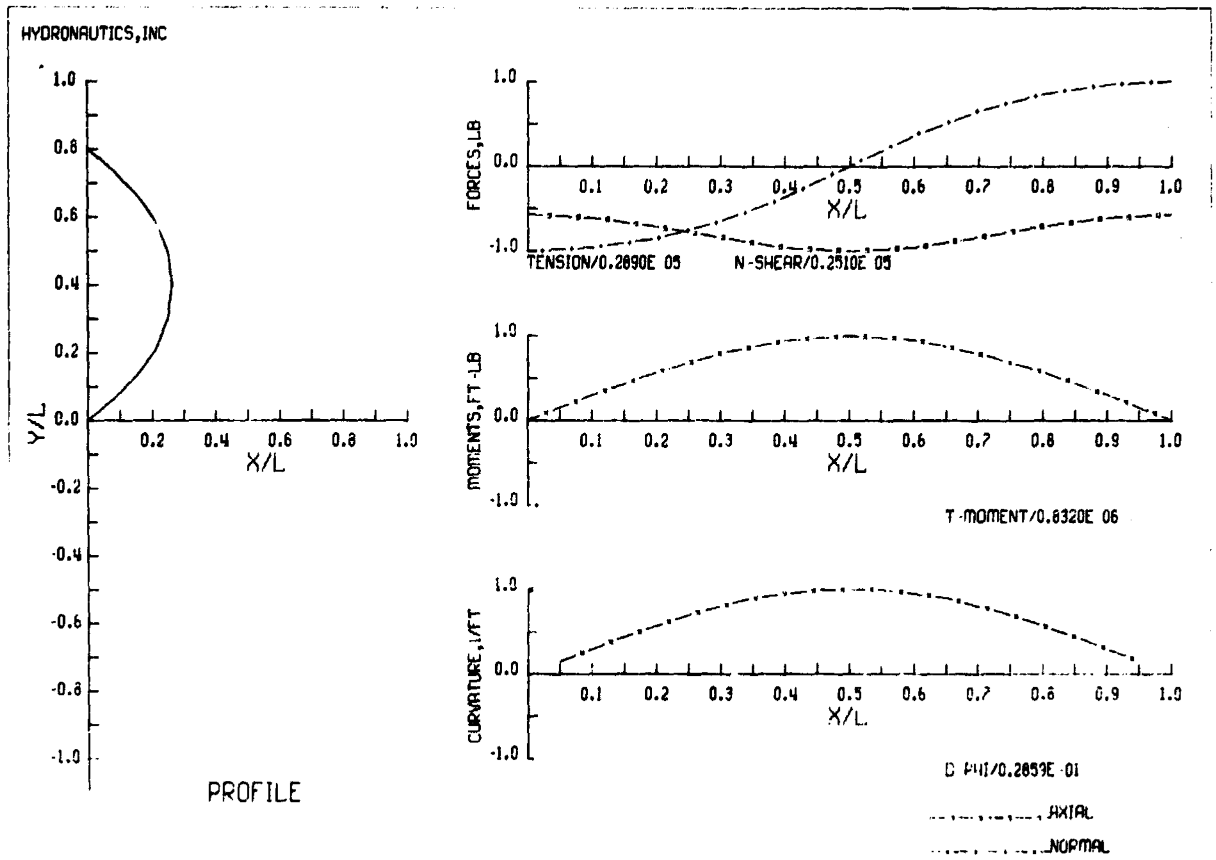

TEST NO. II - 20 - 2 - 90

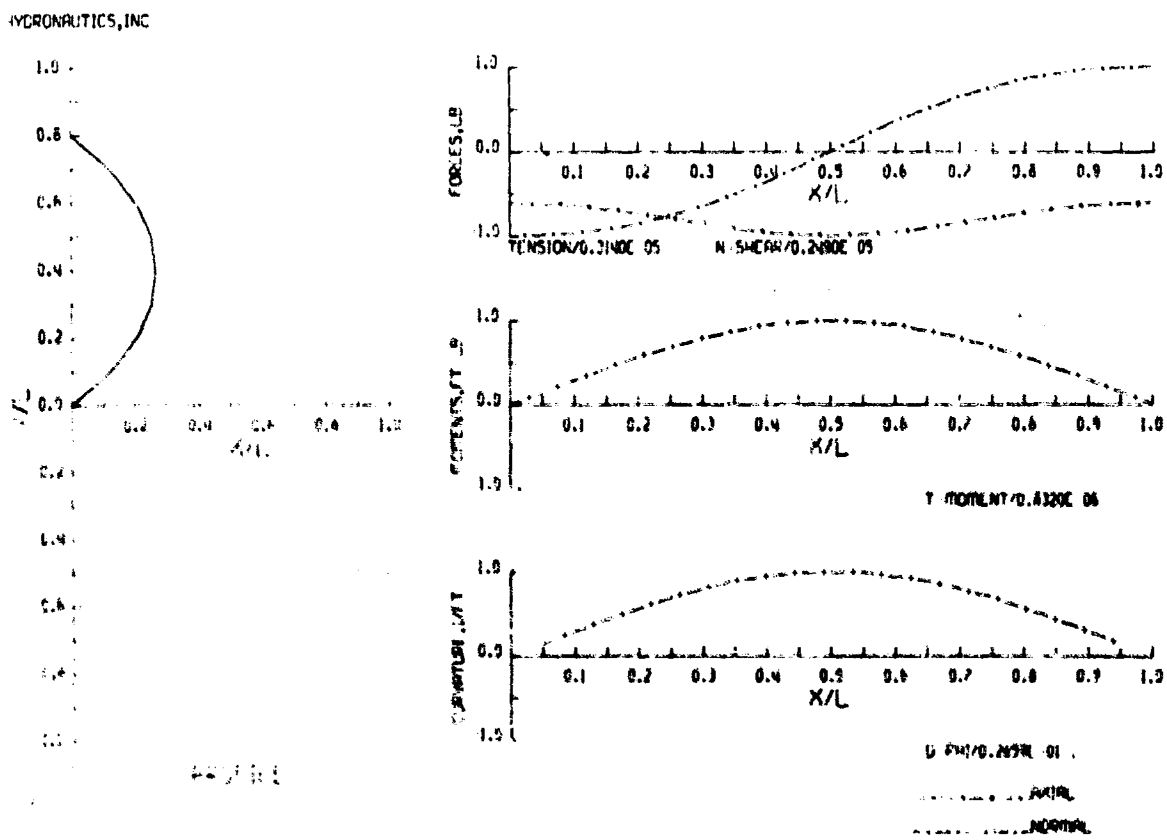

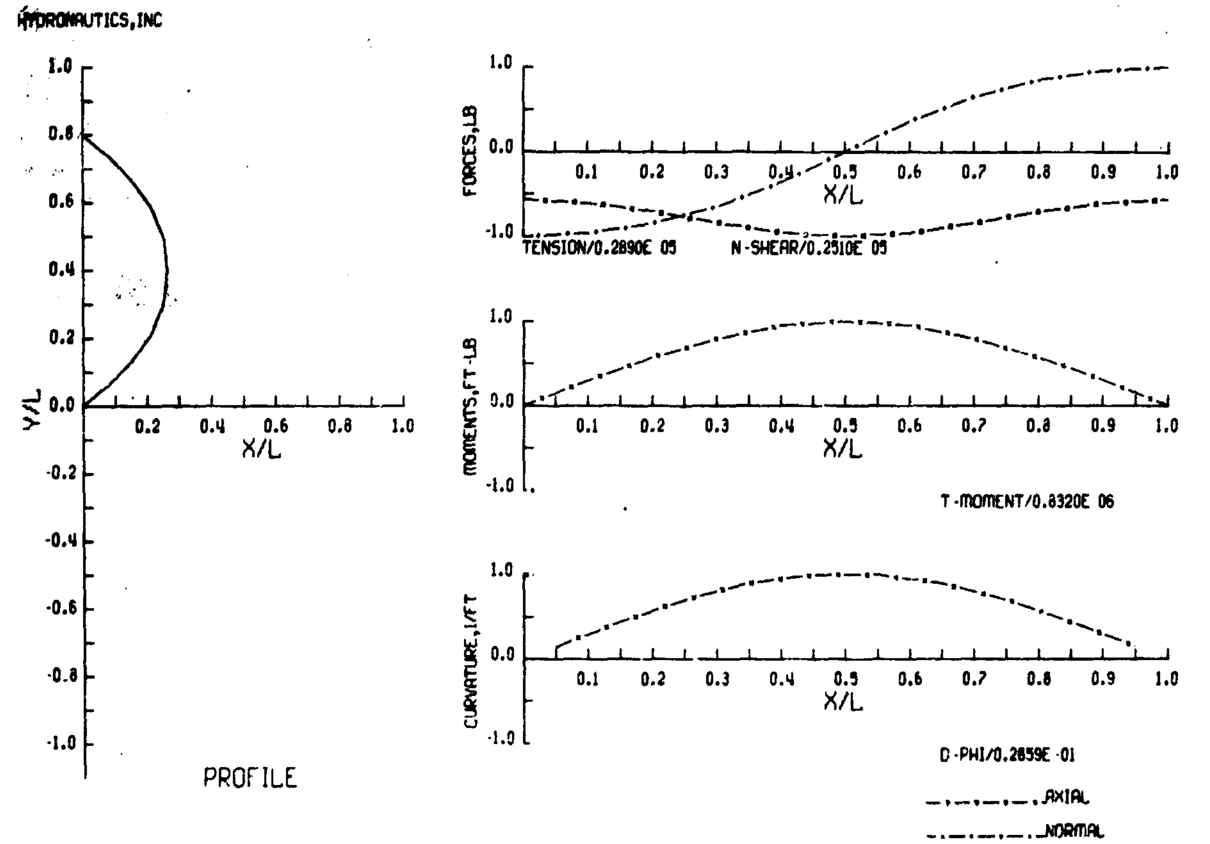

TEST NO. II - 22 - 2 - 90

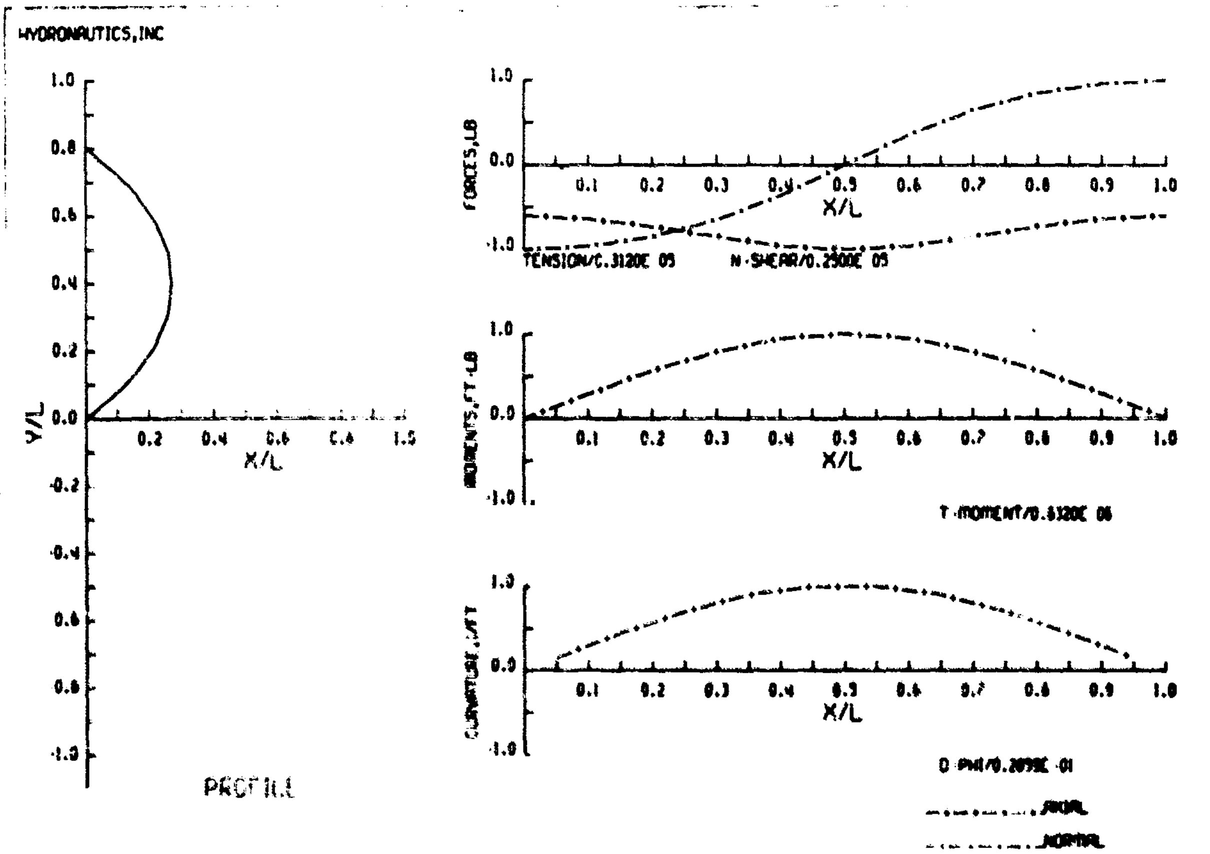

TEST NO. II 40 - 0 - 30

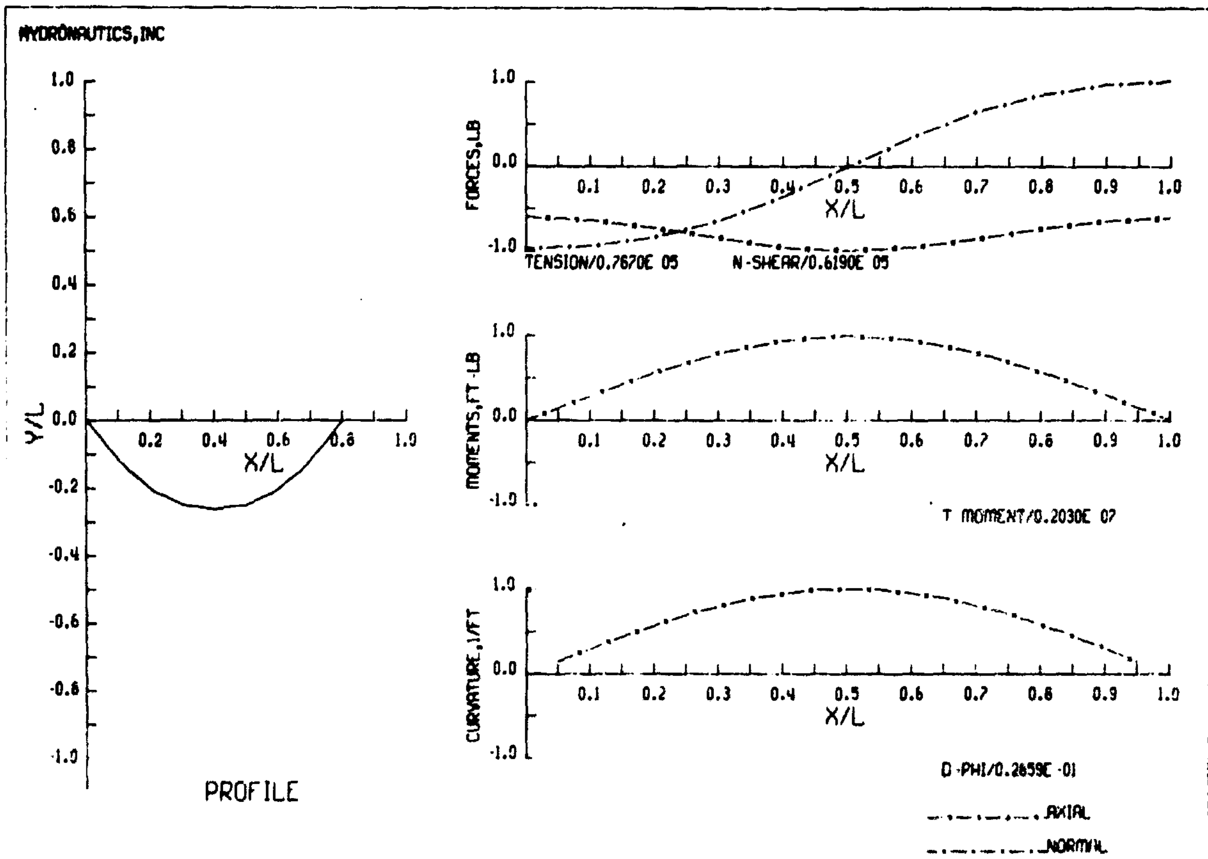

TEST NO. III 0 - 2 - 0

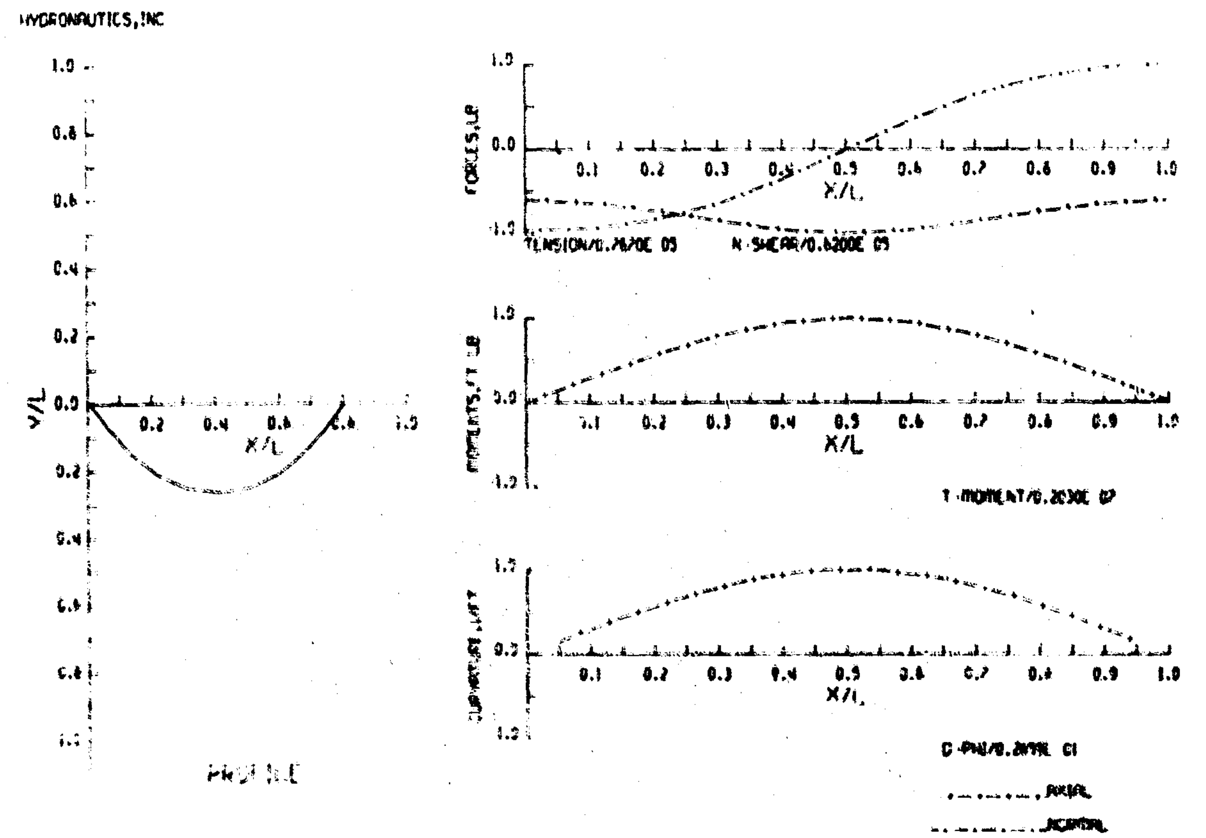

TEST NO. III 20 - 2 0

HYDRONAUTICS, INC

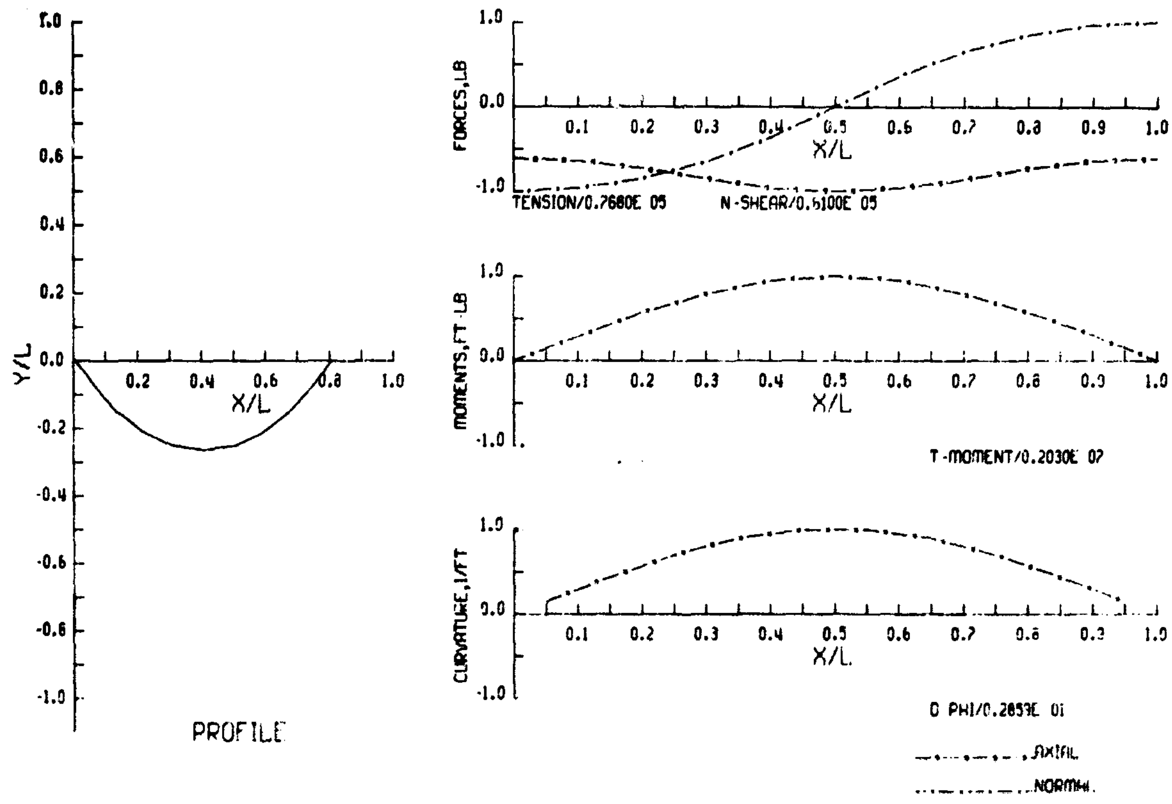

TEST NO. III 22 0 0

HYDRONAUTICS, INC

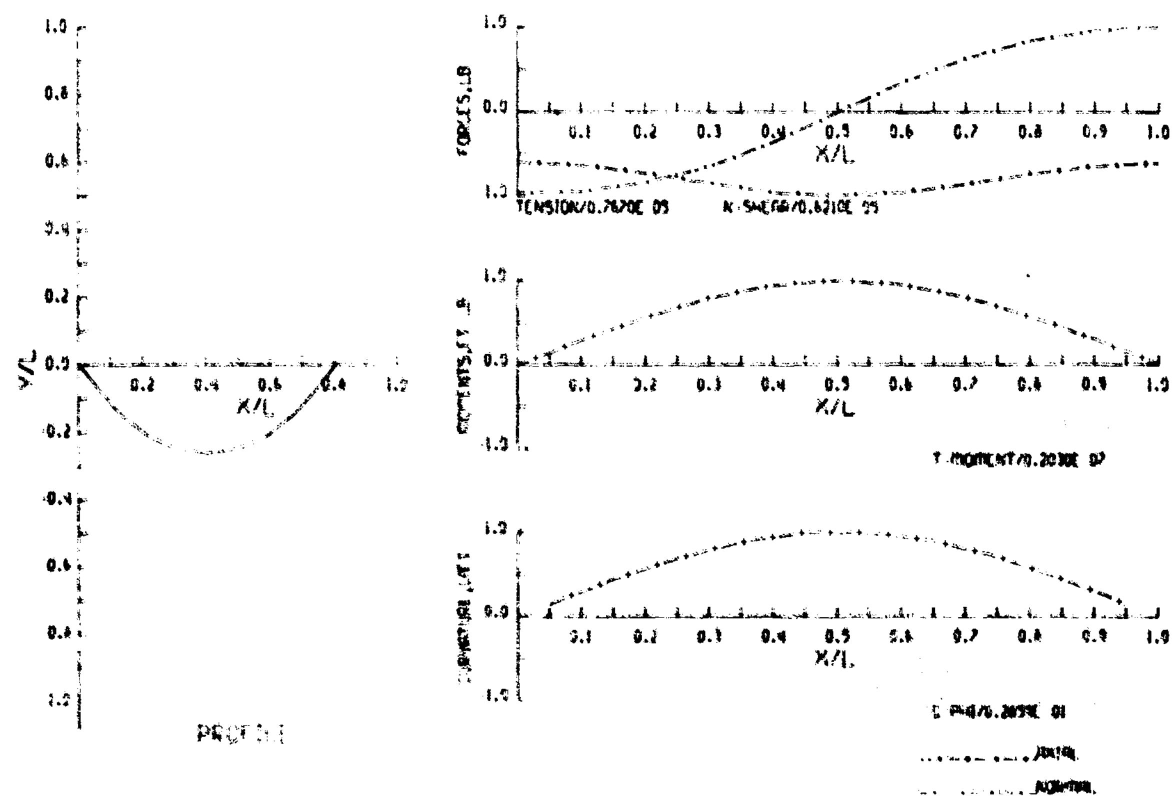

TEST NO. III - 22

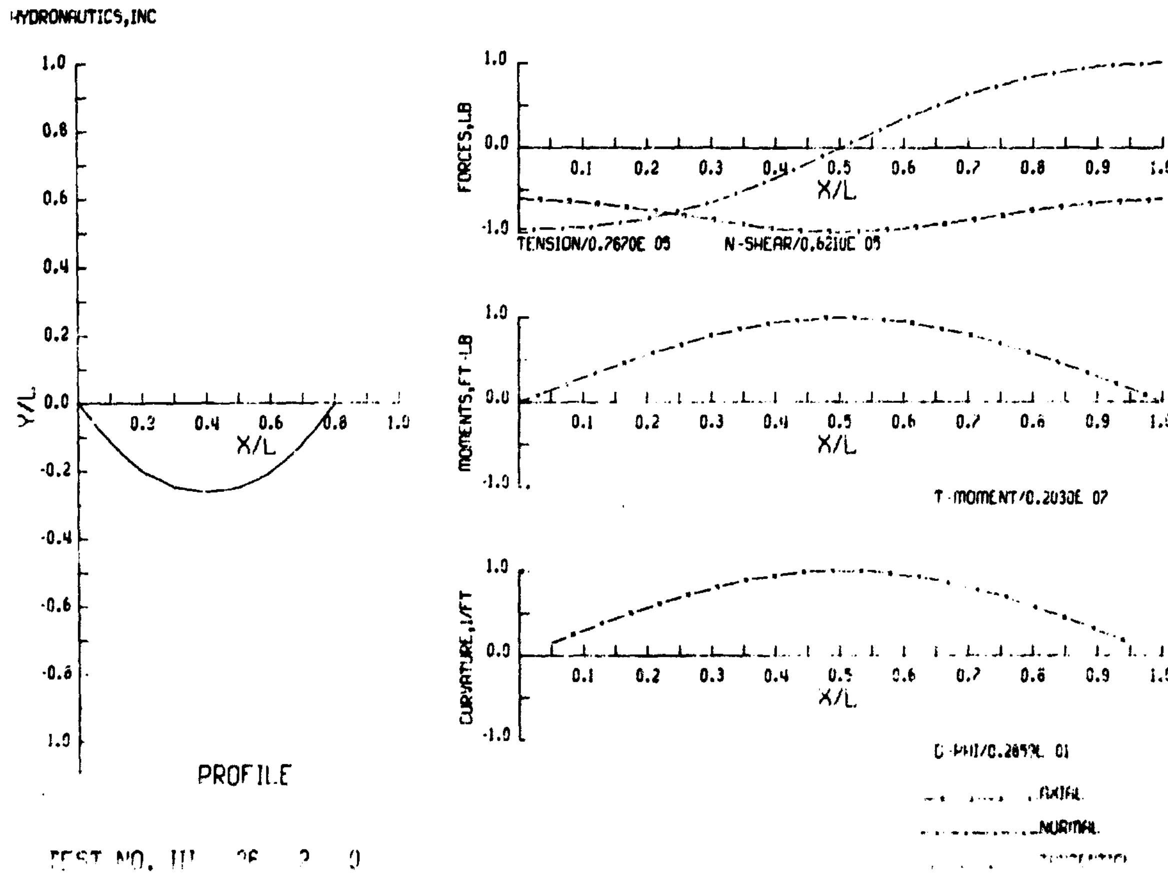
HYDRONAUTICS,INC
Y/L
X/L
PROFILE
FORCES,LB
TENSION/0.7670E 05
N-SHEAR/0.6210E 05
MOMENTS,FT-LB
T-MOMENT/0.2030E 07
CURVATURE,1/FT
AXIAL
NORMAL

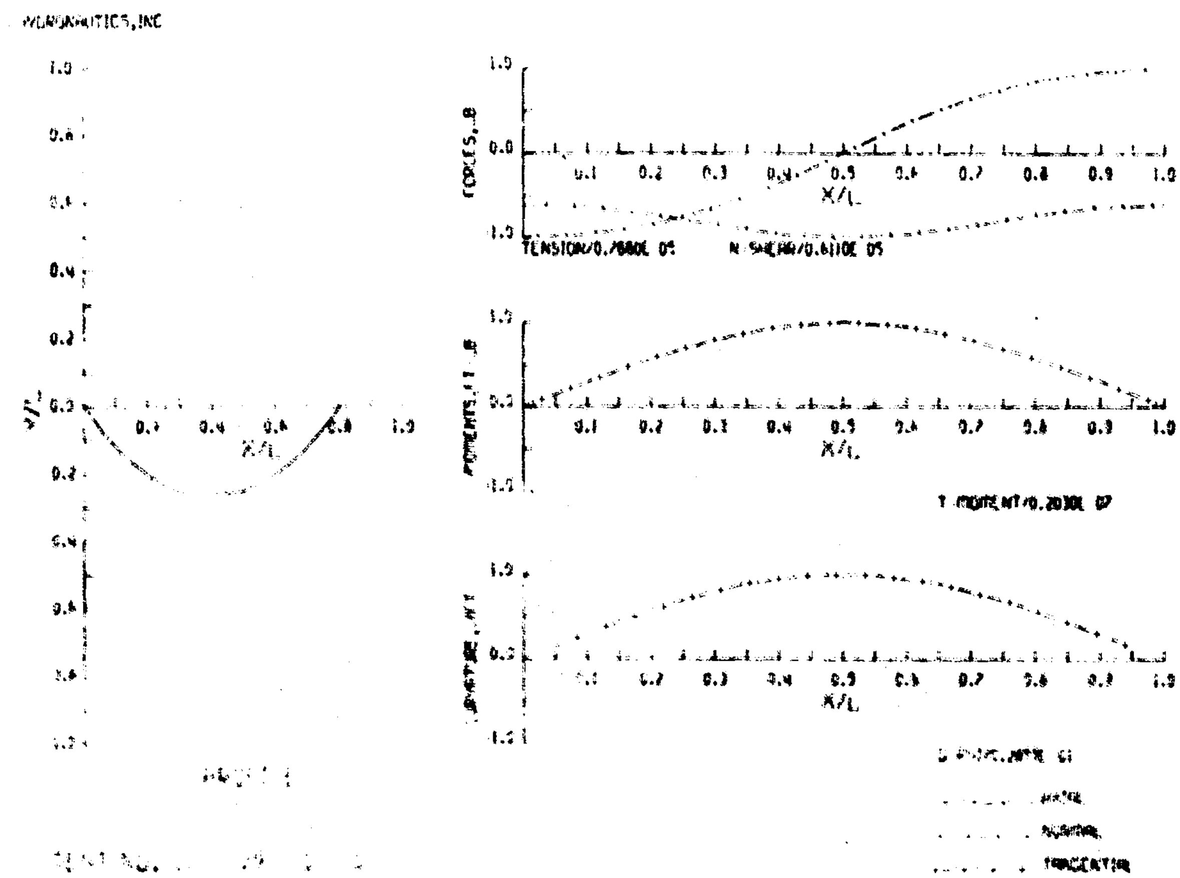
X/L
TENSION/0.7680E 05
N-SHEAR/0.6110E 05
T-MOMENT/0.2030E 07
AXIAL
NORMAL
TANGENTIAL

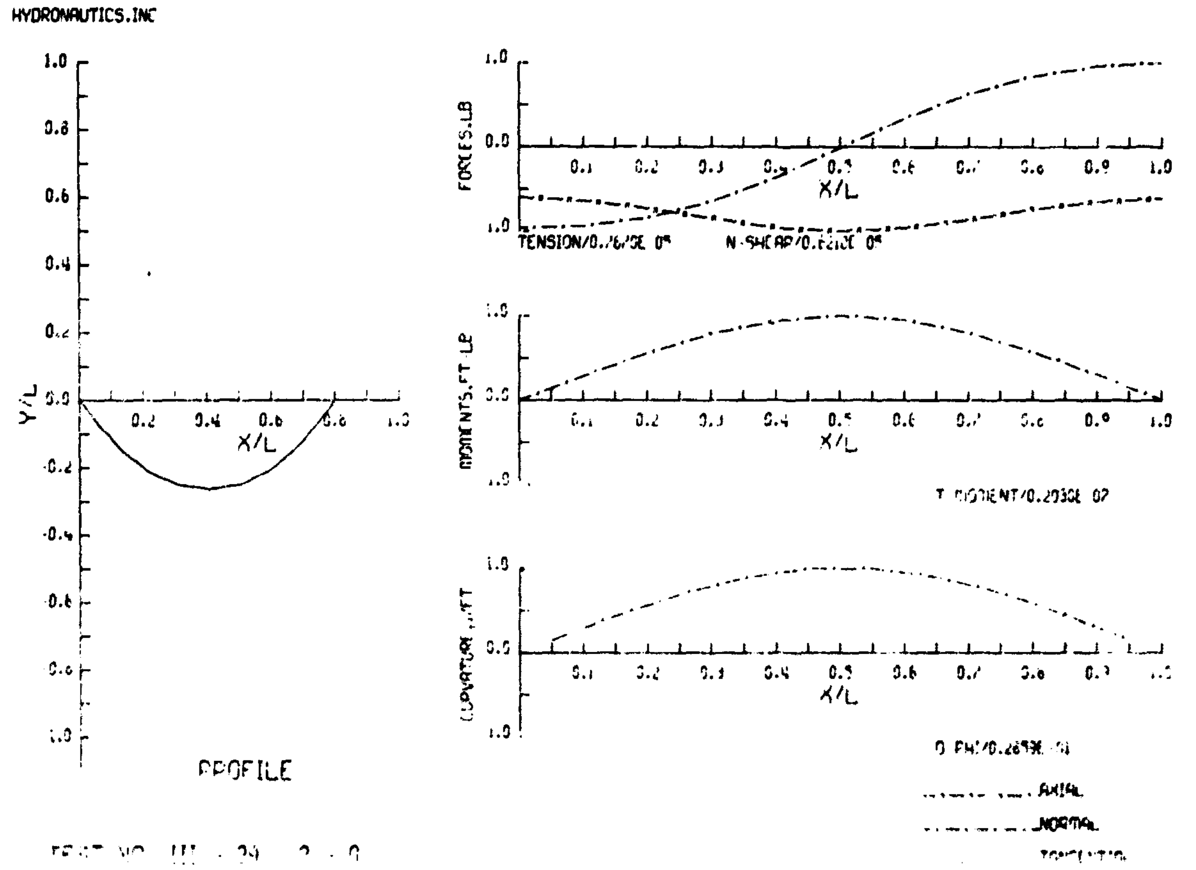
HYDRONAUTICS, INC
Y/L
X/L
PROFILE
FORCES,LB
MOMENTS,FT-LB
T MOMENT/0.2030E 02
0.1 0.2 0.3 0.4 0.5 0.6 0.7 0.8 0.9 1.0
AXIAL
NORMAL

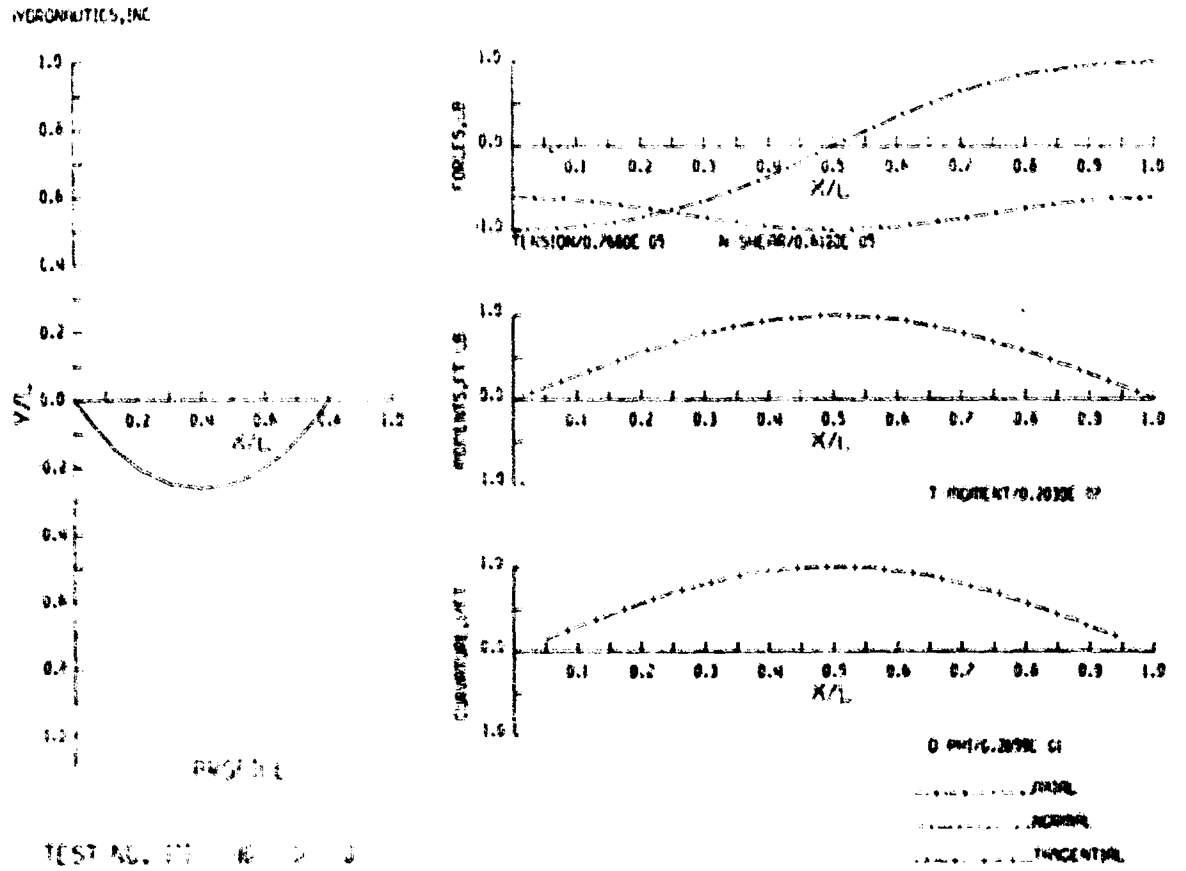
HYDRONAUTICS, INC
Y/L
X/L
FORCES,LB
MOMENTS,FT-LB
T MOMENT/0.2030E 02
0.1 0.2 0.3 0.4 0.5 0.6 0.7 0.8 0.9 1.0
AXIAL
NORMAL
TANGENTIAL

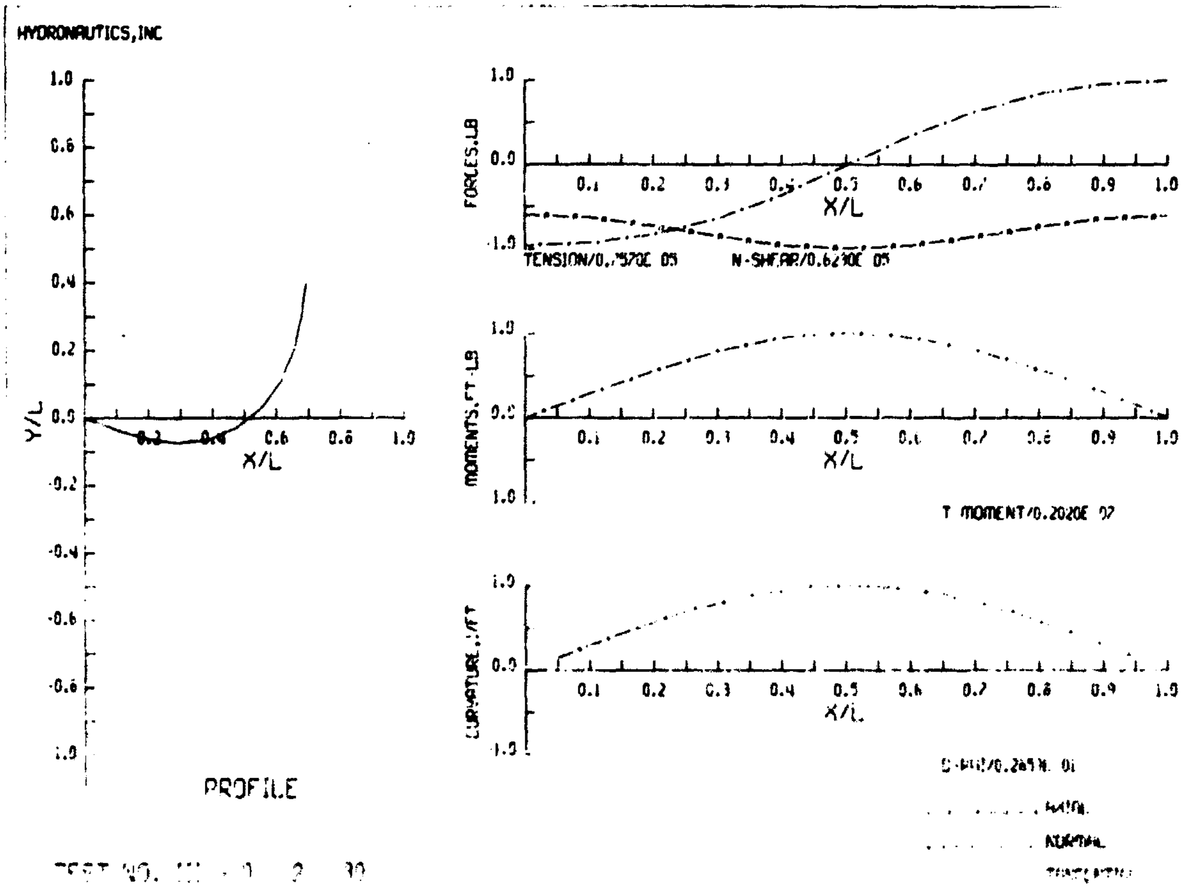
HYDRONAUTICS,INC
Y/L
X/L
PROFILE
FORCES,LB
TENSION/0.7570E 05
N-SHEAR/0.6210E 05
MOMENTS,FT-LB
T MOMENT/0.2020E 07
CURVATURE,1/FT
AXIAL
NORMAL

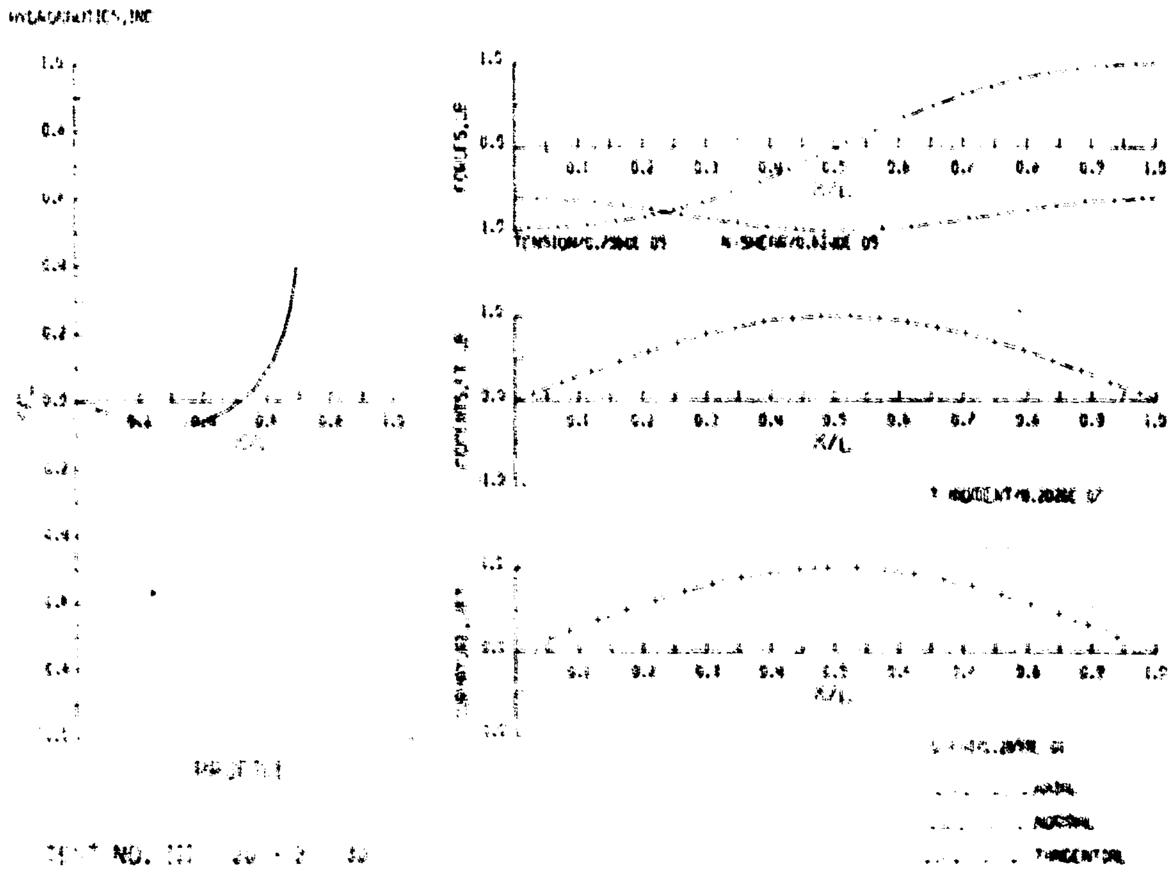
X/L
T MOMENT/0.2020E 07
AXIAL
NORMAL
TANGENTIAL

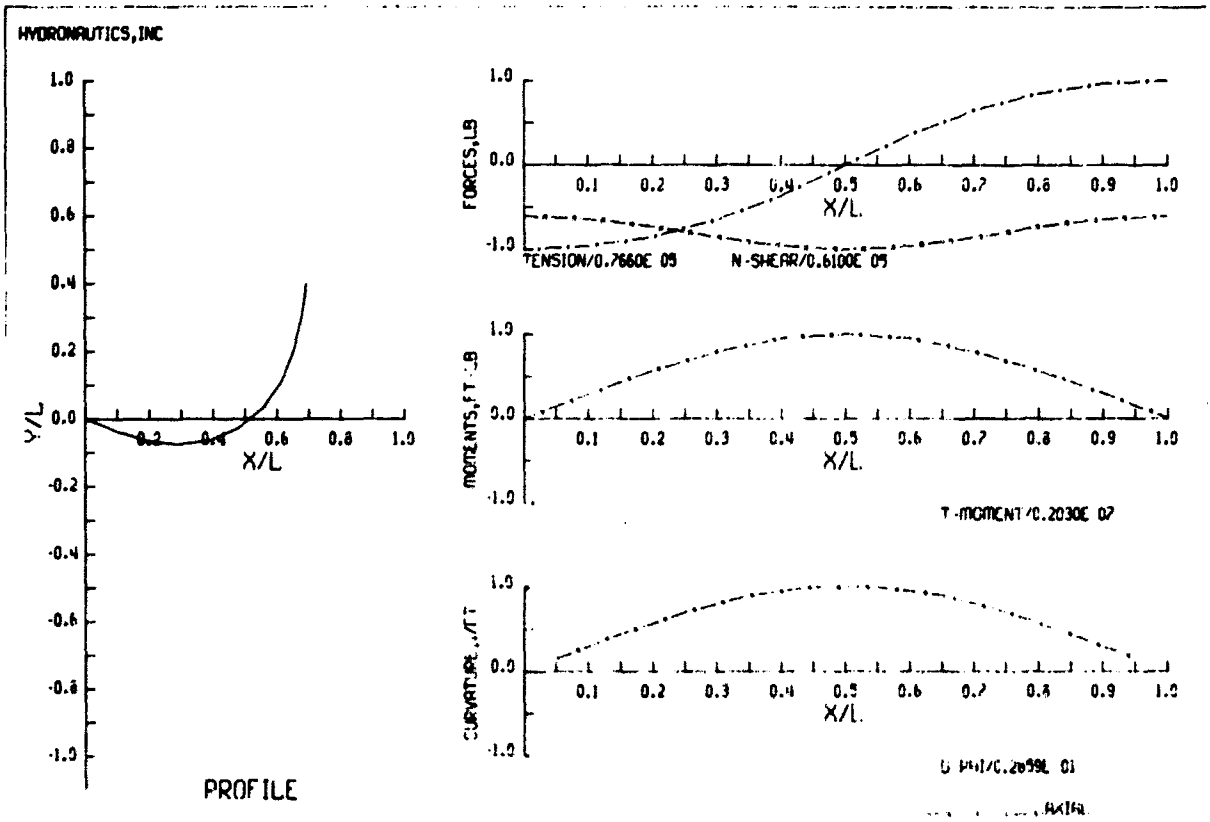

TEST NO. 111 22 0 30

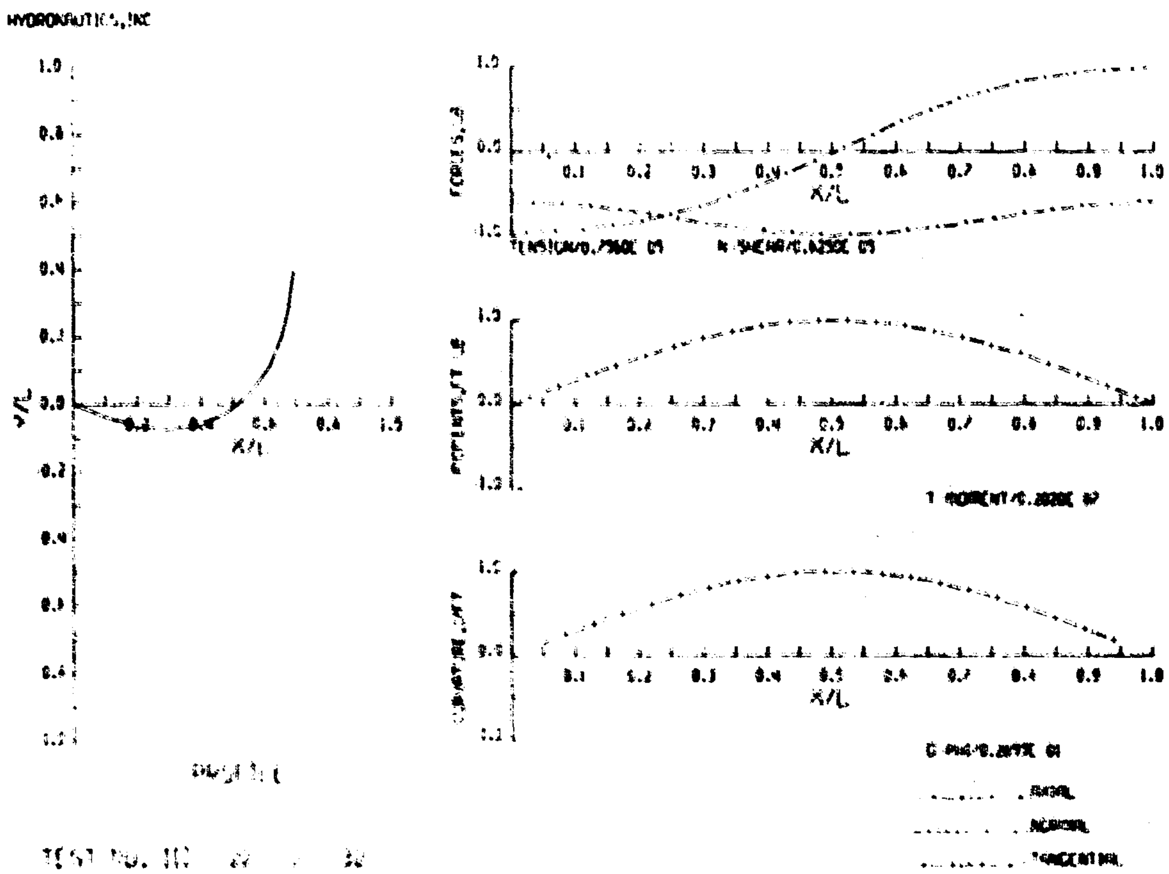

TEST NO. 111 22 32

HYDRONAUTICS,INC

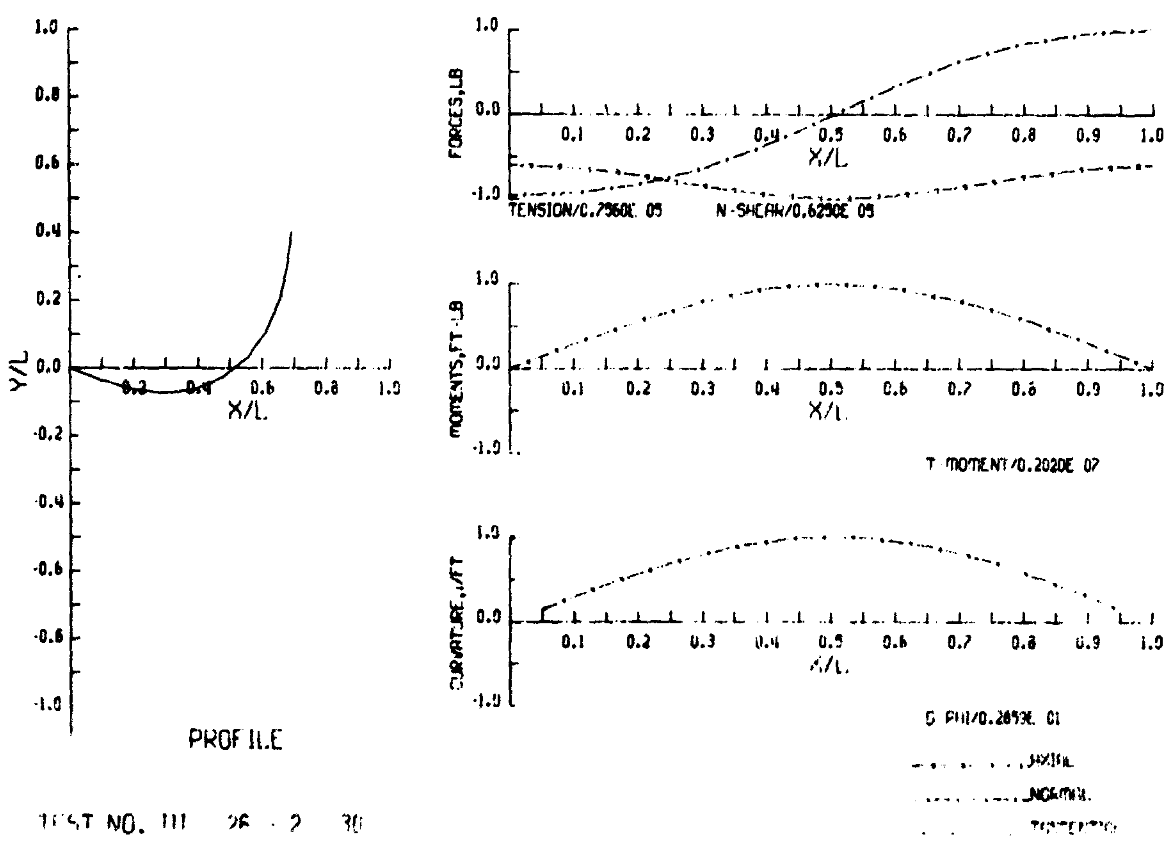

TEST NO. 111 26 - 2 30

HYDRONAUTICS,INC

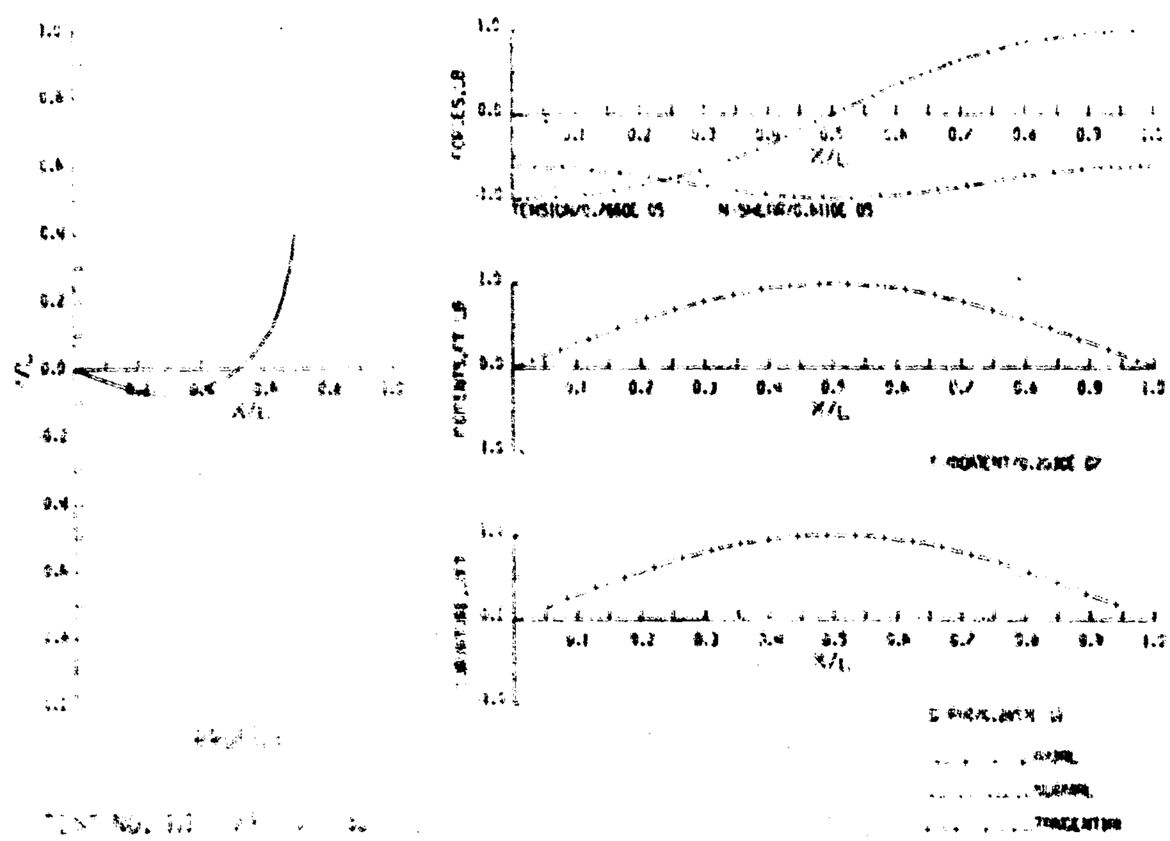

HYDRONAUTICS,INC

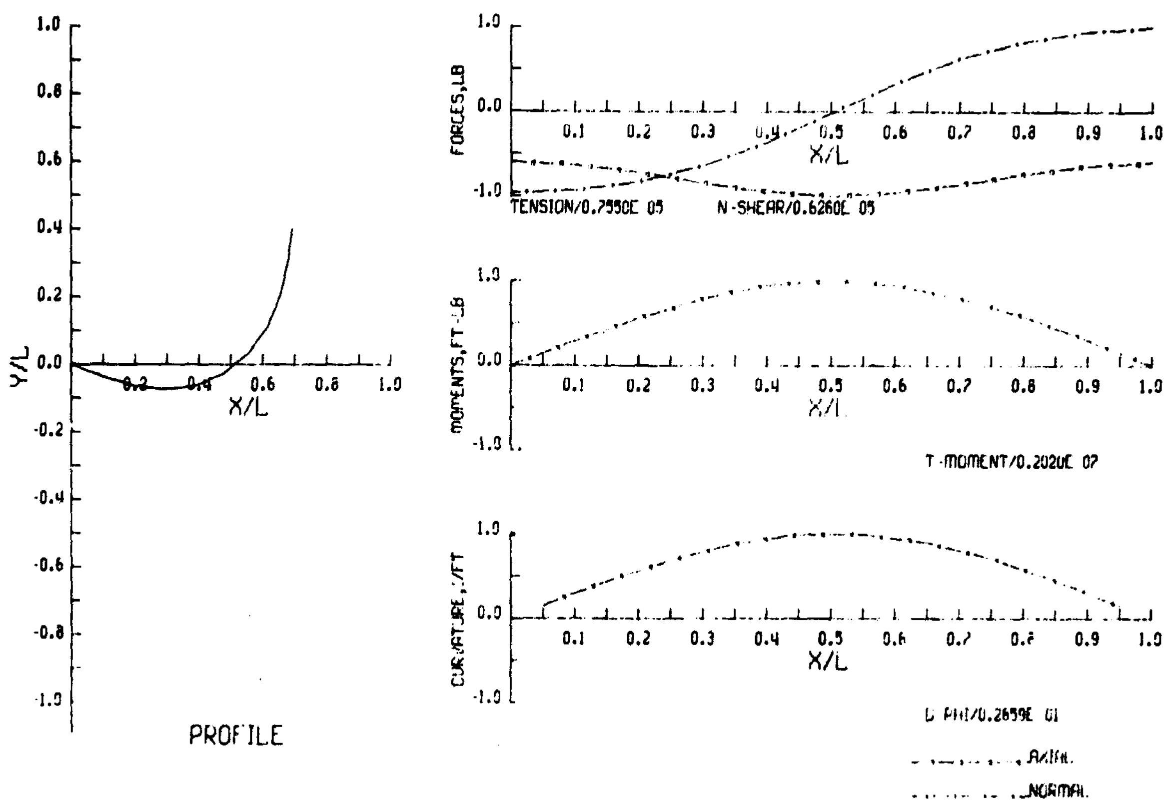

TEST NO. 111 29 2 30

HYDRONAUTICS,INC

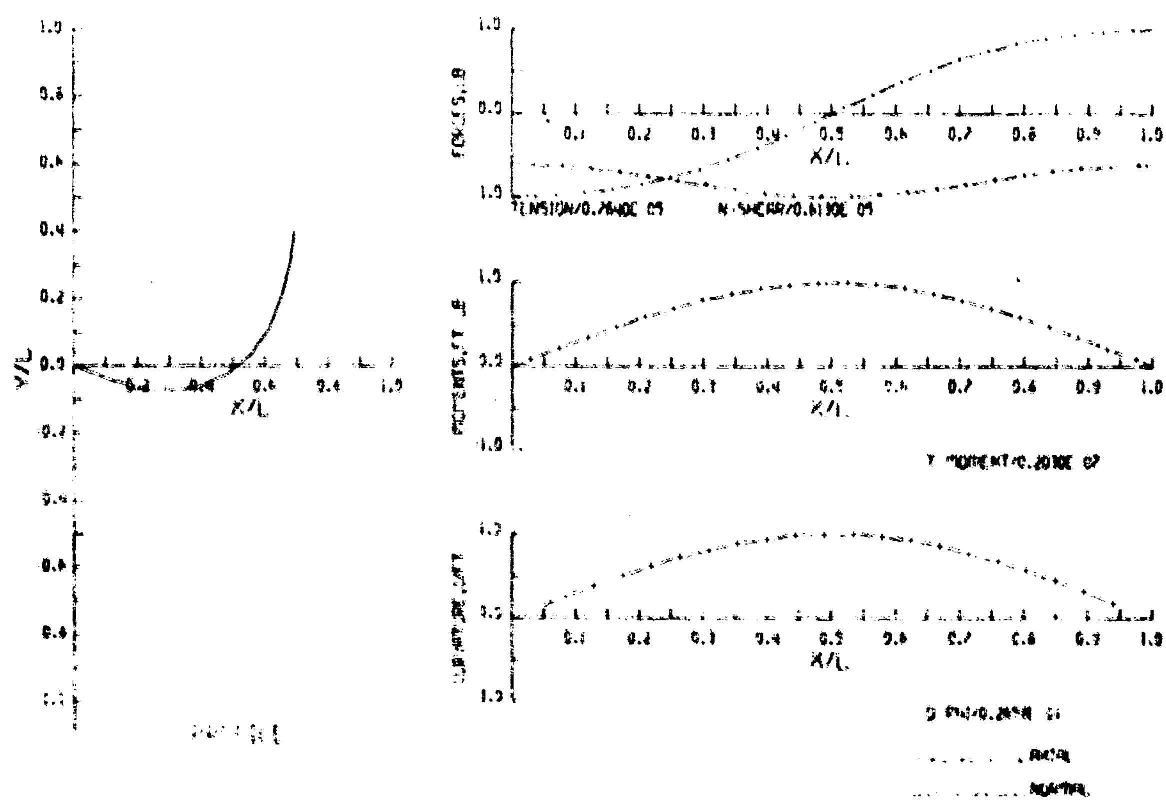

TEST NO. [illegible]

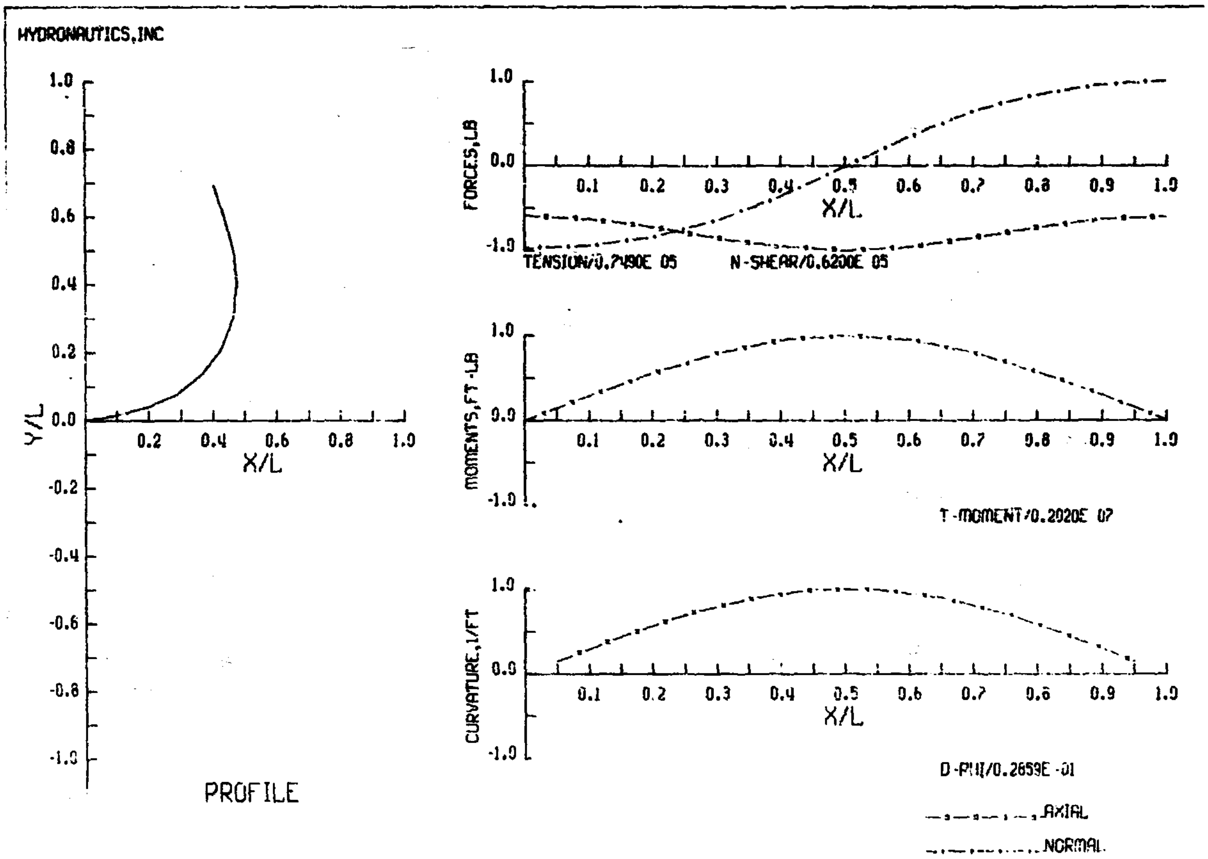

TEST NO. III 0 - 2 - 60

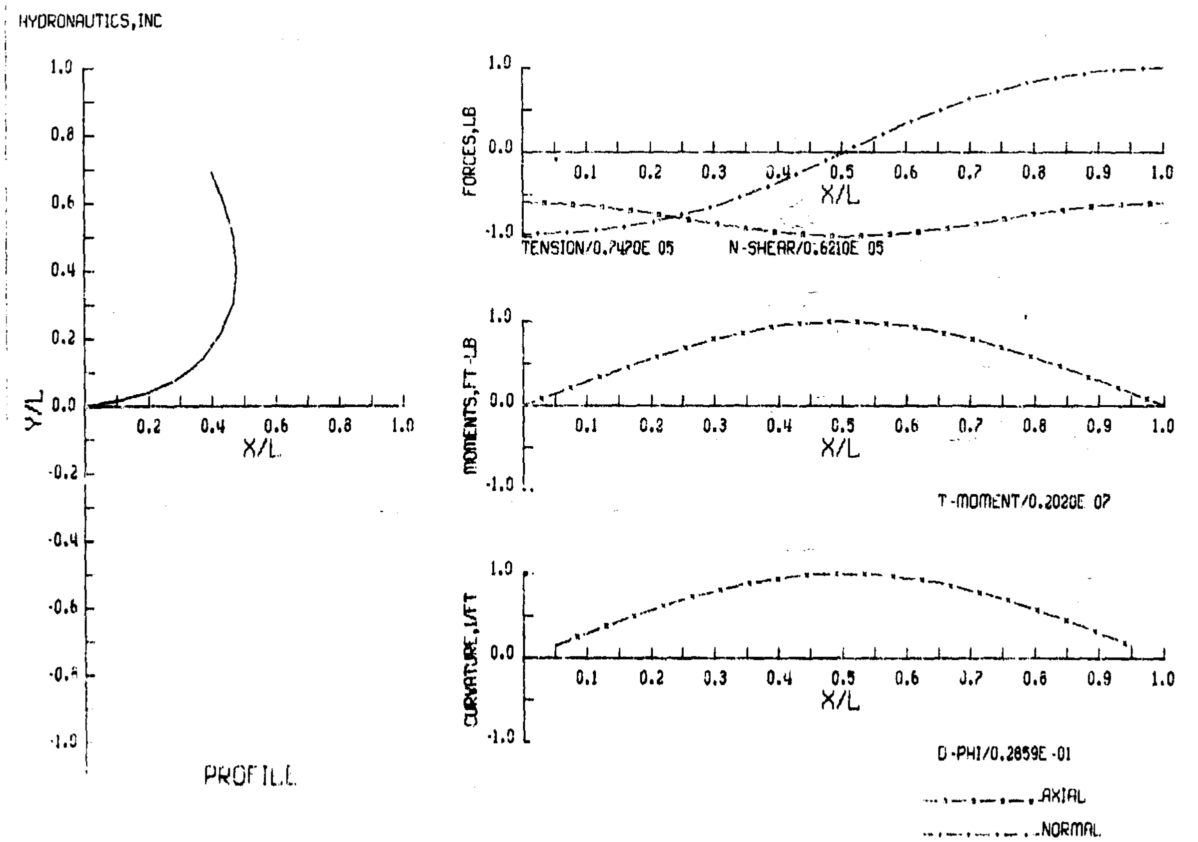

TEST NO. III 20 - 2 - 60

HYDRONAUTICS, INC

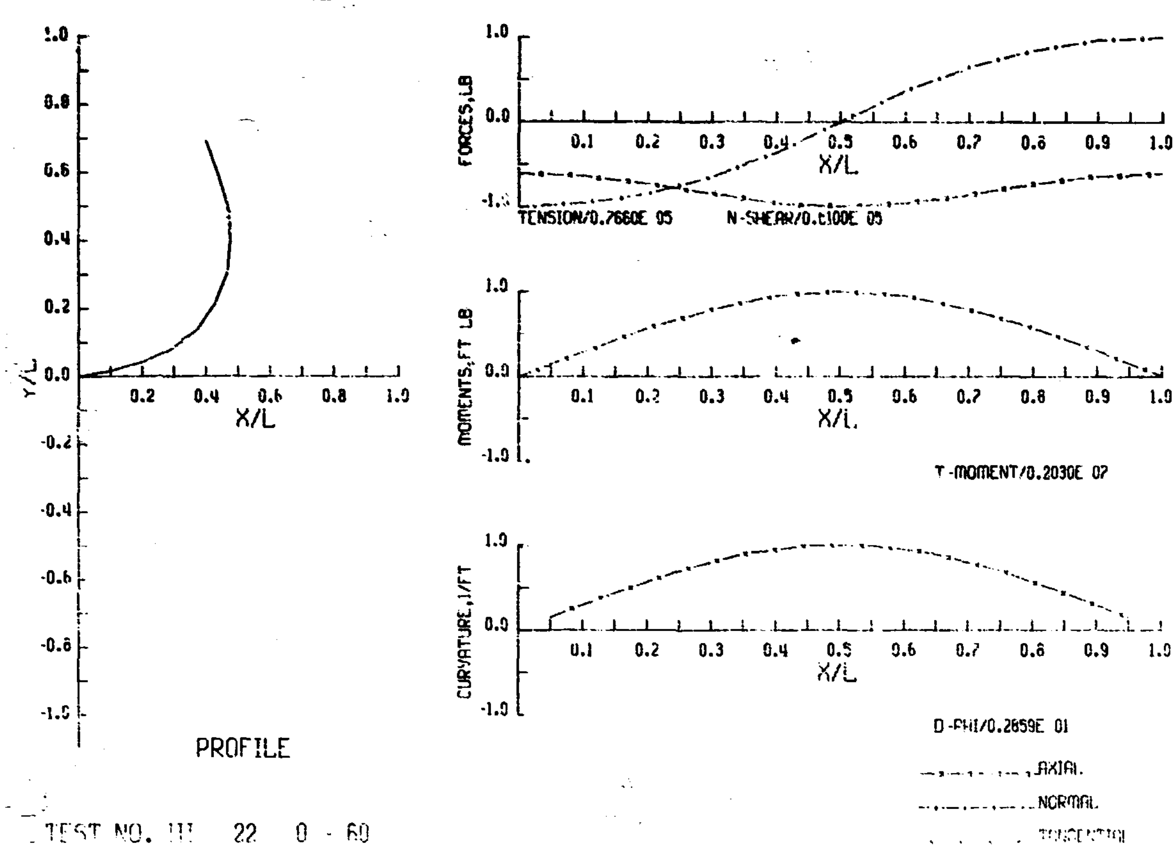

TEST NO. III 22 0 - 60

HYDRONAUTICS, INC

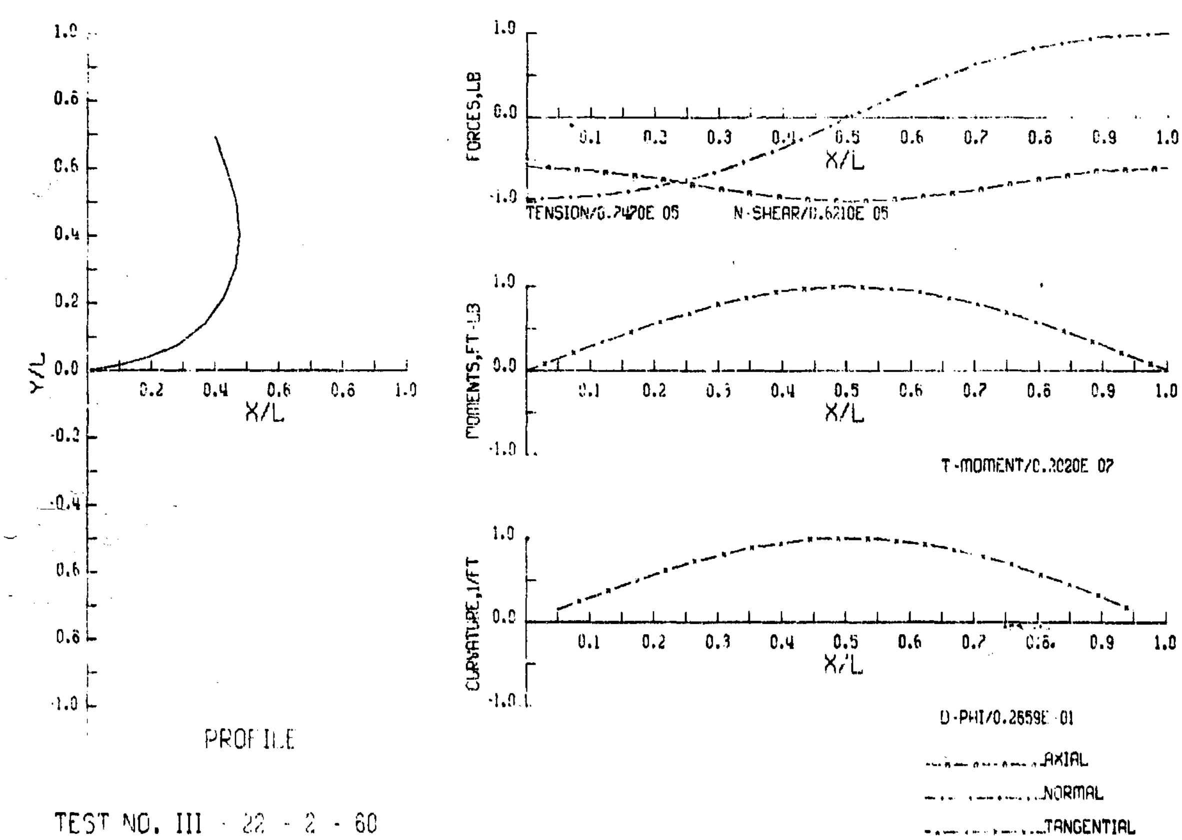

TEST NO. III - 22 - 2 - 60

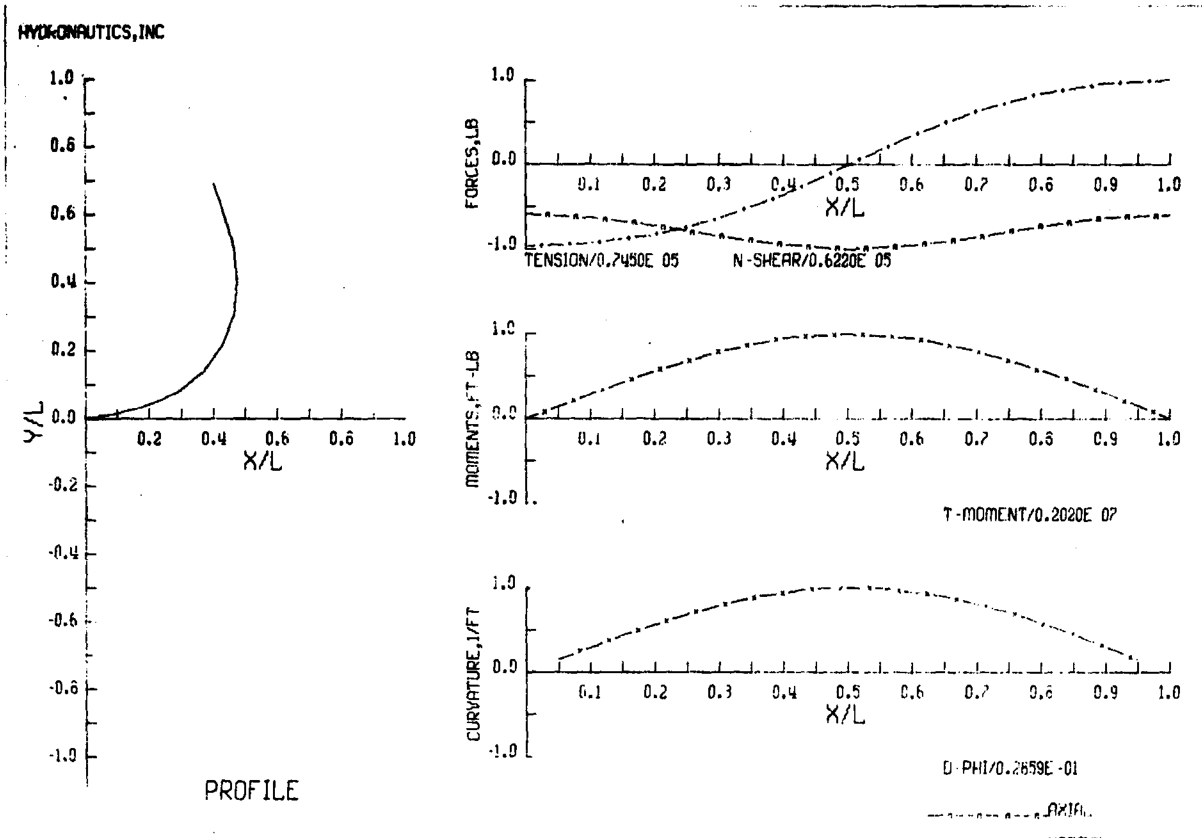

TEST NO. III - 28 - 2 - 60

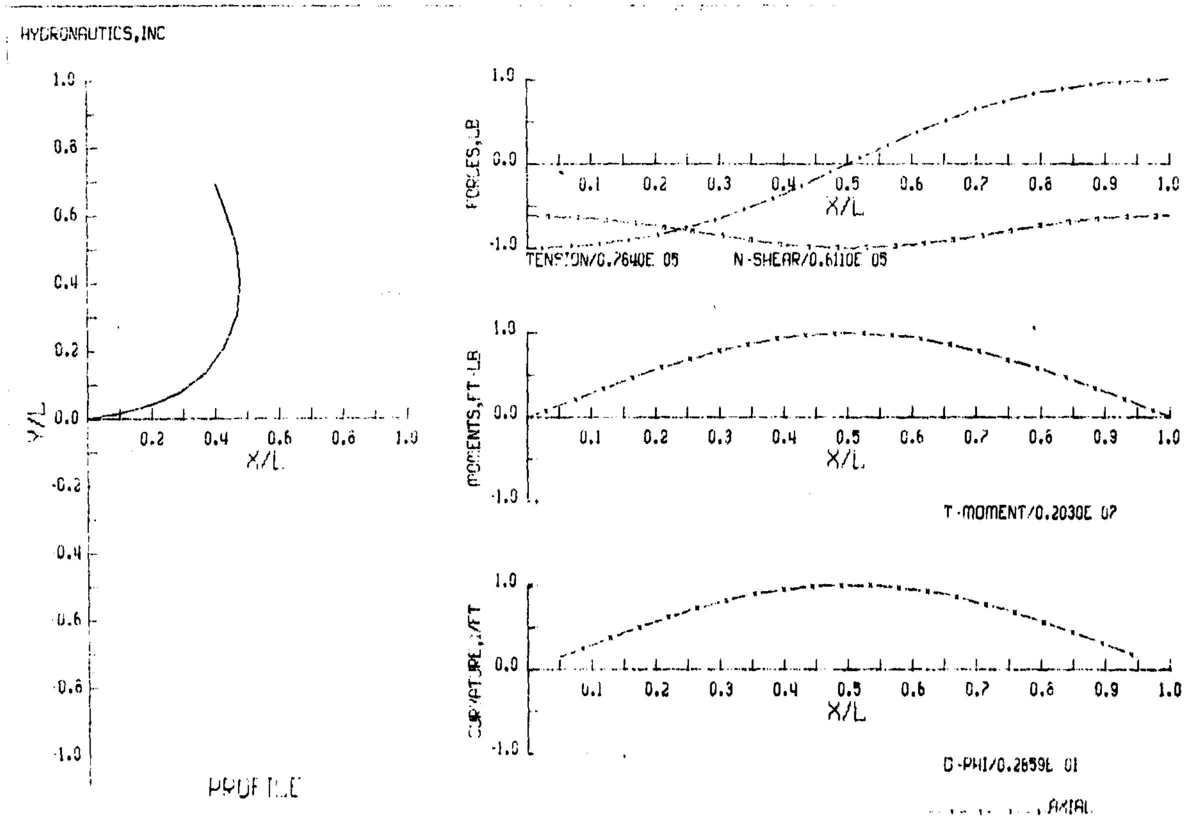

TEST NO. III 29 0 - 60

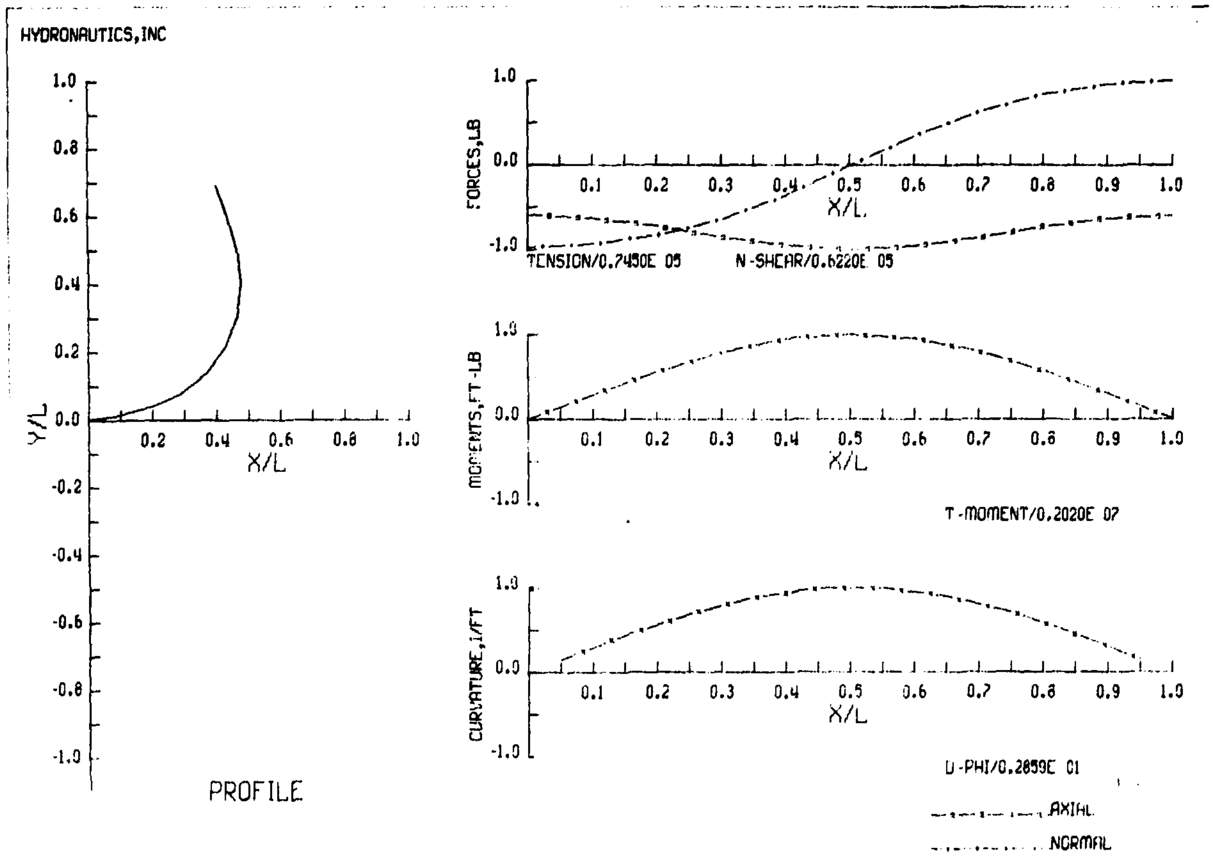

TEST NO. III - 29 2 60

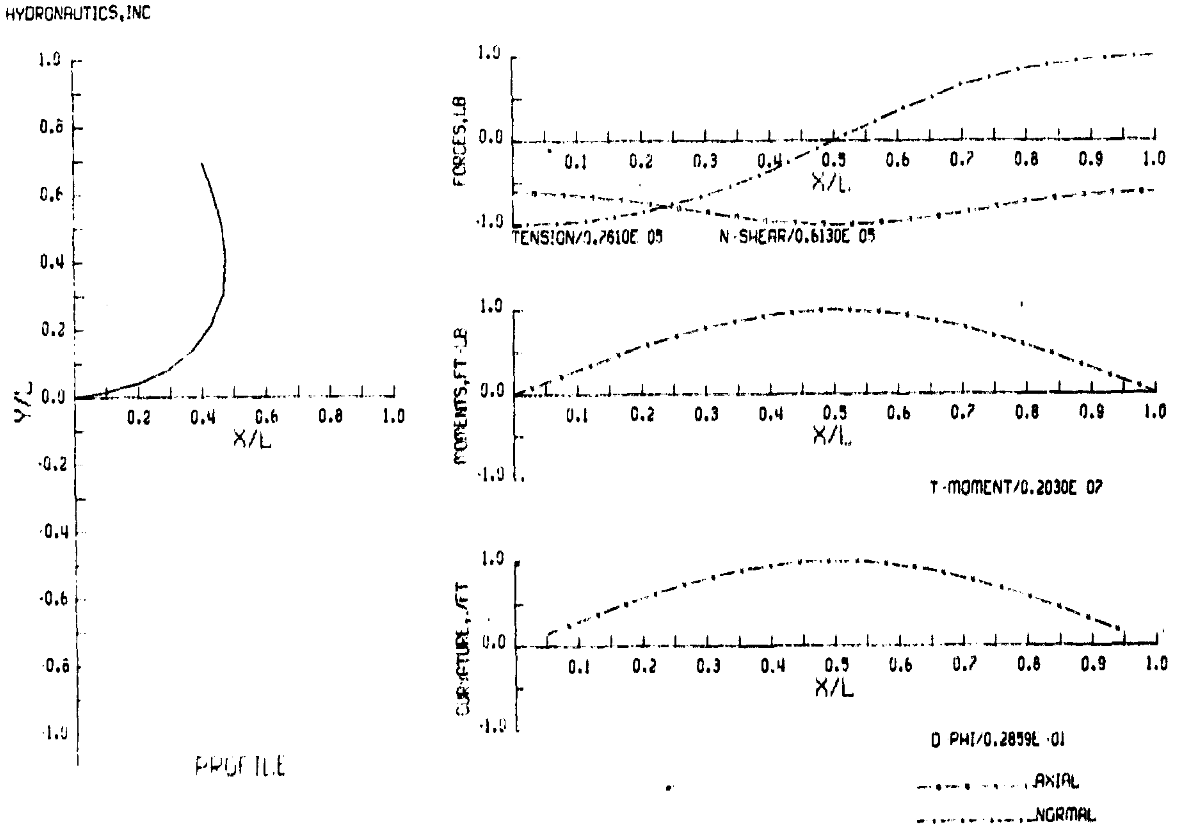

TEST NO. III 46 - 0 - 20

HYDRONAUTICS,INC

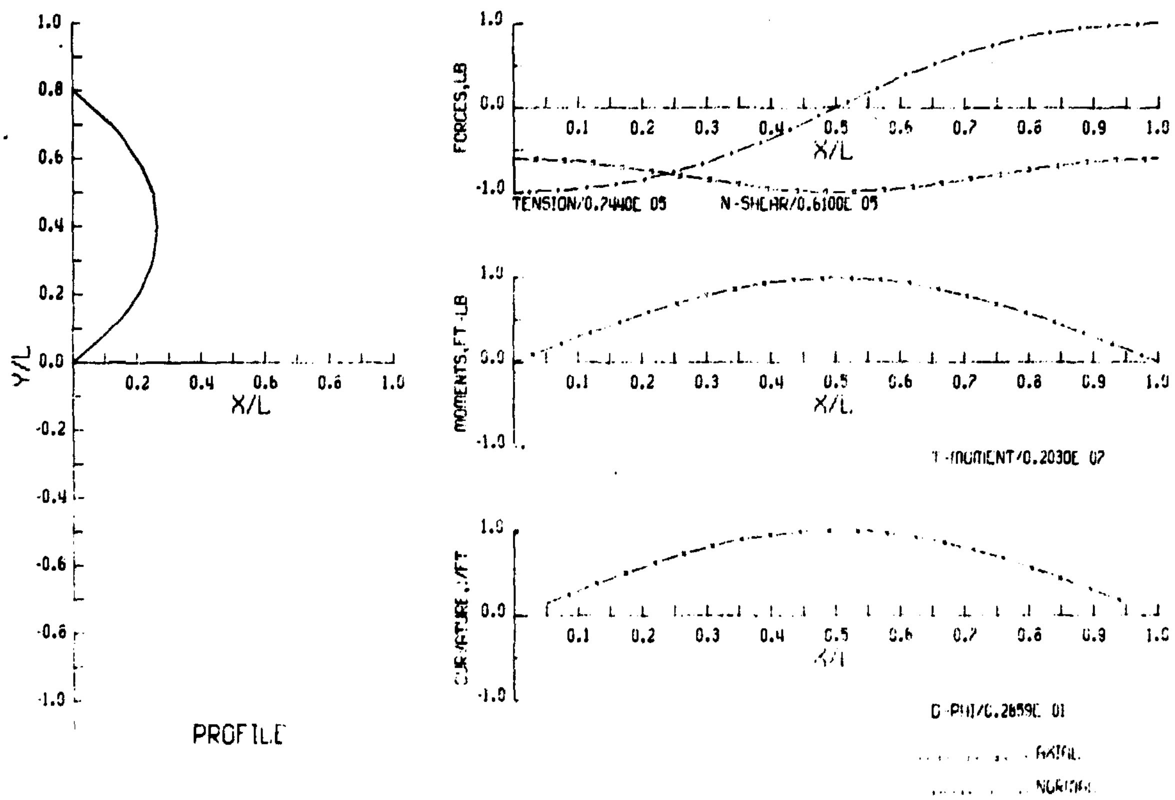

TEST NO. III [illegible] 90

HYDRONAUTICS,INC

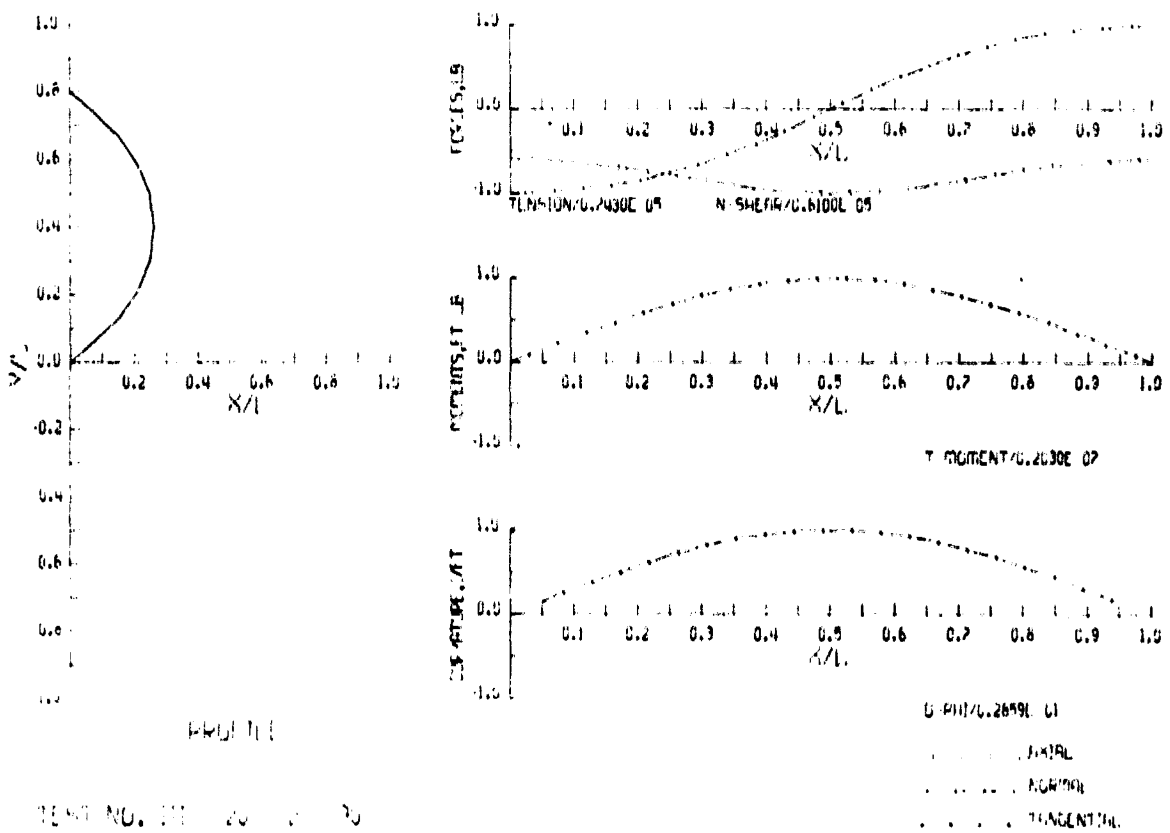

[illegible] NO. III 20 [illegible] 90

HYDRONAUTICS,INC

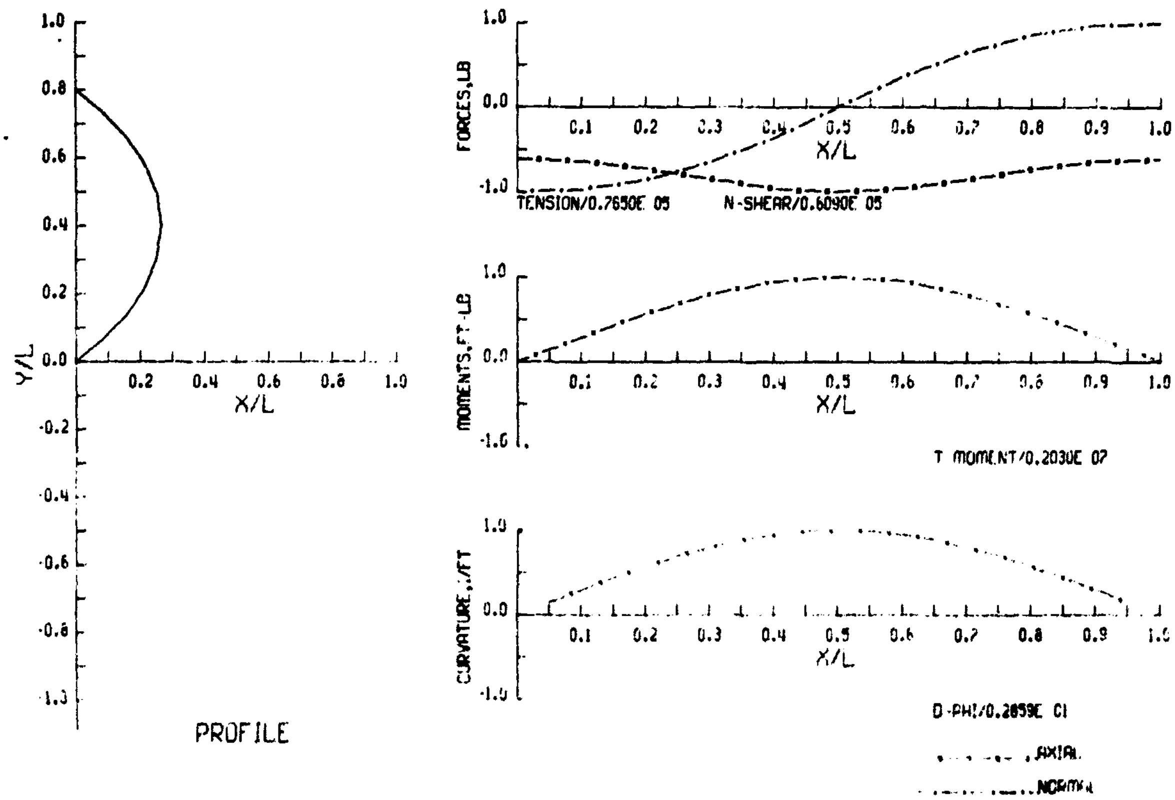

HYDRONAUTICS,INC

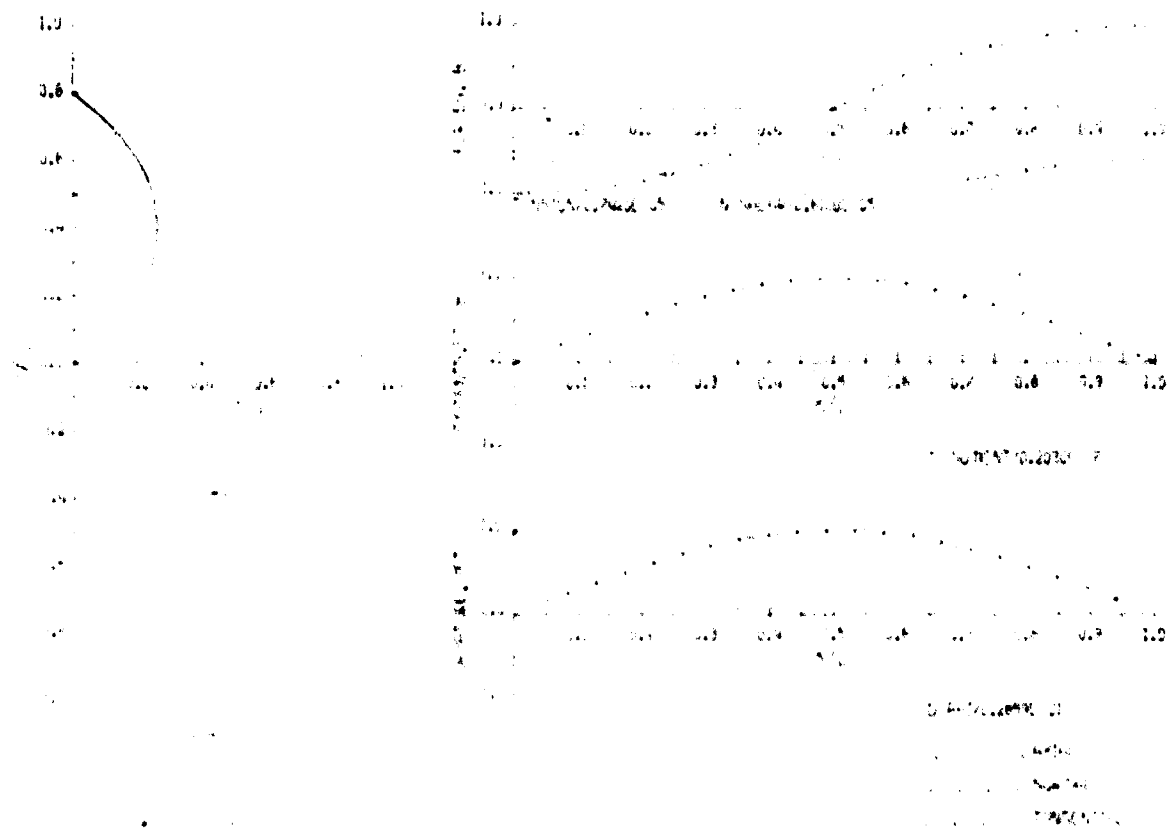

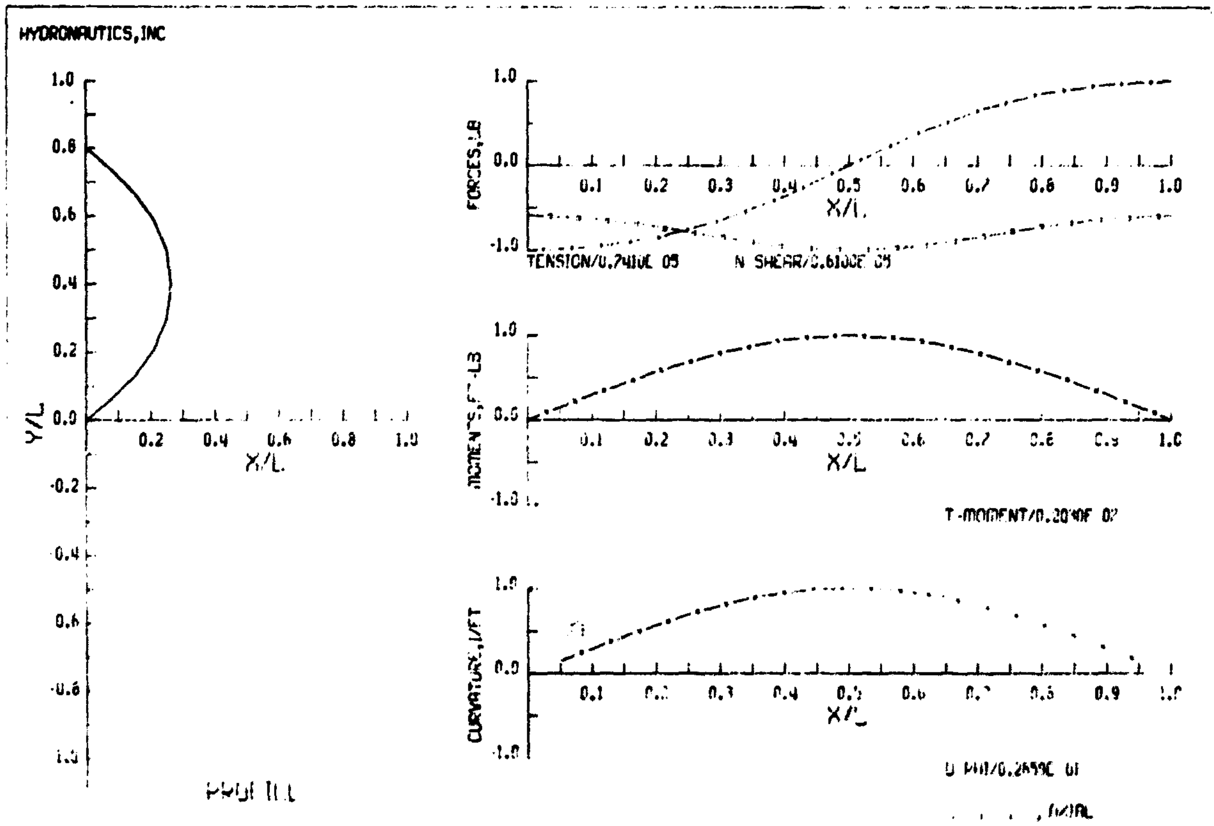
HYDRONAUTICS,INC
Y/L
X/L
PROFILE
FORCES,LB
TENSION/0.2410E 05
N SHEAR/0.6100E 05
T-MOMENT/0.2030E 02
CURVATURE,1/FT
D PHI/0.2659E 01
AXIAL

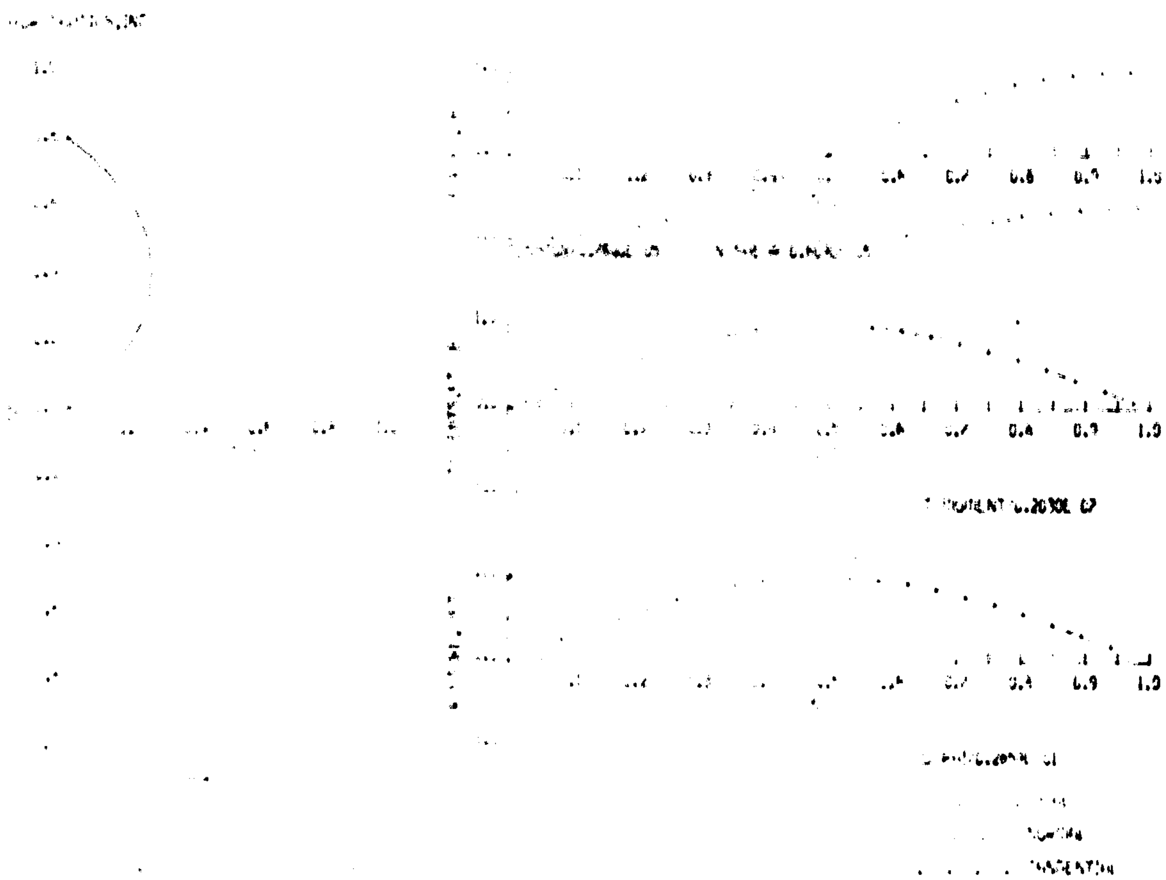

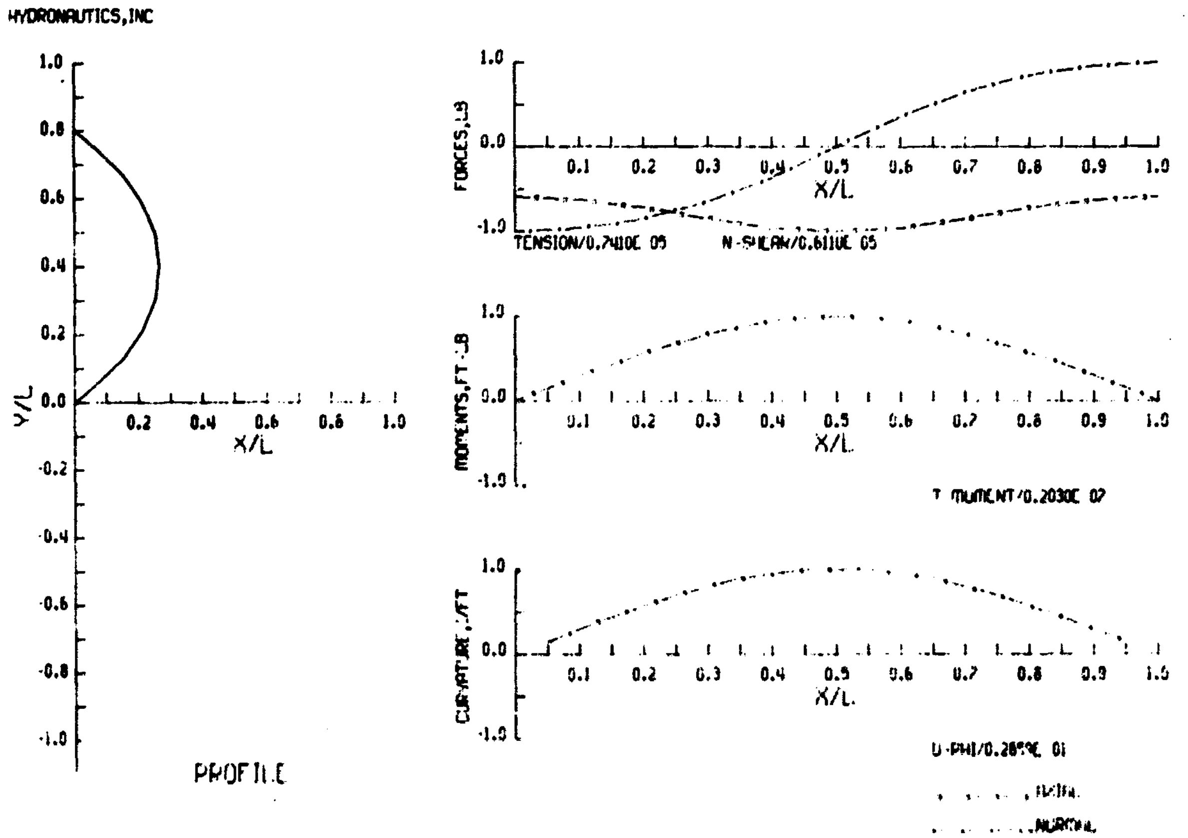

TEST NO. III 20 2 09

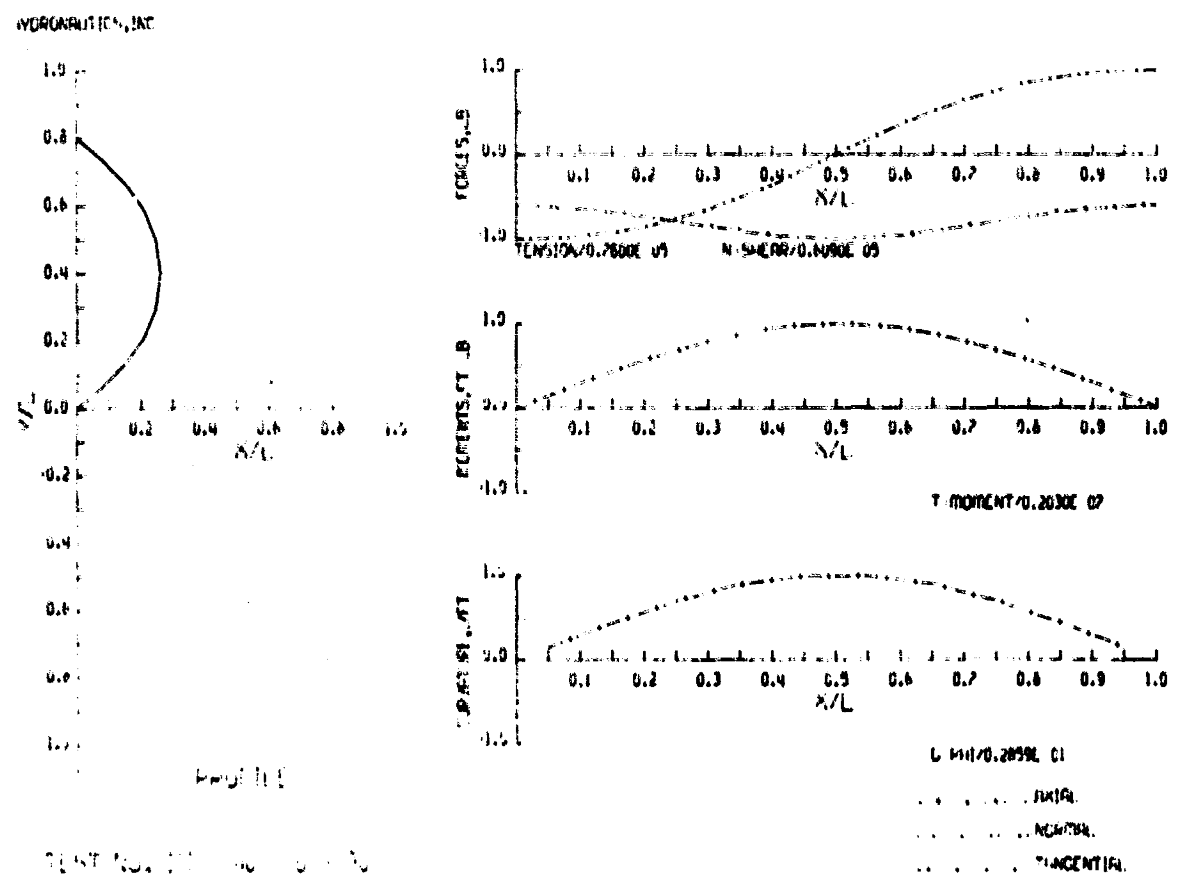

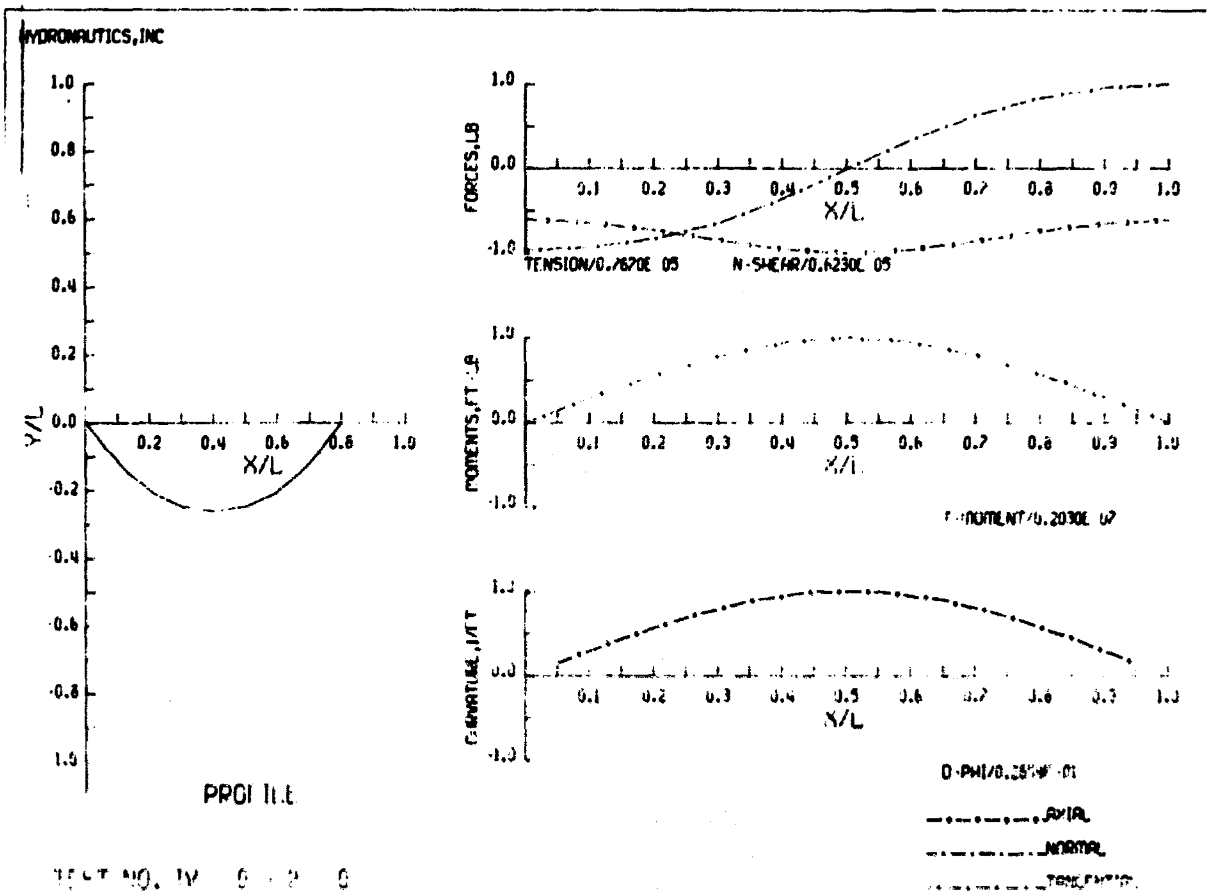
HYDRONAUTICS,INC
Y/L
X/L
PROFILE
FORCES,LB
TENSION/0.7670E 05
N-SHEAR/0.6230E 05
MOMENTS,FT-LB
CURVATURE,1/FT
AXIAL
NORMAL

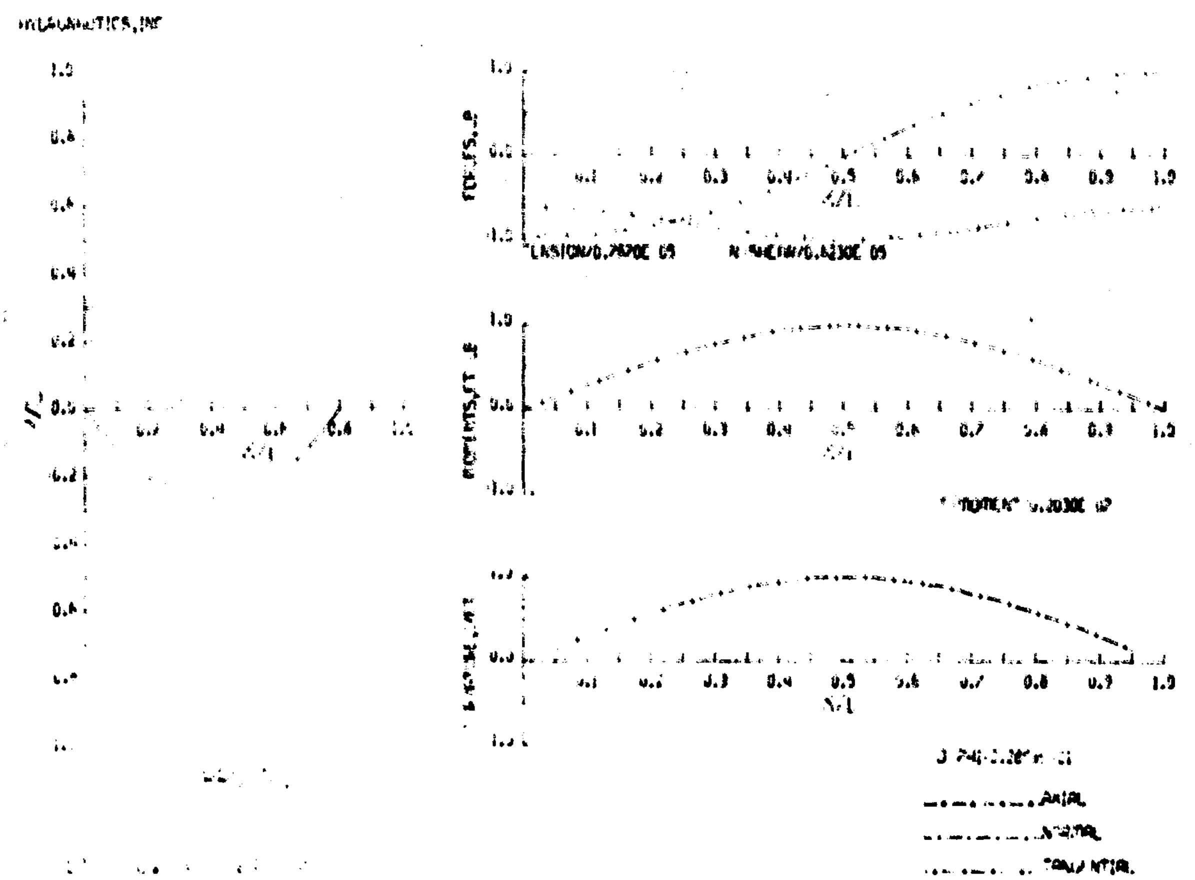
AXIAL

HYDRONAUTICS, INC

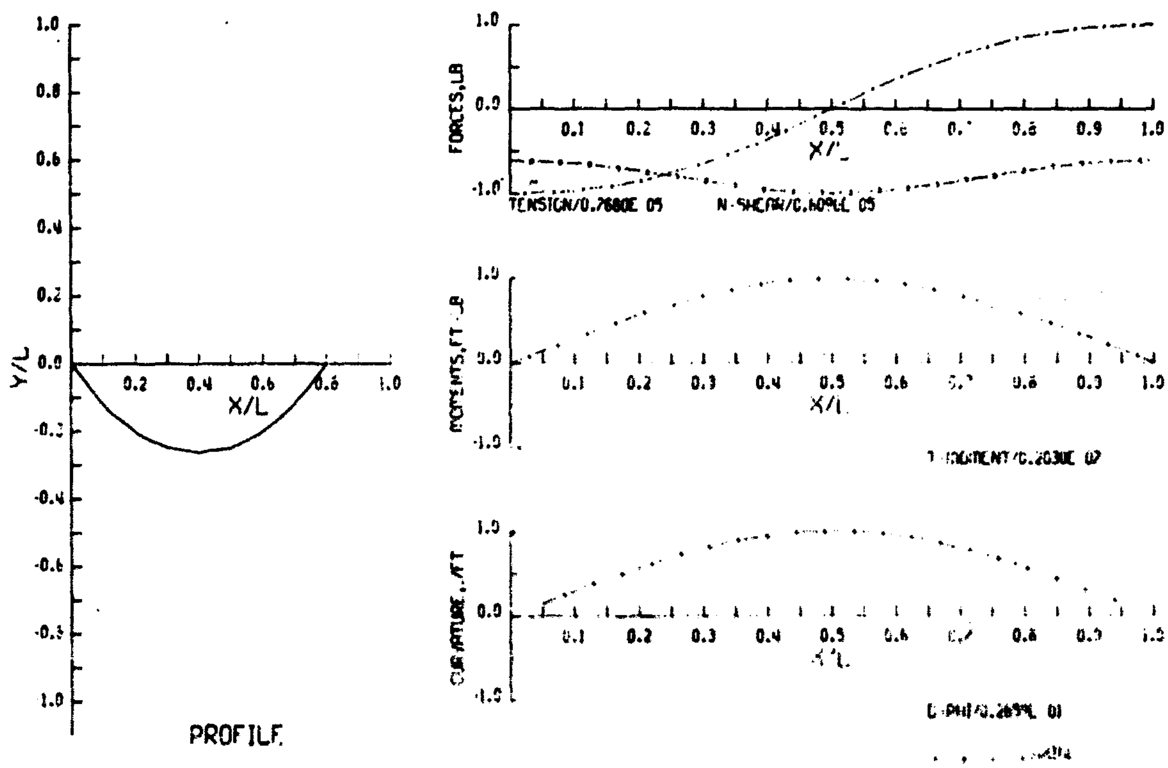

TEST NO. IV - 22 - 0 - 0

HYDRONAUTICS, INC

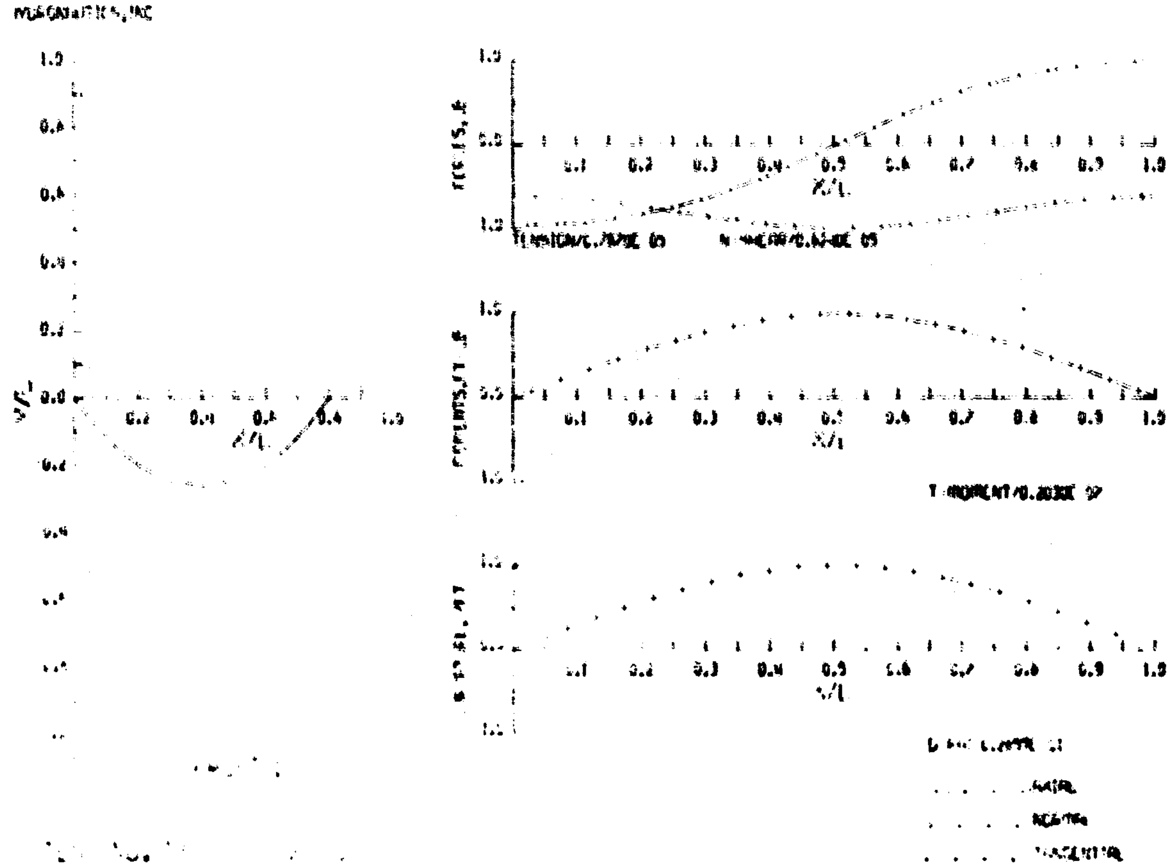

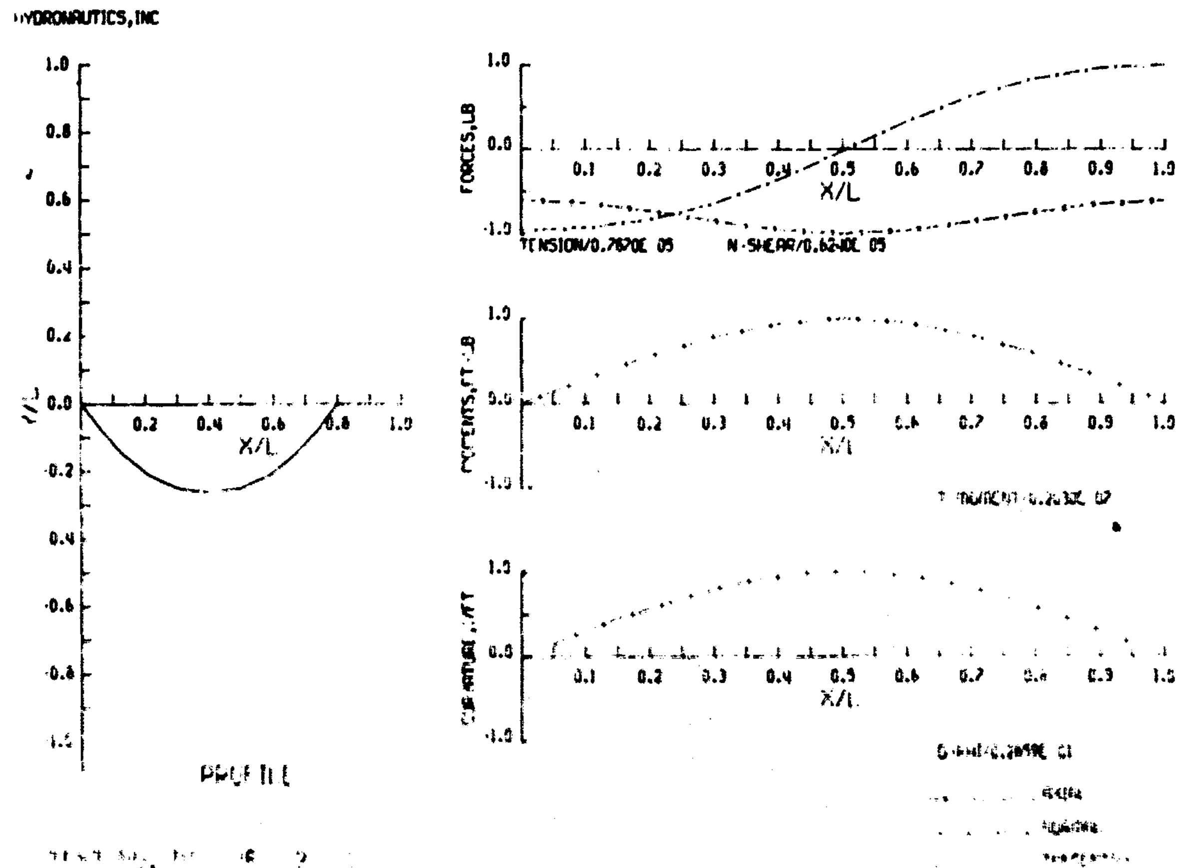

HYDRONAUTICS,INC
FORCES,LB
X/L
TENSION/0.7870E 05
N-SHEAR/0.6240E 05
PROFILE

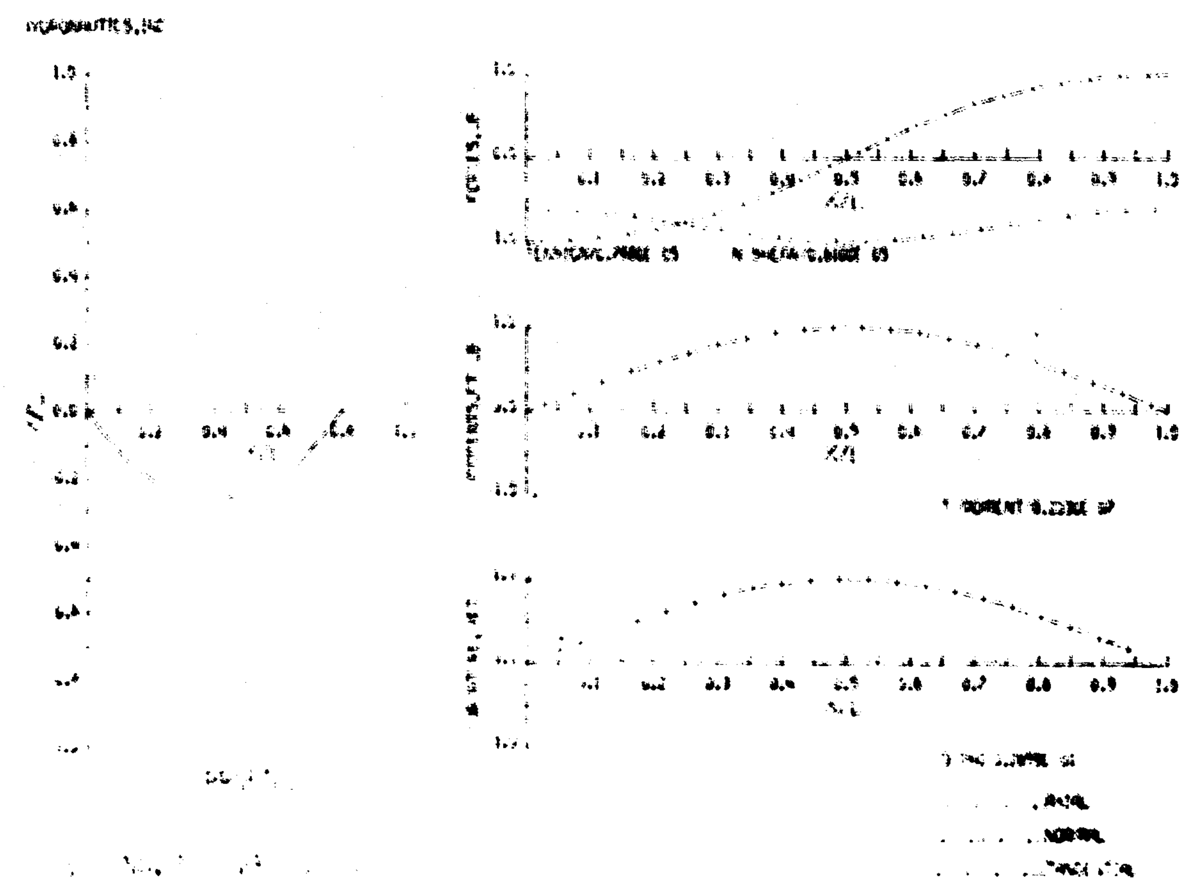

X/L
AXIAL
NORMAL

HYDRONAUTICS, INC

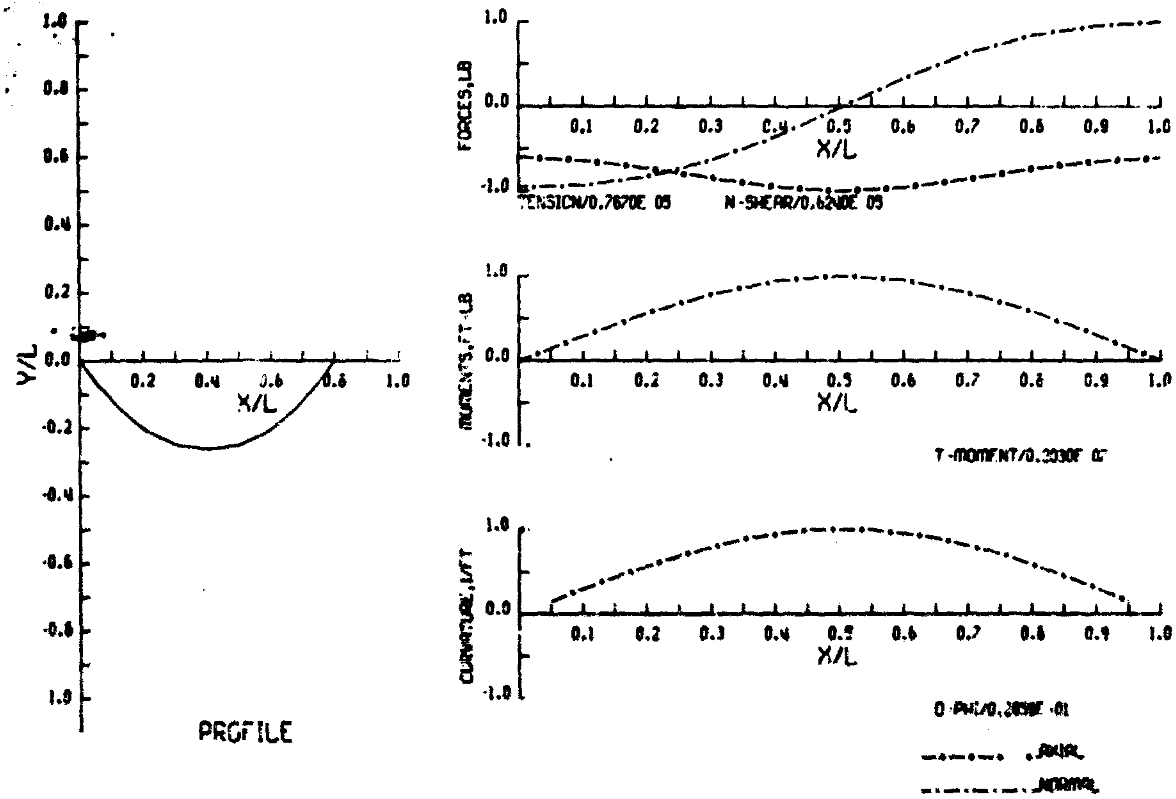

TEST NO. IV - 25 - 3 - 0

HYDRONAUTICS, INC

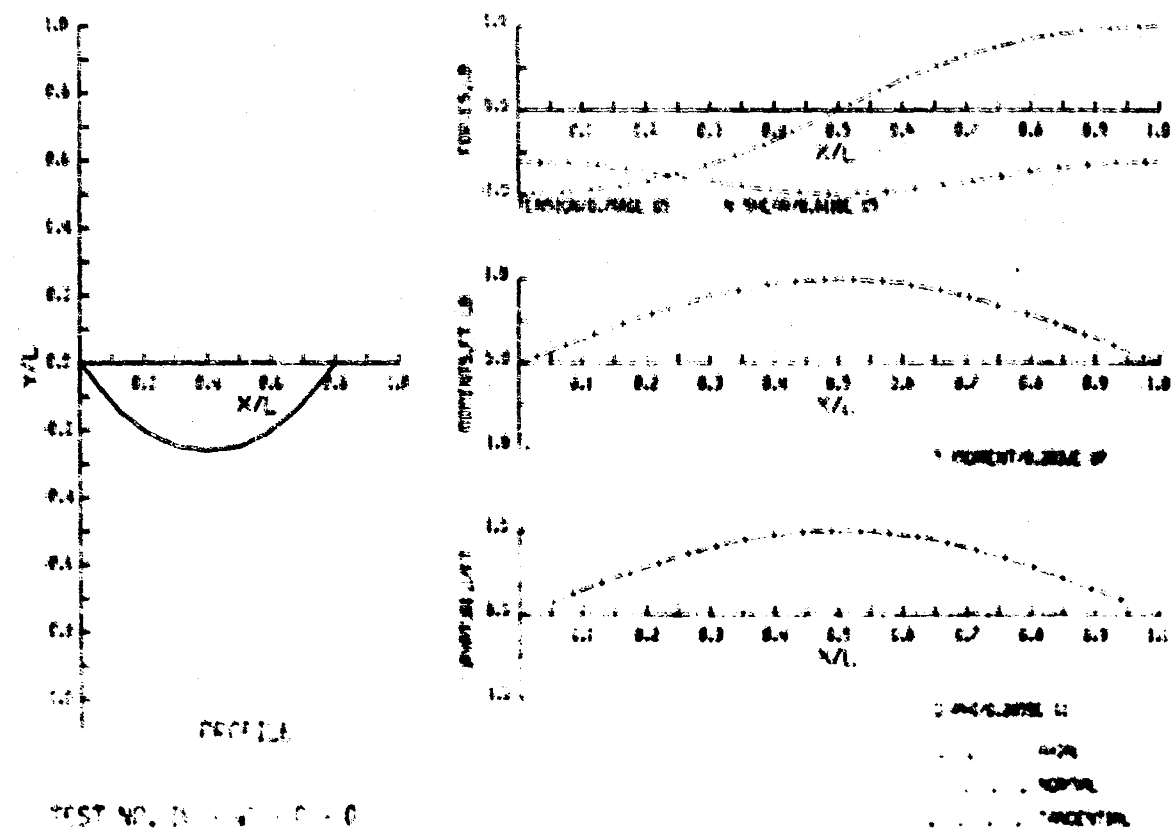

TEST NO. [illegible]

HYDRONAUTICS,INC

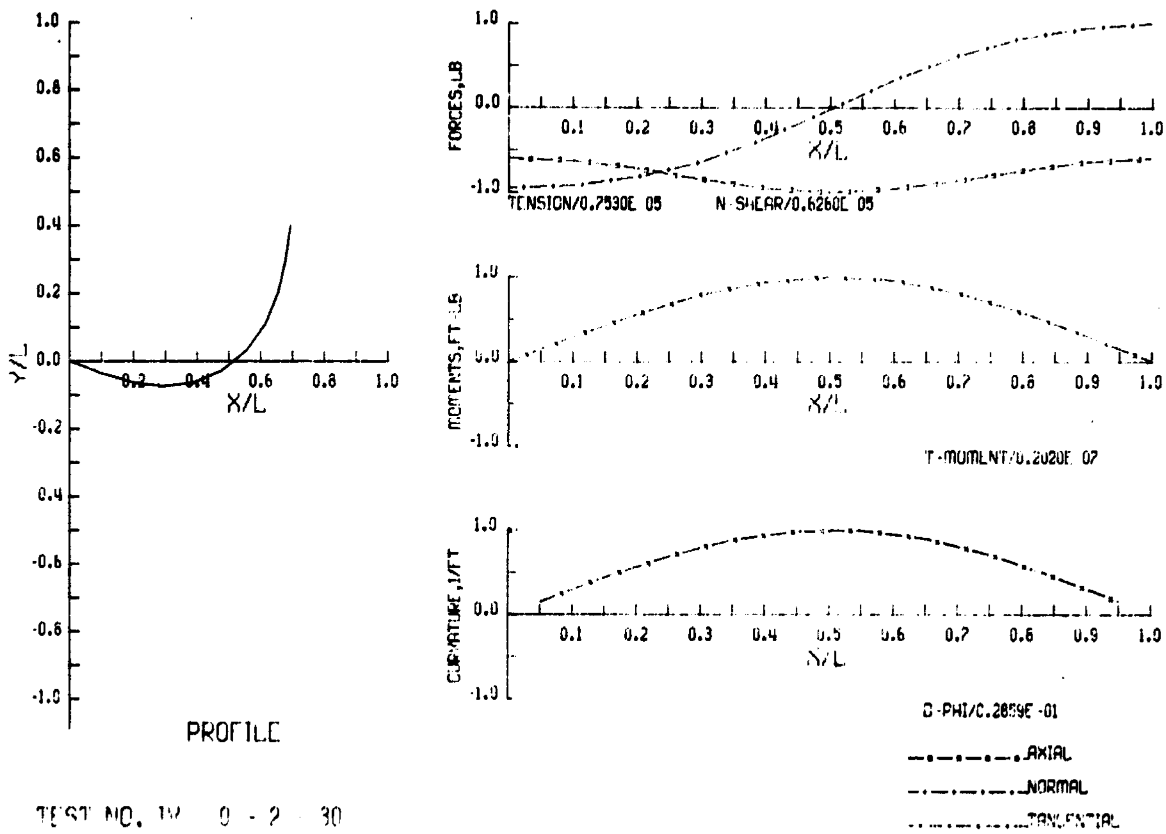

TEST NO. 1V 0 - 2 - 30

HYDRONAUTICS,INC

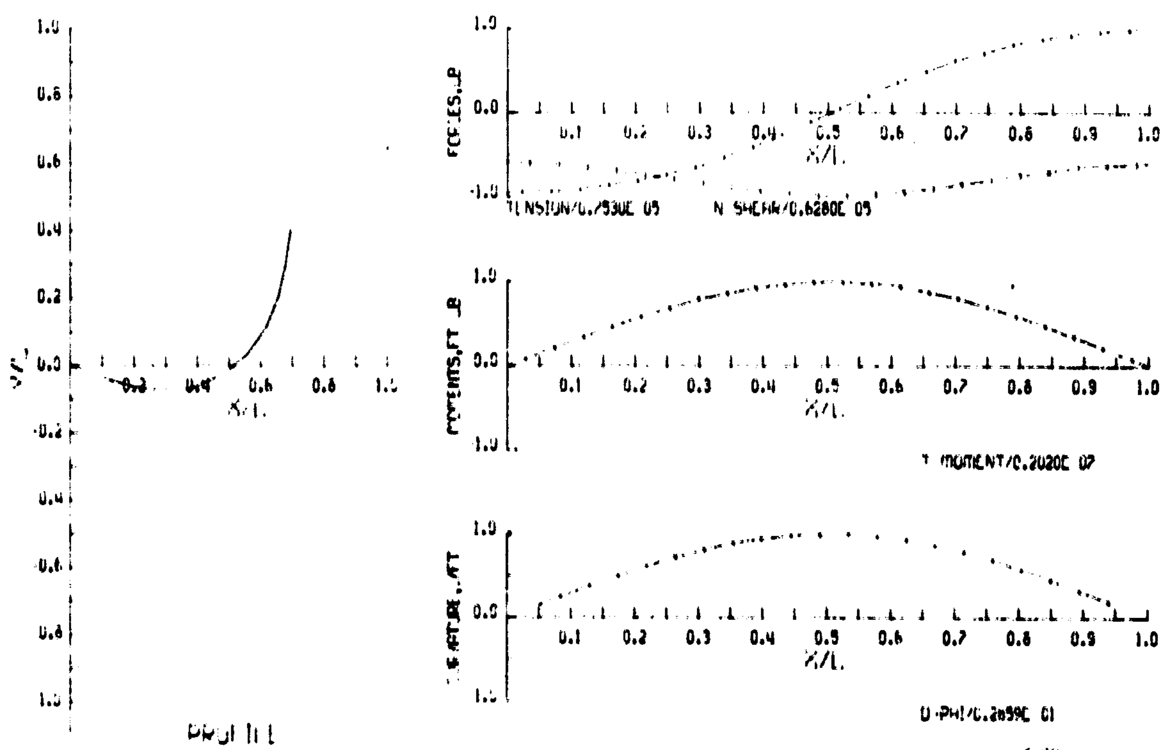

NO. 20 - 2 - 30

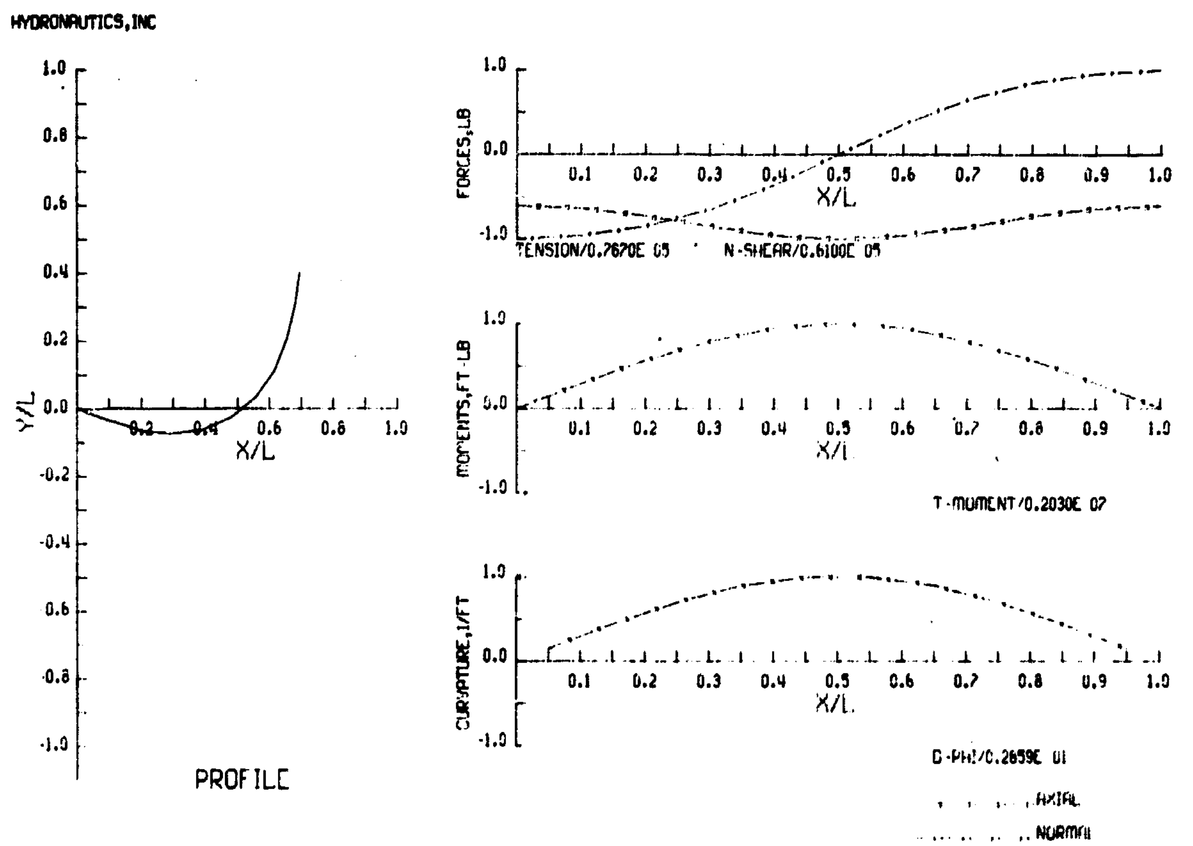

TEST NO. IV 22 - 0 - 30

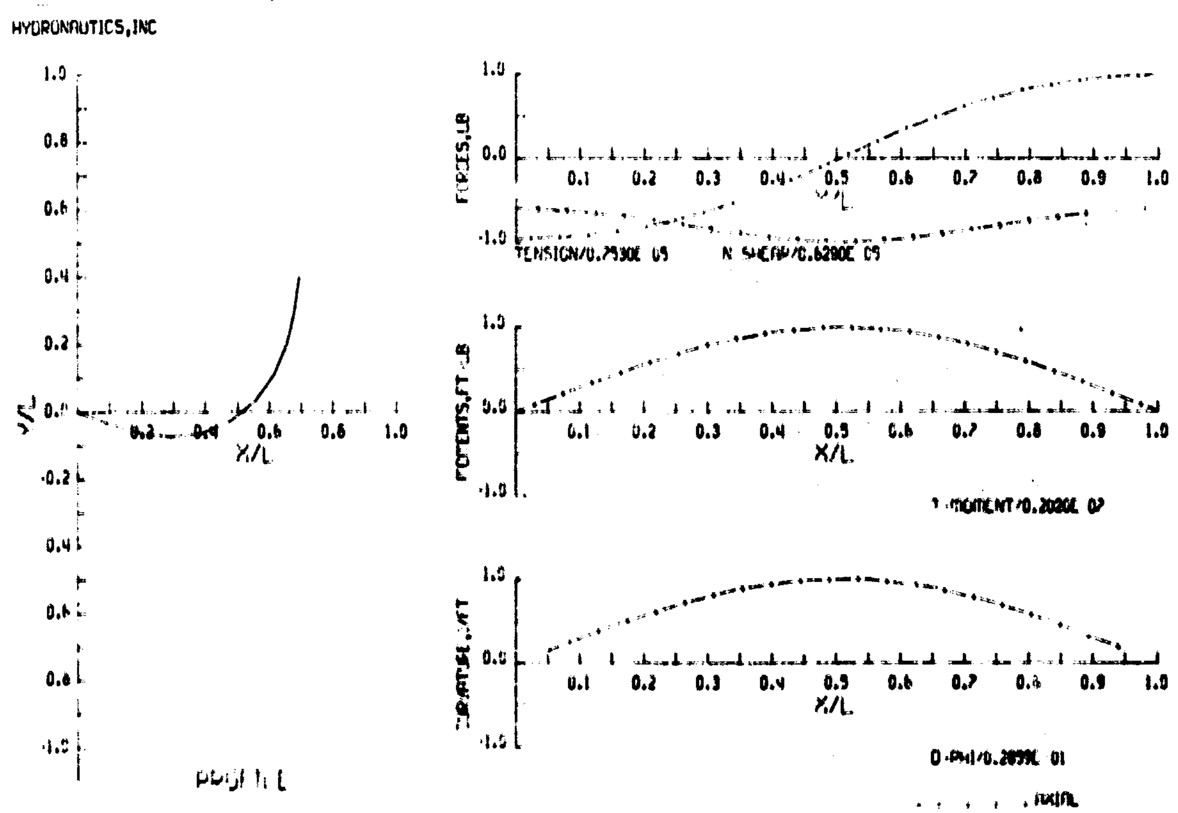

TEST NO. IV 22 2 30

HYDRONAUTICS,INC

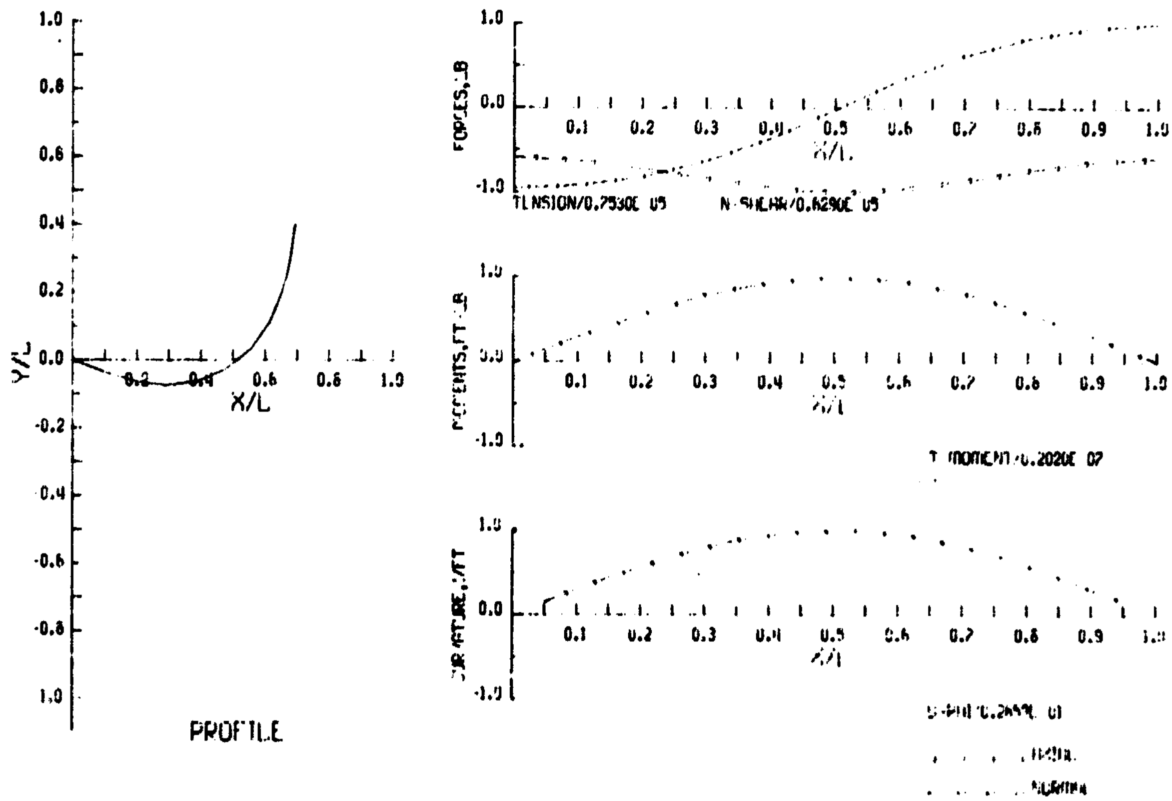

TEST NO. IV - 26 - 2 - 30

HYDRONAUTICS,INC

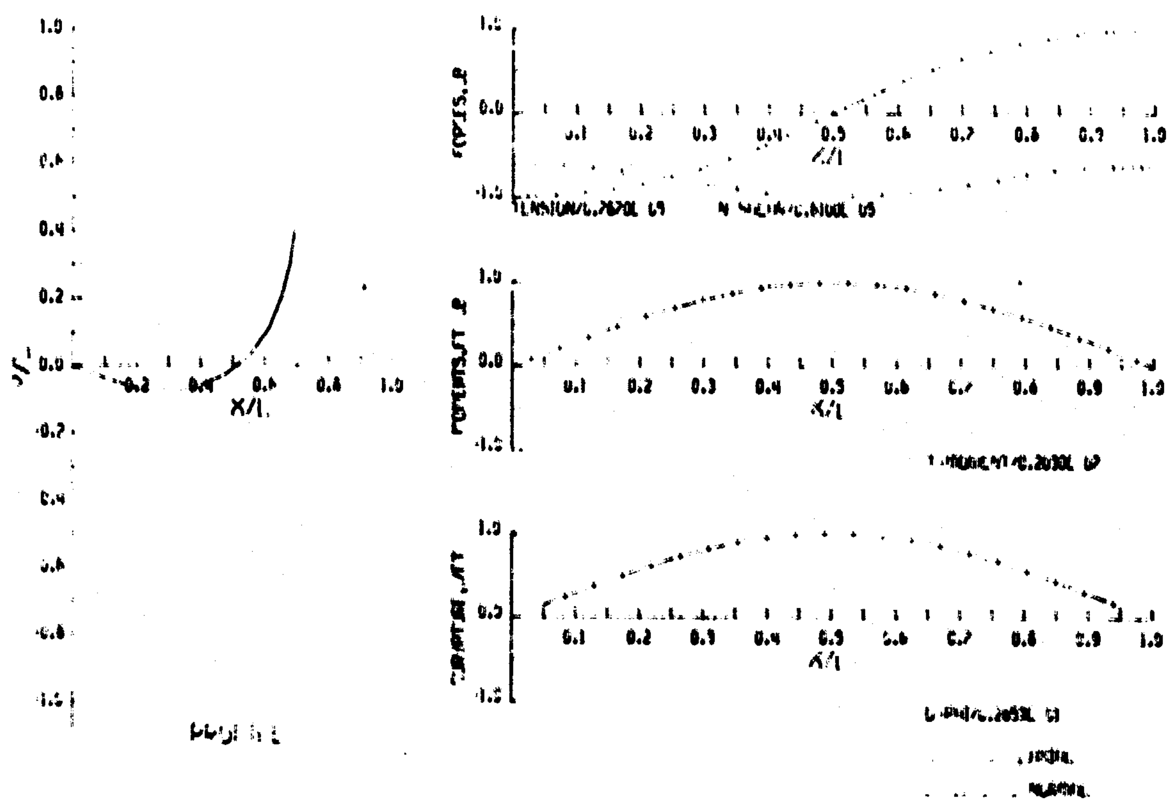

[illegible] NO. [illegible] 27 [illegible] 30

HYDRONAUTICS, INC

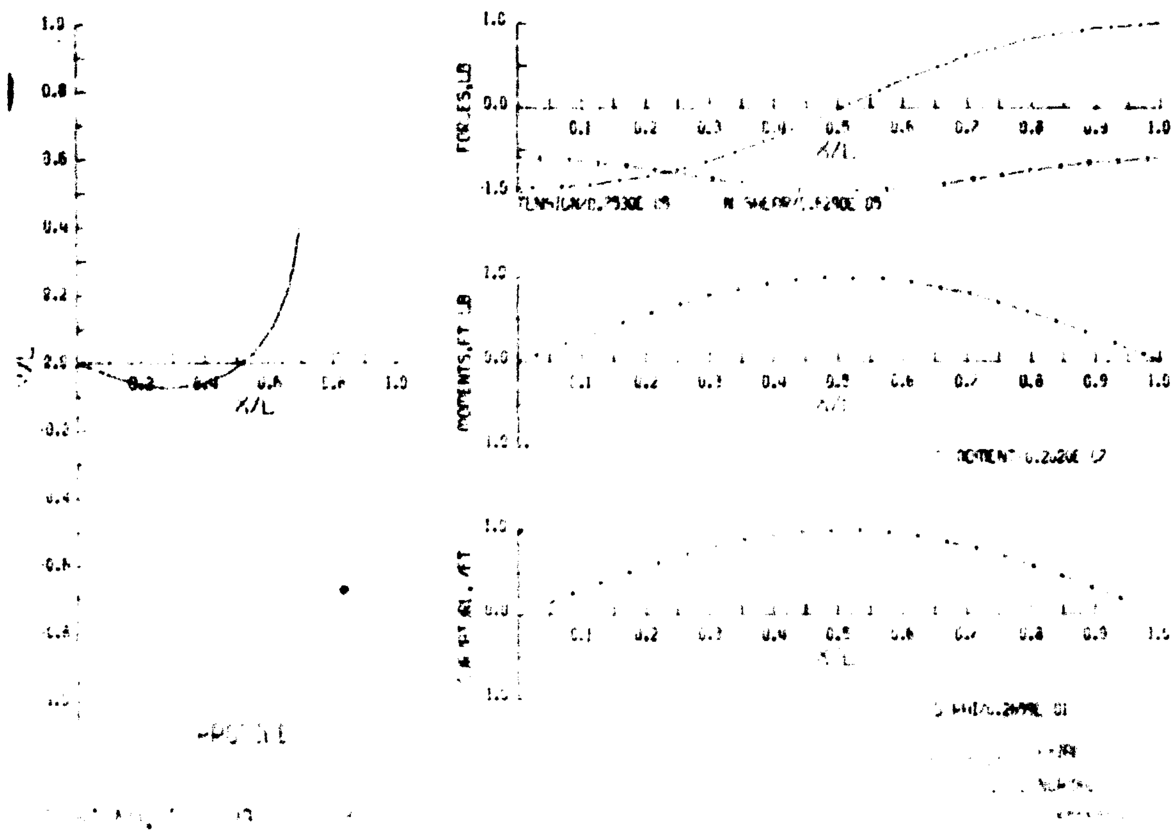

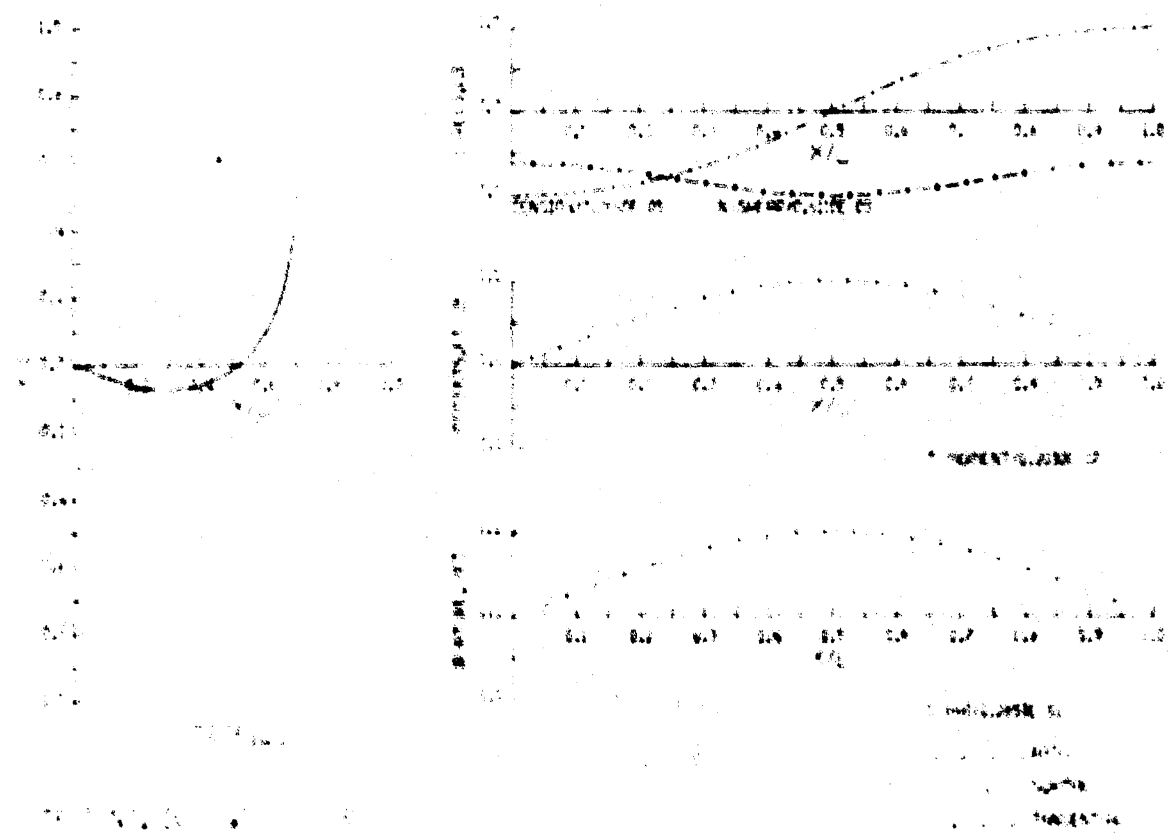

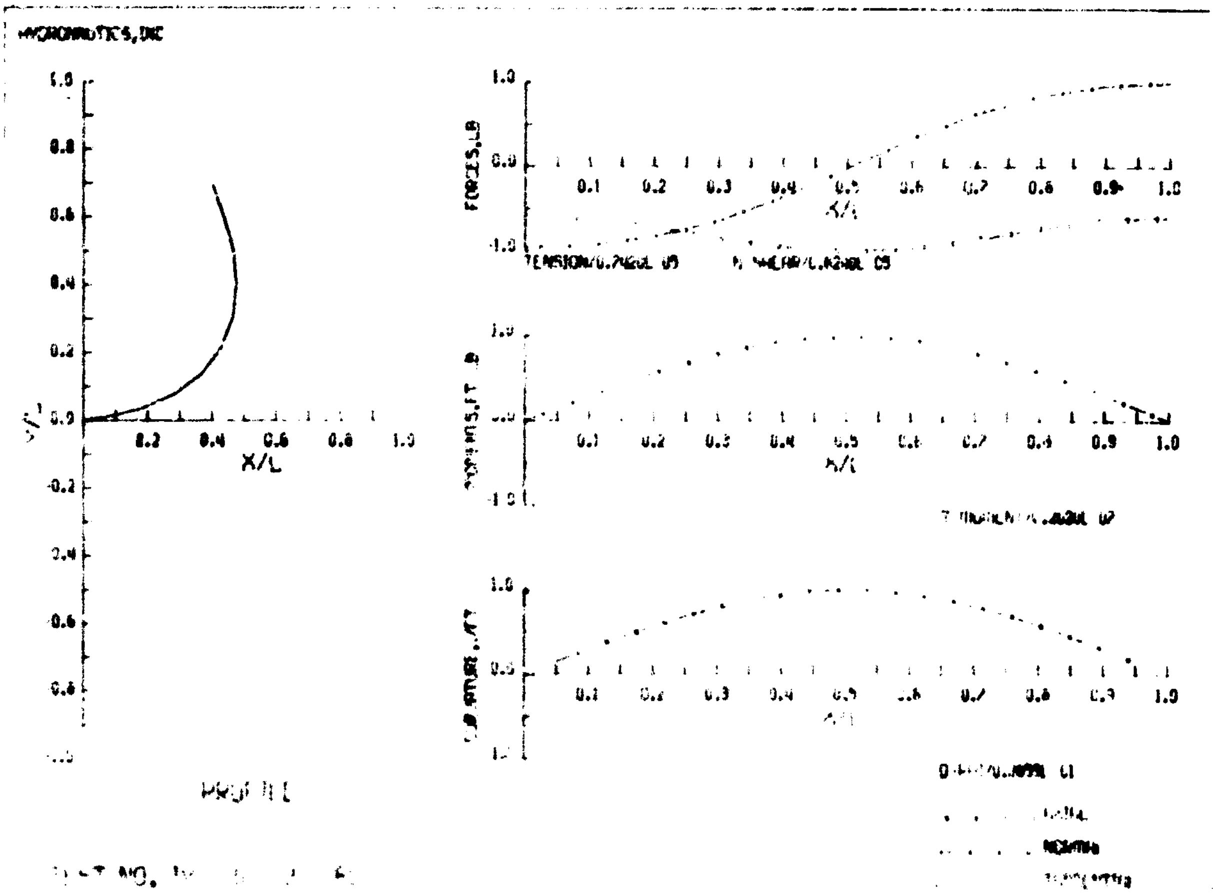
HYDRONAUTICS, INC
FORCES, LB
TENSION/0.7460E 05
PROFILE
X/L
Y/L

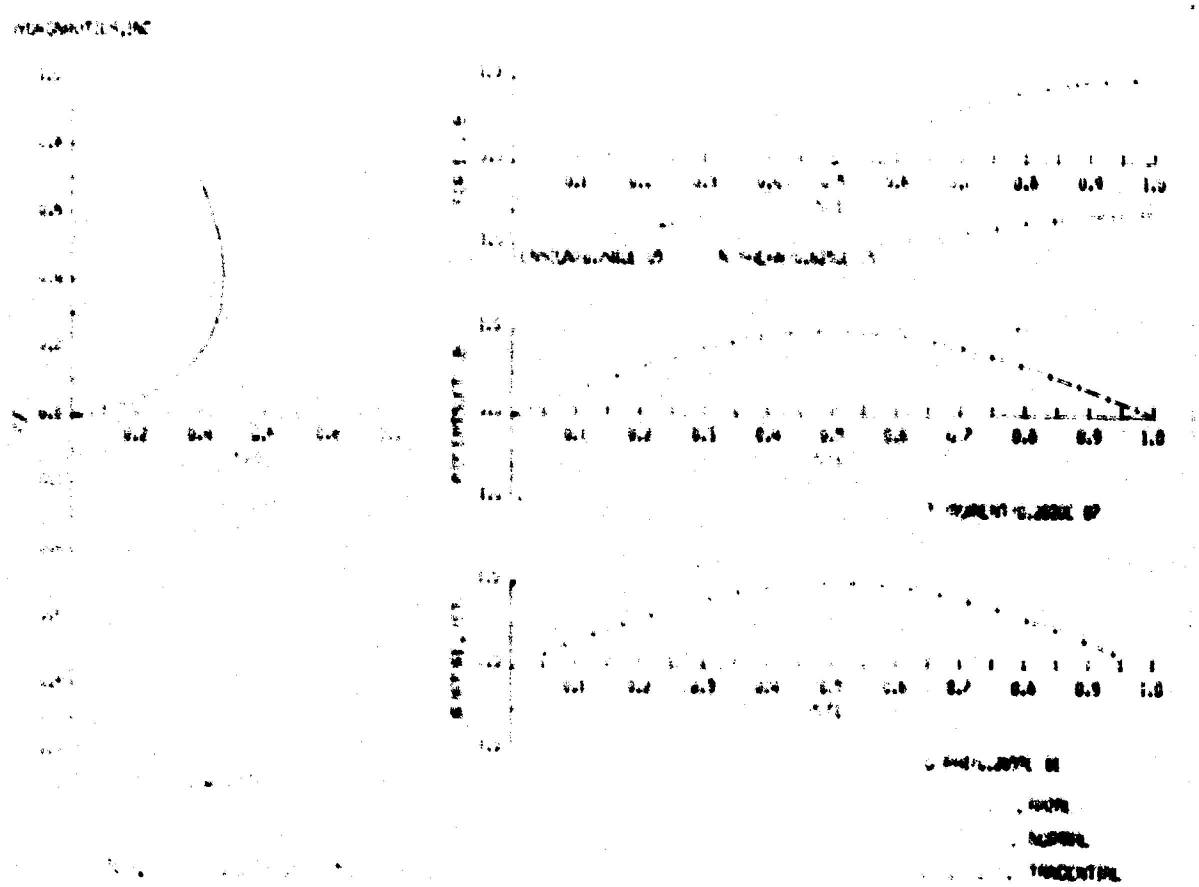
HYDRONAUTICS, INC
NORMAL
TANGENTIAL

HYDRONAUTICS,INC

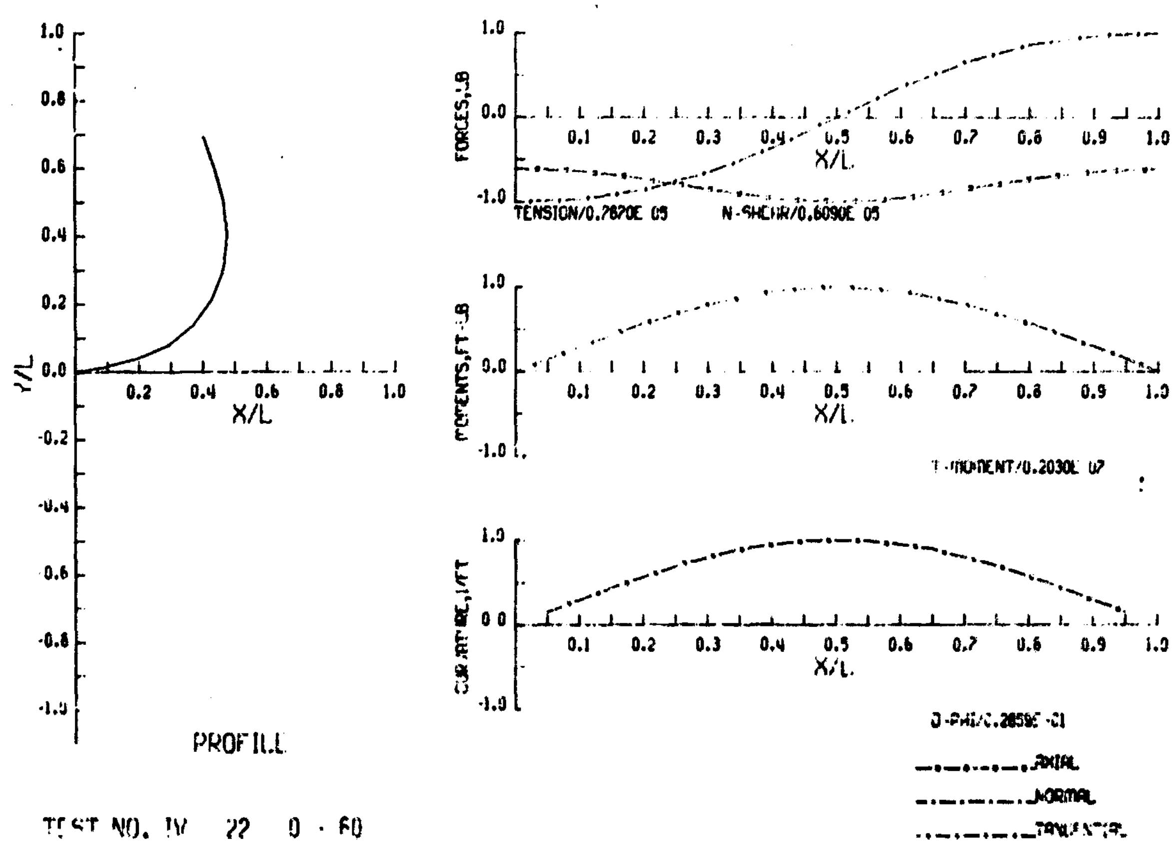

TEST NO. IV 22 0 - 60

HYDRONAUTICS,INC

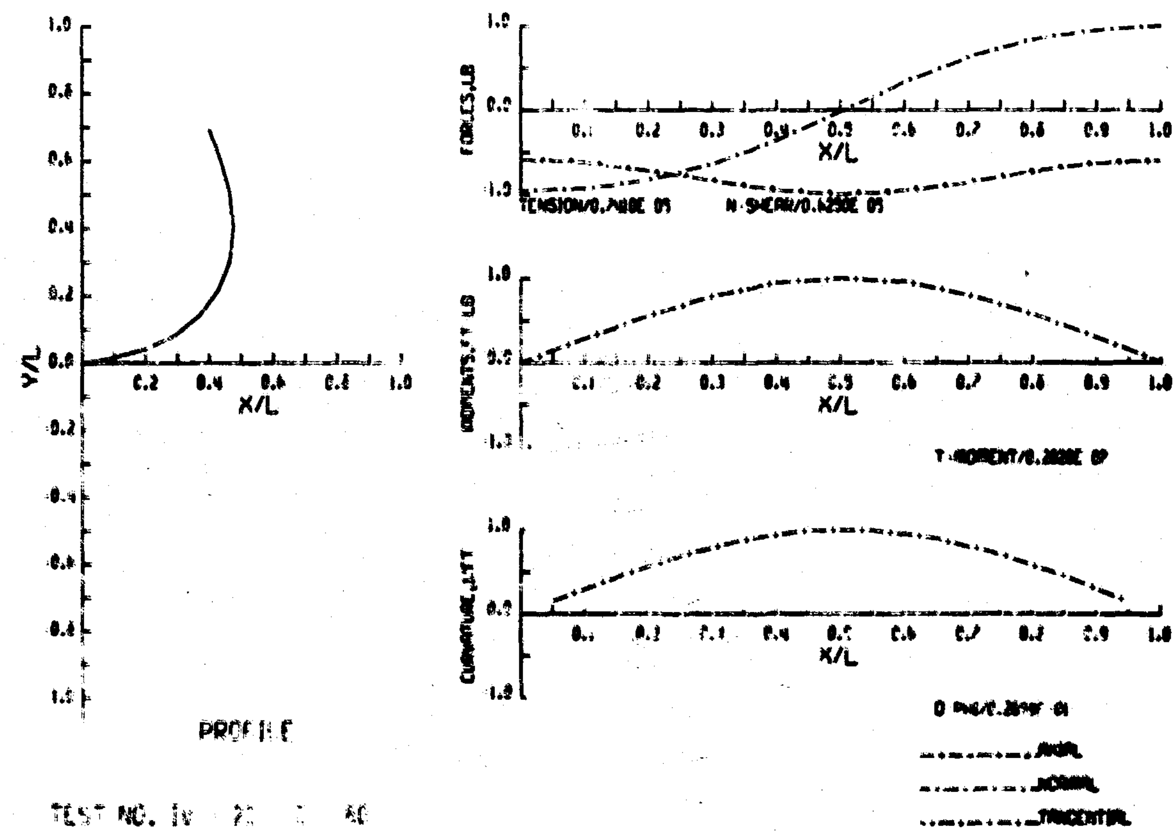

TEST NO. IV 22 0 60

HYDRONAUTICS,INC

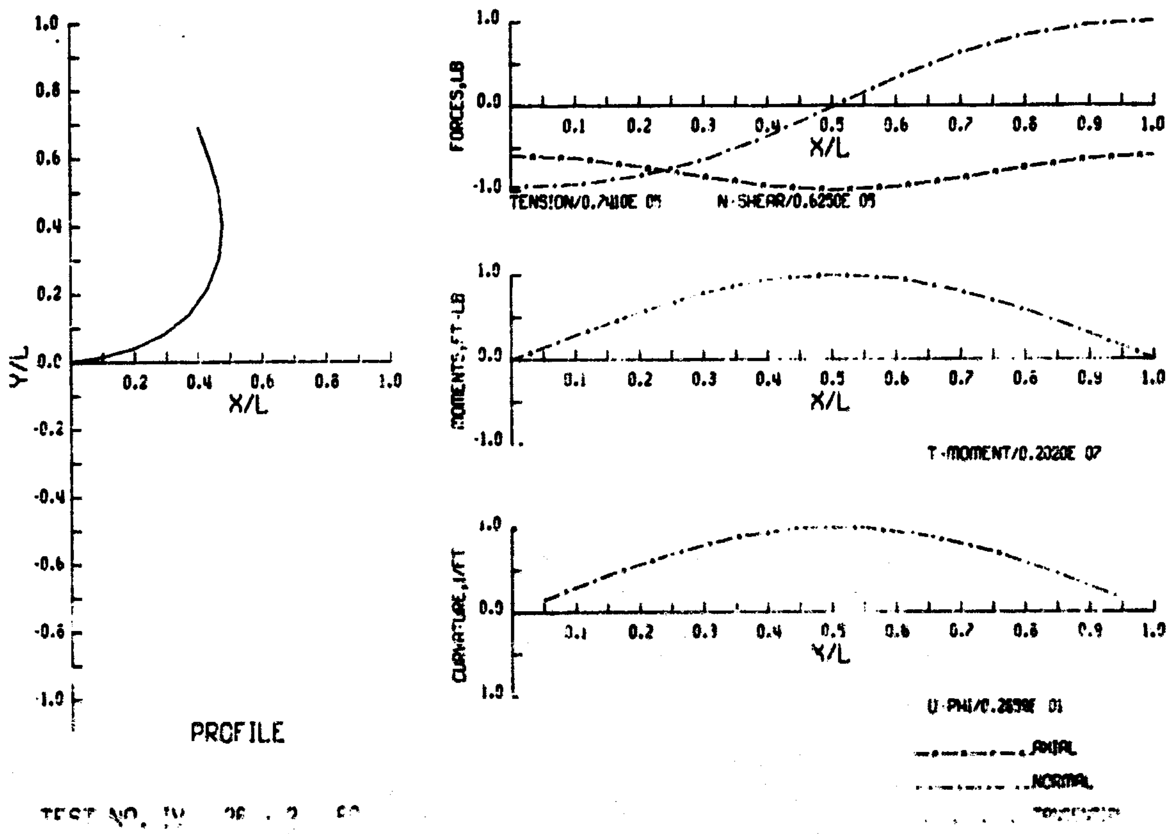

TEST NO. IV [illegible]

HYDRONAUTICS,INC

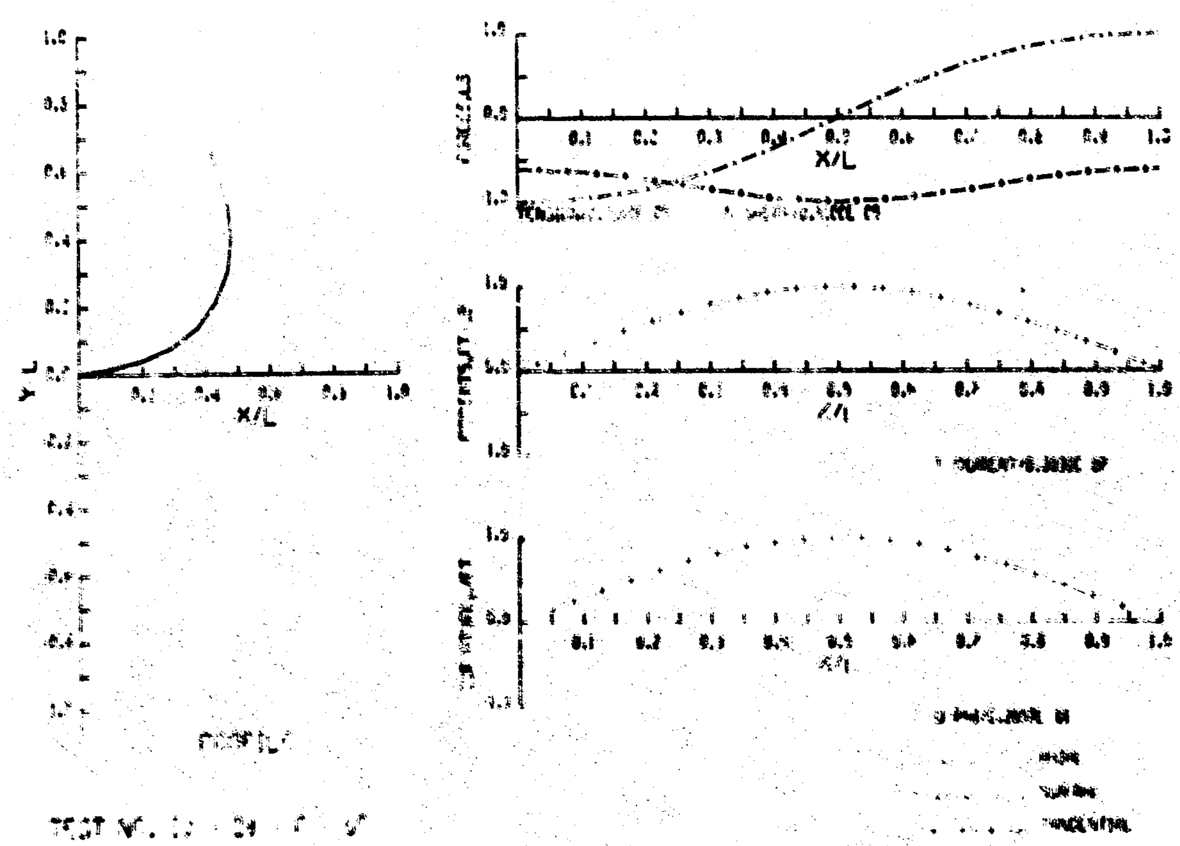

TEST NO. [illegible]

HYDRONAUTICS,INC

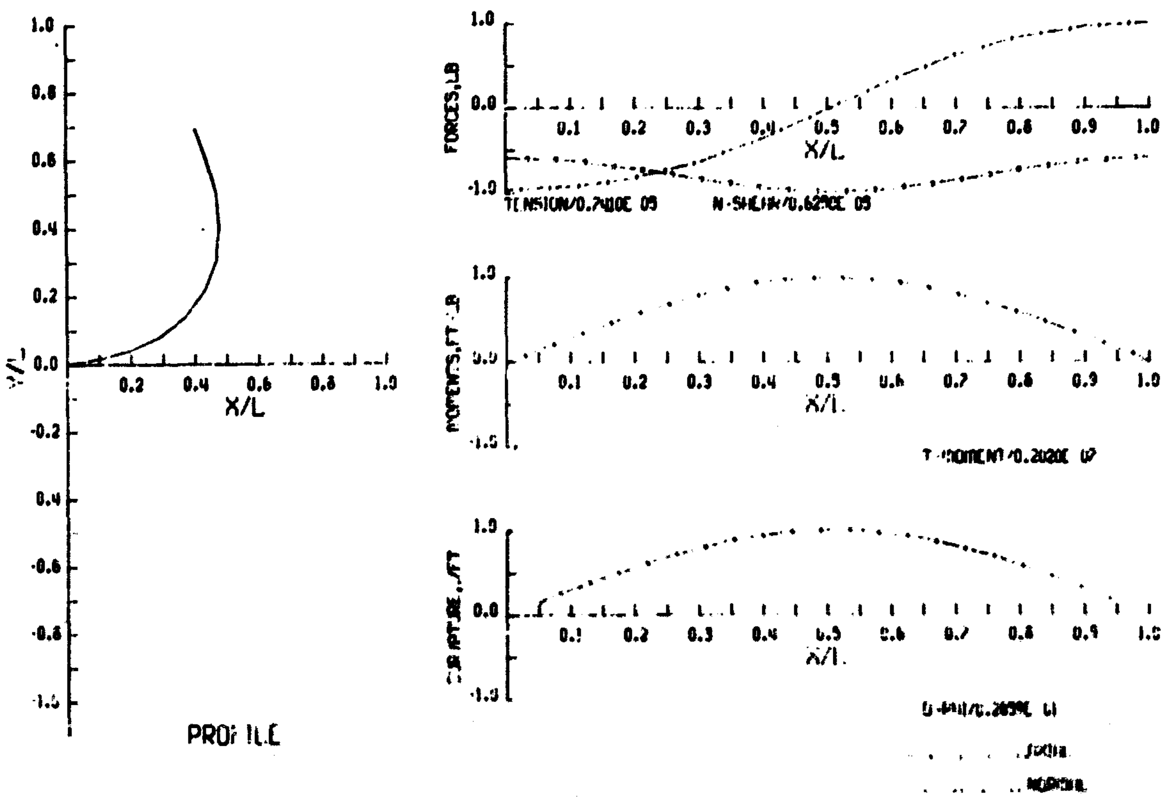

TEST NO. IV 29 - 2 60

HYDRONAUTICS,INC

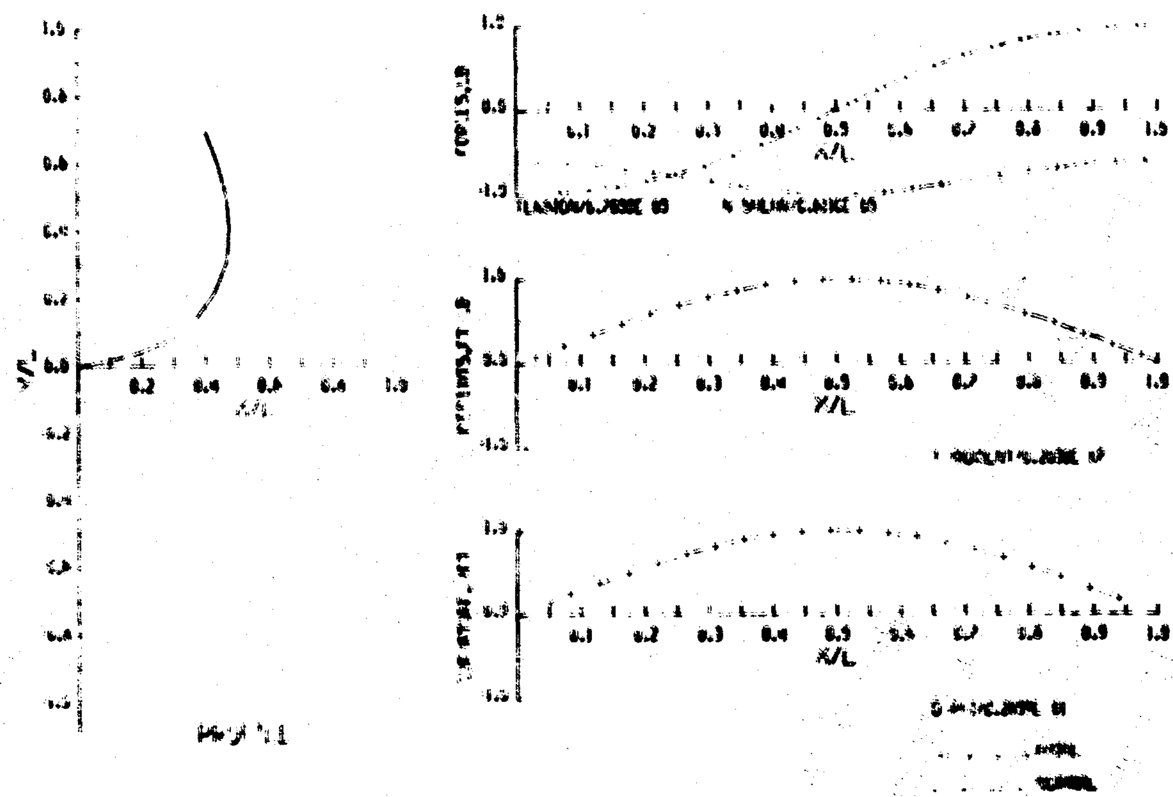

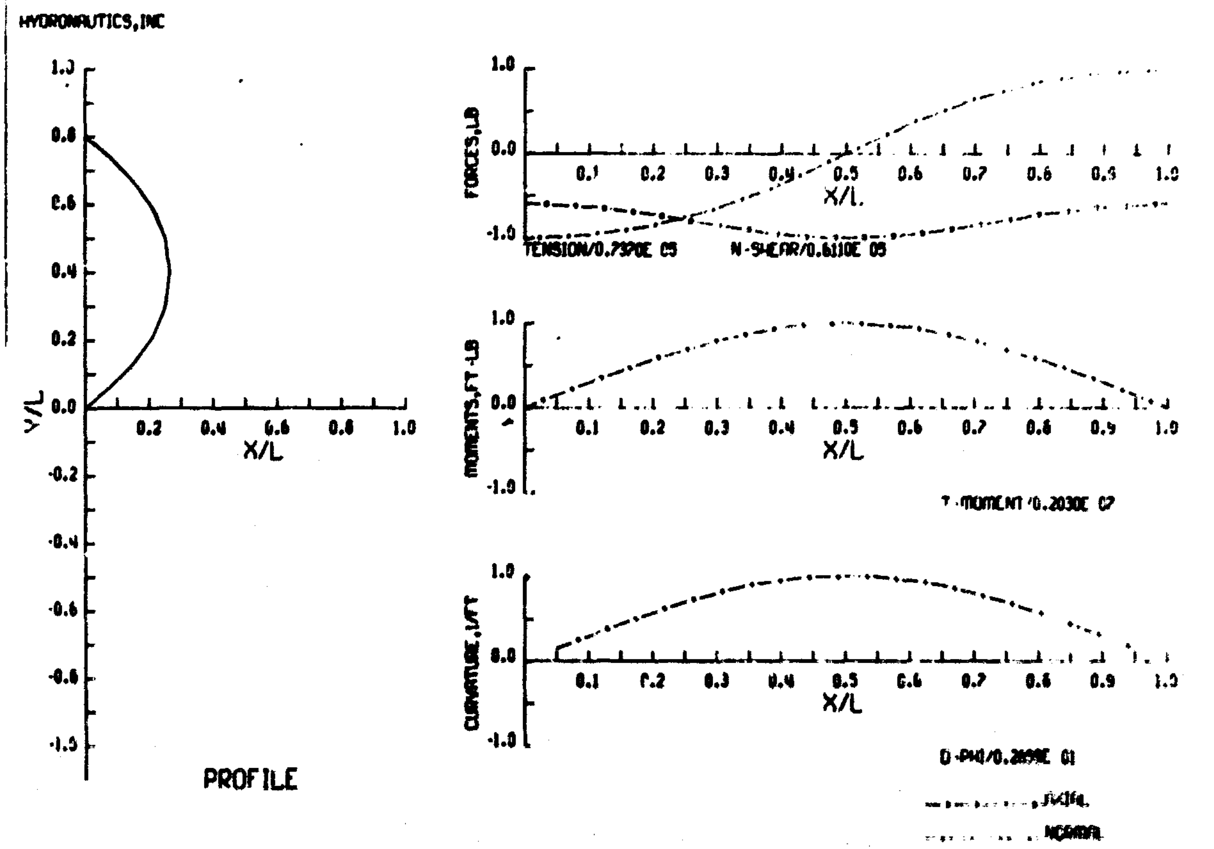

TEST NO. IV 0 - 2 90

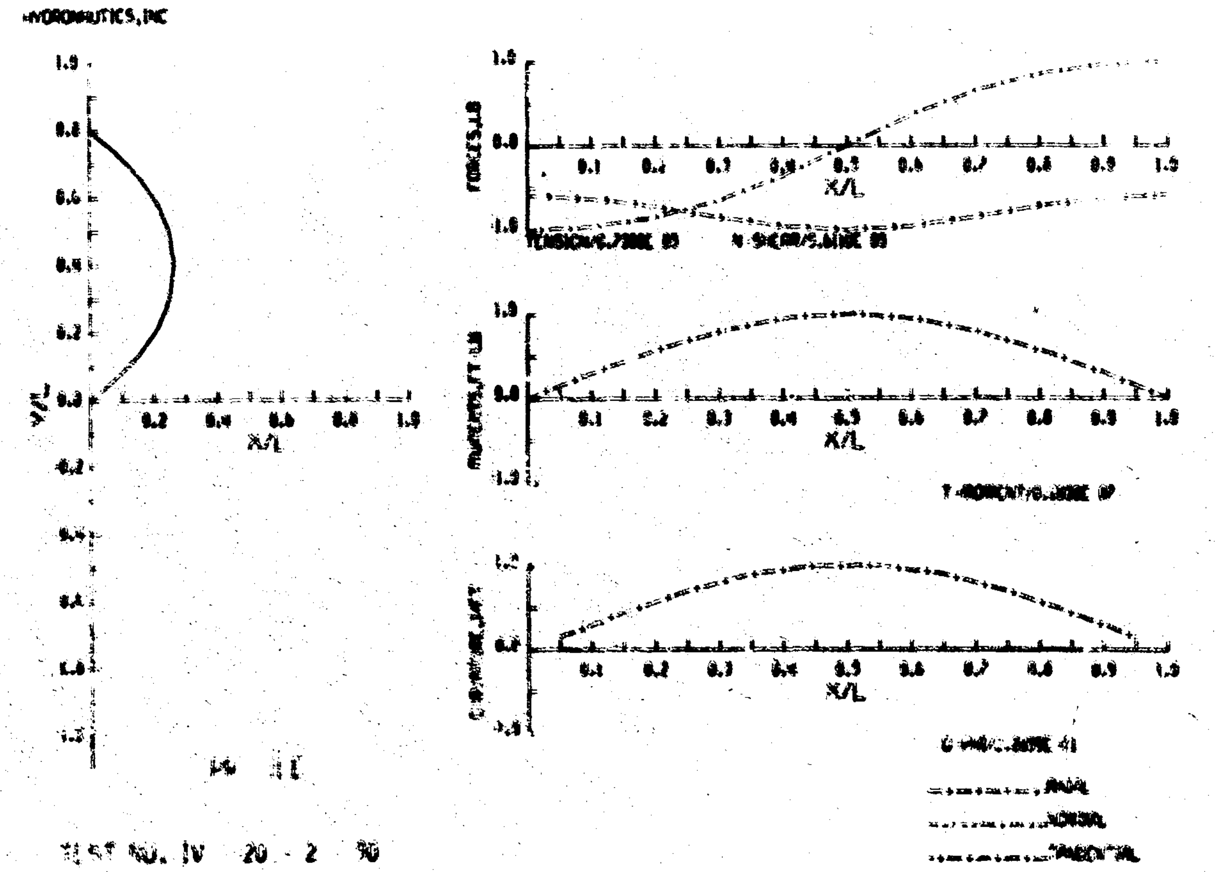

TEST NO. IV 20 - 2 90

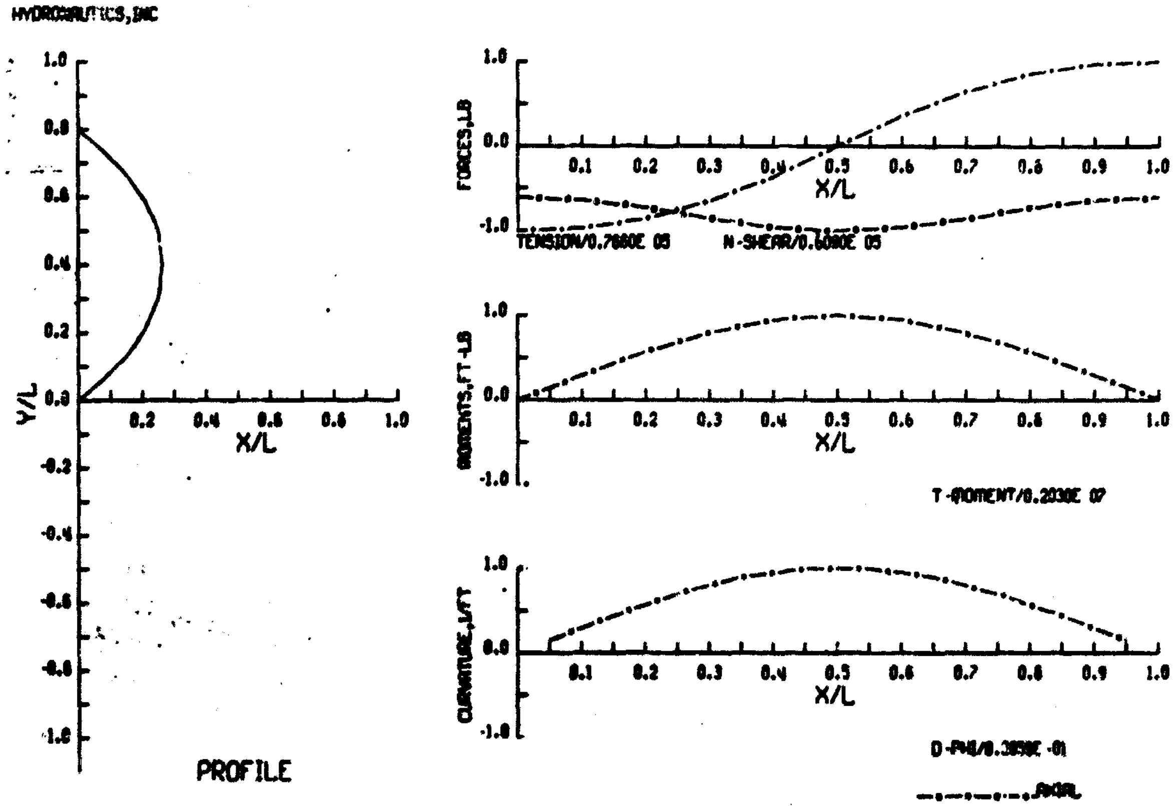

TEST NO. IV - 22 - 0 - 90

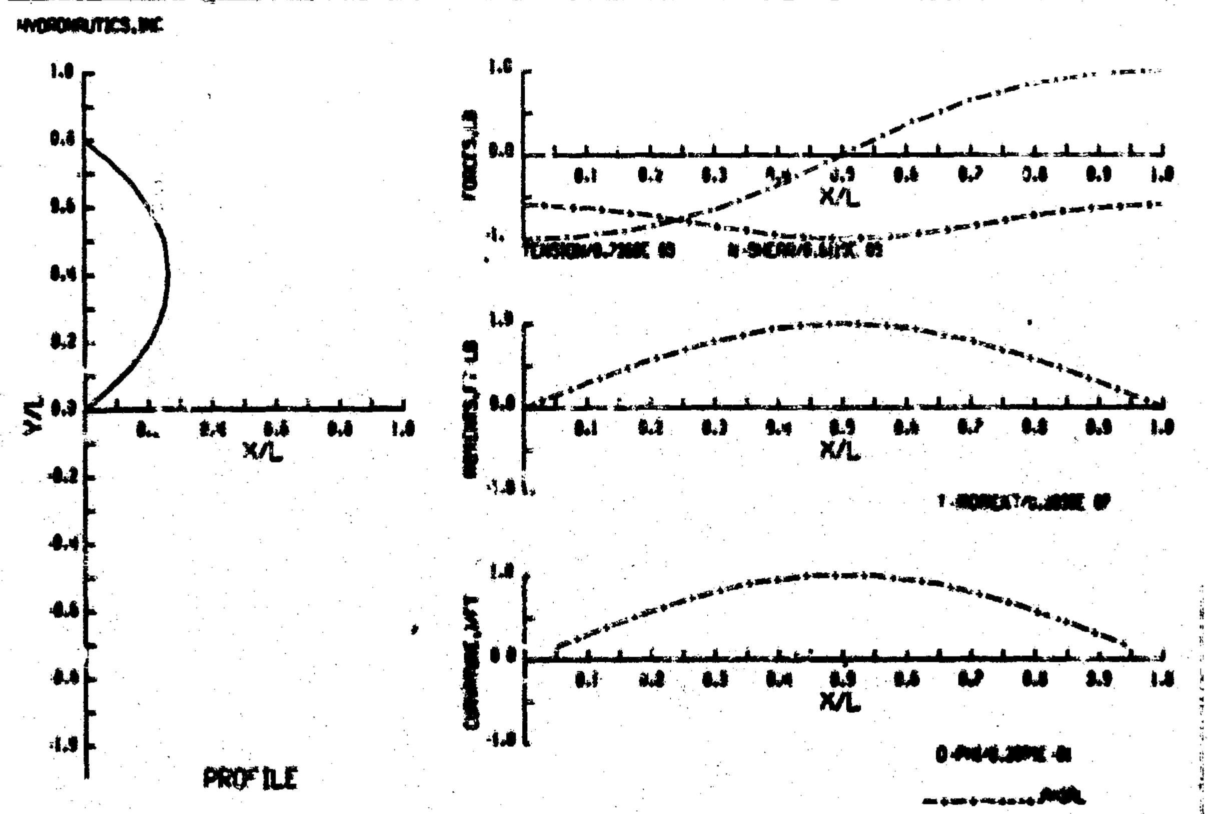

TEST NO. IV - 22 - 2 - 90

HYDRONAUTICS, INC

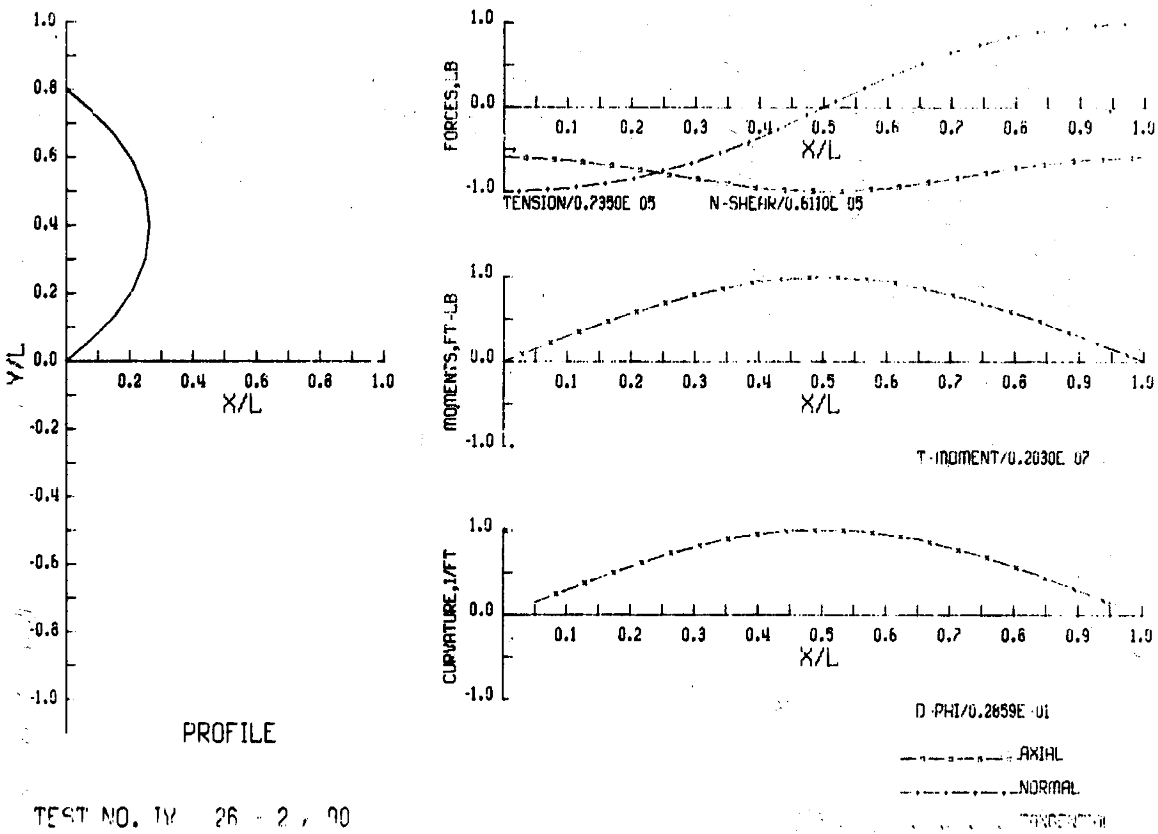

TEST NO. IV 26 - 2 , 90

HYDRONAUTICS, INC

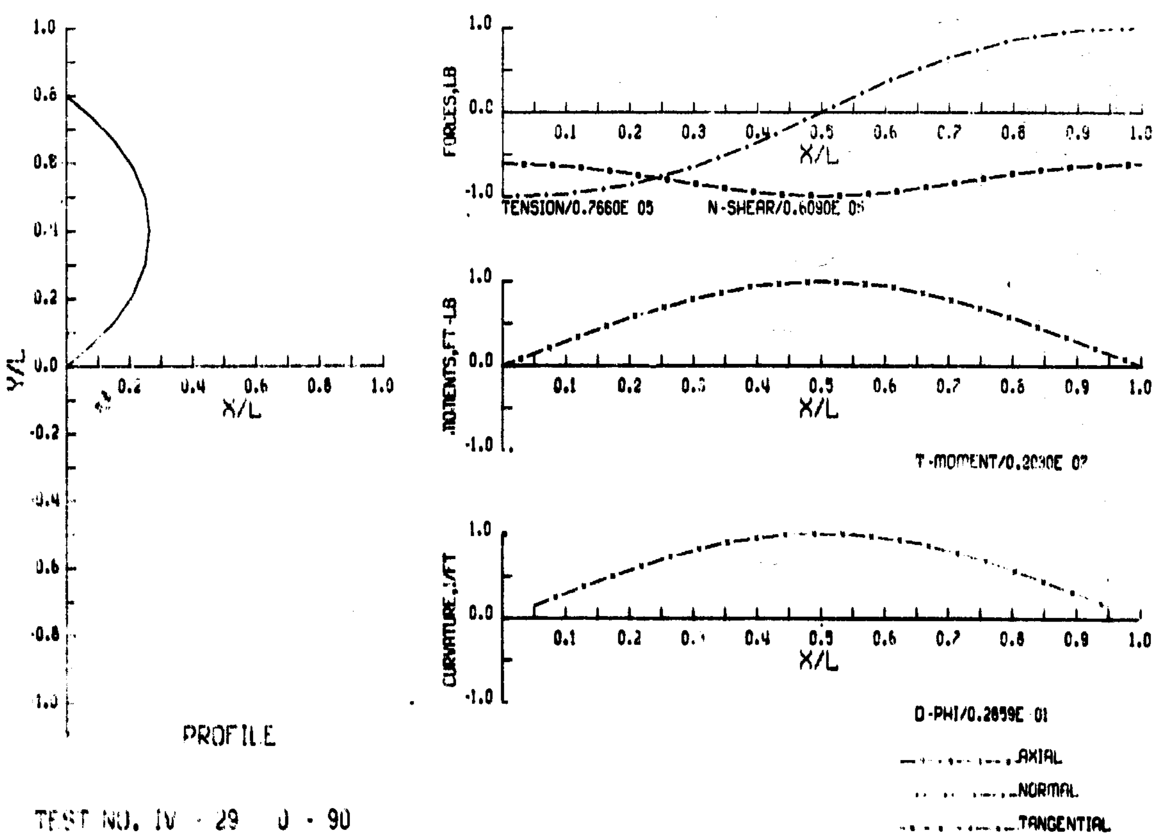

TEST NO. IV - 29 0 - 90

HYDRONAUTICS,INC

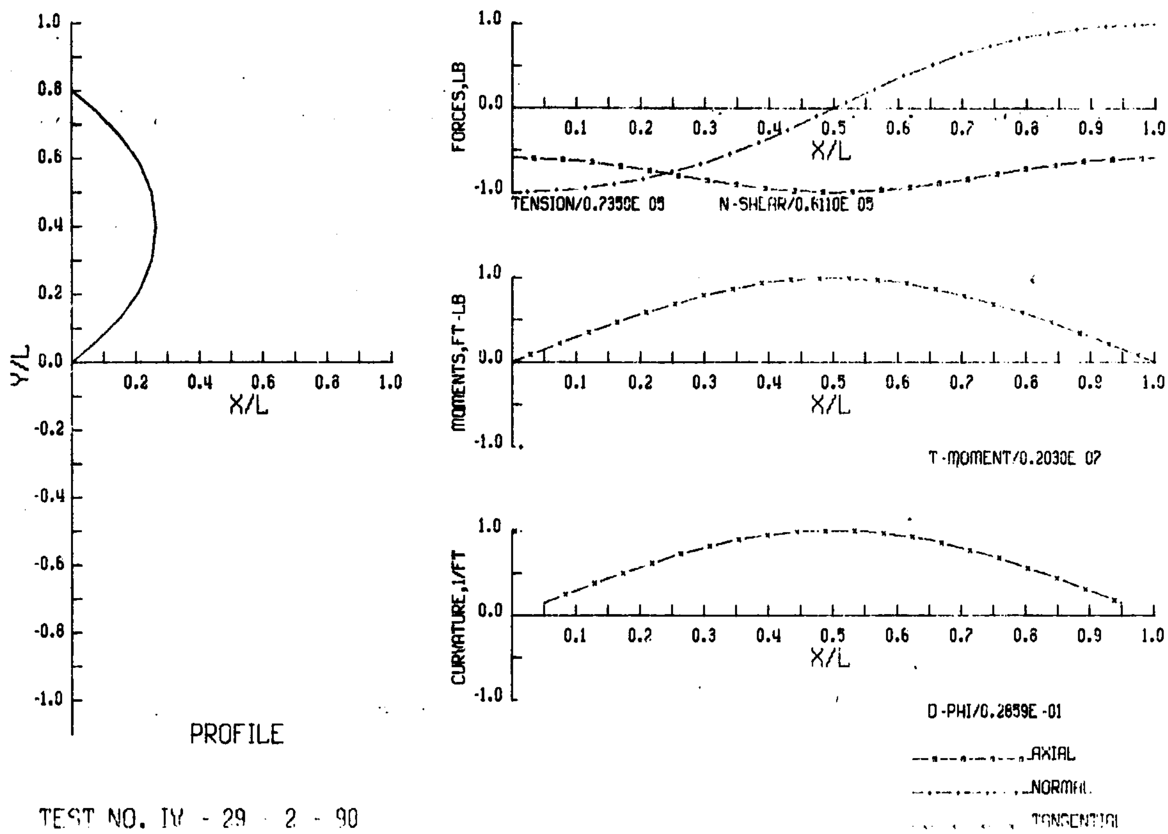

TEST NO. IV - 29 - 2 - 90

HYDRONAUTICS,INC

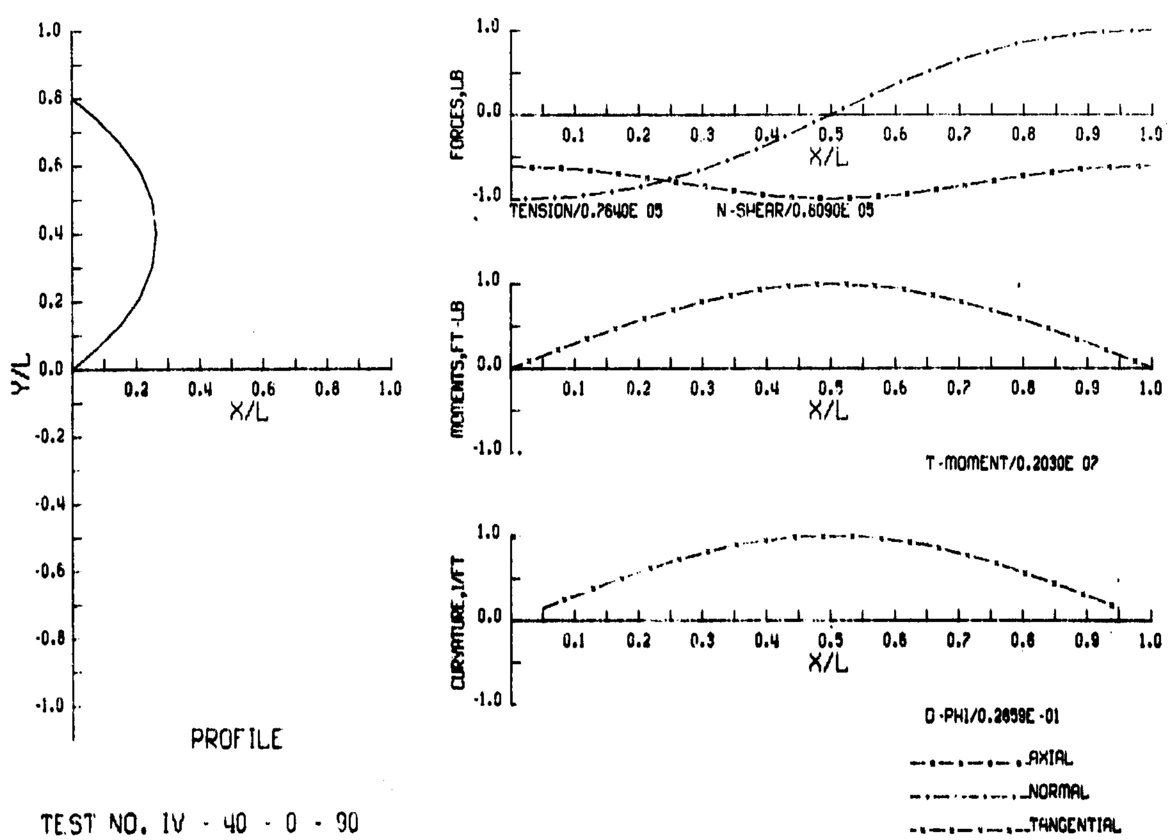

TEST NO. IV - 40 - 0 - 90

HYDRONAUTICS,INC

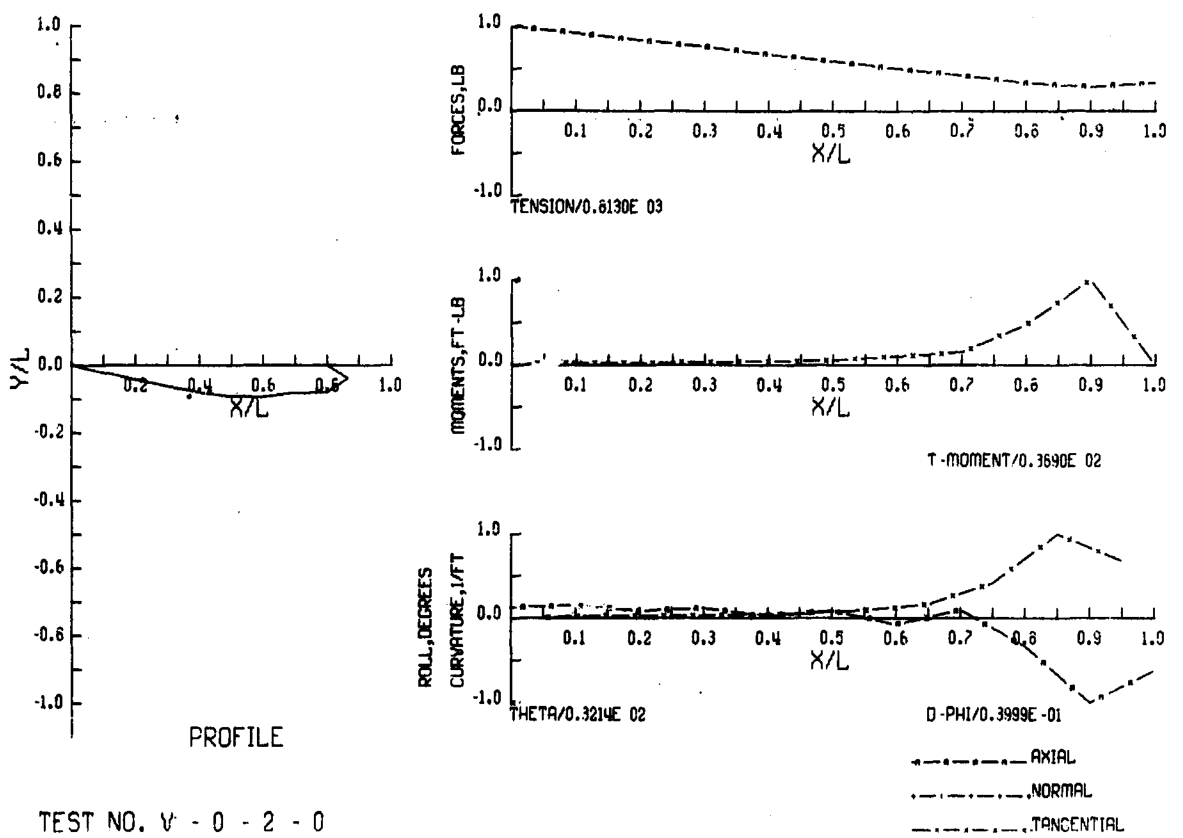

TEST NO. V - 0 - 2 - 0

HYDRONAUTICS,INC

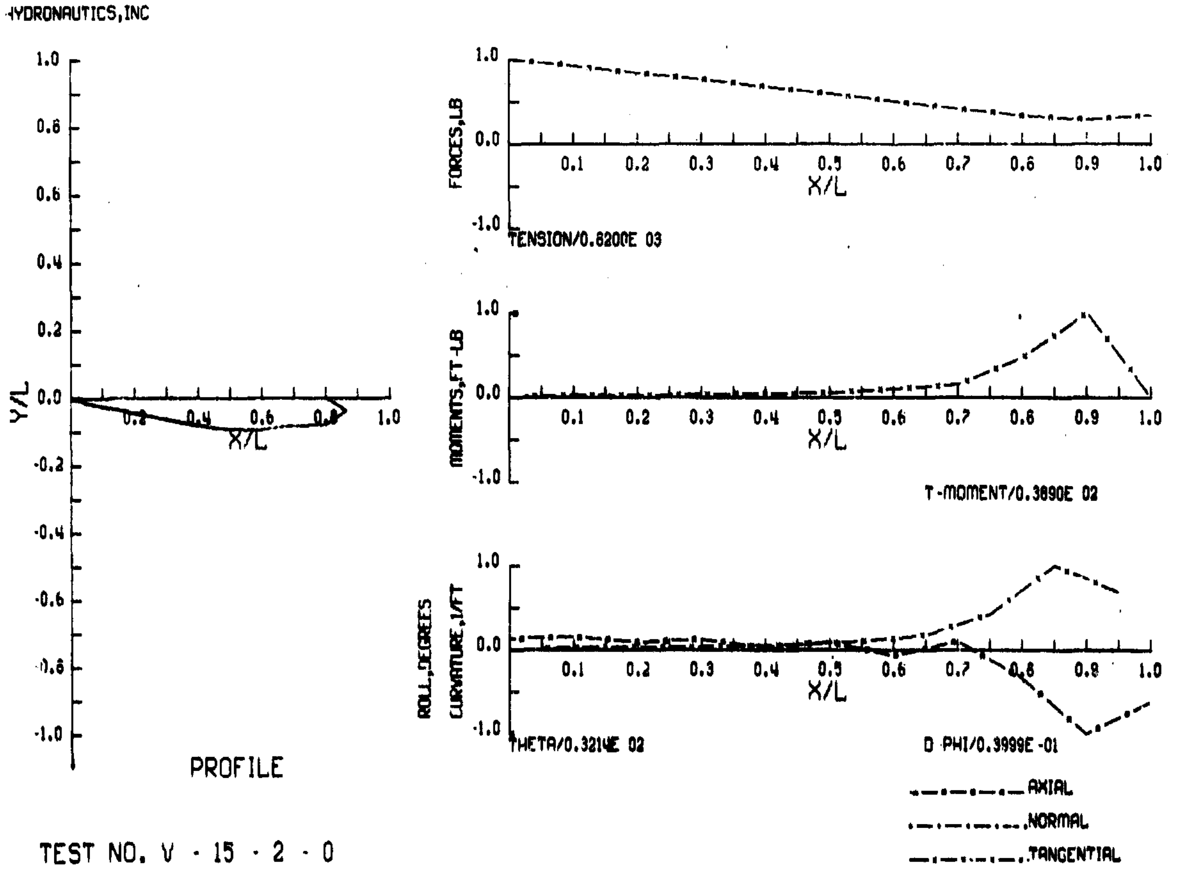

TEST NO. V - 15 - 2 - 0

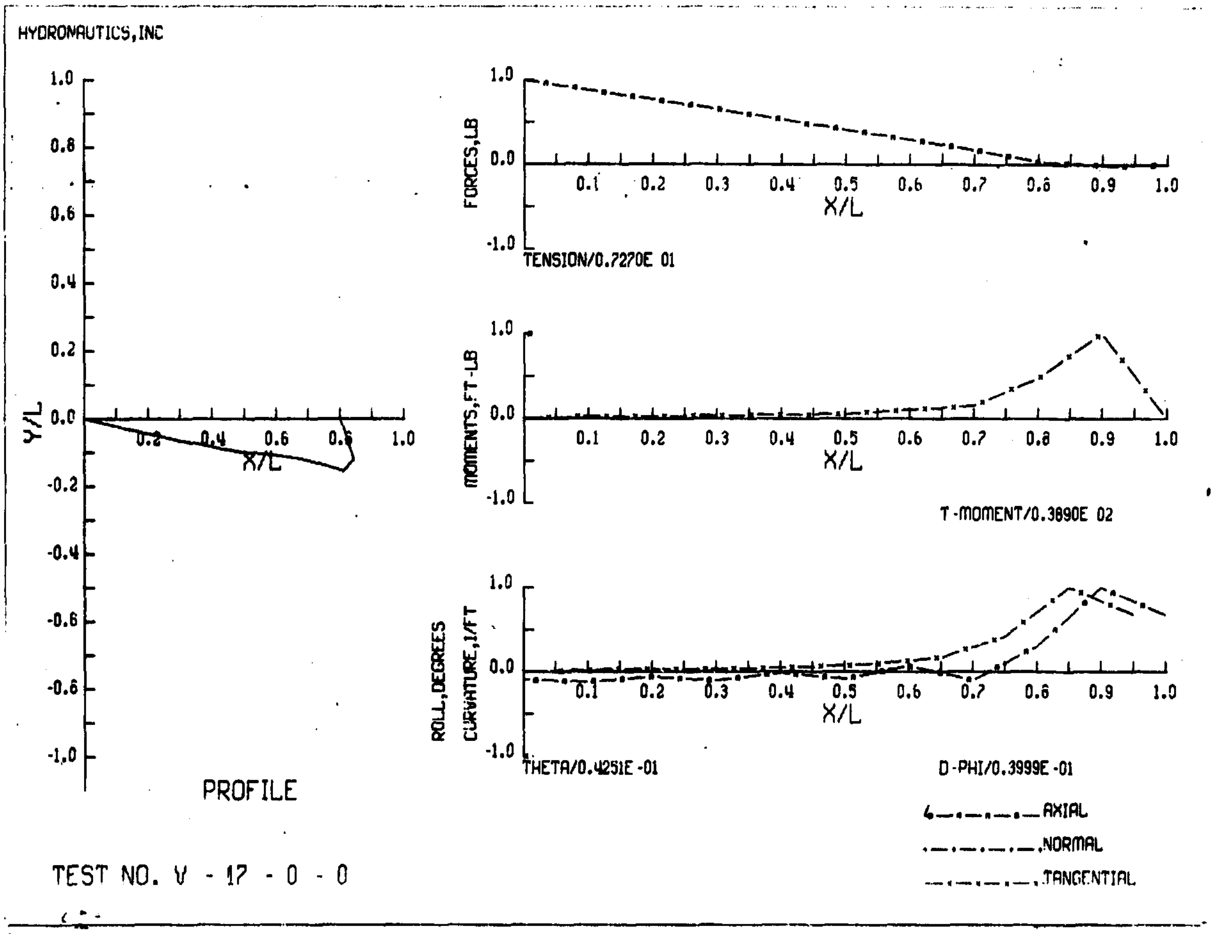
HYDRONAUTICS,INC
Y/L
X/L
PROFILE
FORCES,LB
TENSION/0.7270E 01
MOMENTS,FT-LB
T-MOMENT/0.3890E 02
ROLL,DEGREES
CURVATURE,1/FT
THETA/0.4251E-01
D-PHI/0.3999E-01
AXIAL
NORMAL
TANGENTIAL
TEST NO. V - 17 - 0 - 0

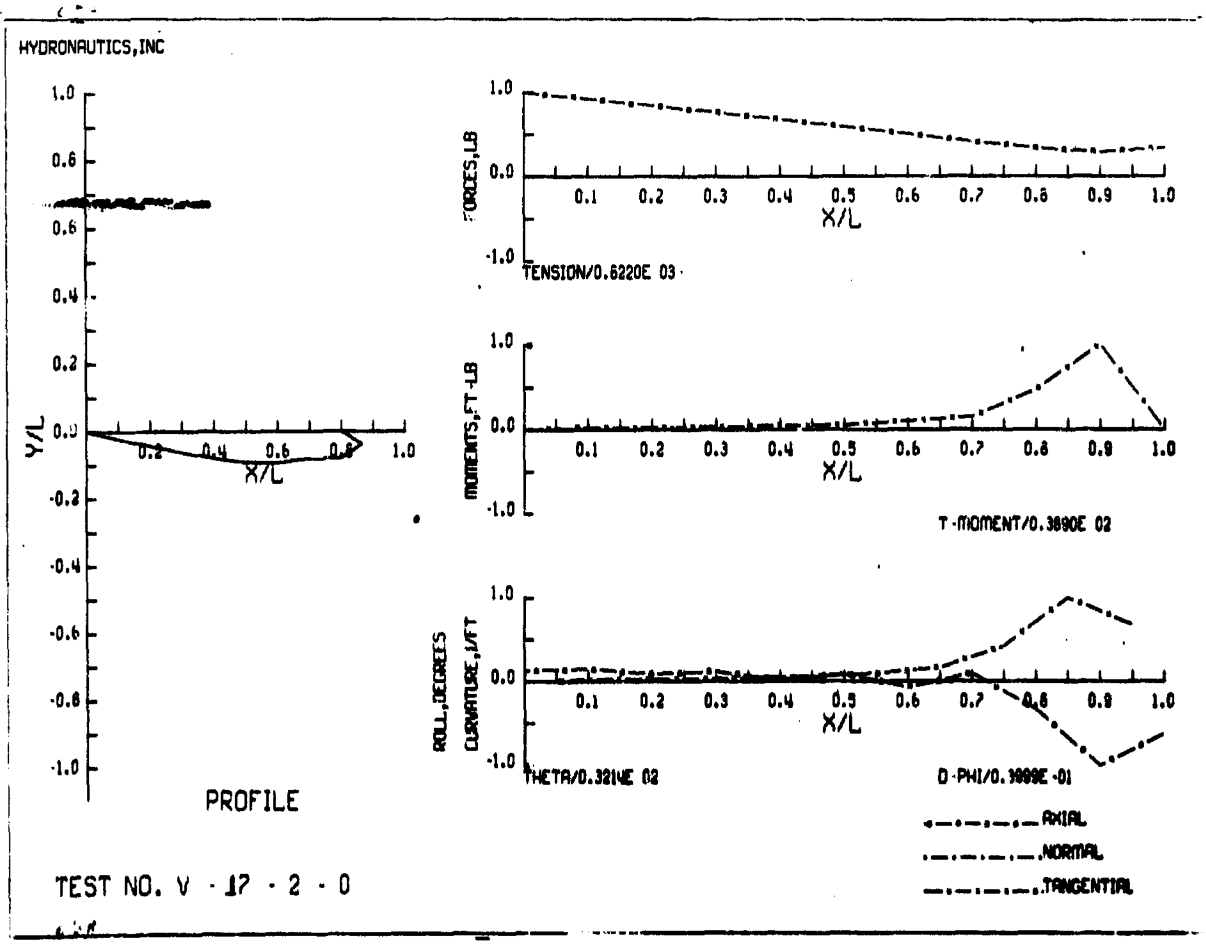
HYDRONAUTICS,INC
Y/L
X/L
PROFILE
FORCES,LB
TENSION/0.6220E 03
MOMENTS,FT-LB
T-MOMENT/0.3890E 02
ROLL,DEGREES
CURVATURE,1/FT
THETA/0.3214E 02
D-PHI/0.3999E-01
AXIAL
NORMAL
TANGENTIAL
TEST NO. V - 17 - 2 - 0

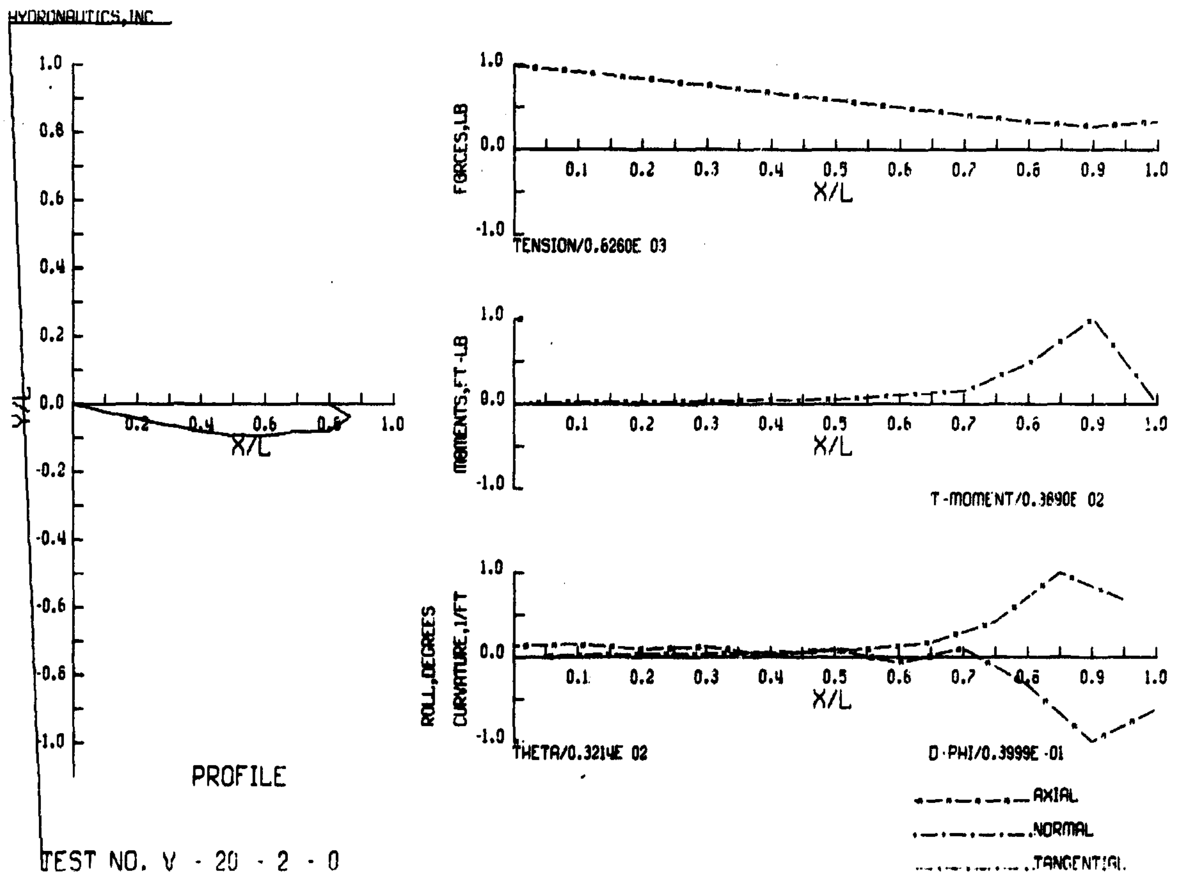
HYDRONAUTICS, INC
Y/L
X/L
PROFILE
FORCES, LB
TENSION/0.6260E 03
MOMENTS, FT-LB
T-MOMENT/0.3890E 02
ROLL, DEGREES
CURVATURE, 1/FT
THETA/0.3214E 02
D-PHI/0.3999E -01
AXIAL
NORMAL
TANGENTIAL
TEST NO. V - 20 - 2 - 0

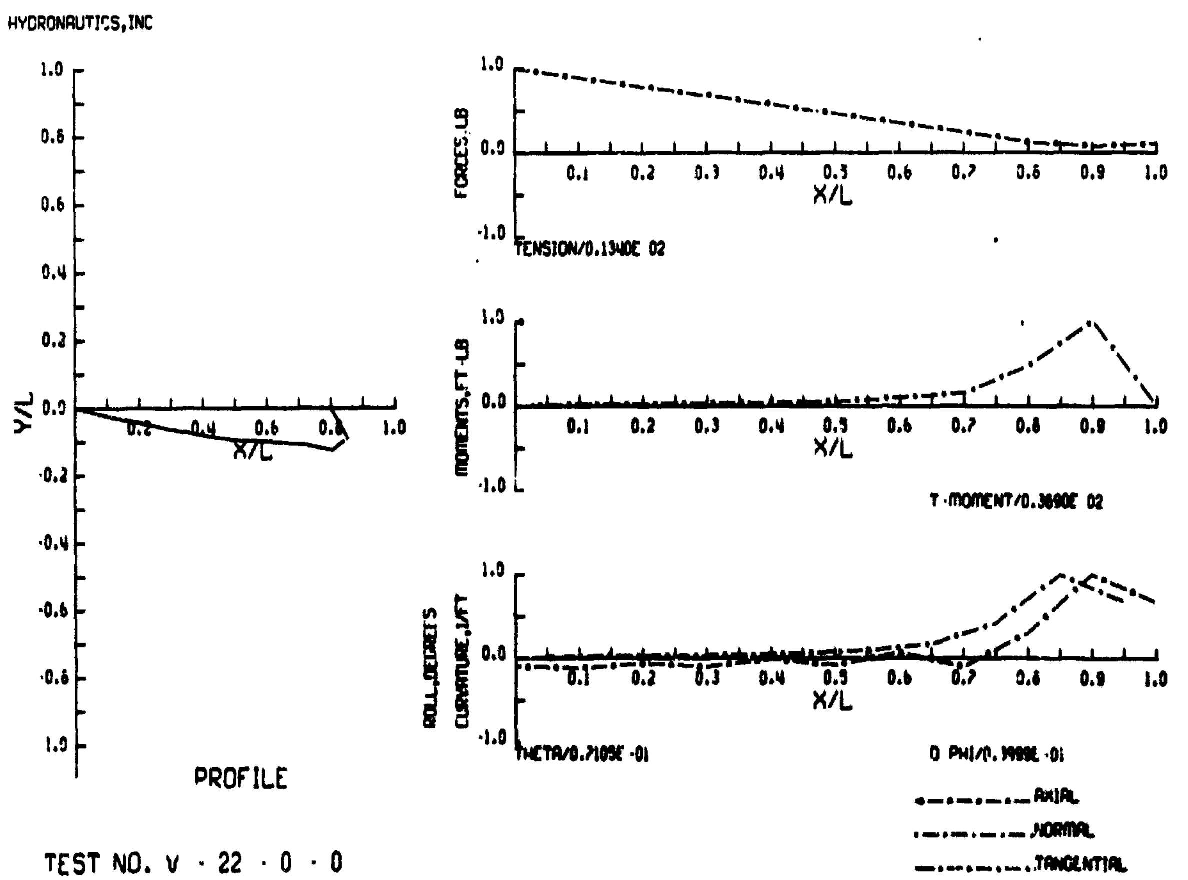
HYDRONAUTICS, INC
Y/L
X/L
PROFILE
FORCES, LB
TENSION/0.1340E 02
MOMENTS, FT-LB
T-MOMENT/0.3890E 02
ROLL, DEGREES
CURVATURE, 1/FT
THETA/0.7105E -01
D PHI/0.3999E -01
AXIAL
NORMAL
TANGENTIAL
TEST NO. V - 22 - 0 - 0

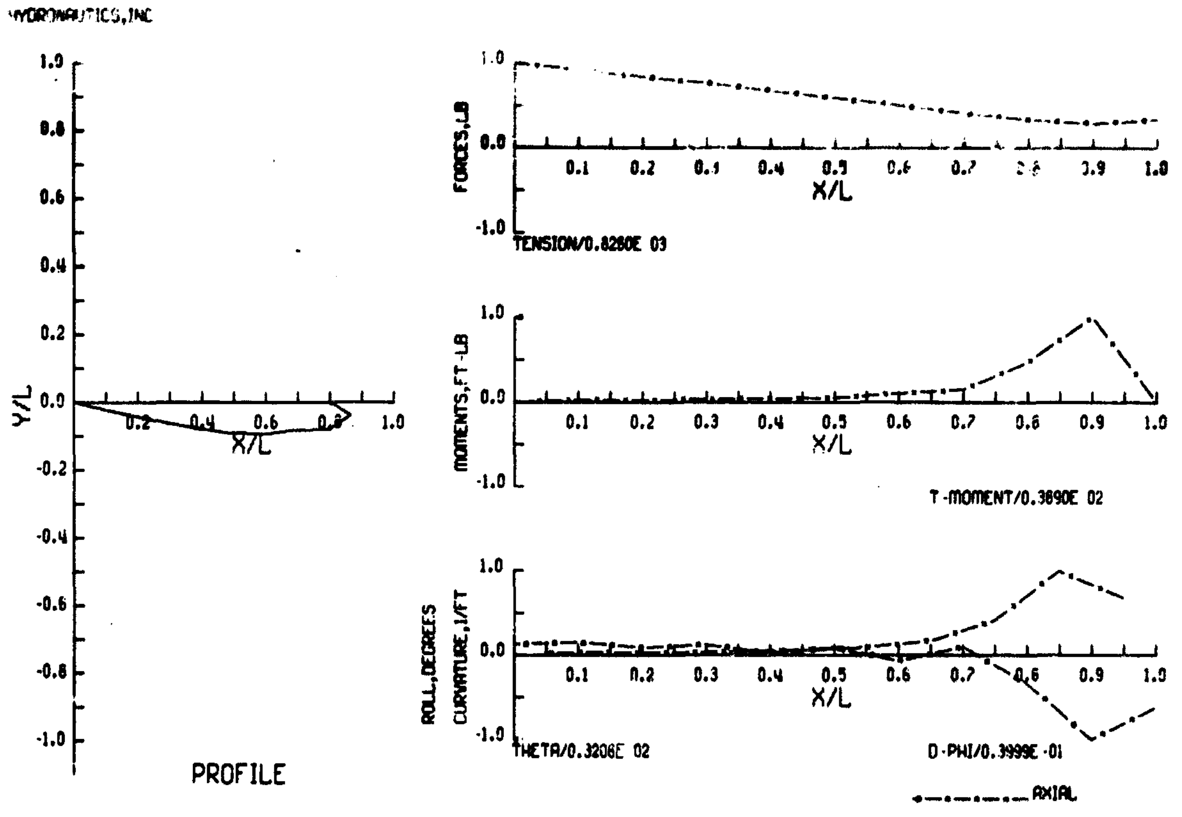

TEST NO. V - 22 - 2 - 0

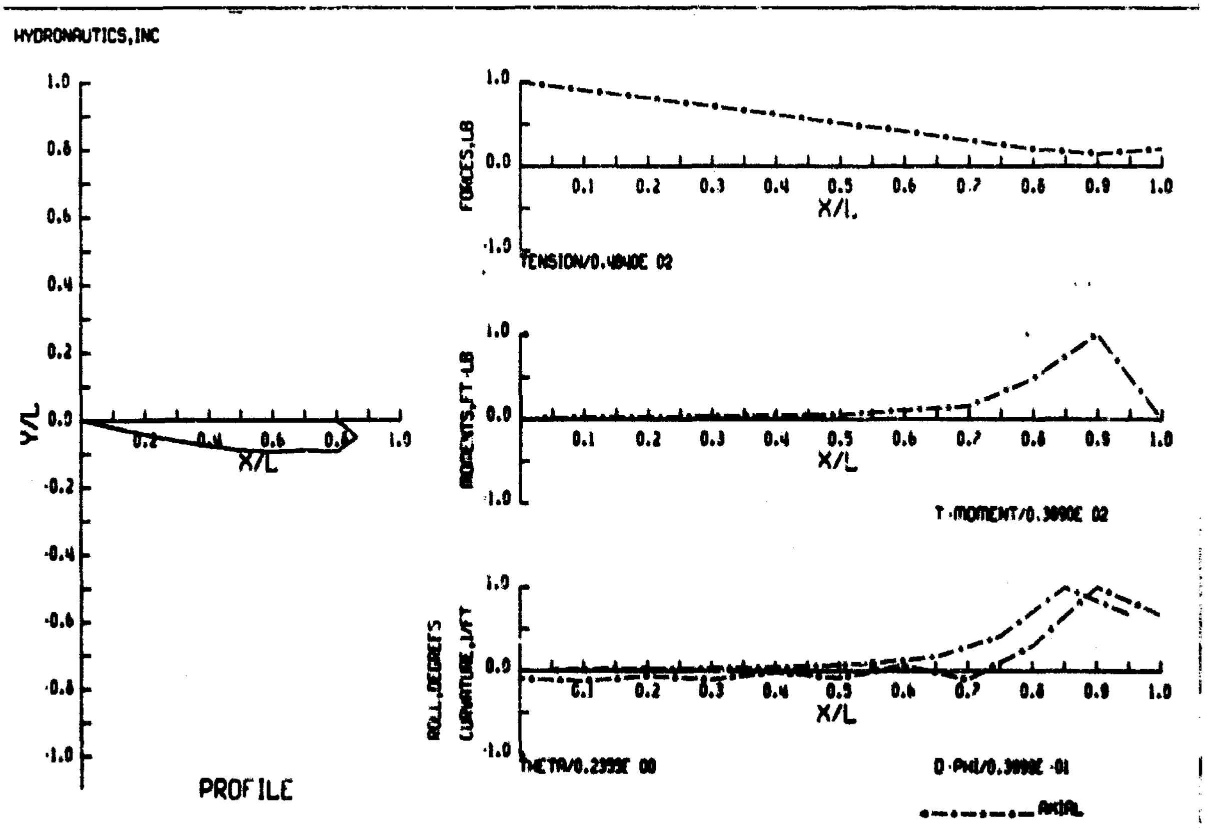

TEST NO. V - 40 - 0 - 0

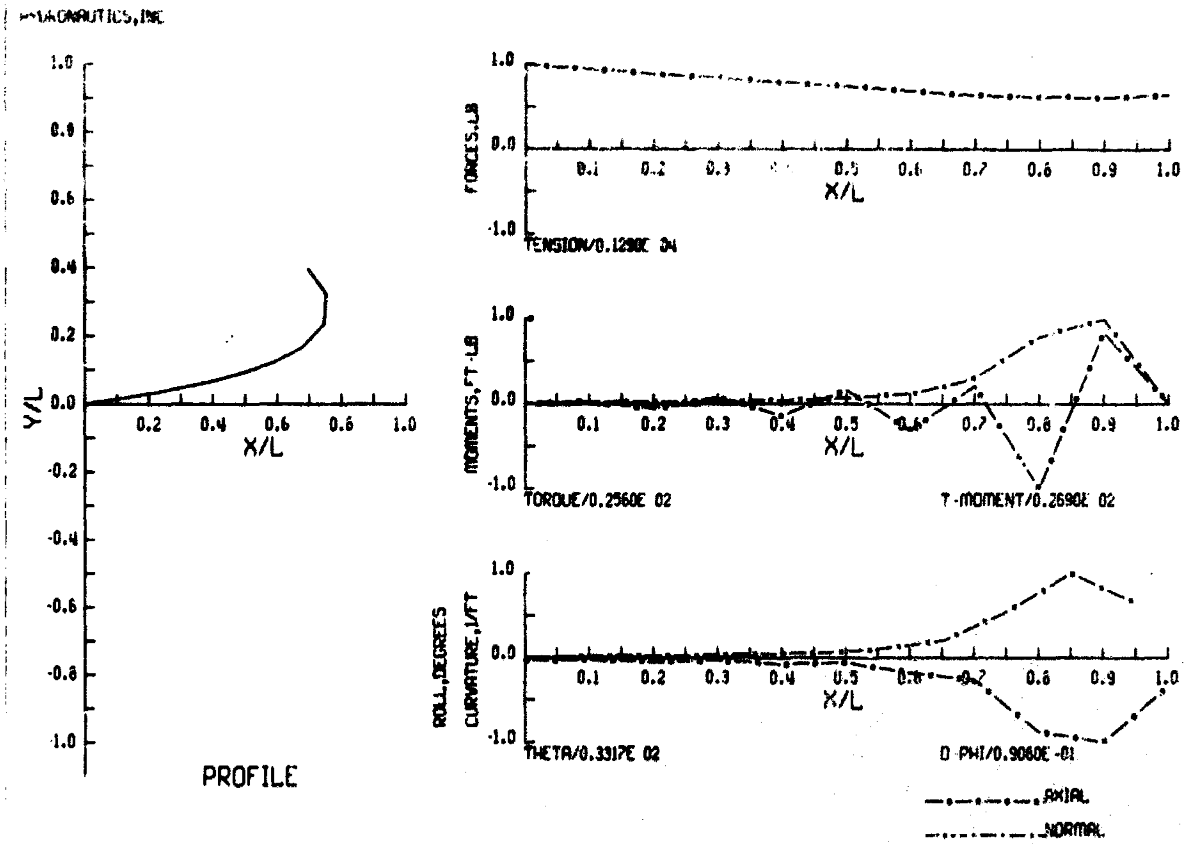

TEST NO. V - 0 - 2 - 30

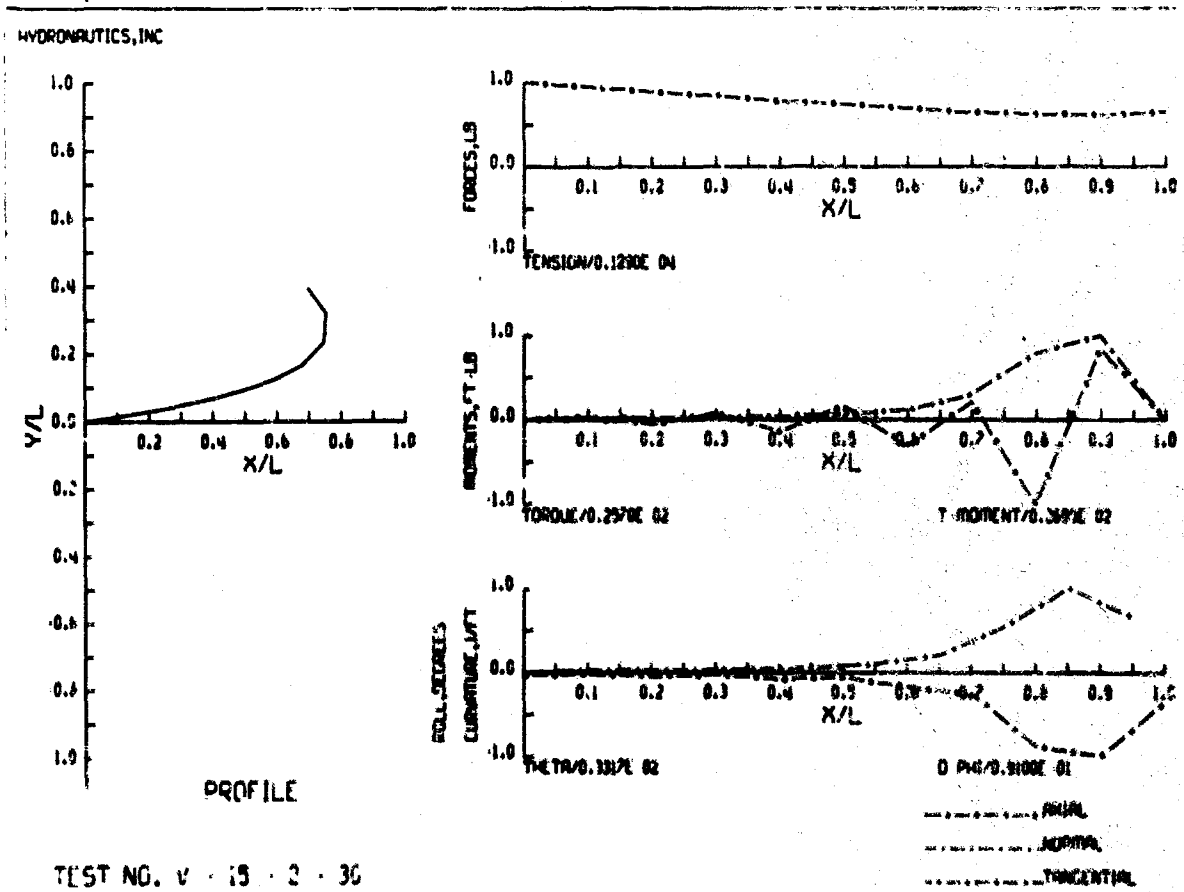

TEST NO. V - 15 - 2 - 30

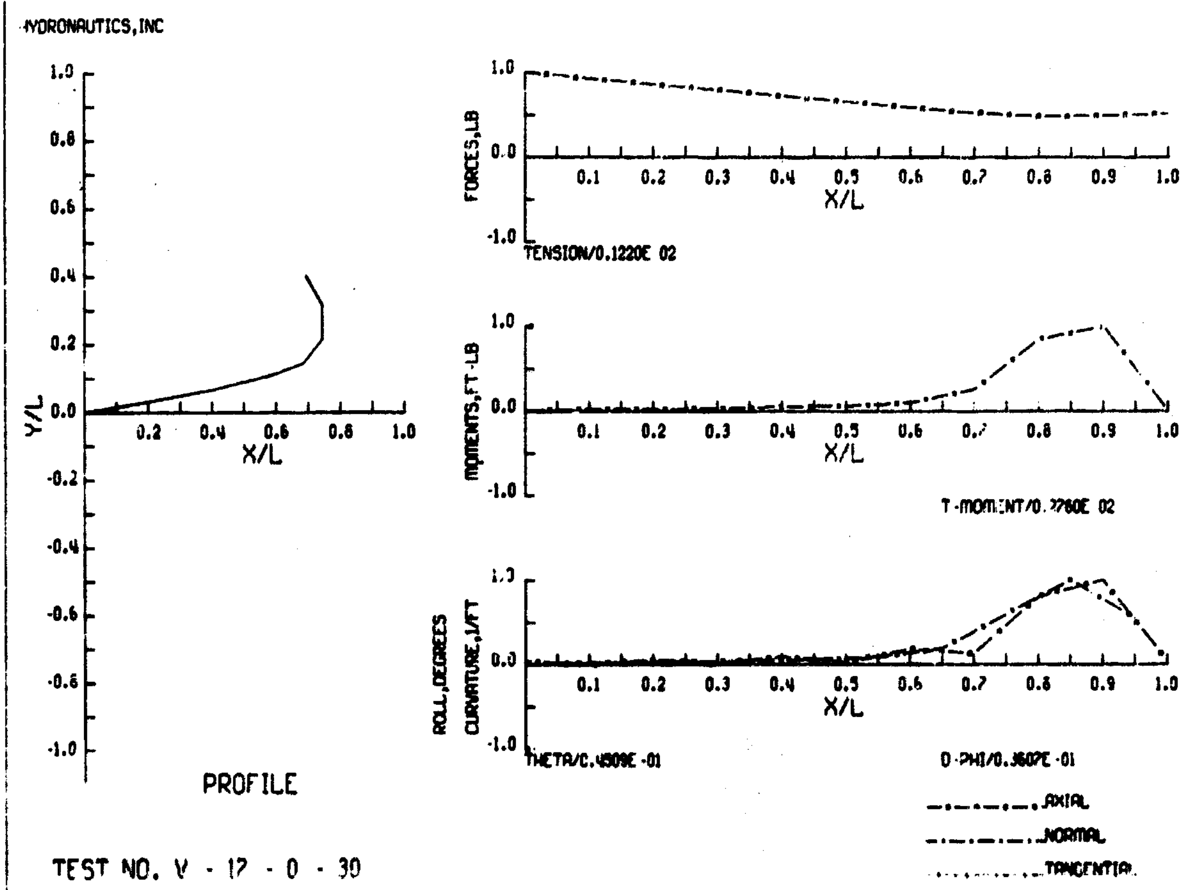

TEST NO. V - 17 - 0 - 30

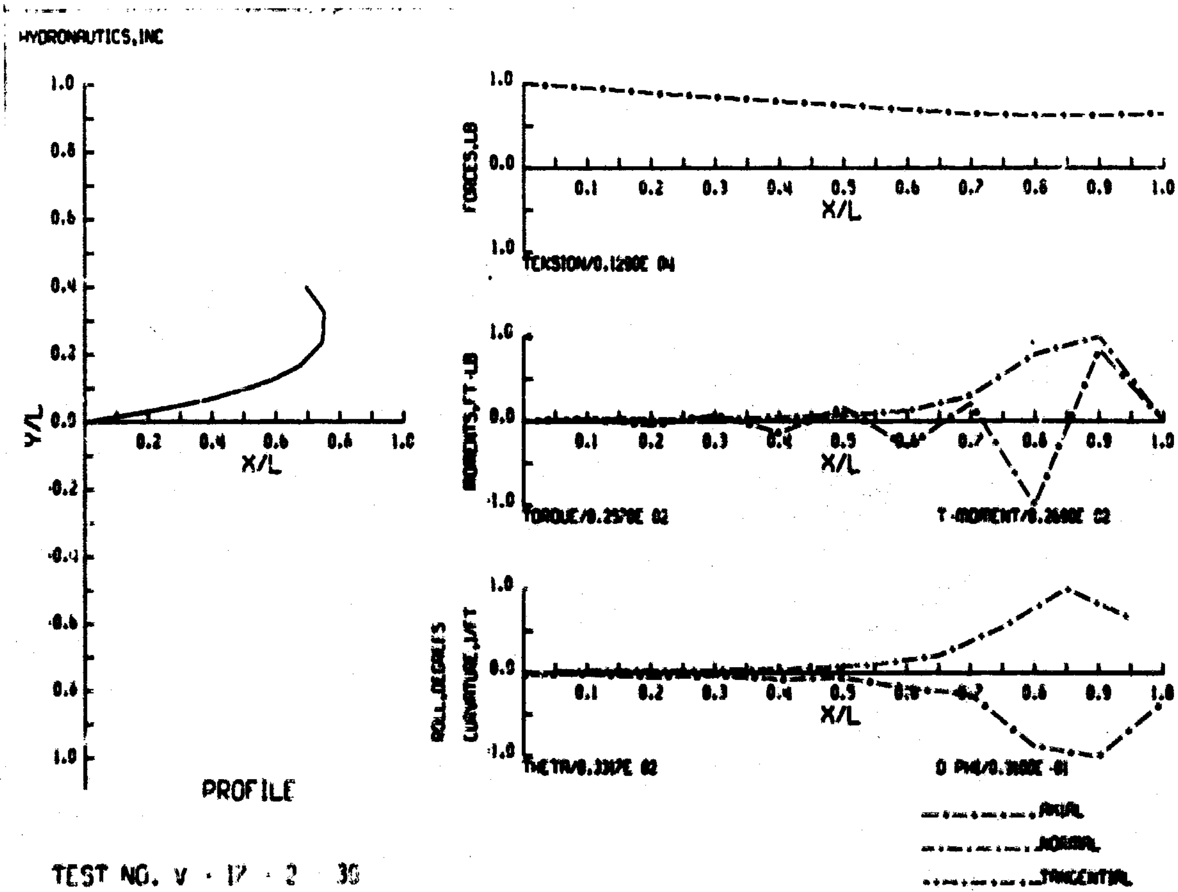

TEST NO. V - 17 - 2 - 30

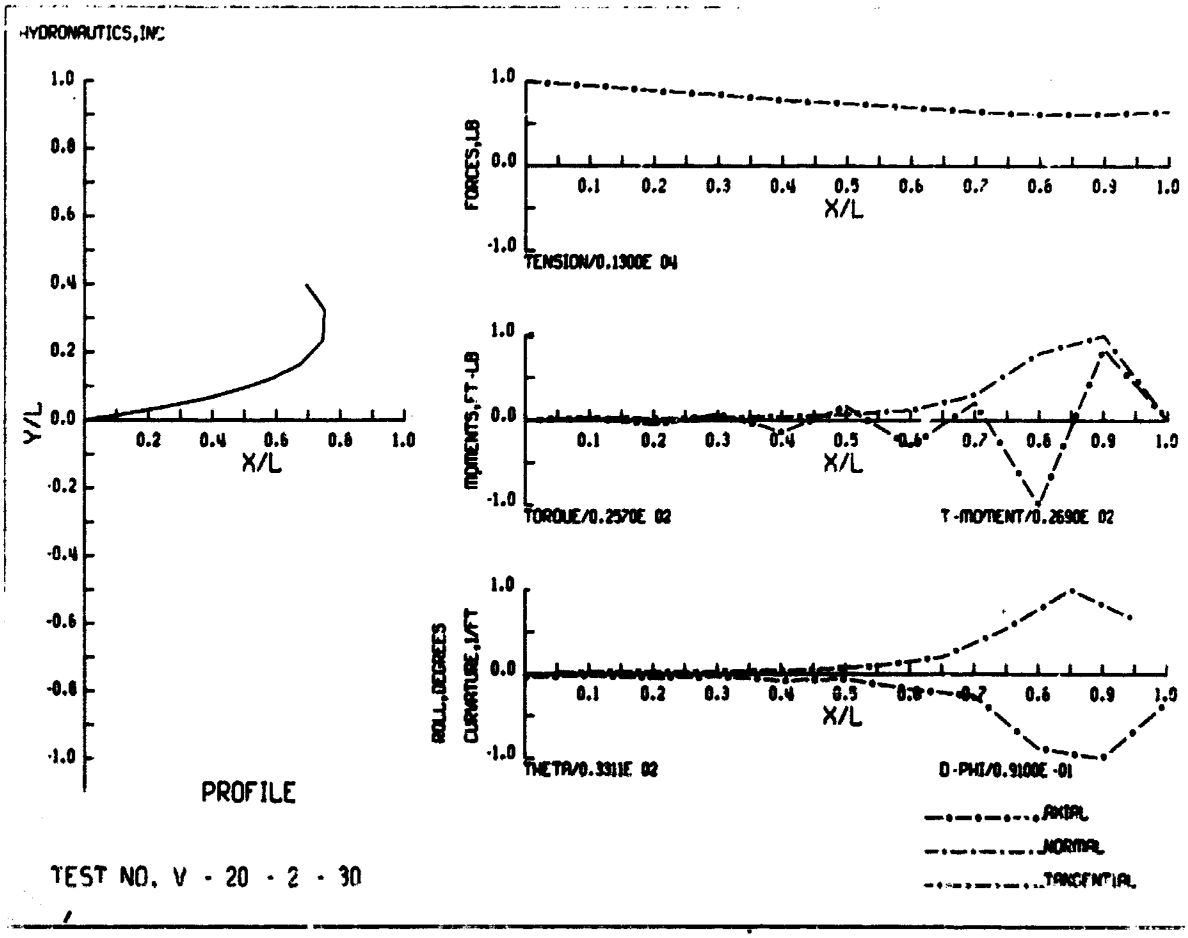
HYDRONAUTICS,INC
Y/L
X/L
PROFILE
FORCES,LB
TENSION/0.1300E 04
MOMENTS,FT-LB
TORQUE/0.2570E 02
T-MOMENT/0.2690E 02
ROLL,DEGREES
CURVATURE,1/FT
THETA/0.3311E 02
D-PHI/0.9100E -01
AXIAL
NORMAL
TANGENTIAL
TEST NO. V - 20 - 2 - 30

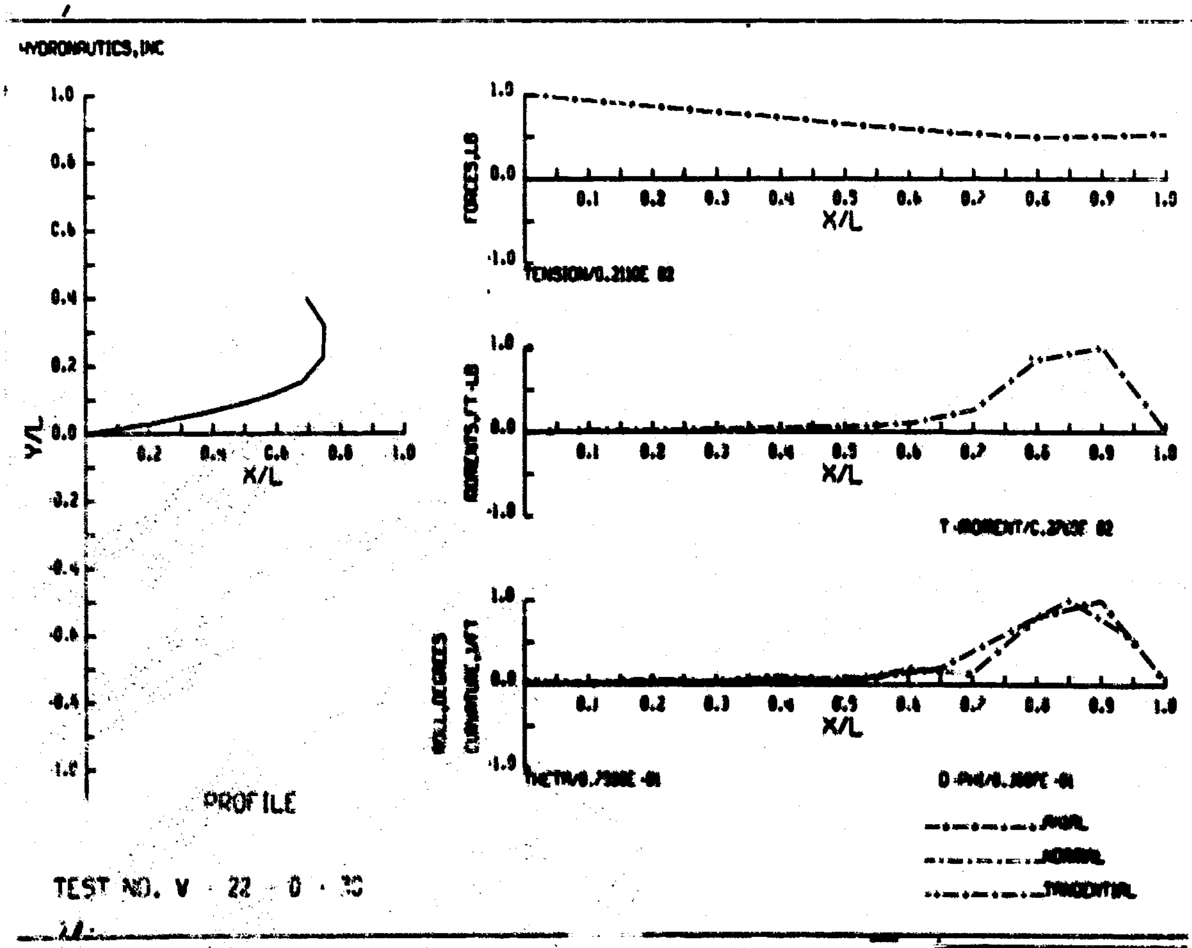
HYDRONAUTICS,INC
Y/L
X/L
PROFILE
FORCES,LB
MOMENTS,FT-LB
ROLL,DEGREES
CURVATURE,1/FT
AXIAL
NORMAL
TANGENTIAL

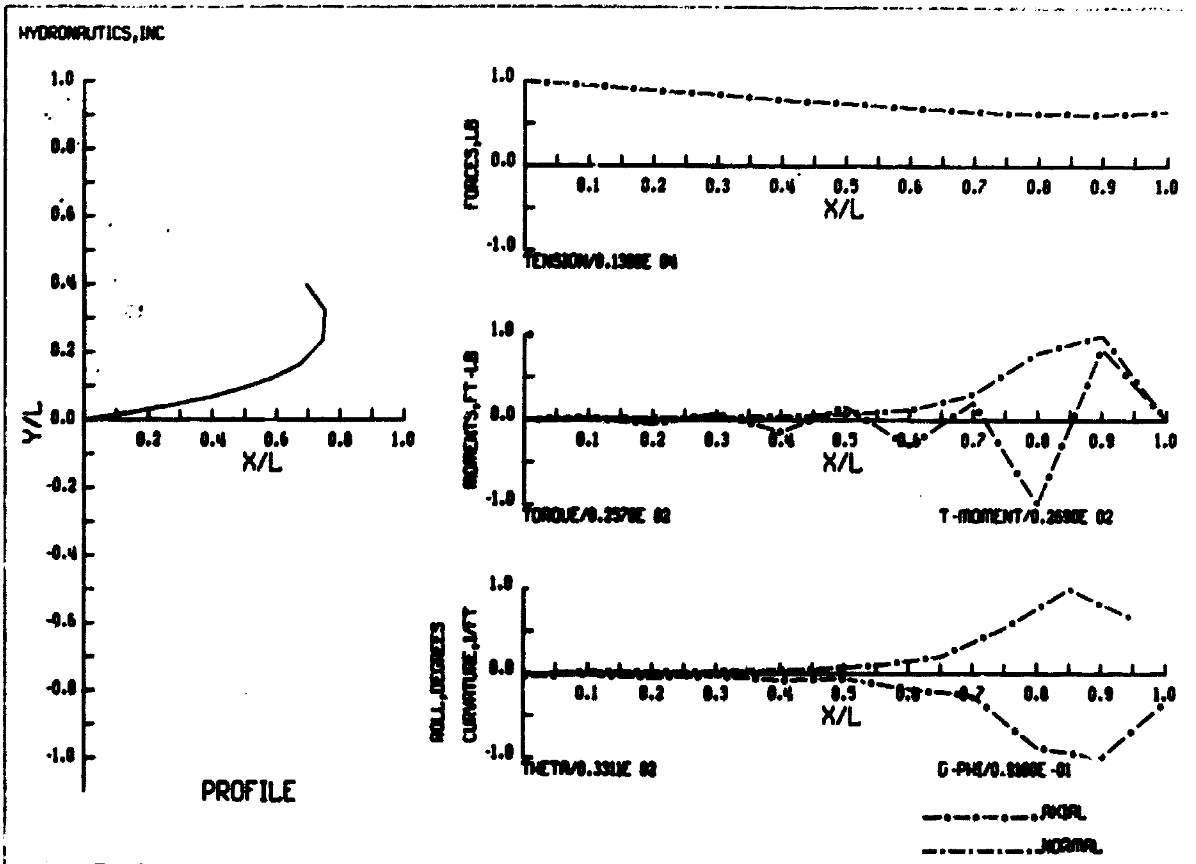

TEST NO. V - 22 - 2 - 30

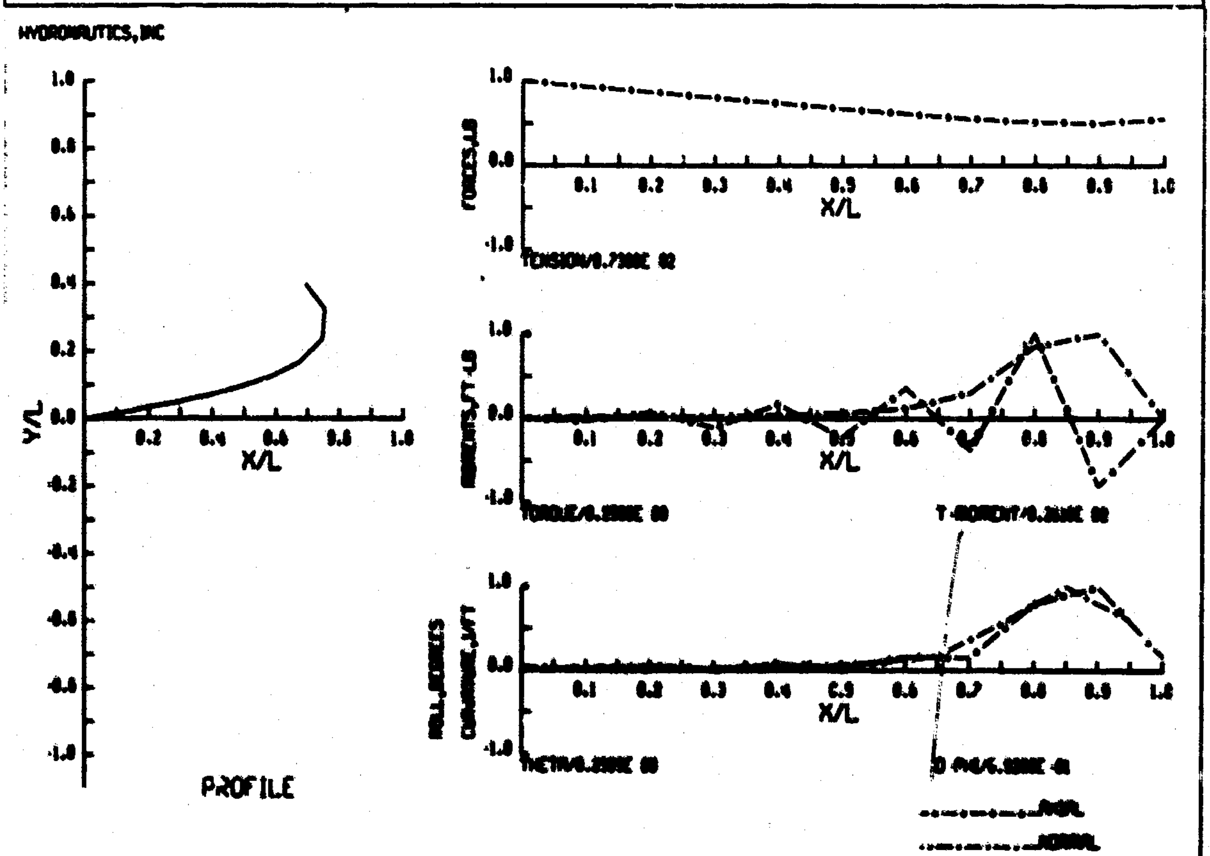

TEST NO. V - 40 - 0 - 30

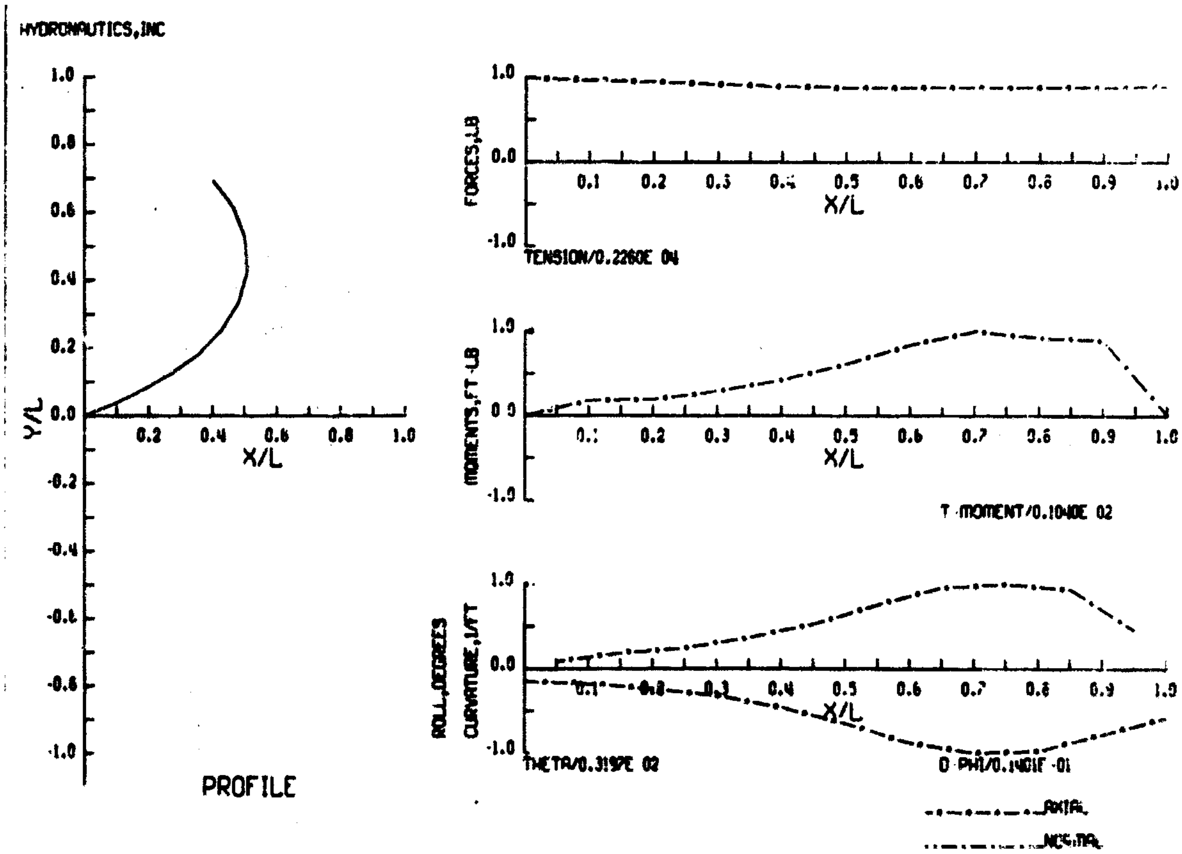

TEST NO. V - 0 - 2 - 60

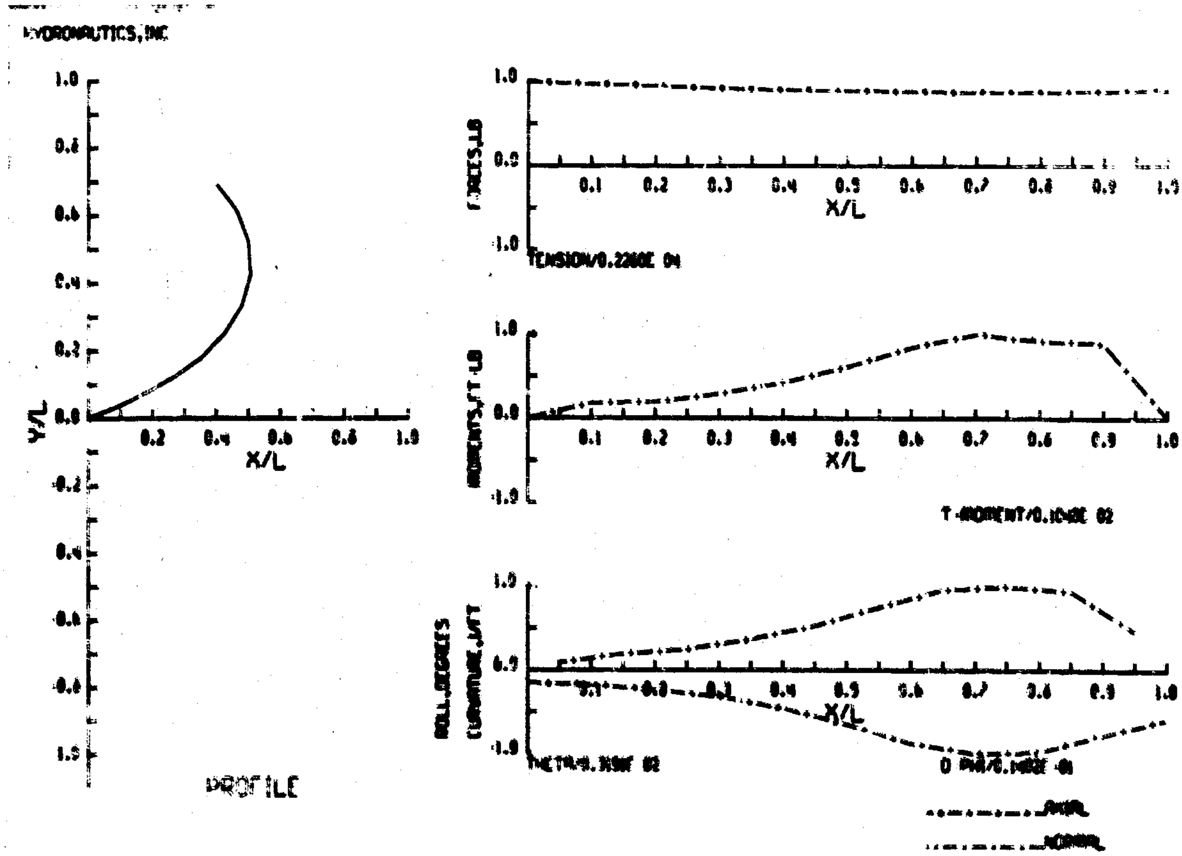

TEST NO. V - 15 - 2 - 60

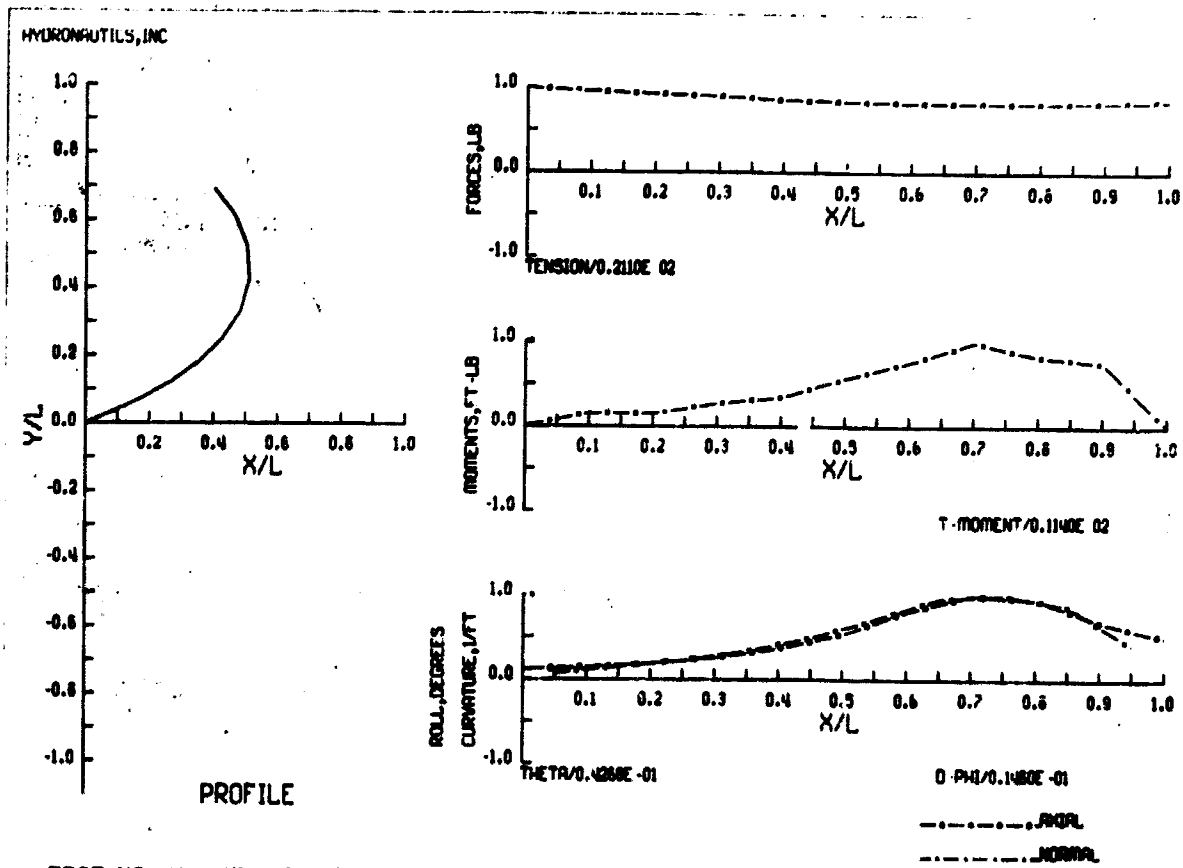

TEST NO. V - 17 - 0 - 60

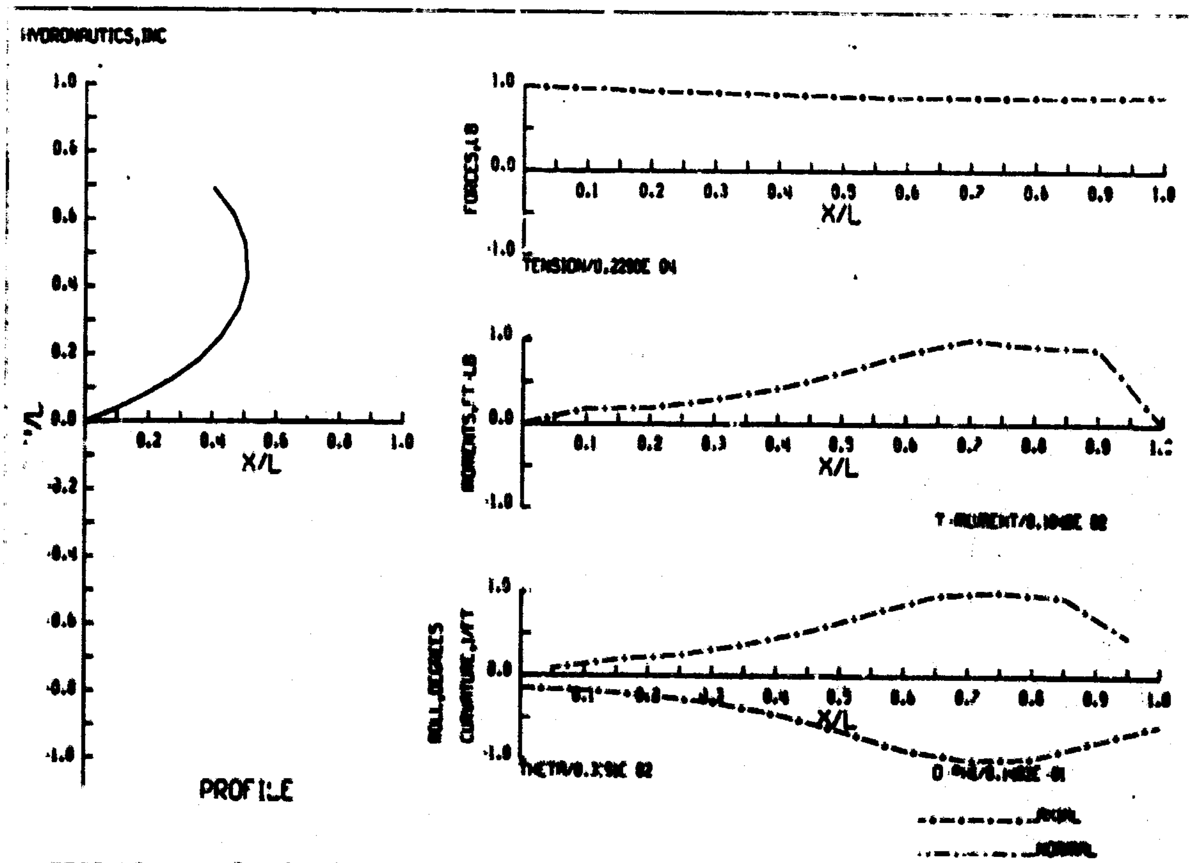

TEST NO. V - 17 - 2 - 60

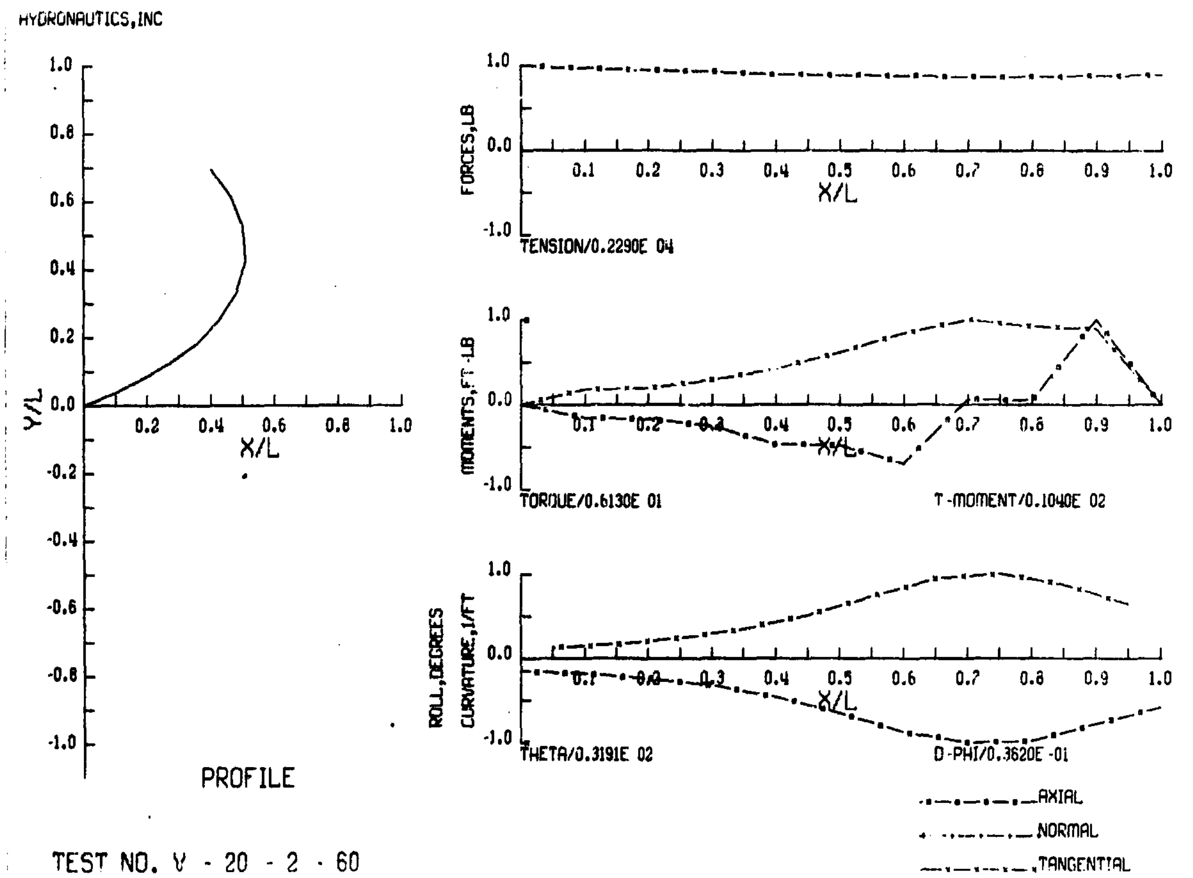
HYDRONAUTICS, INC
Y/L
X/L
PROFILE
FORCES, LB
TENSION/0.2290E 04
MOMENTS, FT-LB
TORQUE/0.6130E 01
T-MOMENT/0.1040E 02
ROLL, DEGREES
CURVATURE, 1/FT
THETA/0.3191E 02
D-PHI/0.3620E -01
AXIAL
NORMAL
TANGENTIAL
TEST NO. V - 20 - 2 - 60

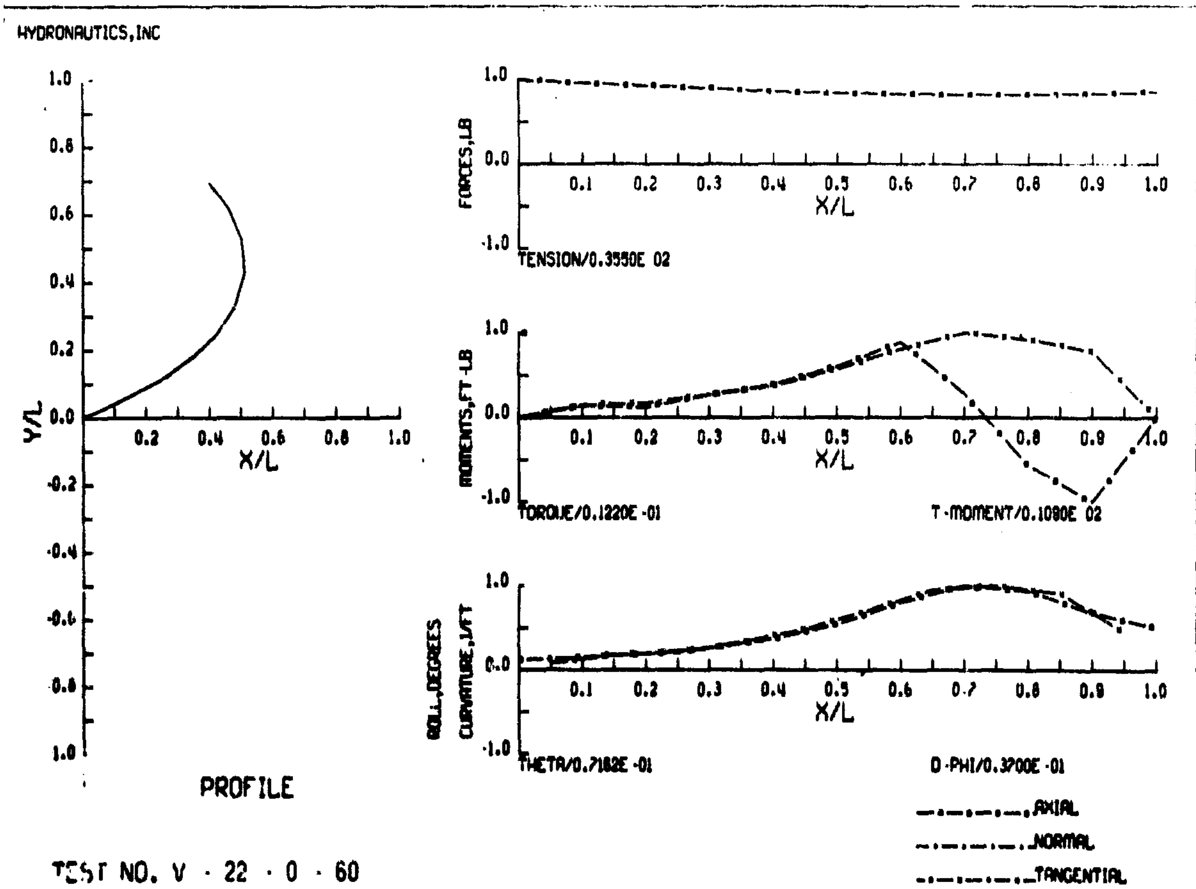
HYDRONAUTICS, INC
Y/L
X/L
PROFILE
FORCES, LB
TENSION/0.3550E 02
MOMENTS, FT-LB
TORQUE/0.1220E -01
T-MOMENT/0.1090E 02
ROLL, DEGREES
CURVATURE, 1/FT
THETA/0.7182E -01
D-PHI/0.3700E -01
AXIAL
NORMAL
TANGENTIAL
TEST NO. V - 22 - 0 - 60

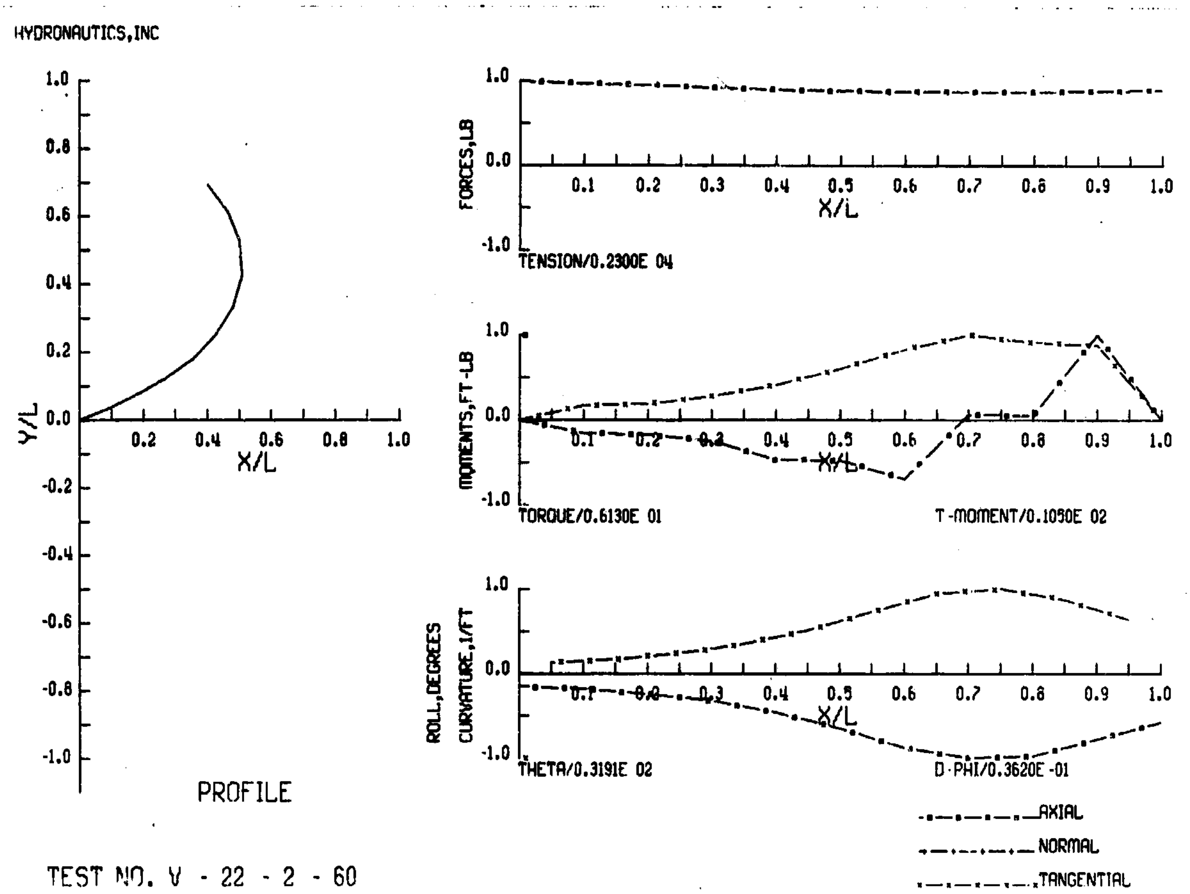
HYDRONAUTICS, INC
Y/L
X/L
PROFILE
FORCES, LB
TENSION/0.2300E 04
MOMENTS, FT-LB
TORQUE/0.6130E 01
T-MOMENT/0.1050E 02
ROLL, DEGREES
CURVATURE, 1/FT
THETA/0.3191E 02
D-PHI/0.3620E -01
AXIAL
NORMAL
TANGENTIAL
TEST NO. V - 22 - 2 - 60

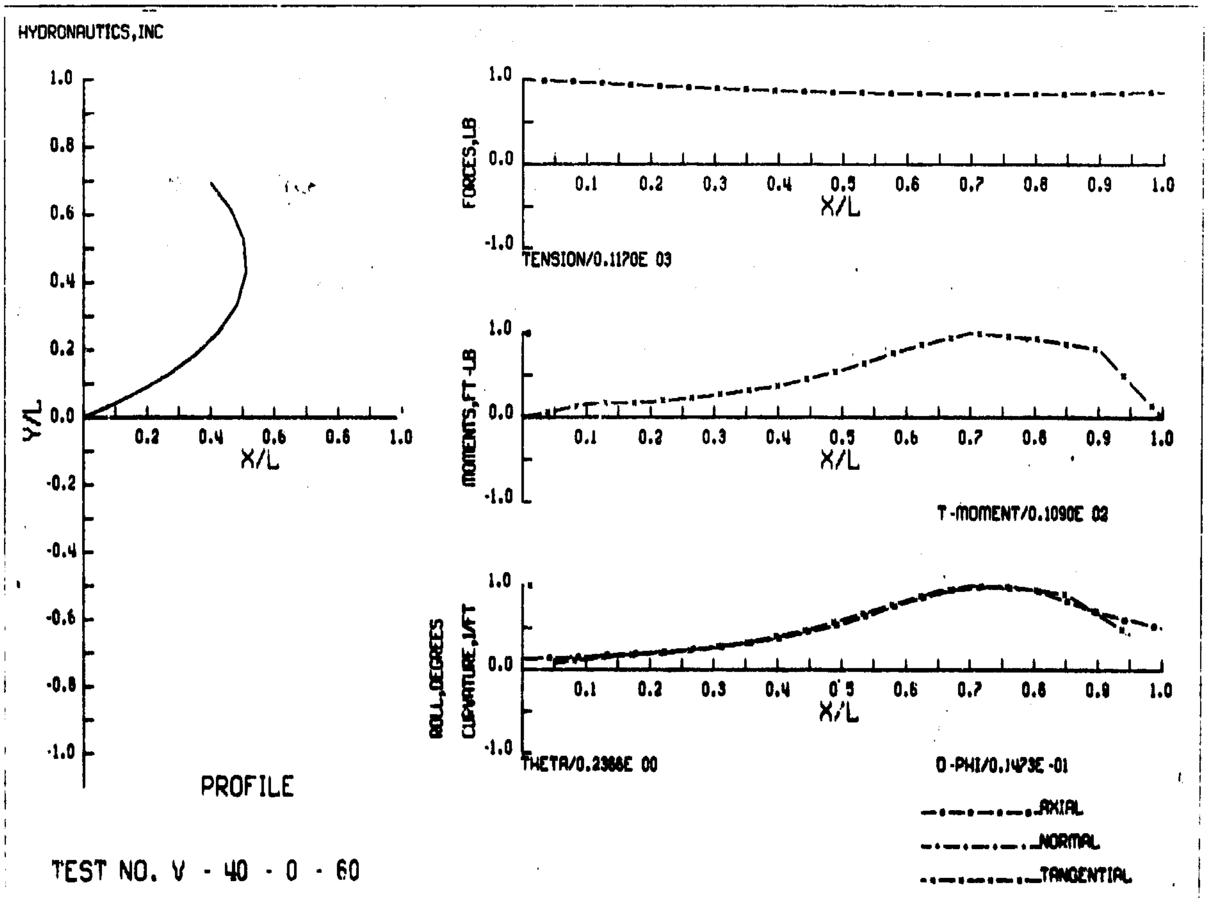
HYDRONAUTICS, INC
Y/L
X/L
PROFILE
FORCES, LB
TENSION/0.1170E 03
MOMENTS, FT-LB
T-MOMENT/0.1090E 02
ROLL, DEGREES
CURVATURE, 1/FT
THETA/0.2366E 00
D-PHI/0.1473E -01
AXIAL
NORMAL
TANGENTIAL
TEST NO. V - 40 - 0 - 60

HYDRONAUTICS,INC

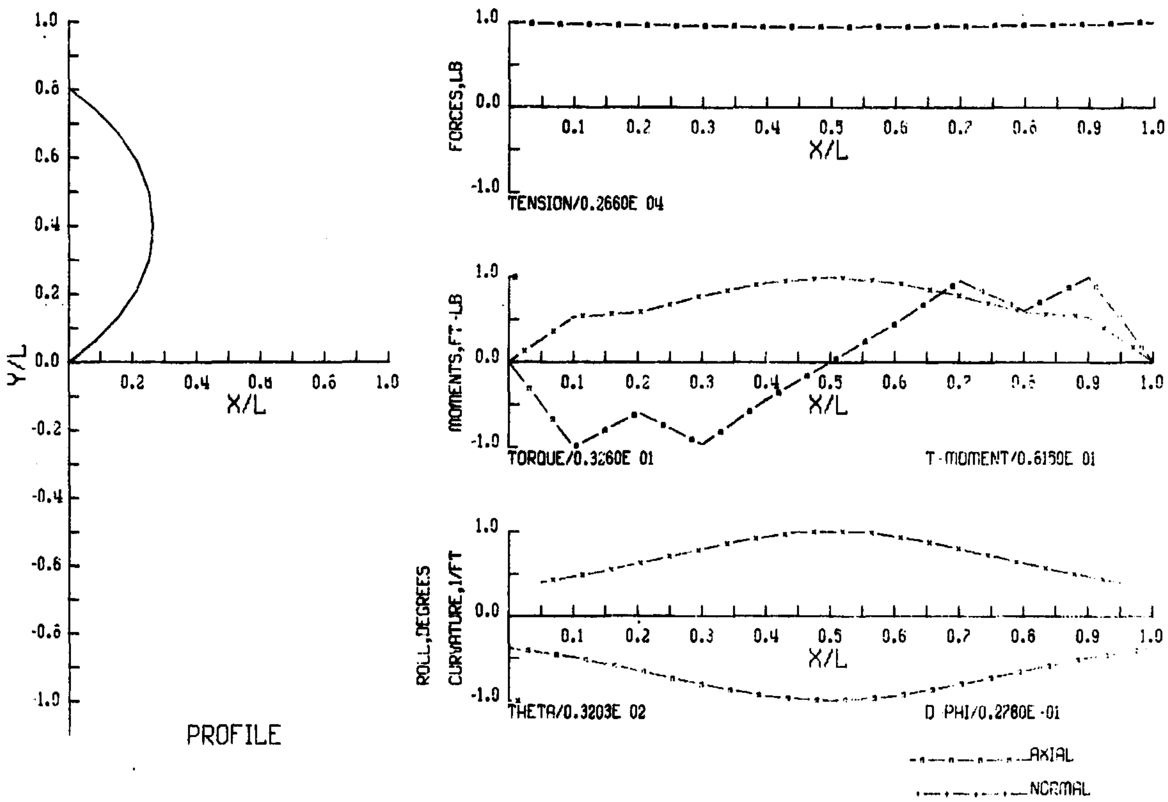

TEST NO. V - 0 - 2 - 90

HYDRONAUTICS,INC

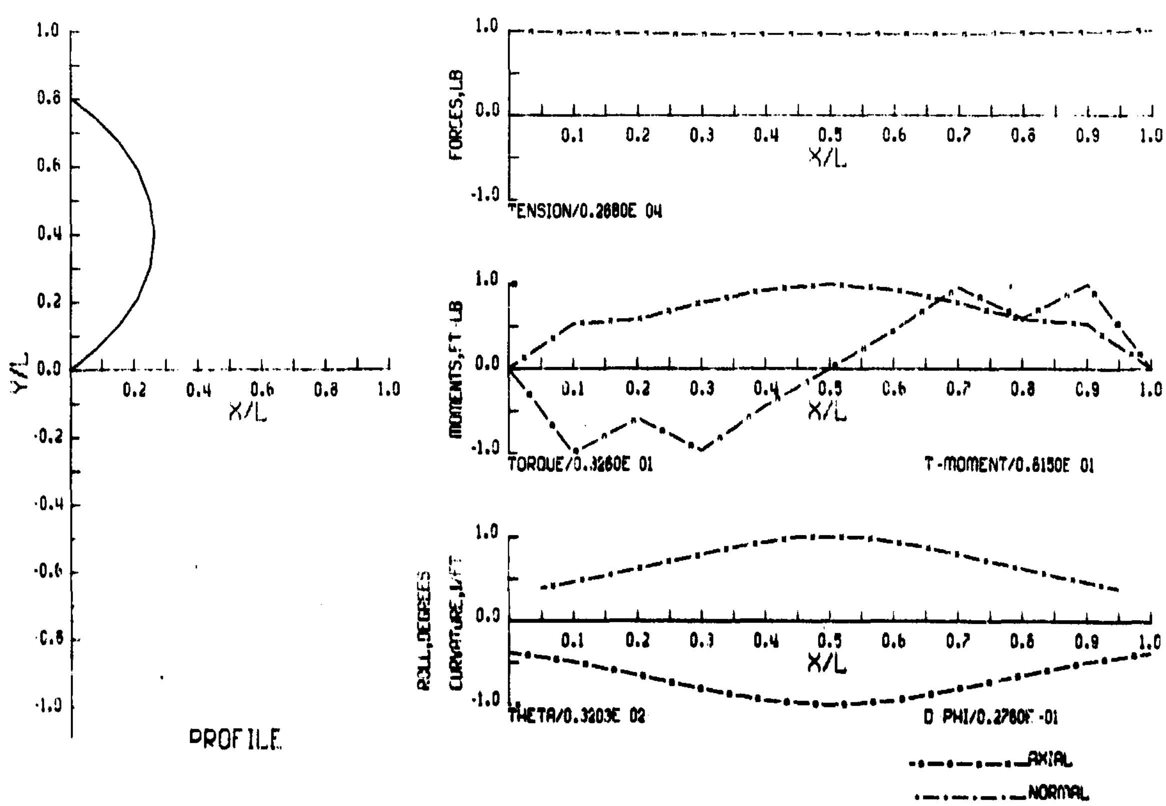

TEST NO. V - 15 - 2 - 90

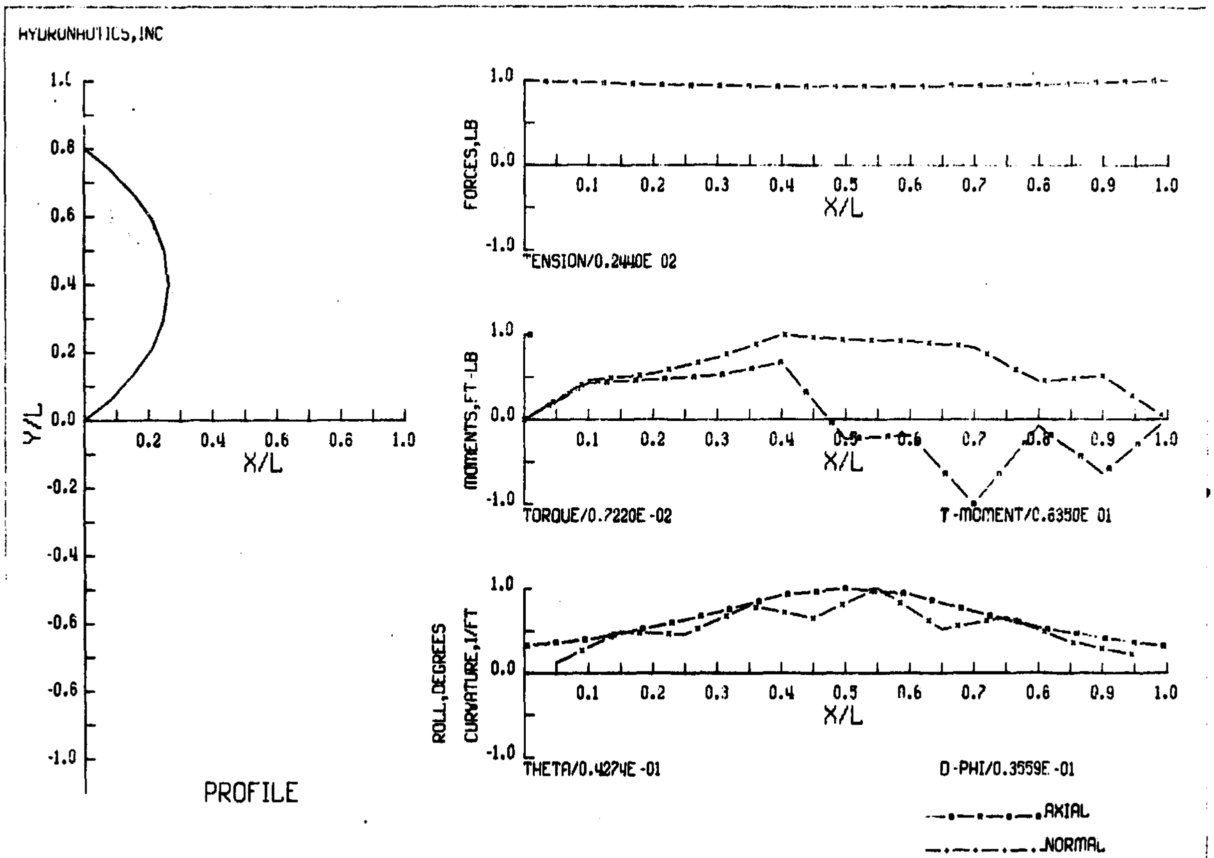

TEST NO. V - 12 - 0 - 90

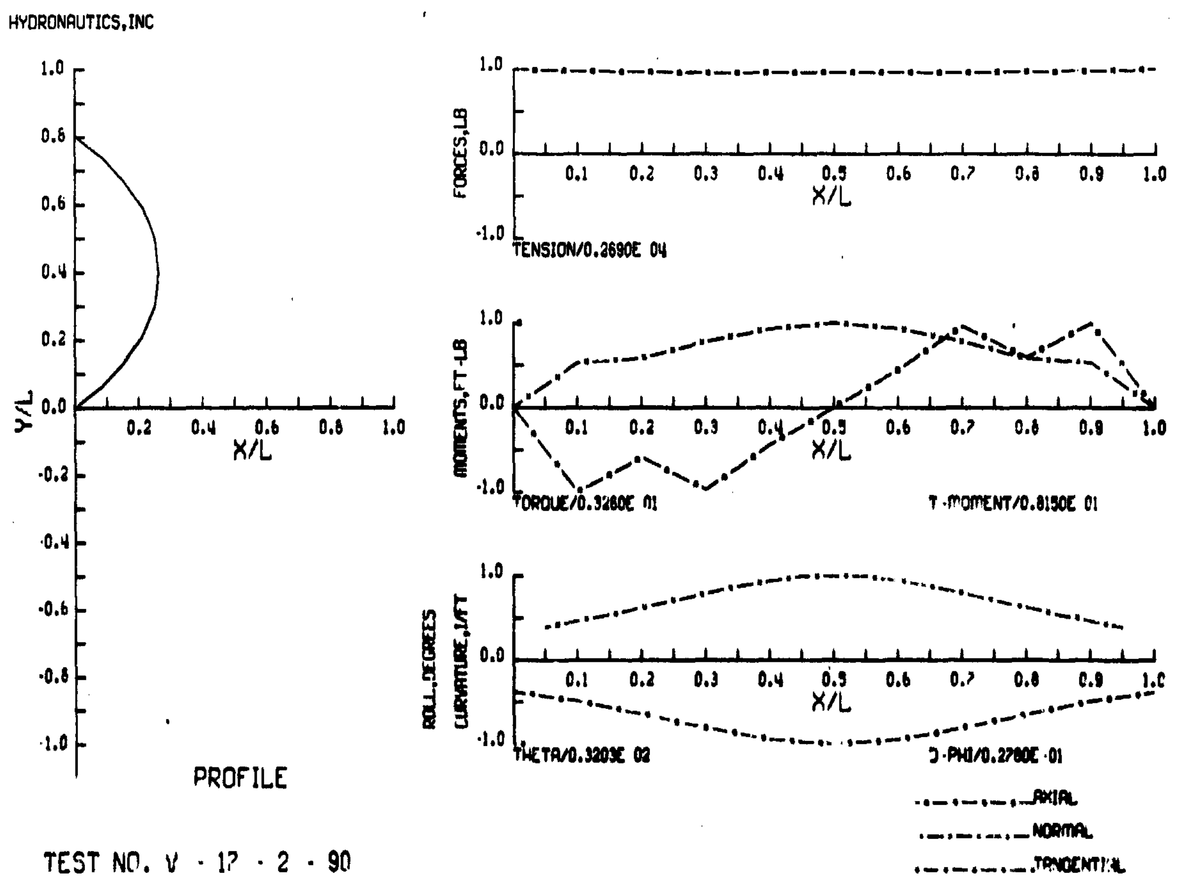

TEST NO. V - 12 - 2 - 90

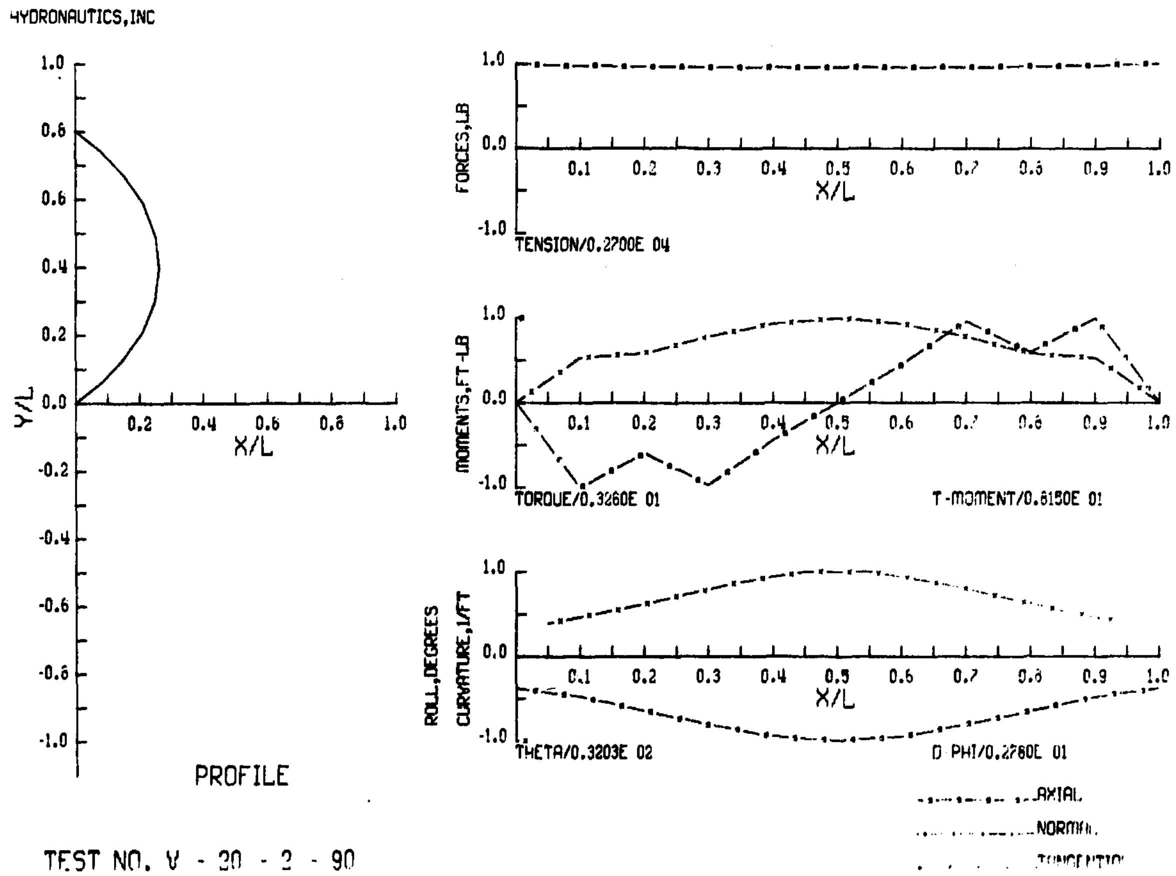
HYDRONAUTICS,INC
PROFILE
Y/L
X/L
FORCES,LB
TENSION/0.2700E 04
MOMENTS,FT-LB
TORQUE/0.3260E 01
T-MOMENT/0.6150E 01
ROLL,DEGREES
CURVATURE,1/FT
THETA/0.3203E 02
D PHI/0.2780E 01
AXIAL
NORMAL
TEST NO. V - 20 - 2 - 90

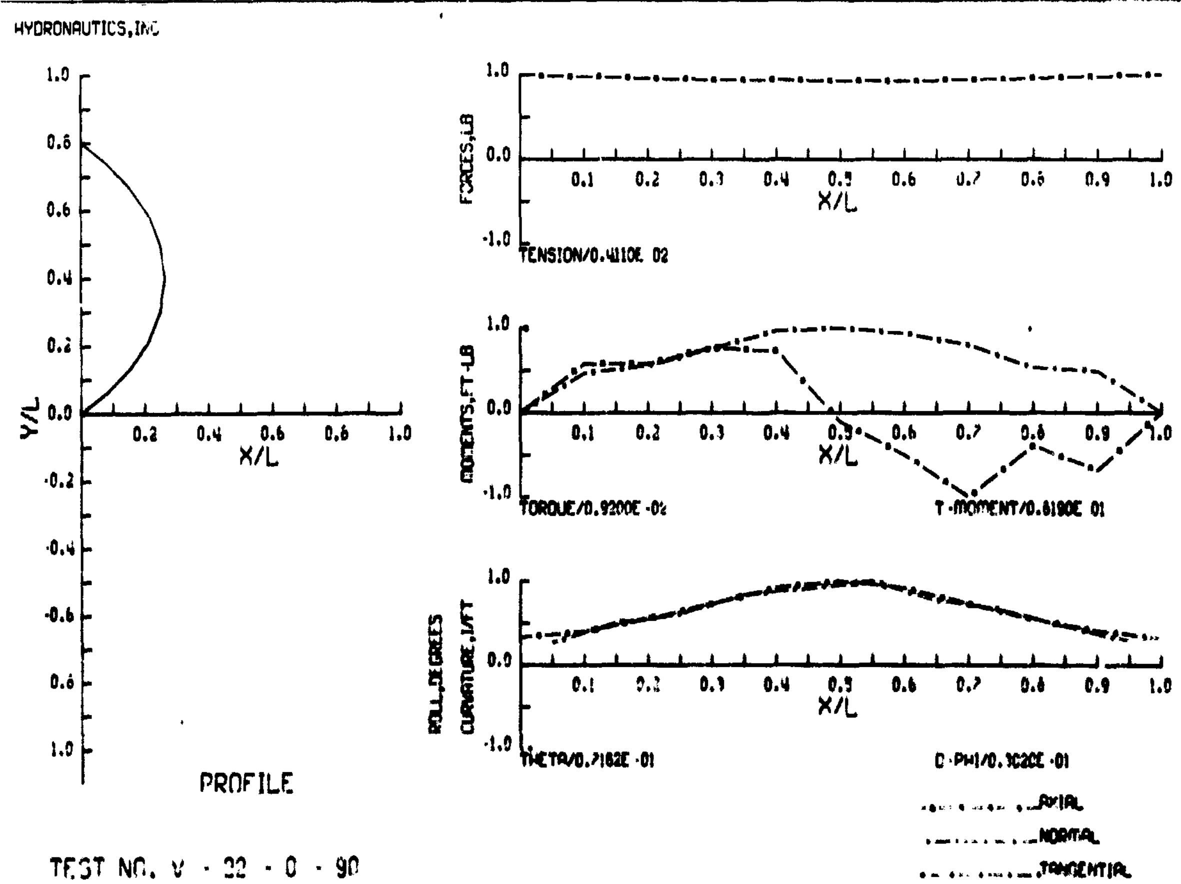
HYDRONAUTICS,INC
PROFILE
Y/L
X/L
FORCES,LB
TENSION/0.4110E 02
MOMENTS,FT-LB
TORQUE/0.9200E -02
T-MOMENT/0.6190E 01
ROLL,DEGREES
CURVATURE,1/FT
THETA/0.7162E -01
D PHI/0.3C2CE -01
AXIAL
NORMAL
TANGENTIAL
TEST NO. V - 22 - 0 - 90

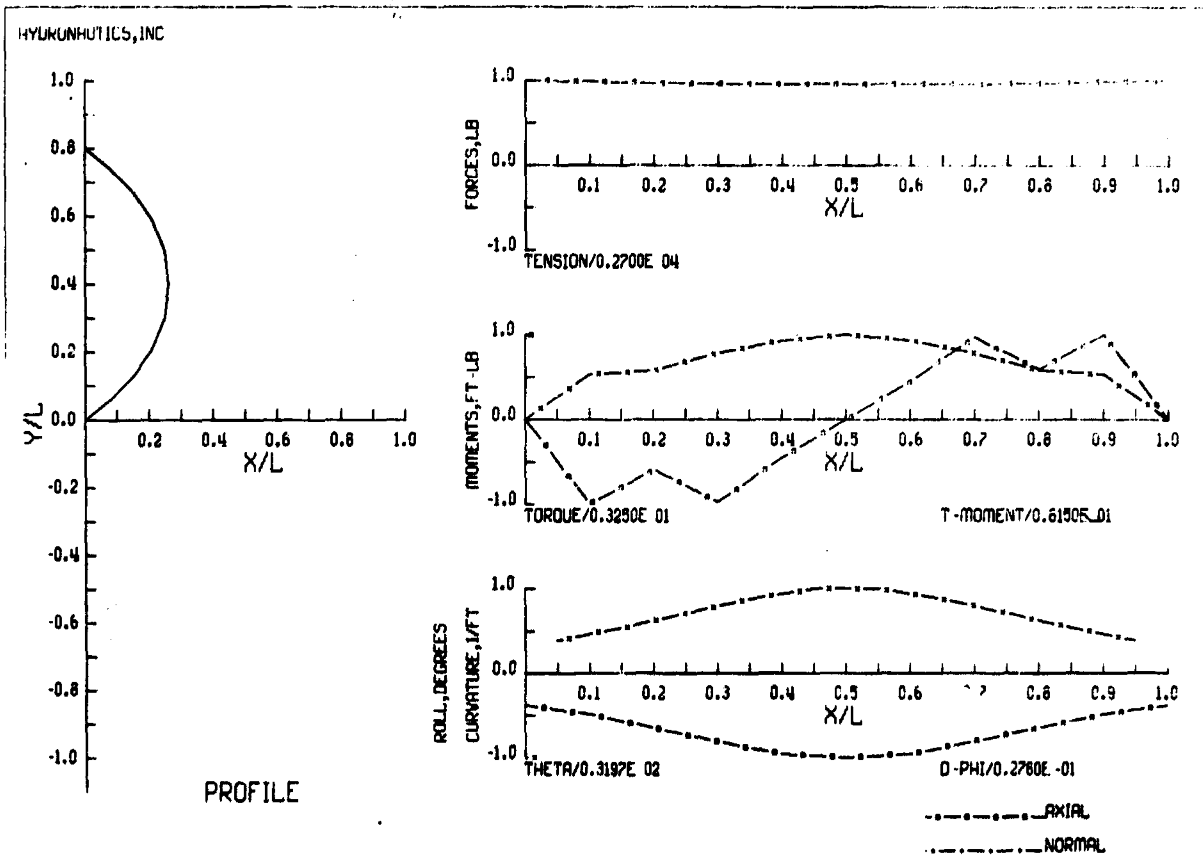

TEST NO. V - 22 - 2 - 90

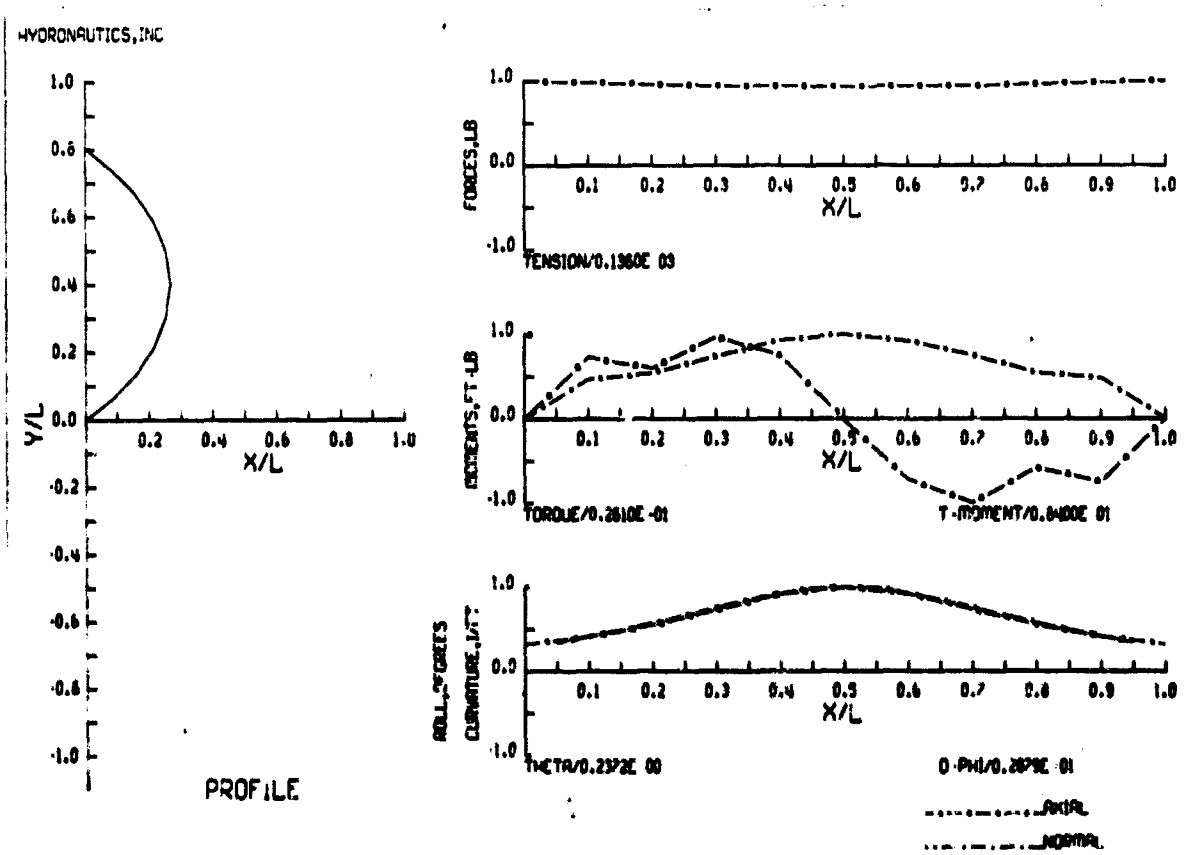

TEST NO. V - 40 - 0 - 90

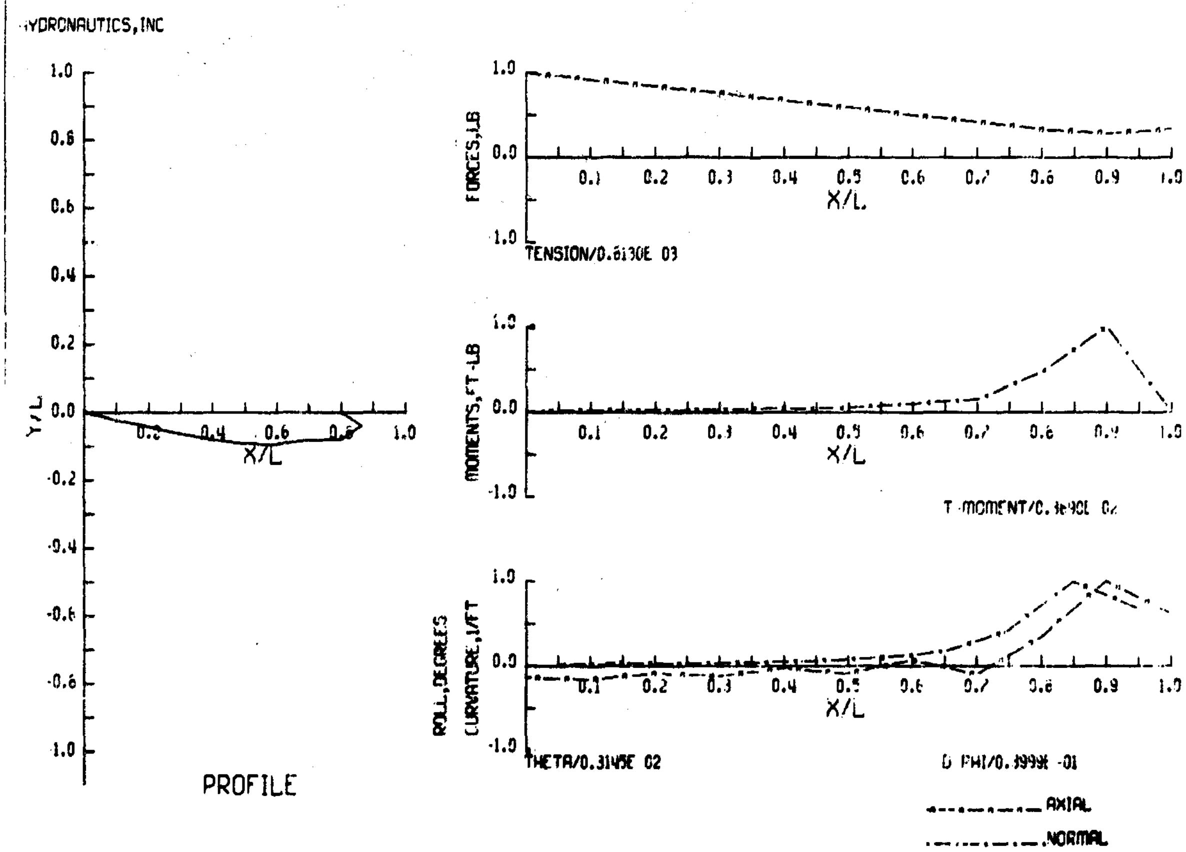

TEST NO. VI - 0 - 2 - 0

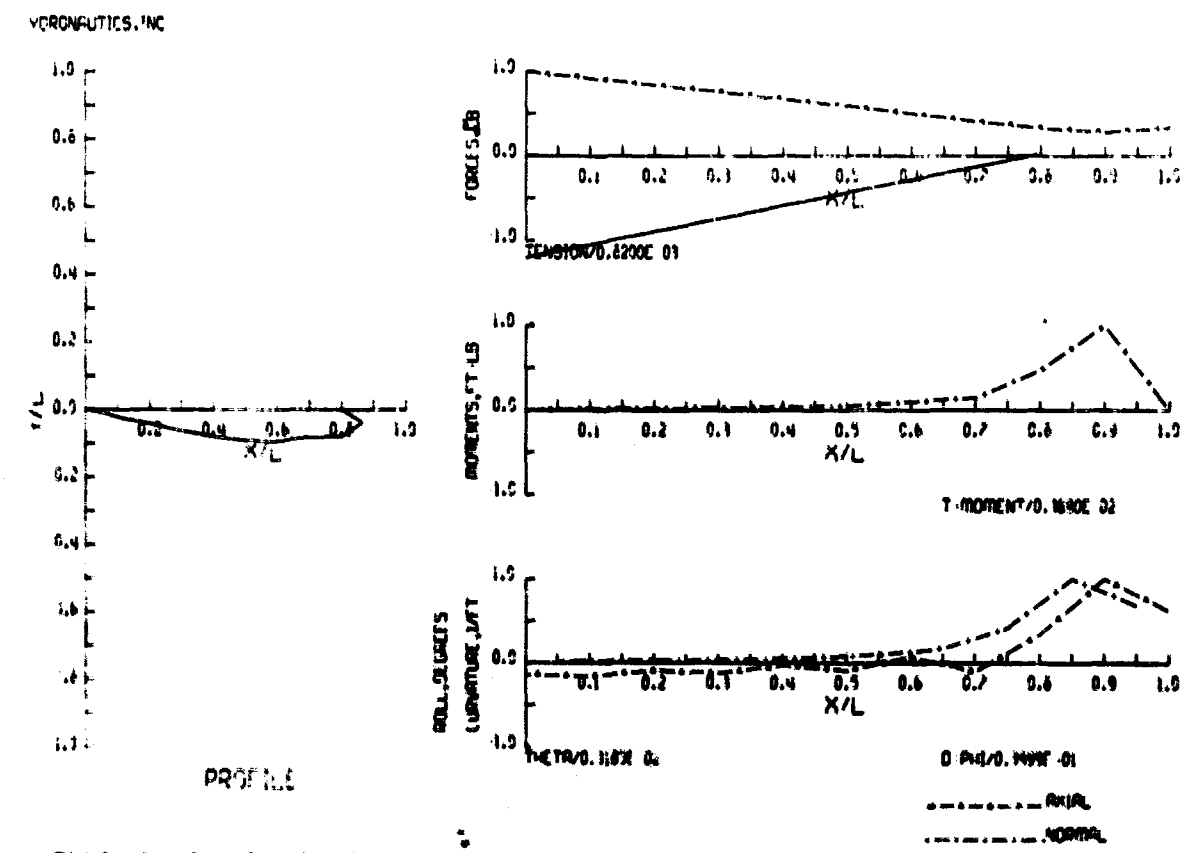

TEST NO. VI [illegible]

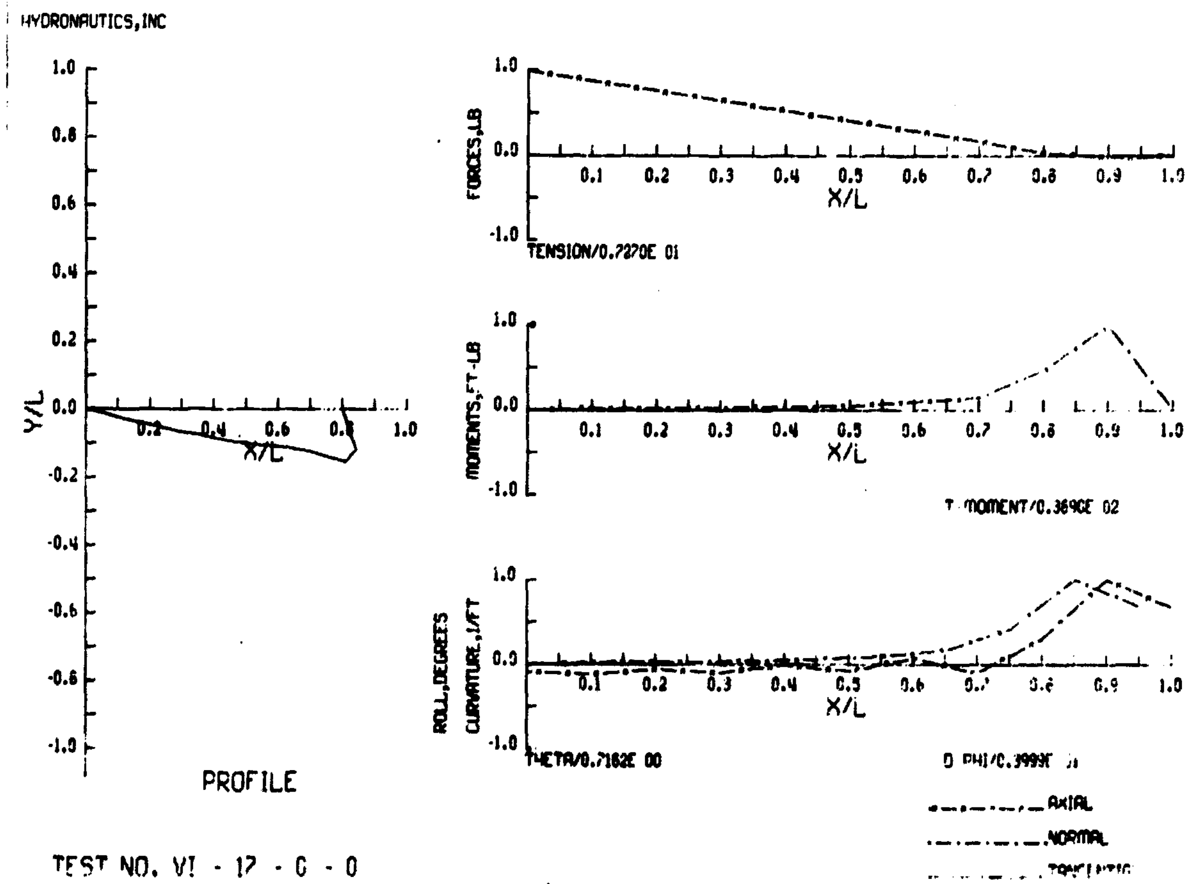

TEST NO. VI - 12 - 0 - 0

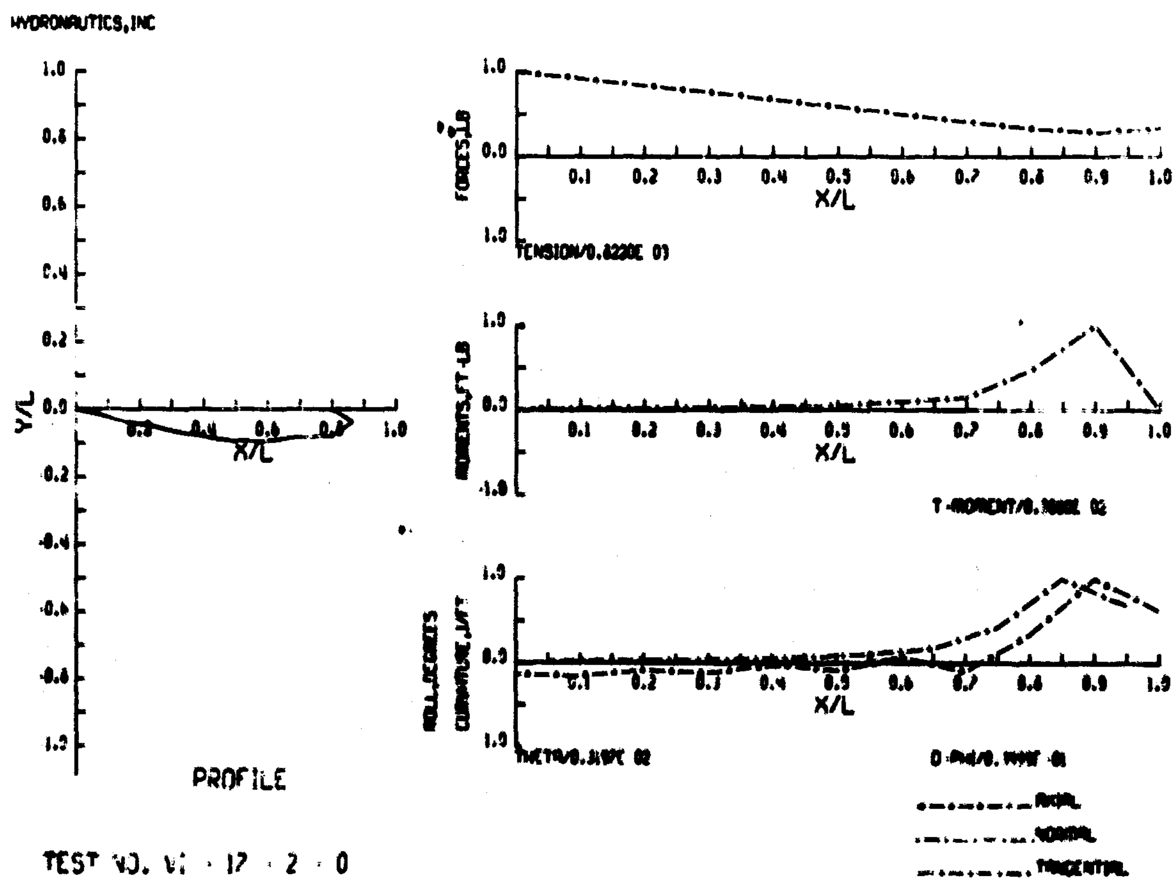

TEST NO. VI - 12 - 2 - 0

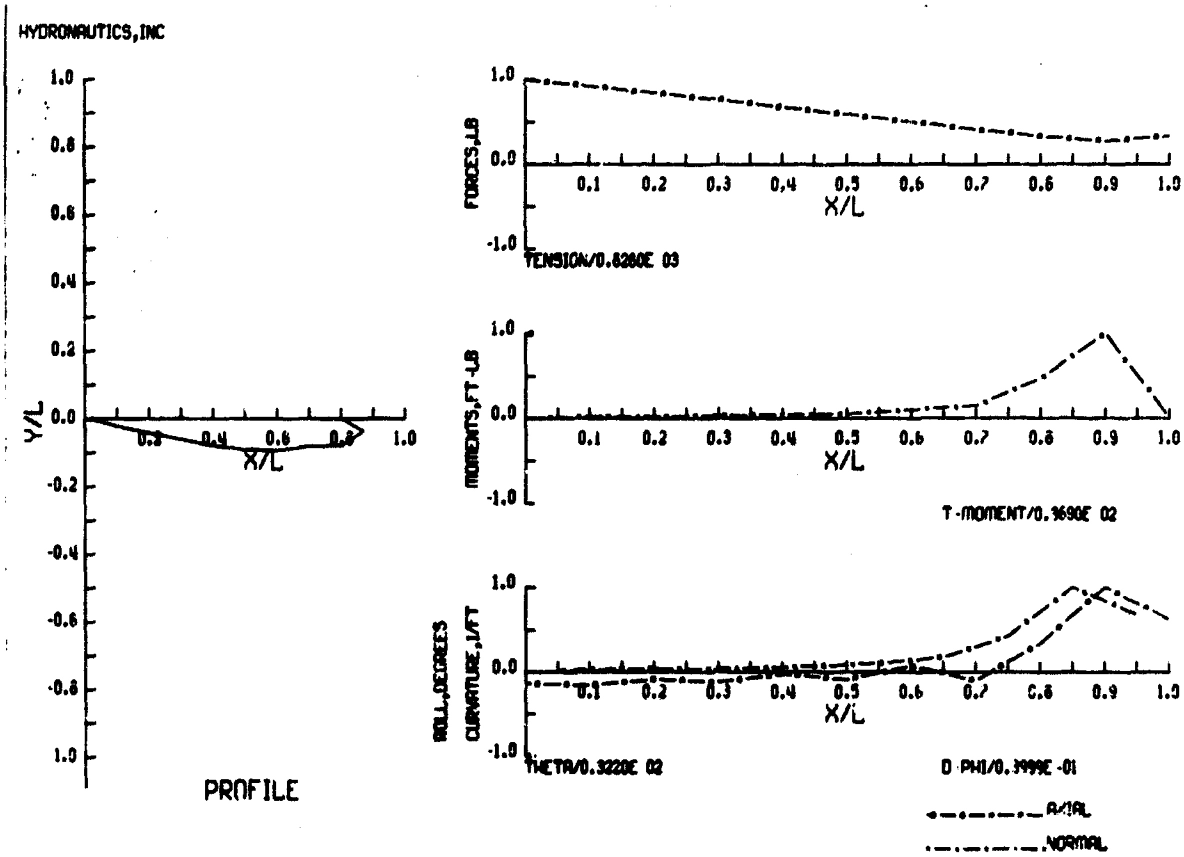

TEST NO. VI - 20 - 2 - 0

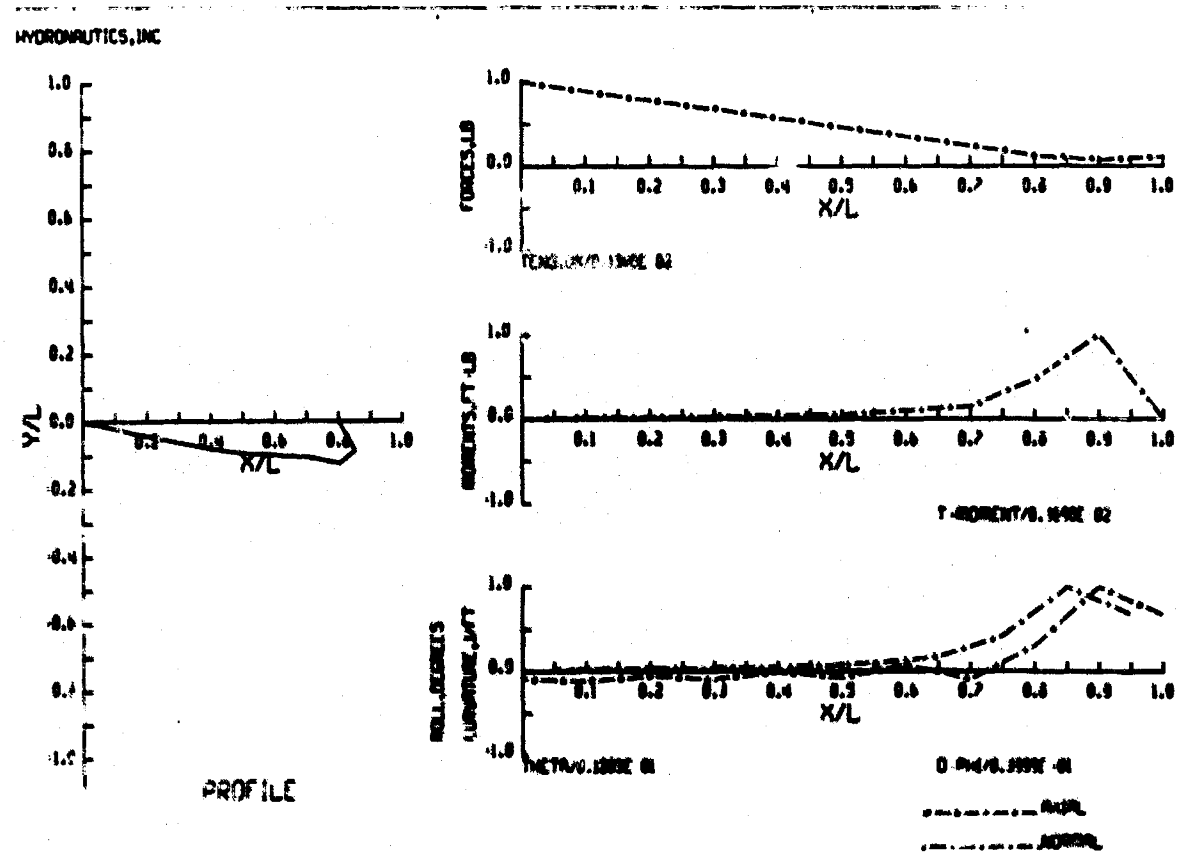

TEST NO. VI - 22 - 0 - 0

HYDRONAUTICS, INC

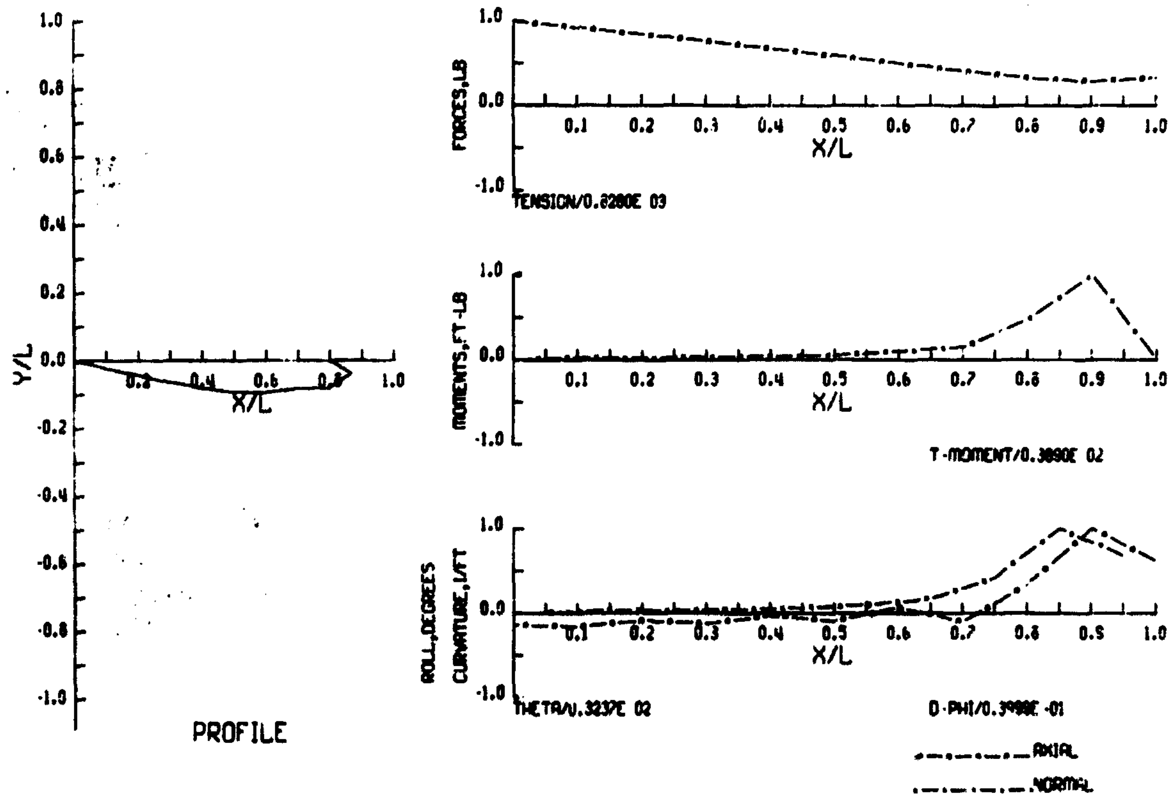

TEST NO. VI - 22 - 2 - 0

HYDRONAUTICS, INC

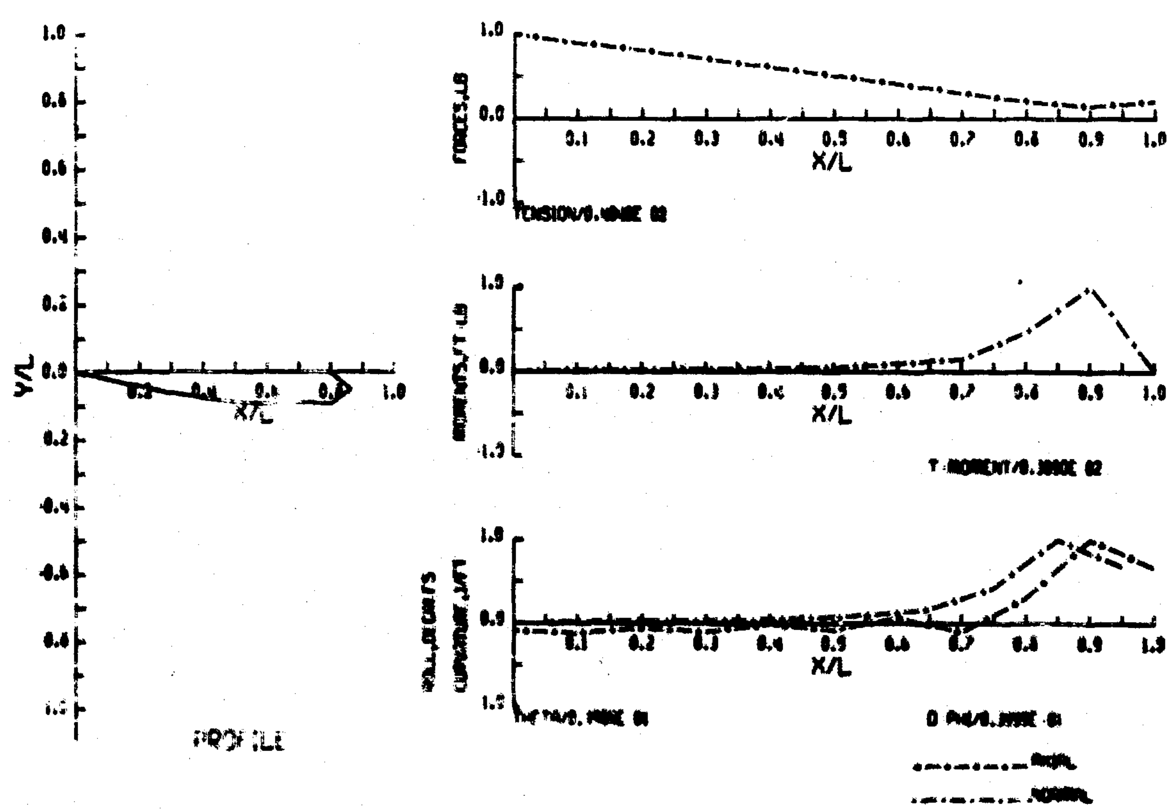

TEST NO. VI - 40 - 0 - 0

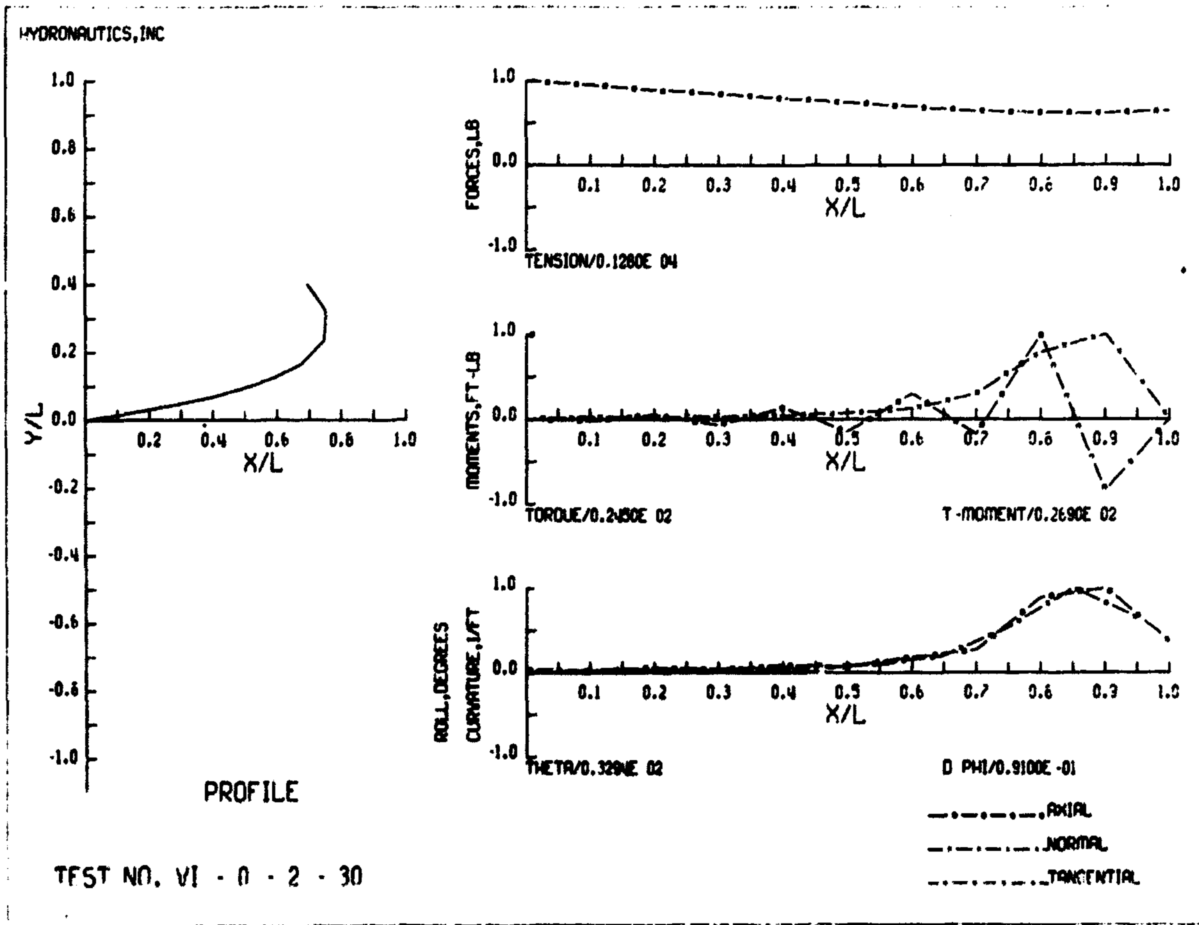

TEST NO. VI - 0 - 2 - 30

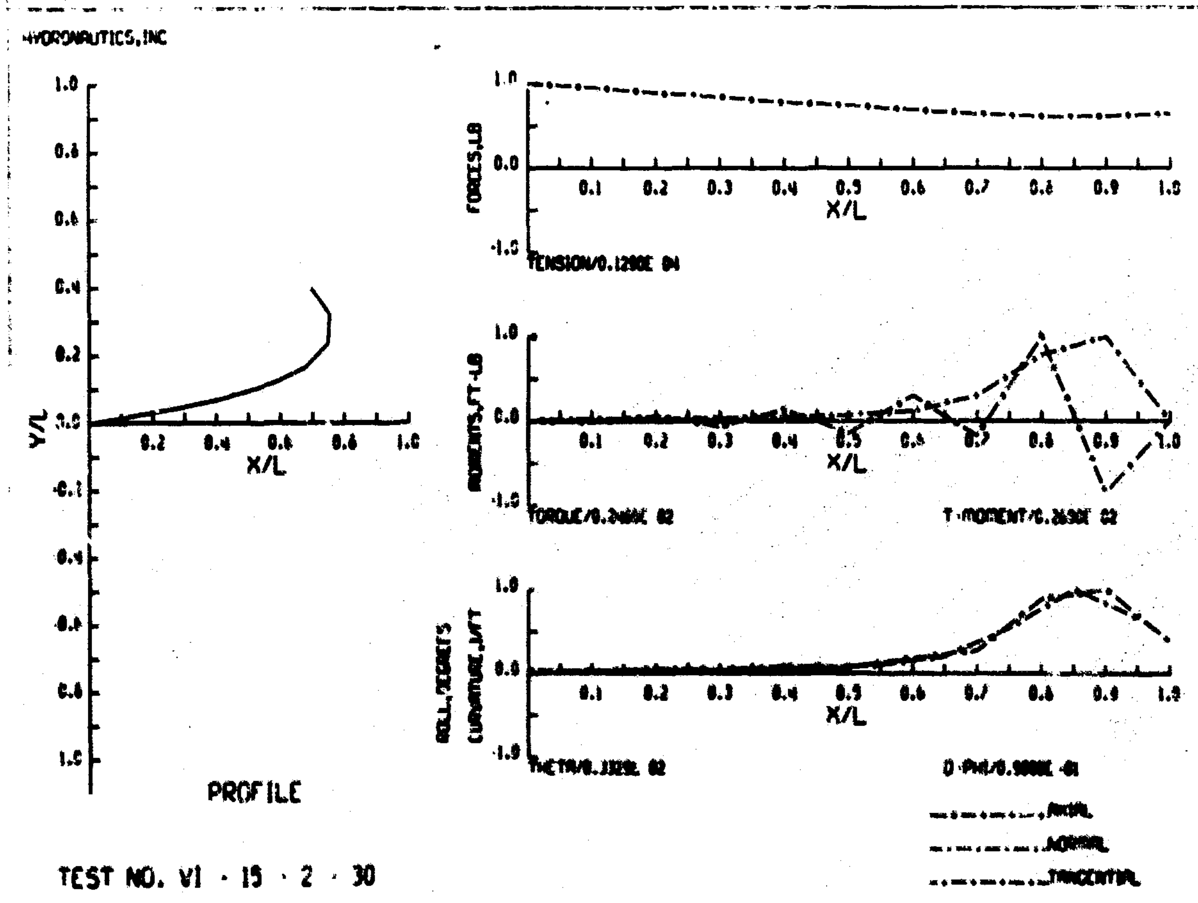

TEST NO. VI - 15 - 2 - 30

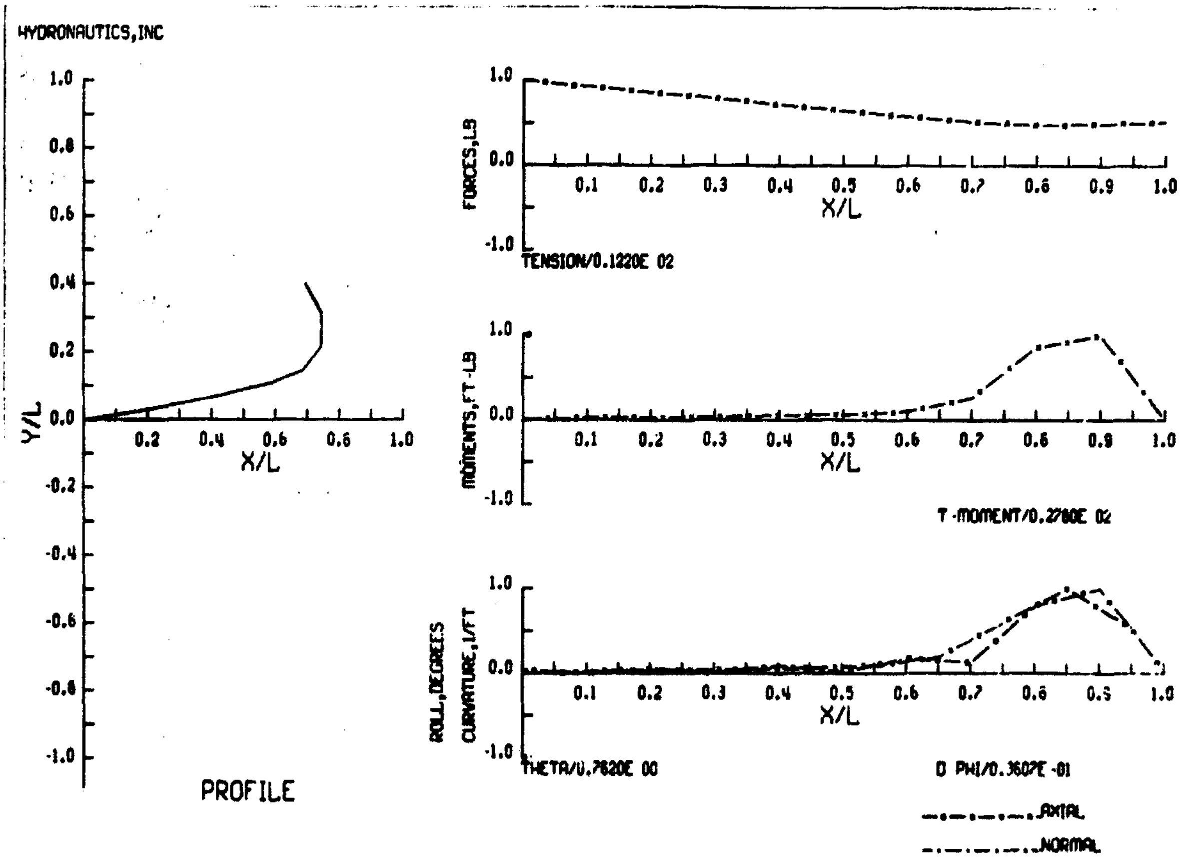

TEST NO. VI - 17 - 0 - 30

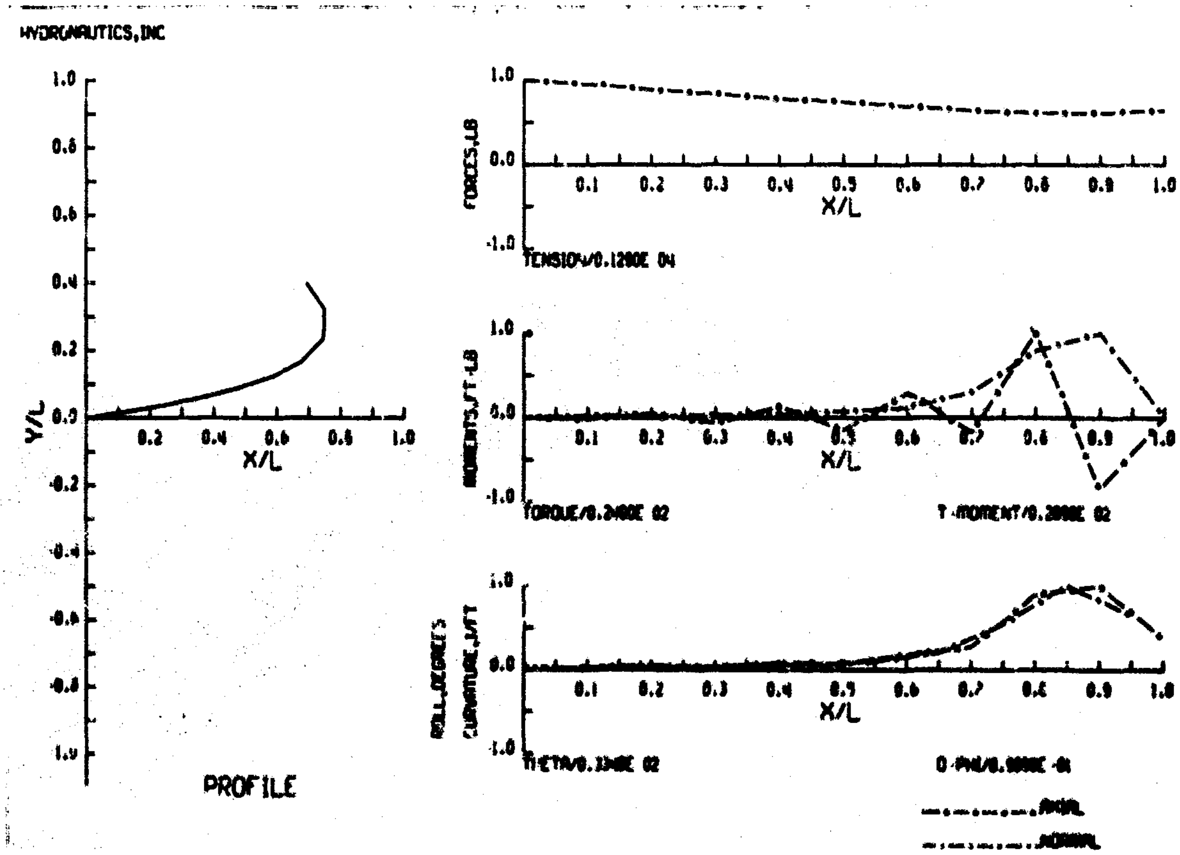

TEST NO. VI - 17 - 2 - 30

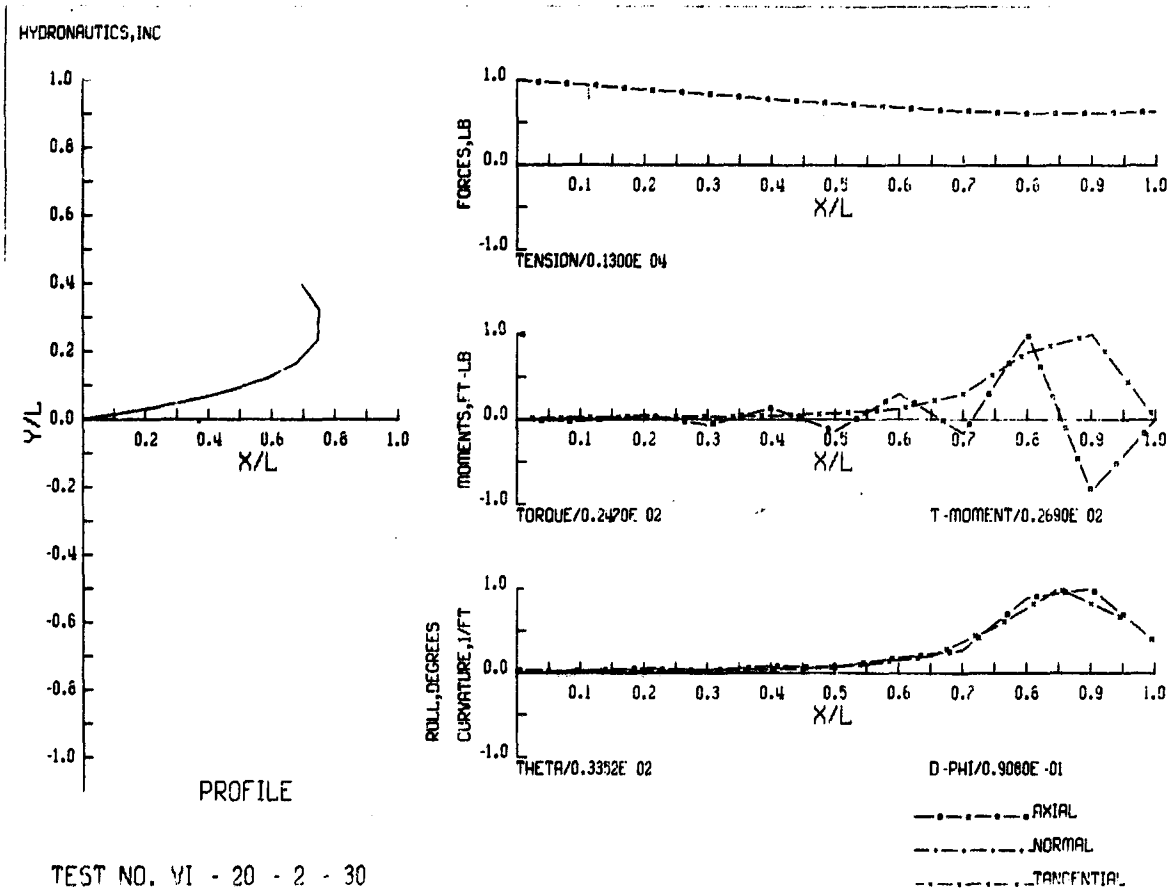

TEST NO. VI - 20 - 2 - 30

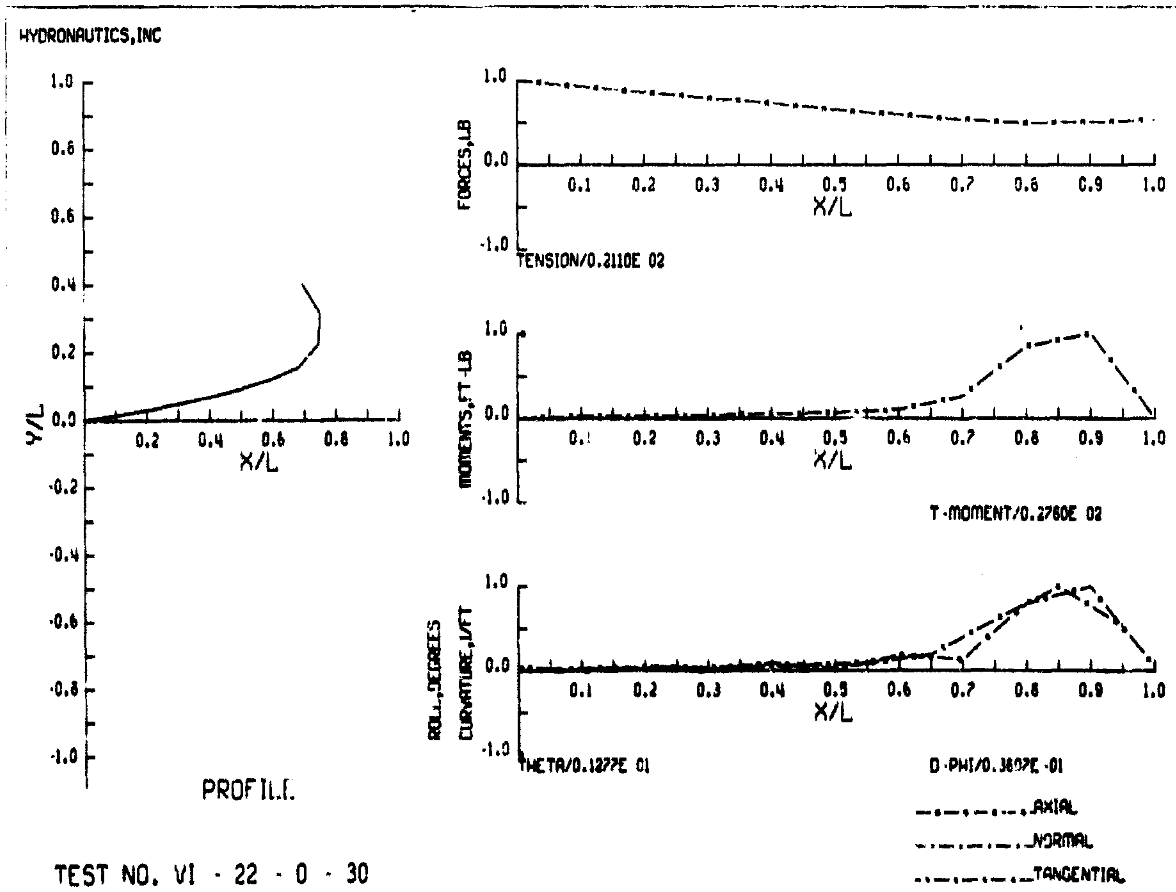

TEST NO. VI - 22 - 0 - 30

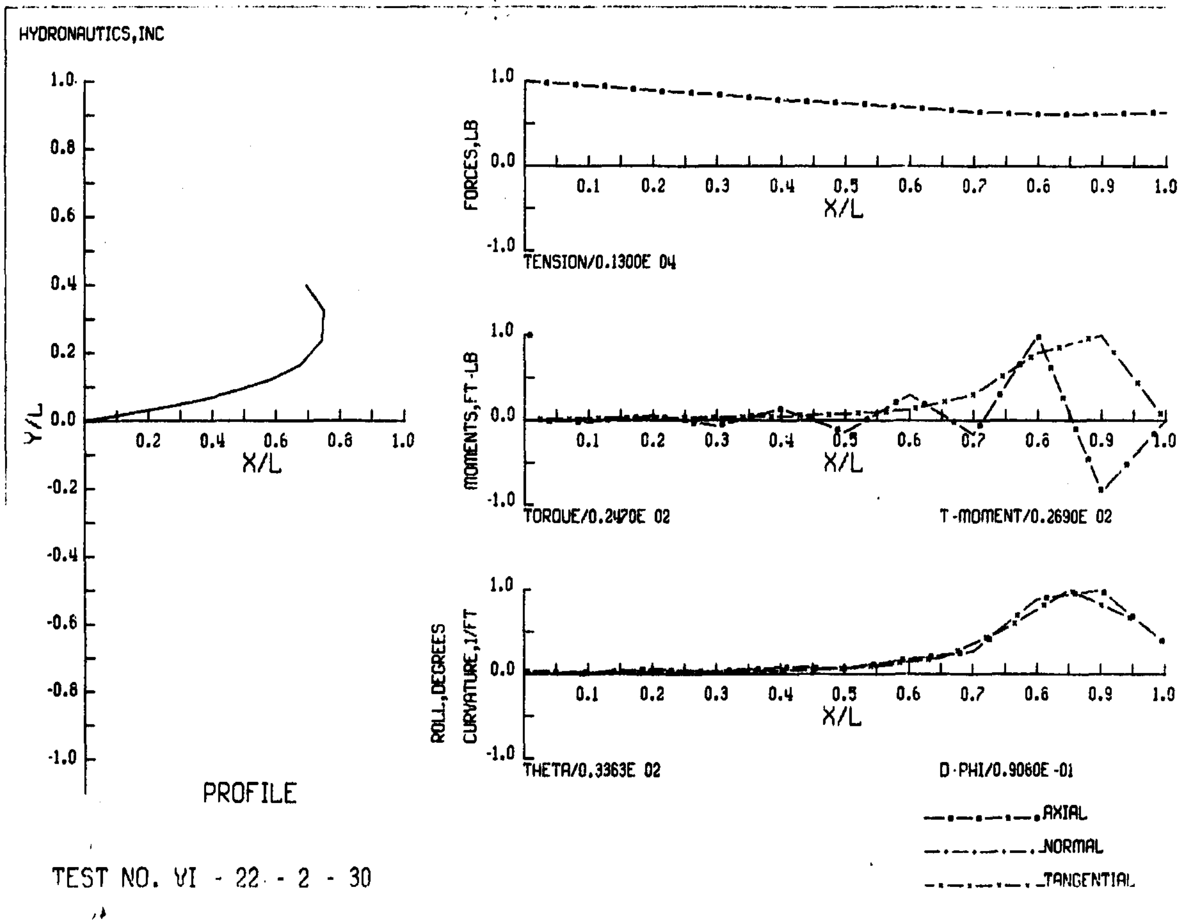
HYDRONAUTICS,INC
Y/L
X/L
PROFILE
FORCES,LB
TENSION/0.1300E 04
MOMENTS,FT-LB
TORQUE/0.2470E 02
T-MOMENT/0.2690E 02
ROLL,DEGREES
CURVATURE,1/FT
THETA/0.3363E 02
D-PHI/0.9060E -01
AXIAL
NORMAL
TANGENTIAL
TEST NO. VI - 22 - 2 - 30

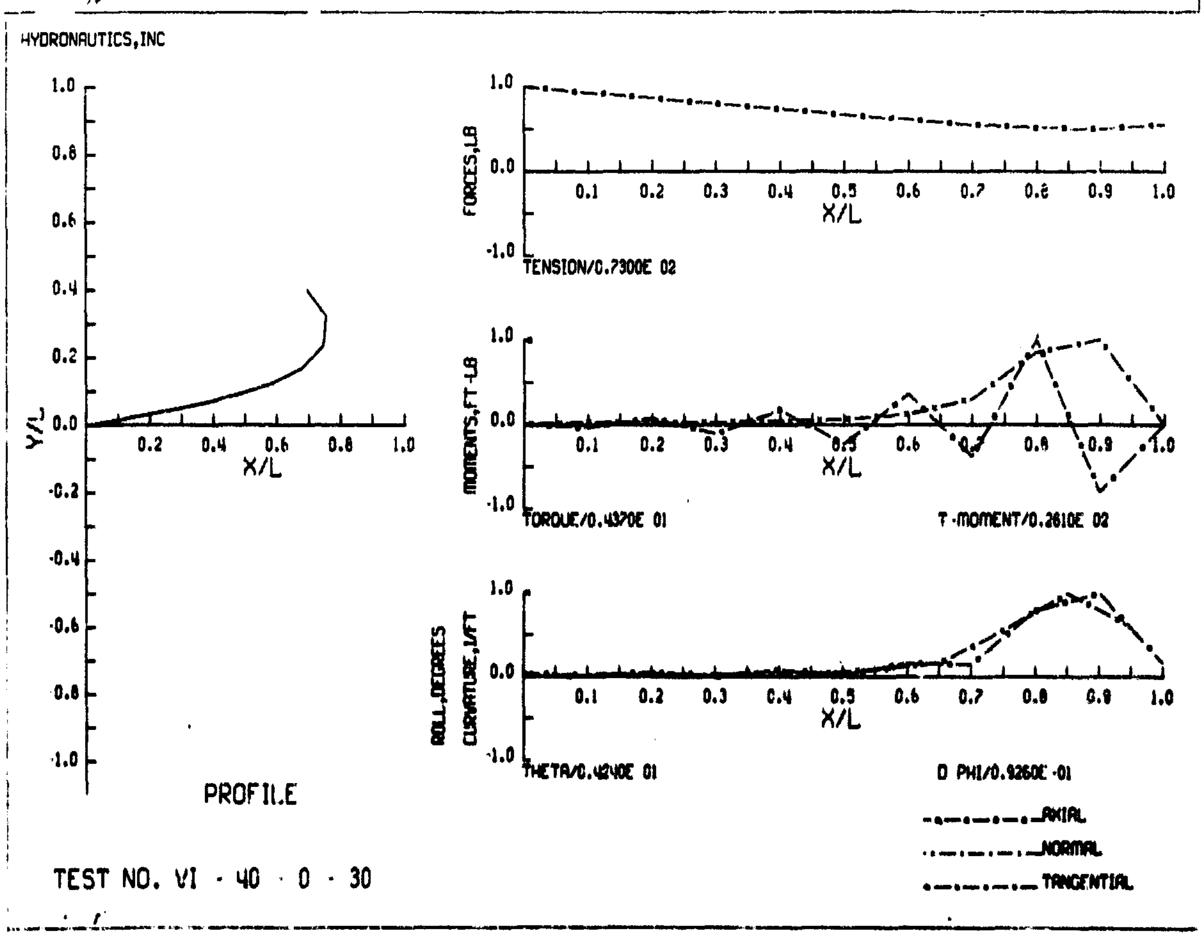
HYDRONAUTICS,INC
Y/L
X/L
PROFILE
FORCES,LB
TENSION/0.7300E 02
MOMENTS,FT-LB
TORQUE/0.4370E 01
T-MOMENT/0.2610E 02
ROLL,DEGREES
CURVATURE,1/FT
THETA/0.4240E 01
D PHI/0.9260E -01
AXIAL
NORMAL
TANGENTIAL
TEST NO. VI - 40 - 0 - 30

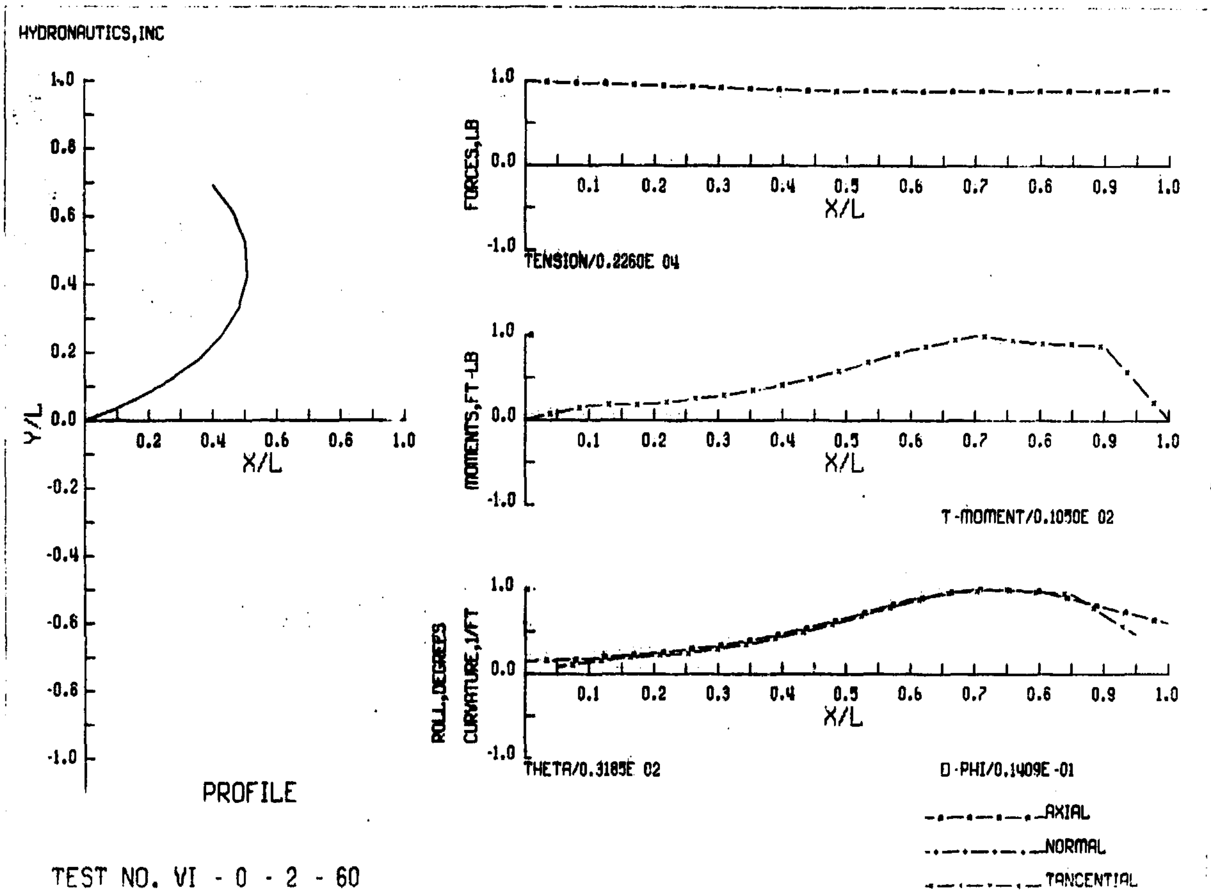

TEST NO. VI - 0 - 2 - 60

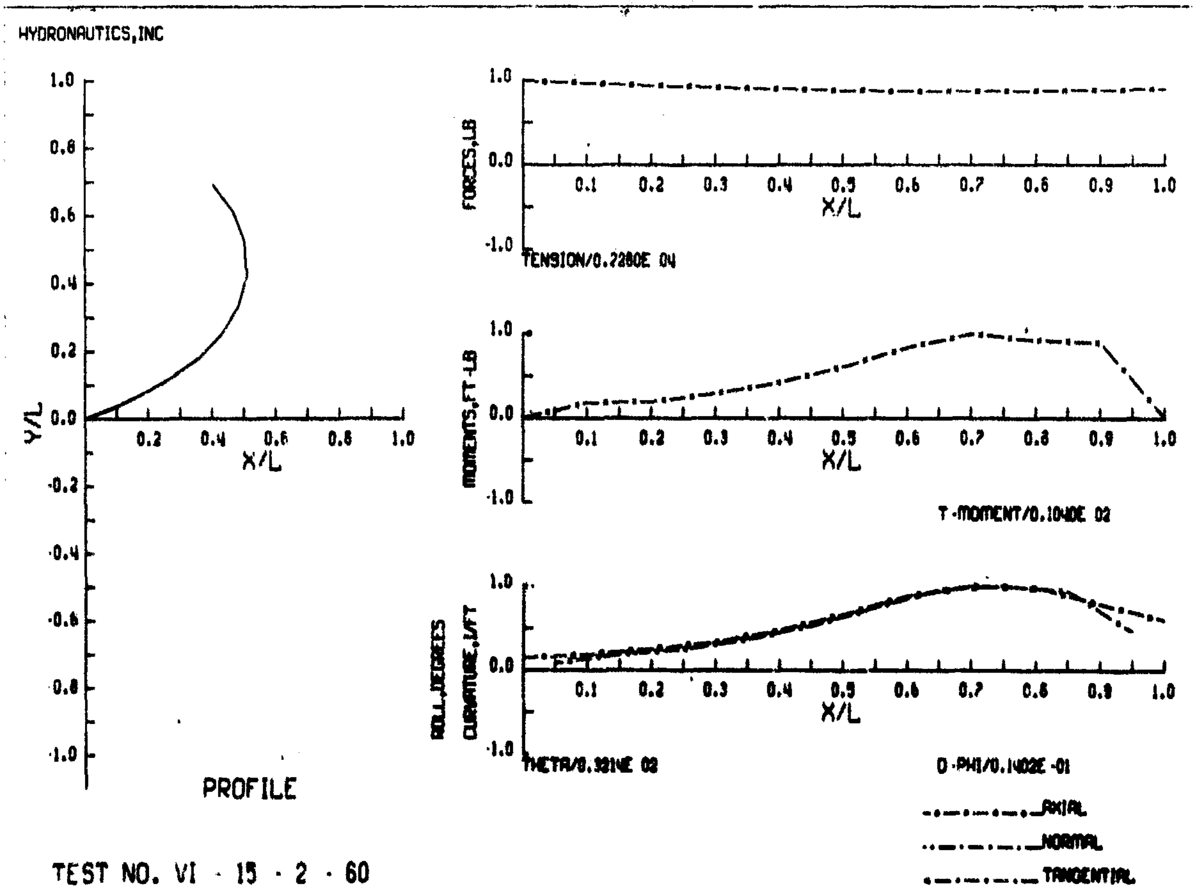

TEST NO. VI - 15 - 2 - 60

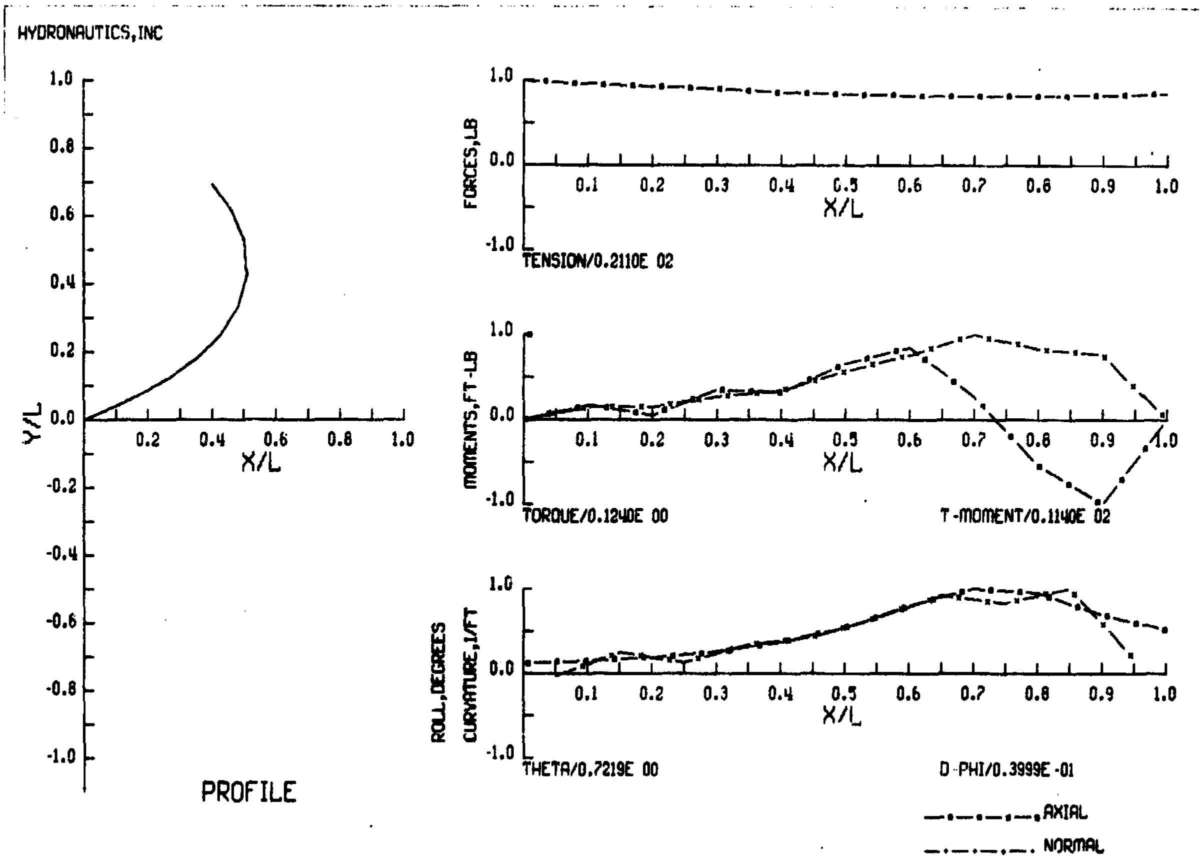

TEST NO. VI - 17 - 0 - 60

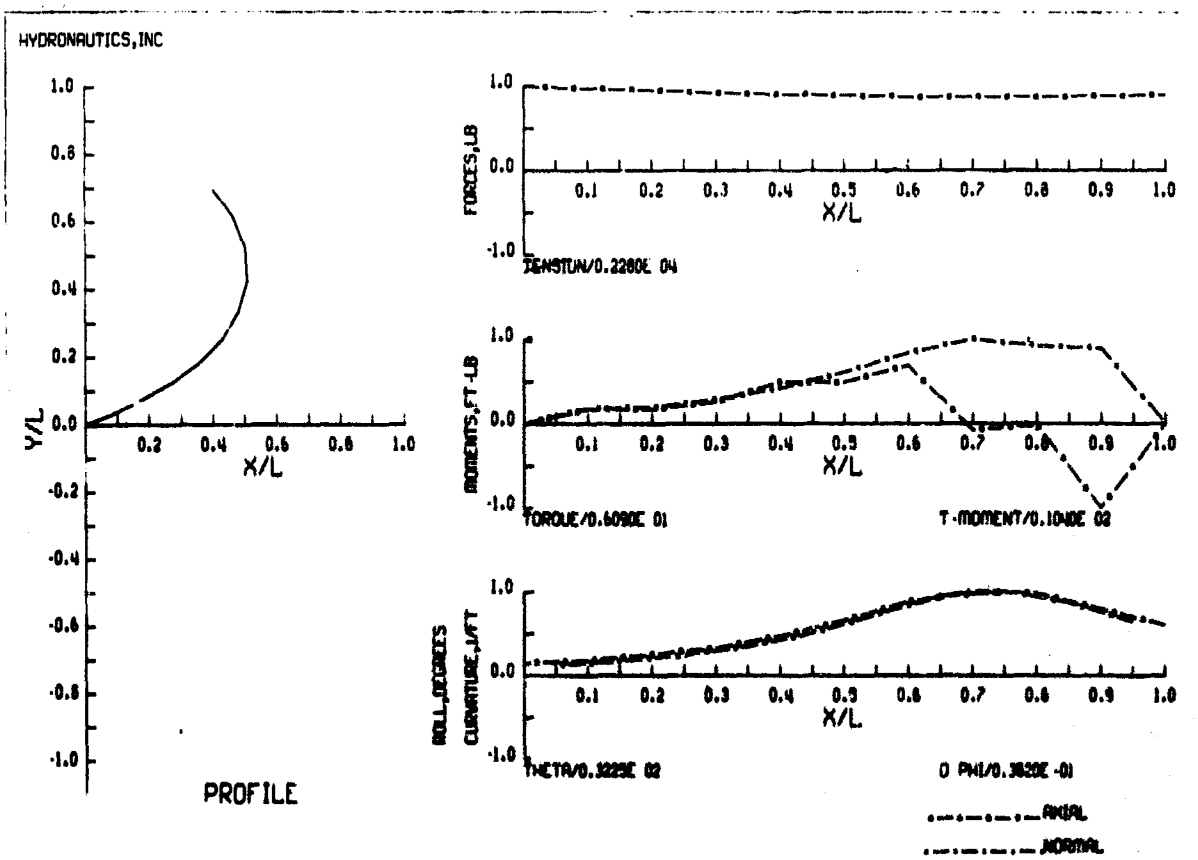

TEST NO. VI - 17 - 2 - 60

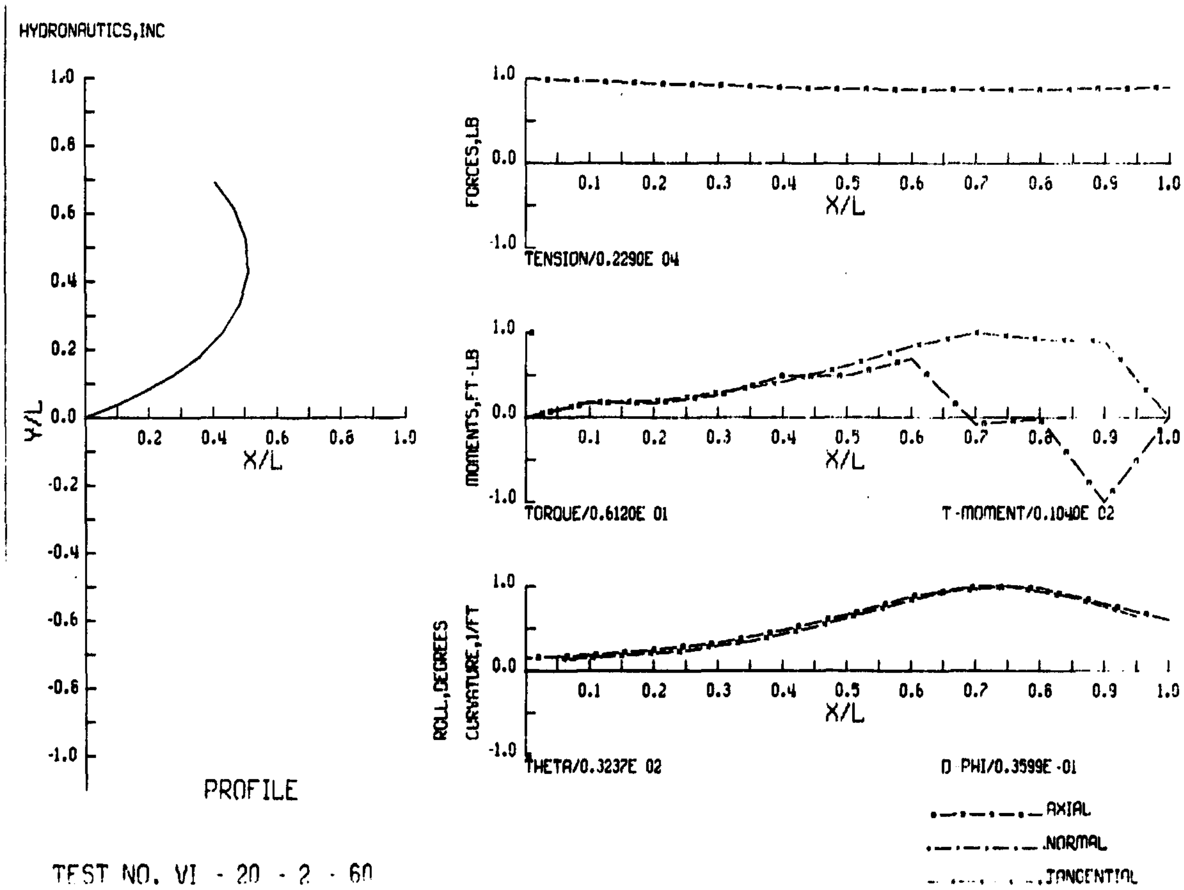

TEST NO. VI - 20 - 2 - 60

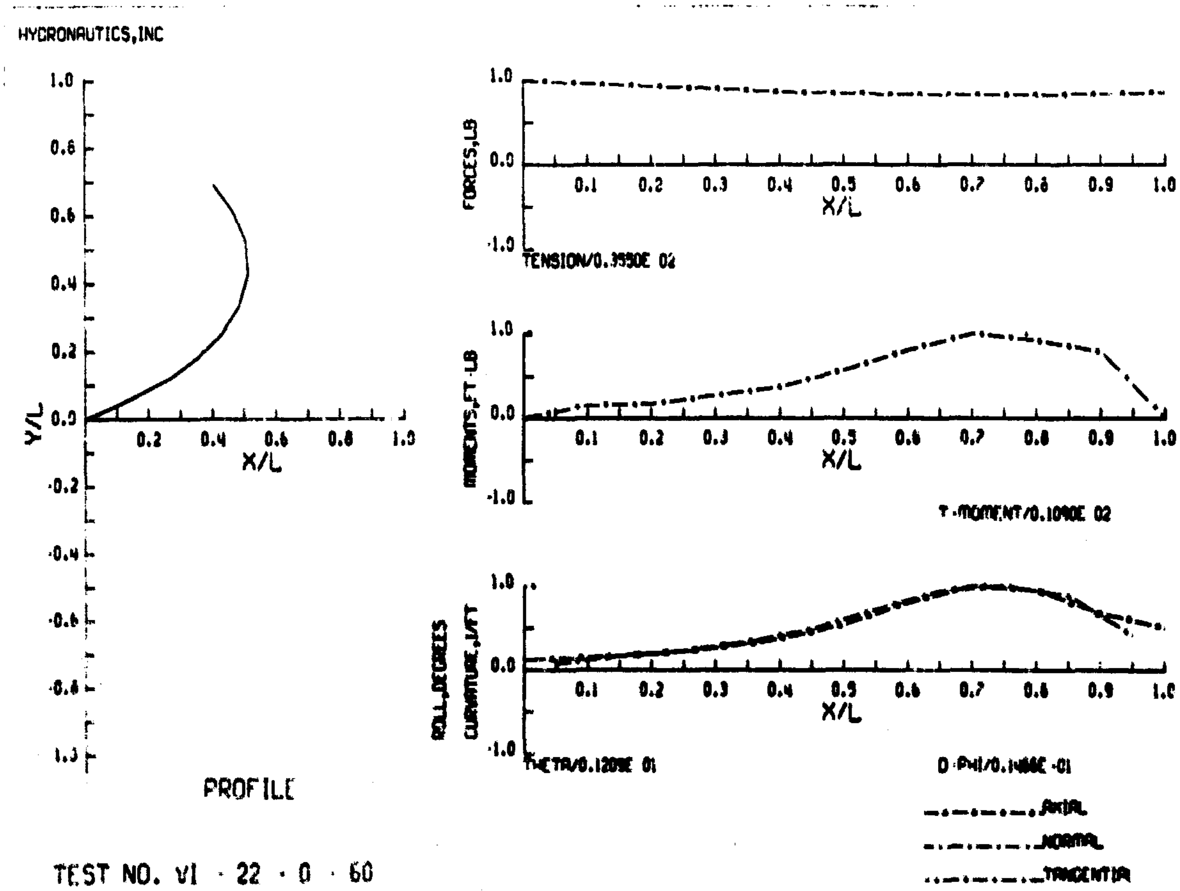

TEST NO. VI - 22 - 0 - 60

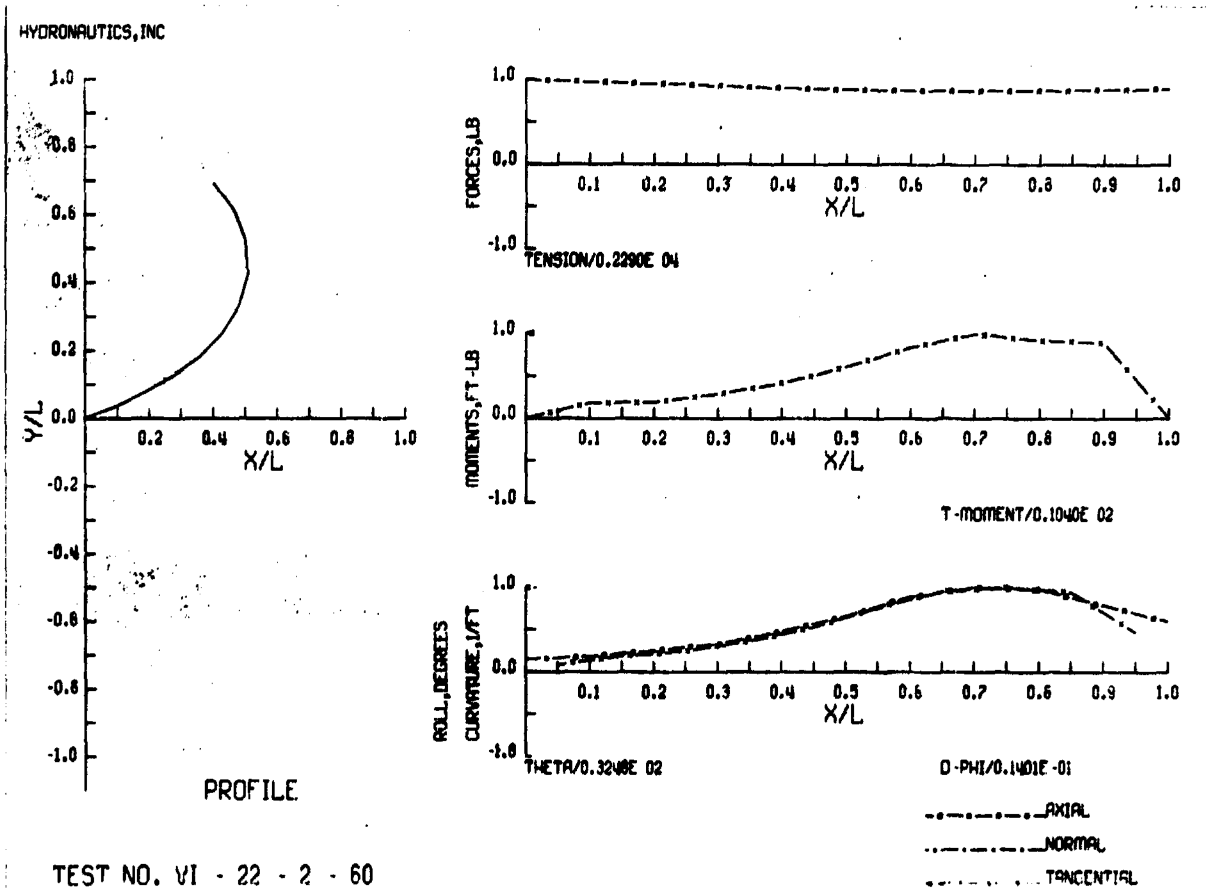

TEST NO. VI - 22 - 2 - 60

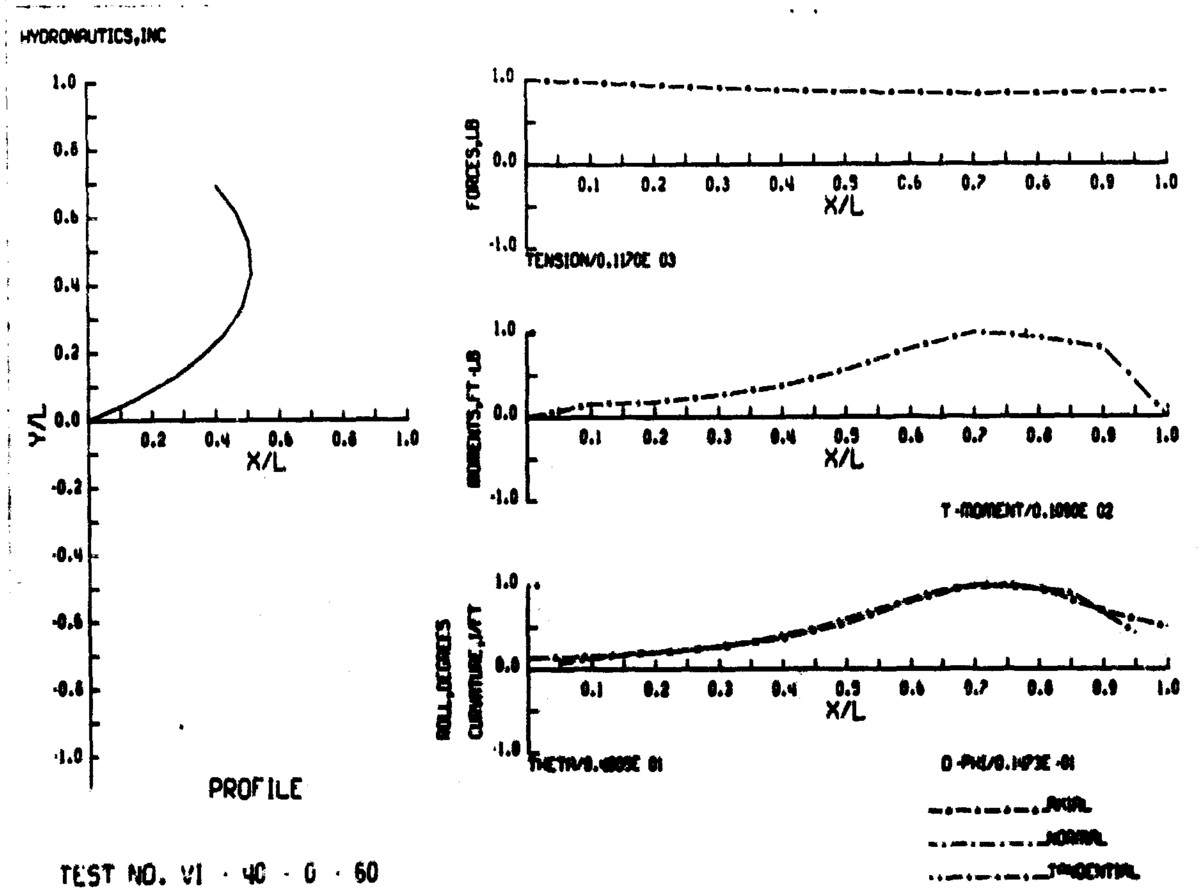

TEST NO. VI - 40 - 0 - 60

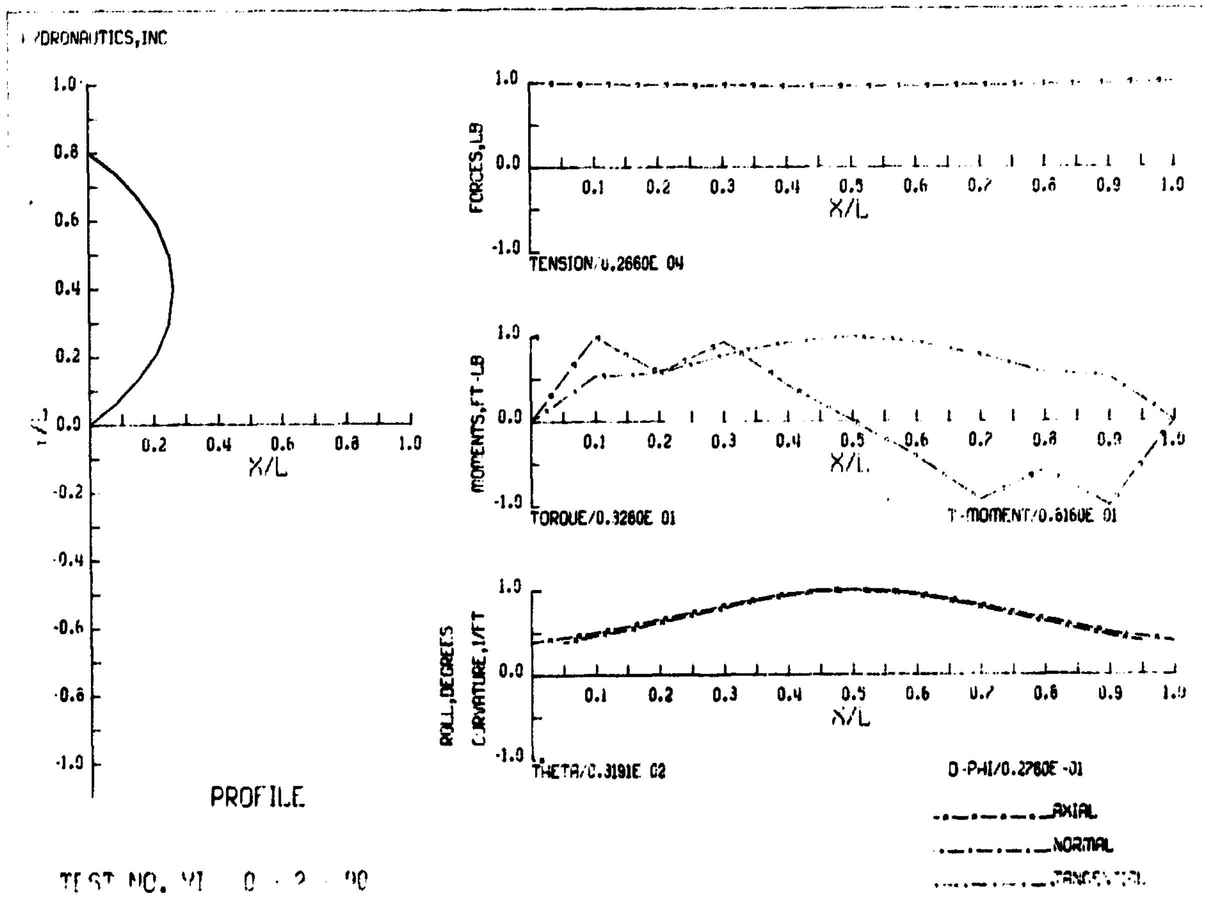
HYDRONAUTICS,INC
Y/L
X/L
PROFILE
FORCES,LB
TENSION/0.2660E 04
MOMENTS,FT-LB
TORQUE/0.3260E 01
T-MOMENT/0.6160E 01
ROLL,DEGREES
CURVATURE,1/FT
THETA/0.3191E 02
D-PHI/0.2780E -01
AXIAL
NORMAL
TANGENTIAL
TEST NO. VI 0 - 2 - 90

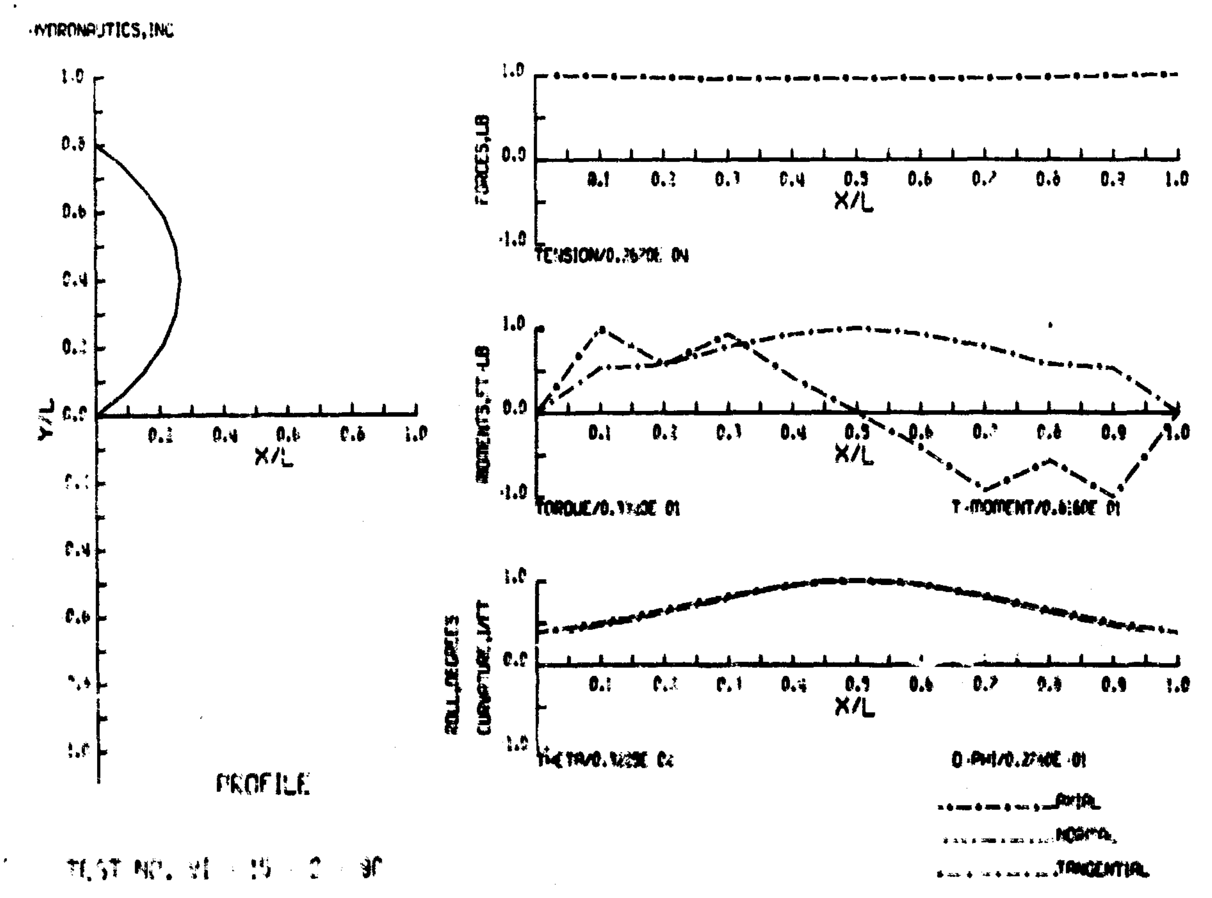
HYDRONAUTICS,INC
Y/L
X/L
PROFILE
FORCES,LB
MOMENTS,FT-LB
T-MOMENT
ROLL,DEGREES
CURVATURE,1/FT
AXIAL
TANGENTIAL

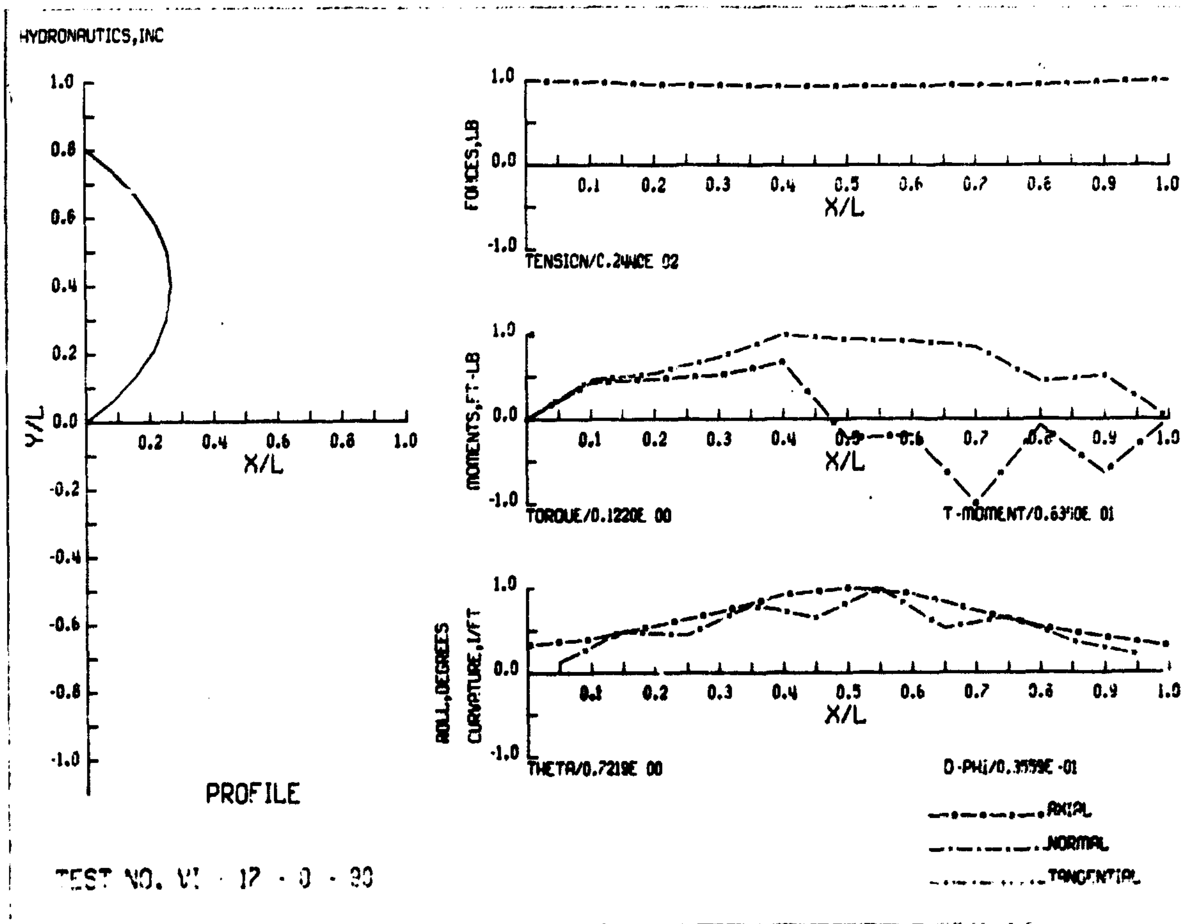
HYDRONAUTICS,INC
Y/L
X/L
PROFILE
FORCES,LB
MOMENTS,FT-LB
ROLL,DEGREES
CURVATURE,1/FT
AXIAL
NORMAL
TANGENTIAL

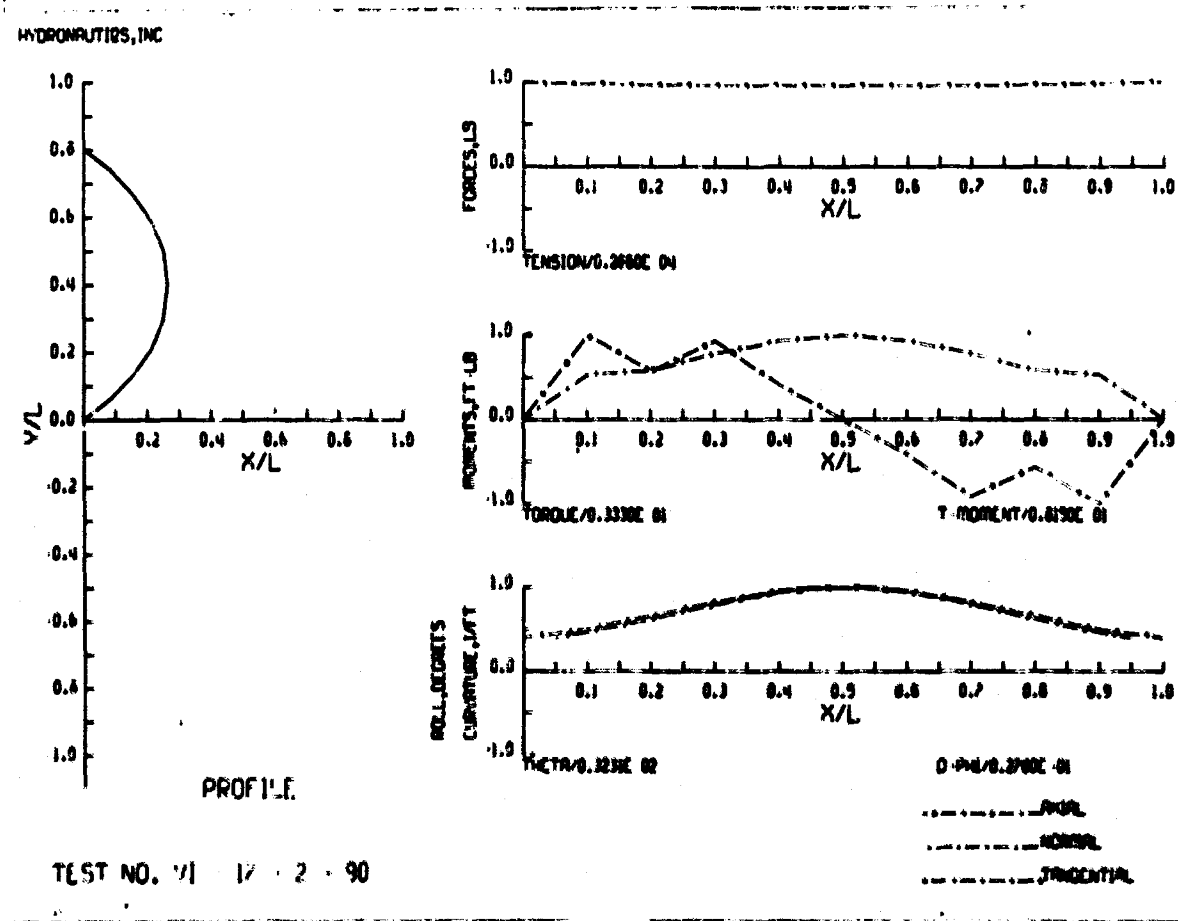
HYDRONAUTICS,INC
Y/L
X/L
PROFILE
FORCES,LB
MOMENTS,FT-LB
ROLL,DEGREES
CURVATURE,1/FT
AXIAL
NORMAL
TANGENTIAL
TEST NO. VI - 17 - 2 - 90

HYDRONAUTICS,INC

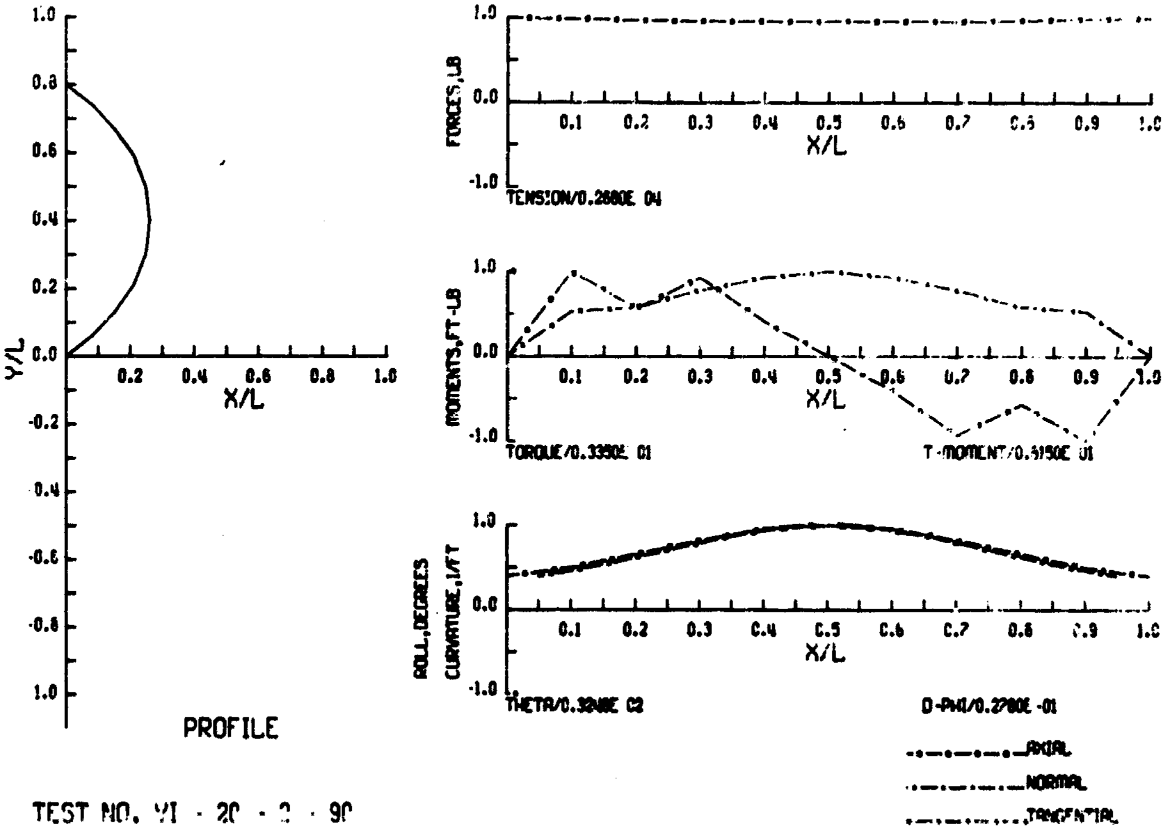

TEST NO. VI - 20 - 0 - 90

HYDRONAUTICS,INC

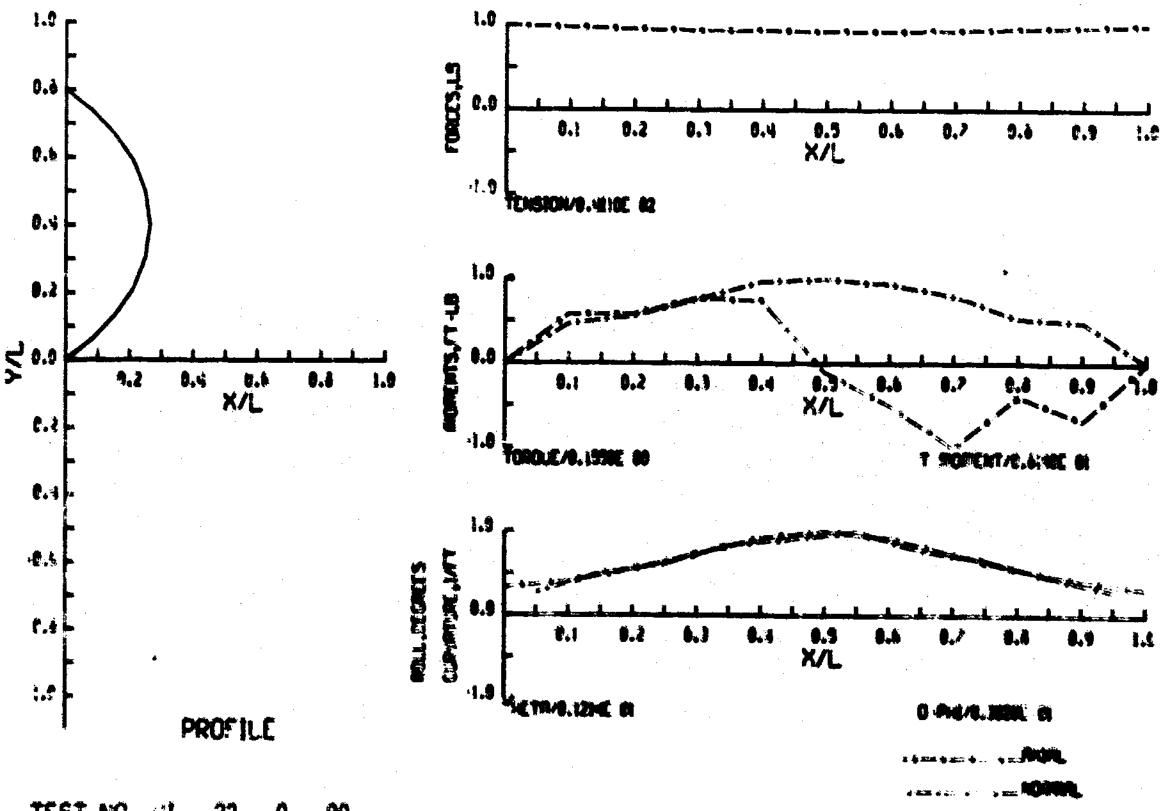

TEST NO. VI - 22 - 0 - 90

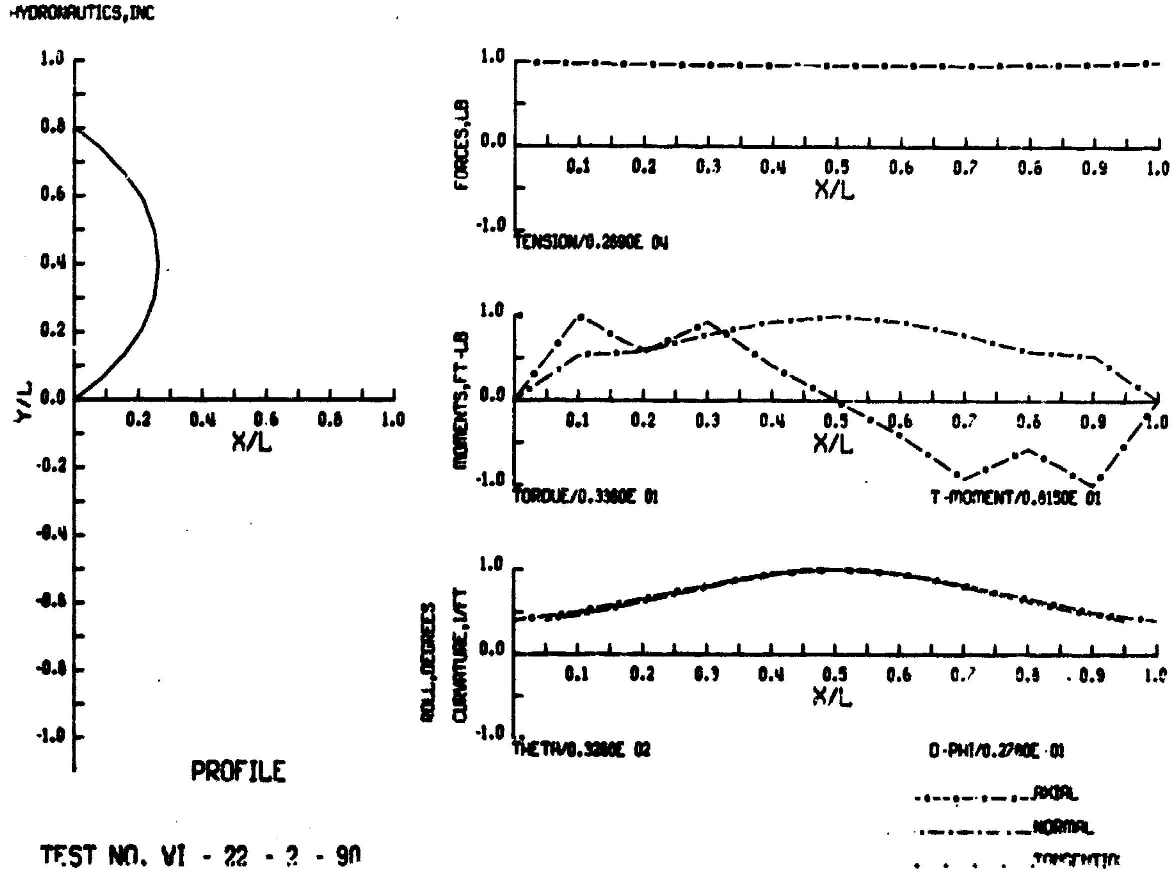

TEST NO. VI - 22 - 2 - 90

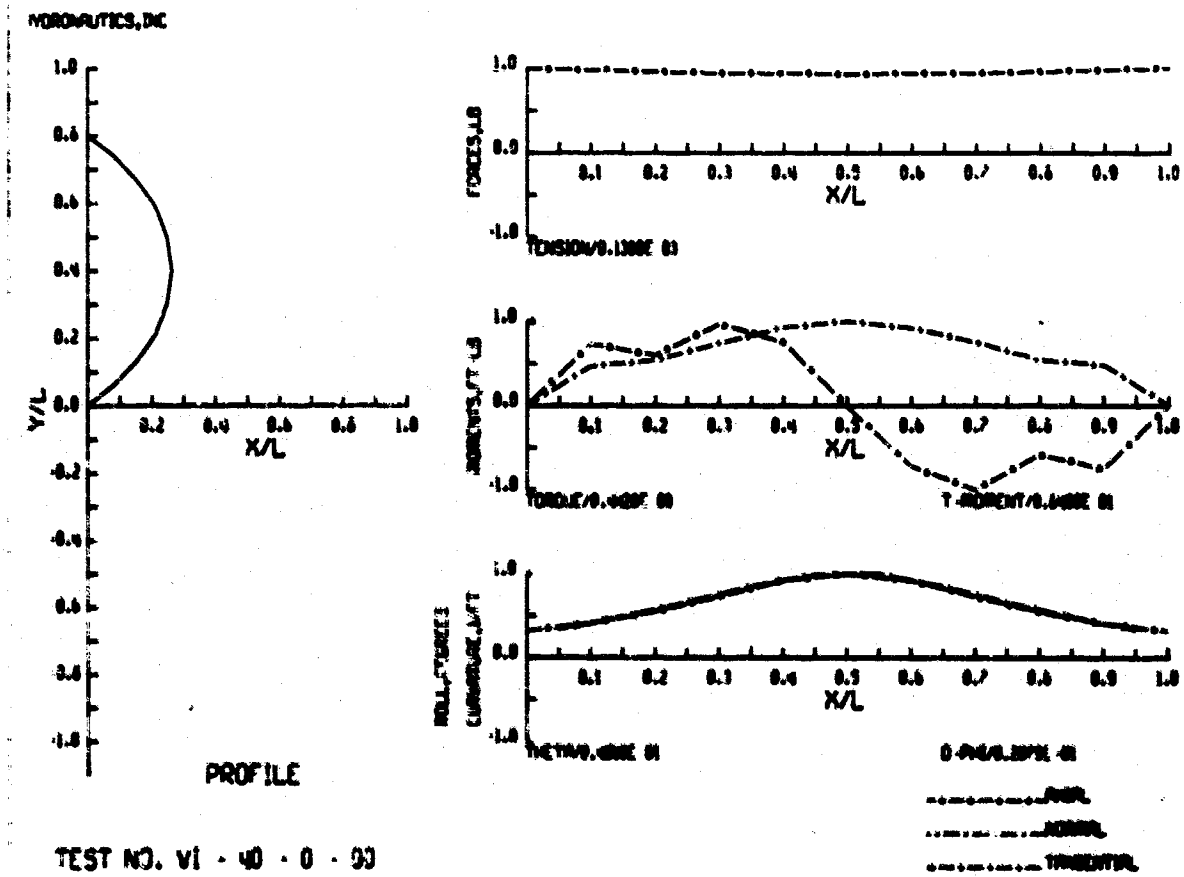

TEST NO. VI - 40 - 0 - 90

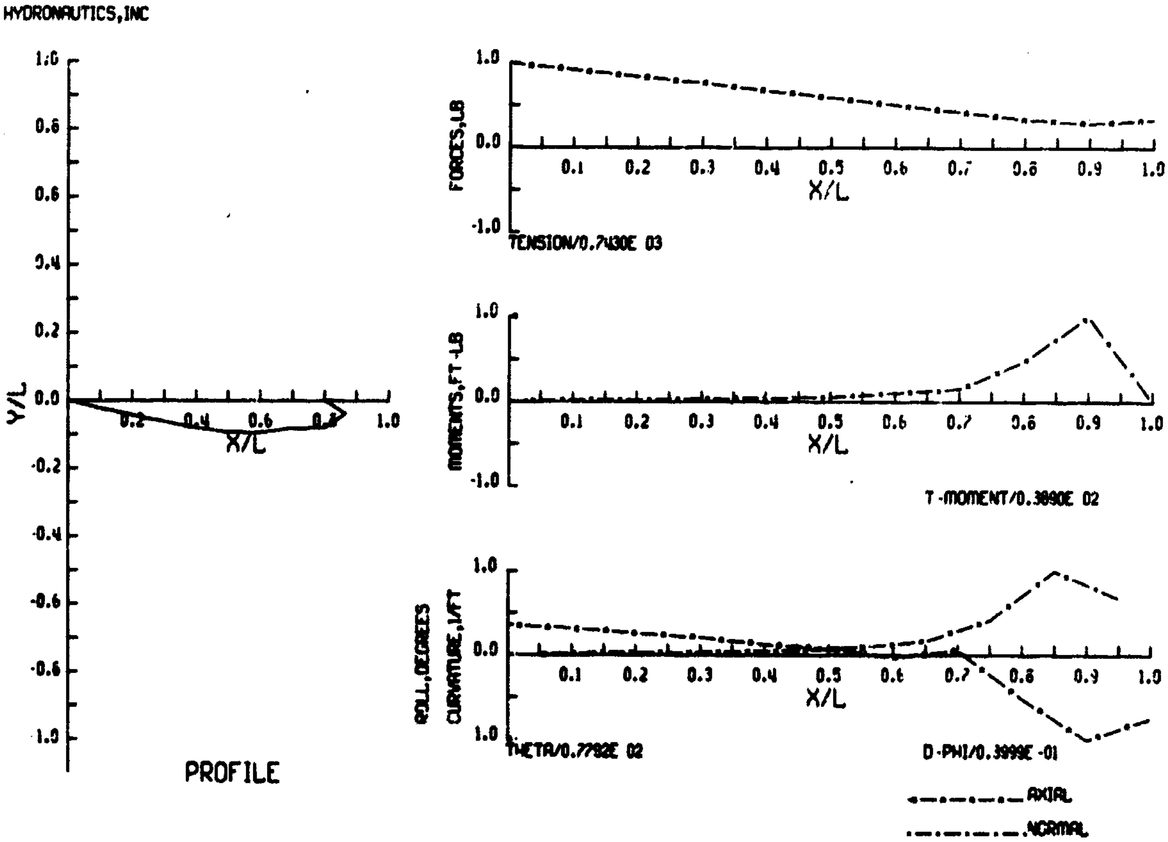

TEST NO. VII - 0 - 2 - 0

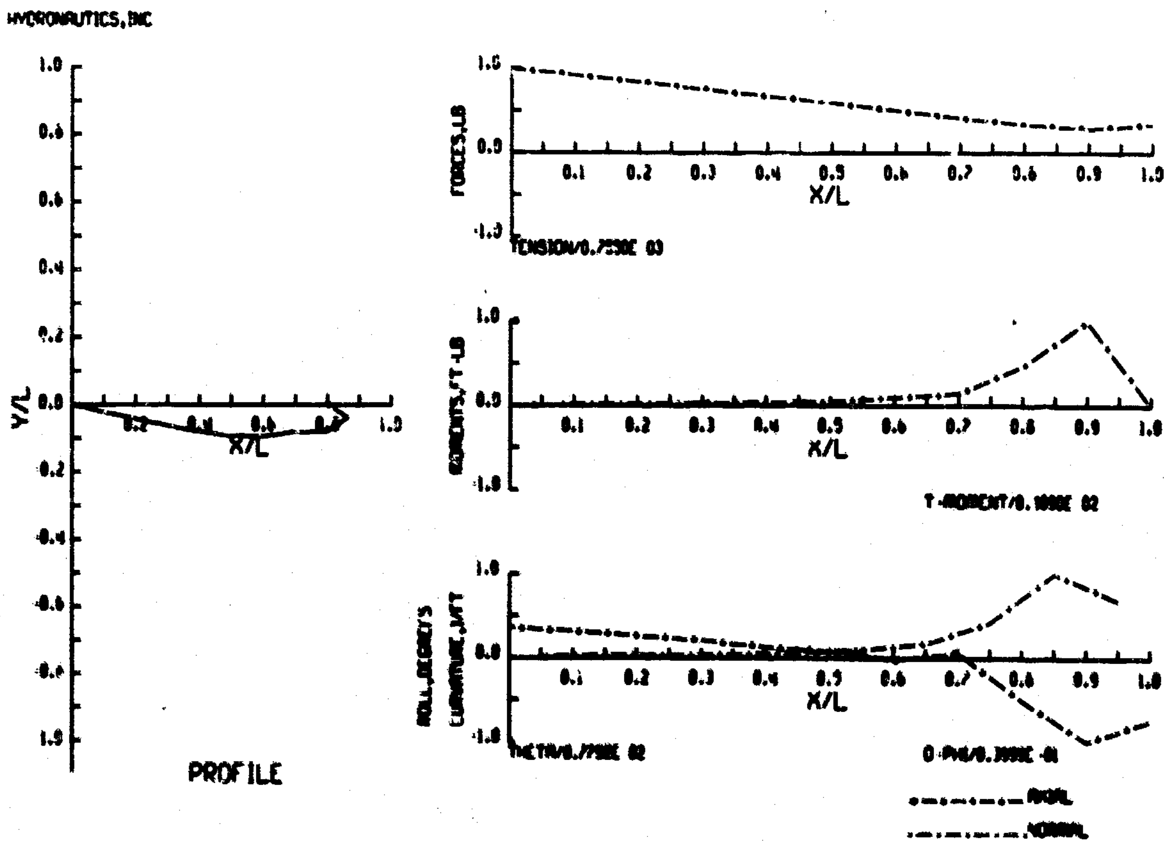

TEST NO. VII - 15 - 2 - 0

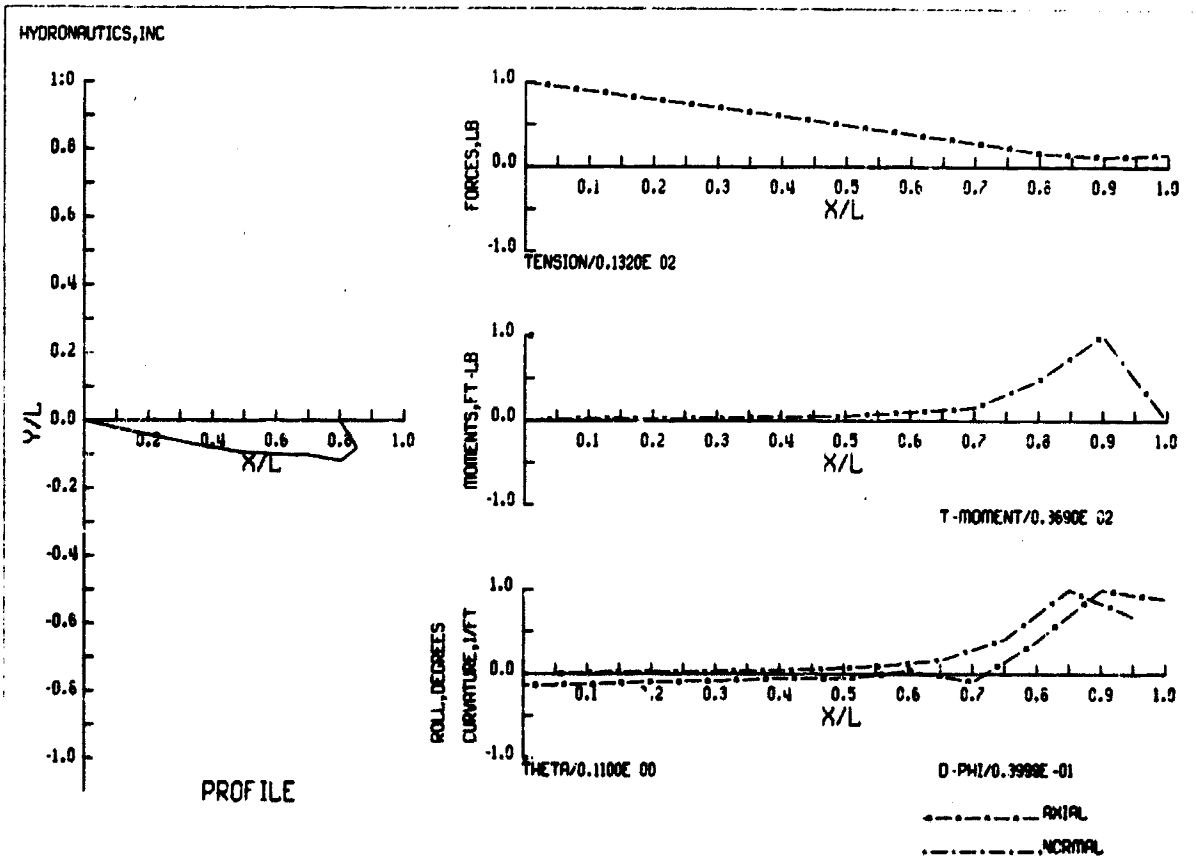

TEST NO. VII - 17 - 0 - 0

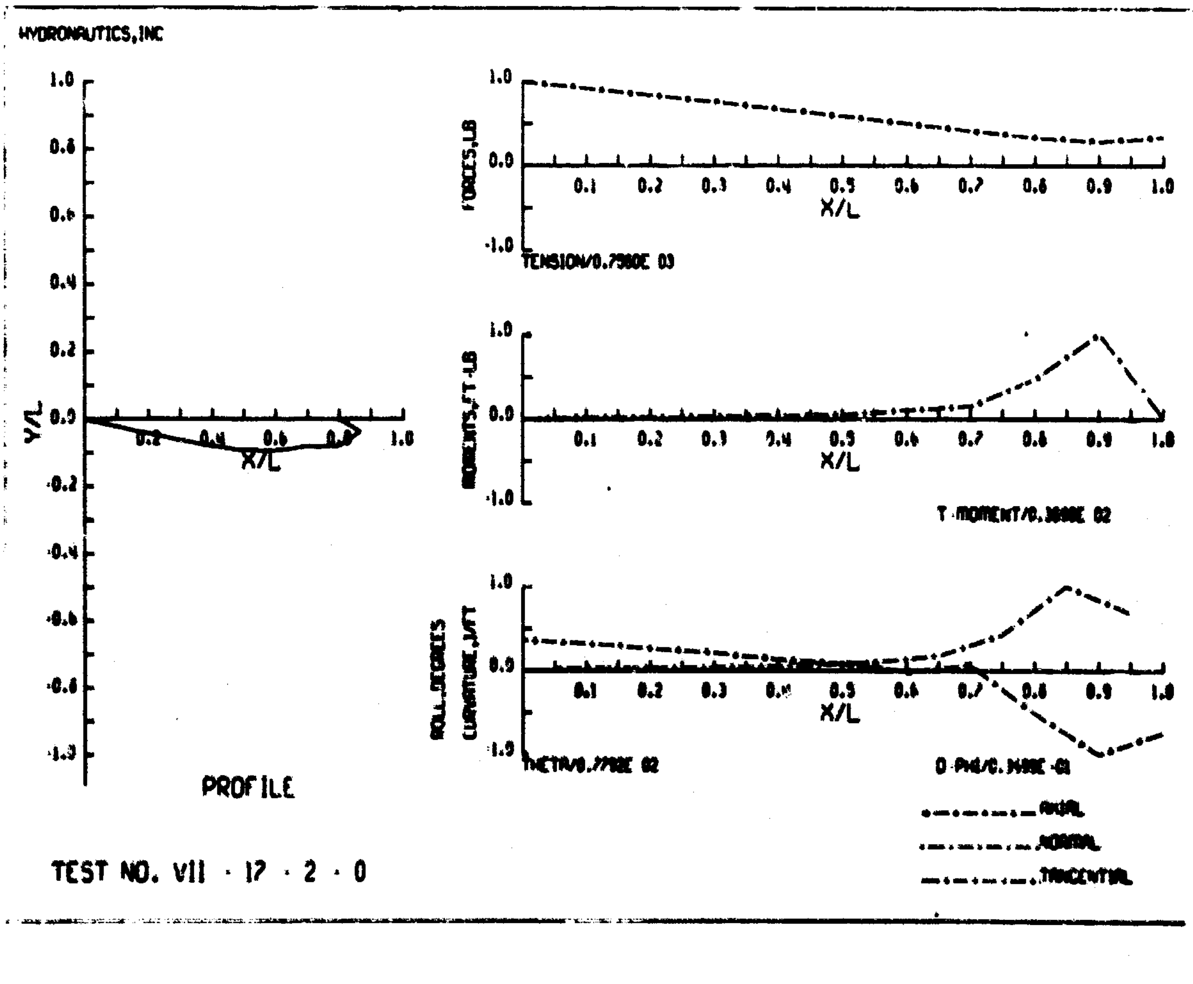

TEST NO. VII - 17 - 2 - 0

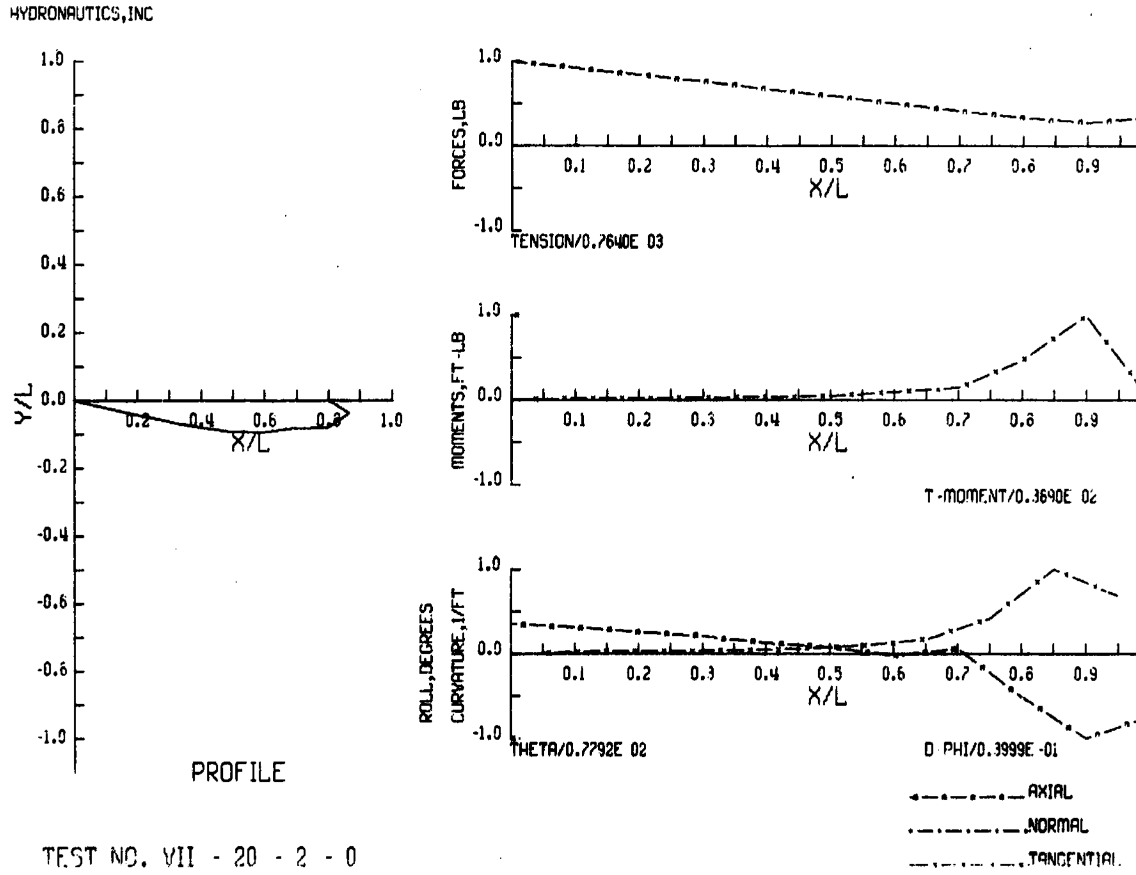
HYDRONAUTICS,INC
Y/L
X/L
PROFILE
FORCES,LB
TENSION/0.7640E 03
MOMENTS,FT-LB
T-MOMENT/0.3690E 02
ROLL,DEGREES
CURVATURE,1/FT
THETA/0.7792E 02
D PHI/0.3999E-01
AXIAL
NORMAL
TANGENTIAL
TEST NO. VII - 20 - 2 - 0

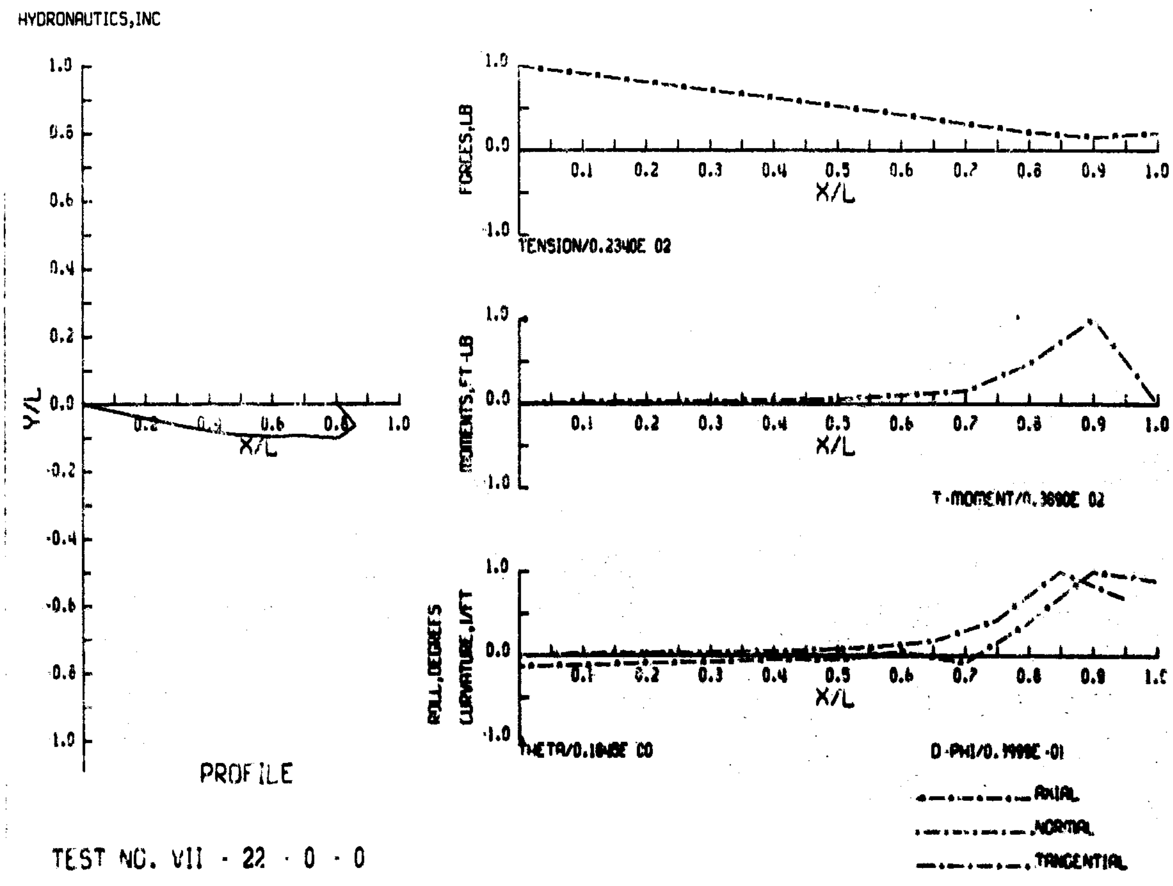
HYDRONAUTICS,INC
Y/L
X/L
PROFILE
FORCES,LB
TENSION/0.2340E 02
MOMENTS,FT-LB
T-MOMENT/0.3690E 02
ROLL,DEGREES
CURVATURE,1/FT
AXIAL
NORMAL
TANGENTIAL
TEST NO. VII - 22 - 0 - 0

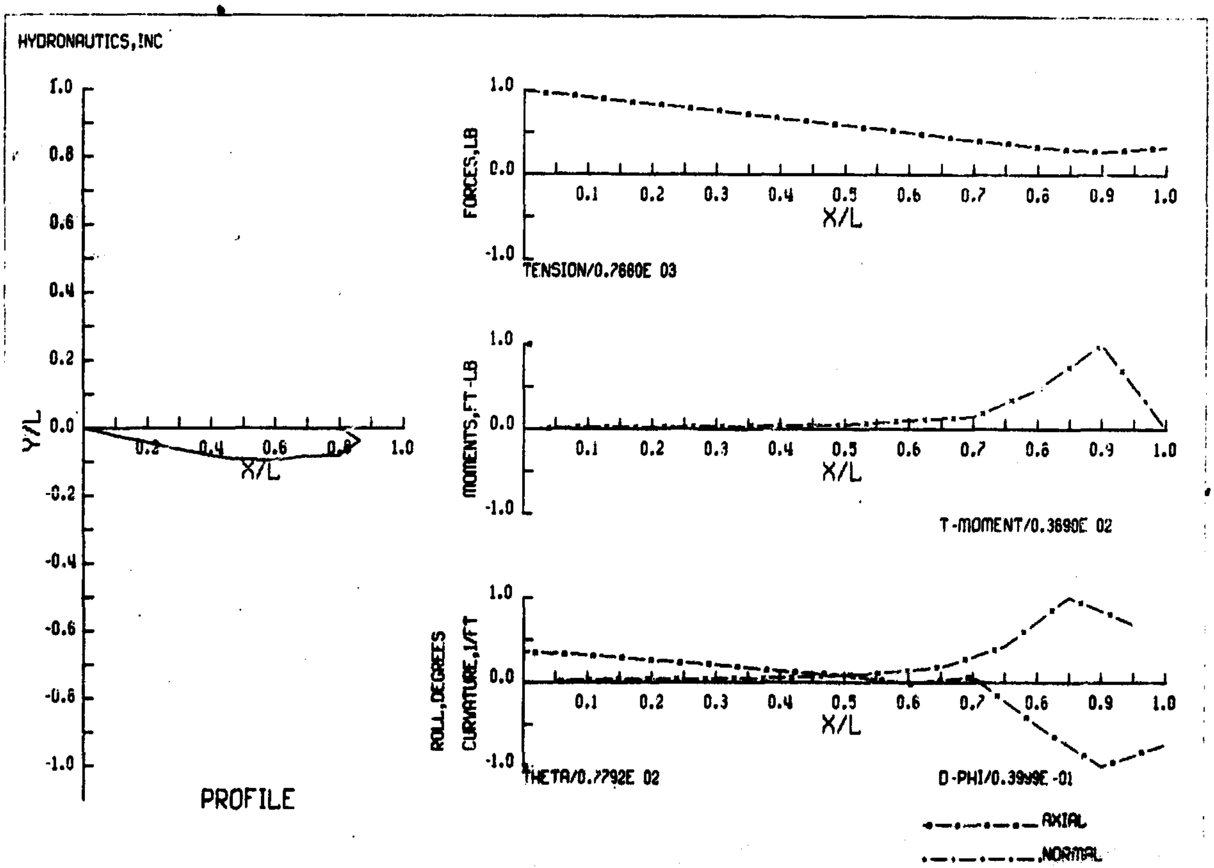

TEST NO. VII - 22 - 2 - 0

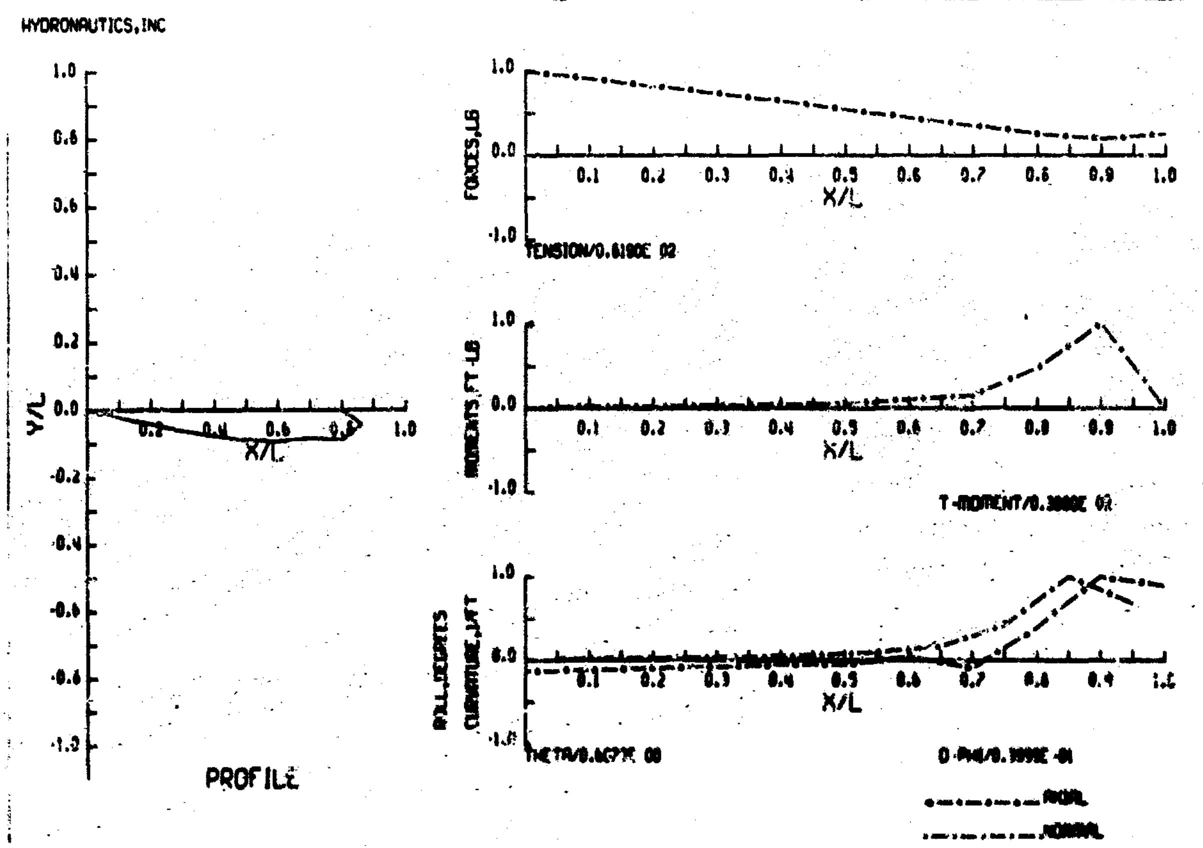

TEST NO. VII - 40 - 0 - 0

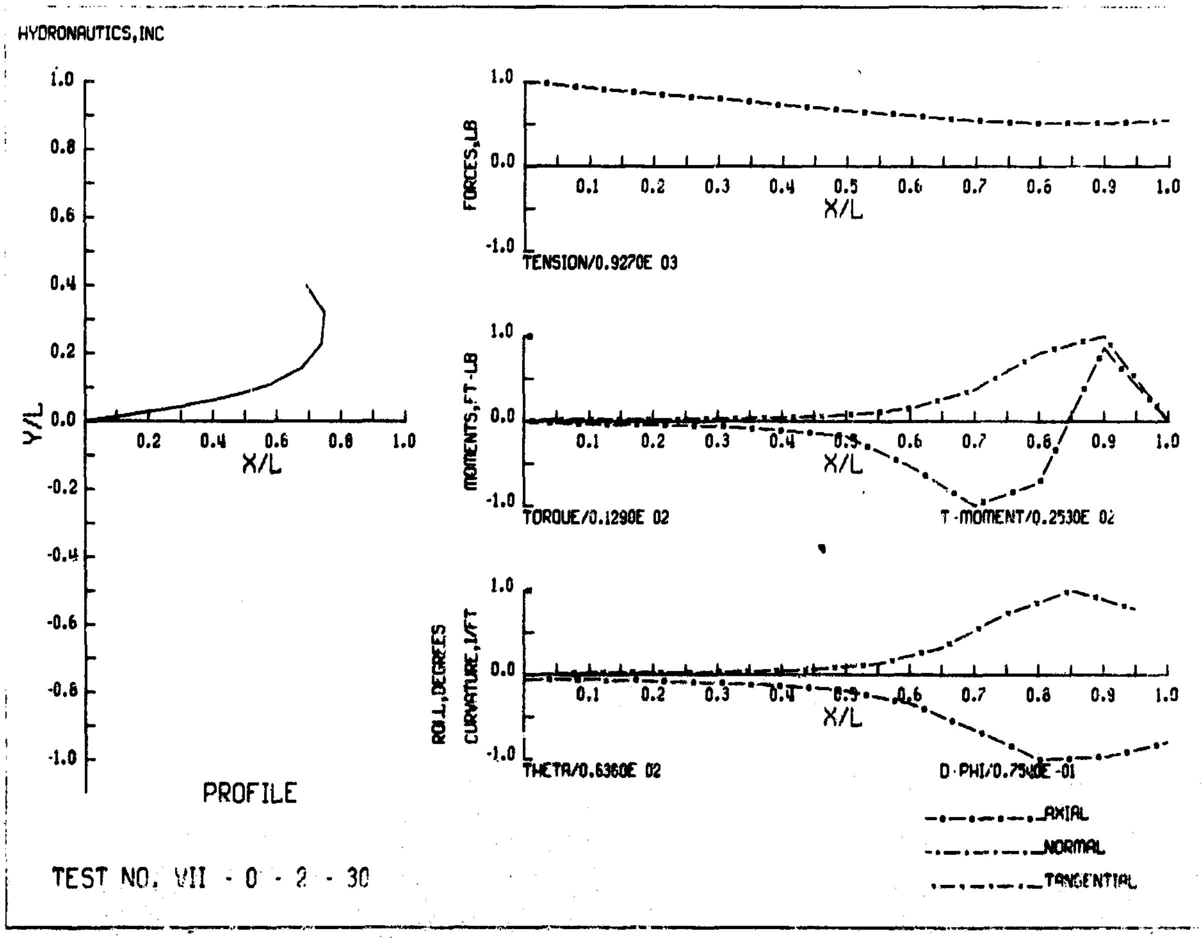
HYDRONAUTICS,INC
Y/L
X/L
PROFILE
FORCES,LB
TENSION/0.9270E 03
MOMENTS,FT-LB
TORQUE/0.1290E 02
T-MOMENT/0.2530E 02
ROLL,DEGREES
CURVATURE,1/FT
THETA/0.6360E 02
D-PHI/0.754E -01
AXIAL
NORMAL
TANGENTIAL
TEST NO. VII - 0 - 2 - 30

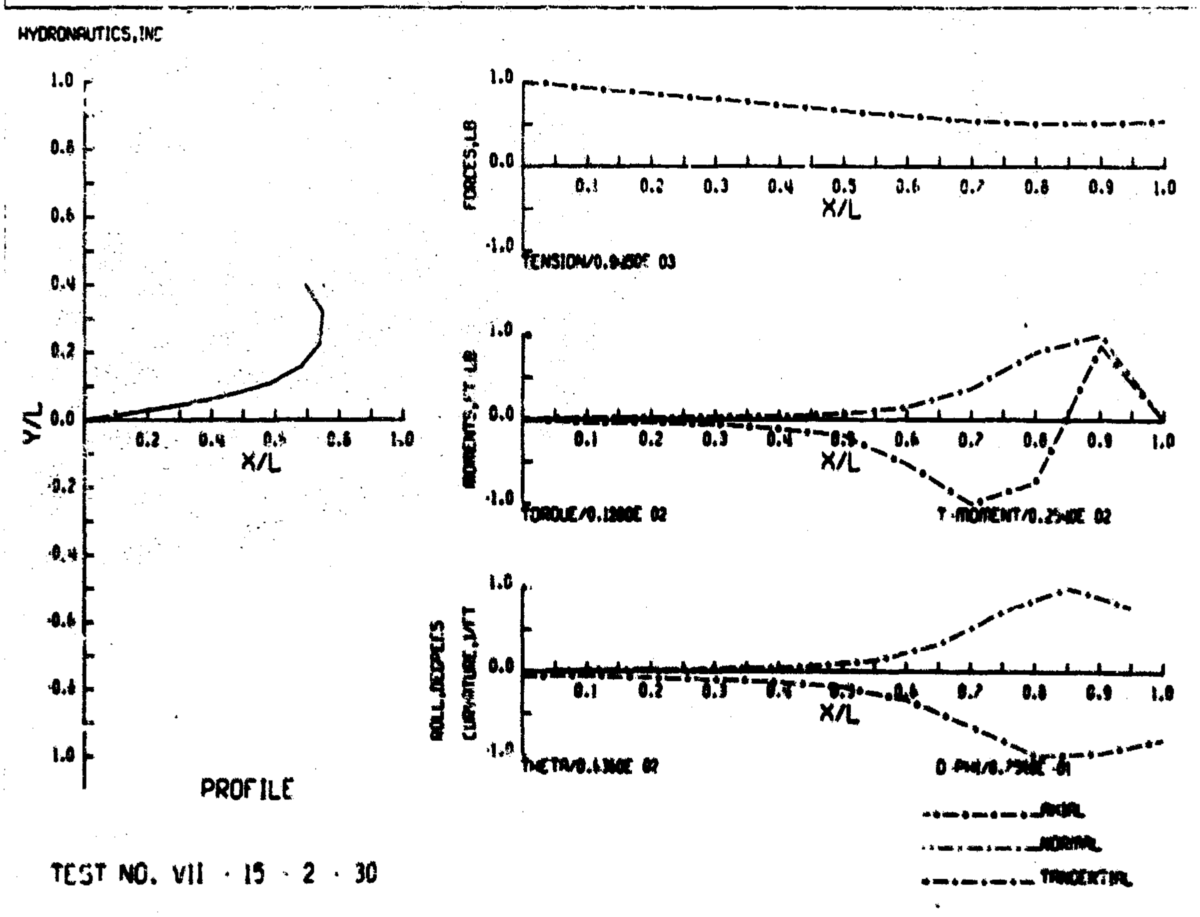
HYDRONAUTICS,INC
Y/L
X/L
PROFILE
FORCES,LB
MOMENTS,FT-LB
TORQUE/0.1280E 02
ROLL,DEGREES
CURVATURE,1/FT
AXIAL
NORMAL
TANGENTIAL
TEST NO. VII - 15 - 2 - 30

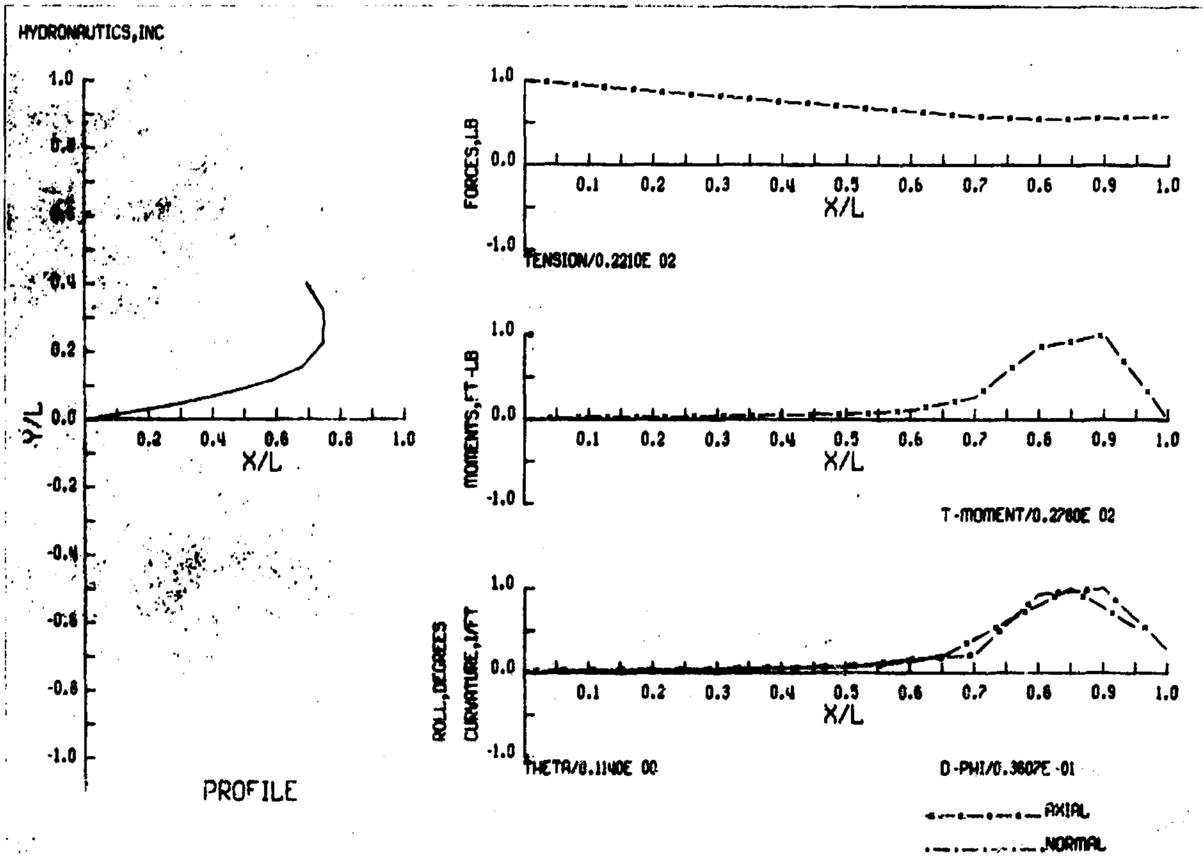

TEST NO. VII - 17 - 0 - 30

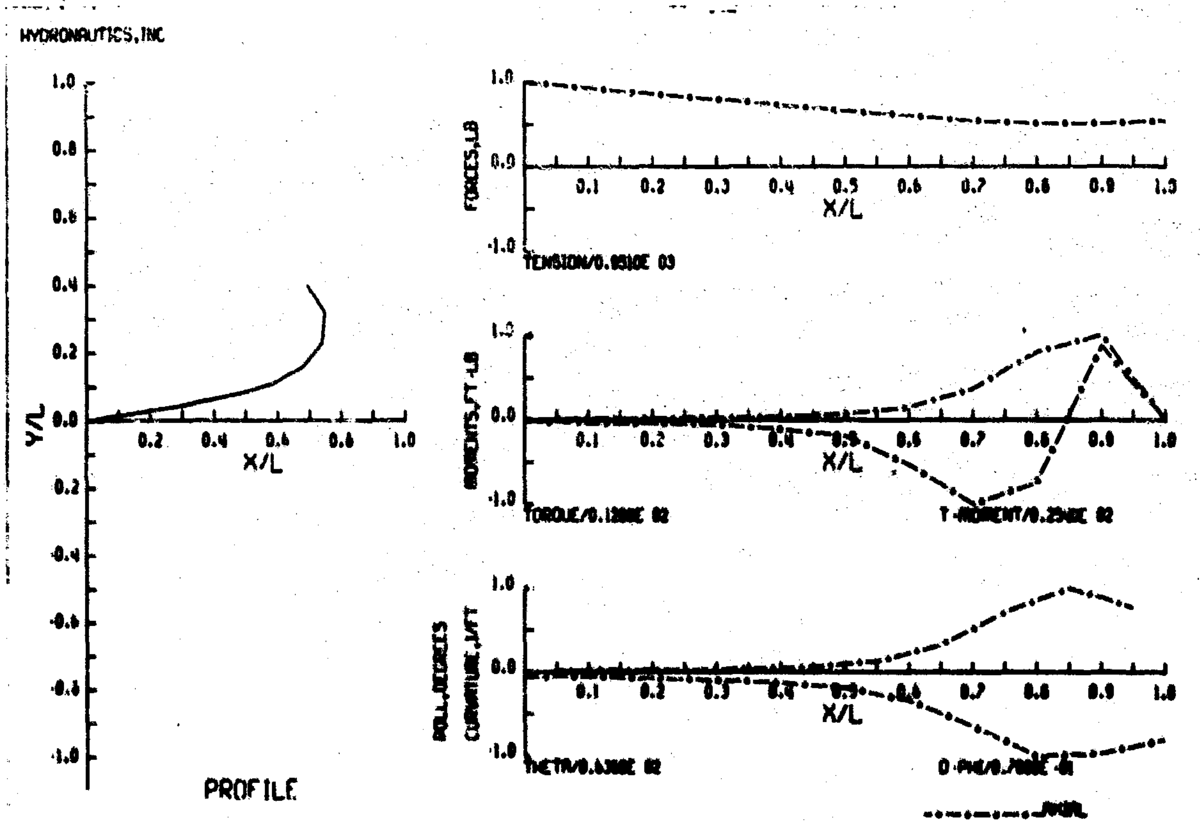

TEST NO. VII - 17 - 2 - 30

HYDRONAUTICS,INC

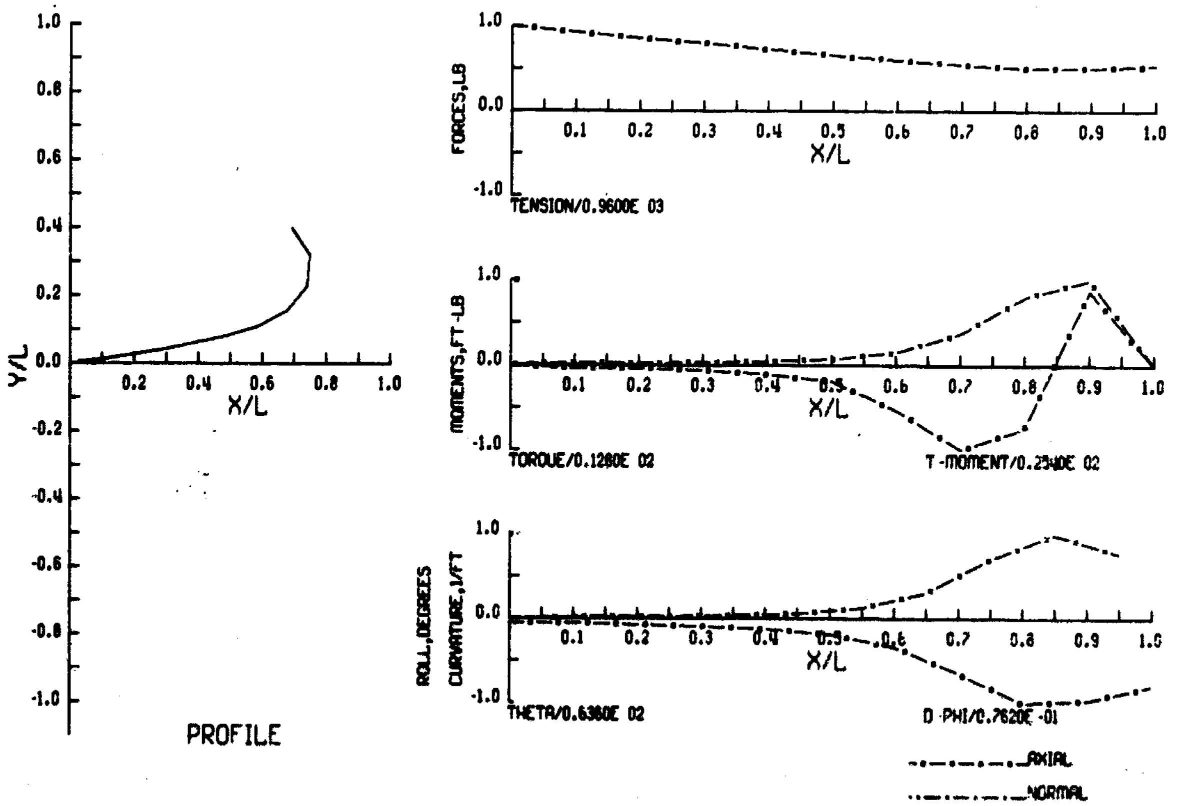

TEST NO. VII - 20 - 2 - 30

HYDRONAUTICS,INC

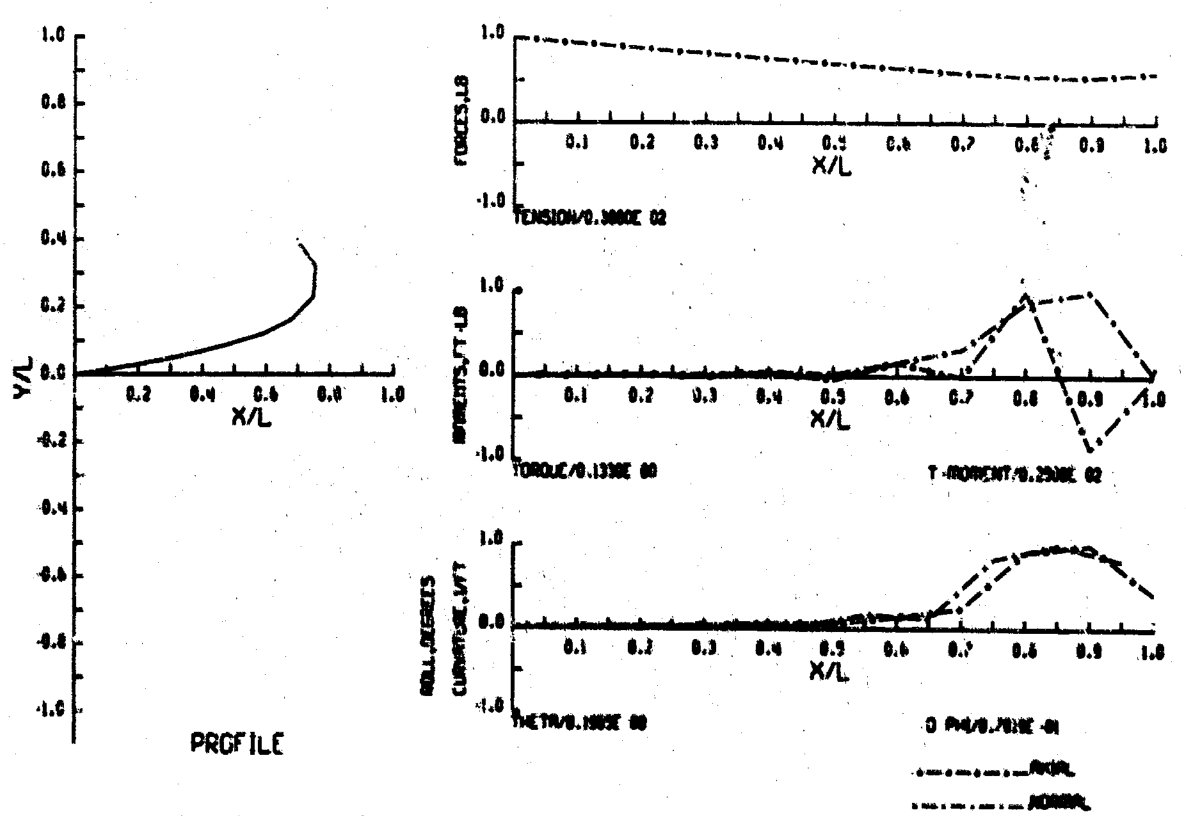

TEST NO. VII - 22 - 0 - 30

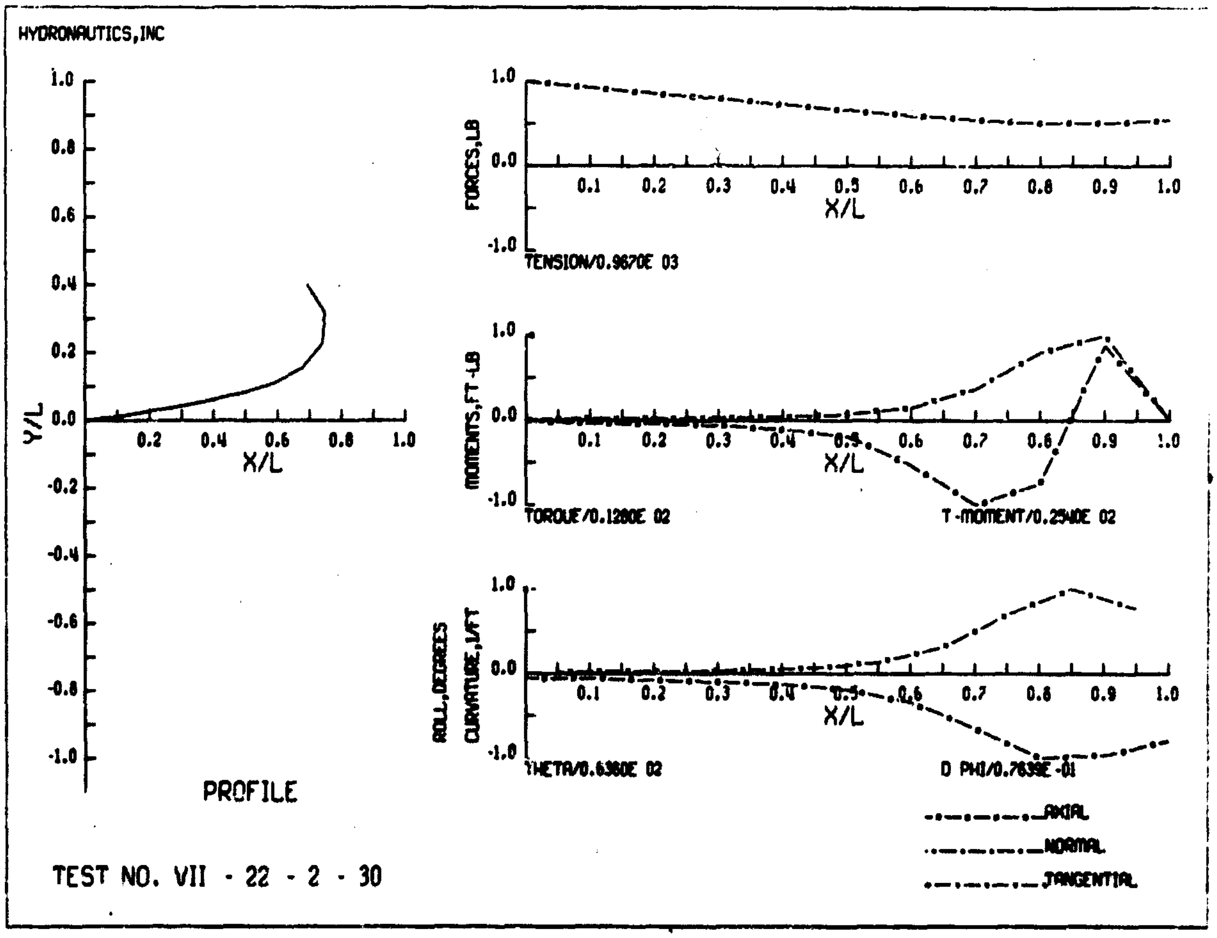
HYDRONAUTICS,INC
Y/L
X/L
PROFILE
FORCES,LB
TENSION/0.9670E 03
MOMENTS,FT-LB
TORQUE/0.1280E 02
T-MOMENT/0.2540E 02
ROLL,DEGREES
CURVATURE,1/FT
THETA/0.6360E 02
D PHI/0.7639E-01
AXIAL
NORMAL
TANGENTIAL
TEST NO. VII - 22 - 2 - 30

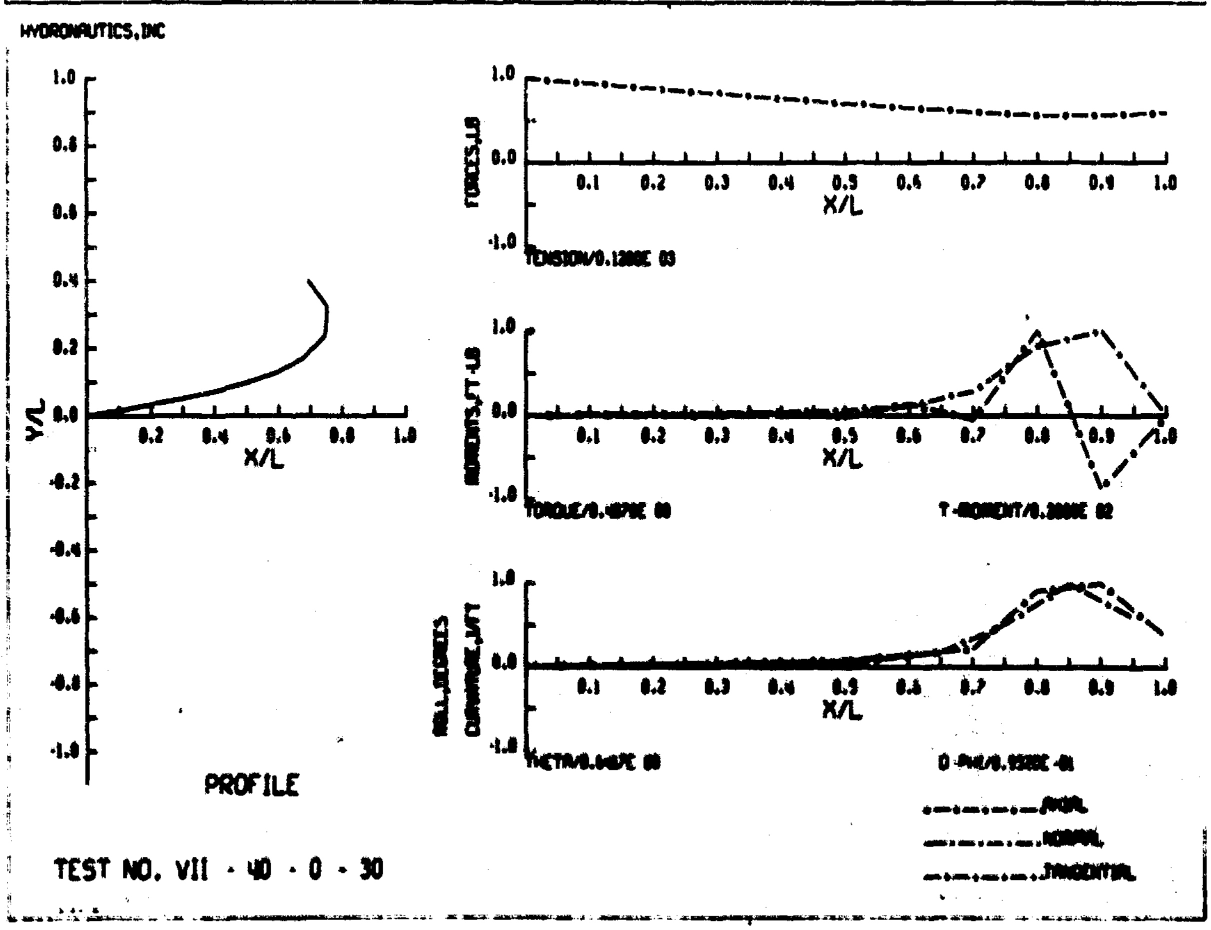
HYDRONAUTICS,INC
Y/L
X/L
PROFILE
FORCES,LB
MOMENTS,FT-LB
ROLL,DEGREES
CURVATURE,1/FT
AXIAL
NORMAL
TANGENTIAL
TEST NO. VII - 40 - 0 - 30

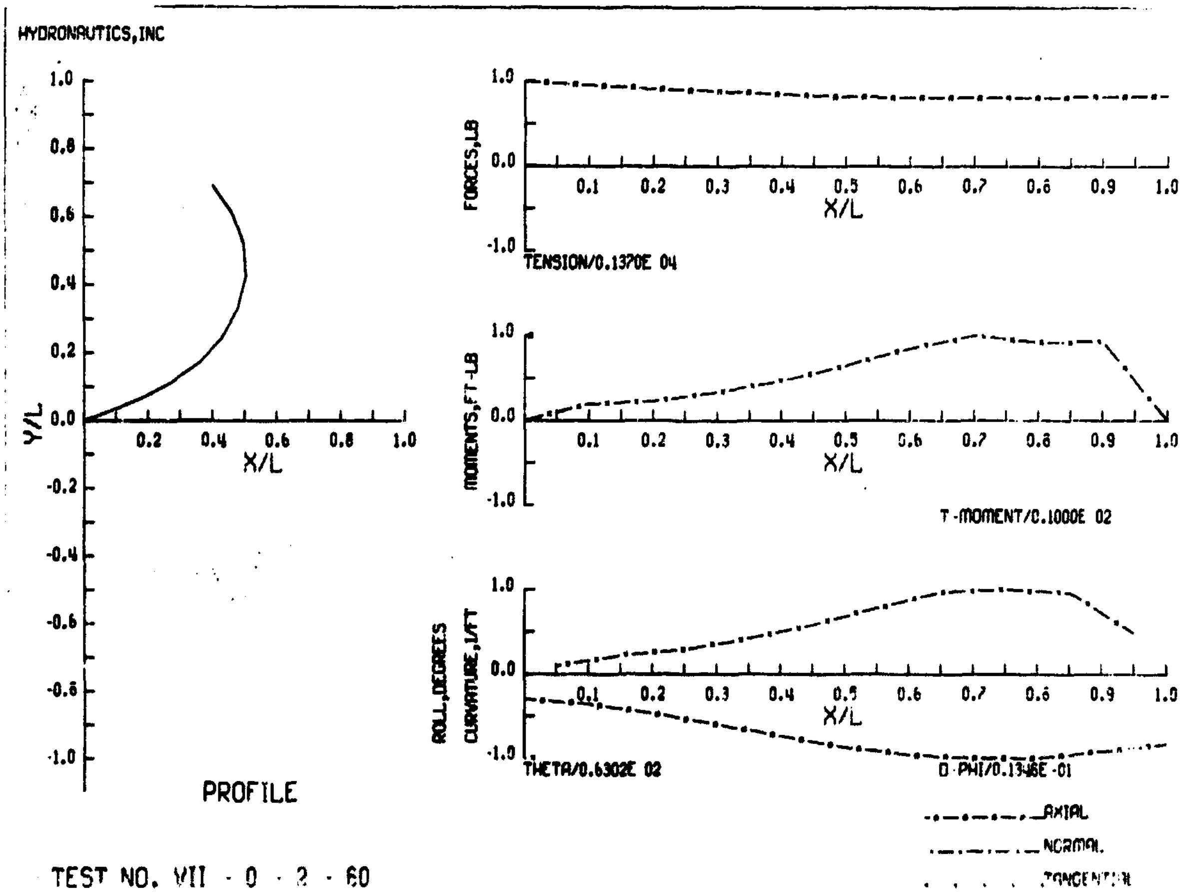

TEST NO. VII - 0 - 2 - 60

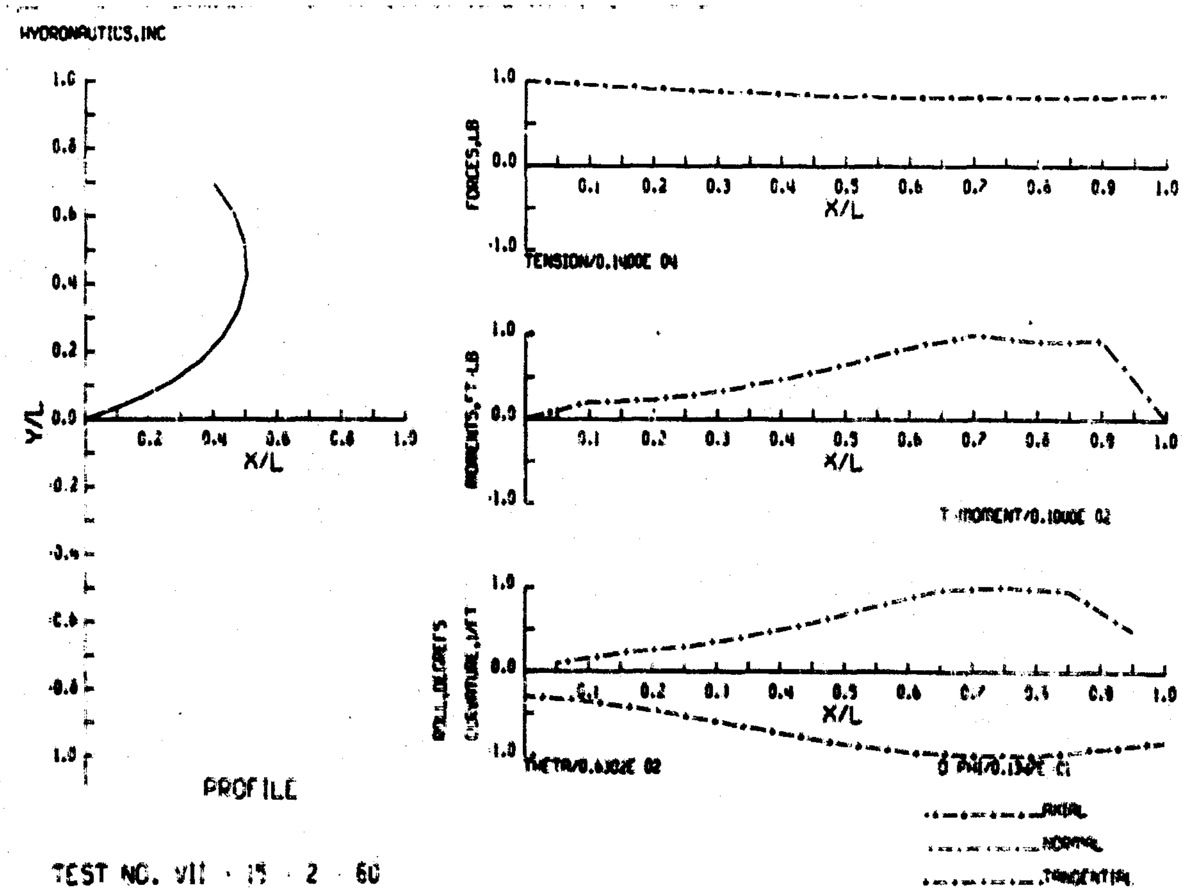

TEST NO. VII - 15 - 2 - 60

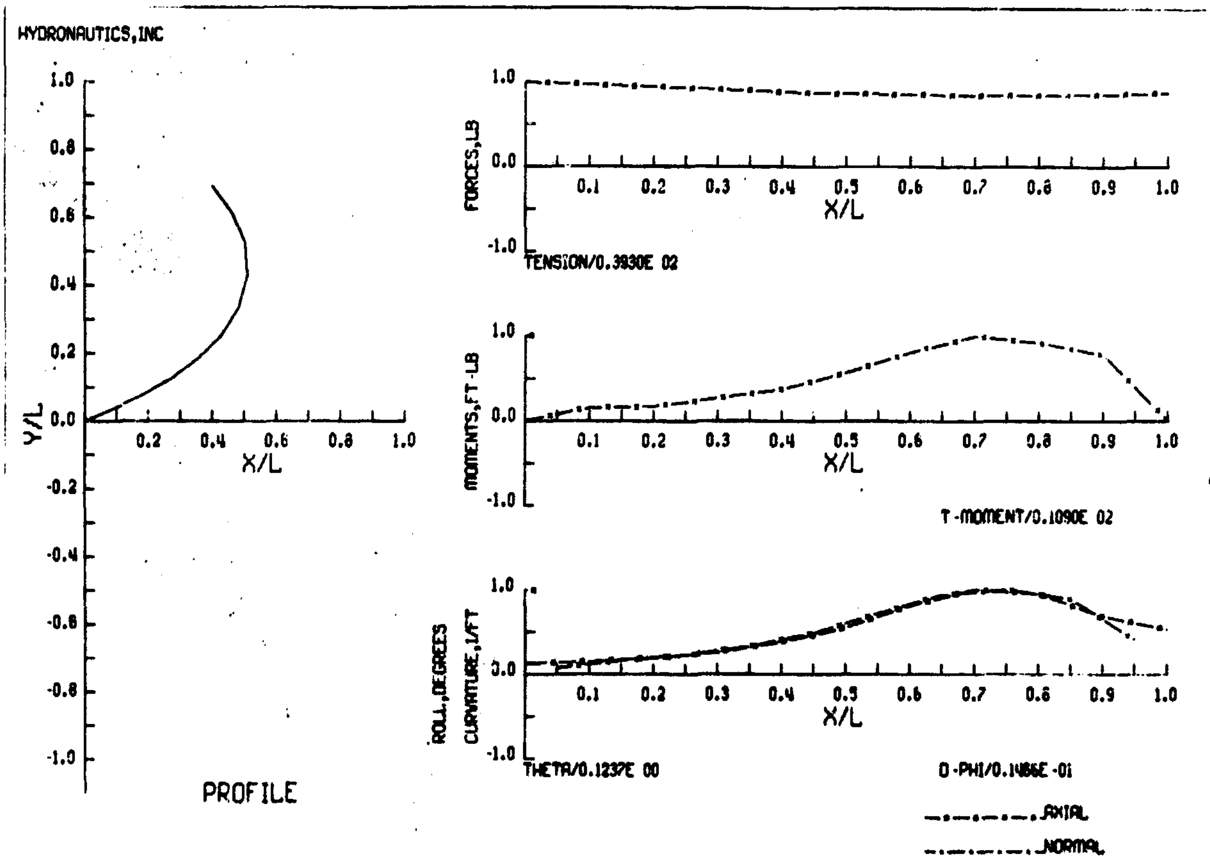

TEST NO. VII - 17 - 0 - 60

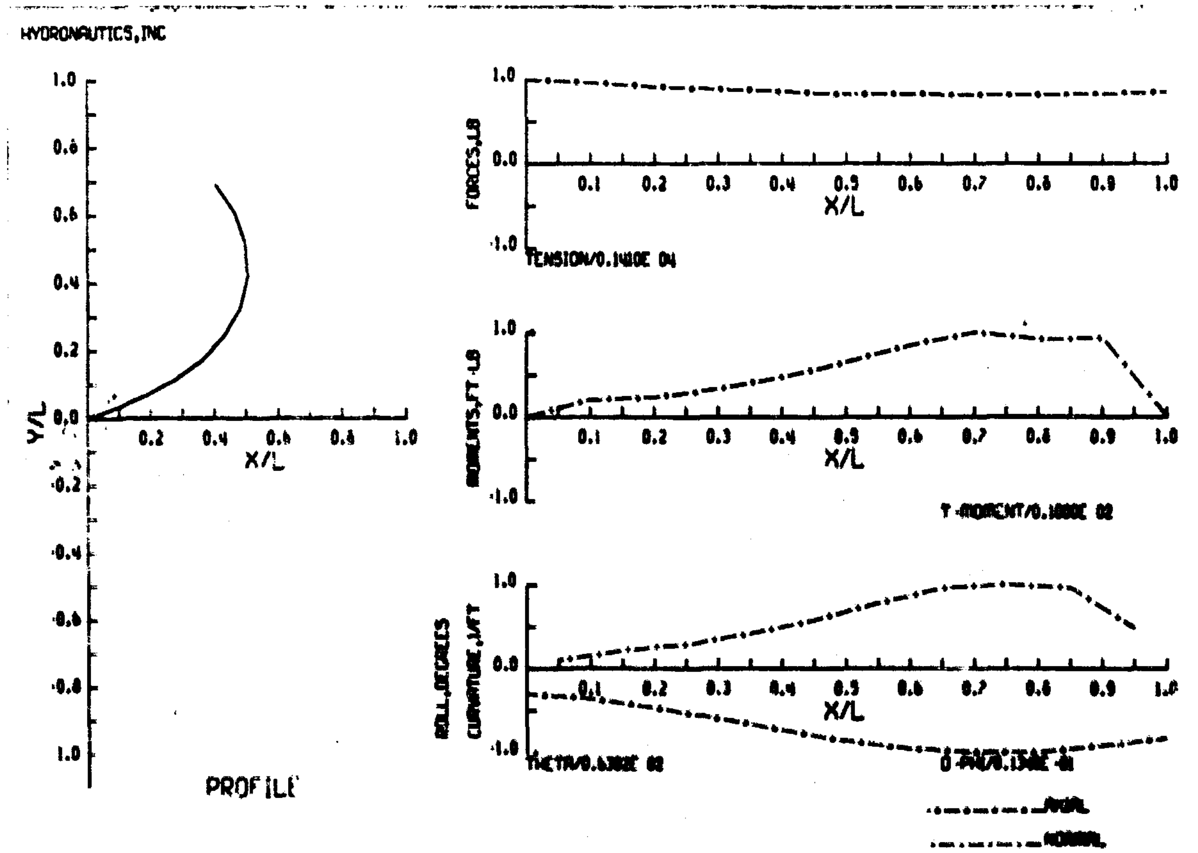

TEST NO. VII - 17 - 2 - 60

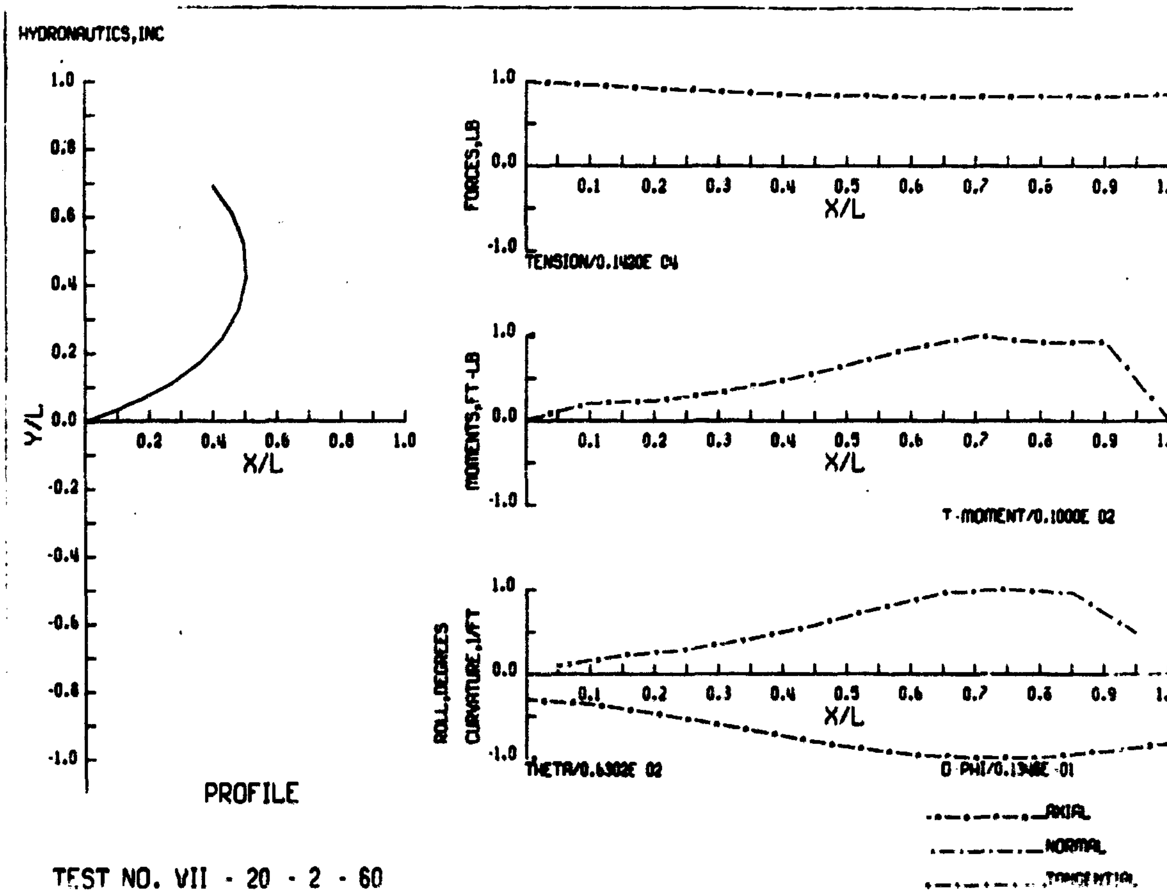

TEST NO. VII - 20 - 2 - 60

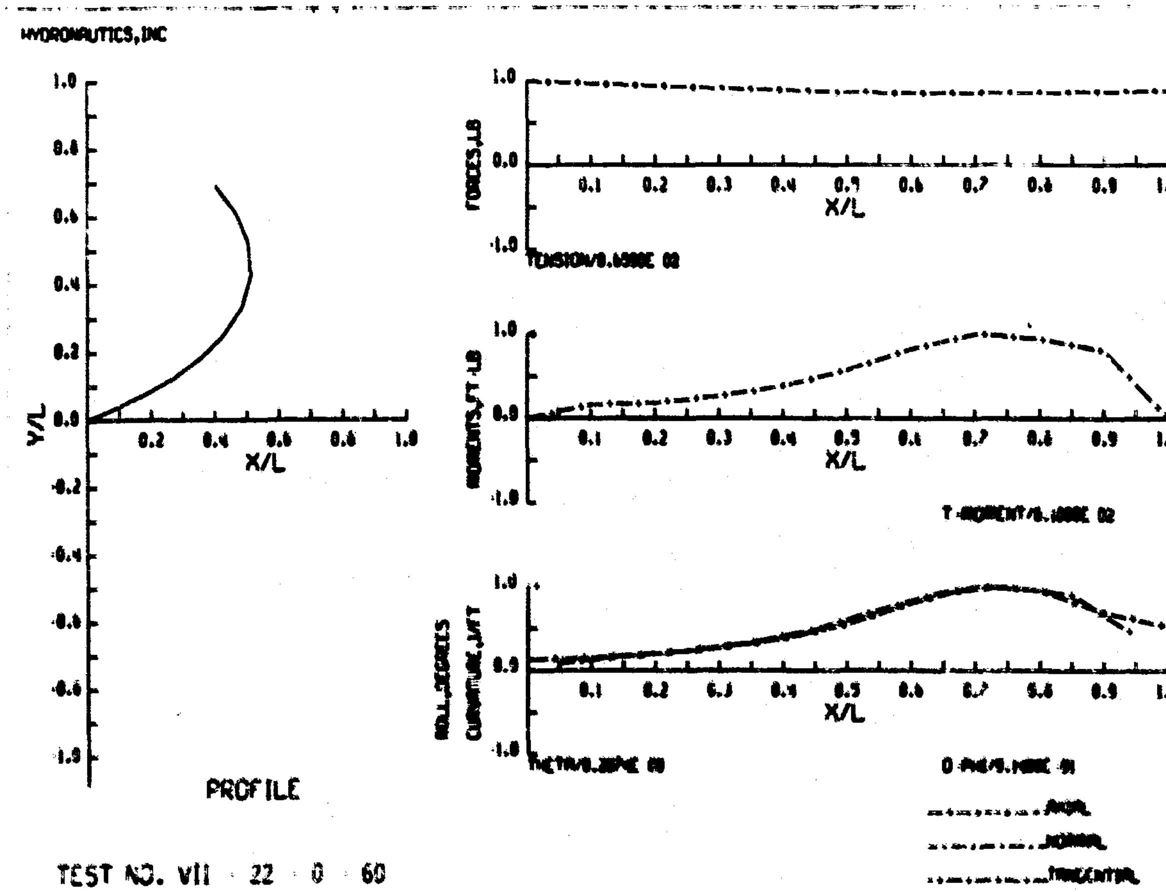

TEST NO. VII - 22 - 0 - 60

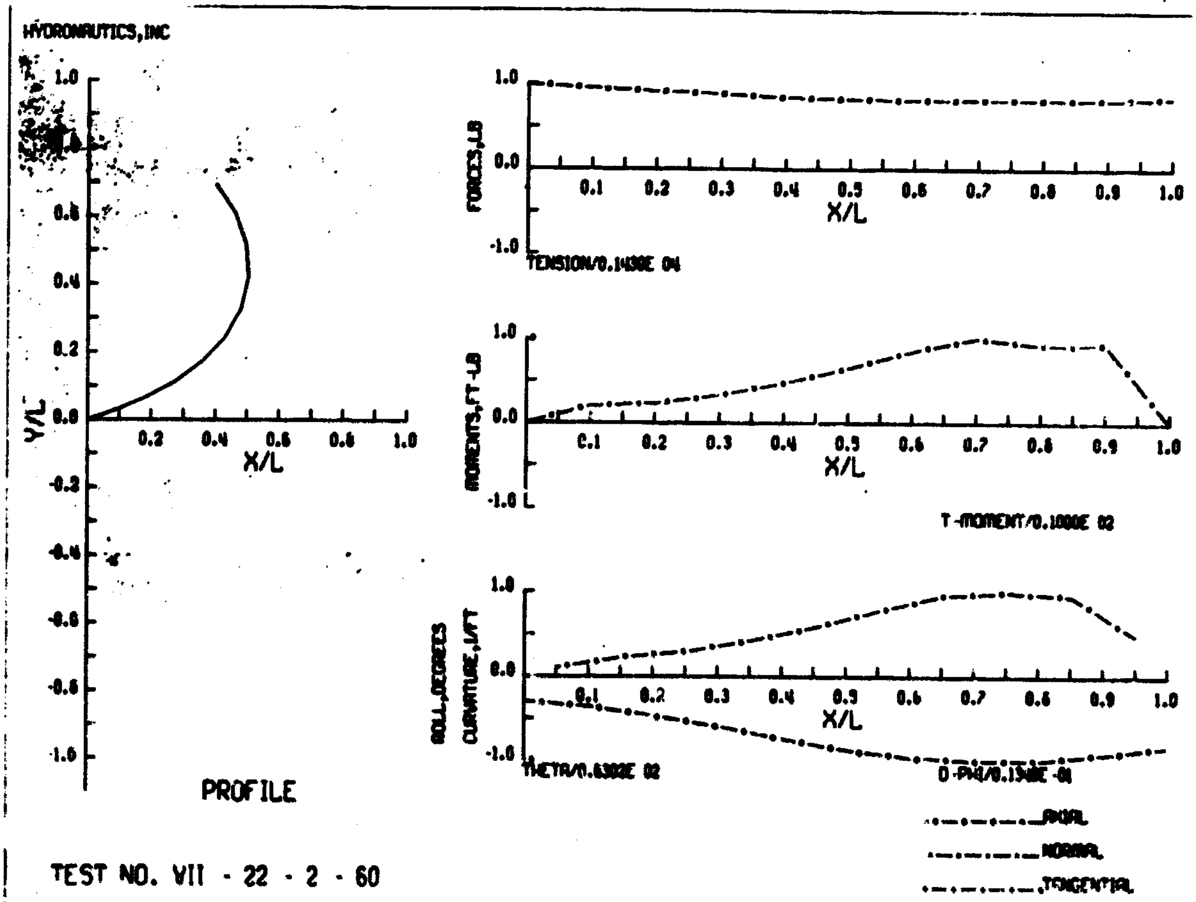

TEST NO. VII - 22 - 2 - 60

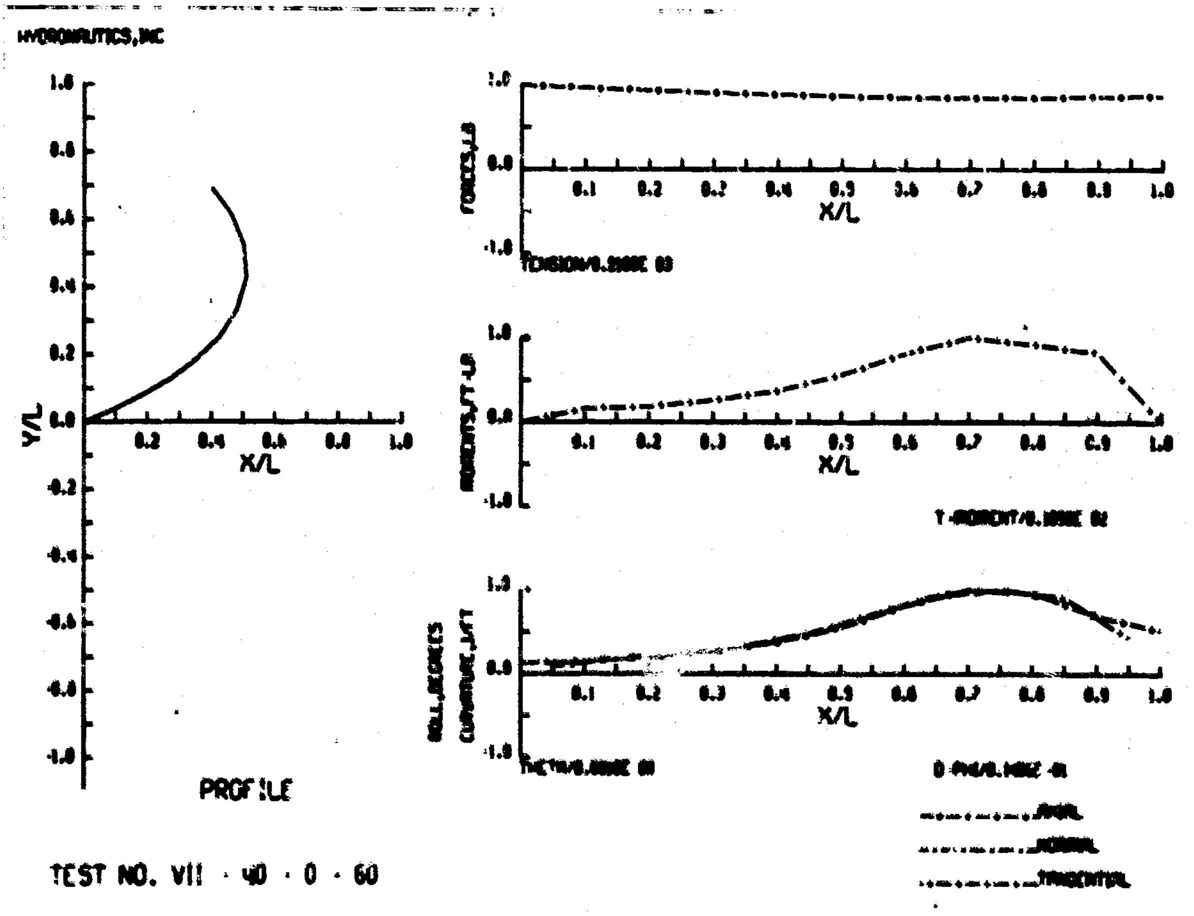

TEST NO. VII - 40 - 0 - 60

HYDRONAUTICS,INC

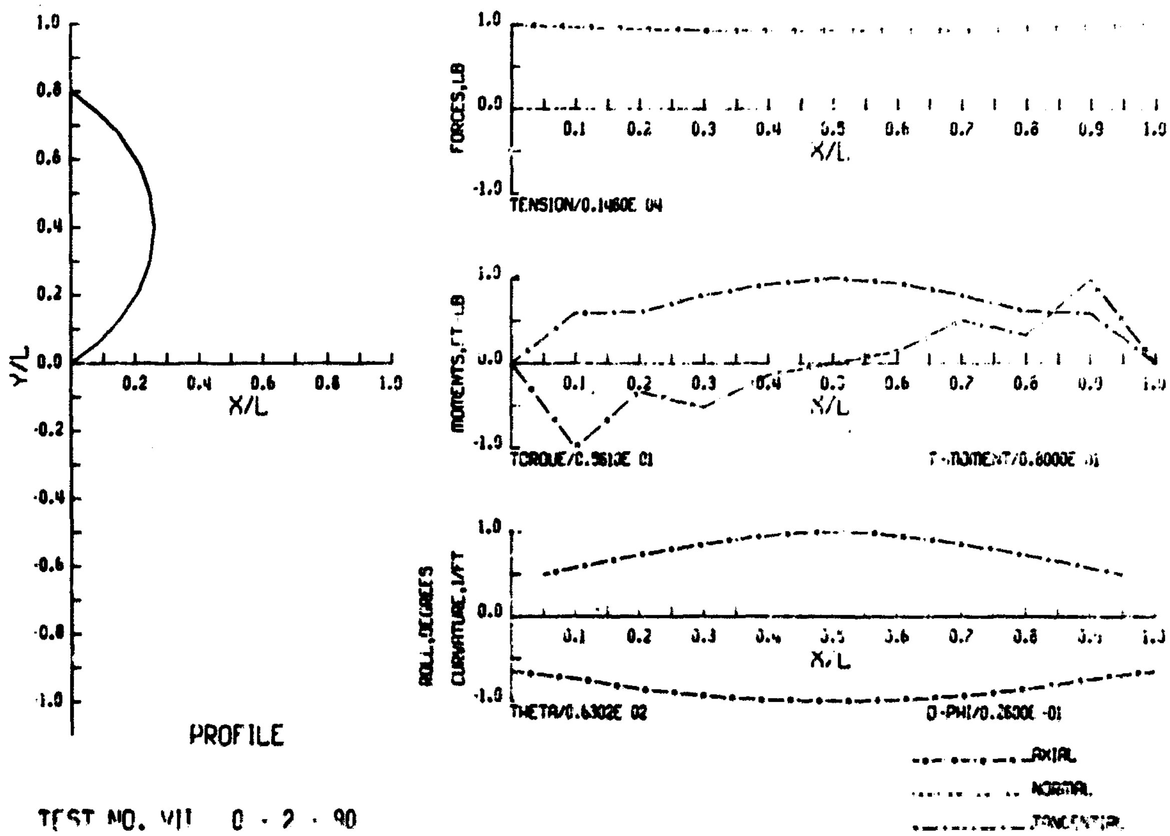

HYDRONAUTICS,INC

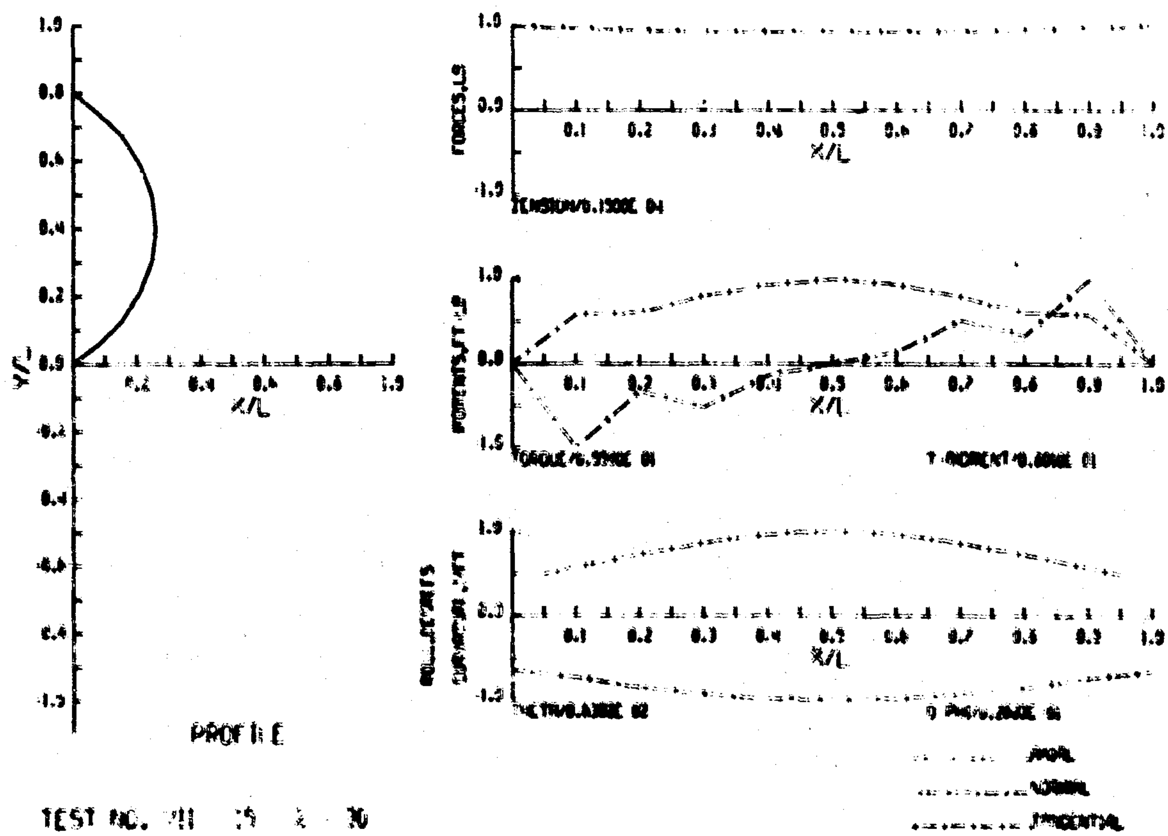

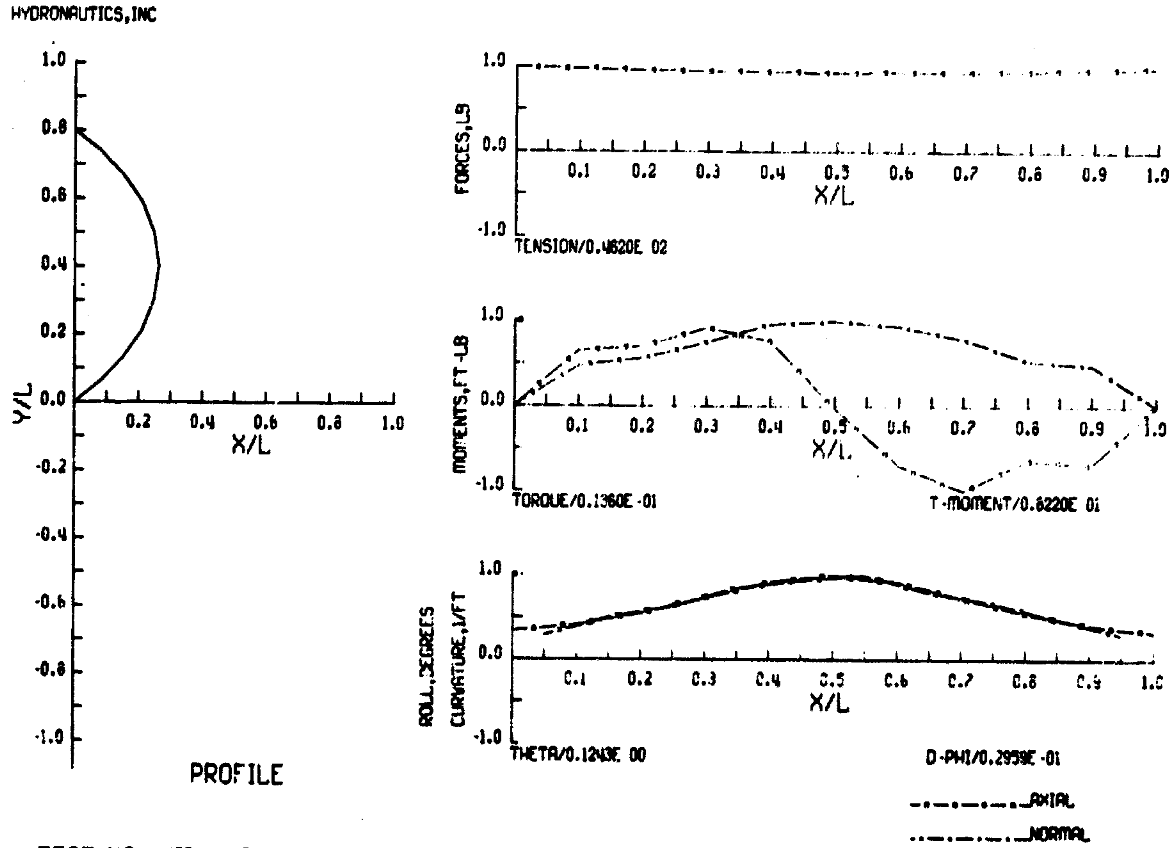

TEST NO. VII - 12 - 0 - 90

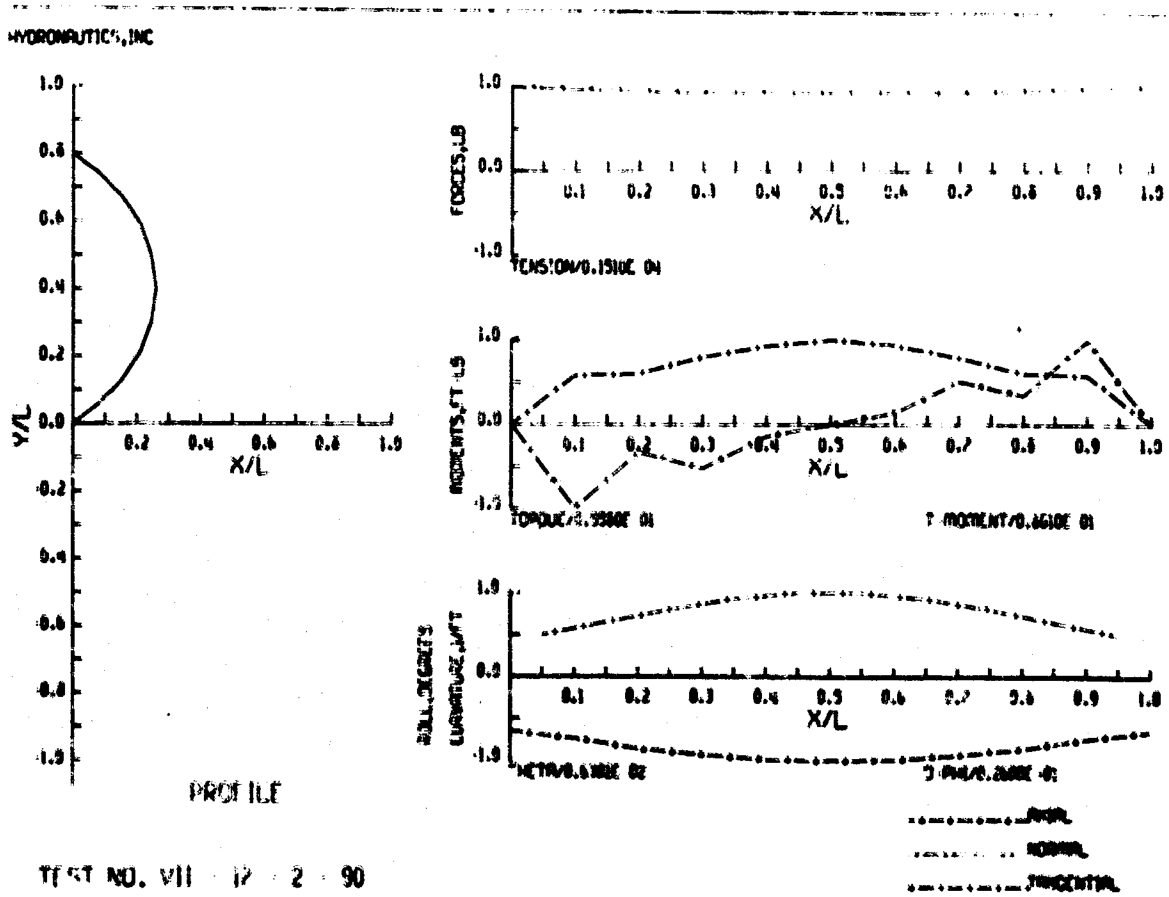

TEST NO. VII - 12 - 2 - 90

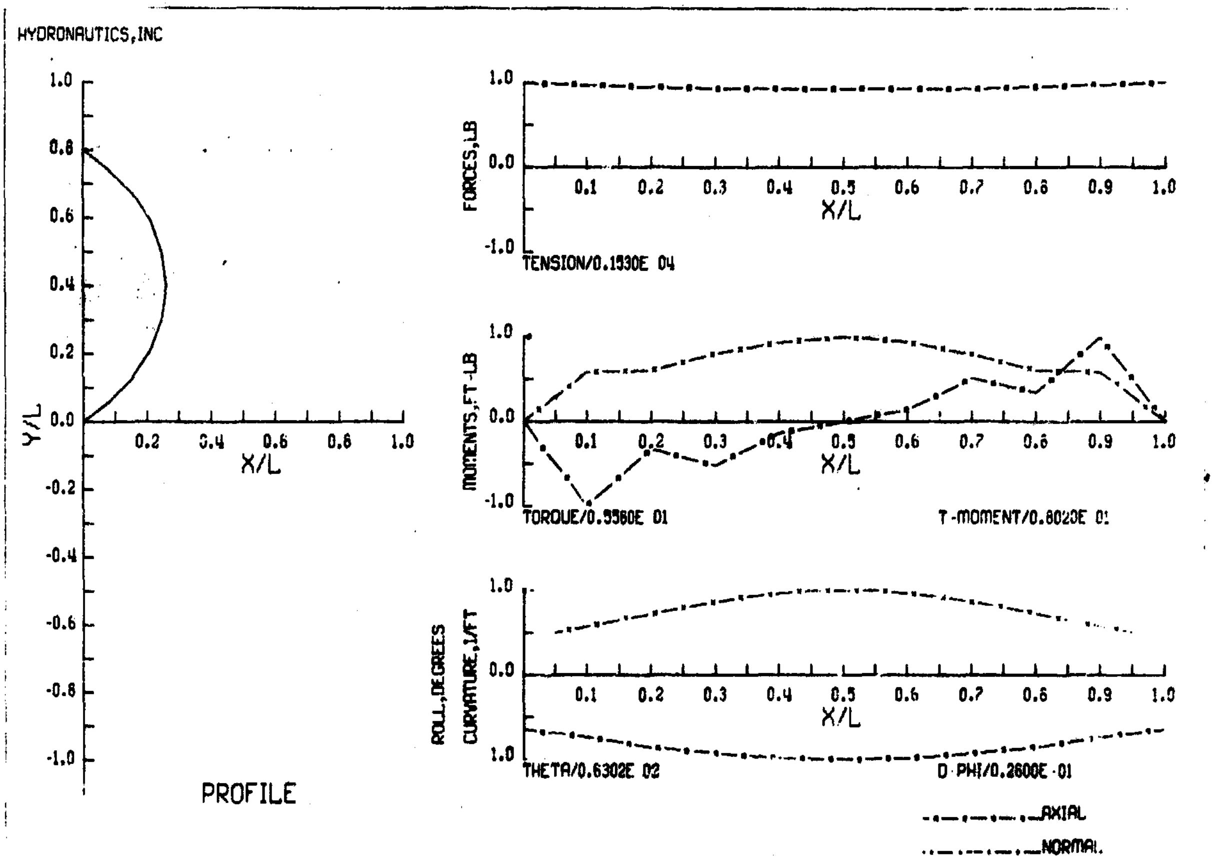

TEST NO. VII - 20 - 2 - 90

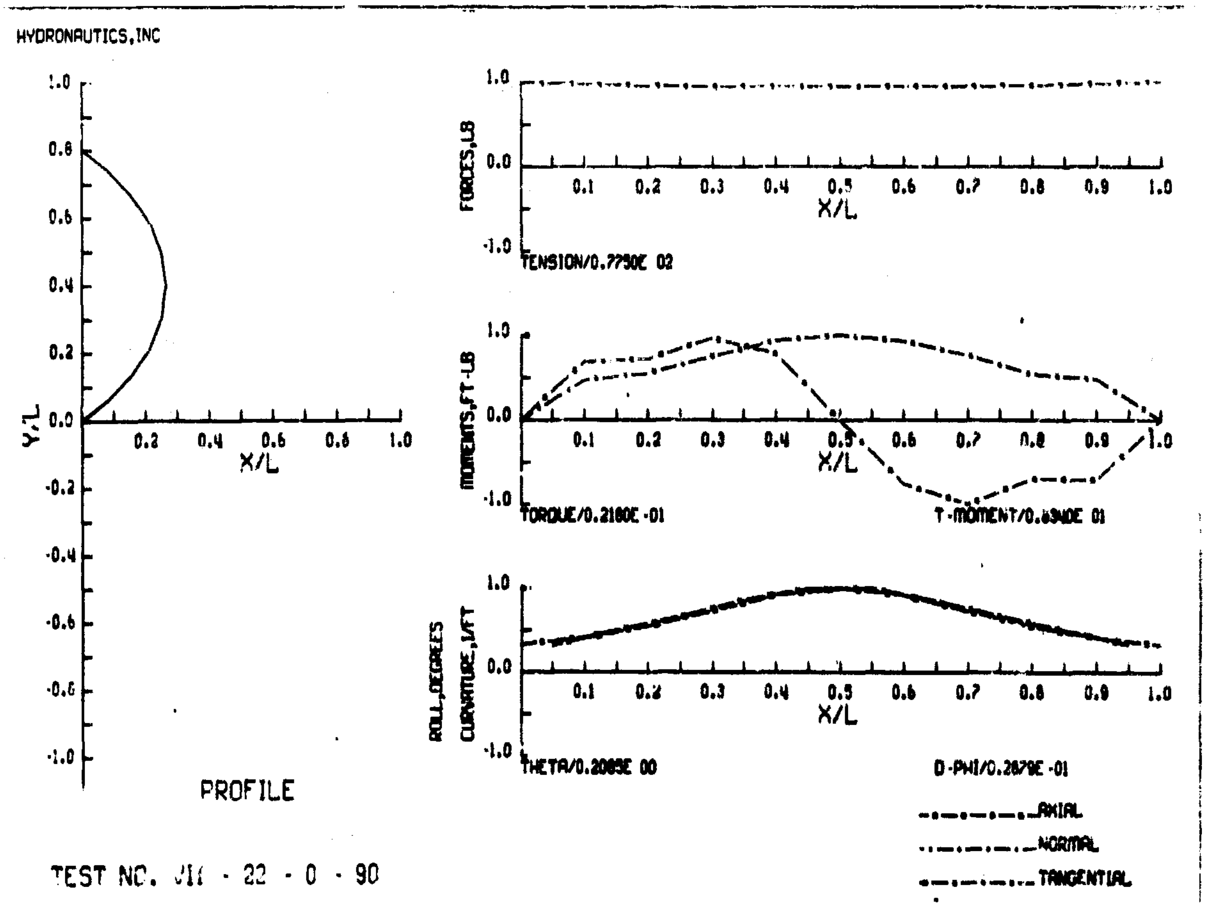

TEST NO. VII - 22 - 0 - 90

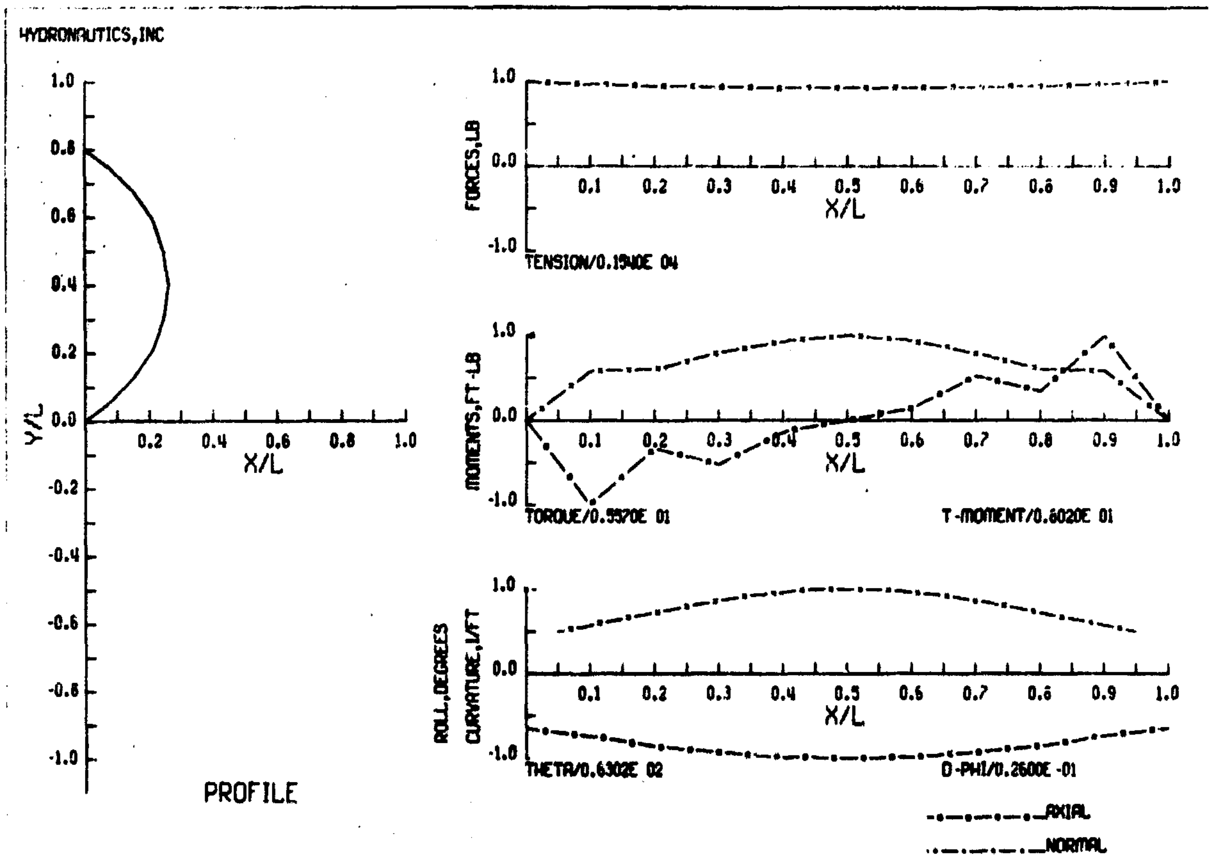

TEST NO. VII - 22 - 2 - 90

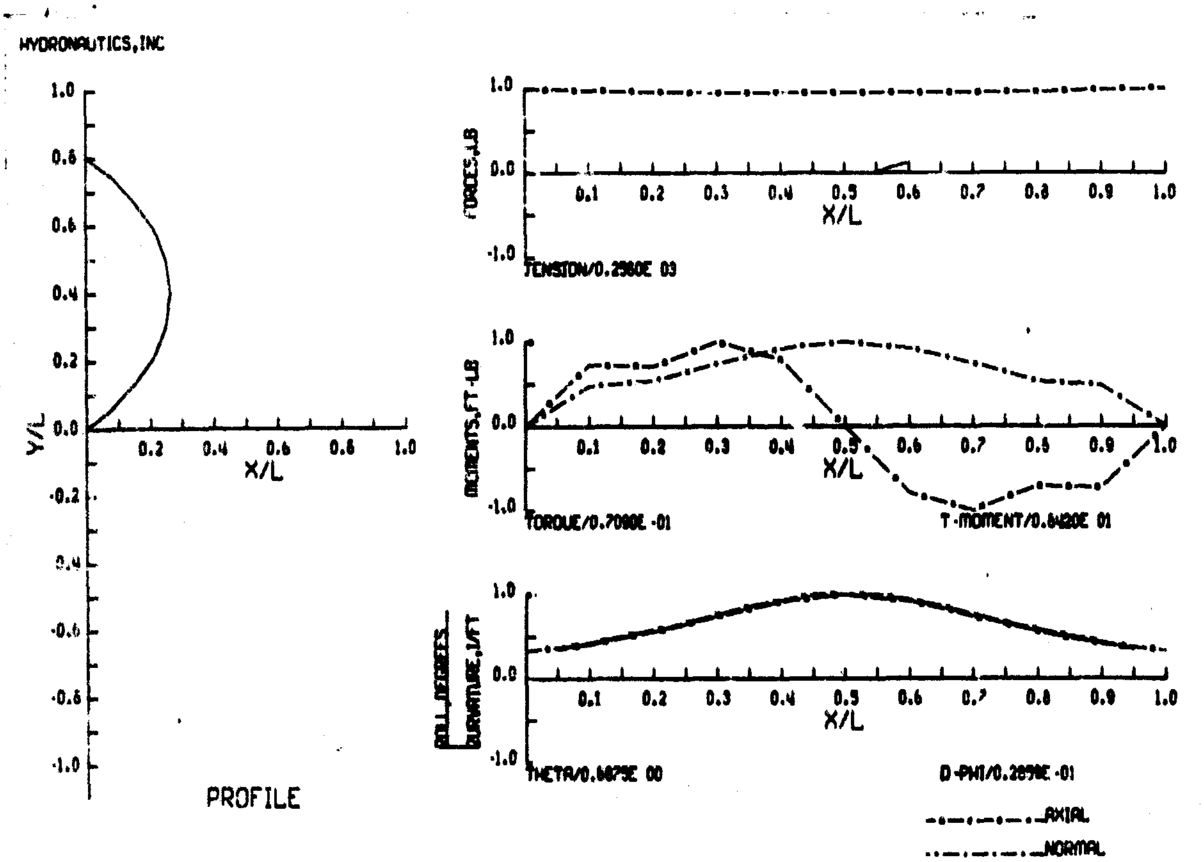

TEST NO. VII - 40 - 0 - 90

HYDRONAUTICS,INC

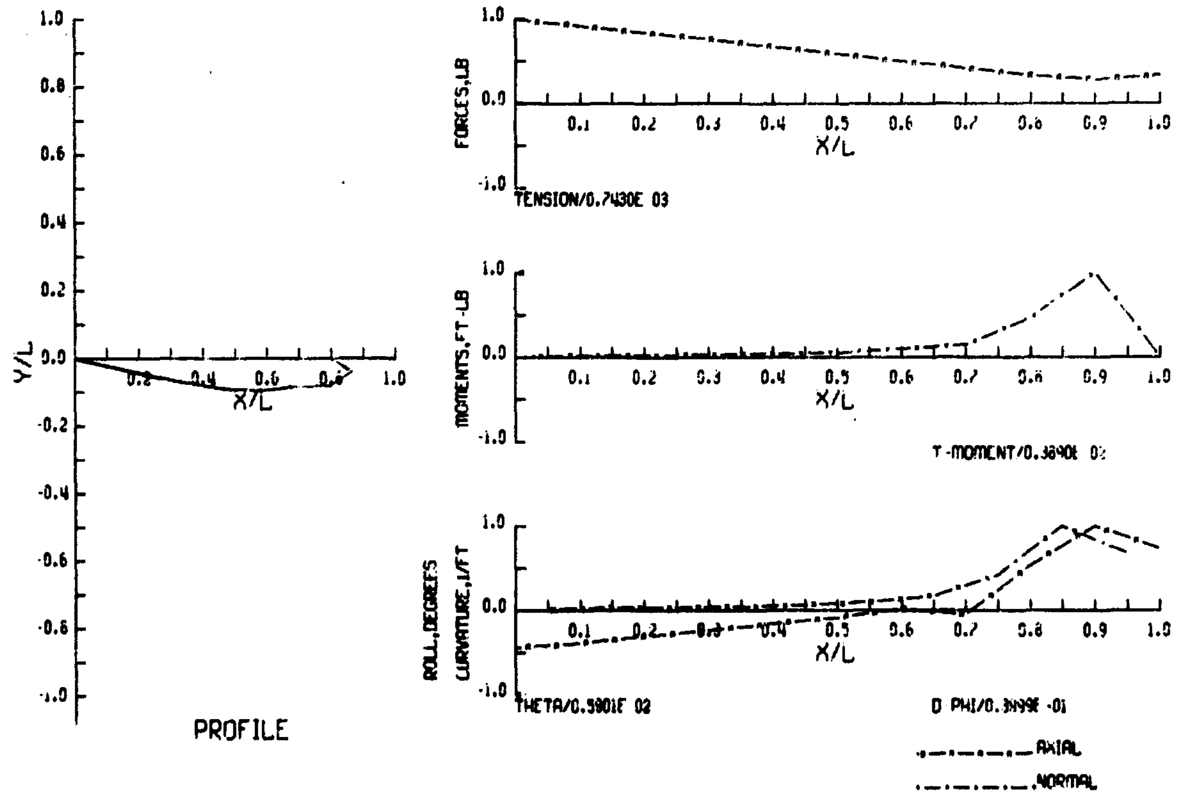

TEST NO. VIII - 0 - 2 - 0

HYDRONAUTICS,INC

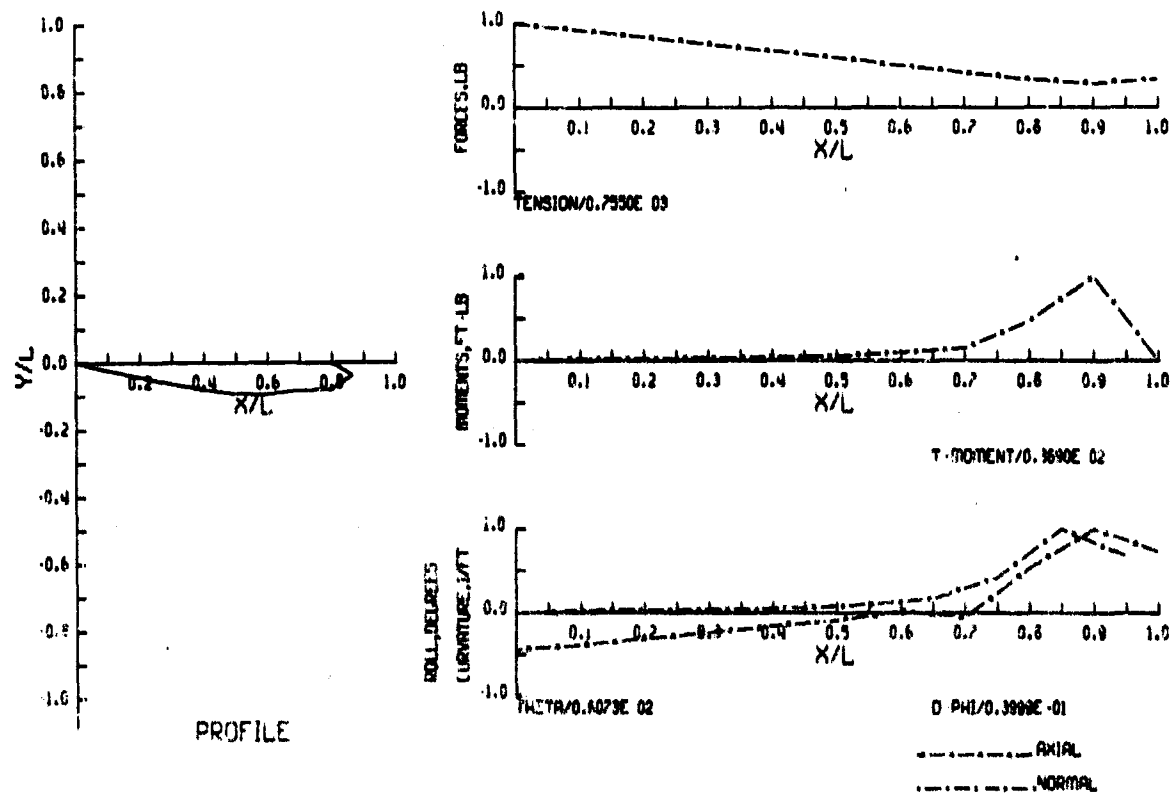

TEST NO. VIII - 15 - 2 - 0

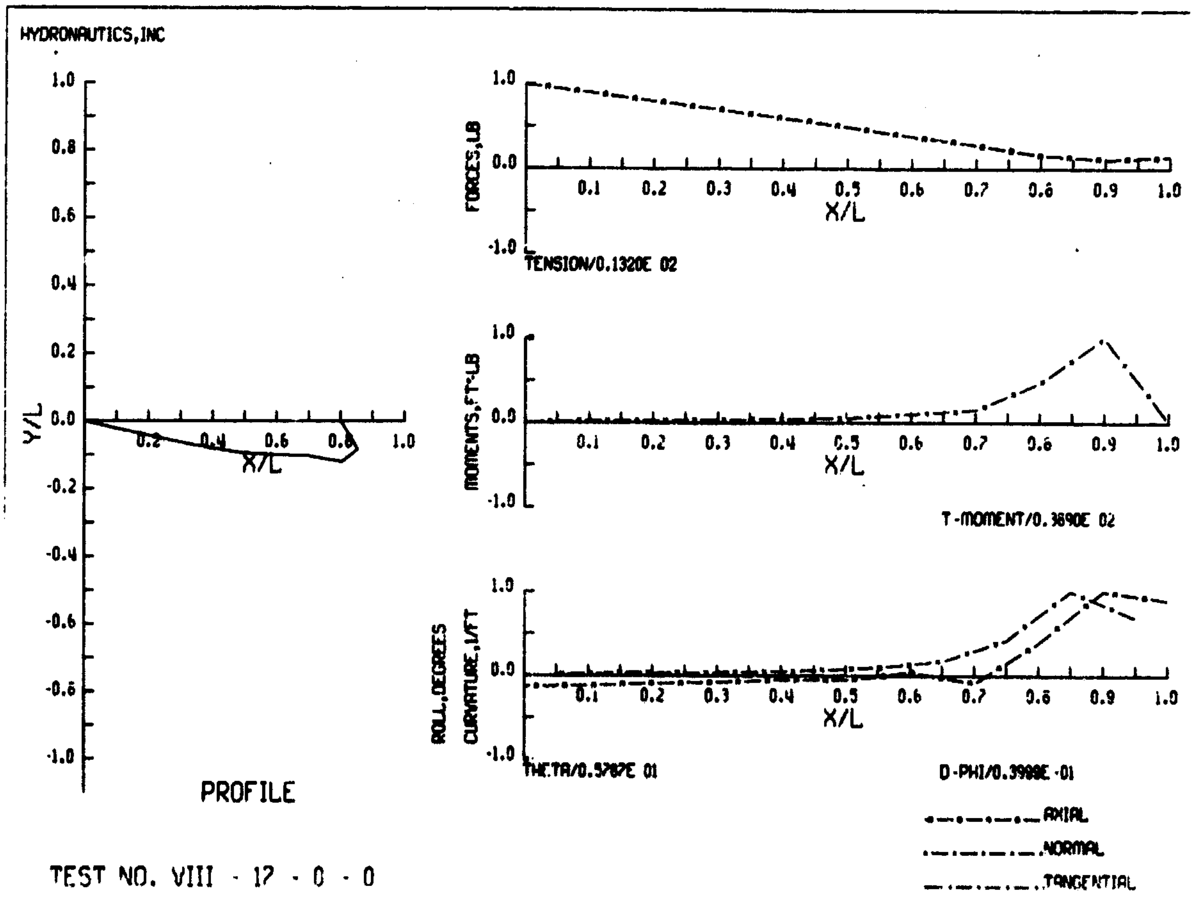

TEST NO. VIII - 17 - 0 - 0

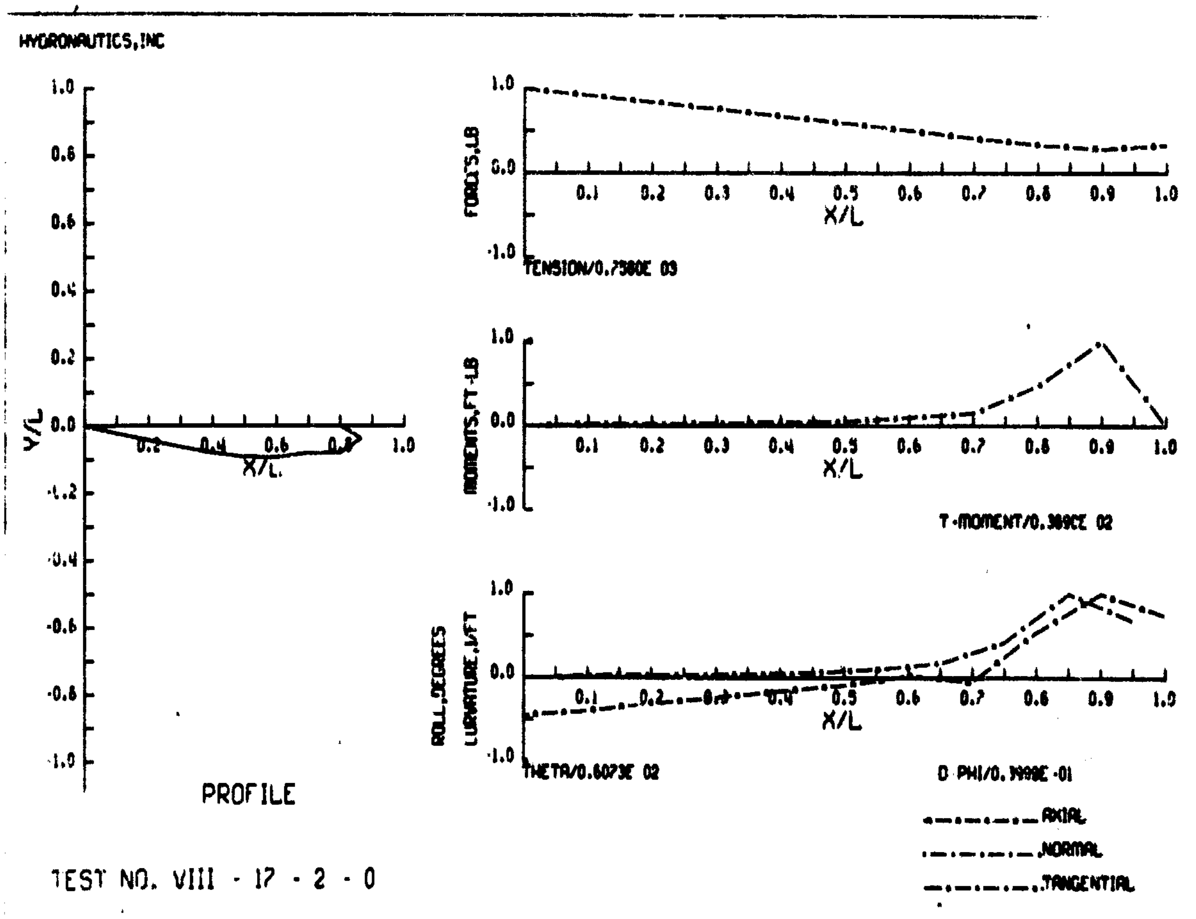

TEST NO. VIII - 17 - 2 - 0

HYDRONAUTICS,INC

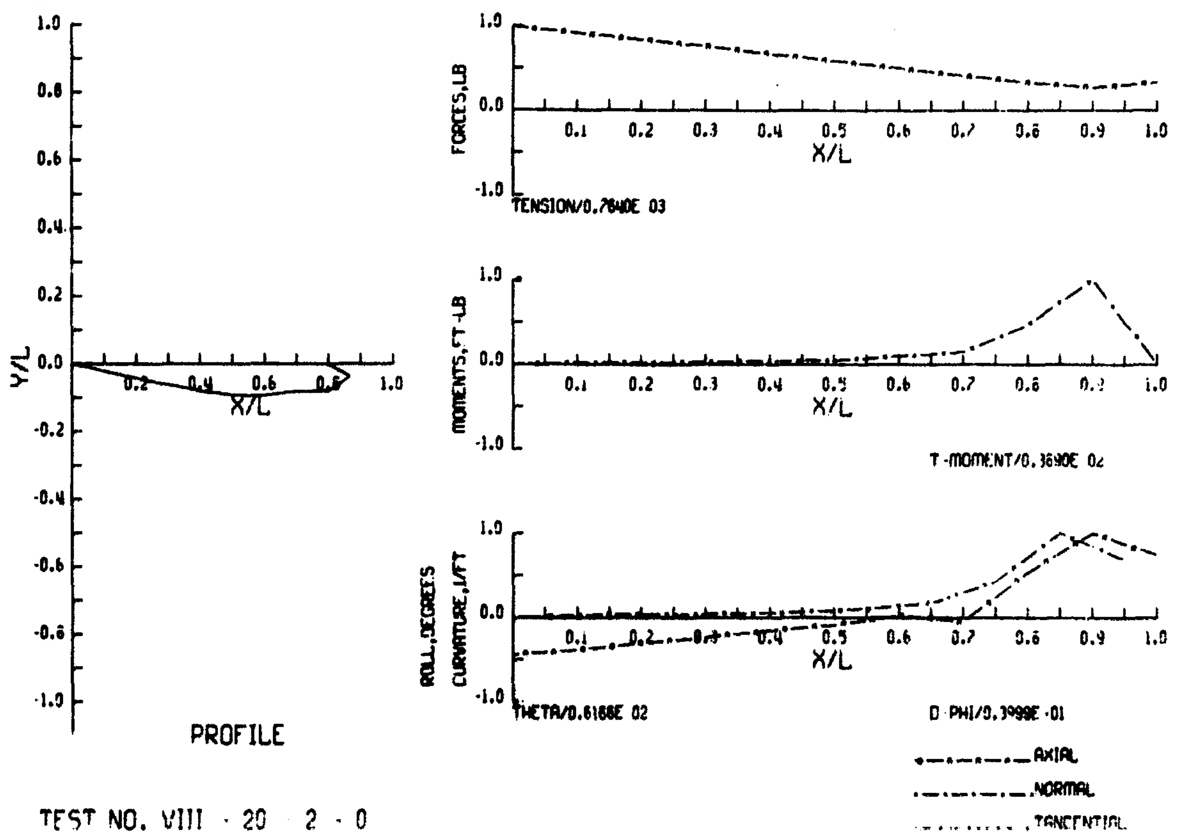

TEST NO. VIII - 20 - 2 - 0

HYDRONAUTICS,INC

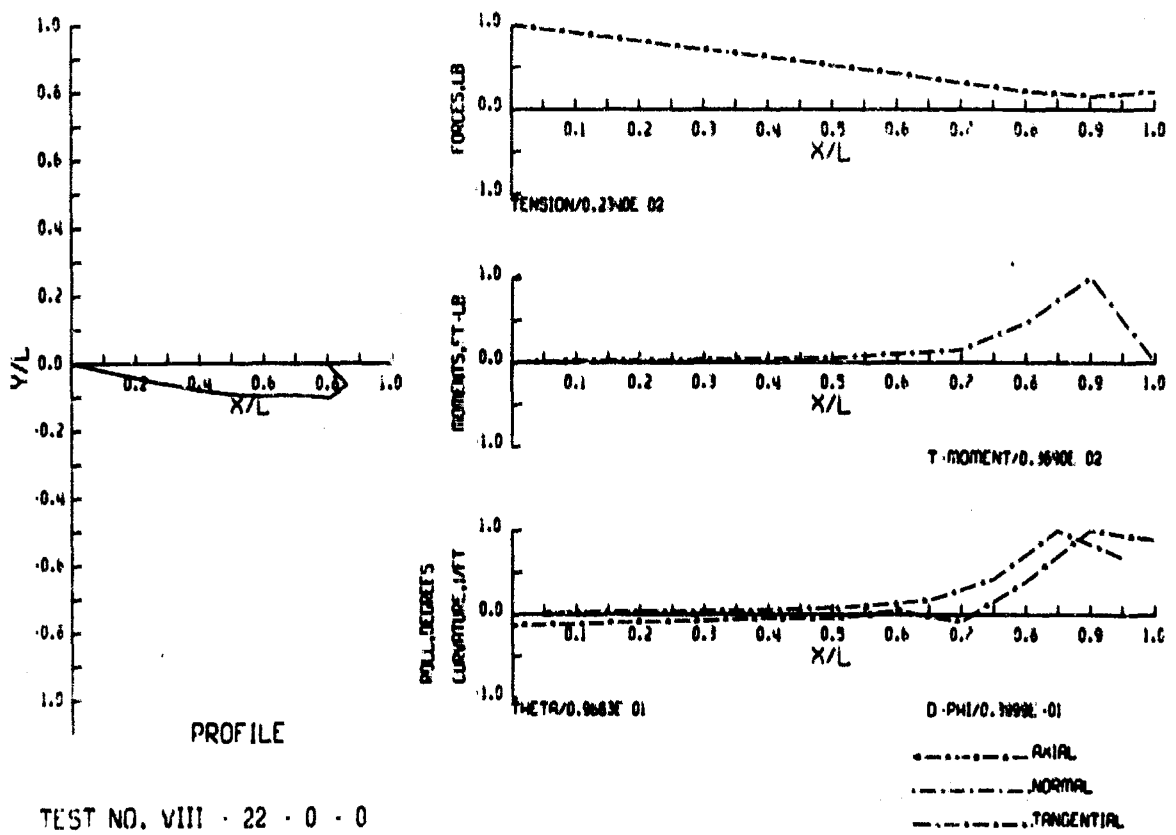

TEST NO. VIII - 22 - 0 - 0

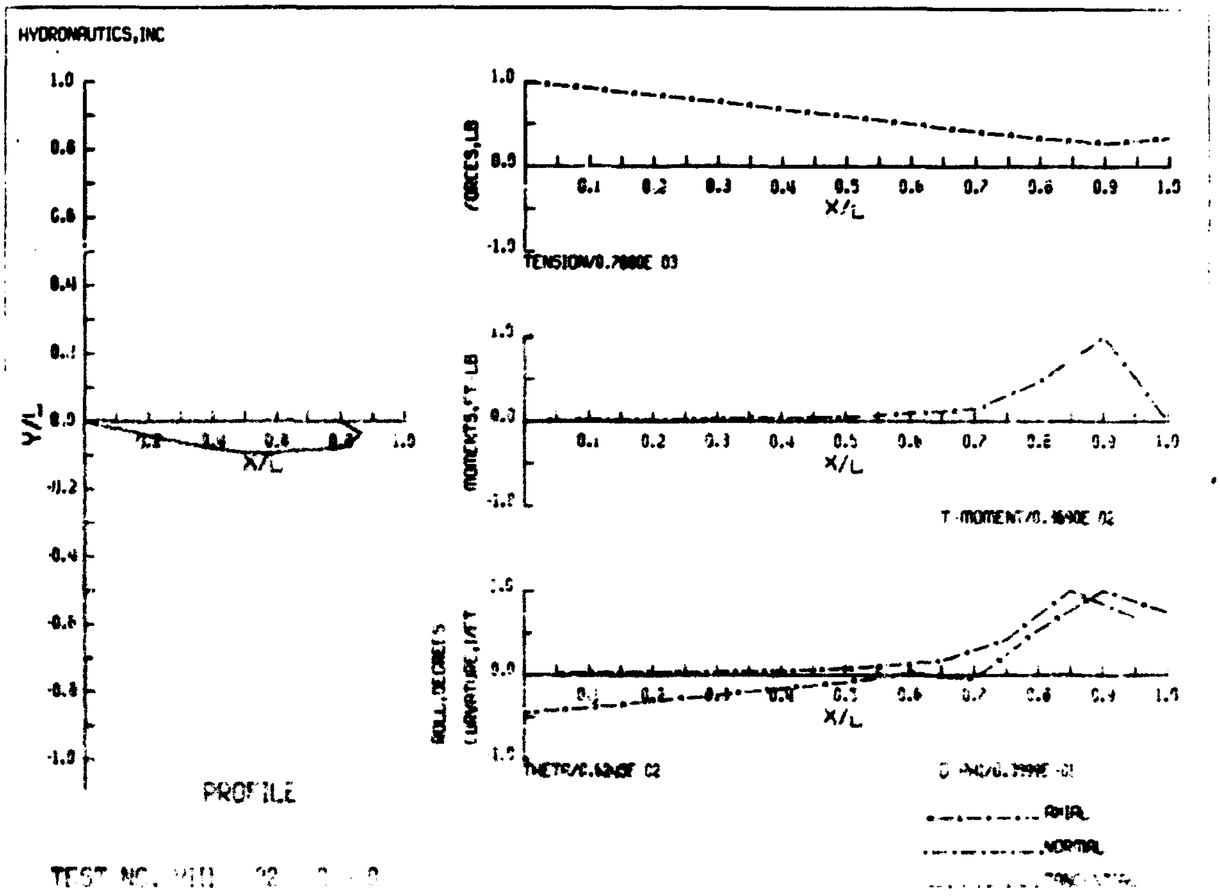
HYDRONAUTICS,INC
Y/L
X/L
PROFILE
FORCES,LB
MOMENTS,FT-LB
ROLL,DEGREES
CURVATURE,1/FT
AXIAL
NORMAL

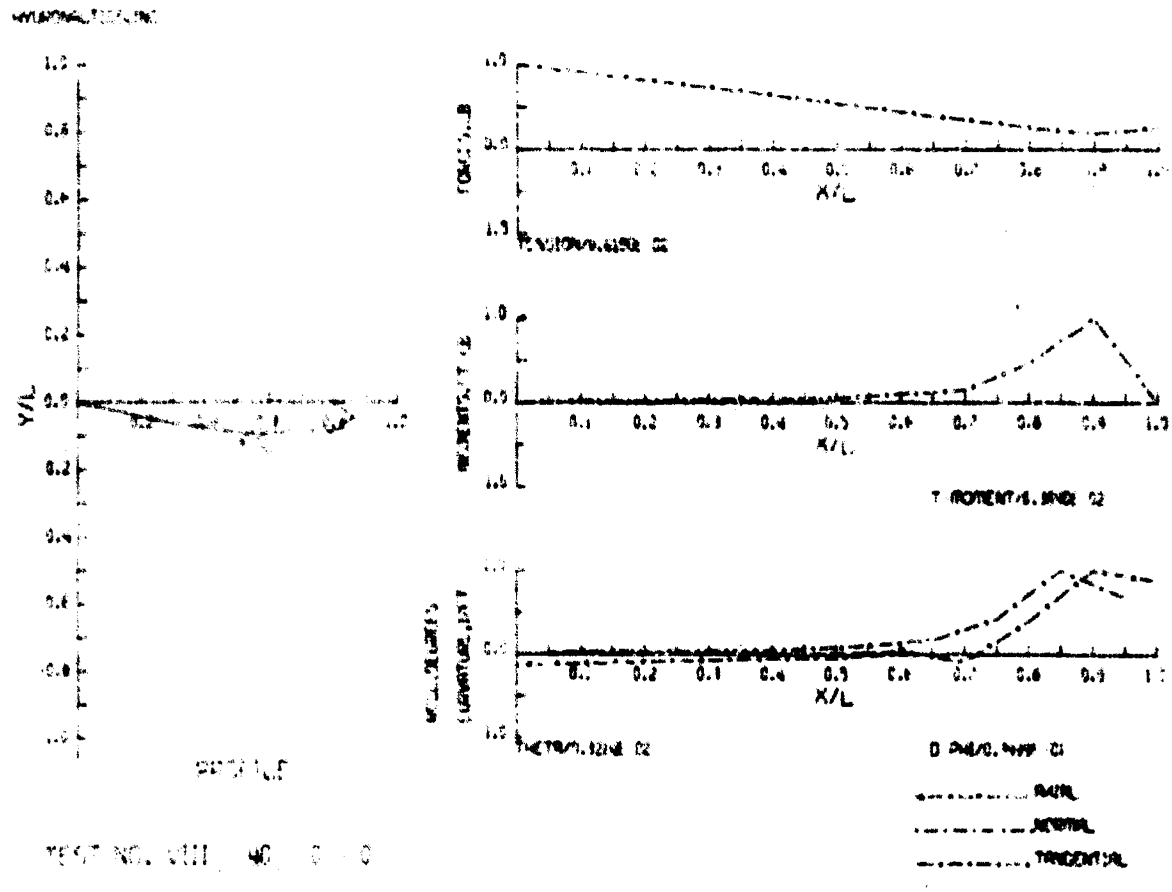
Y/L
X/L
AXIAL
NORMAL
TANGENTIAL

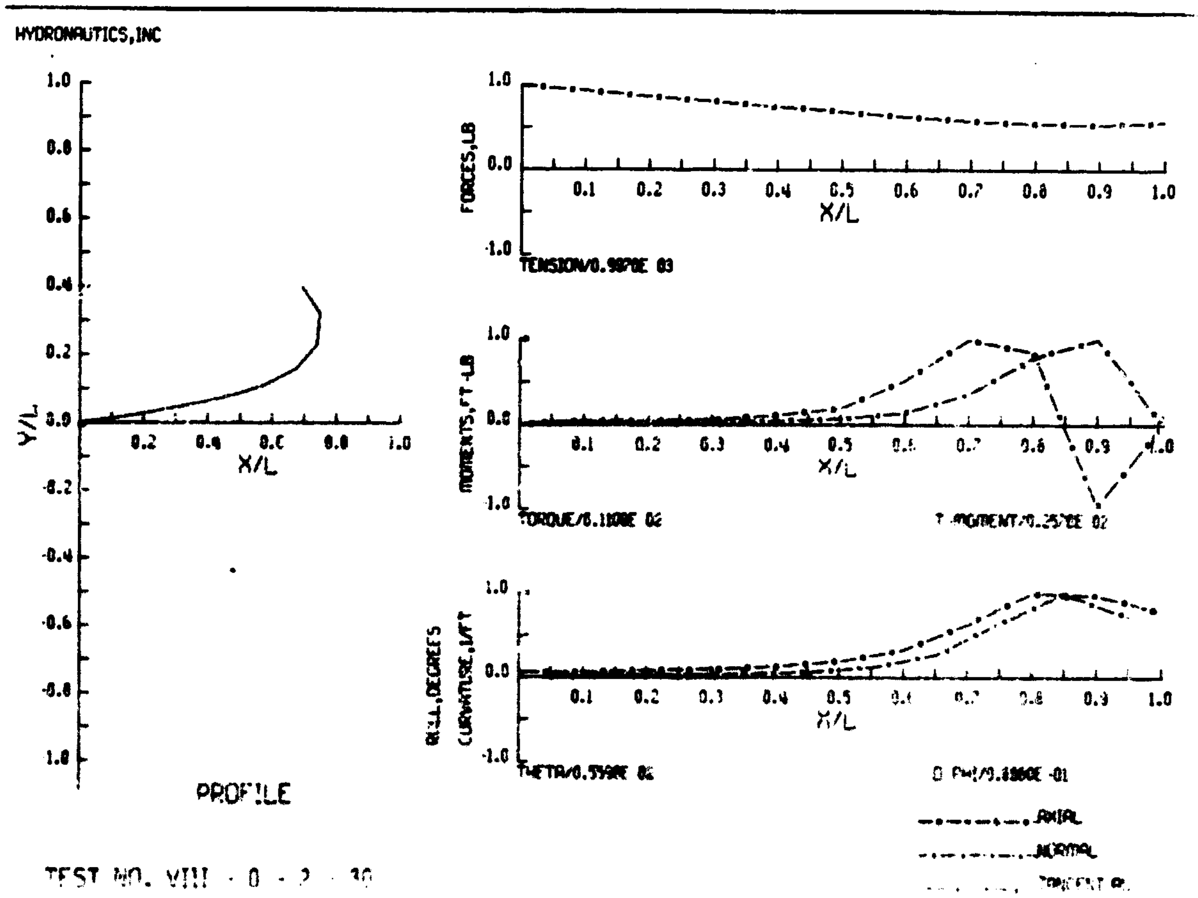
HYDRONAUTICS,INC
Y/L
X/L
PROFILE
FORCES,LB
MOMENTS,FT-LB
ROLL,DEGREES
CURVATURE,1/FT
AXIAL
NORMAL

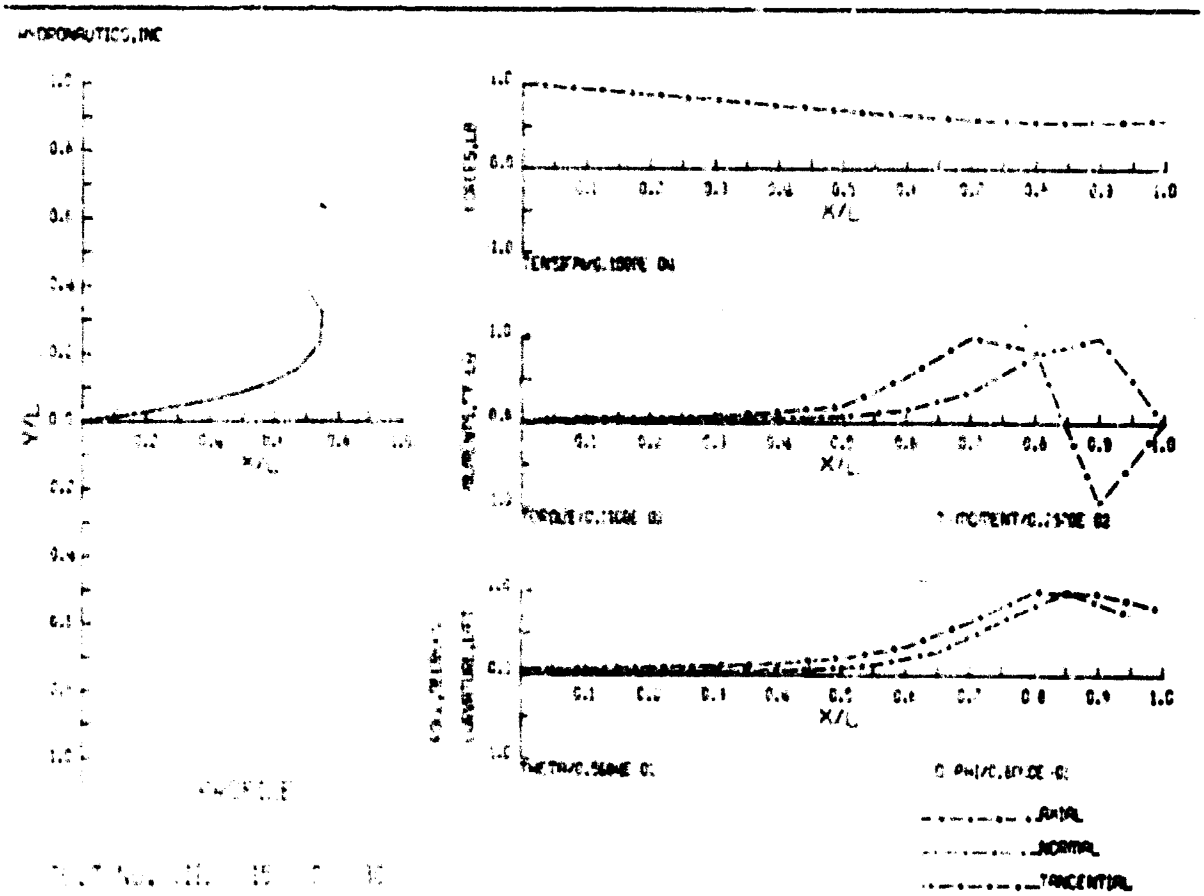
X/L
AXIAL
NORMAL
TANGENTIAL

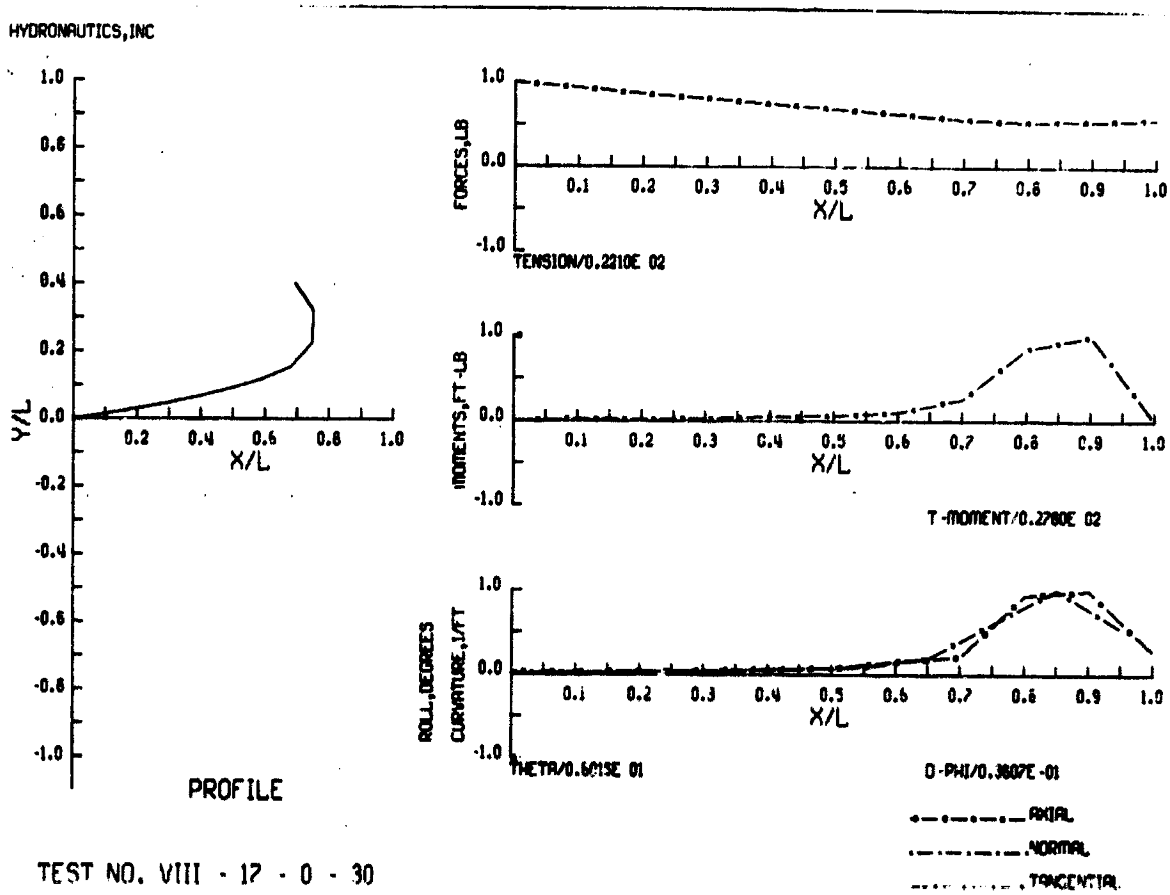

TEST NO. VIII - 17 - 0 - 30

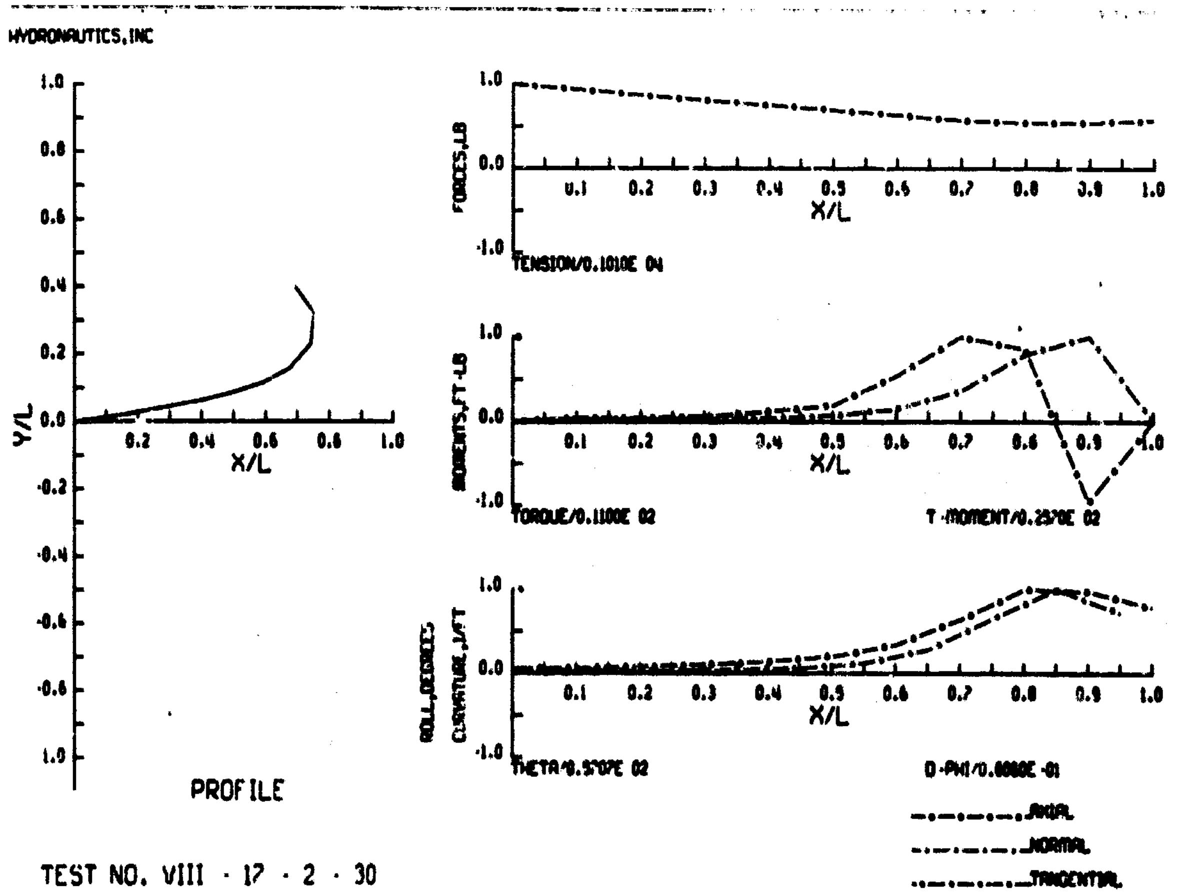

TEST NO. VIII - 17 - 2 - 30

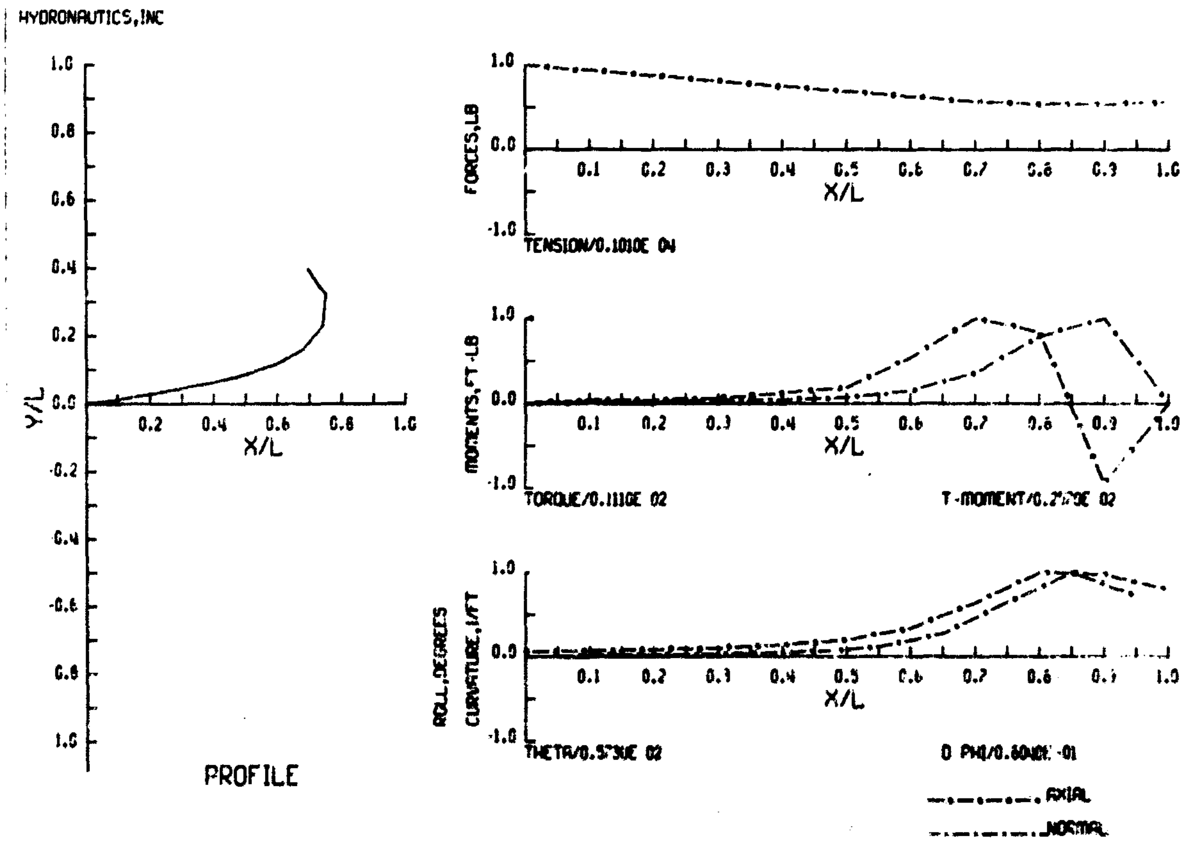

TEST NO. VIII - 20 - 2 - 30

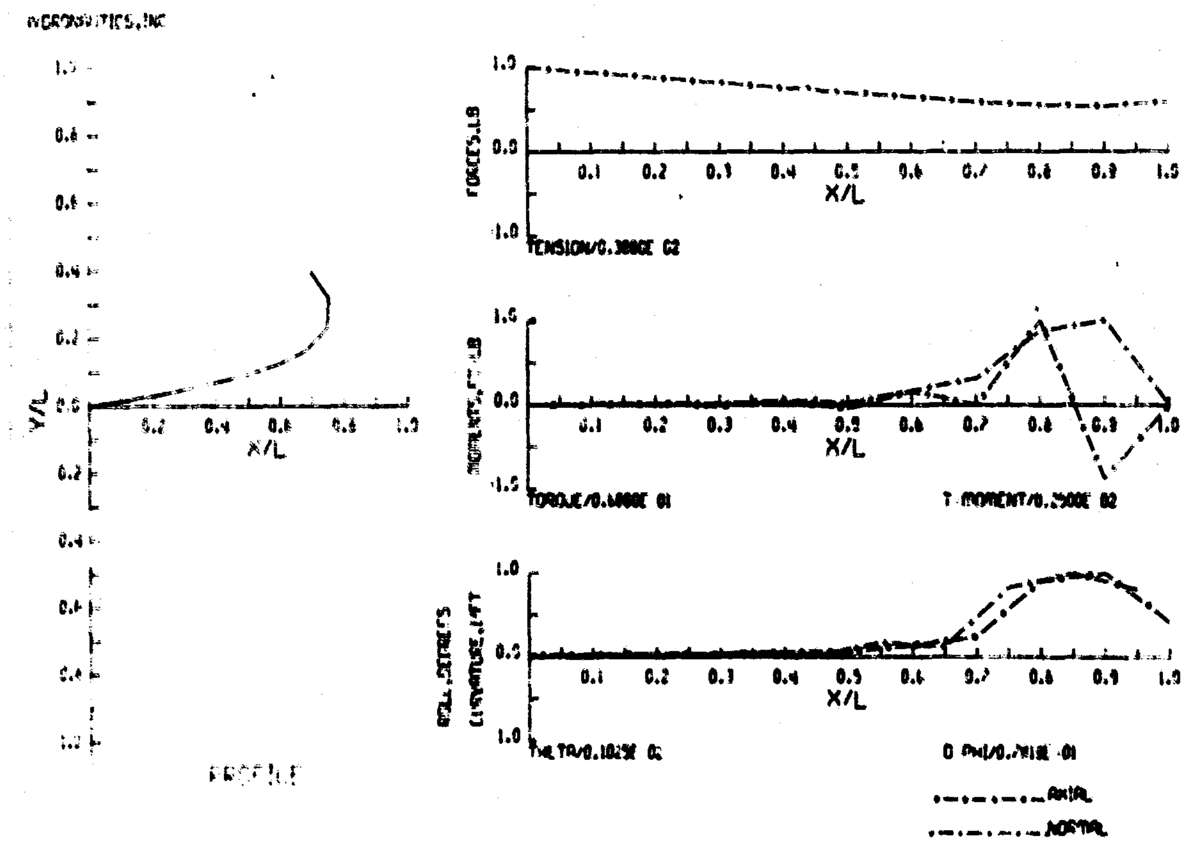

TEST NO. VIII [illegible] 30

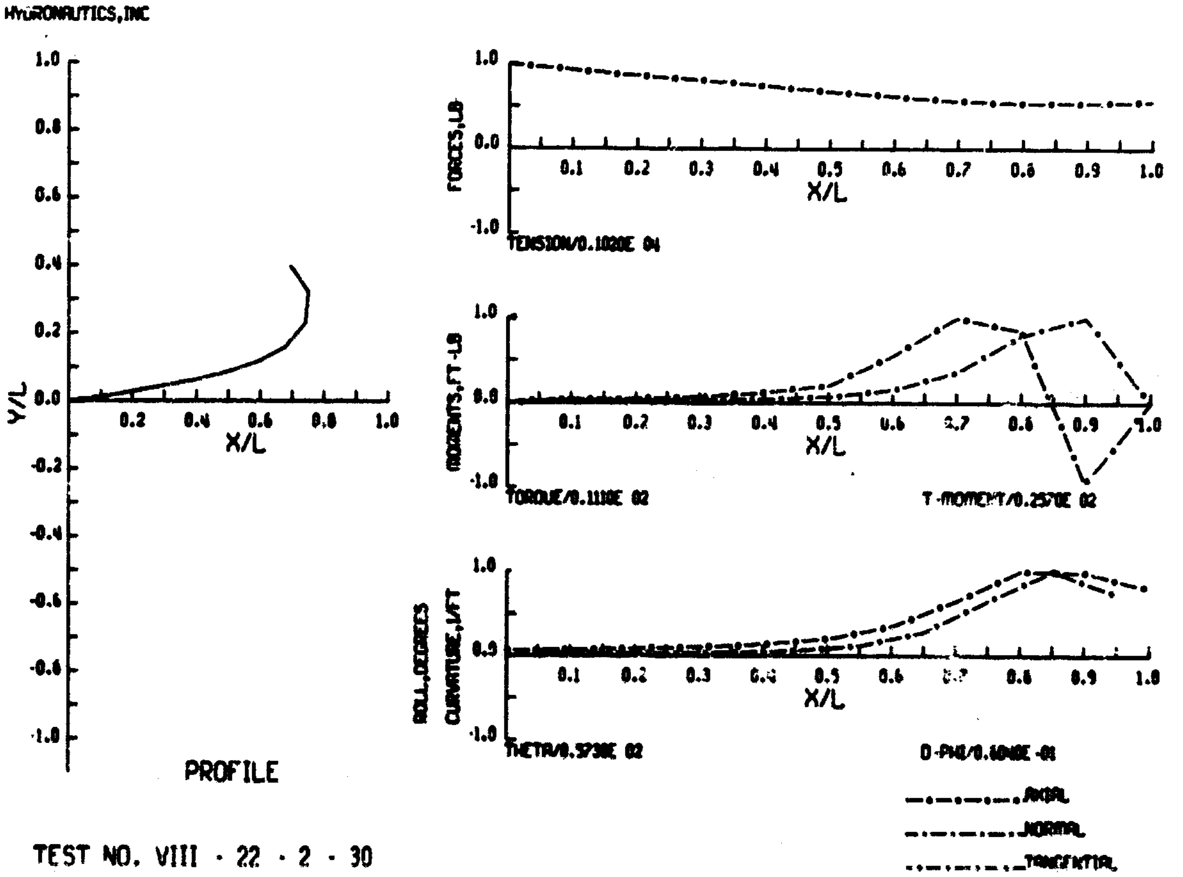

TEST NO. VIII - 22 - 2 - 30

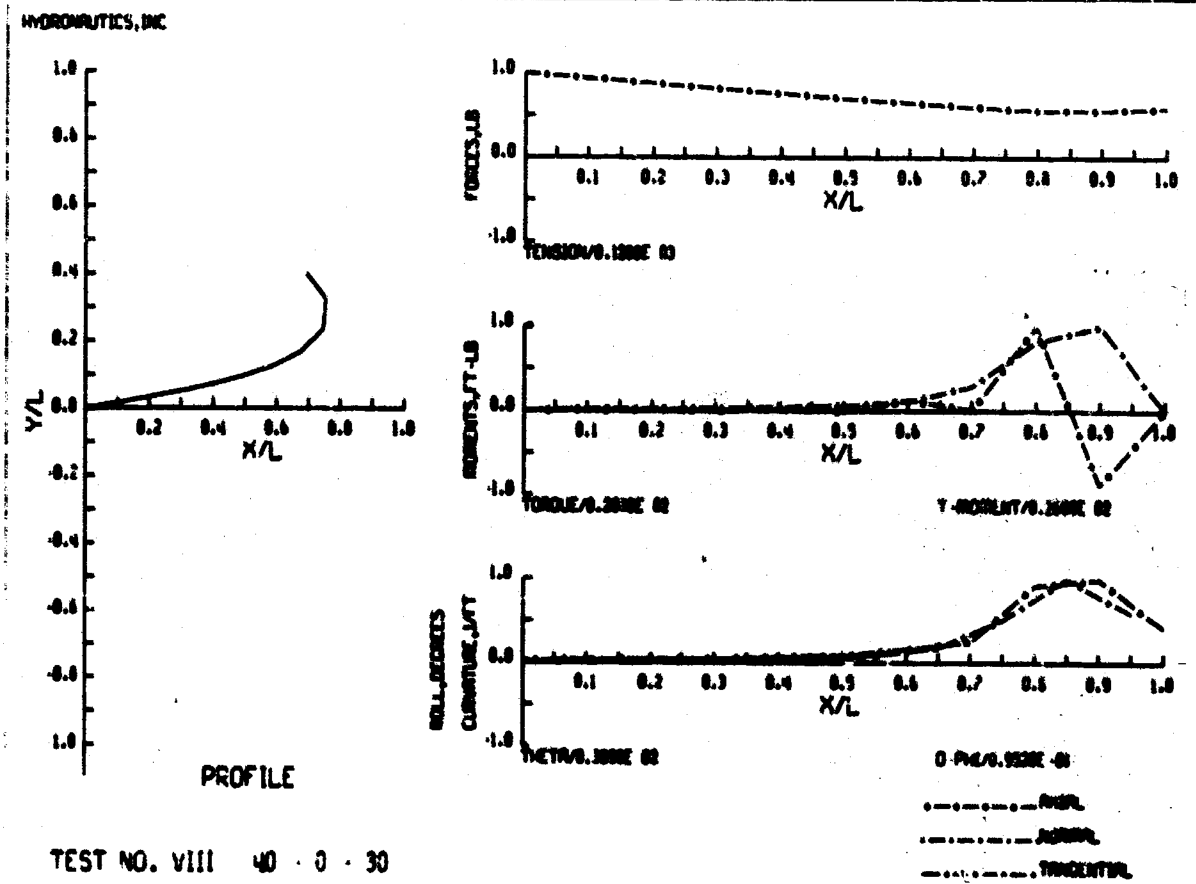

TEST NO. VIII 40 - 0 - 30

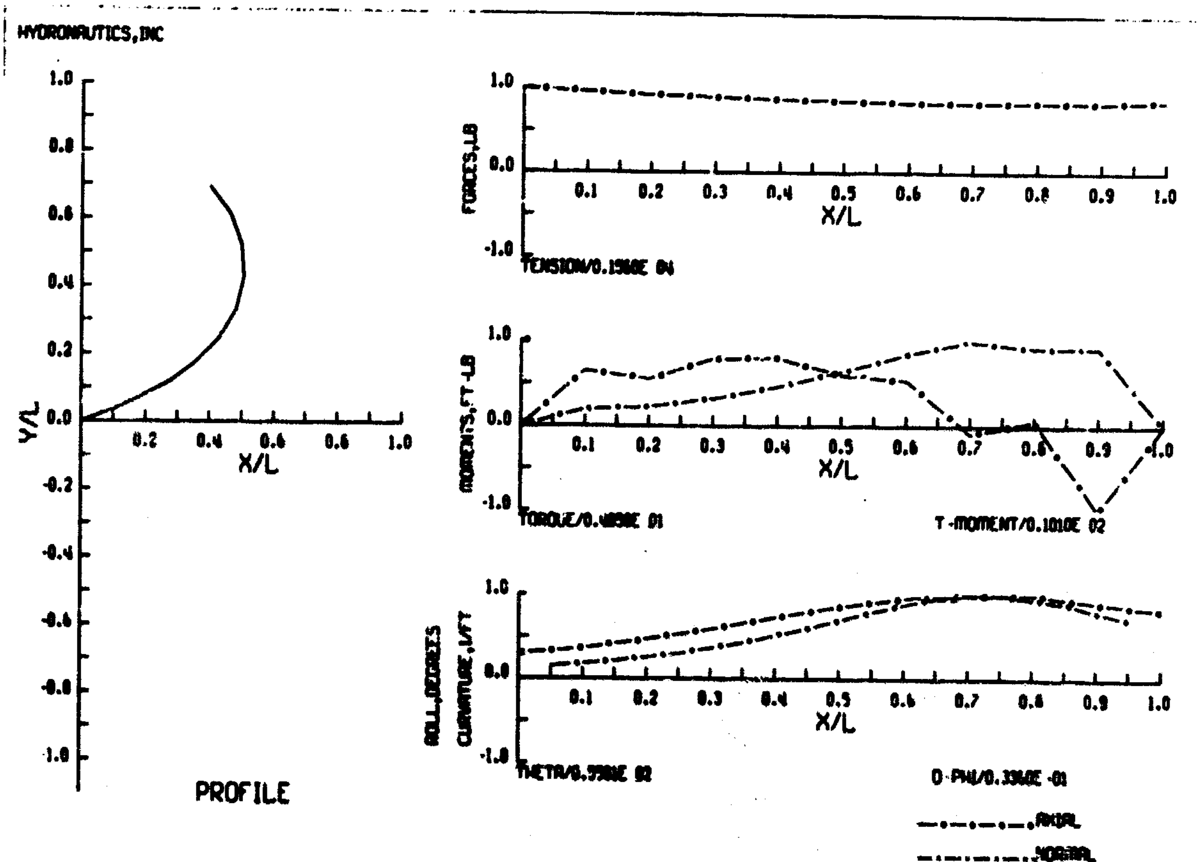

TEST NO. VIII - 0 - 2 - 60

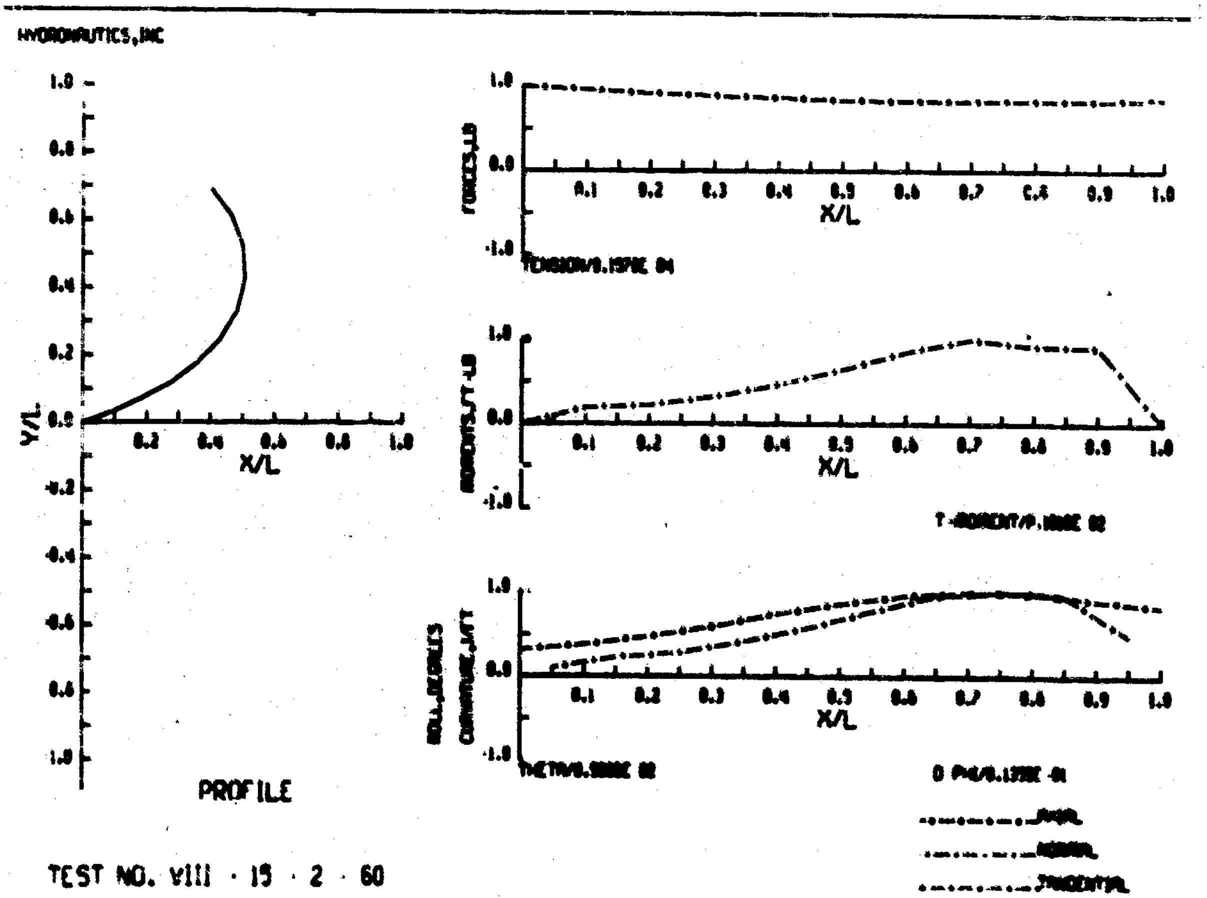

TEST NO. VIII - 15 - 2 - 60

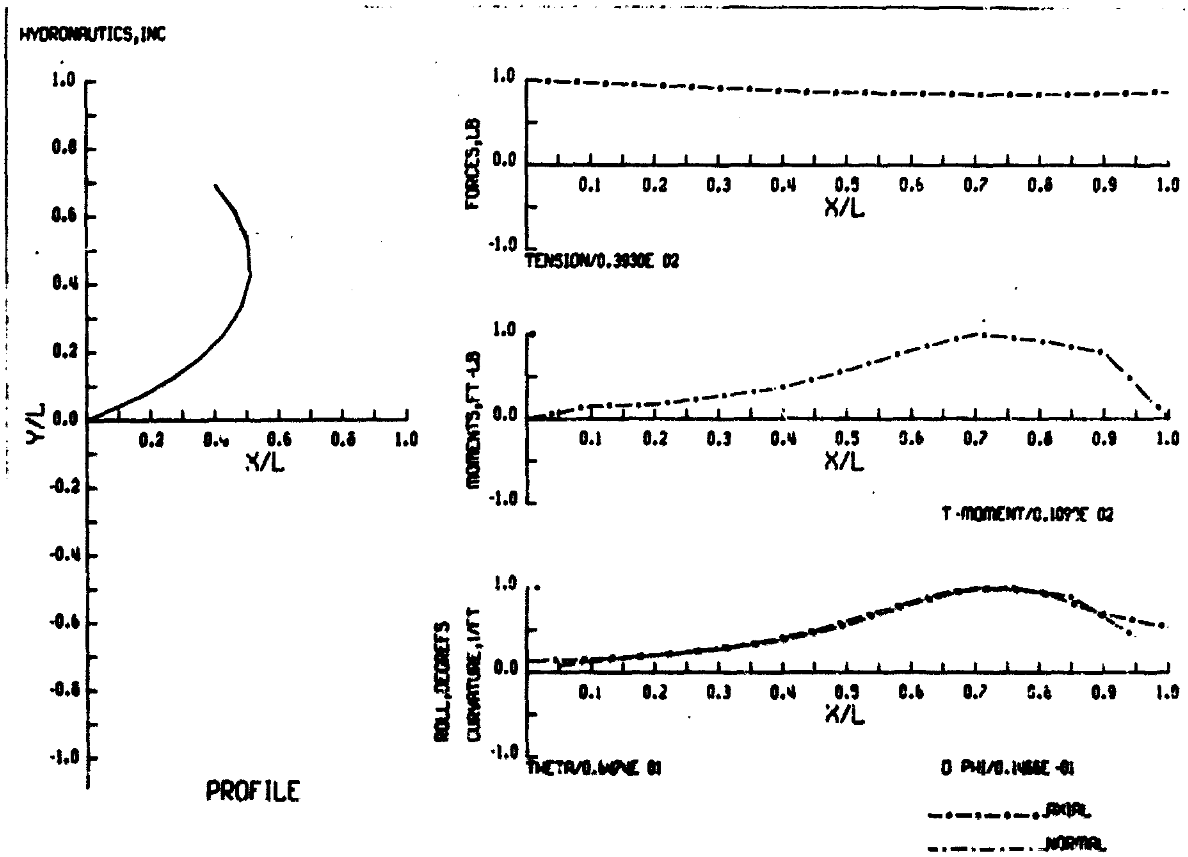

TEST NO. VIII - 17 - 0 - 60

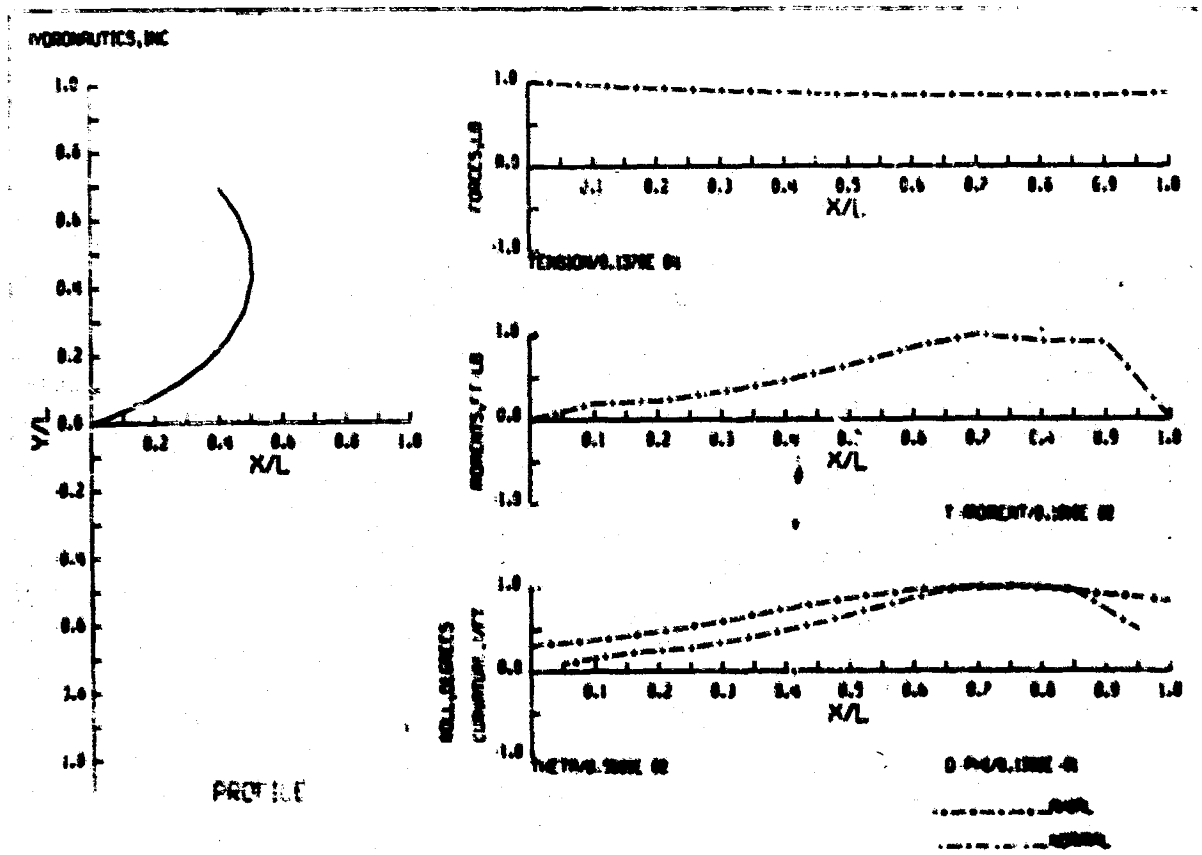

TEST NO. VIII - 17 - 2 - 60

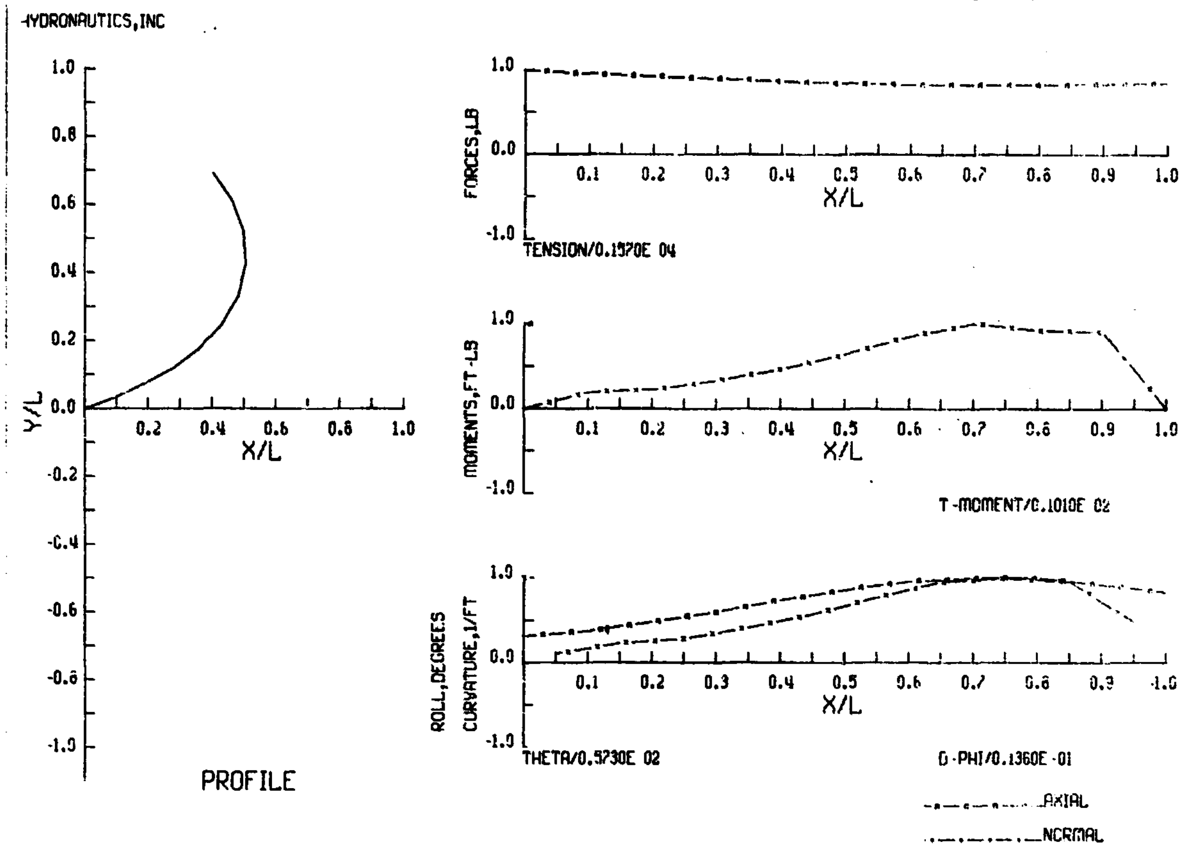

TEST NO. VIII - 20 - 2 - 60

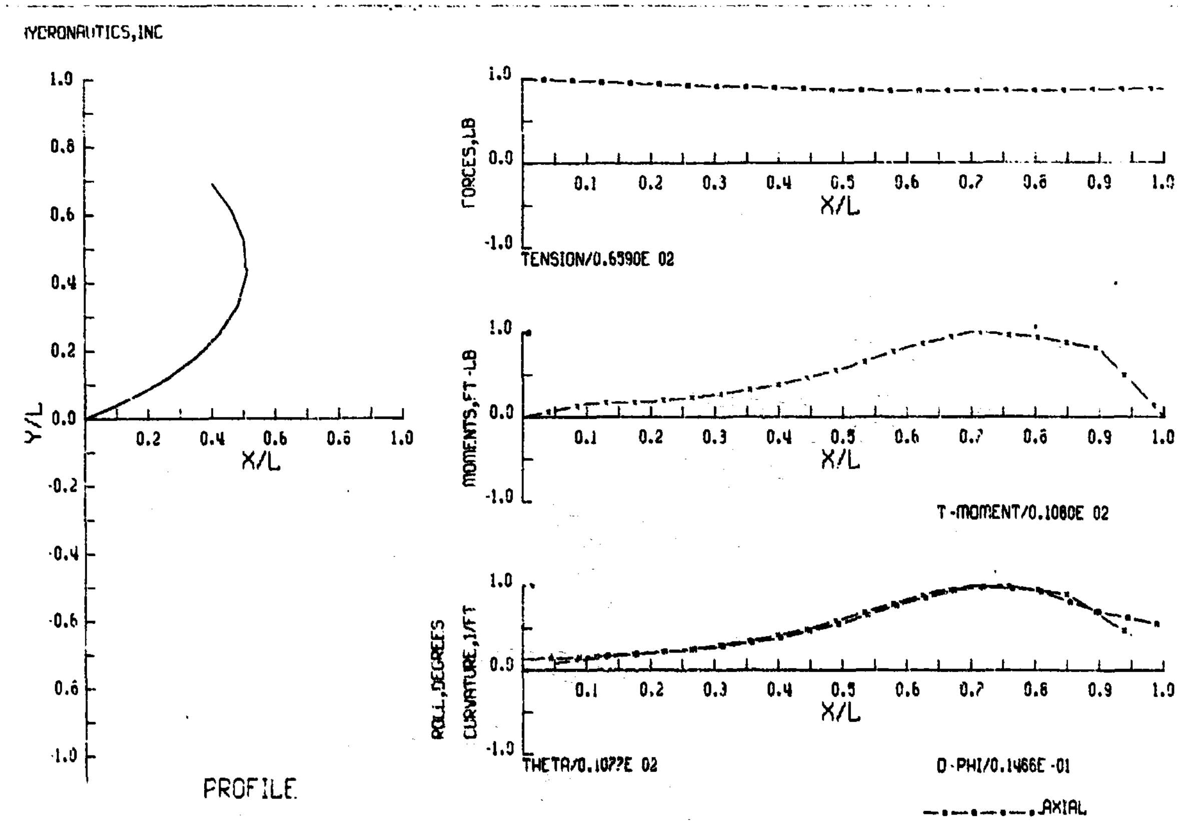

TEST NO. VIII - 22 - 0 - 60

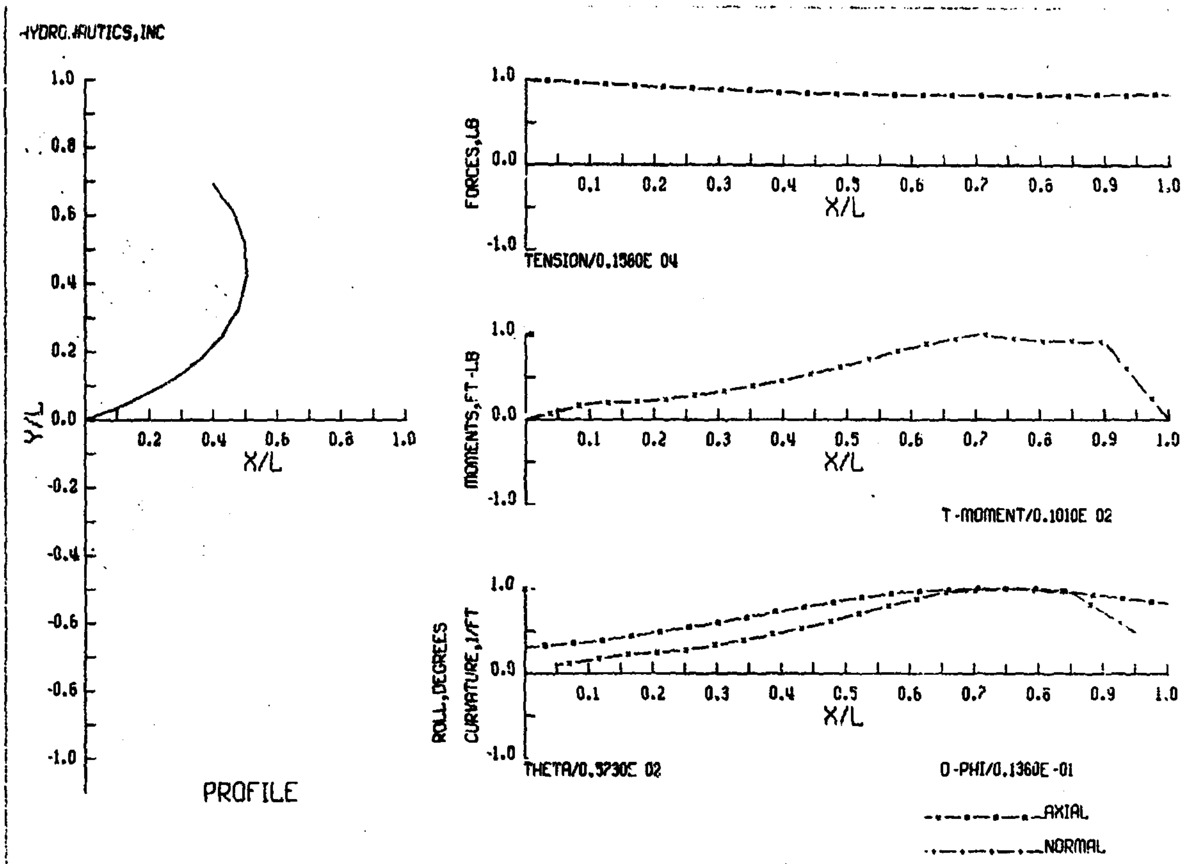

TEST NO. VIII - 22 - 2 - 60

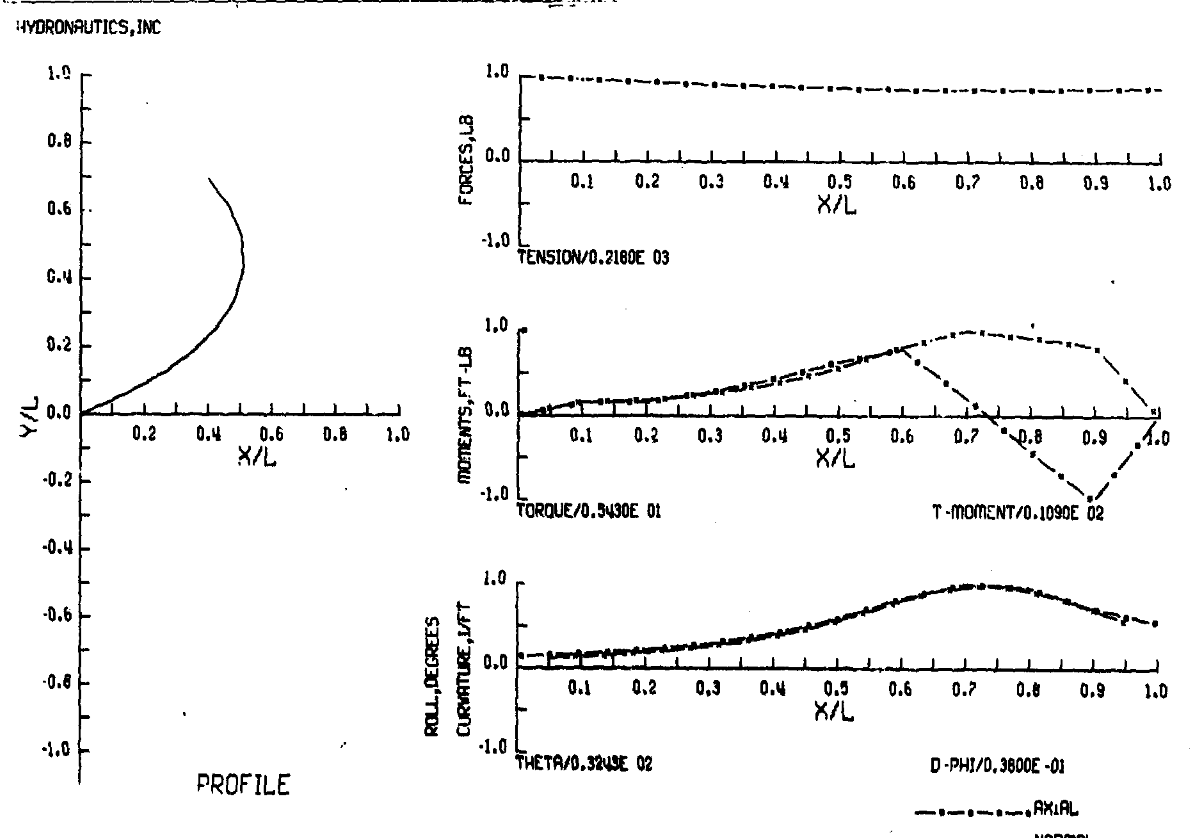

TEST NO. VIII - 40 - 0 - 60

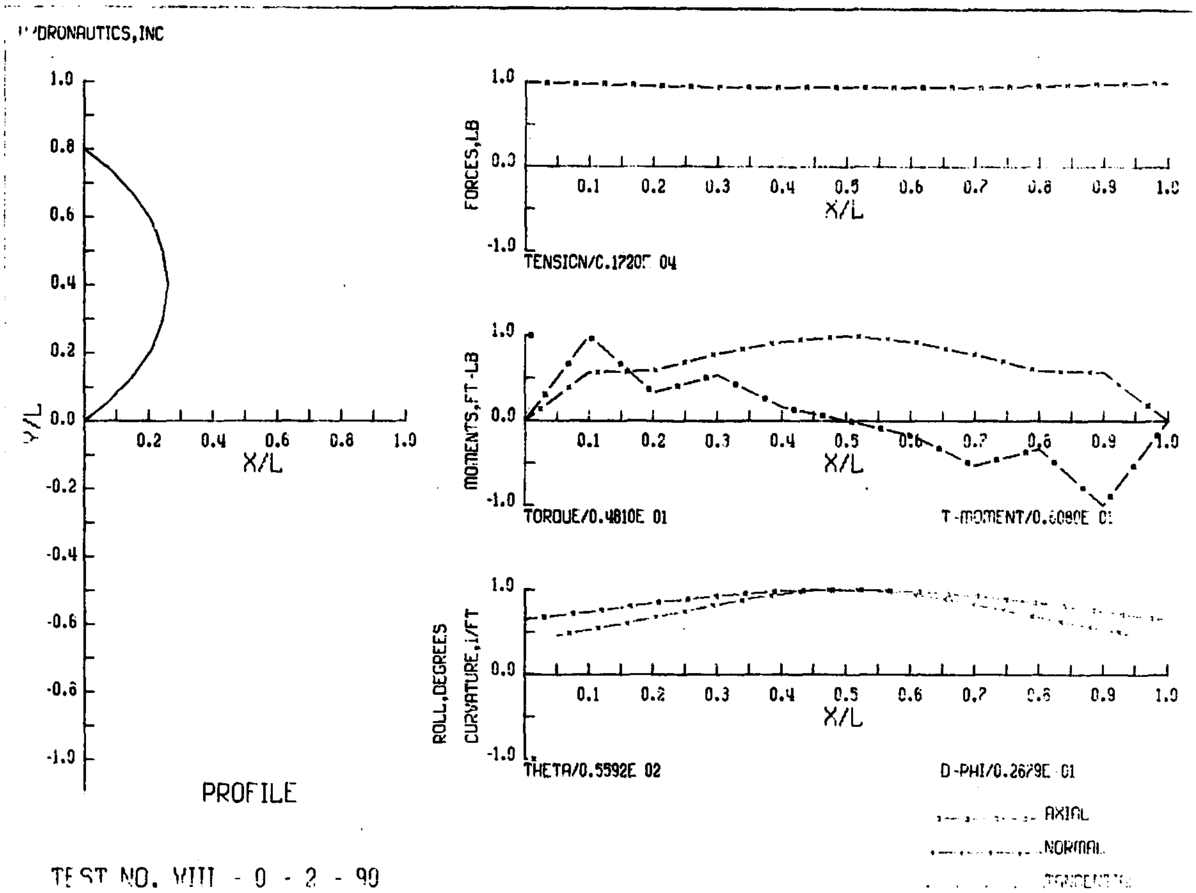

TEST NO. VIII - 0 - 2 - 90

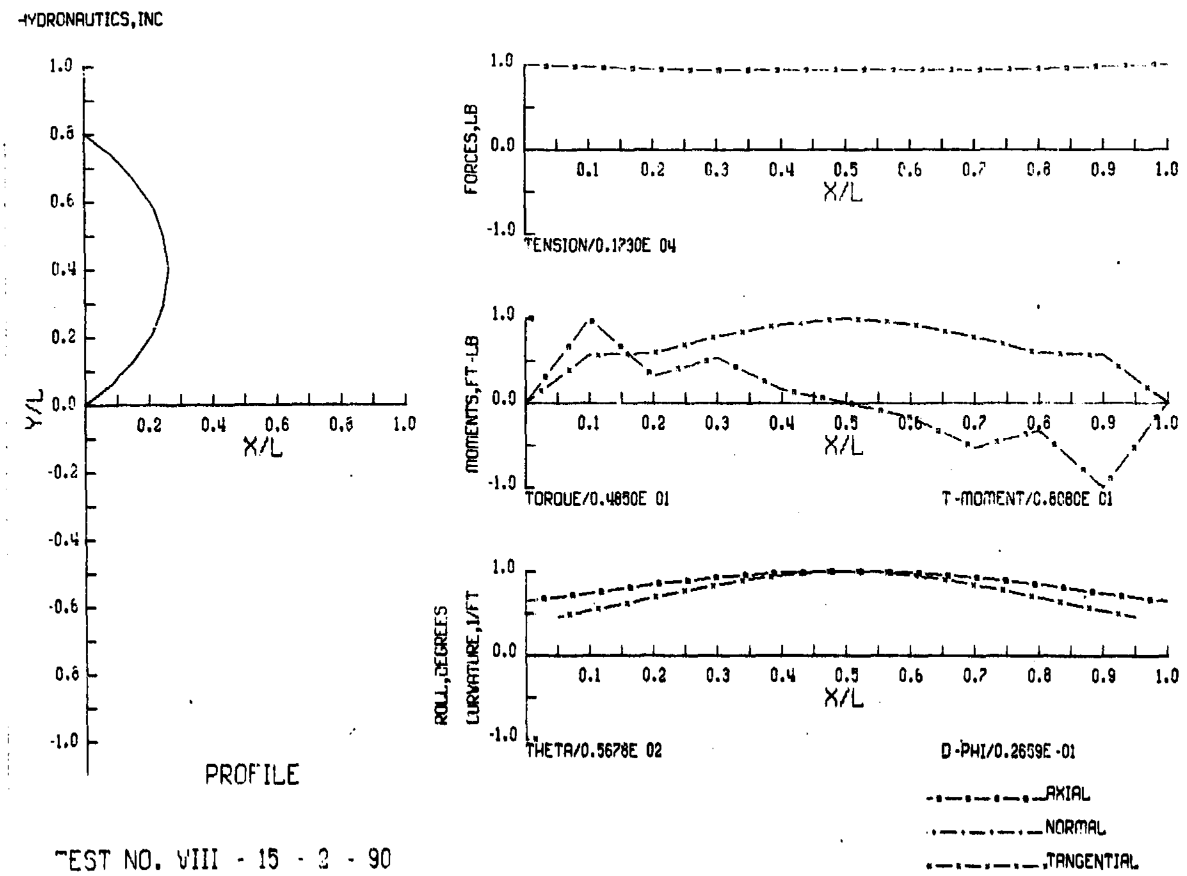

TEST NO. VIII - 15 - 2 - 90

HYDRONAUTICS,INC

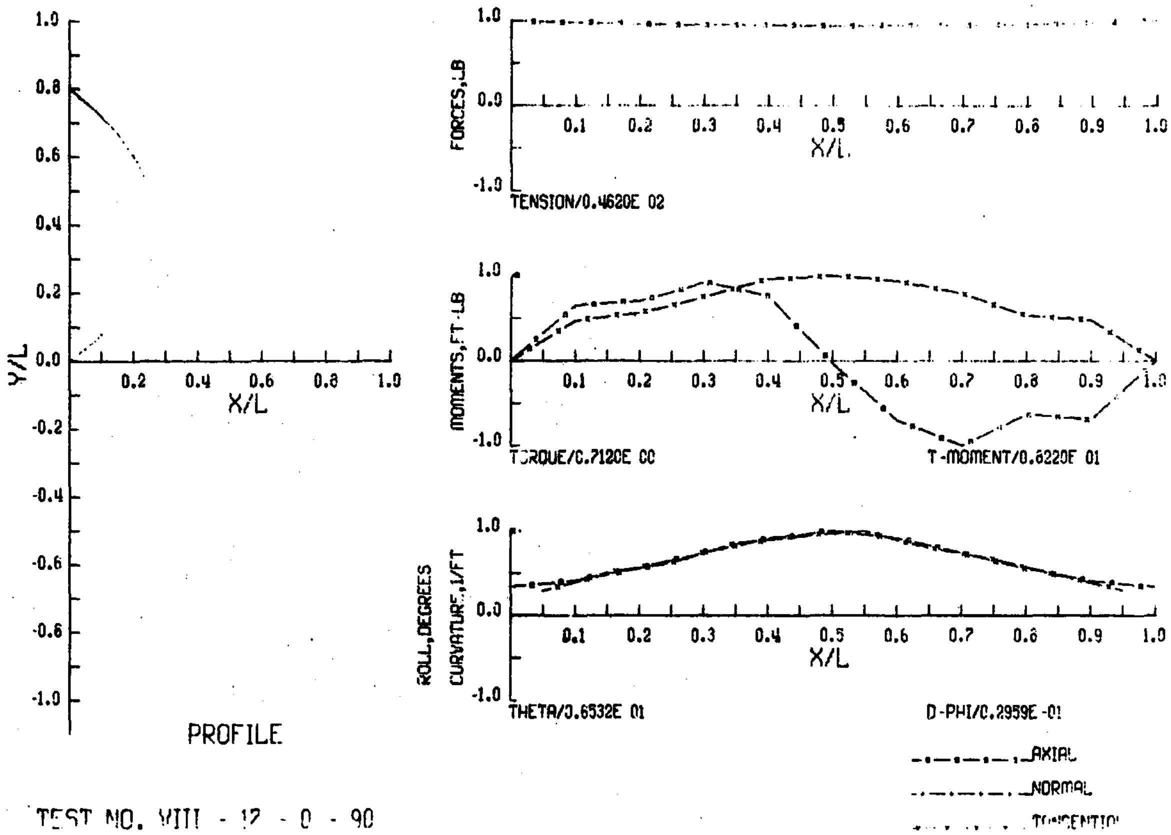

TEST NO. VIII - 17 - 0 - 90

HYDRONAUTICS,INC

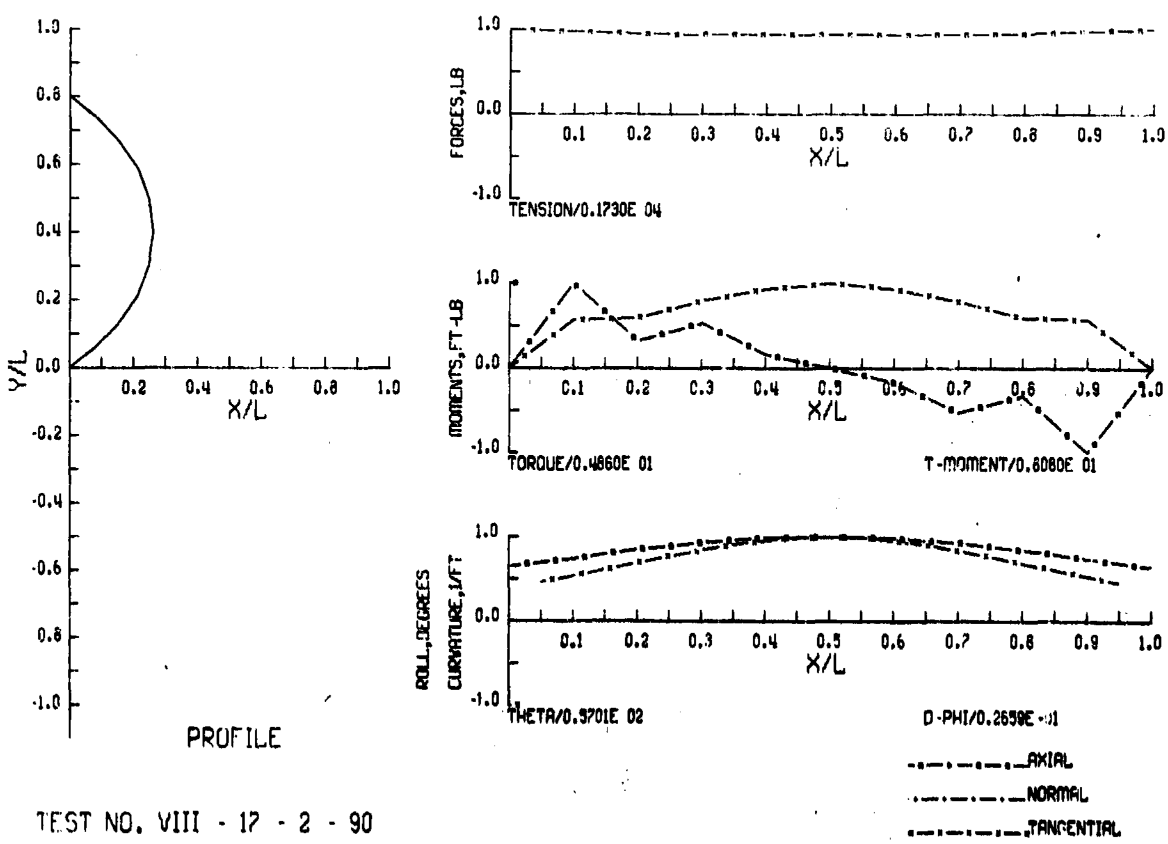

TEST NO. VIII - 17 - 2 - 90

HYDRONAUTICS, INC

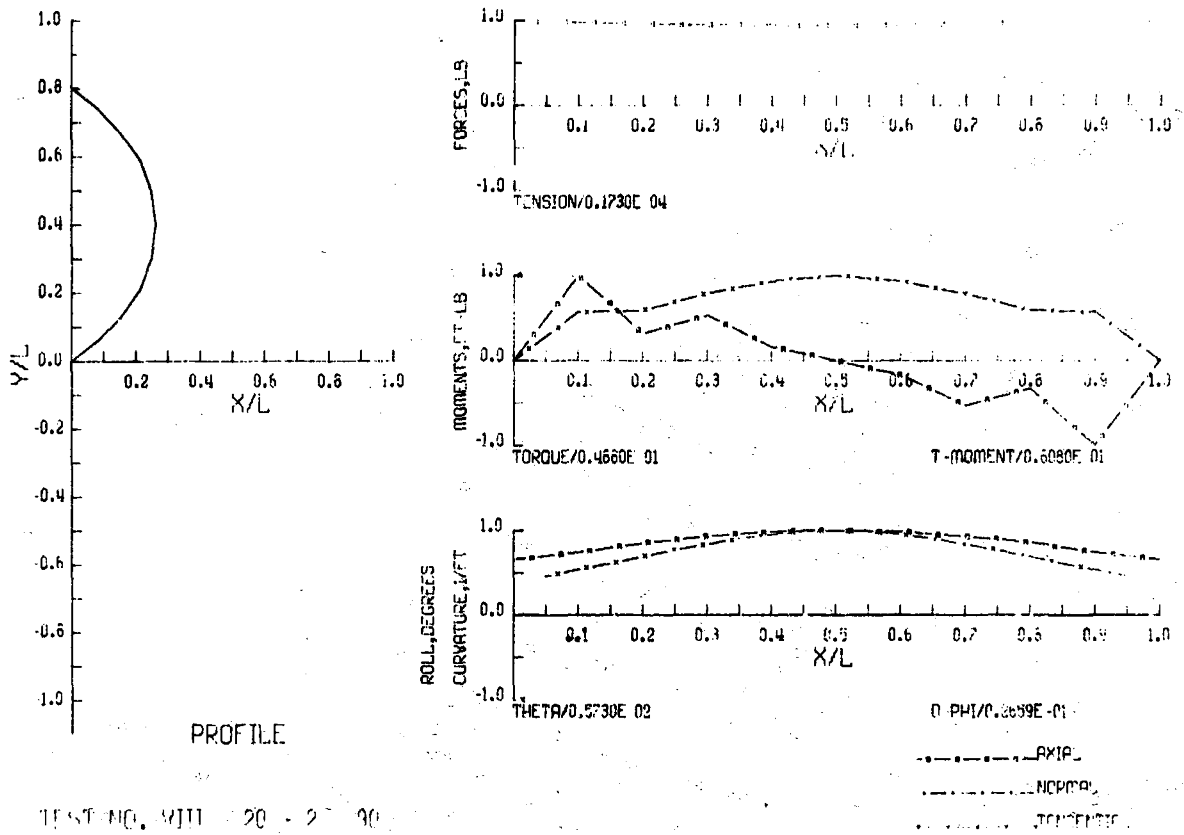

TEST NO. VIII - 20 - 2[illegible] - 90

HYDRONAUTICS, INC

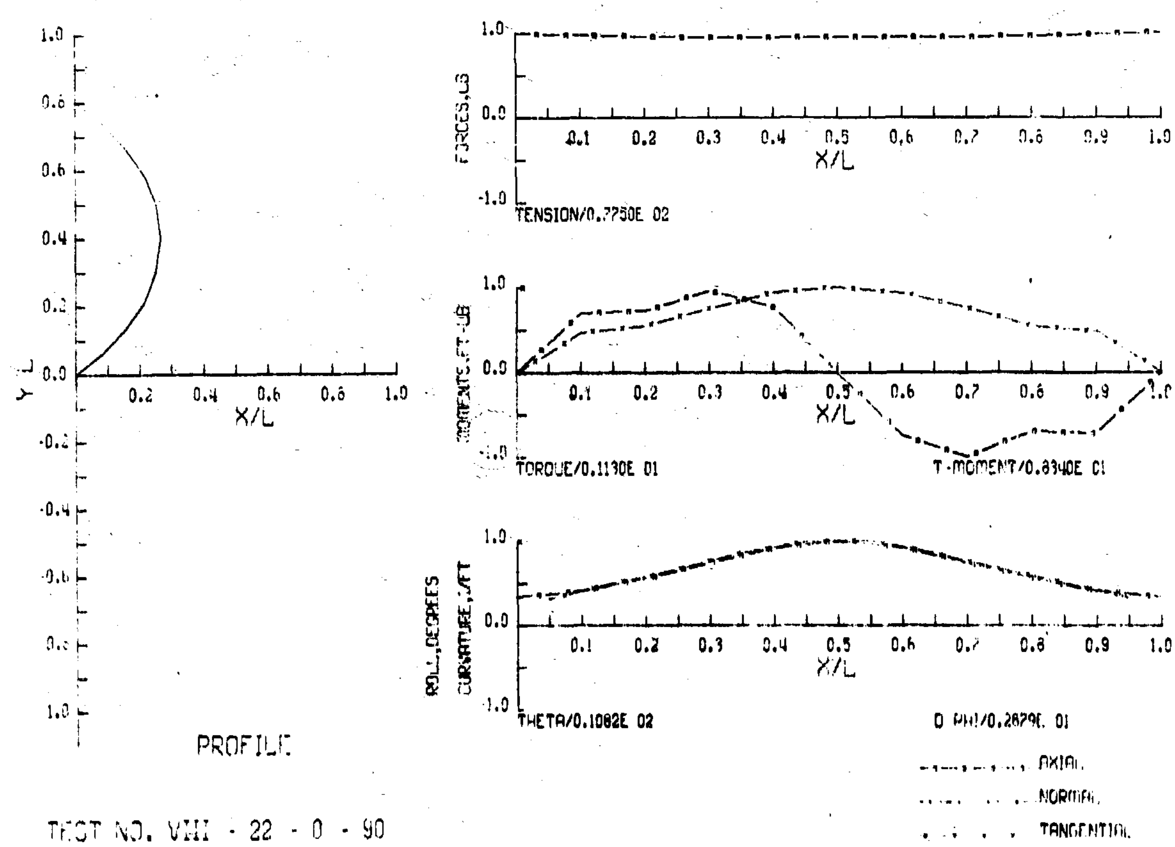

TEST NO. VIII - 22 - 0 - 90

HYDRONAUTICS,INC

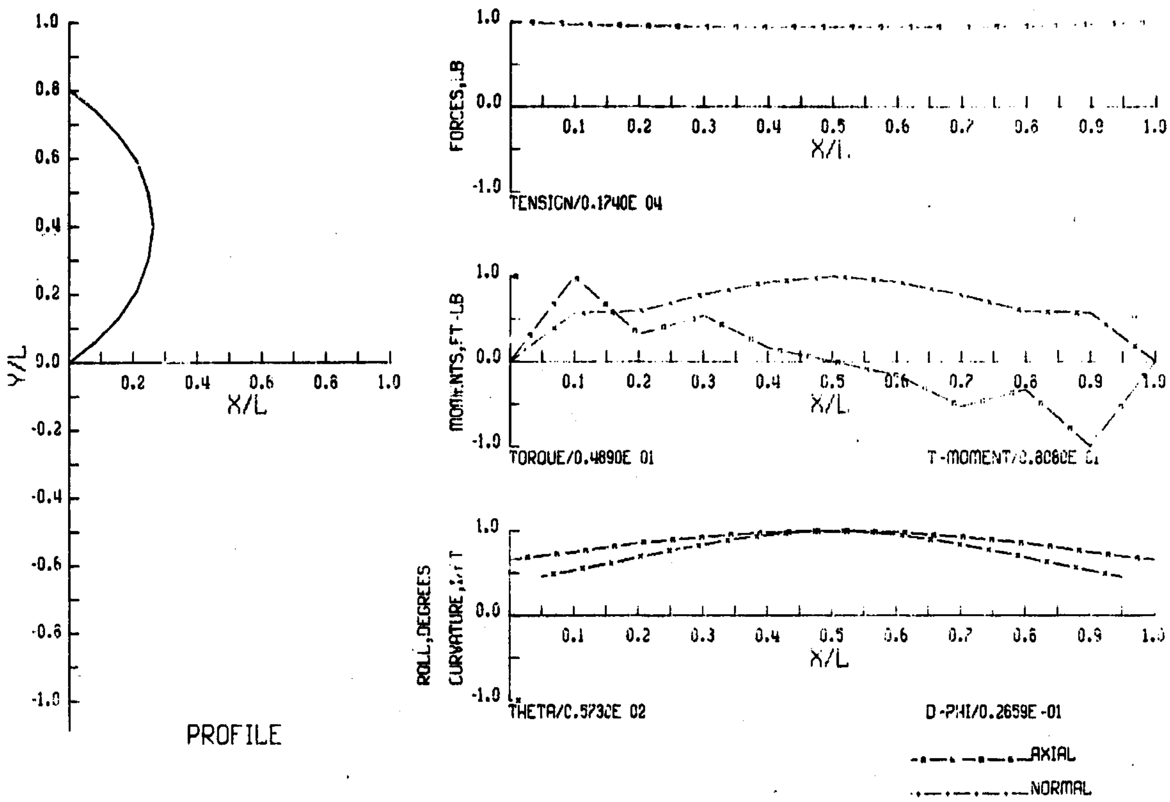

TEST NO. VIII - 22 - 2 - 90

HYDRONAUTICS,INC

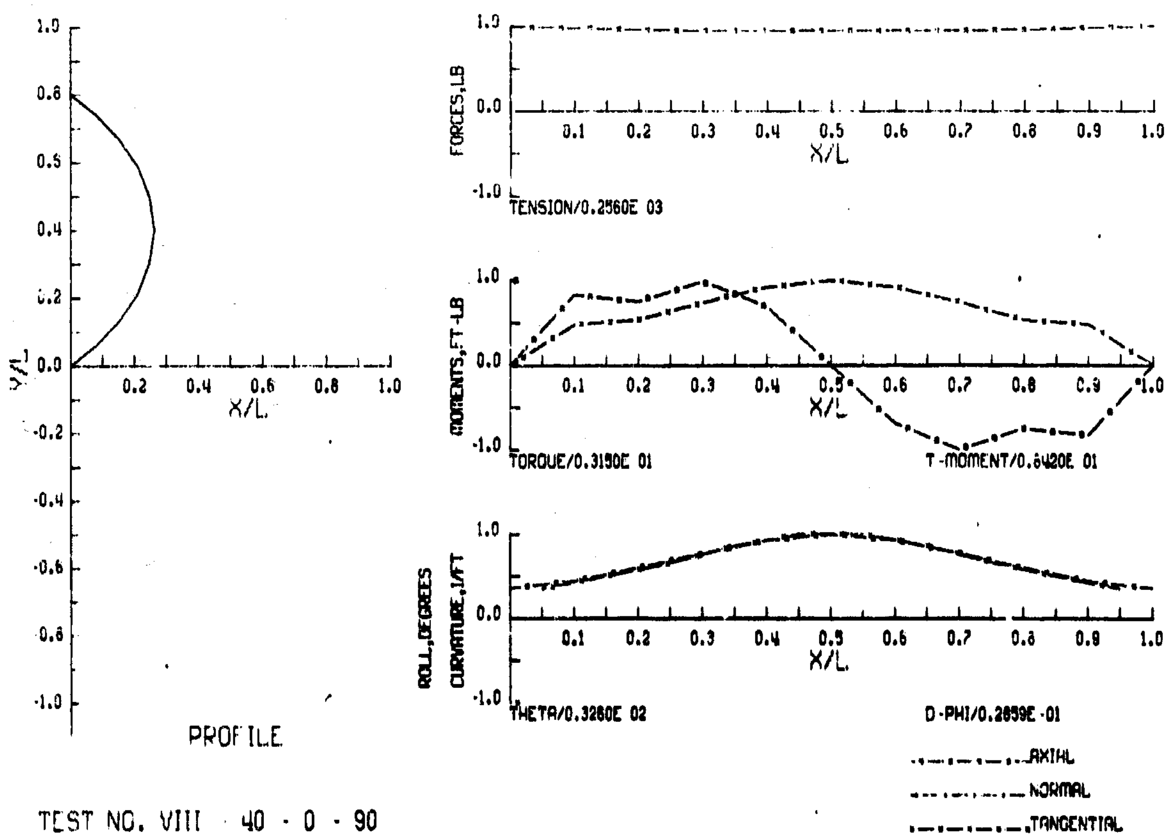

TEST NO. VIII - 40 - 0 - 90

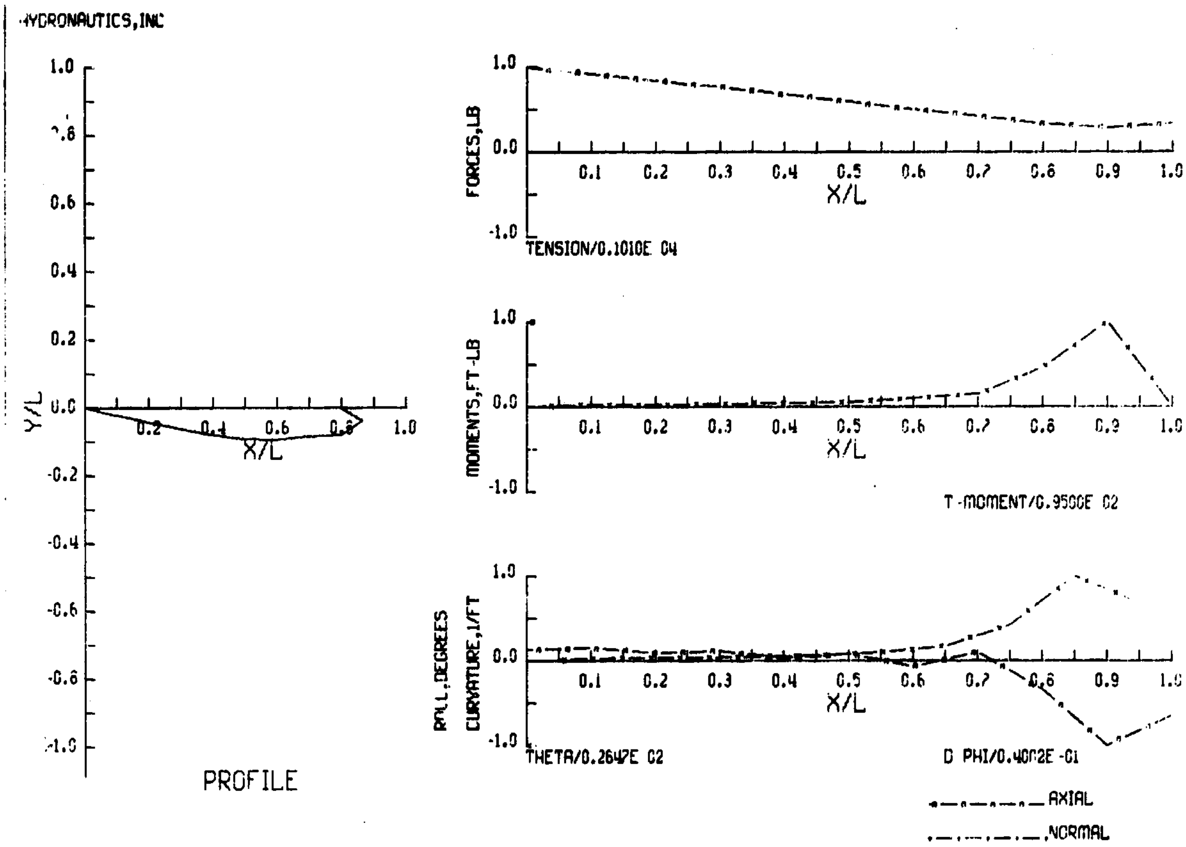

TEST NO. IX - 0 - 2 - 0

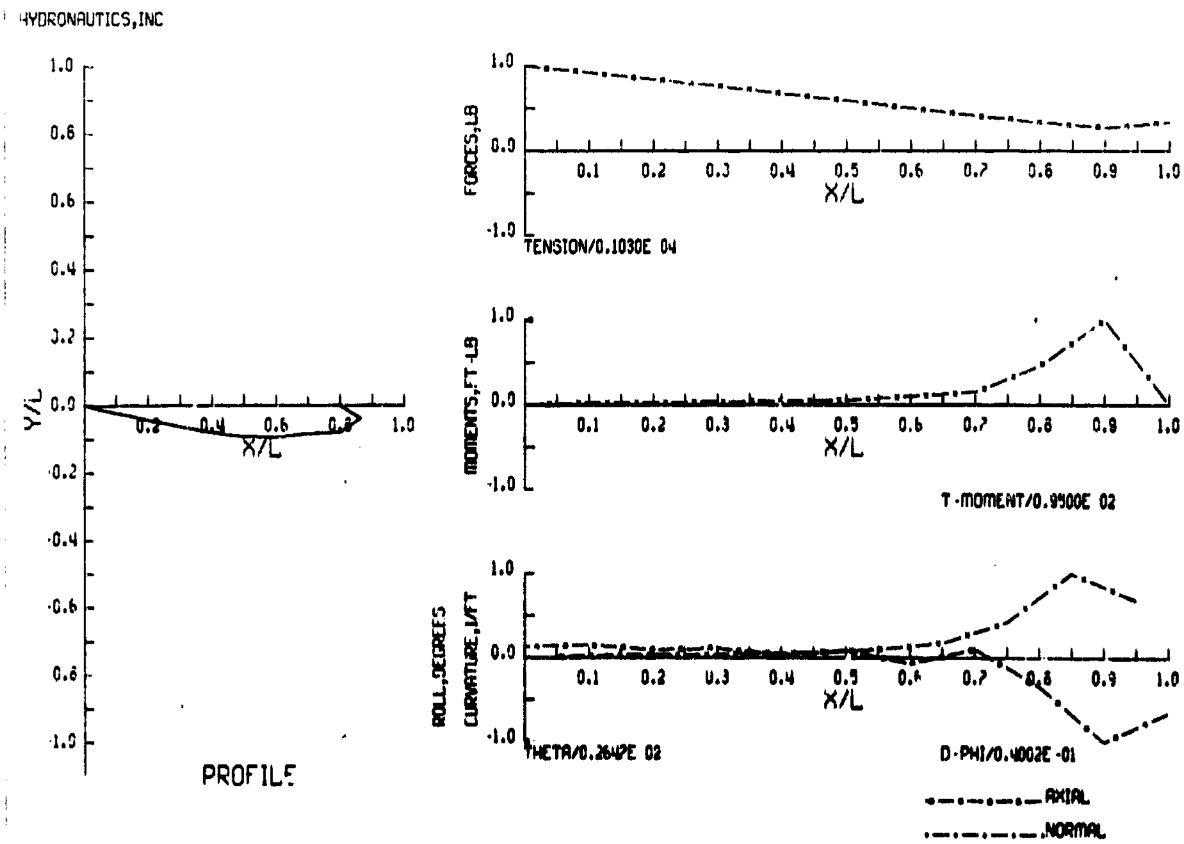

TEST NO. IX - 20 - 2 - 0

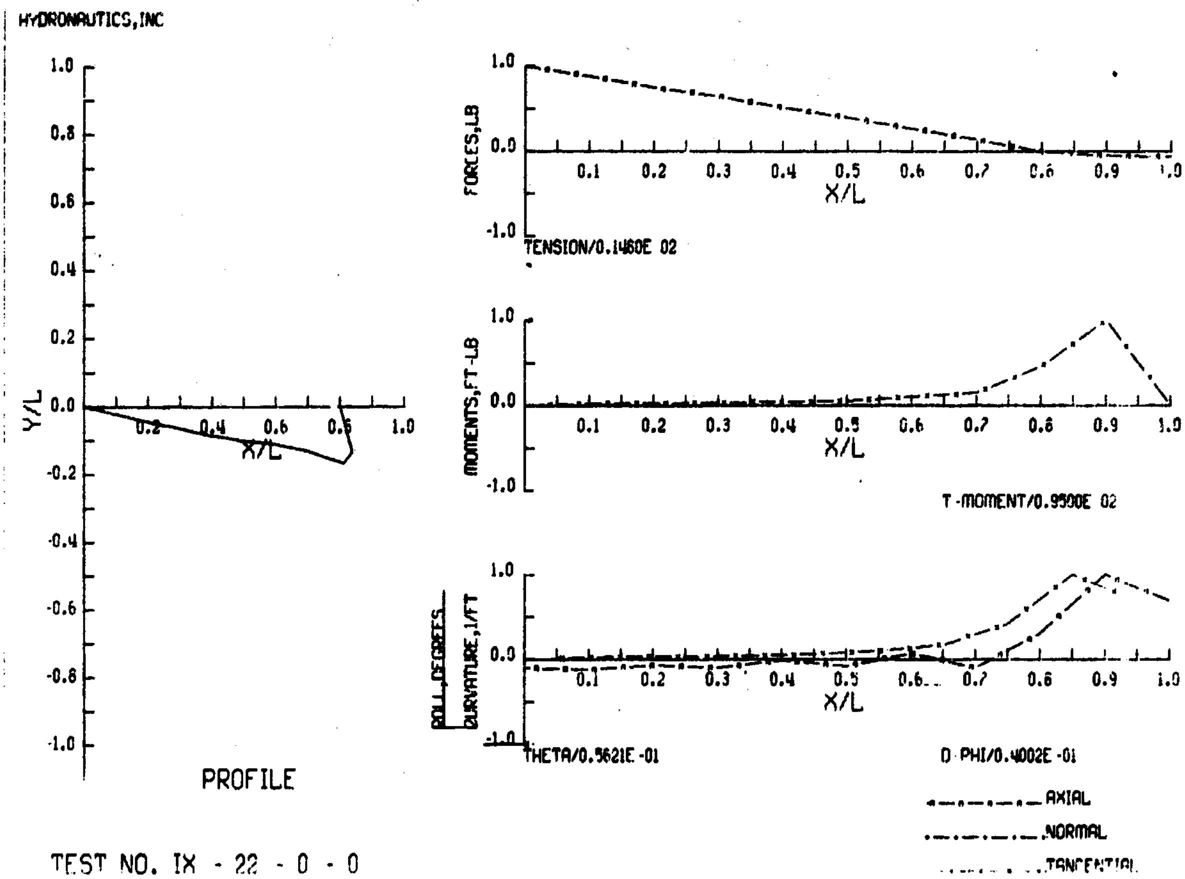

TEST NO. IX - 22 - 0 - 0

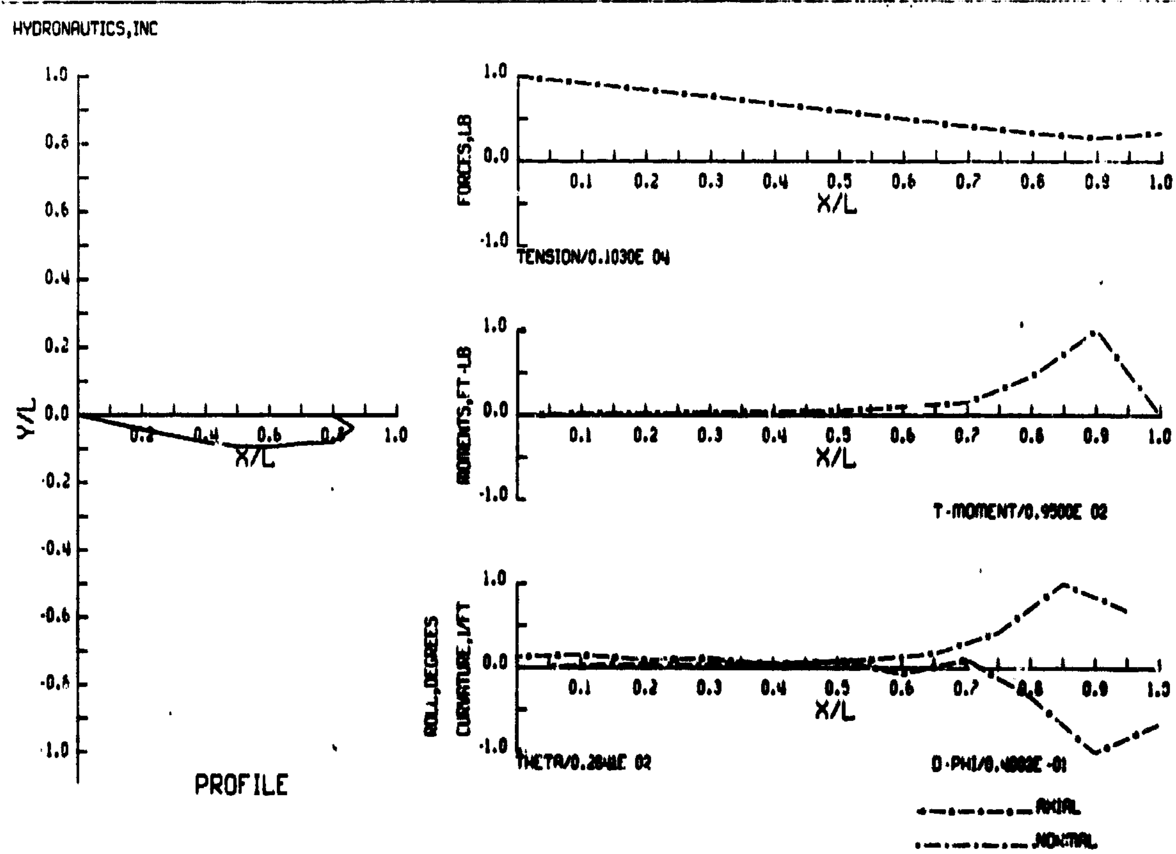

TEST NO. IX - 22 - 2 - 0

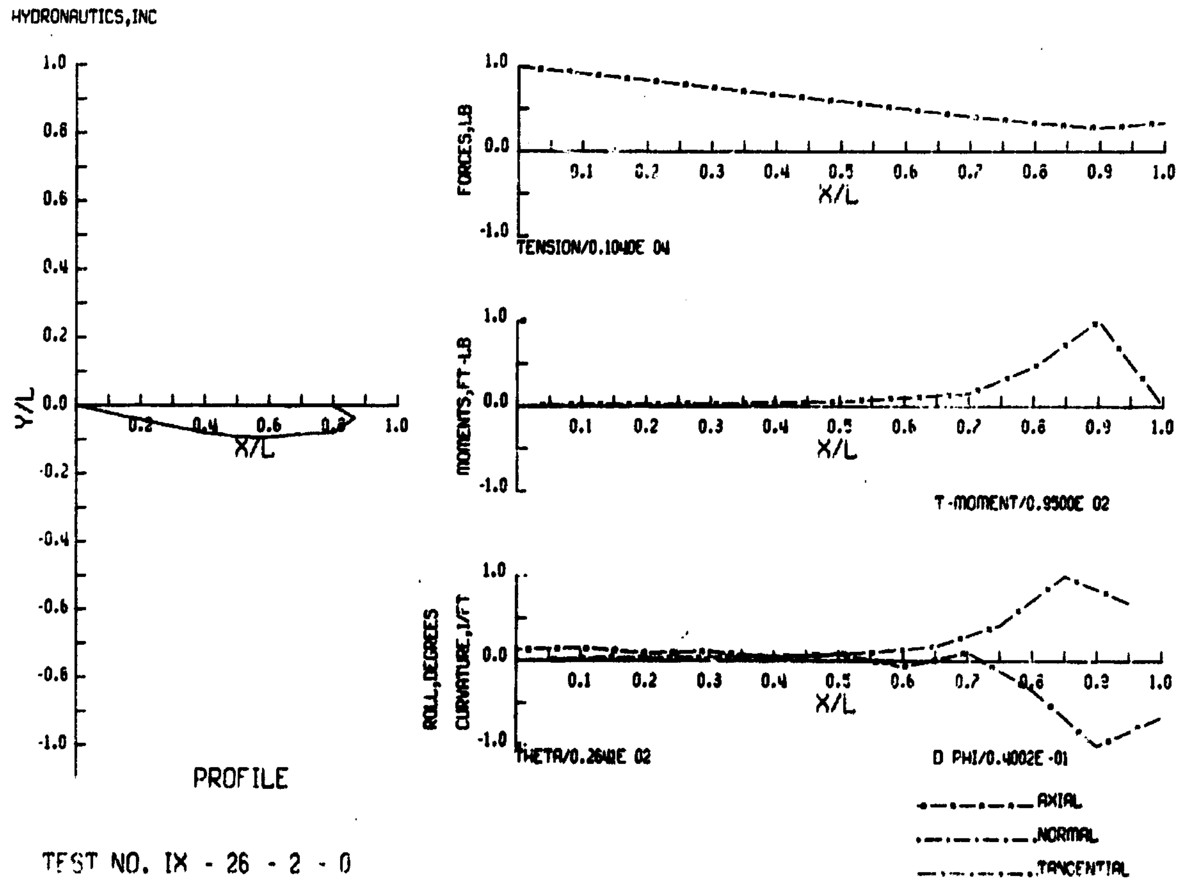

TEST NO. IX - 26 - 2 - 0

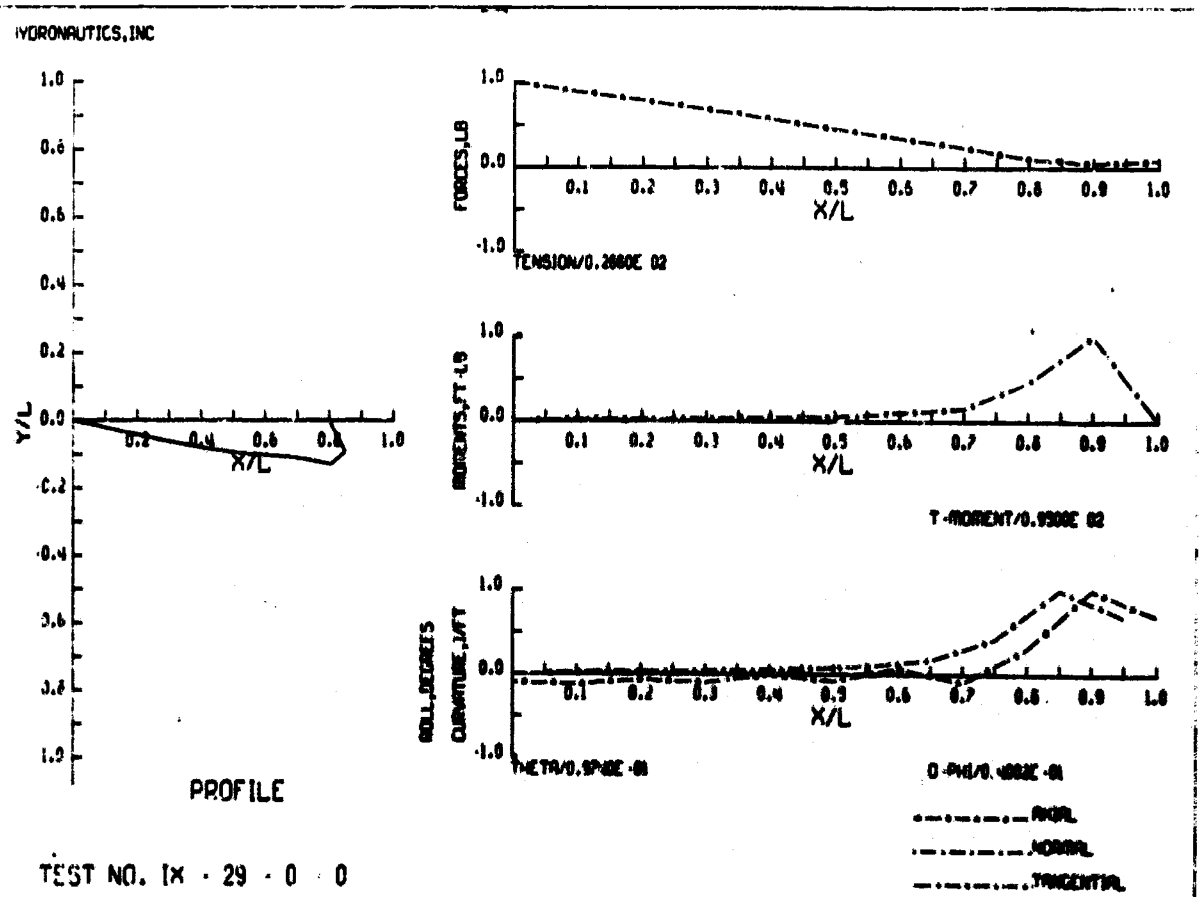

TEST NO. IX - 29 - 0 - 0

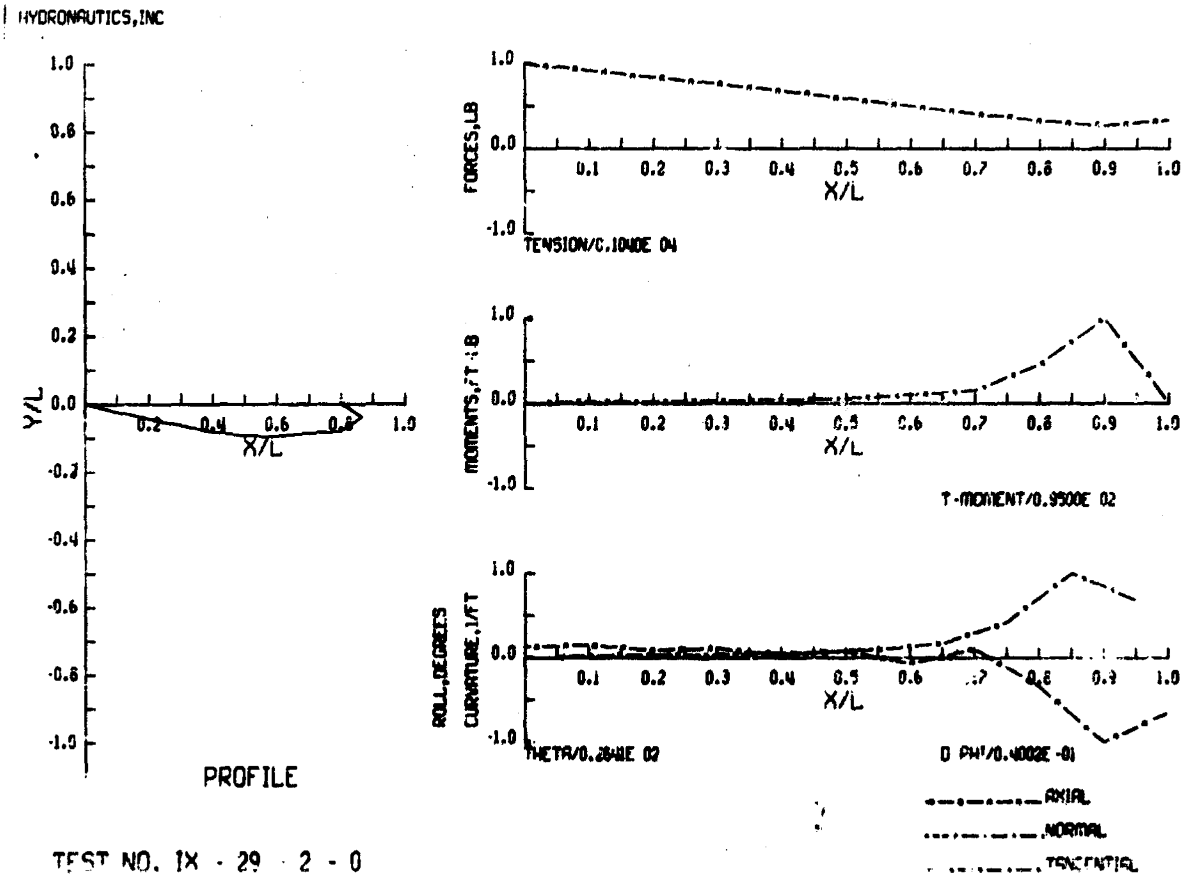

TEST NO. IX - 29 - 2 - 0

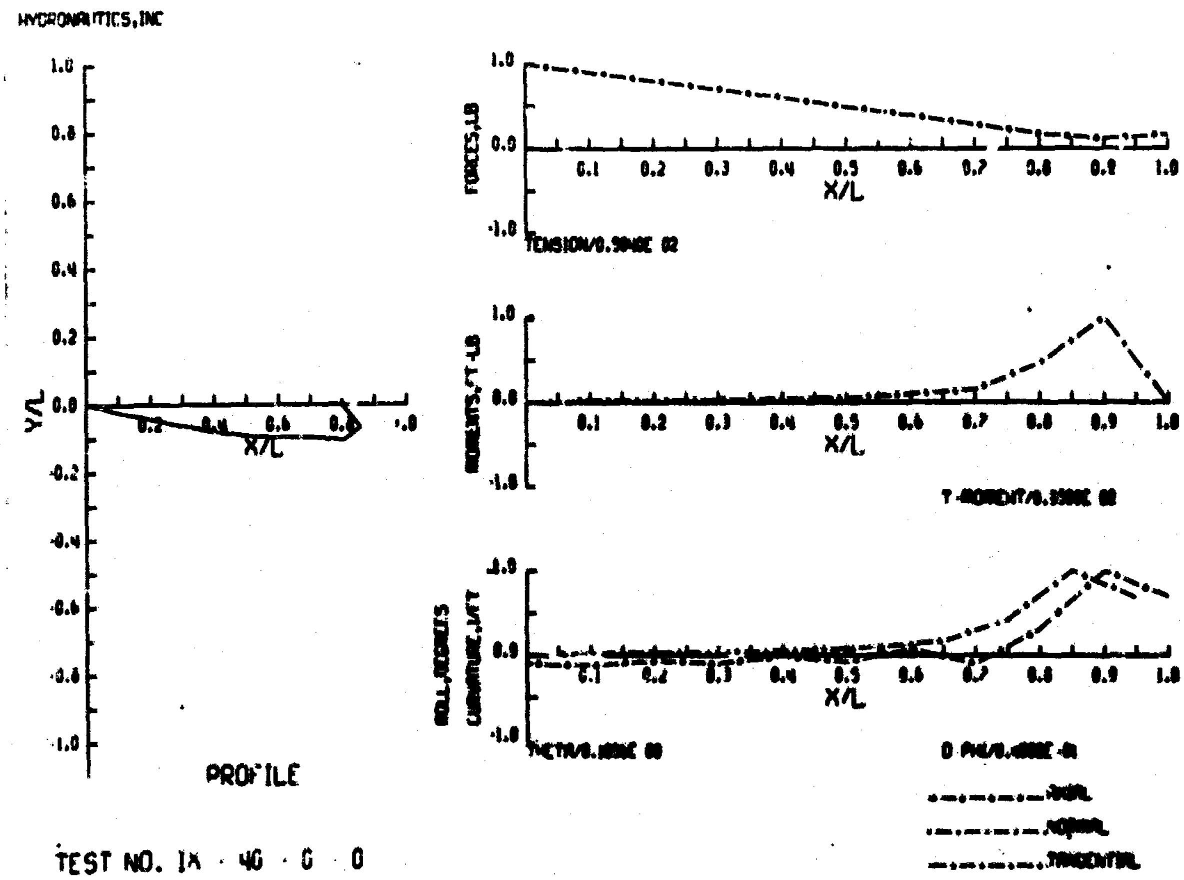

TEST NO. IX - 40 - 0 - 0

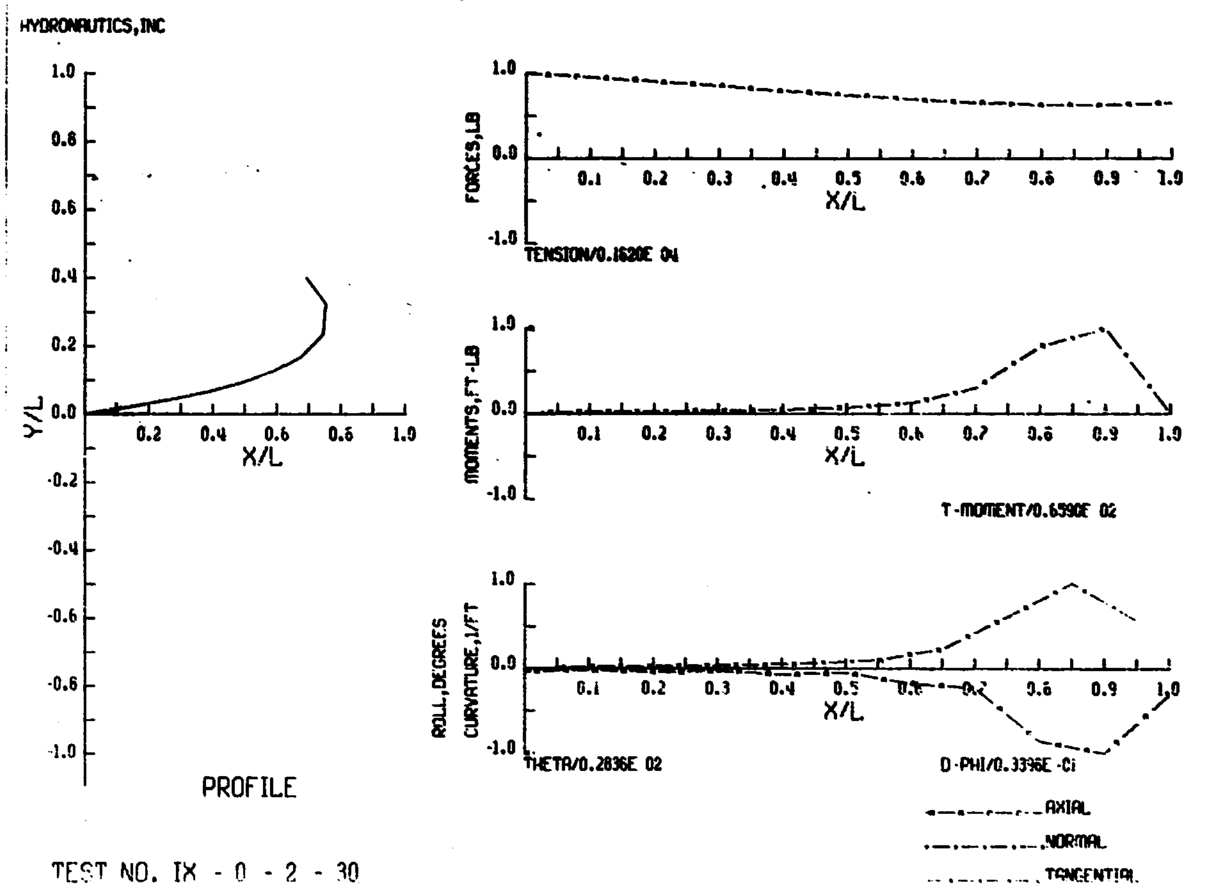

TEST NO. IX - 0 - 2 - 30

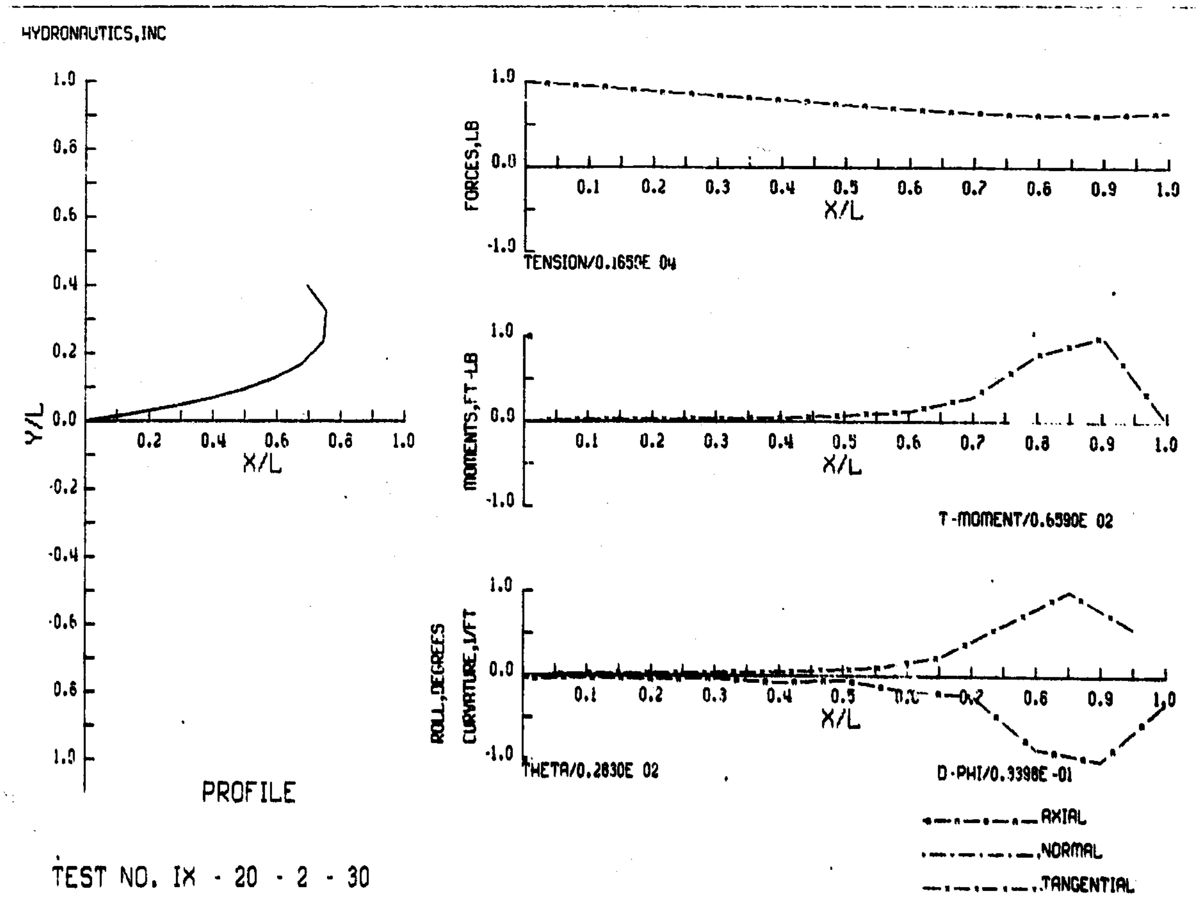

TEST NO. IX - 20 - 2 - 30

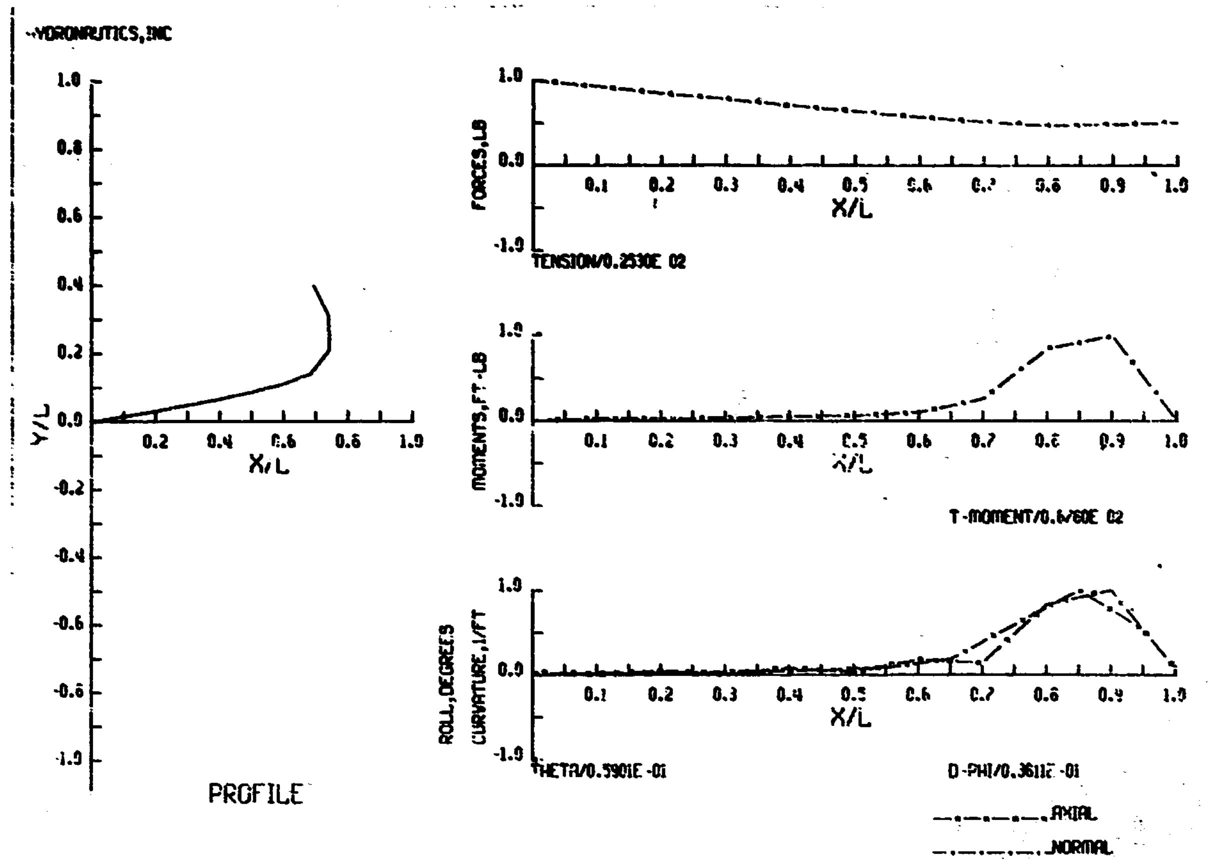

TEST NO. IX - 22 - 0 - 30

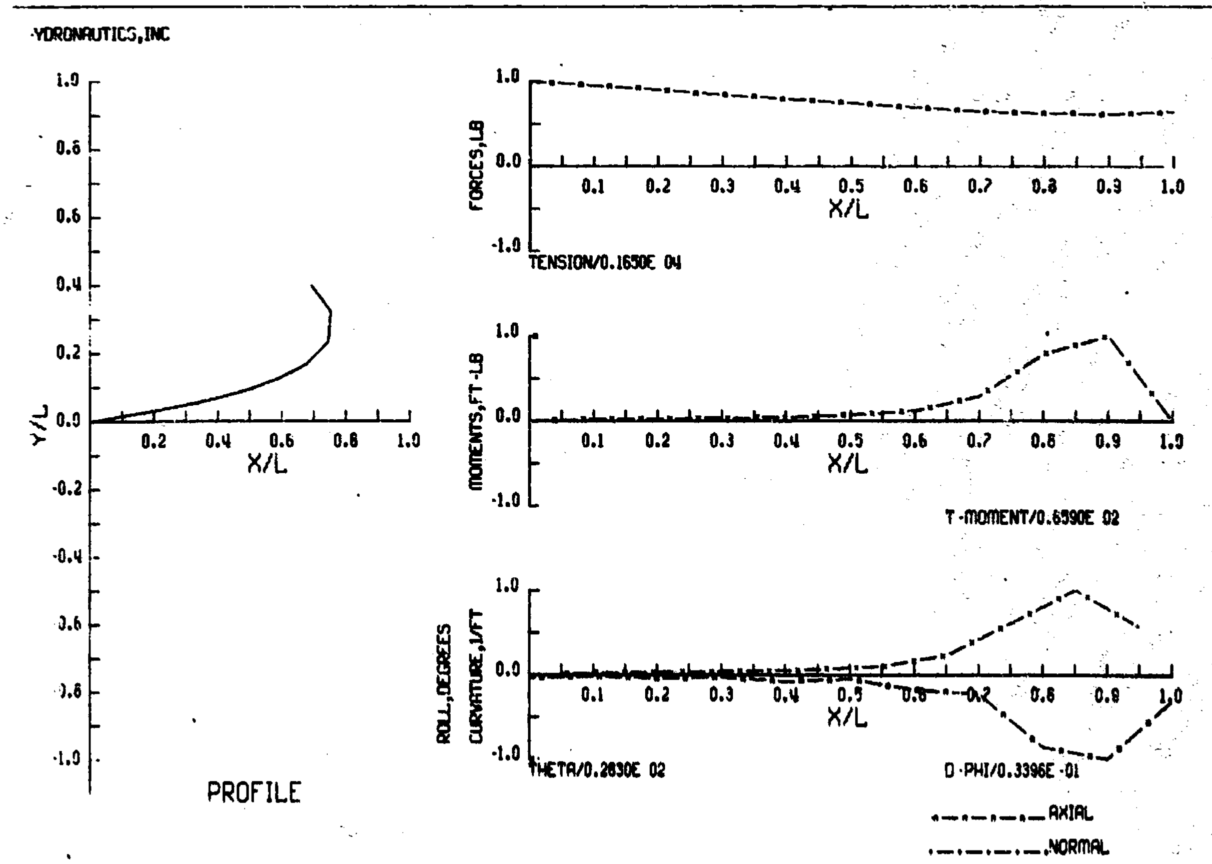

TEST NO. IX - 22 - 2 - 30

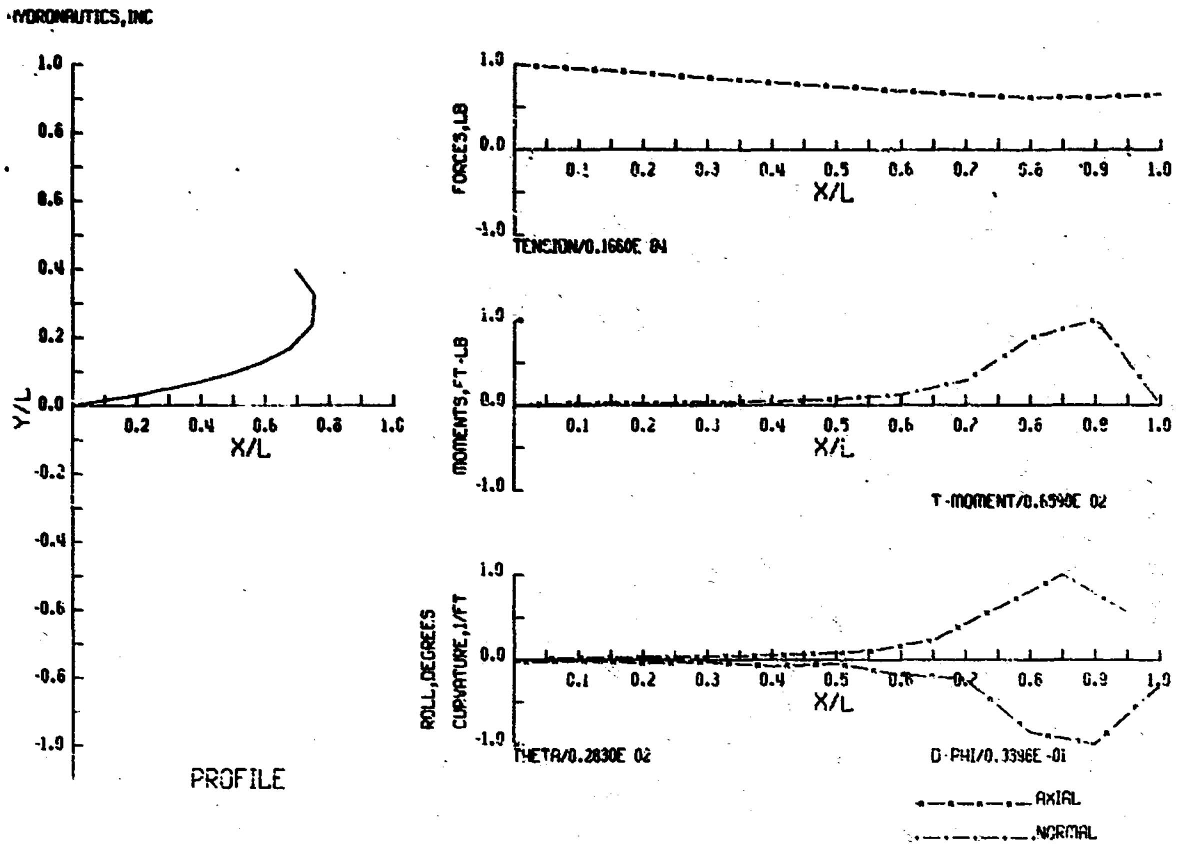

TEST NO. IX - 26 - 2 - 30

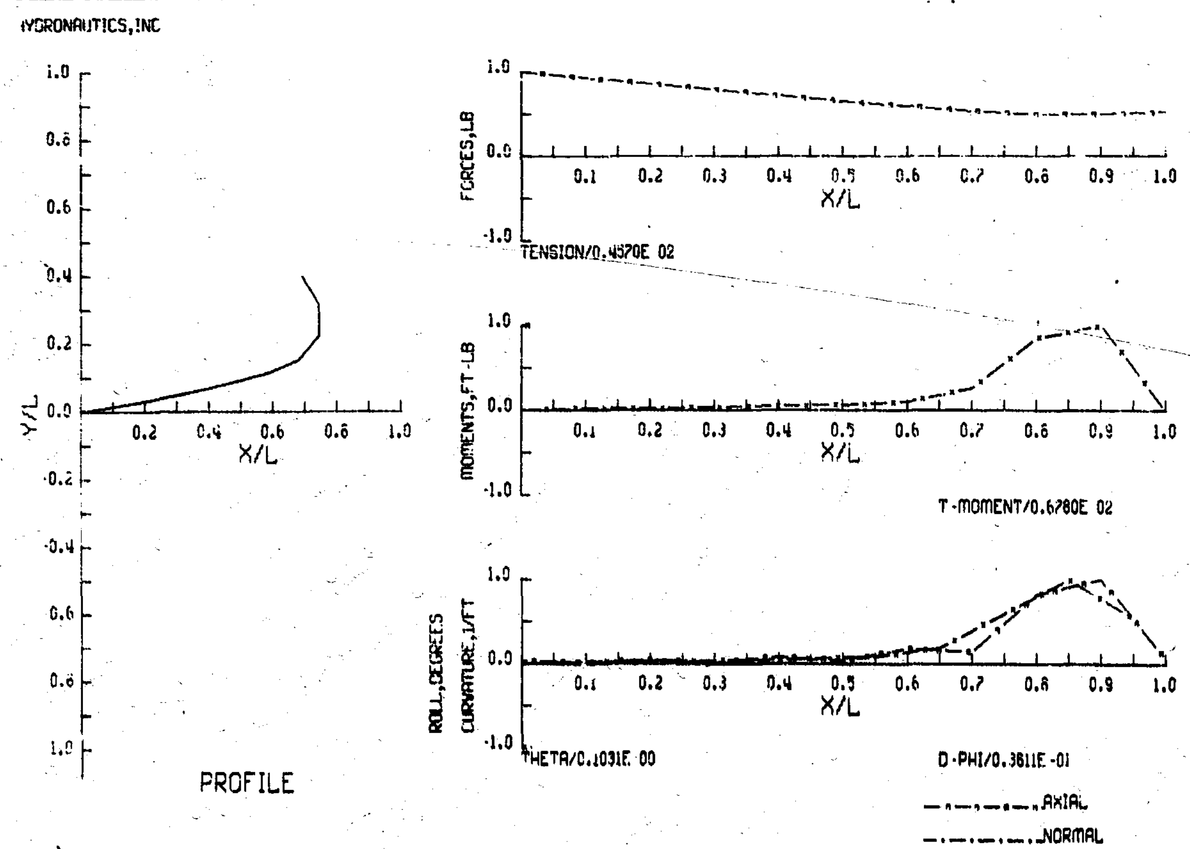

TEST NO. IX - 29 - 0 - 30

HYDRONAUTICS,INC

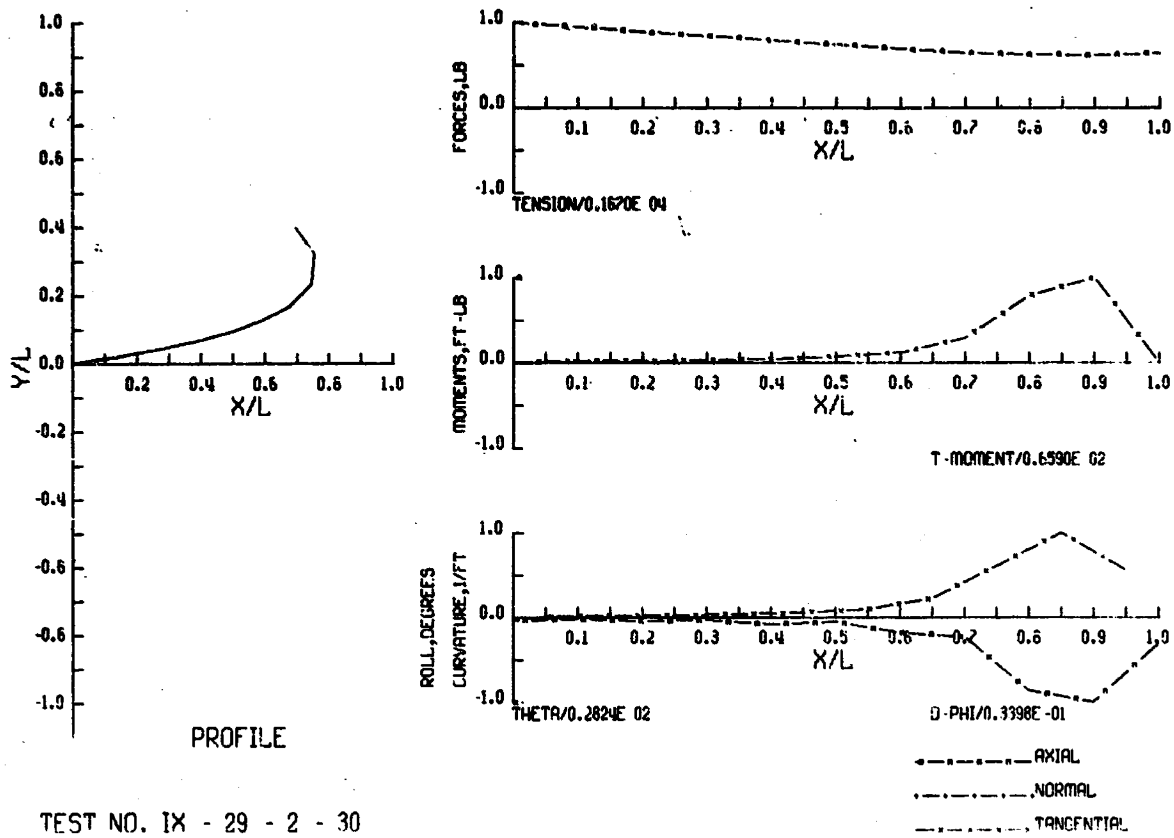

TEST NO. IX - 29 - 2 - 30

HYDRONAUTICS,INC

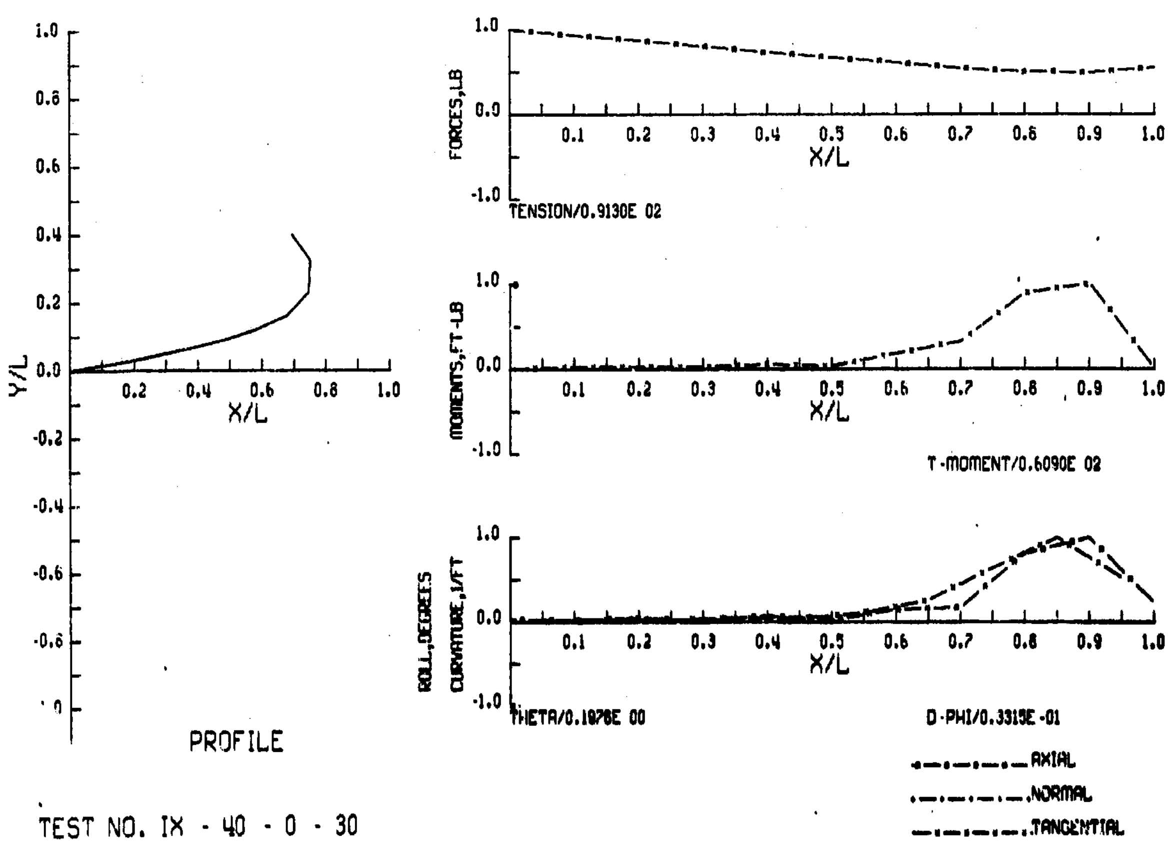

TEST NO. IX - 40 - 0 - 30

HYDRONAUTICS, INC

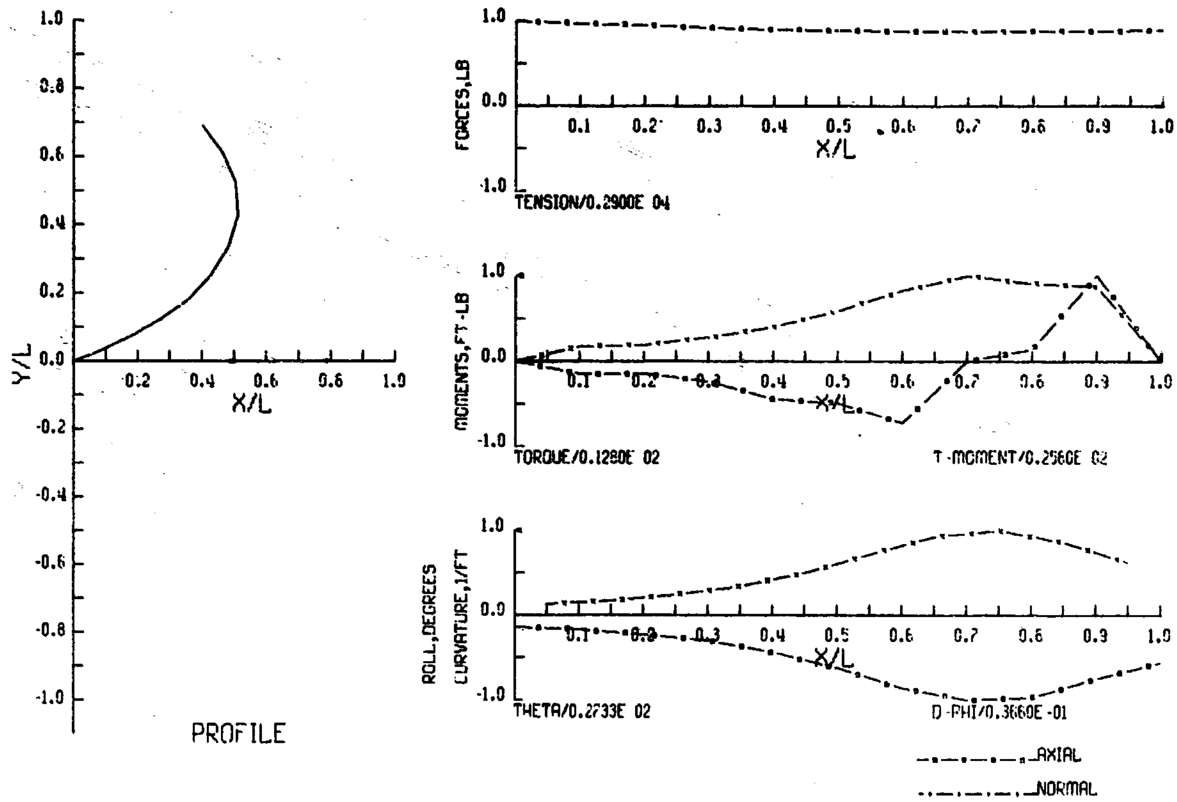

TEST NO. IX - 0 2 60

HYDRONAUTICS, INC

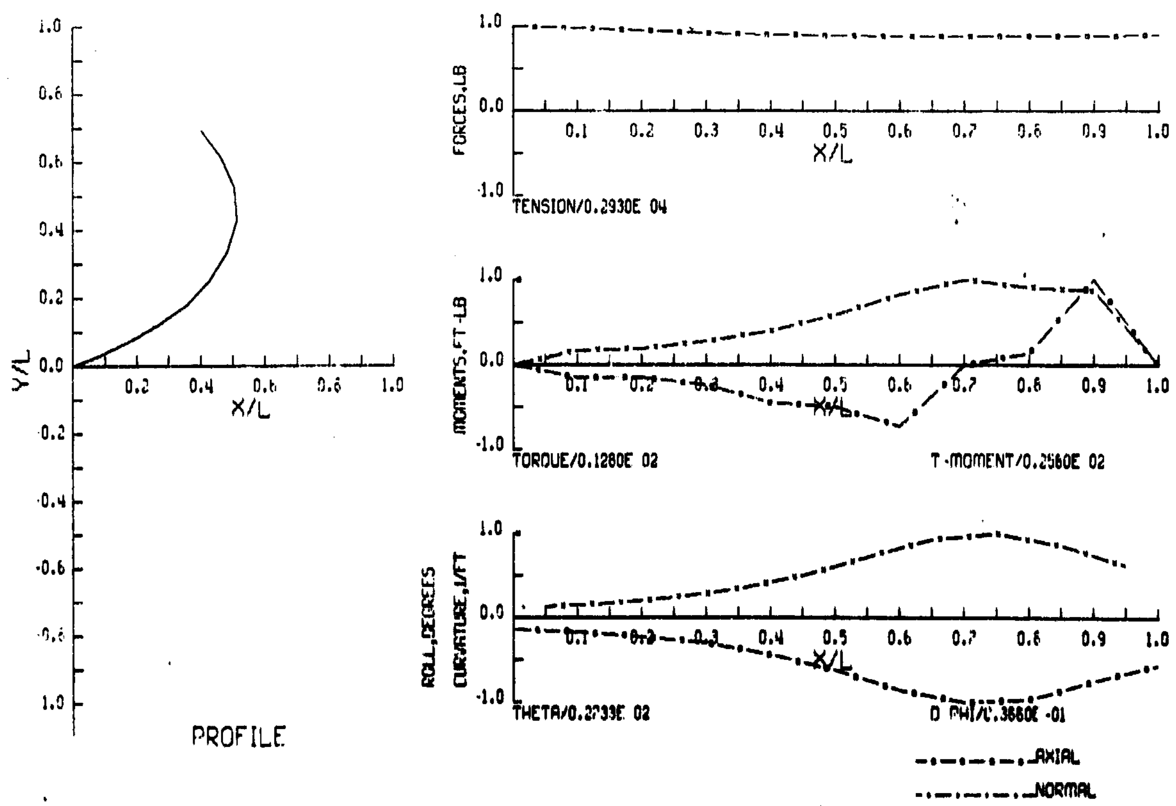

TEST NO. IX - 20 2 - 60

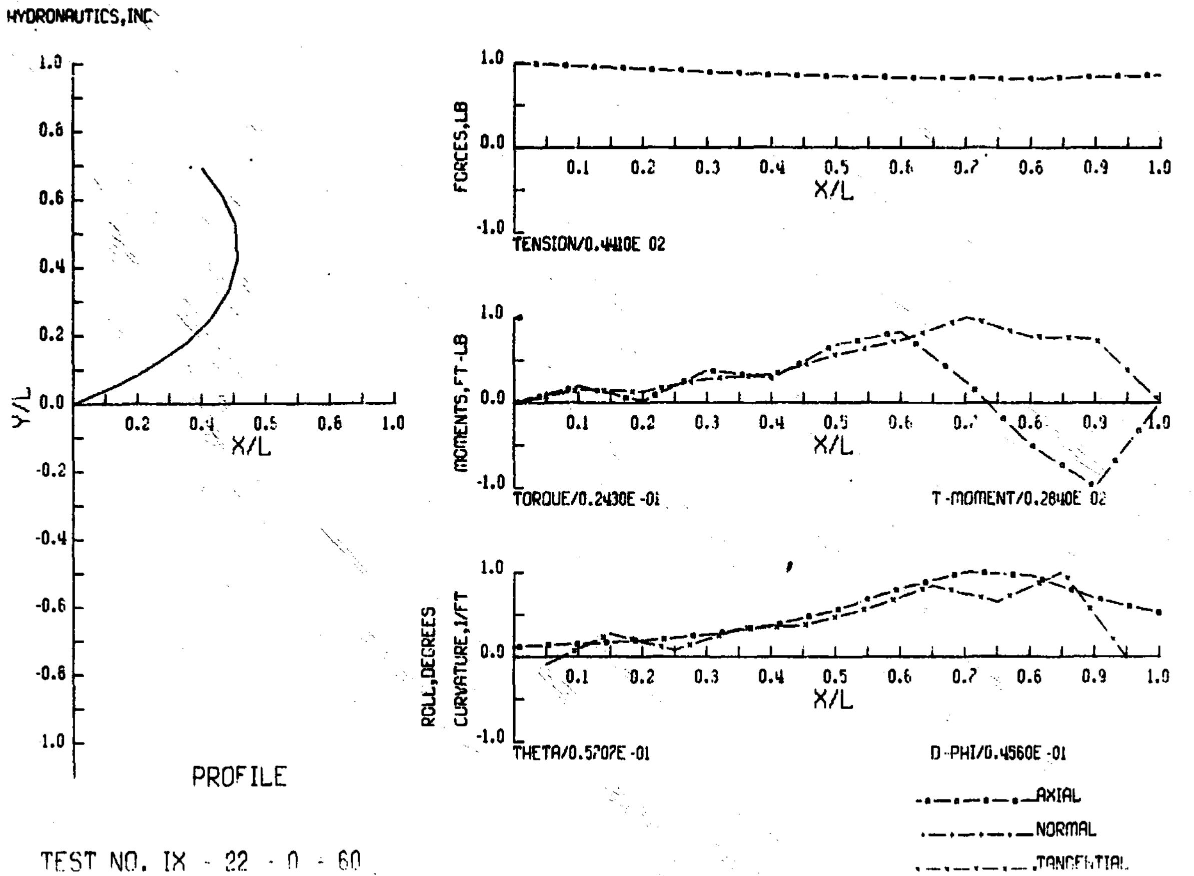

TEST NO. IX - 22 - 0 - 60

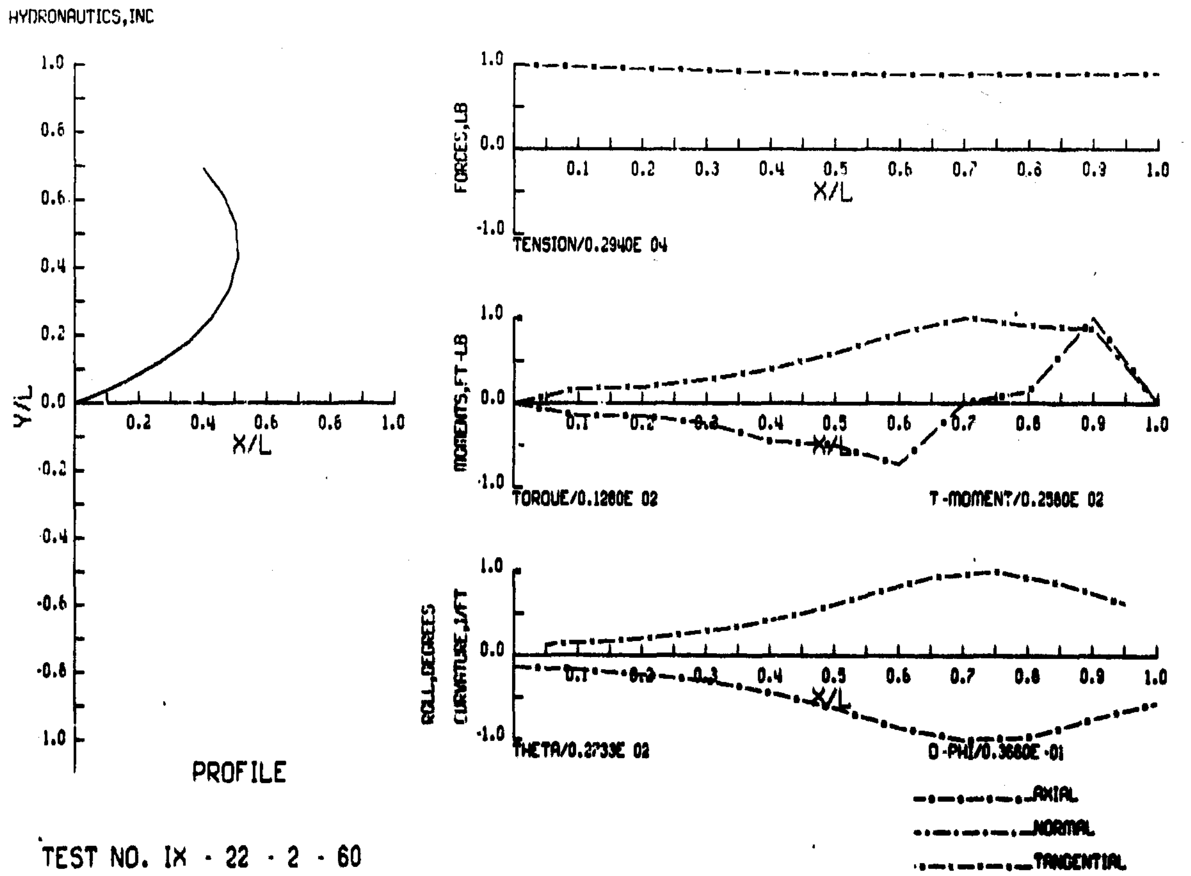

TEST NO. IX - 22 - 2 - 60

HYDRONAUTICS,INC

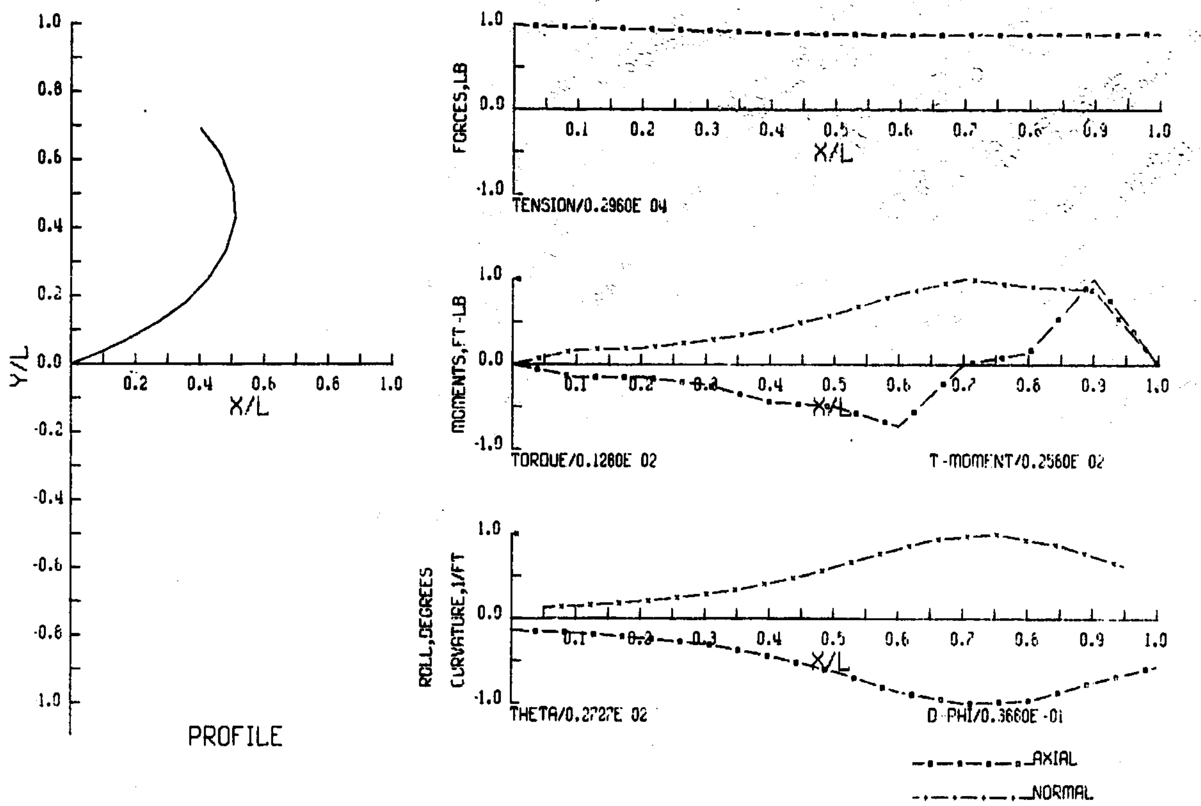

TEST NO. IX - 26 - 0 - 60

HYDRONAUTICS,INC

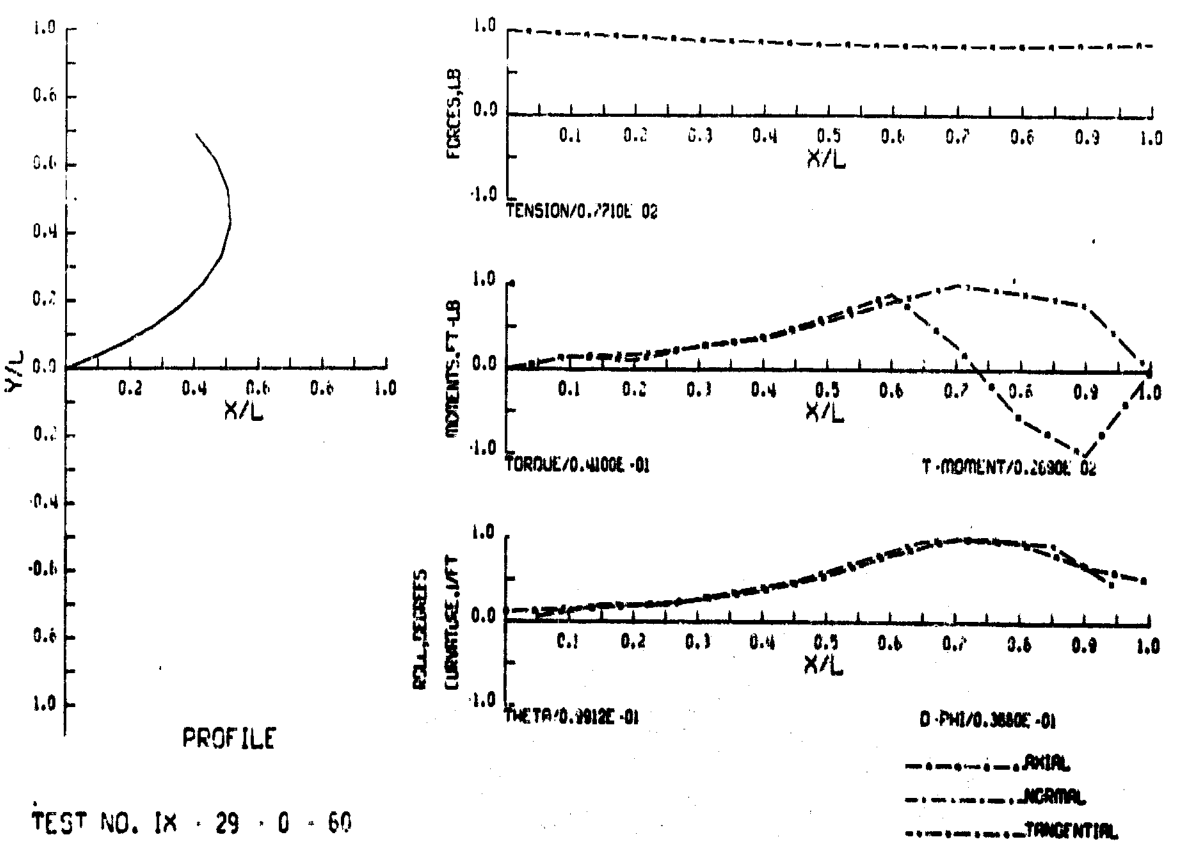

TEST NO. IX - 29 - 0 - 60

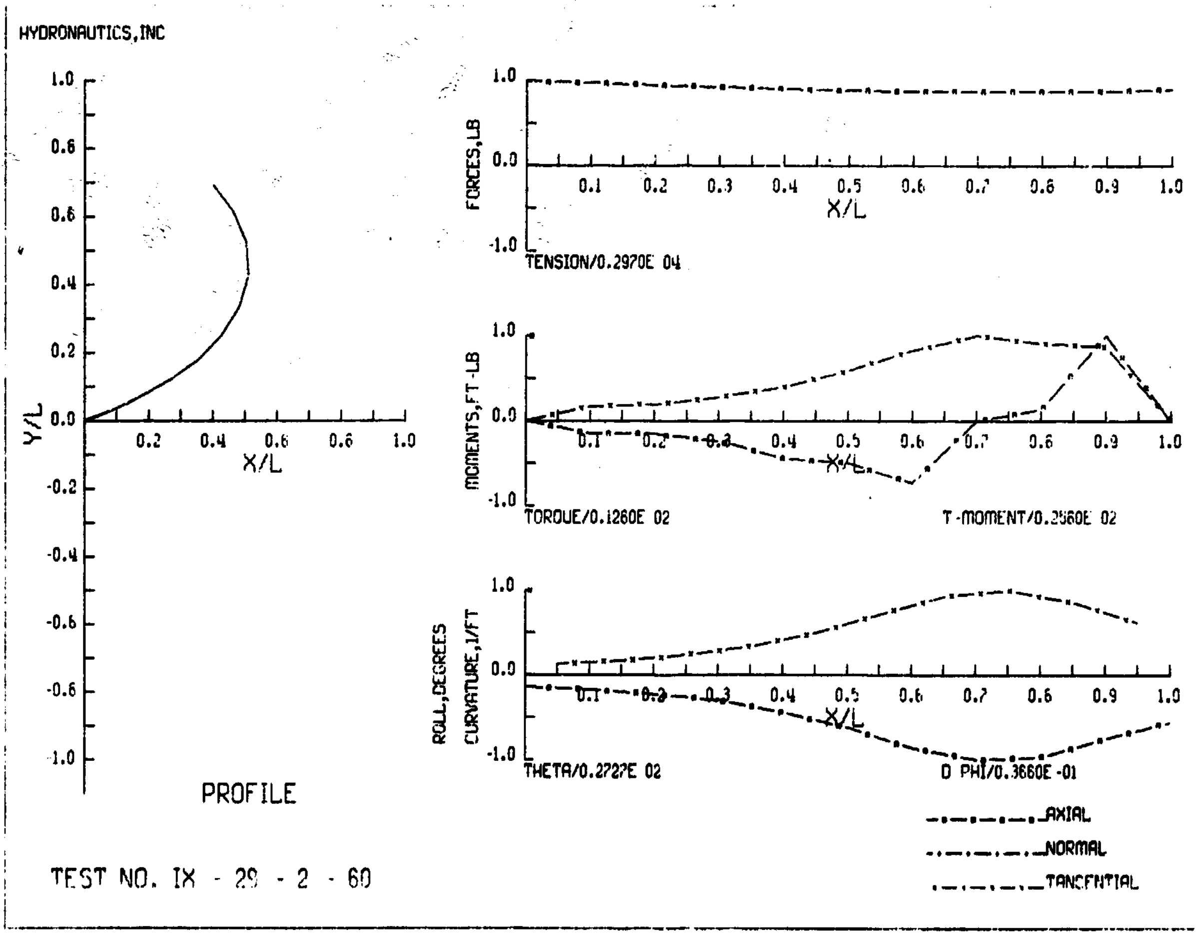
HYDRONAUTICS, INC
Y/L
X/L
PROFILE
FORCES, LB
TENSION/0.2970E 04
MOMENTS, FT-LB
TORQUE/0.1260E 02
T-MOMENT/0.2560E 02
ROLL, DEGREES
CURVATURE, 1/FT
THETA/0.2727E 02
D PHI/0.3660E -01
AXIAL
NORMAL
TANGENTIAL
TEST NO. IX - 29 - 2 - 60

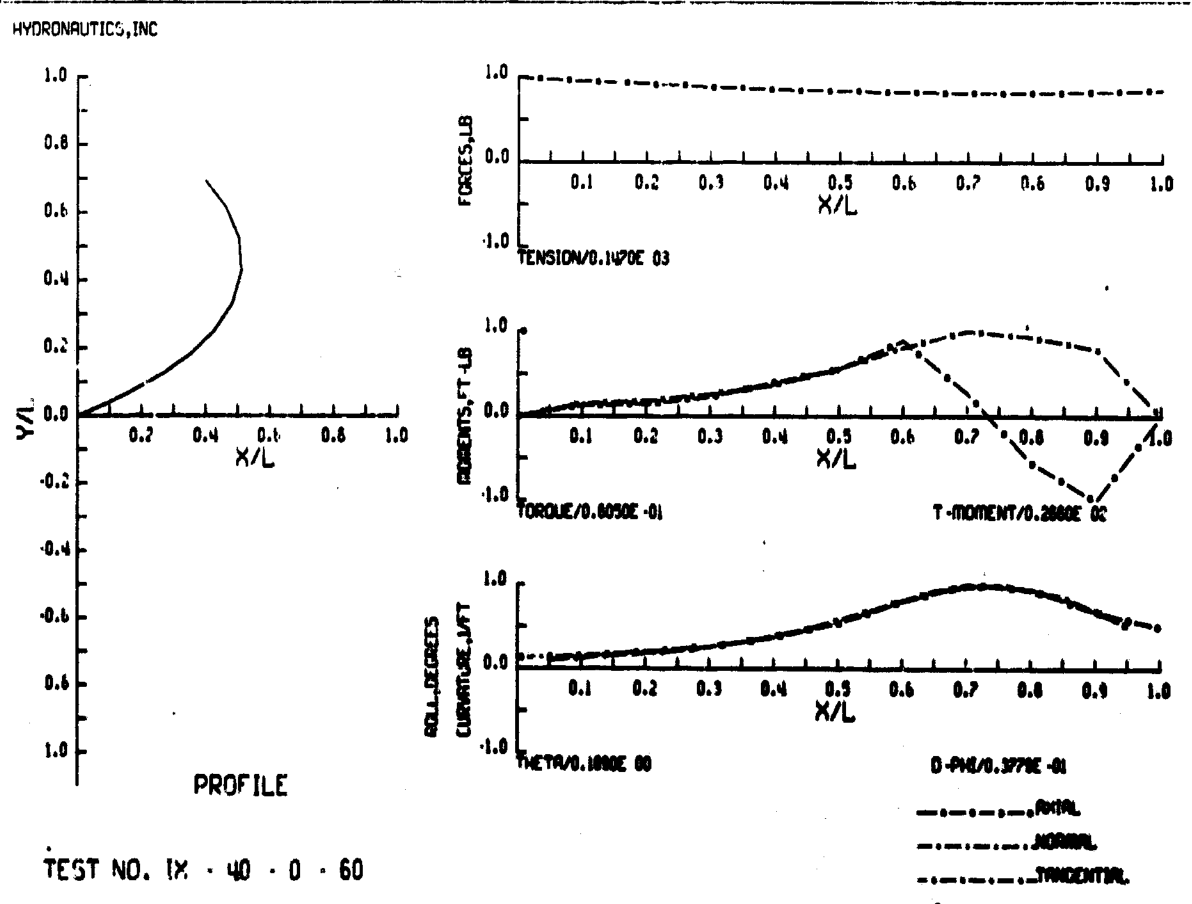
HYDRONAUTICS, INC
Y/L
X/L
PROFILE
FORCES, LB
TENSION/0.1470E 03
MOMENTS, FT-LB
TORQUE/0.6050E -01
T-MOMENT/0.2860E 02
ROLL, DEGREES
CURVATURE, 1/FT
THETA/0.1000E 00
D-PHI/0.3770E -01
AXIAL
NORMAL
TANGENTIAL
TEST NO. IX - 40 - 0 - 60

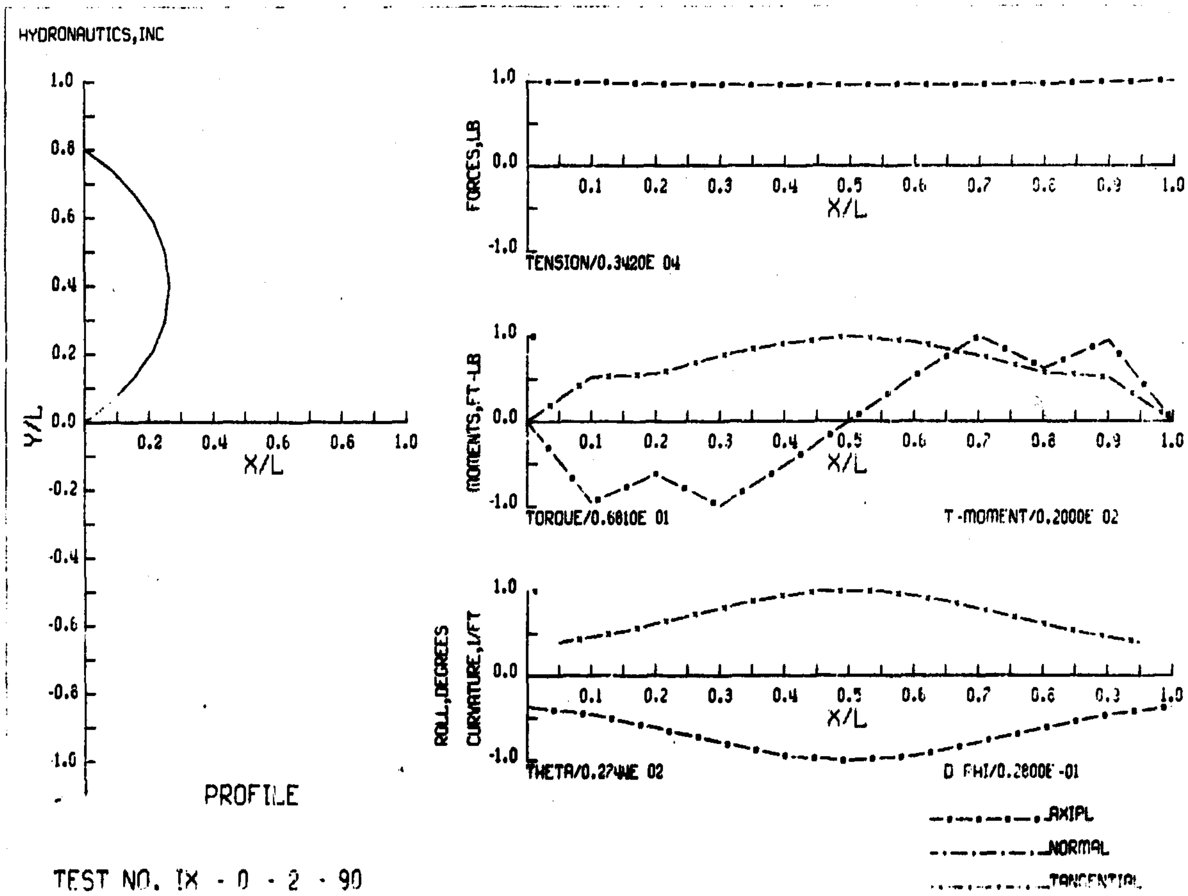
HYDRONAUTICS,INC
Y/L
X/L
PROFILE
FORCES,LB
TENSION/0.3420E 04
MOMENTS,FT-LB
TORQUE/0.6810E 01
T-MOMENT/0.2000E 02
ROLL,DEGREES
CURVATURE,1/FT
THETA/0.274E 02
D PHI/0.2800E -01
AXIAL
NORMAL
TANGENTIAL
TEST NO. IX - 0 - 2 - 90

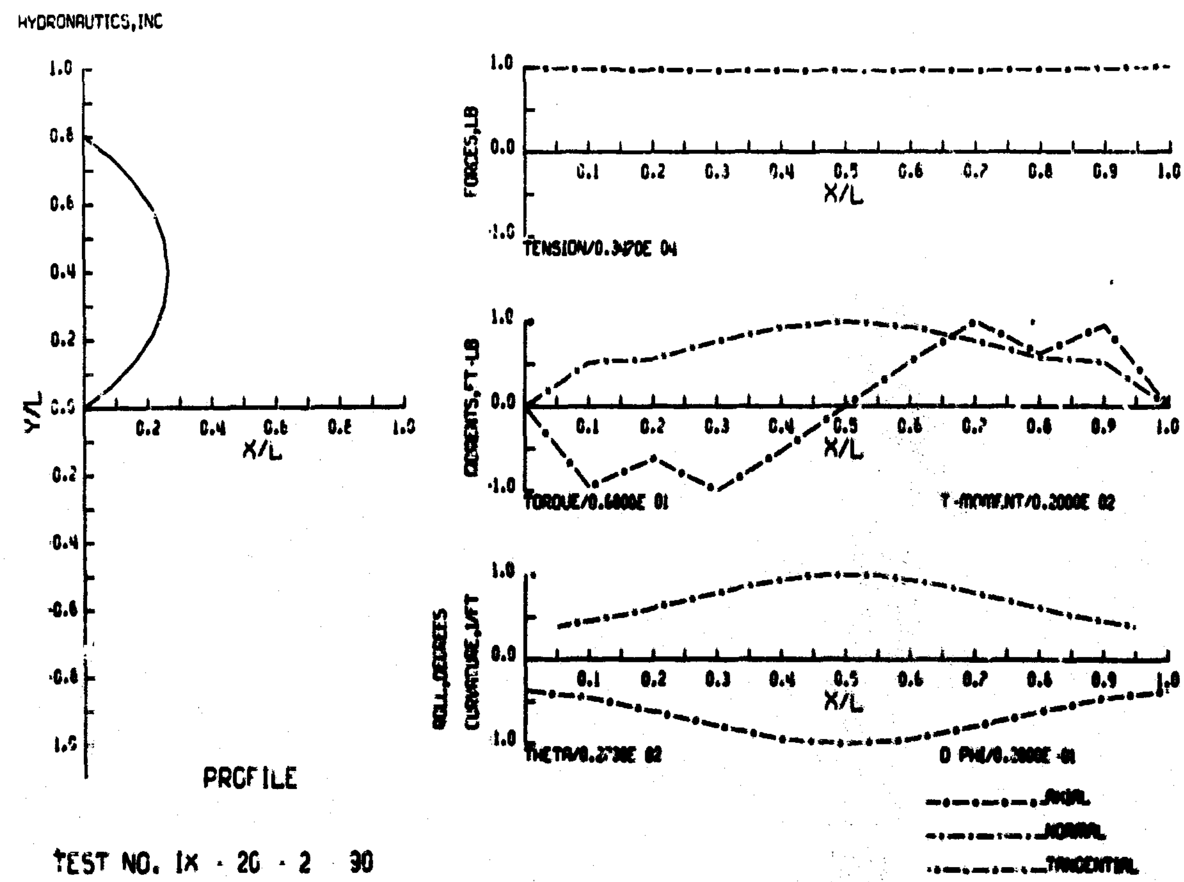
HYDRONAUTICS,INC
Y/L
X/L
PROFILE
FORCES,LB
TENSION/0.3420E 04
MOMENTS,FT-LB
TORQUE/0.6800E 01
T-MOMENT/0.2000E 02
ROLL,DEGREES
CURVATURE,1/FT
D PHI/0.2800E -01
AXIAL
NORMAL
TANGENTIAL
TEST NO. IX - 20 - 2 - 90

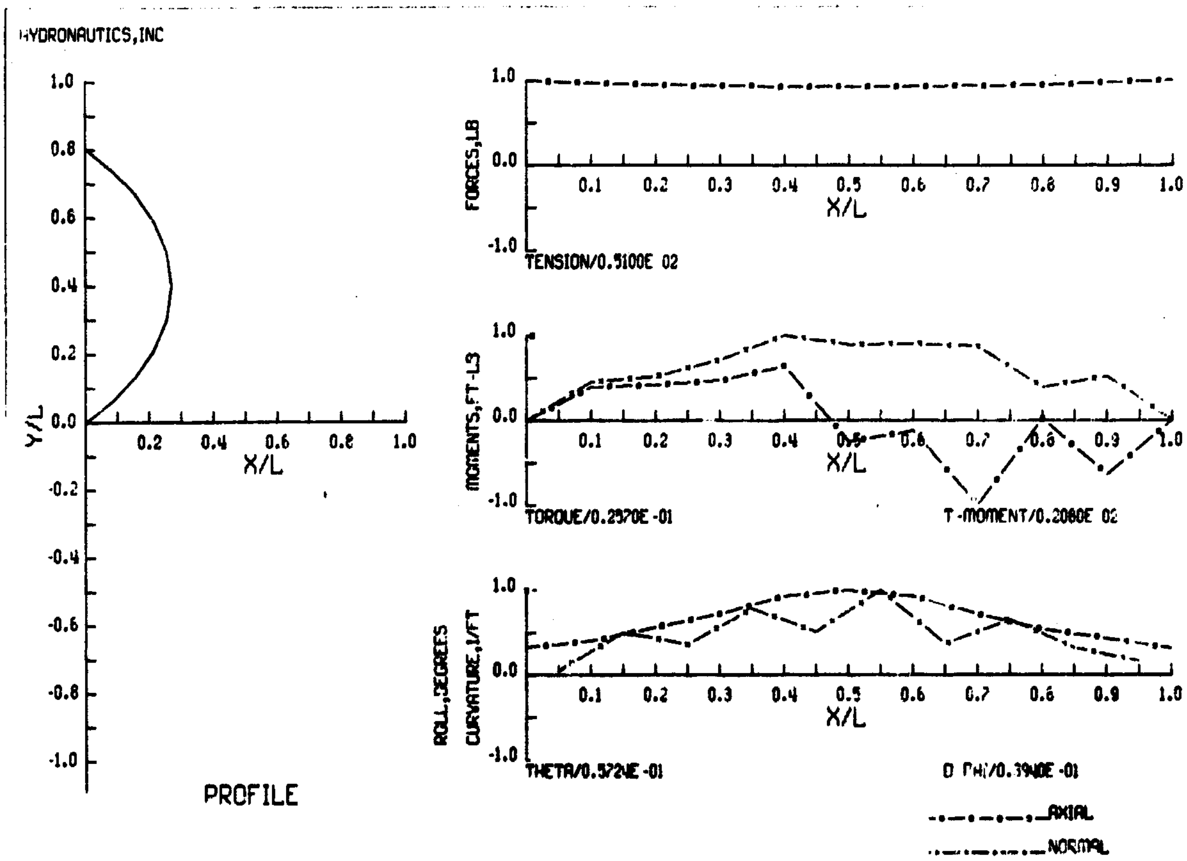

TEST NO. IX - 22 - 0 - 90

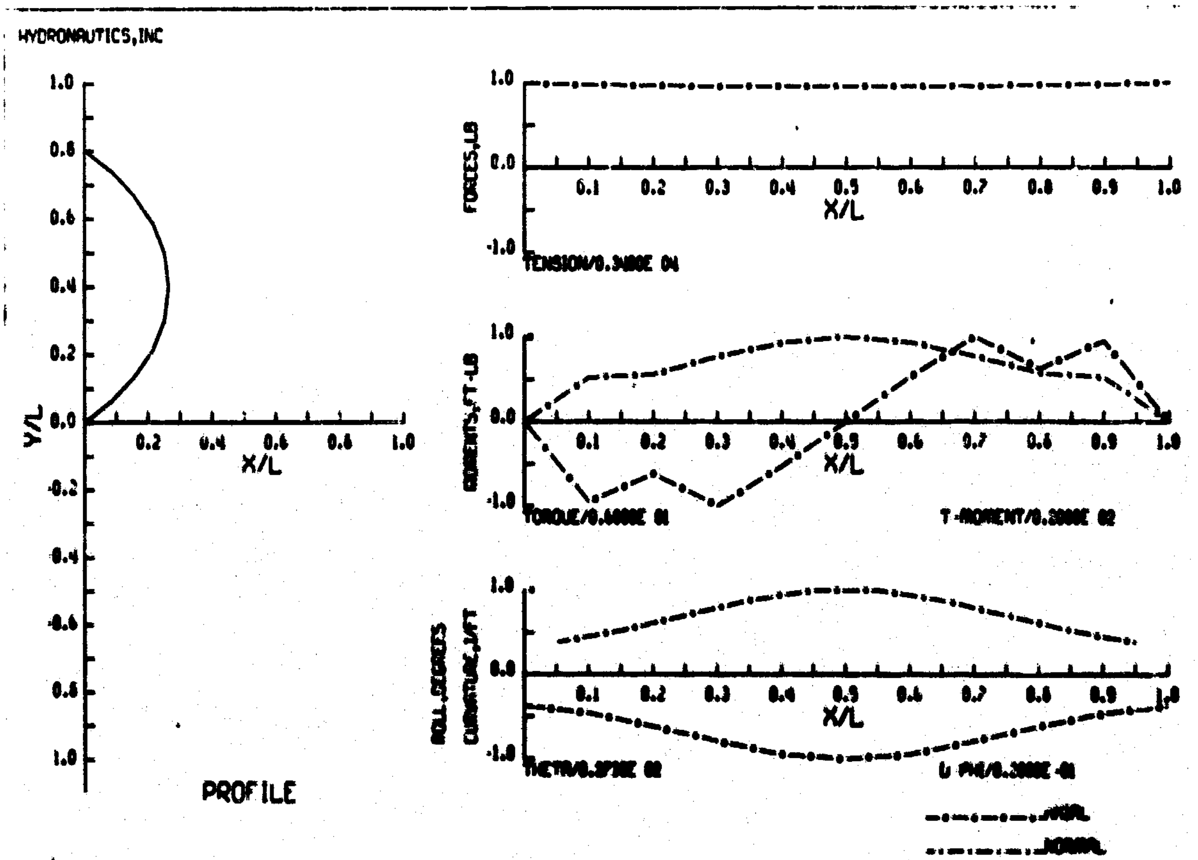

TEST NO. IX - 22 - 2 - 90

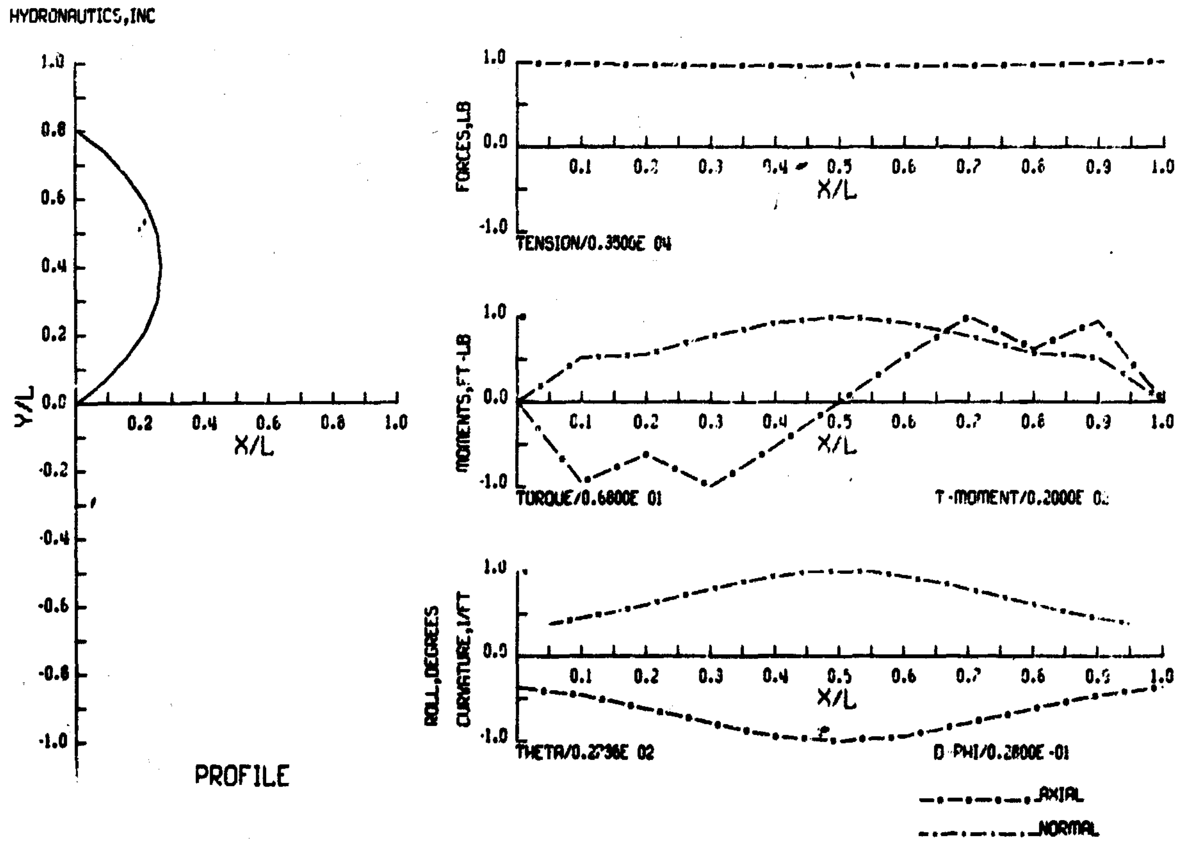

TEST NO. IX - 26 - 2 - 90

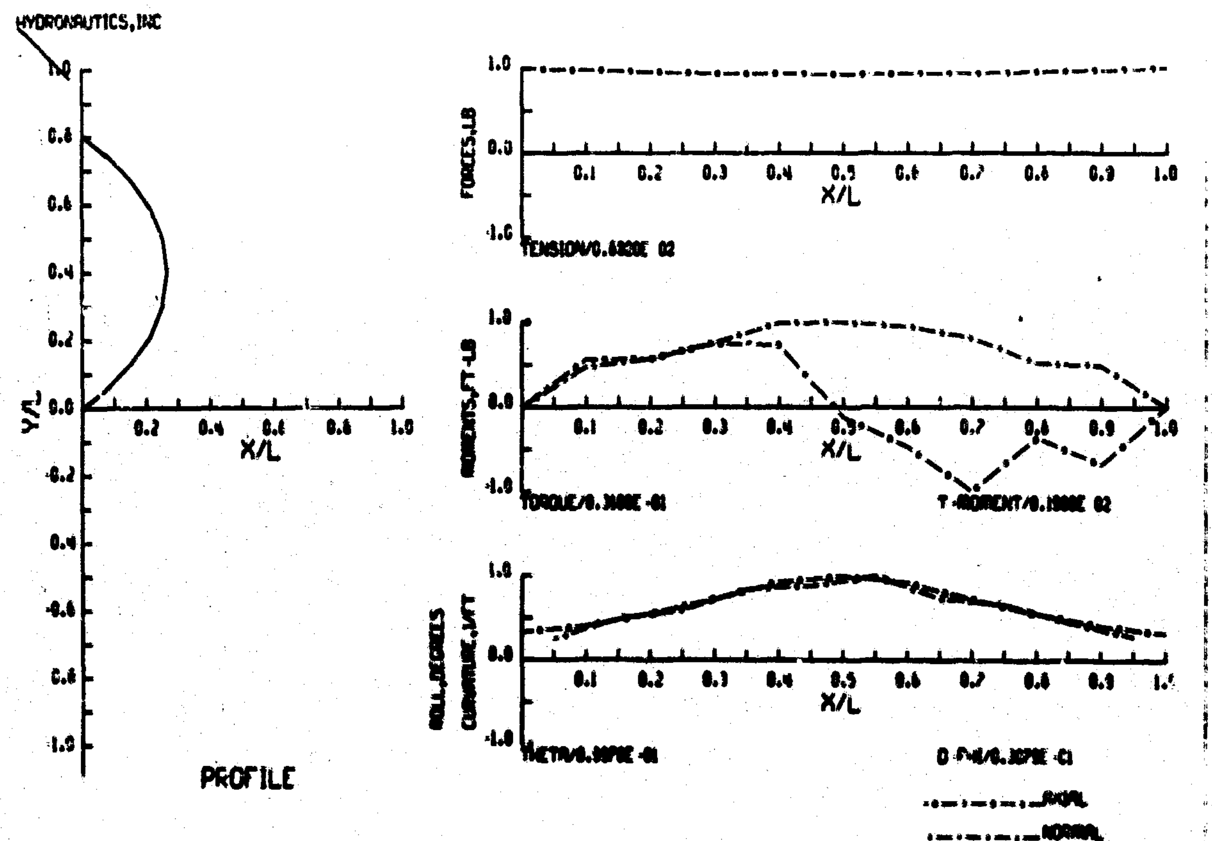

TEST NO. IX - 29 - 0 - 90

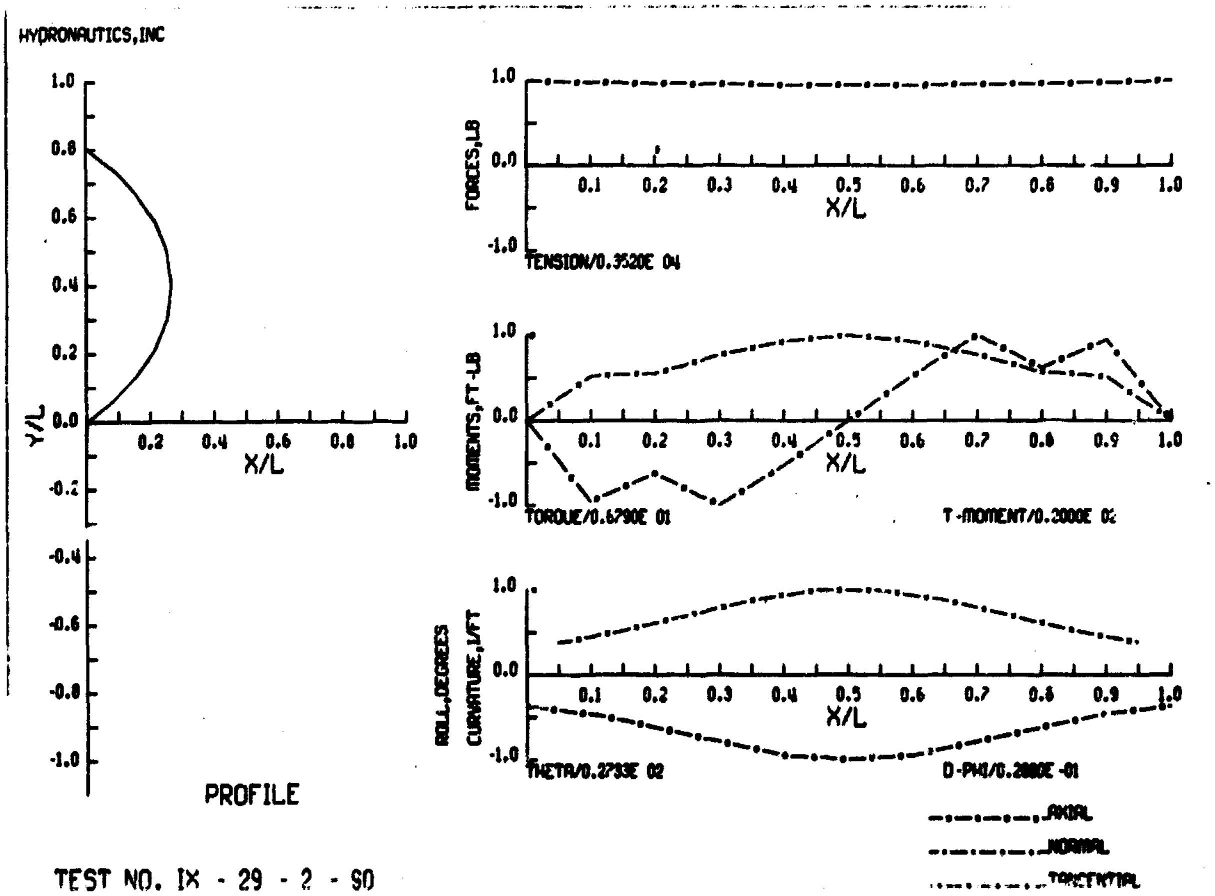

TEST NO. IX - 29 - 2 - 90

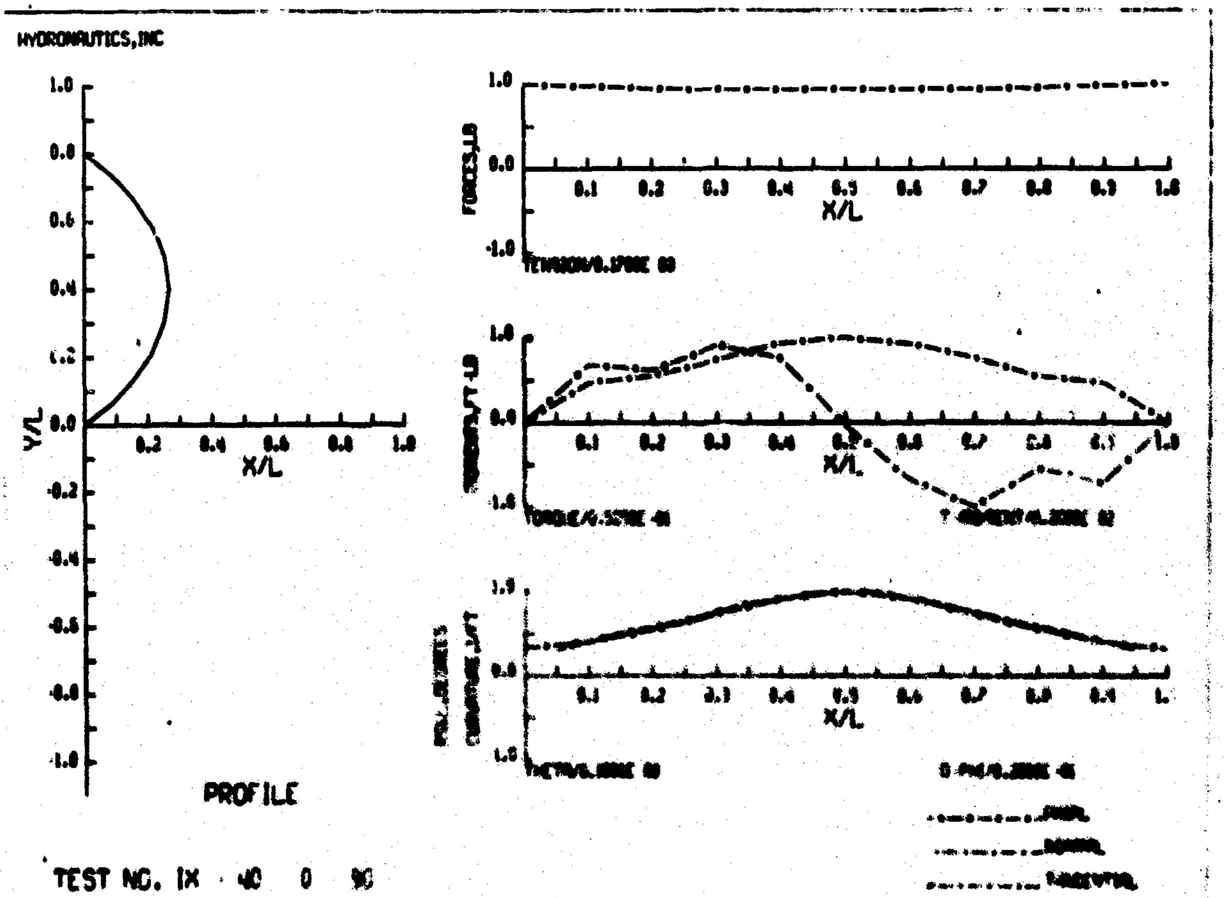

TEST NO. IX - 40 - 0 - 90

HYDRONAUTICS,INC

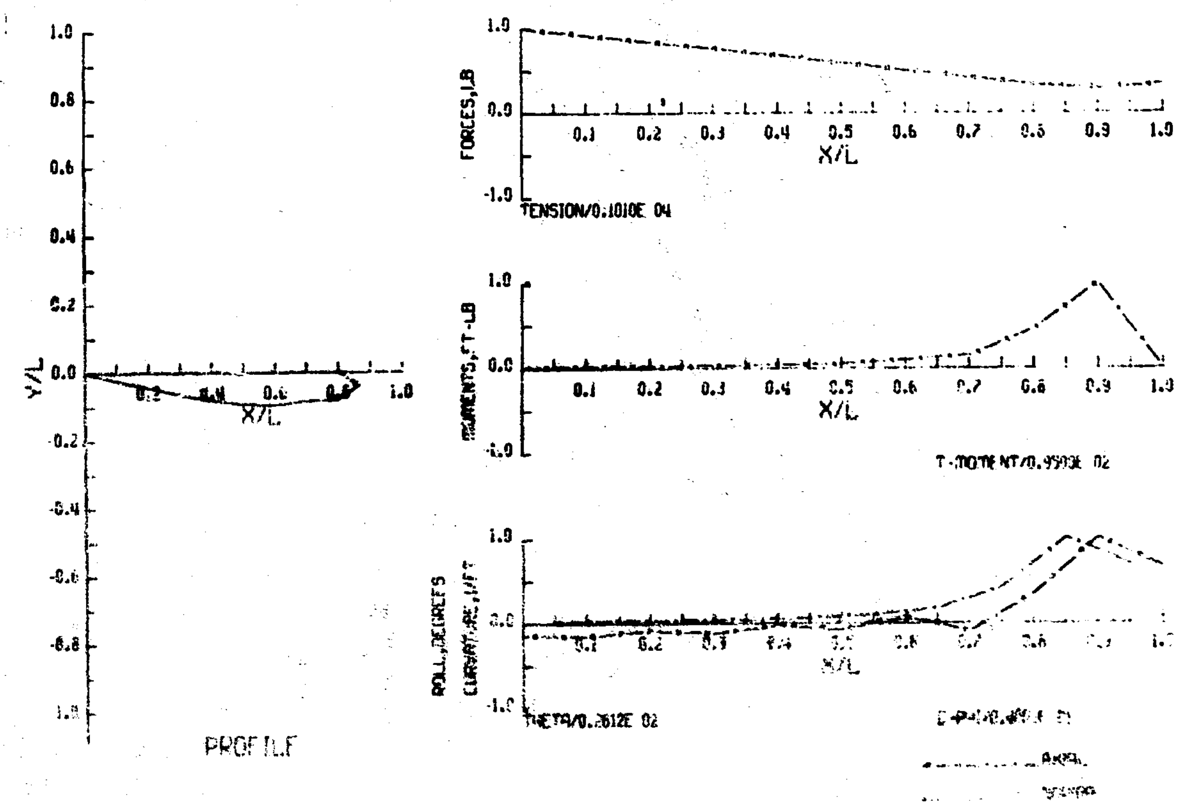

TEST NO. X - 0 - 2 - 0

HYDRONAUTICS,INC

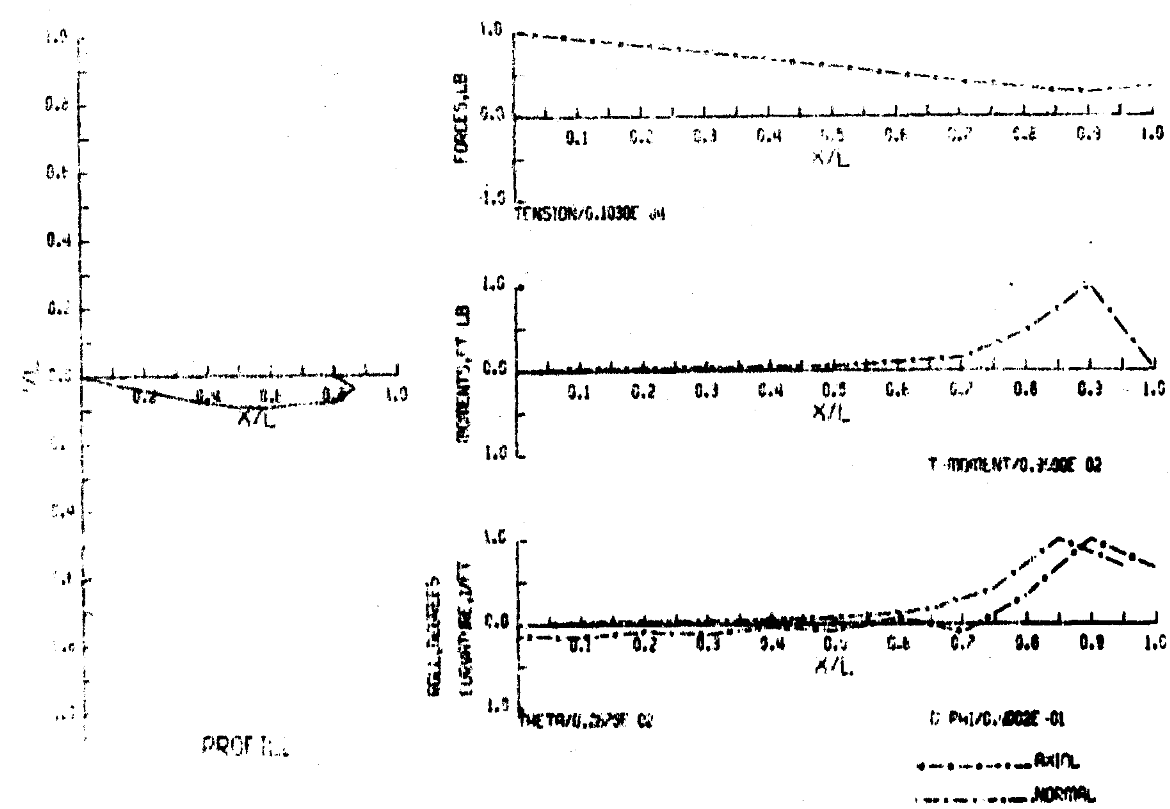

TEST NO. X

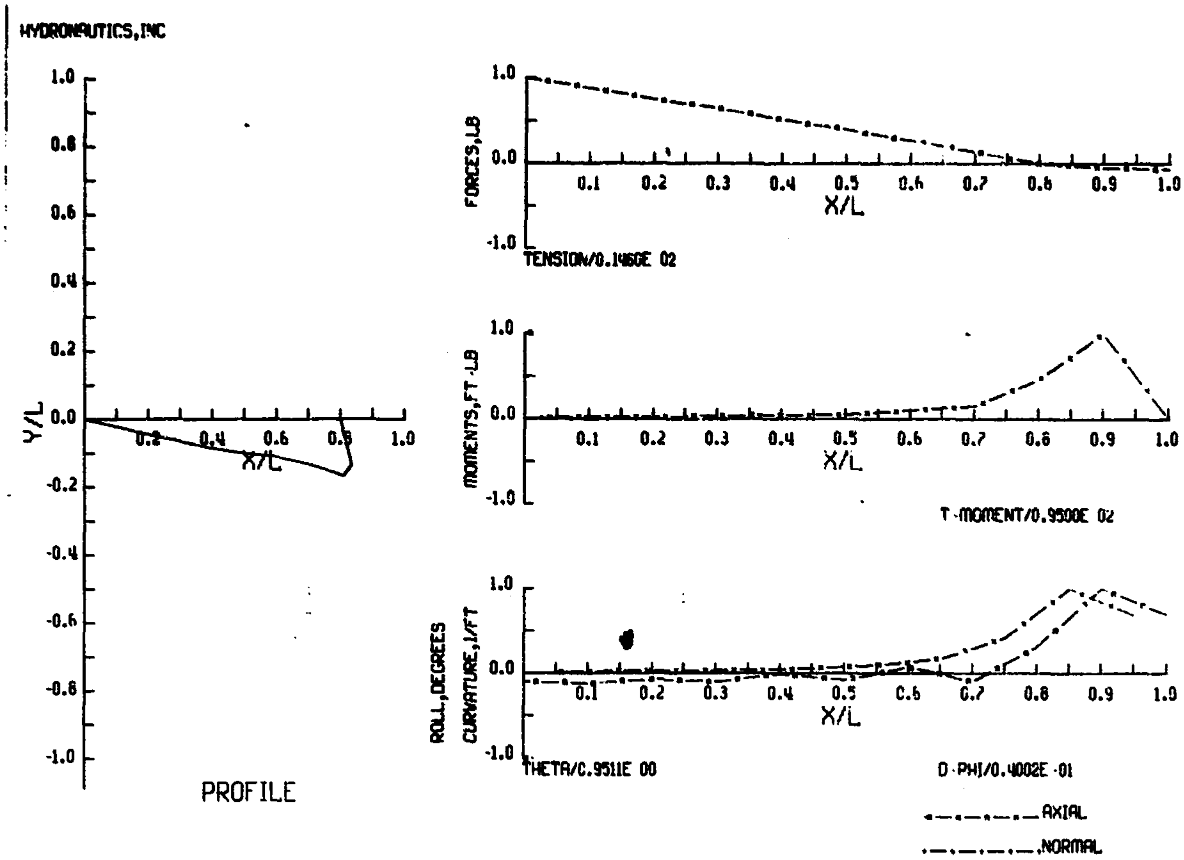

TEST NO. X - 22 - 0 - 0

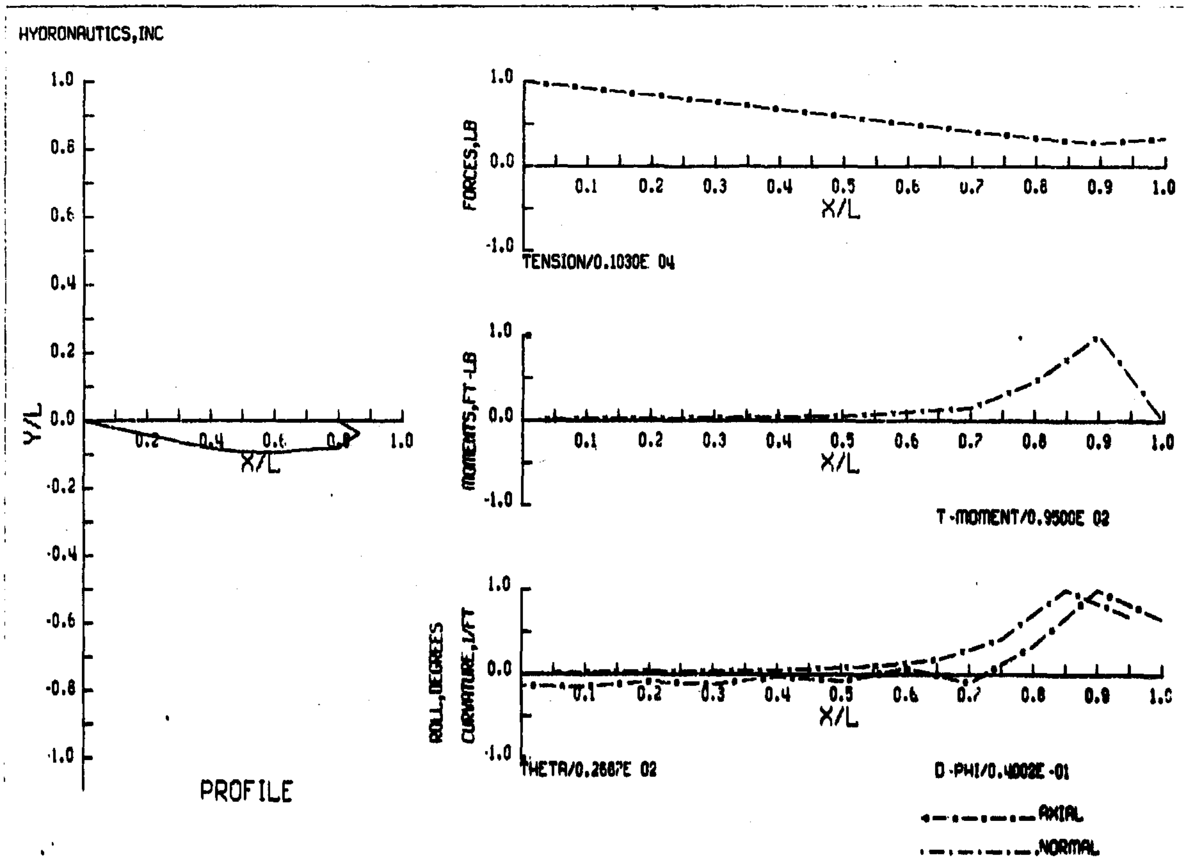

TEST NO. X - 22 - 2 - 0

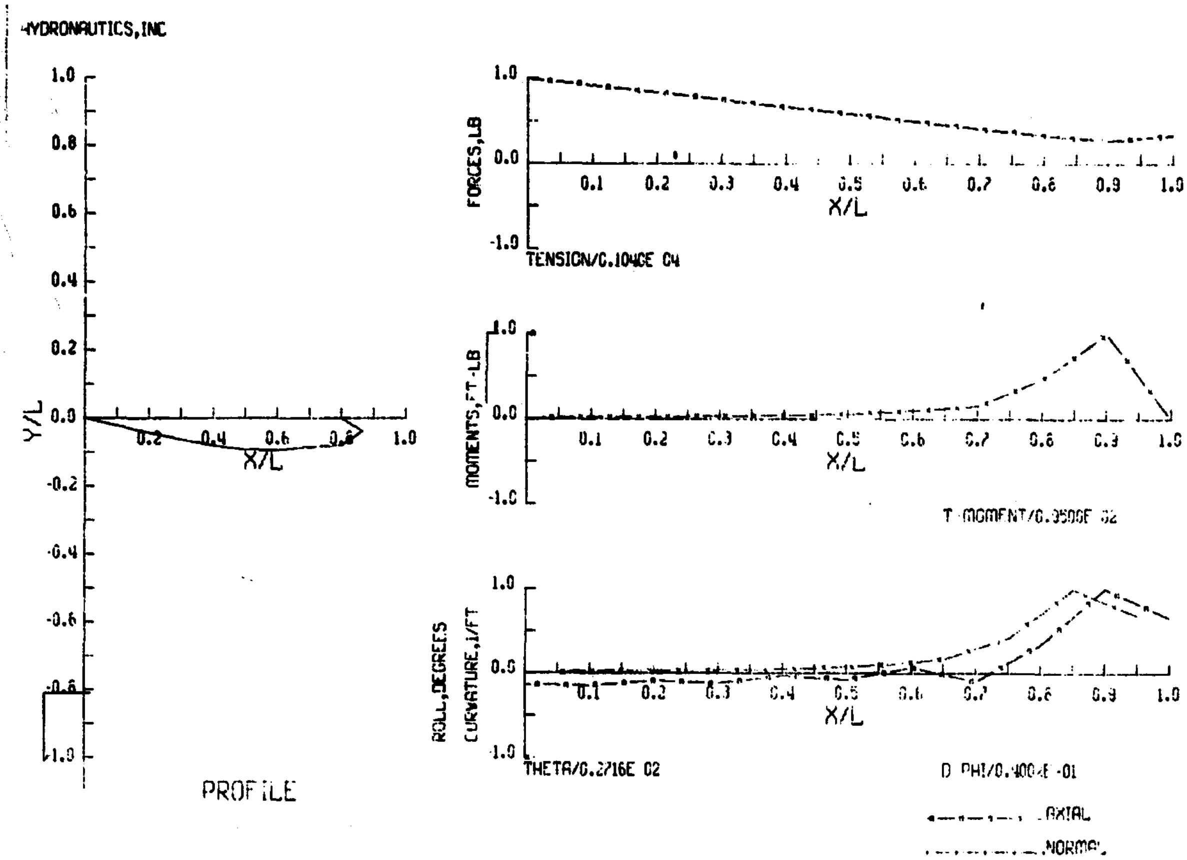

TEST NO. X - 26 - 2 - 0

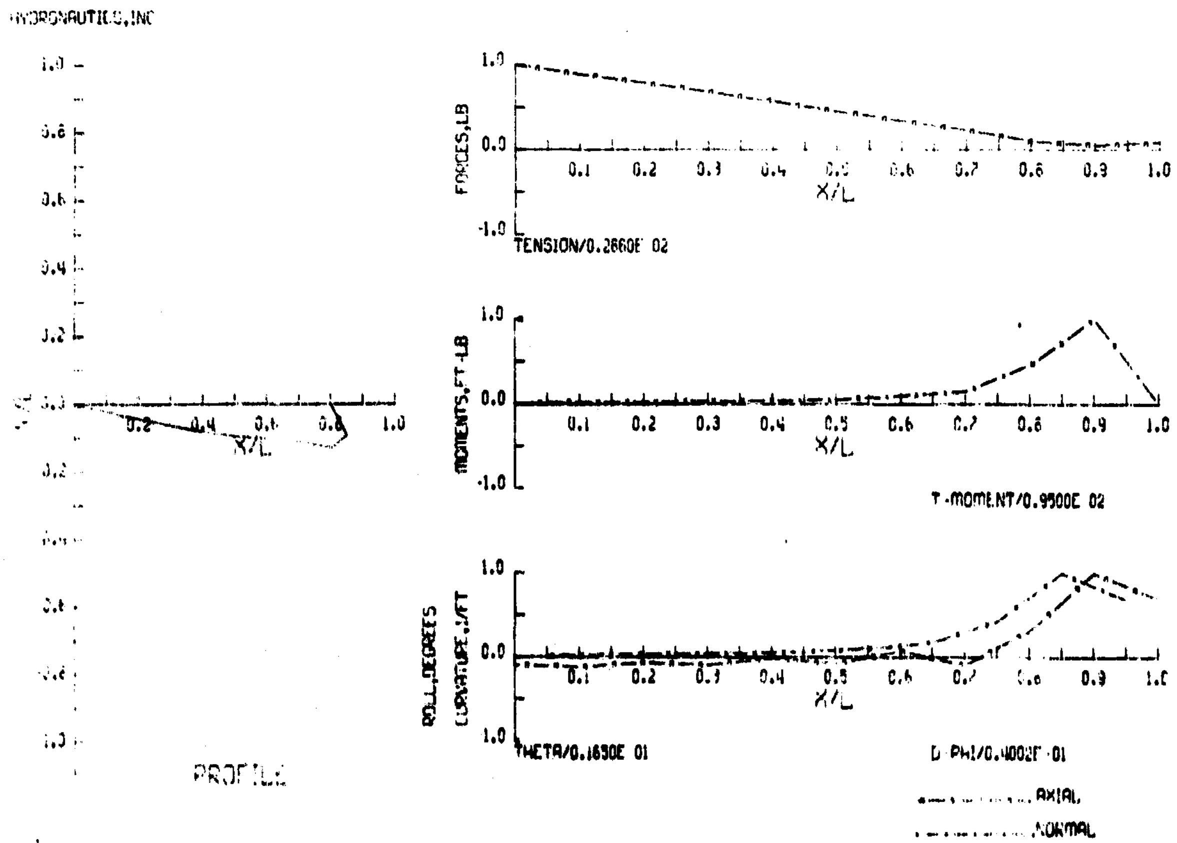

TEST NO. X - 29 - 0 - 0

HYDRONAUTICS,INC

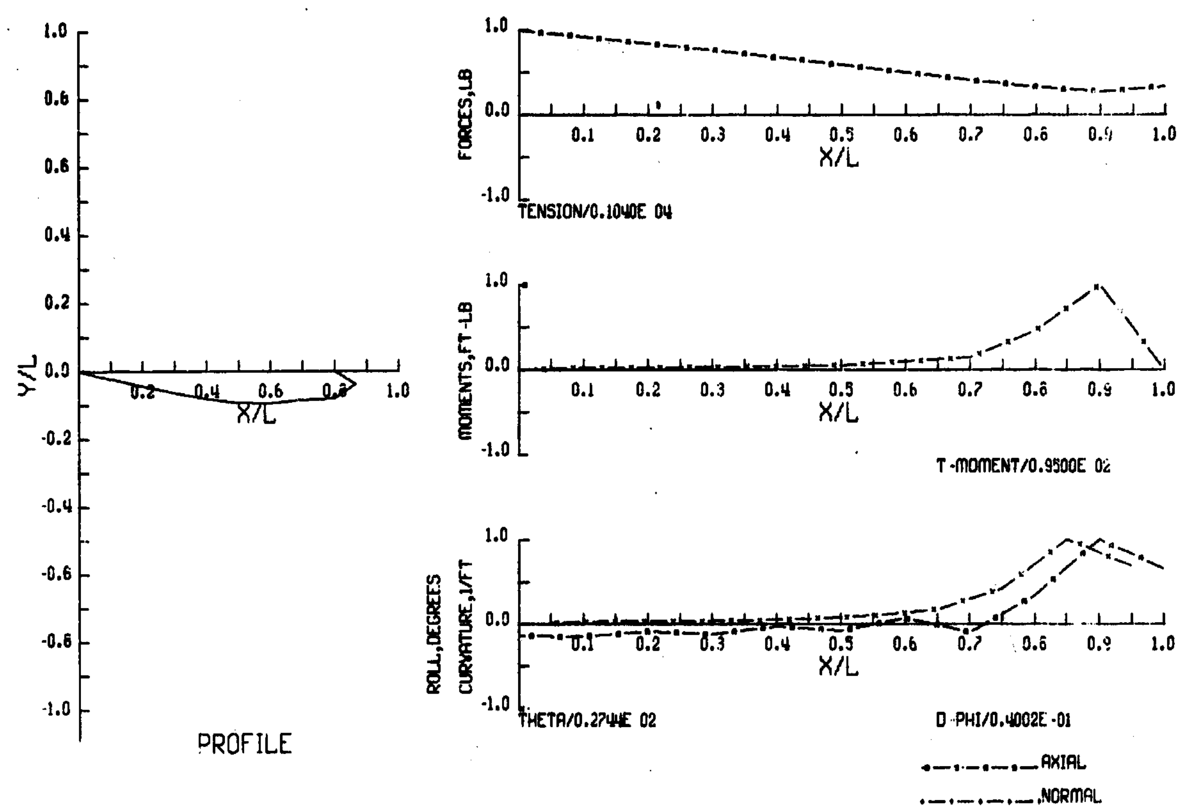

TEST NO. X -29 - 2 - 0

HYDRONAUTICS,INC

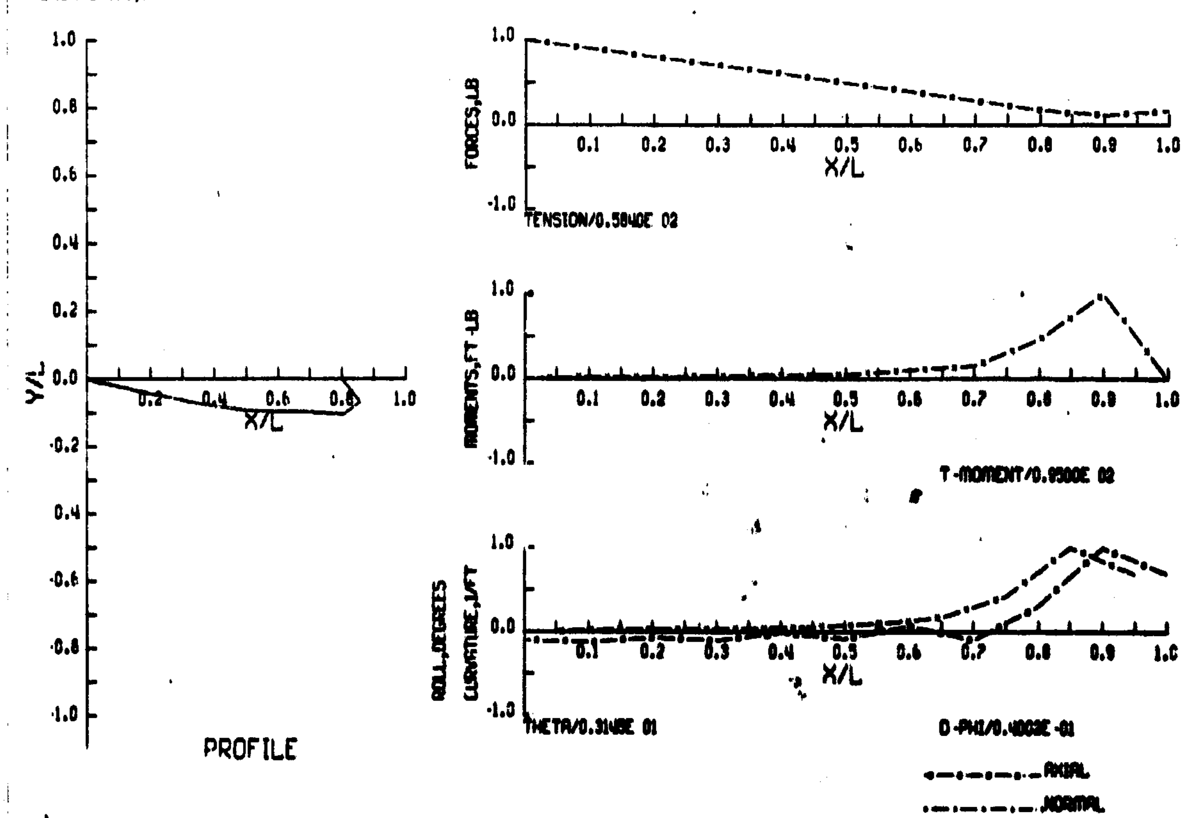

TEST NO. X - 40 - 0 - 0

HYDRONAUTICS,INC

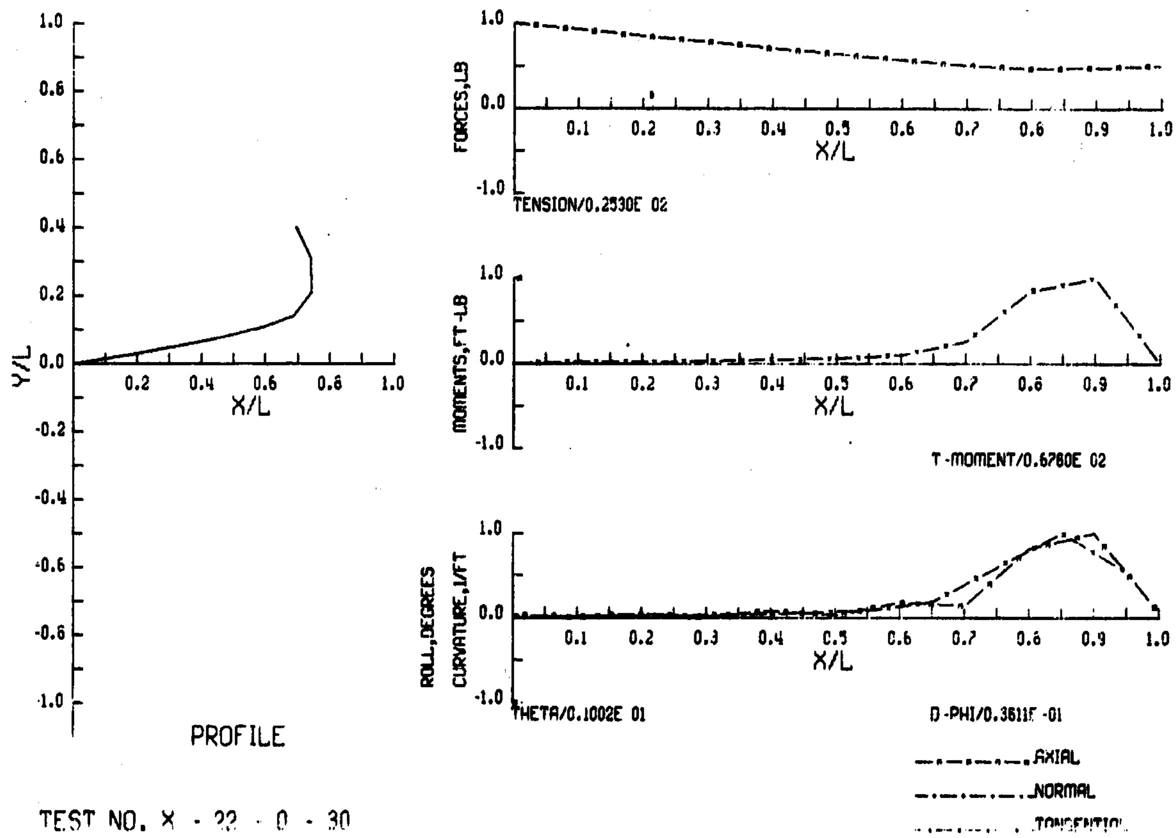

TEST NO. X - 22 - 0 - 30

HYDRONAUTICS,INC

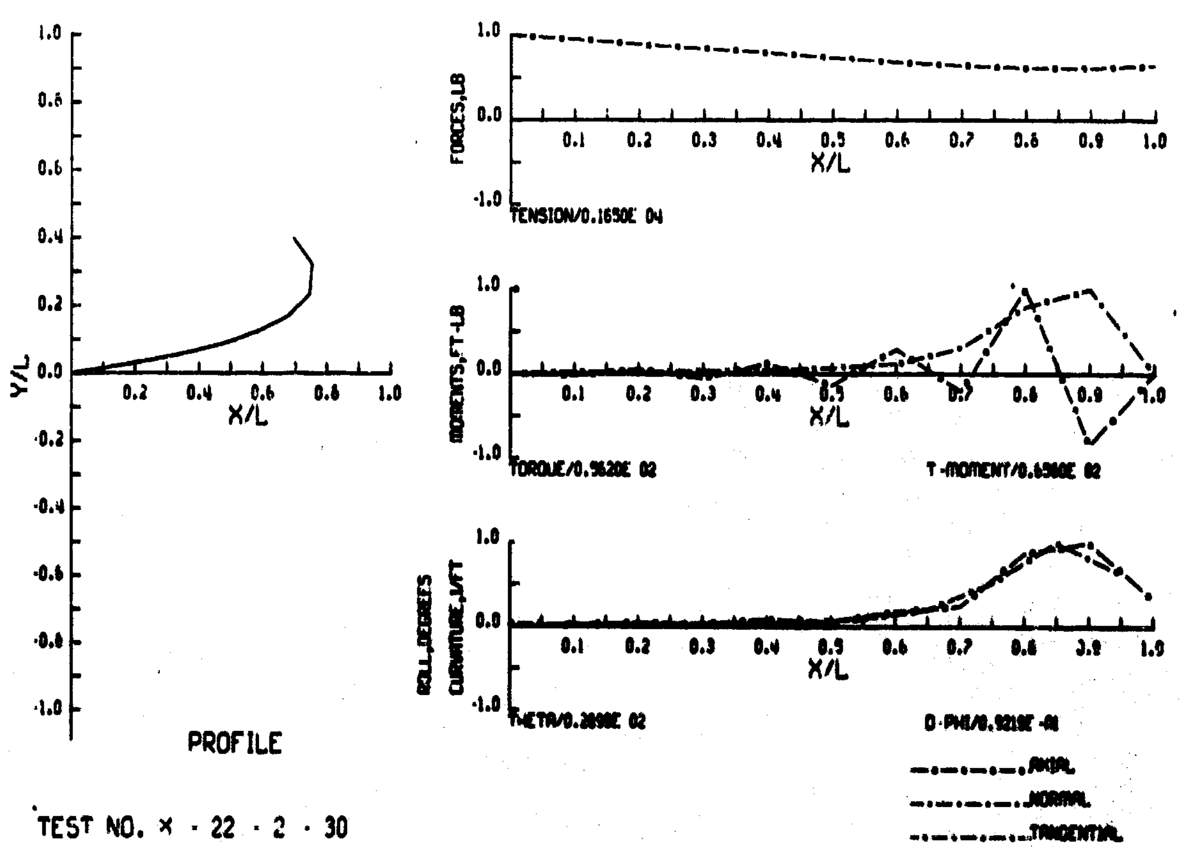

TEST NO. X - 22 - 2 - 30

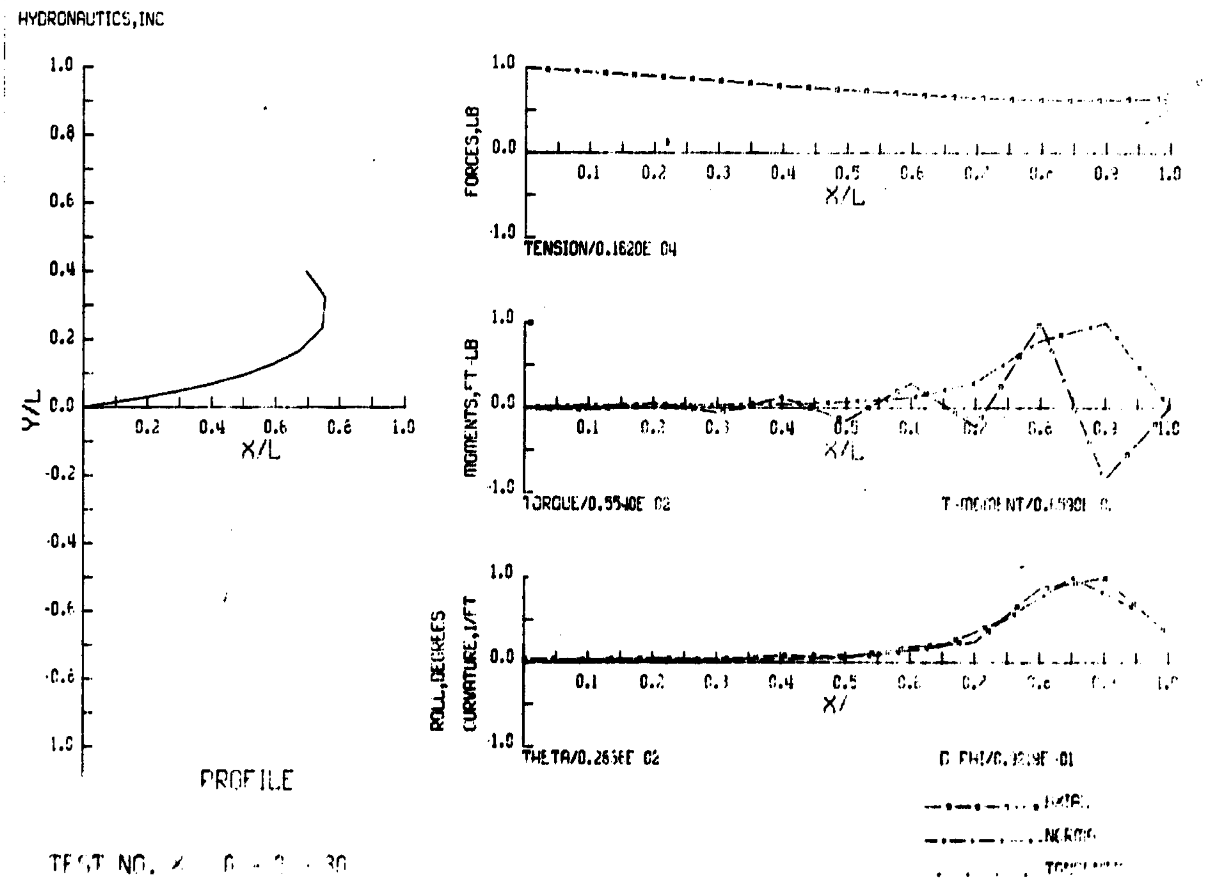
HYDRONAUTICS,INC
Y/L
X/L
PROFILE
FORCES,LB
TENSION/0.1620E 04
MOMENTS,FT-LB
TORQUE/0.5540E 02
ROLL,DEGREES
CURVATURE,1/FT
THETA/0.2656E 02

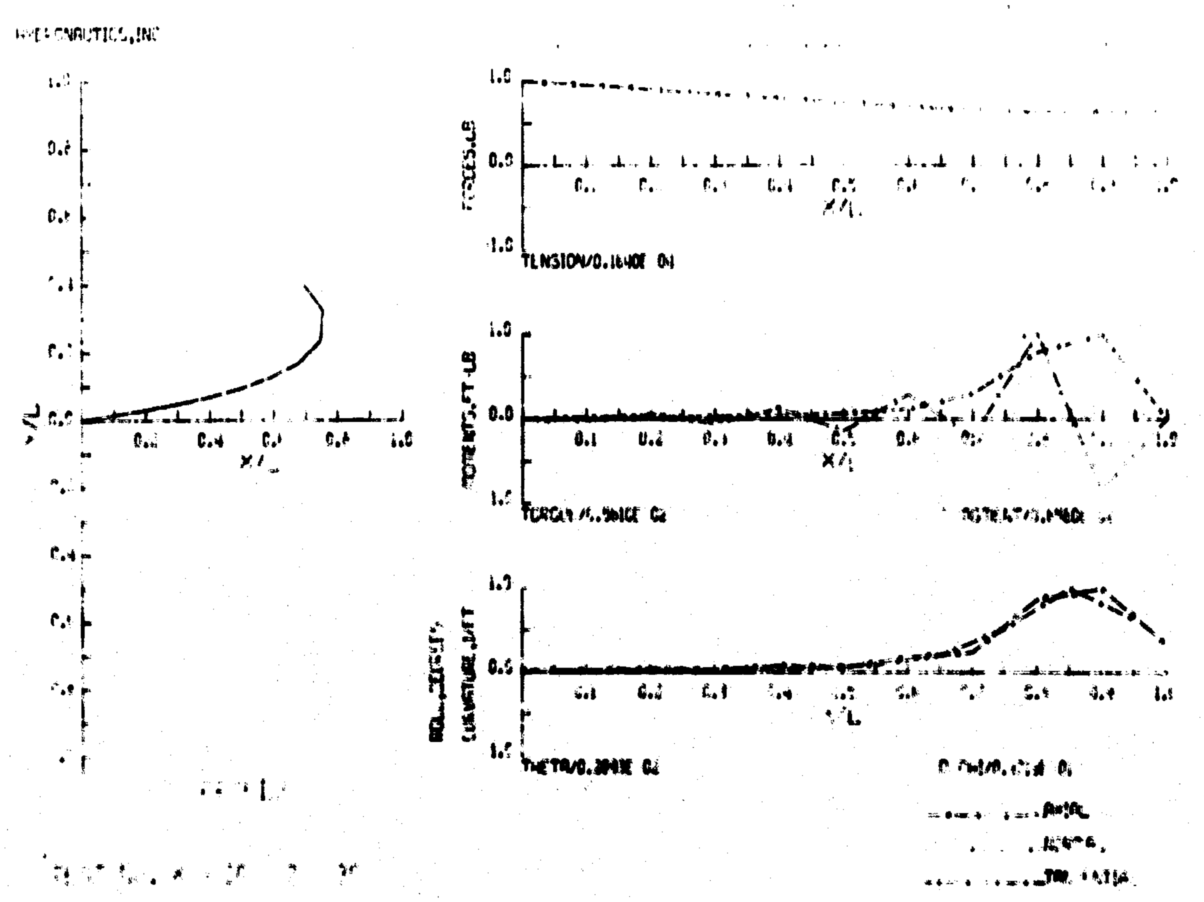
HYDRONAUTICS,INC
TENSION/0.1640E 04

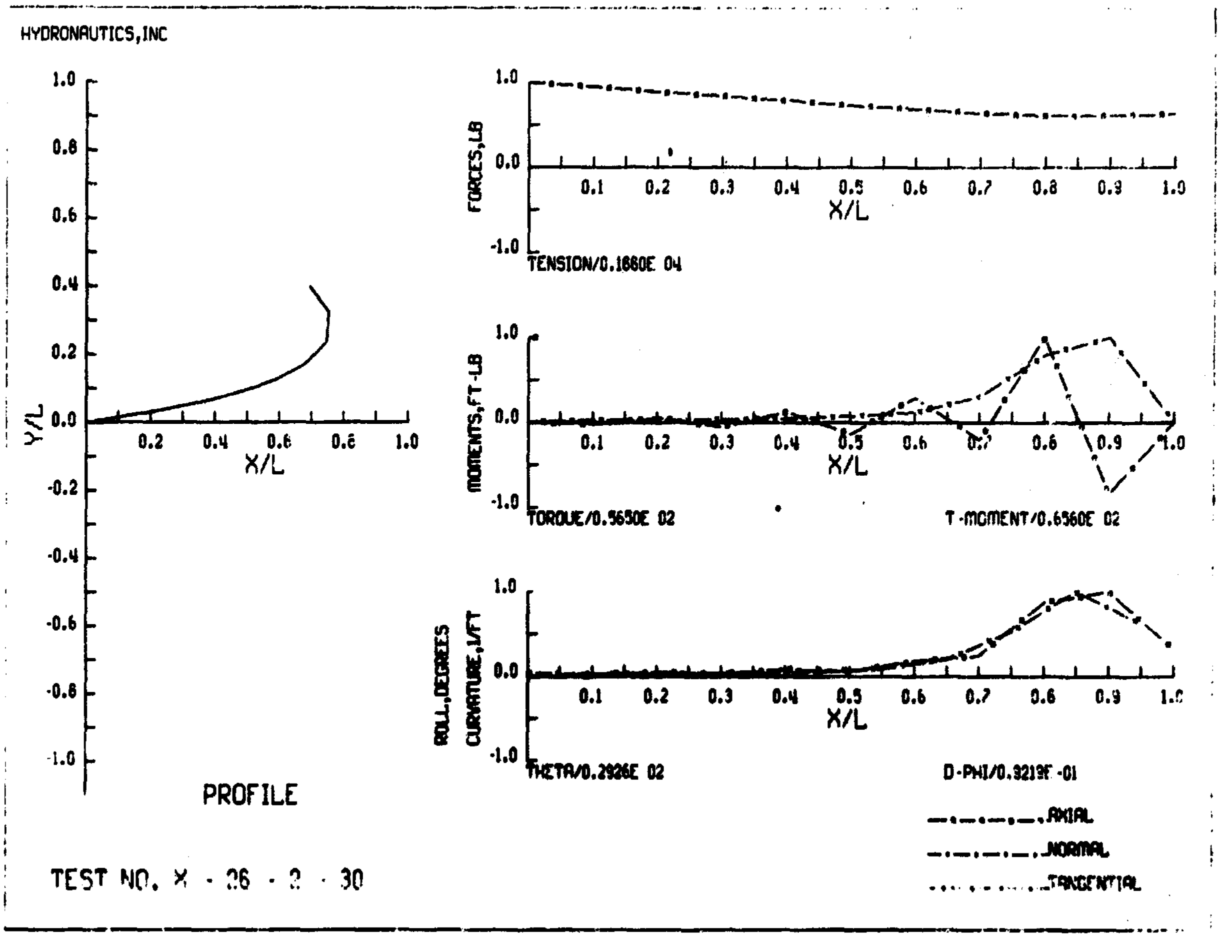
HYDRONAUTICS,INC
Y/L
X/L
PROFILE
TEST NO. X - 26 - 2 - 30
FORCES,LB
TENSION/0.1660E 04
MOMENTS,FT-LB
TORQUE/0.5650E 02
T-MOMENT/0.6560E 02
ROLL,DEGREES
CURVATURE,1/FT
THETA/0.2926E 02
AXIAL
NORMAL
TANGENTIAL

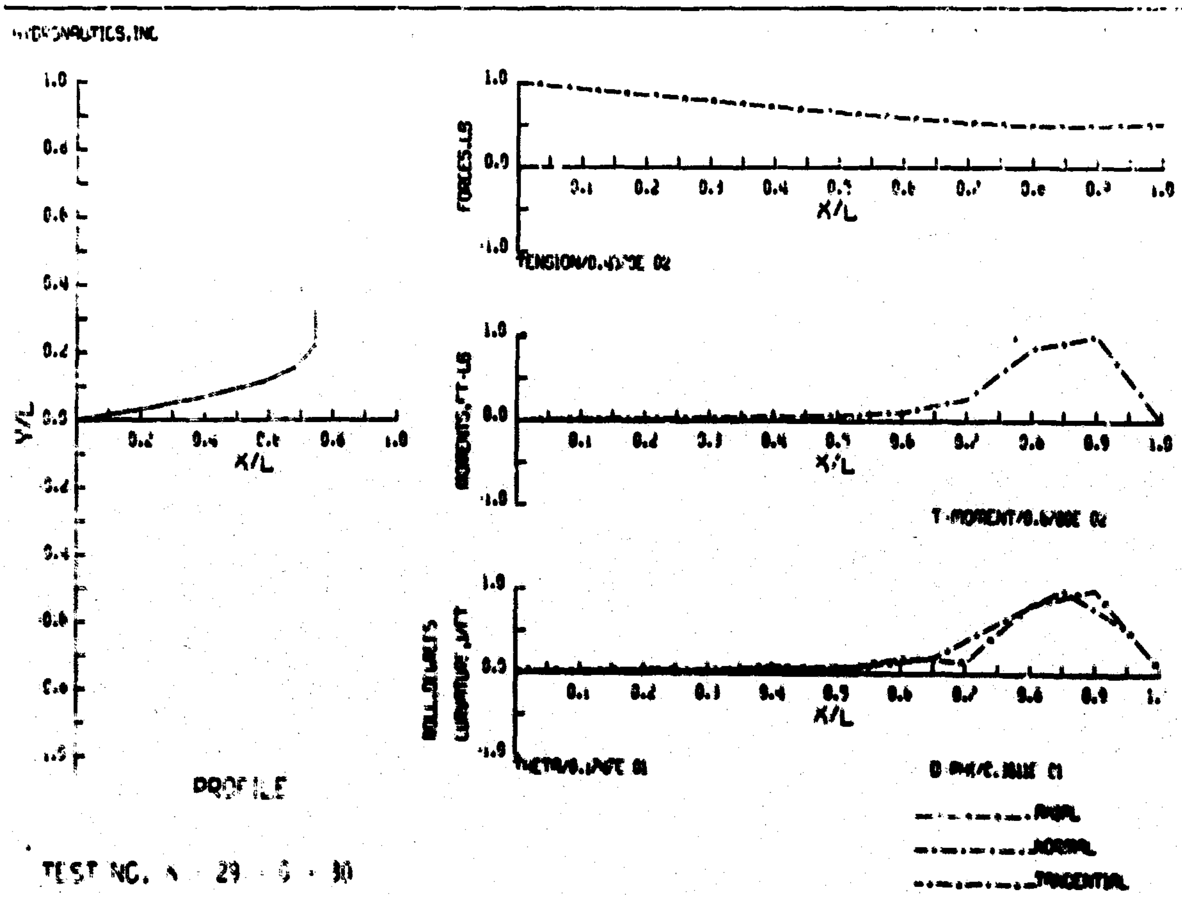
Y/L
X/L
FORCES,LB
MOMENTS,FT-LB
T-MOMENT
AXIAL
NORMAL
TANGENTIAL

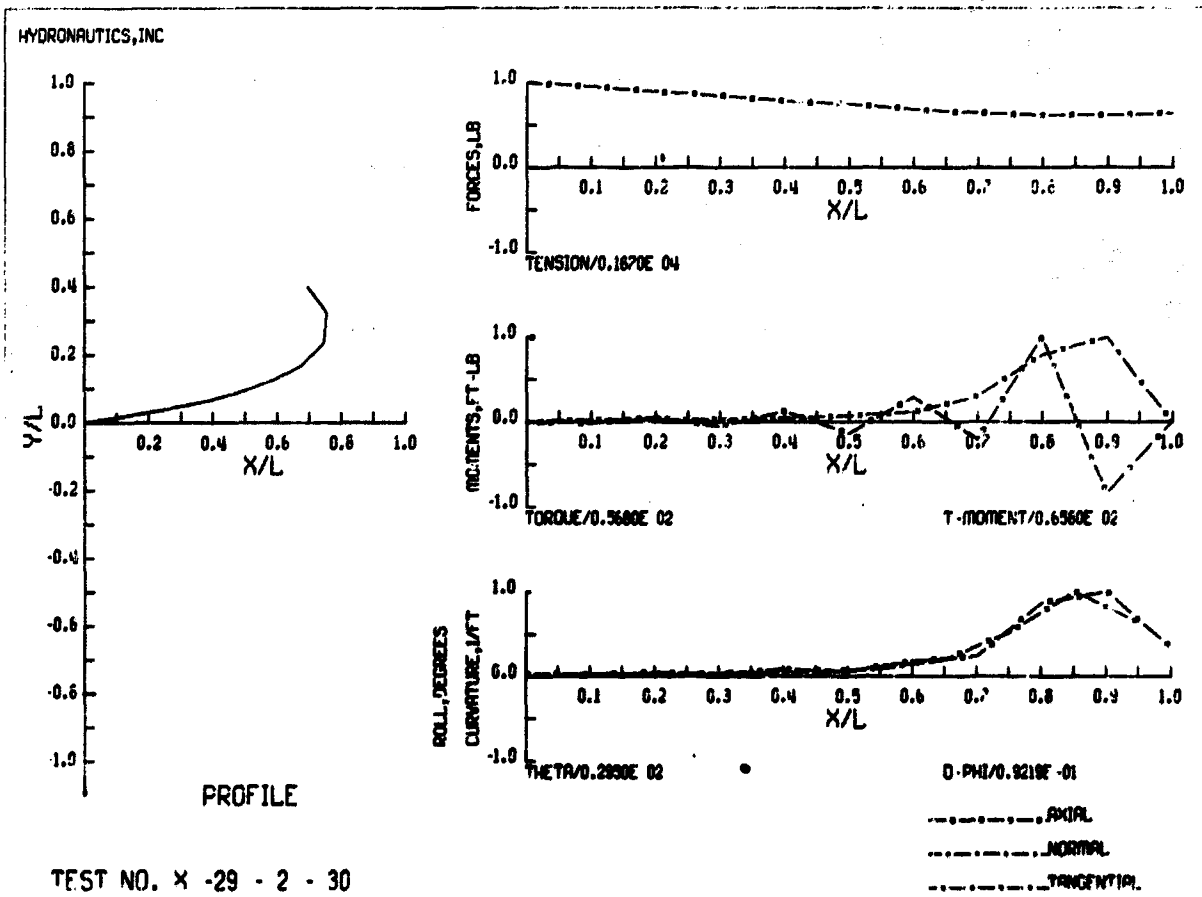
HYDRONAUTICS,INC
Y/L
X/L
PROFILE
FORCES,LB
TENSION/0.1670E 04
MOMENTS,FT-LB
TORQUE/0.5680E 02
T-MOMENT/0.6560E 02
ROLL,DEGREES
CURVATURE,1/FT
THETA/0.2930E 02
D-PHI/0.9219E -01
AXIAL
NORMAL
TANGENTIAL
TEST NO. X -29 - 2 - 30

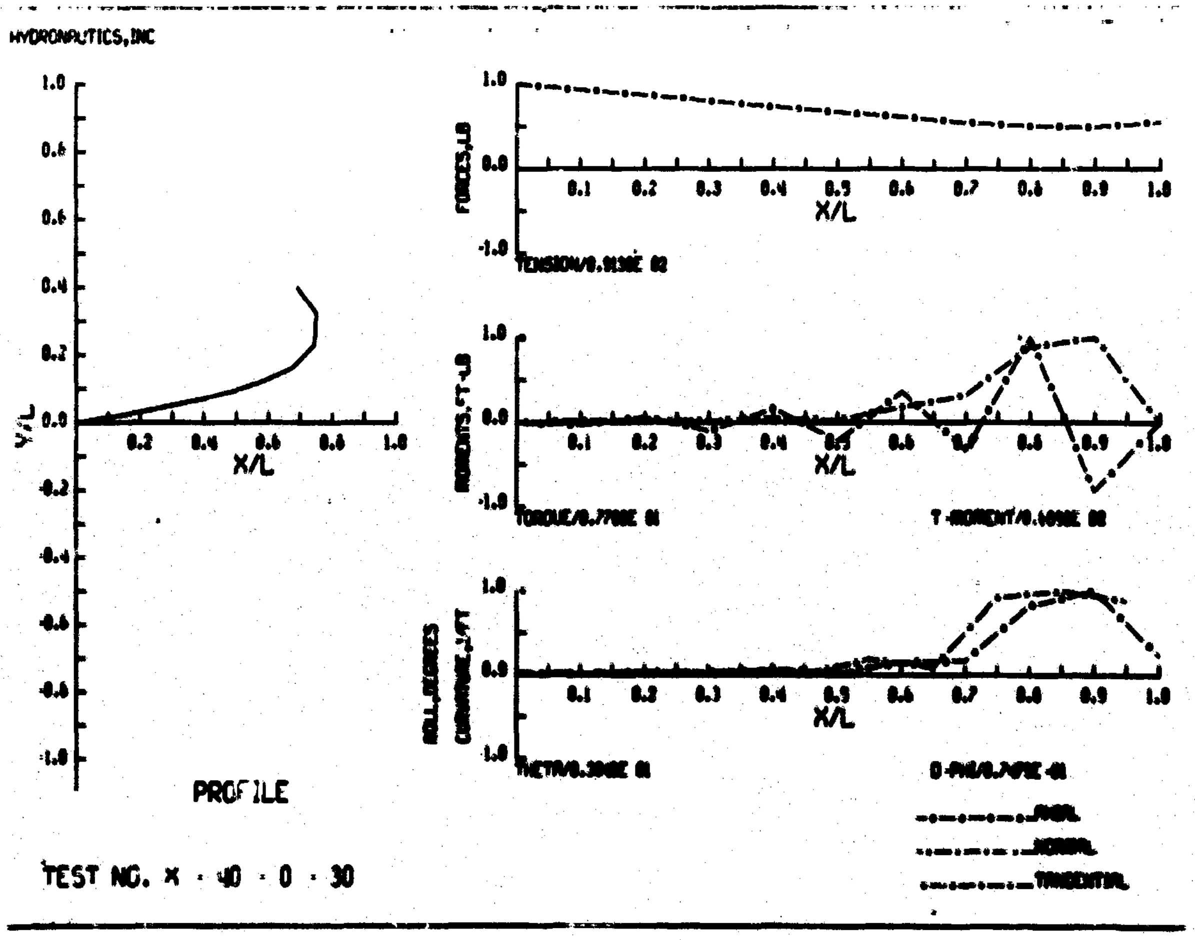
HYDRONAUTICS,INC
Y/L
X/L
PROFILE
FORCES,LB
MOMENTS,FT-LB
ROLL,DEGREES
CURVATURE,1/FT
AXIAL
NORMAL
TANGENTIAL
TEST NO. X - 40 - 0 - 30

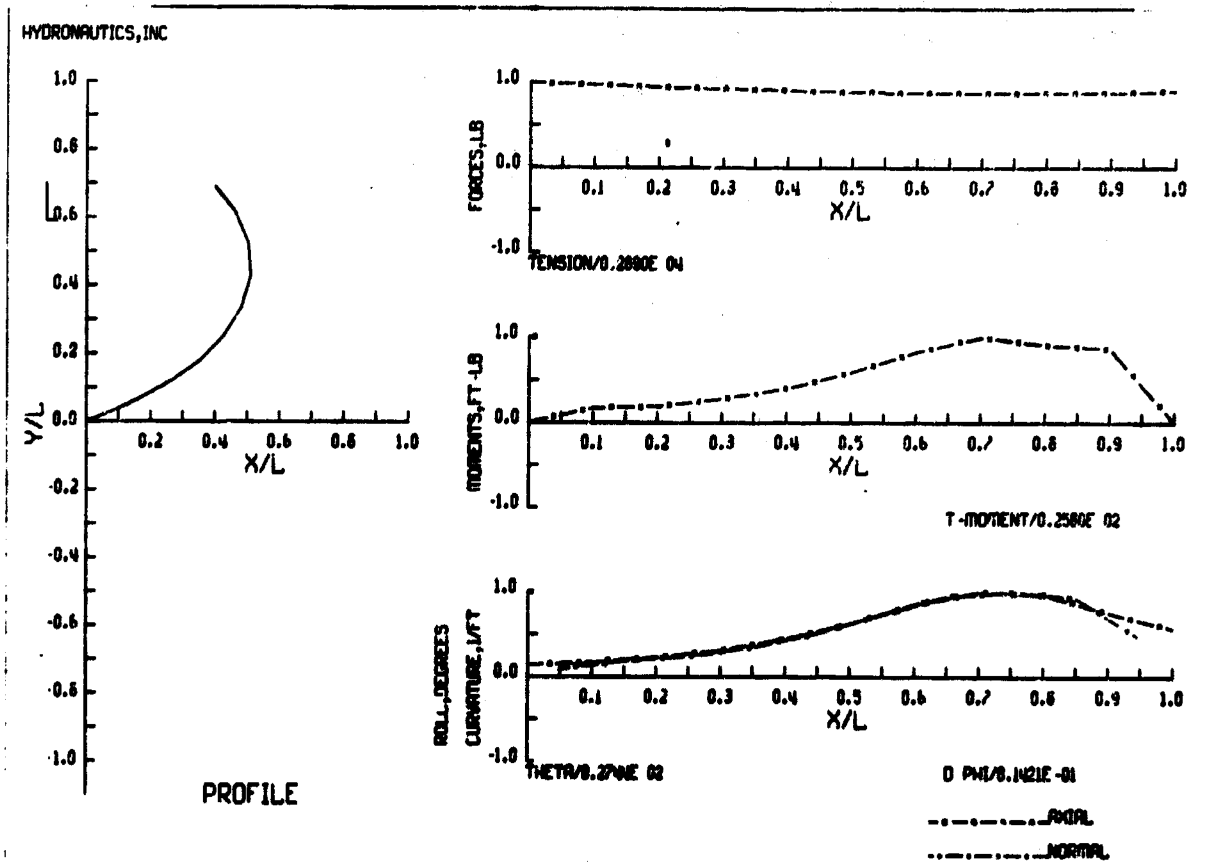

TEST NO. X - 0 - 2 - 60

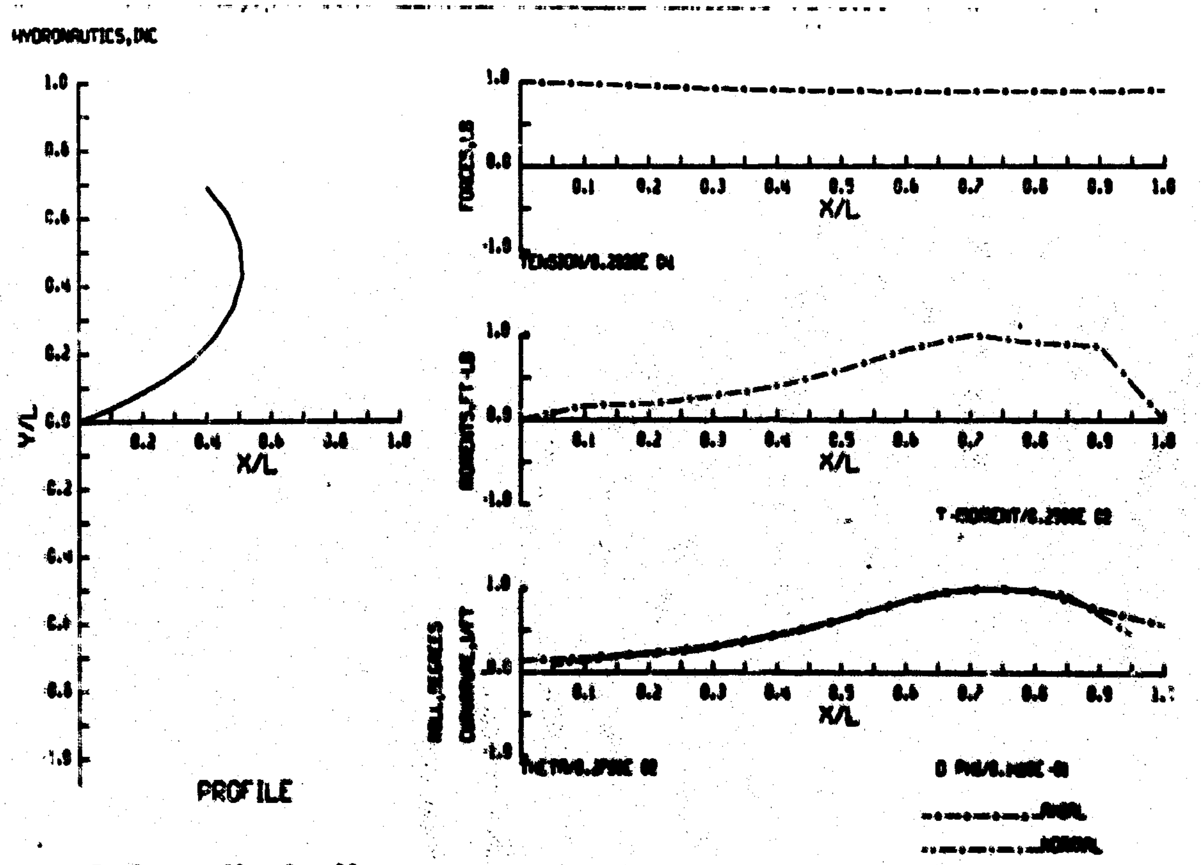

TEST NO. X - 20 - 2 - 60

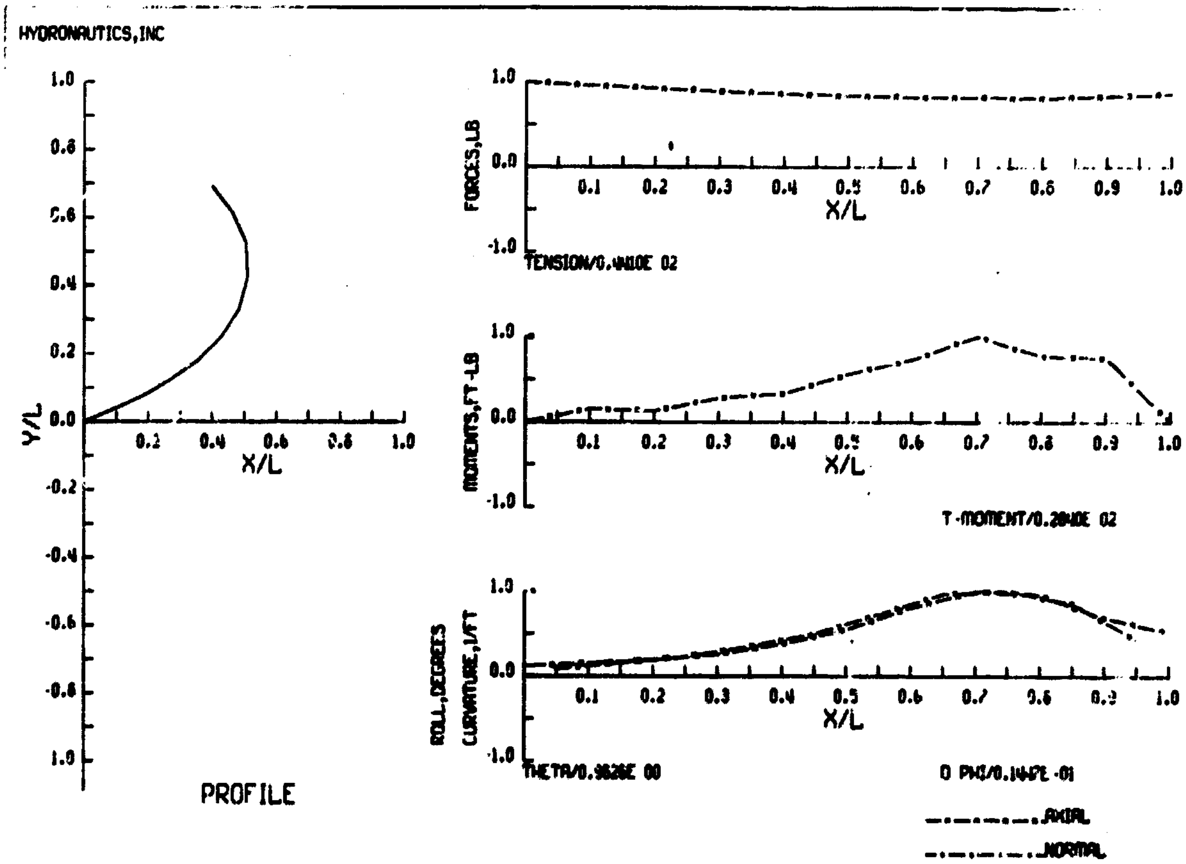

TEST NO. X - 22 - 0 - 60

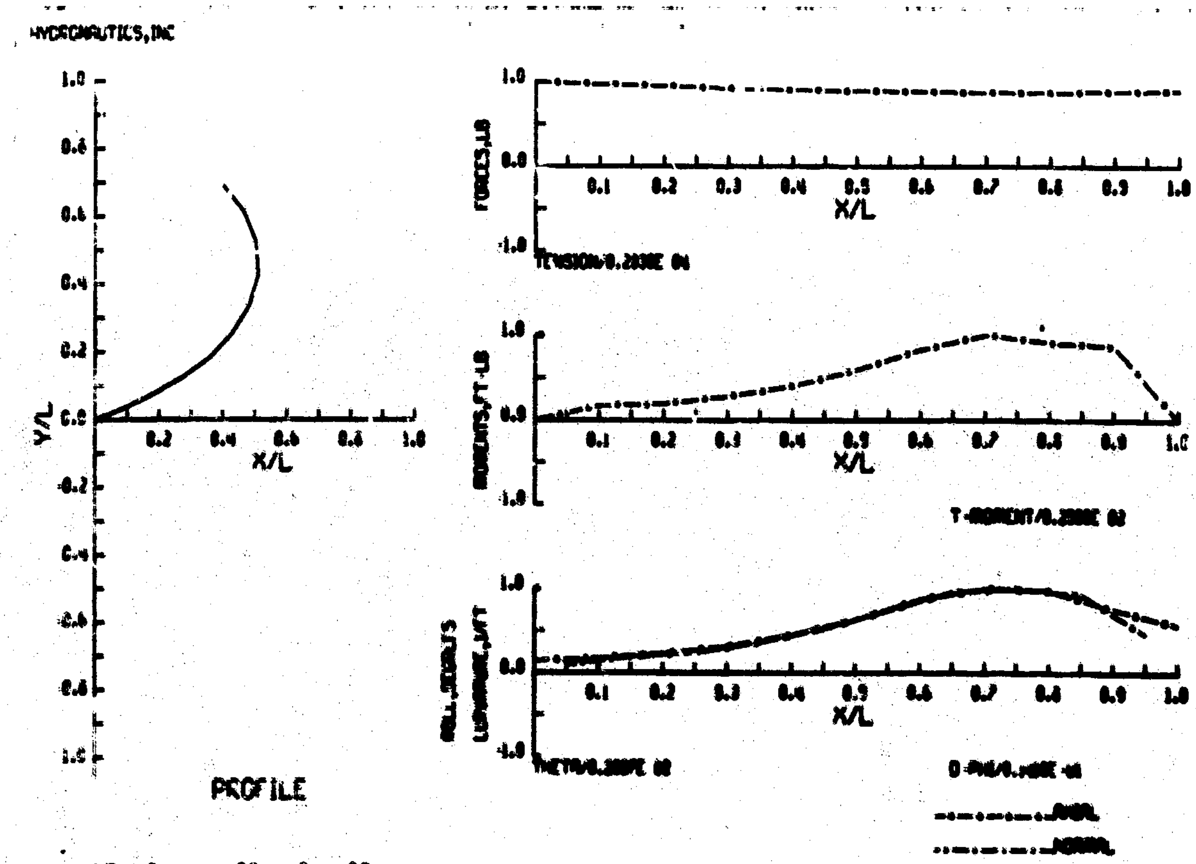

TEST NO. X - 22 - 2 - 60

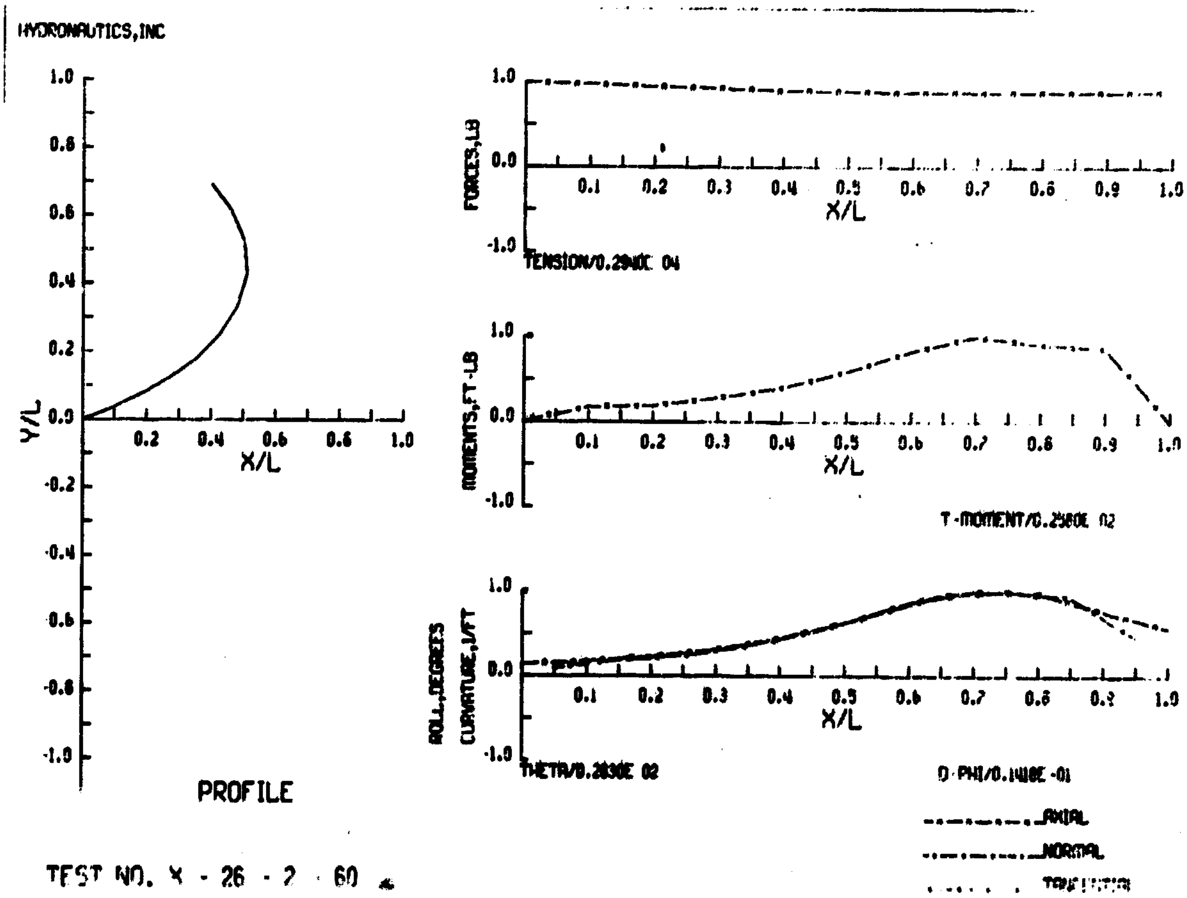

TEST NO. X - 26 - 2 - 60

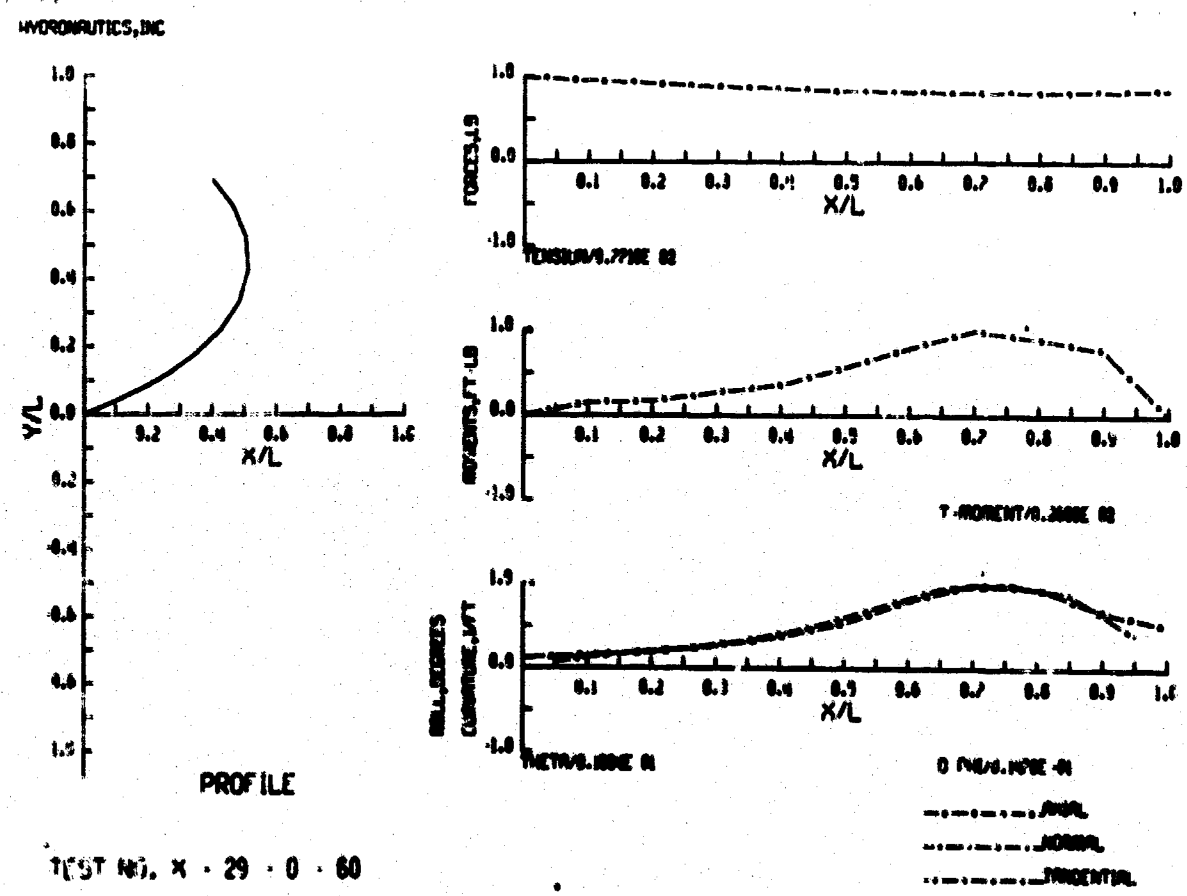

TEST NO. X - 29 - 0 - 60

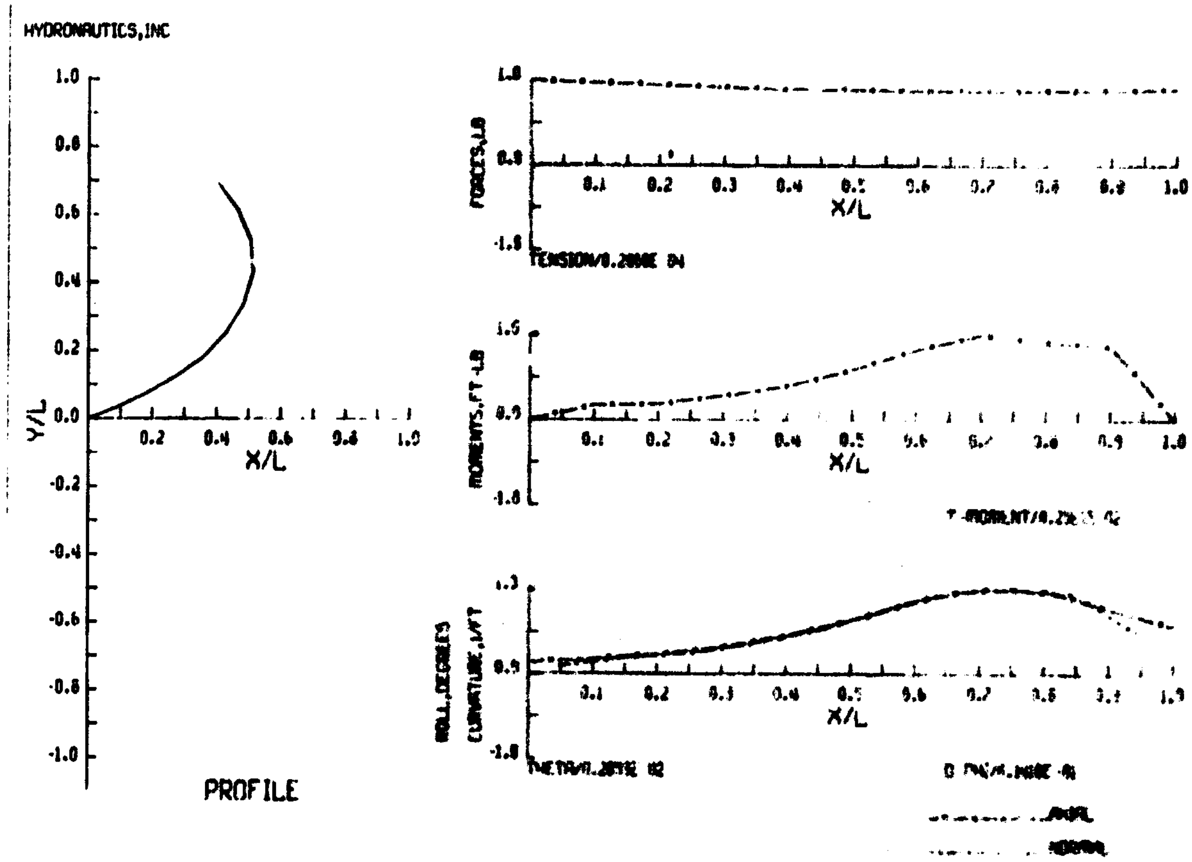

TEST NO. X - 29 - 2 - 60

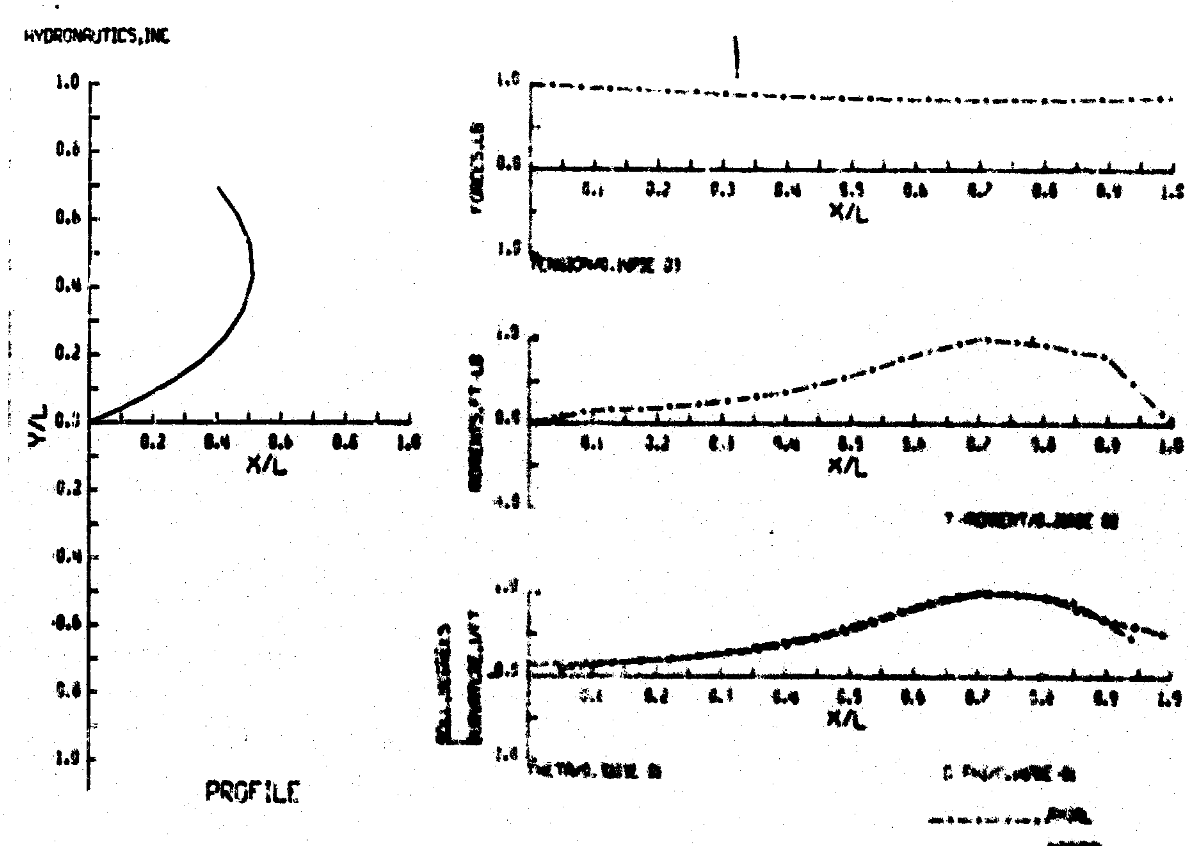

TEST NO. X - 4? - 0 - 60

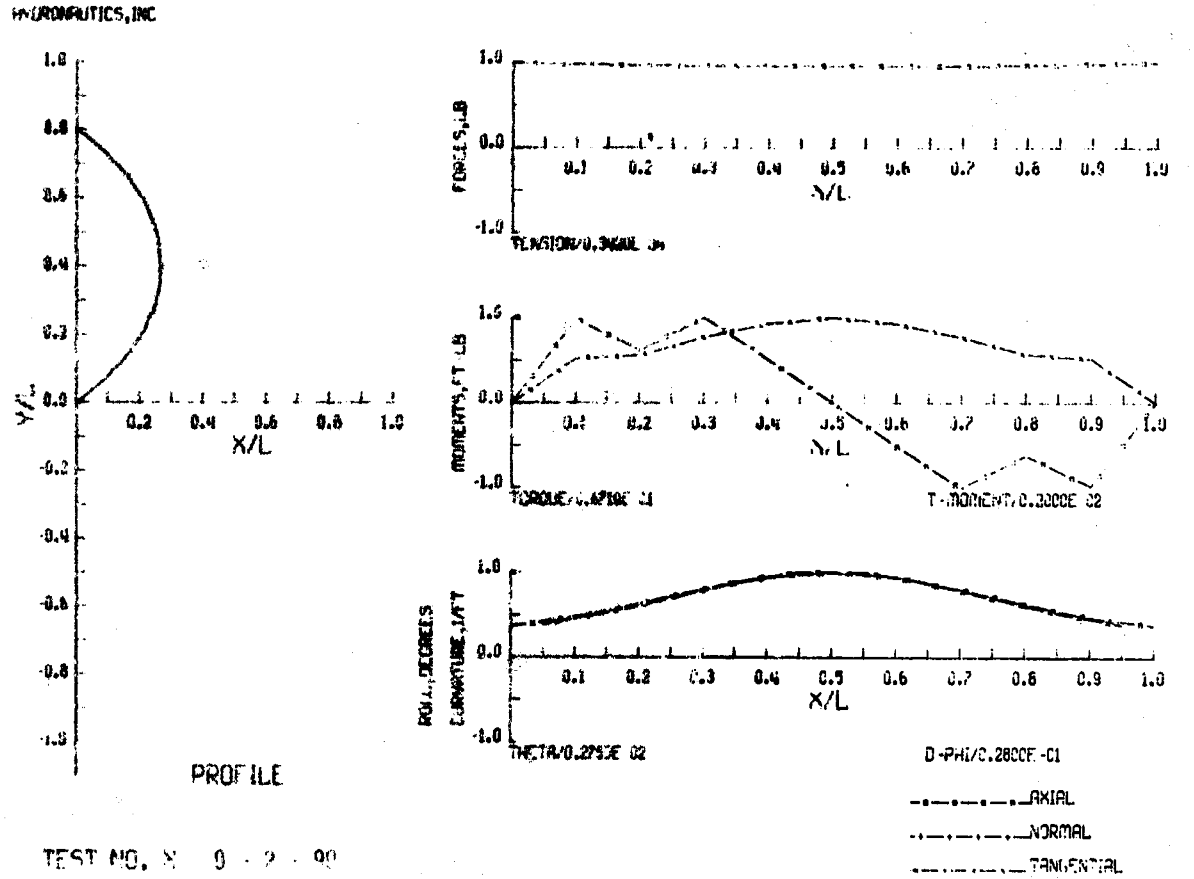

TEST NO. X 0 - 2 - 90

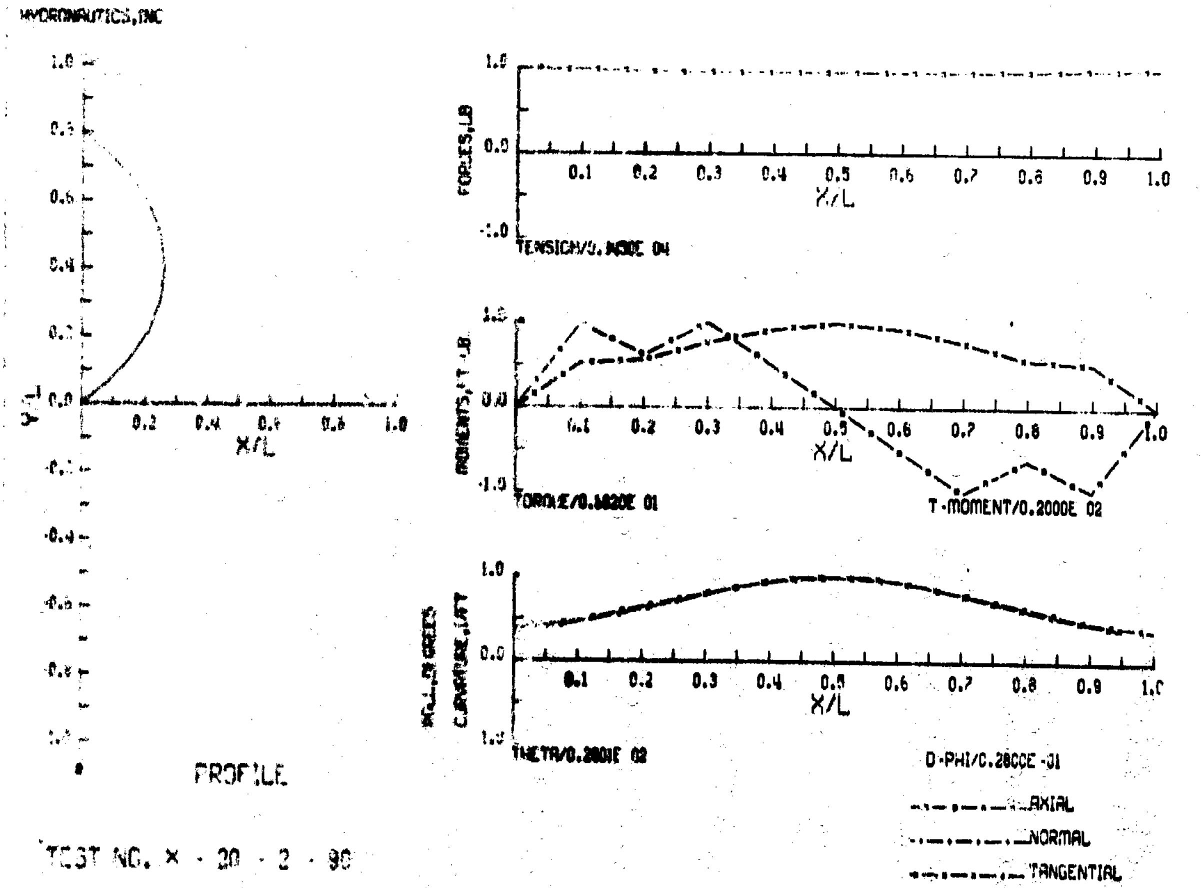

TEST NO. X - 20 - 2 - 90

HYDRONAUTICS,INC

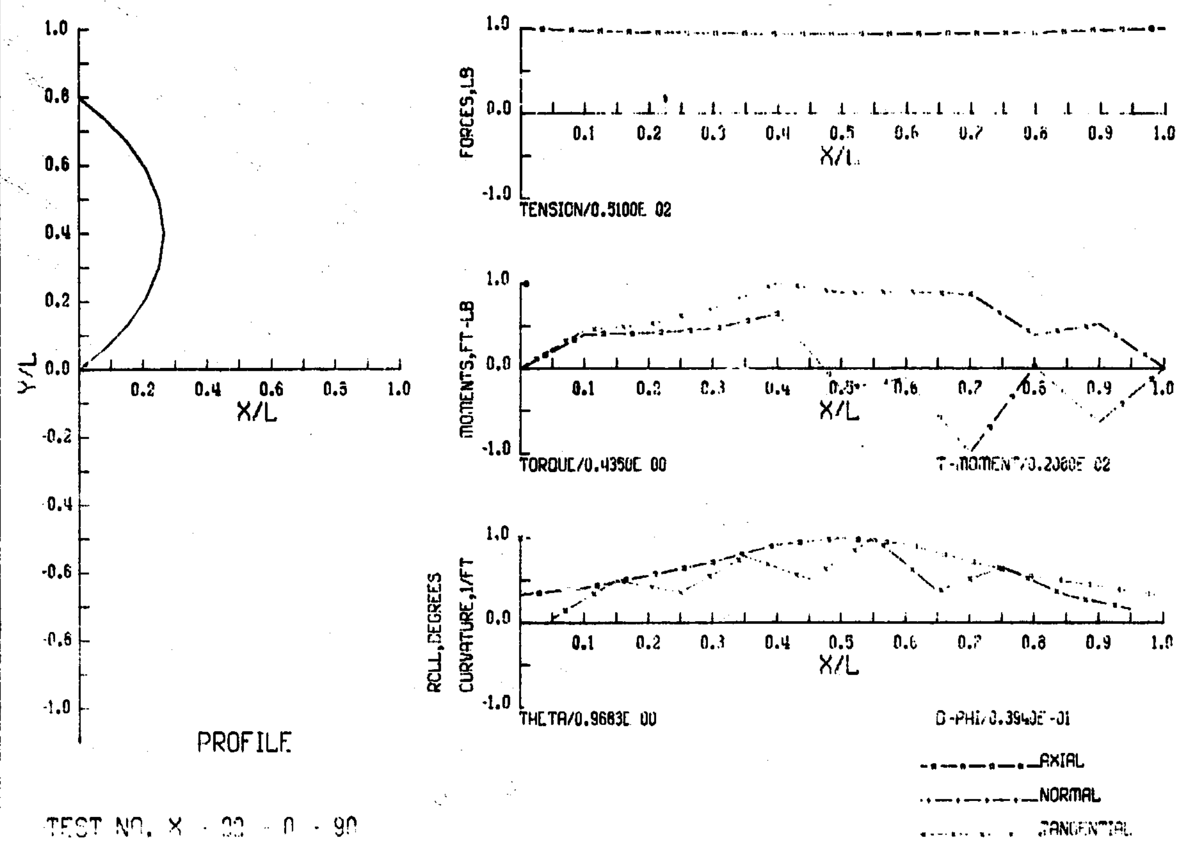

TEST NO. X - 22 - 0 - 90

HYDRONAUTICS,INC

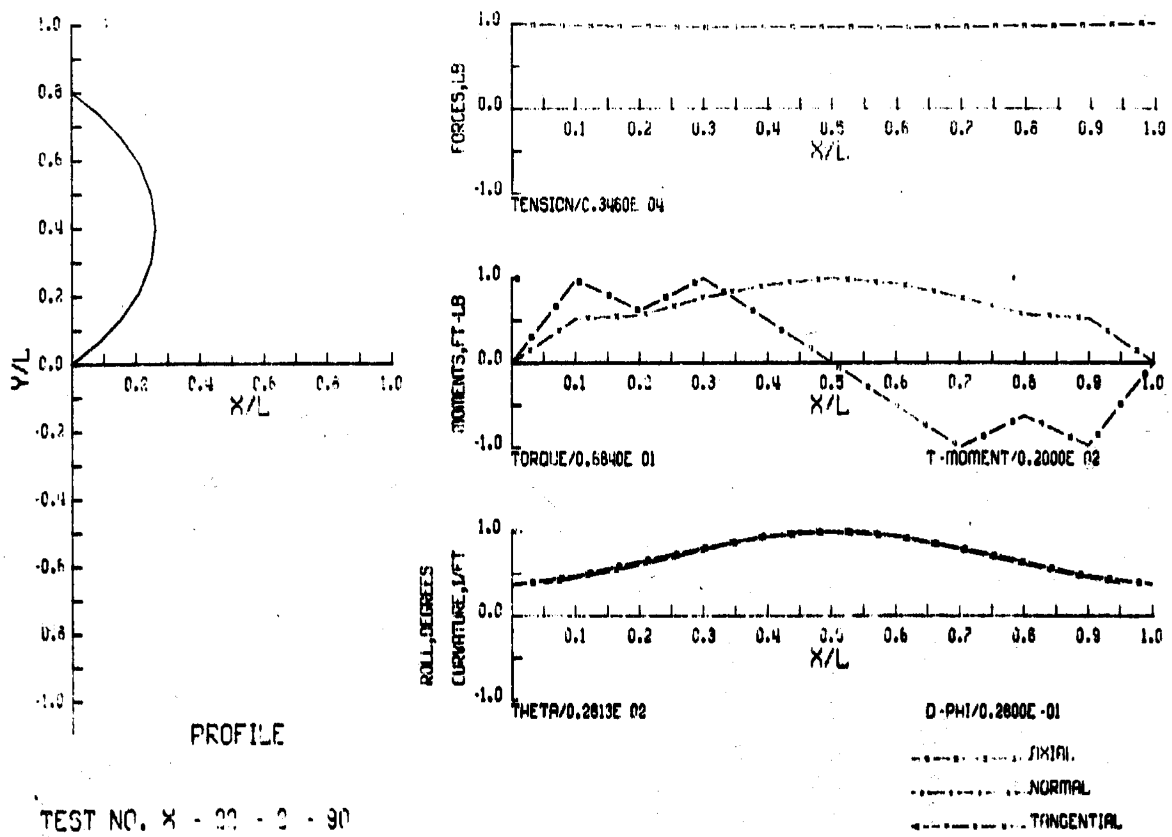

TEST NO. X - 22 - 2 - 90

HYDRONAUTICS,INC

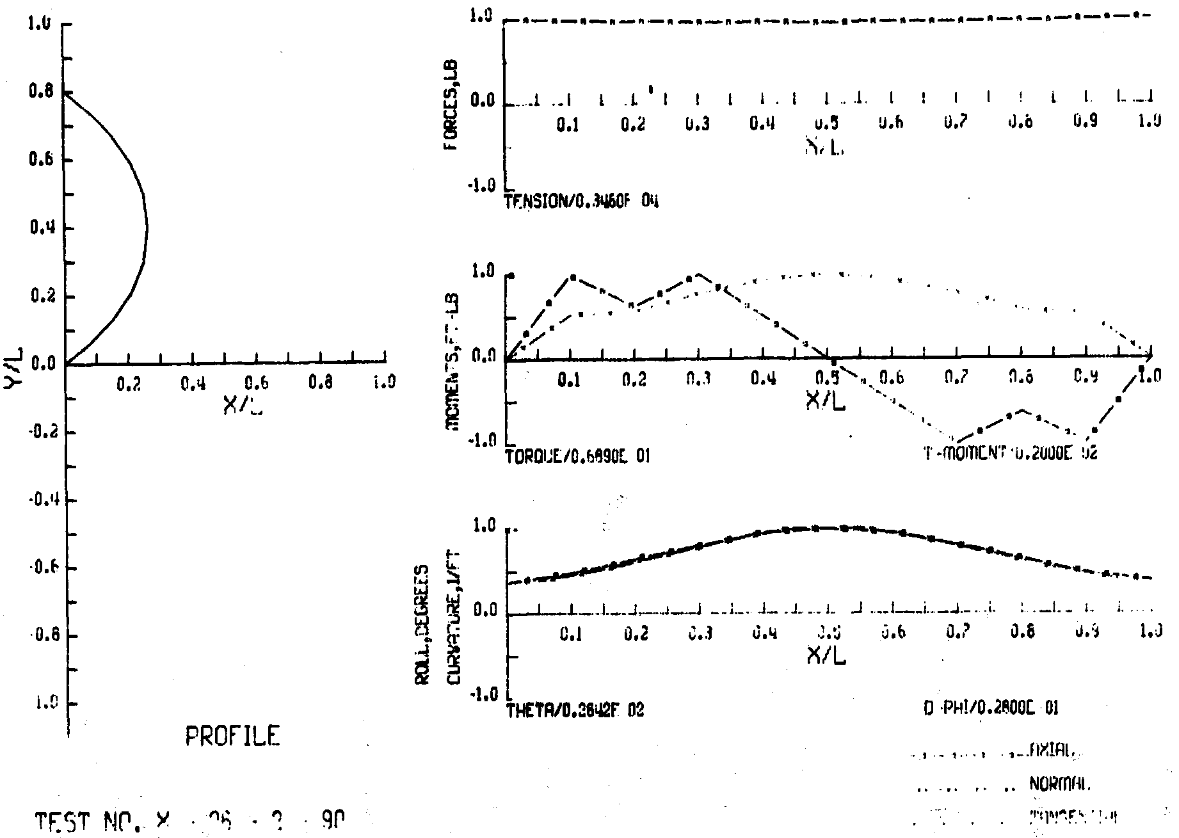

TEST NO. X - 26 - 2 - 90

HYDRONAUTICS,INC

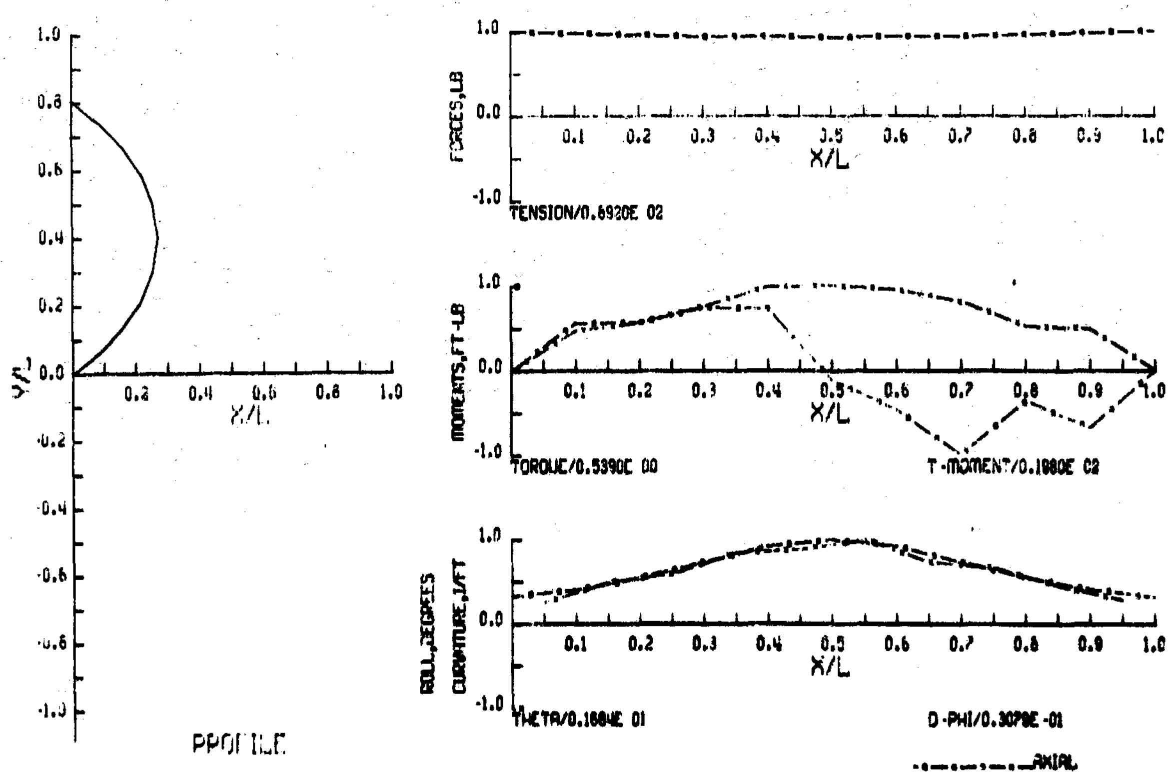

TEST NO. Z - 29 - 0 - 90

HYDRONAUTICS,INC

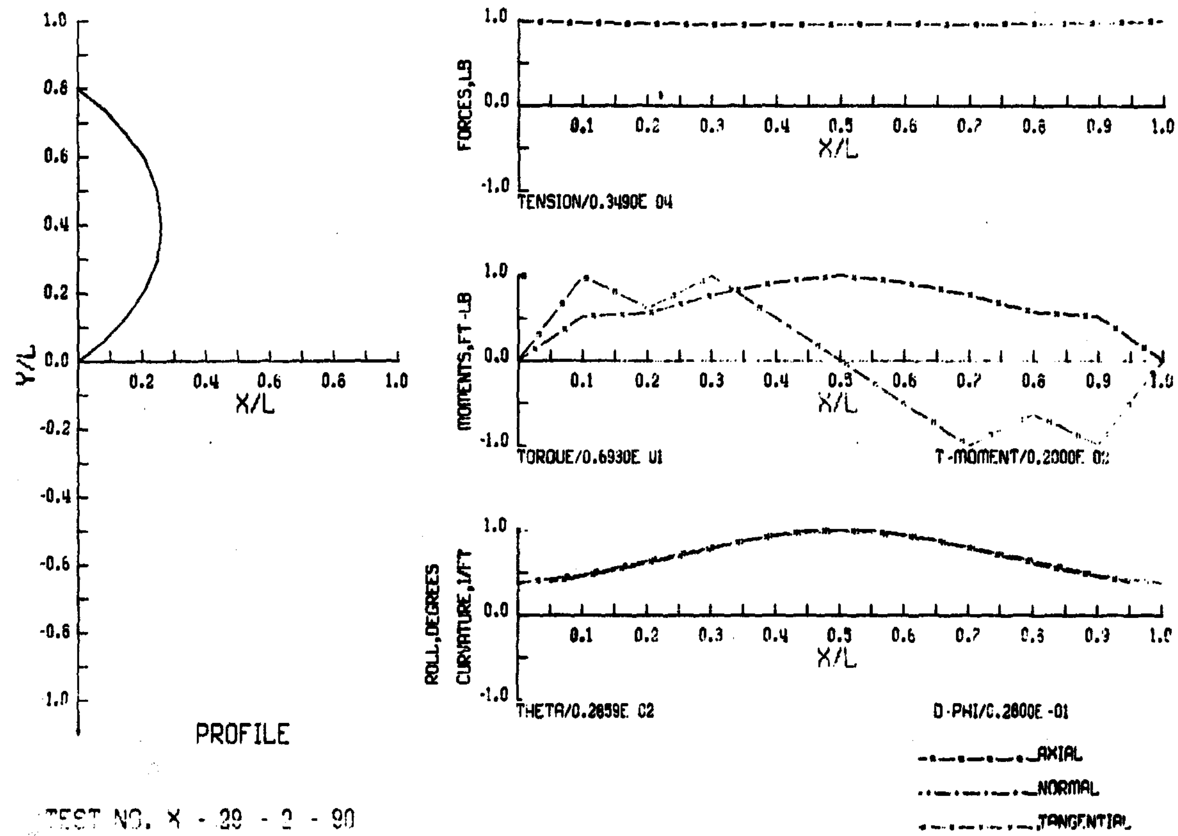

TEST NO. X - 29 - 2 - 90

HYDRONAUTICS,INC

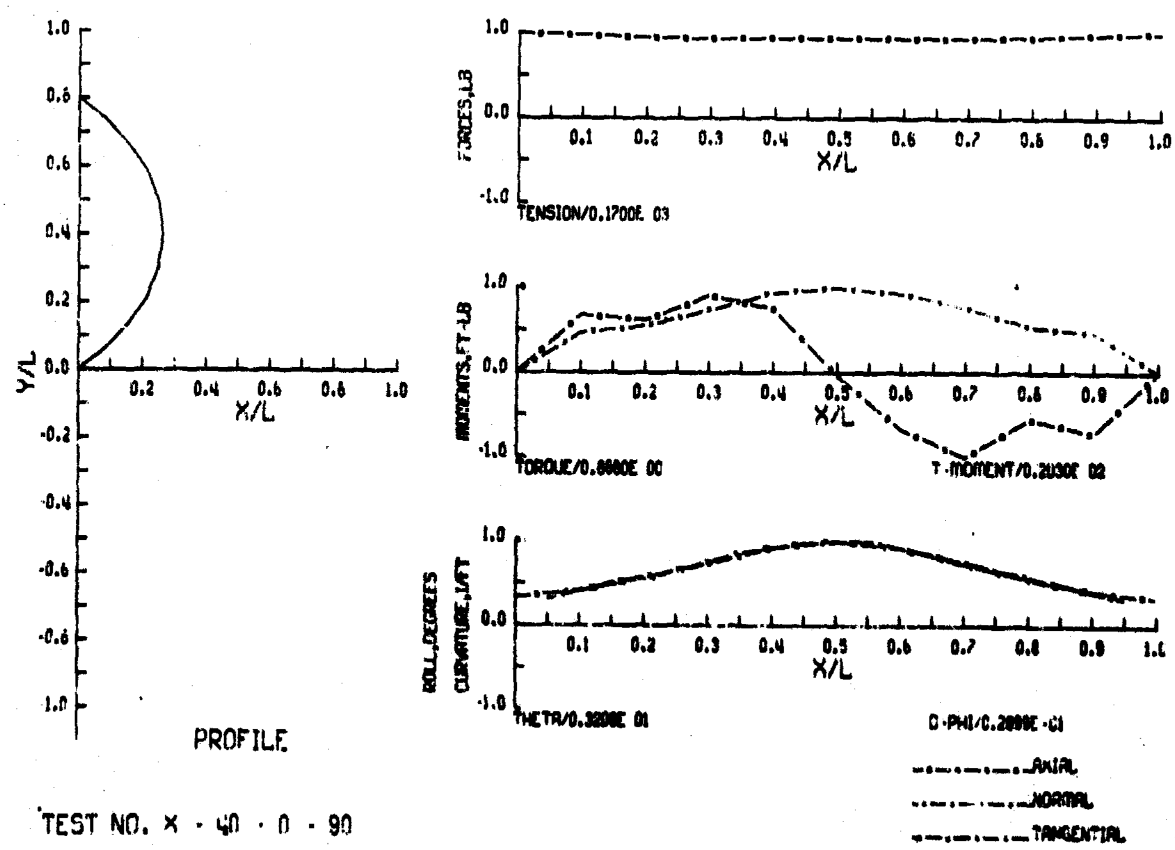

TEST NO. X - 40 - 0 - 90

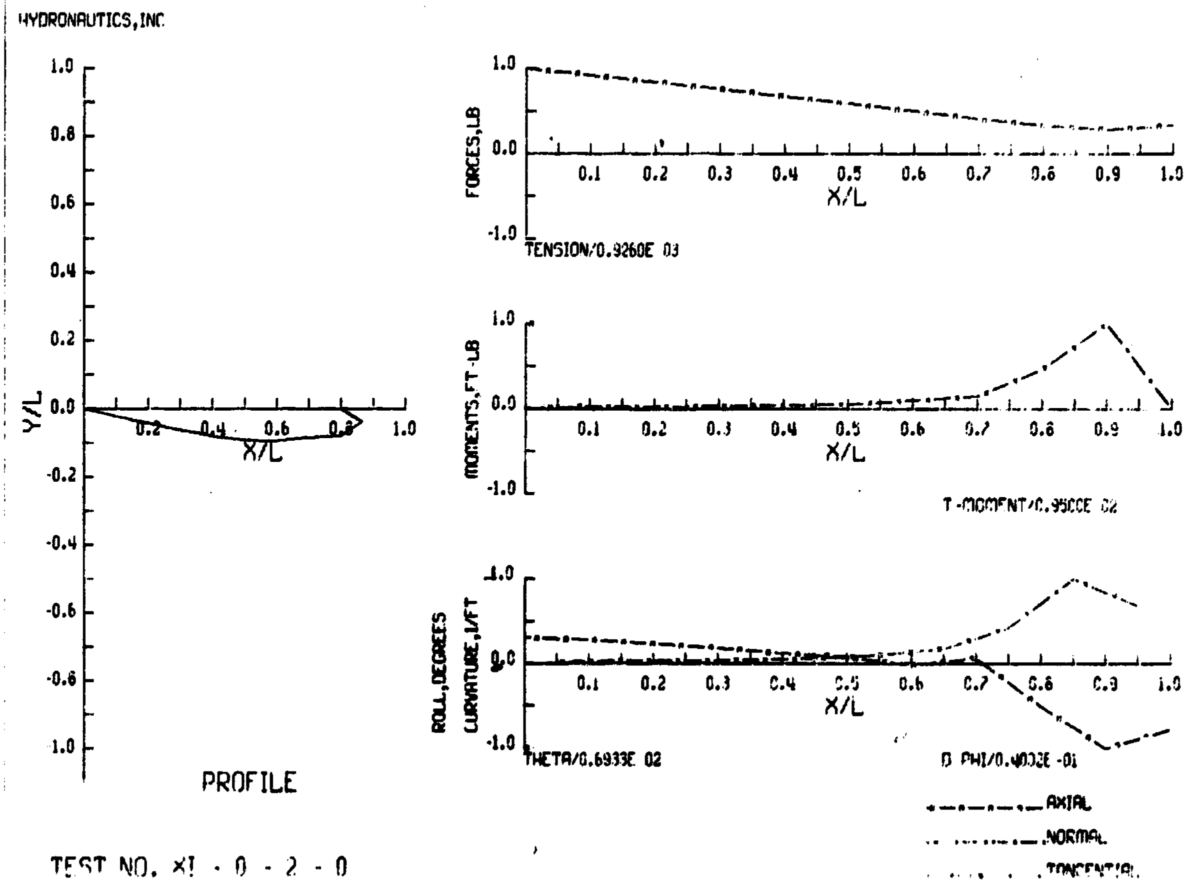

TEST NO. XI - 0 - 2 - 0

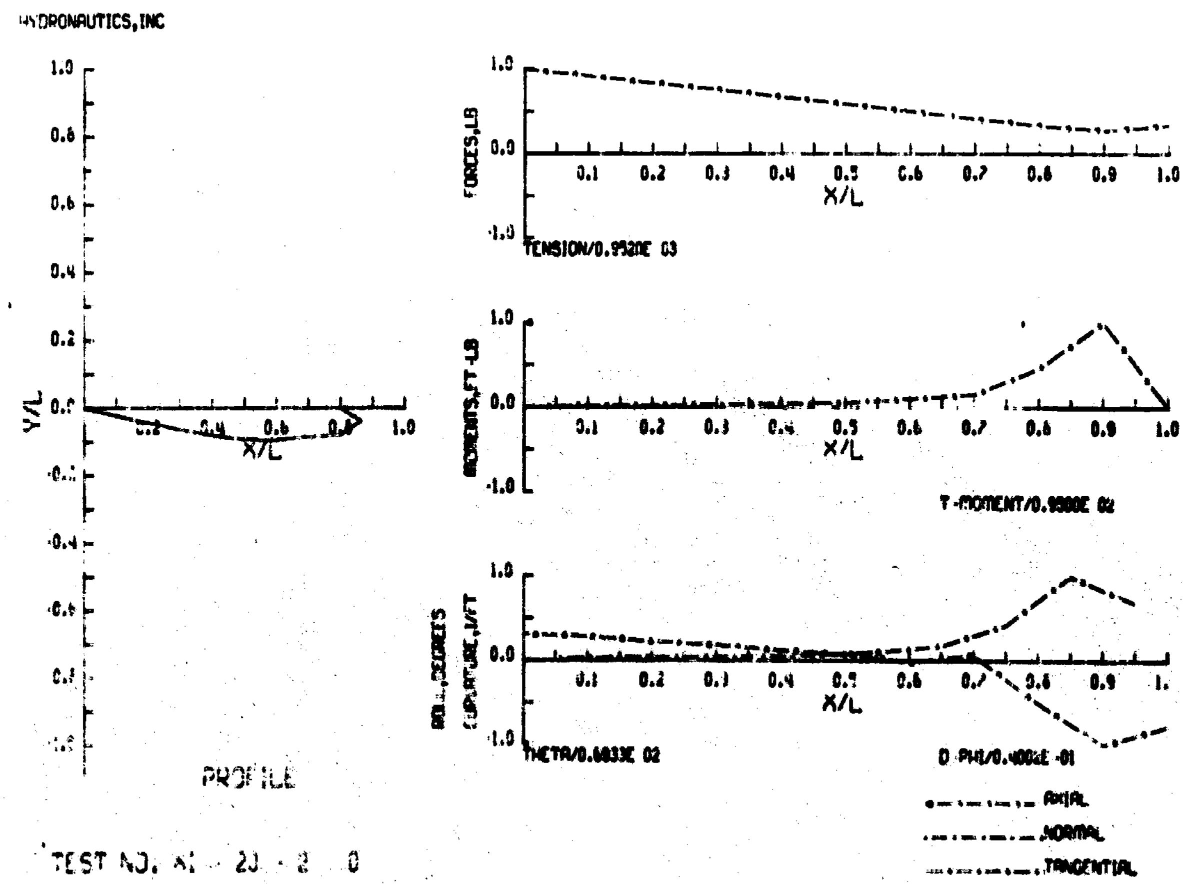

TEST NO. XI - 20 - 2 - 0

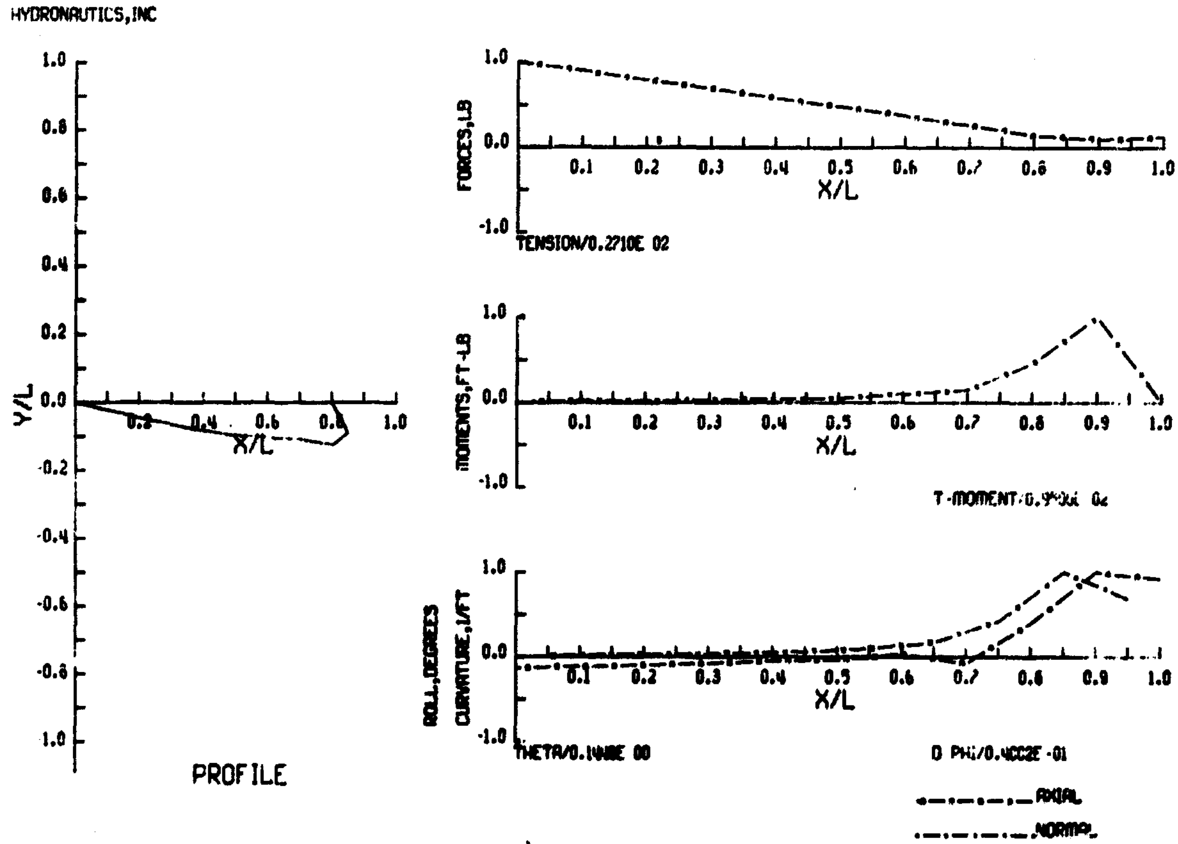

TEST NO. XI 22 0 0

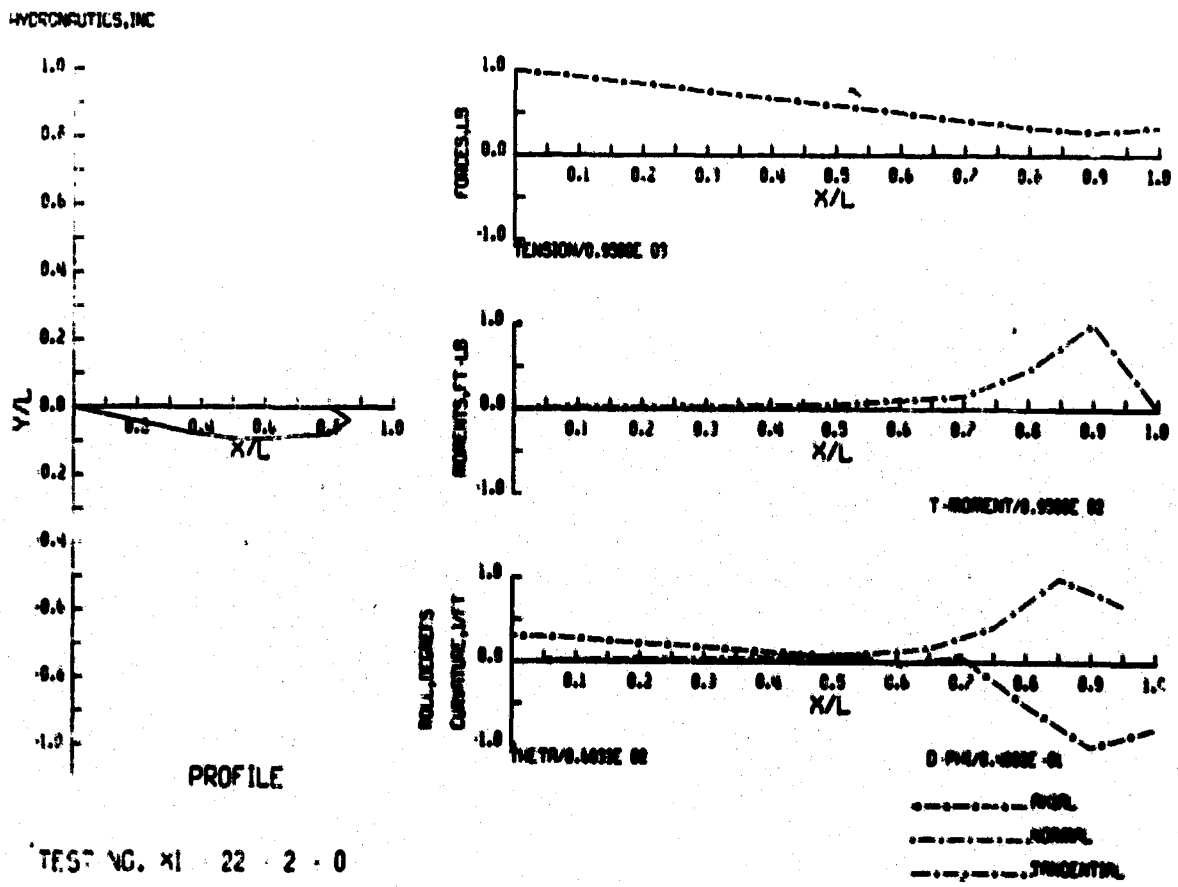

TEST NO. XI 22 2 0

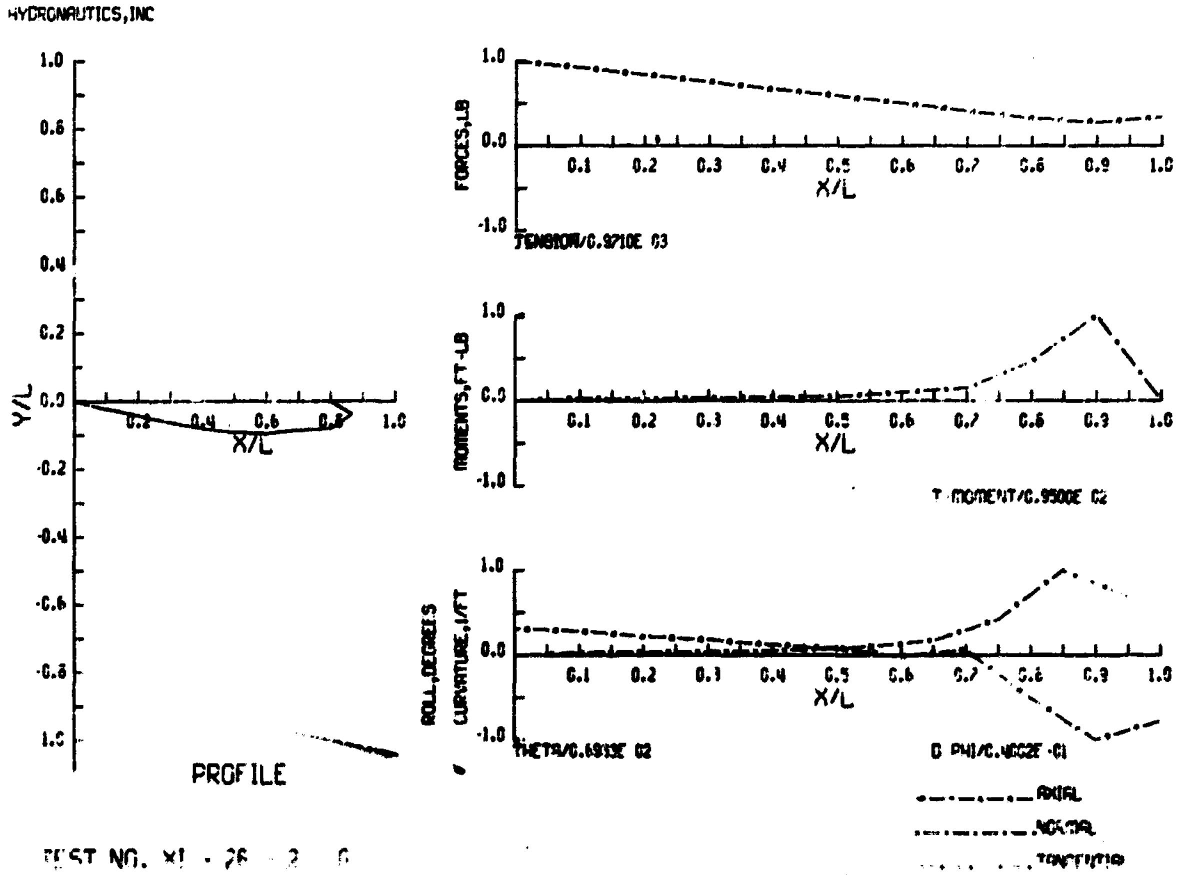
HYDRONAUTICS,INC
Y/L
X/L
PROFILE
FORCES,LB
TENSION/0.9710E 03
MOMENTS,FT-LB
ROLL,DEGREES
CURVATURE,1/FT
AXIAL

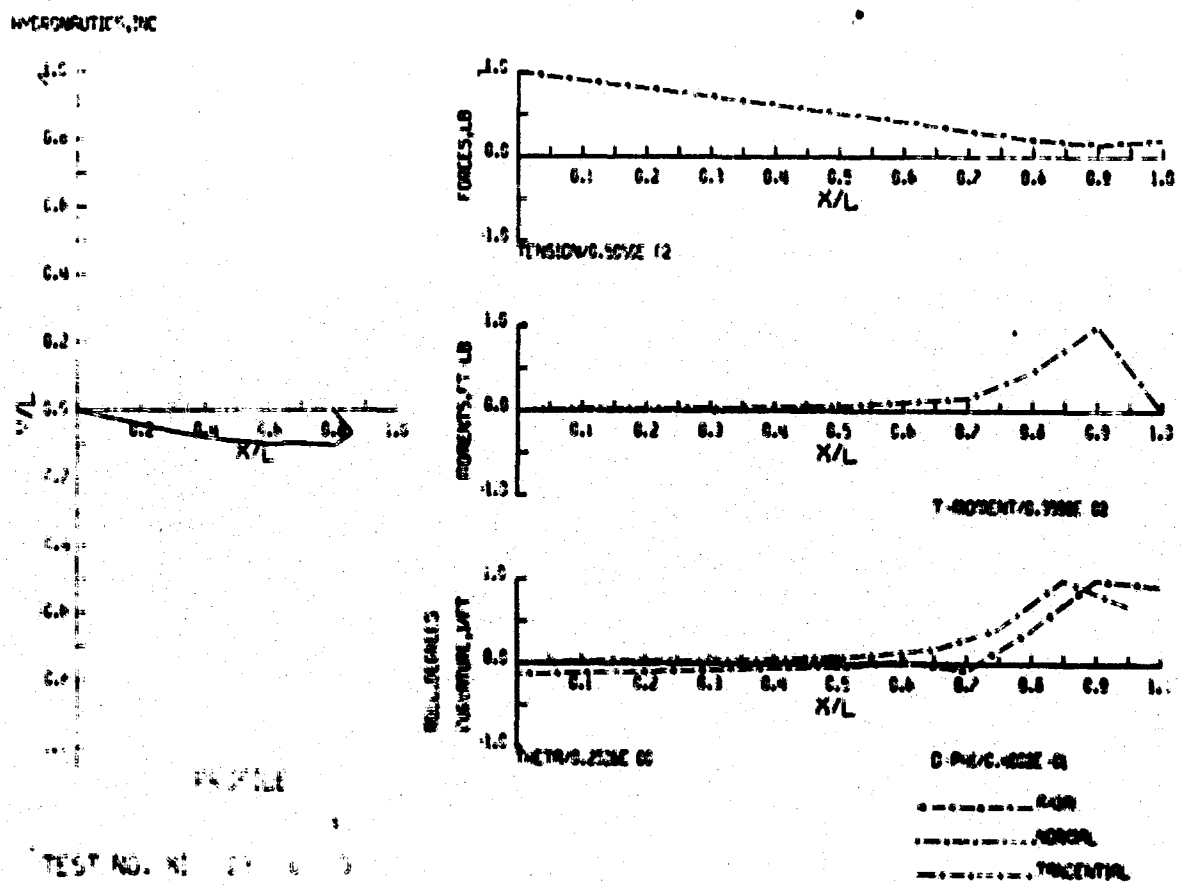
FORCES,LB
X/L
TANGENTIAL

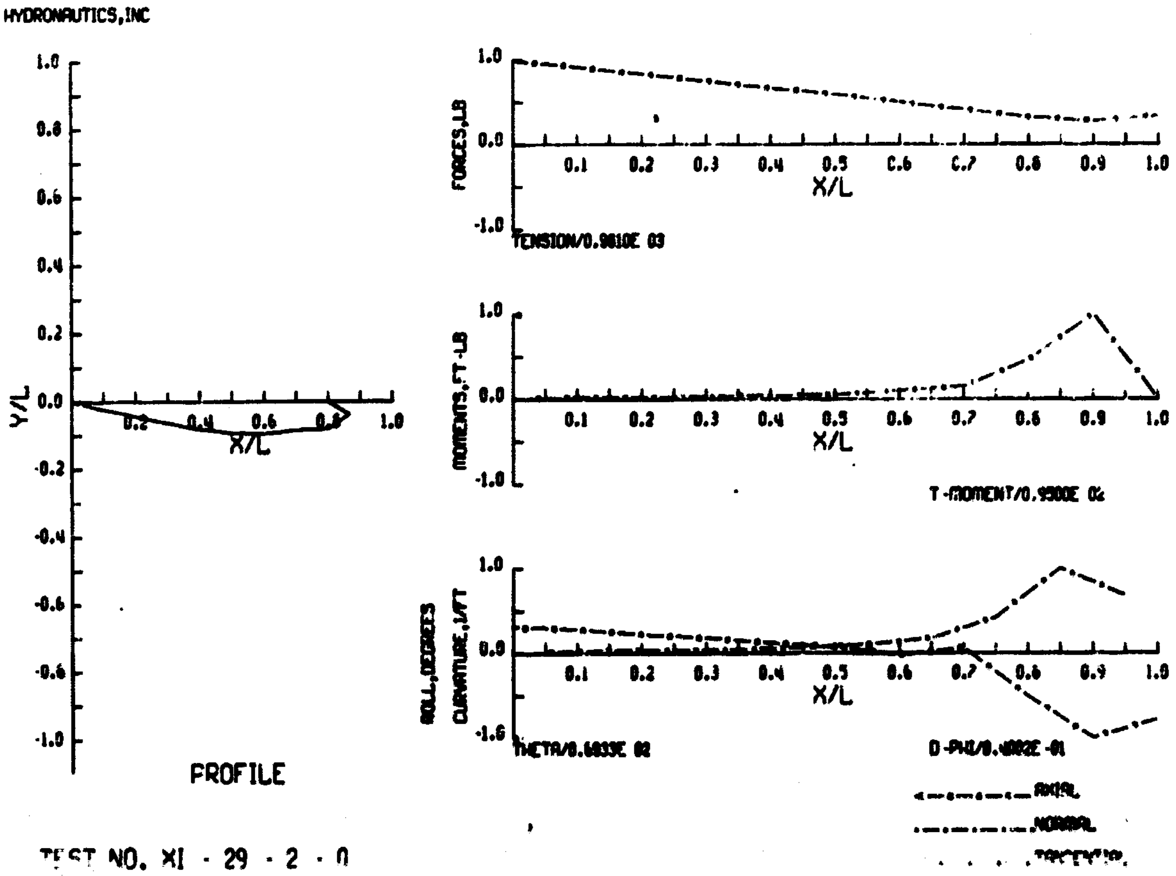

TEST NO. XI - 29 - 2 - 0

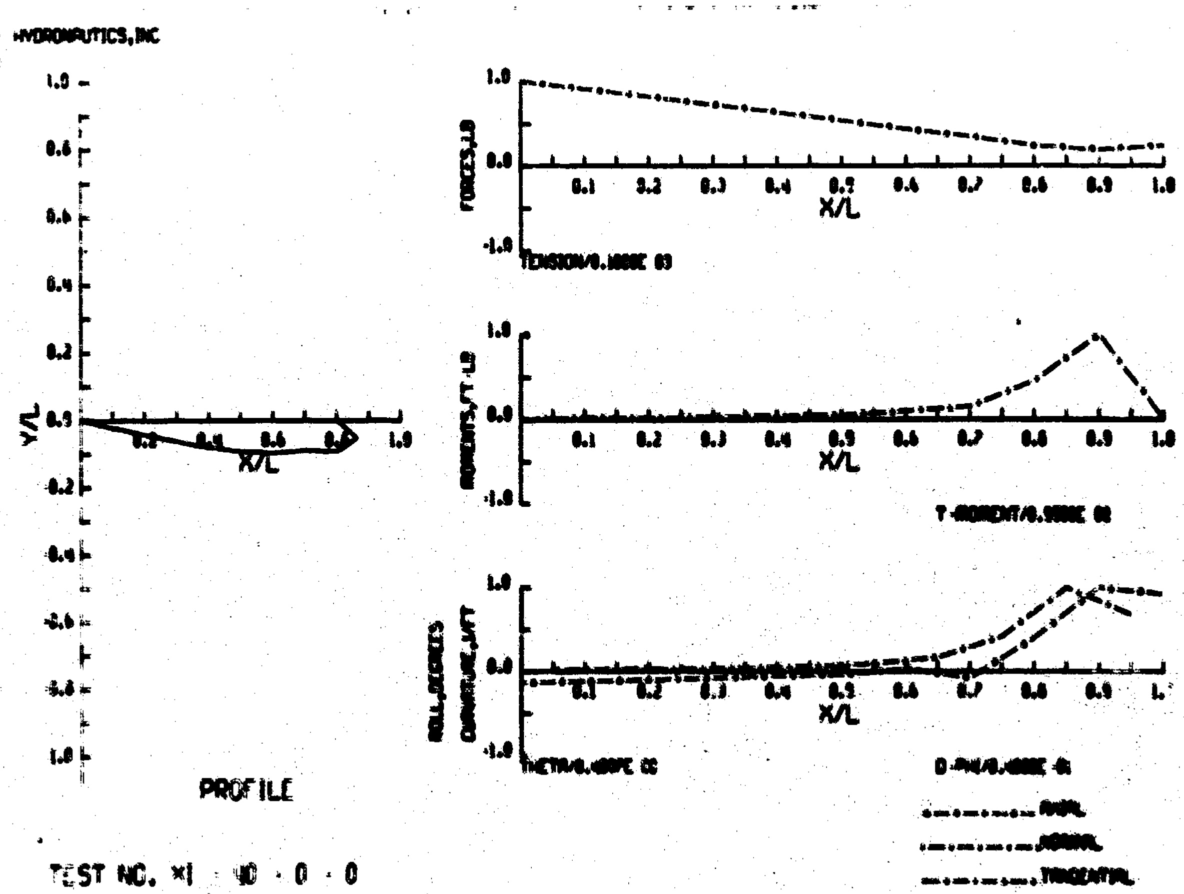

TEST NO. XI - 40 - 0 - 0

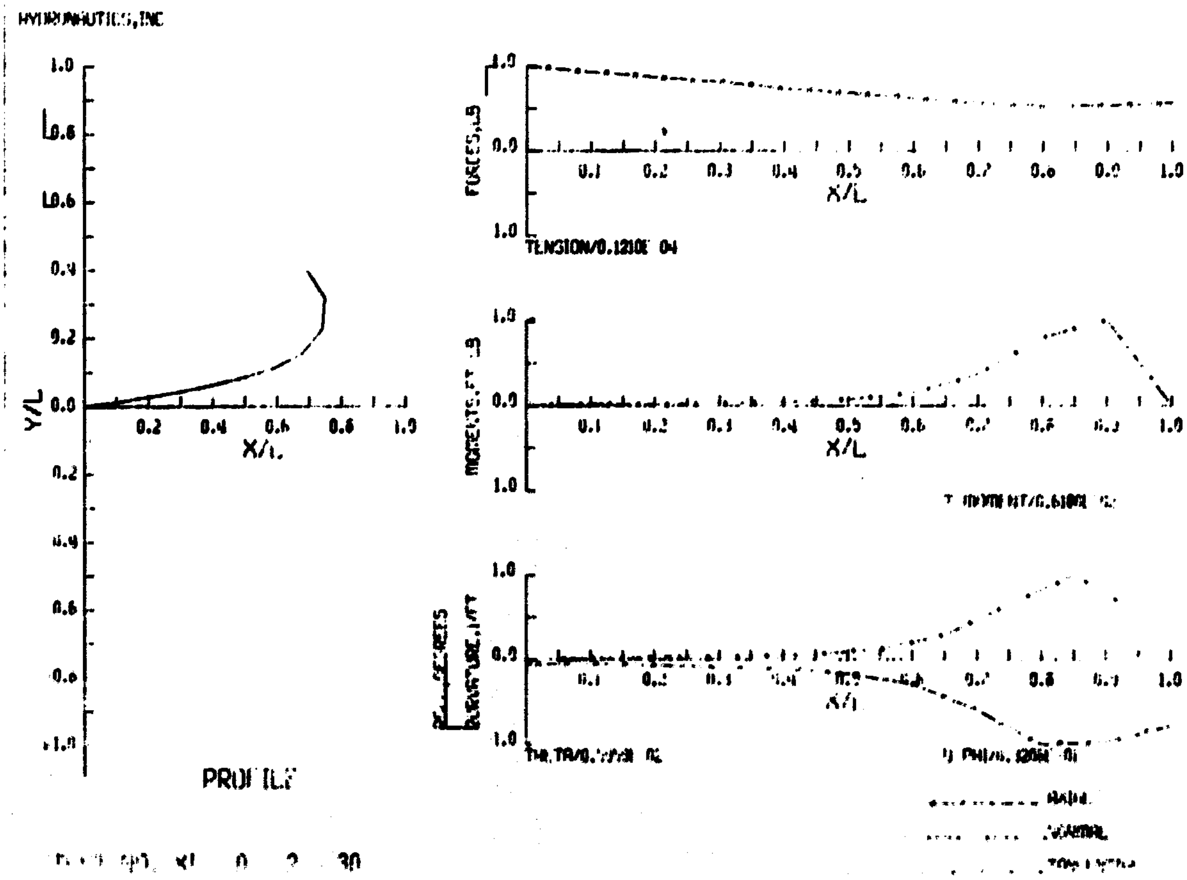
HYDRONAUTICS,INC
Y/L
X/L
PROFILE
FORCES,LB
TENSION/0.1210E 04
MOMENTS,FT-LB
AXIAL
NORMAL

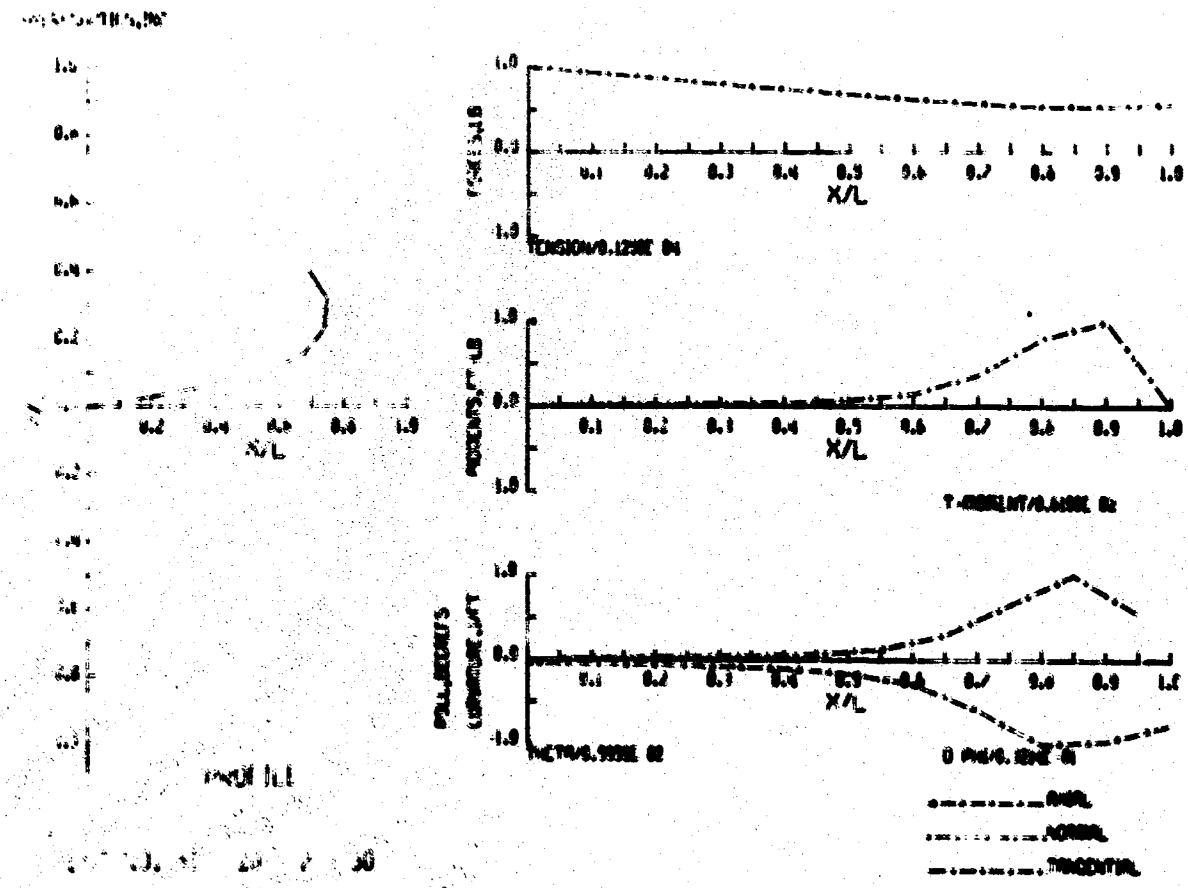
X/L
PROFILE
TENSION/0.1209E 04
MOMENTS,FT-LB
AXIAL
NORMAL
TANGENTIAL

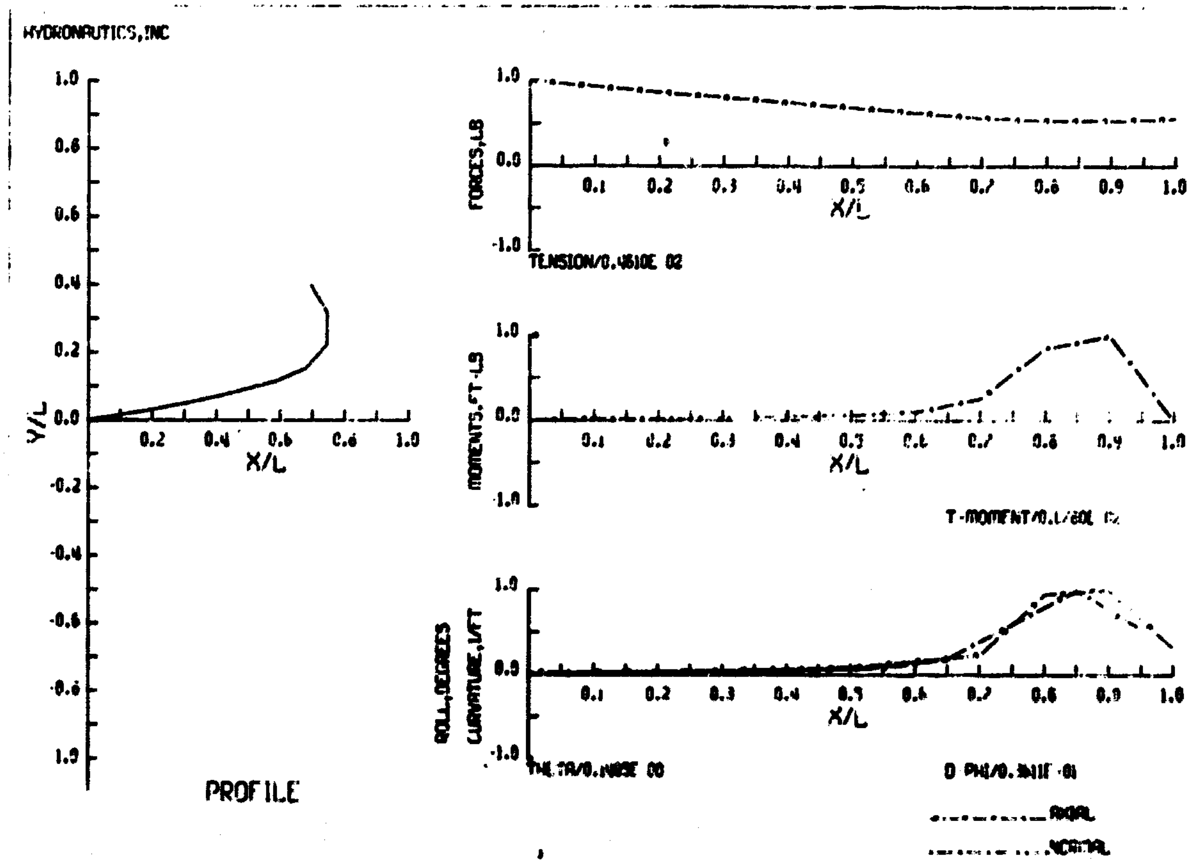

TEST NO. XI - 22 - 0 - 30

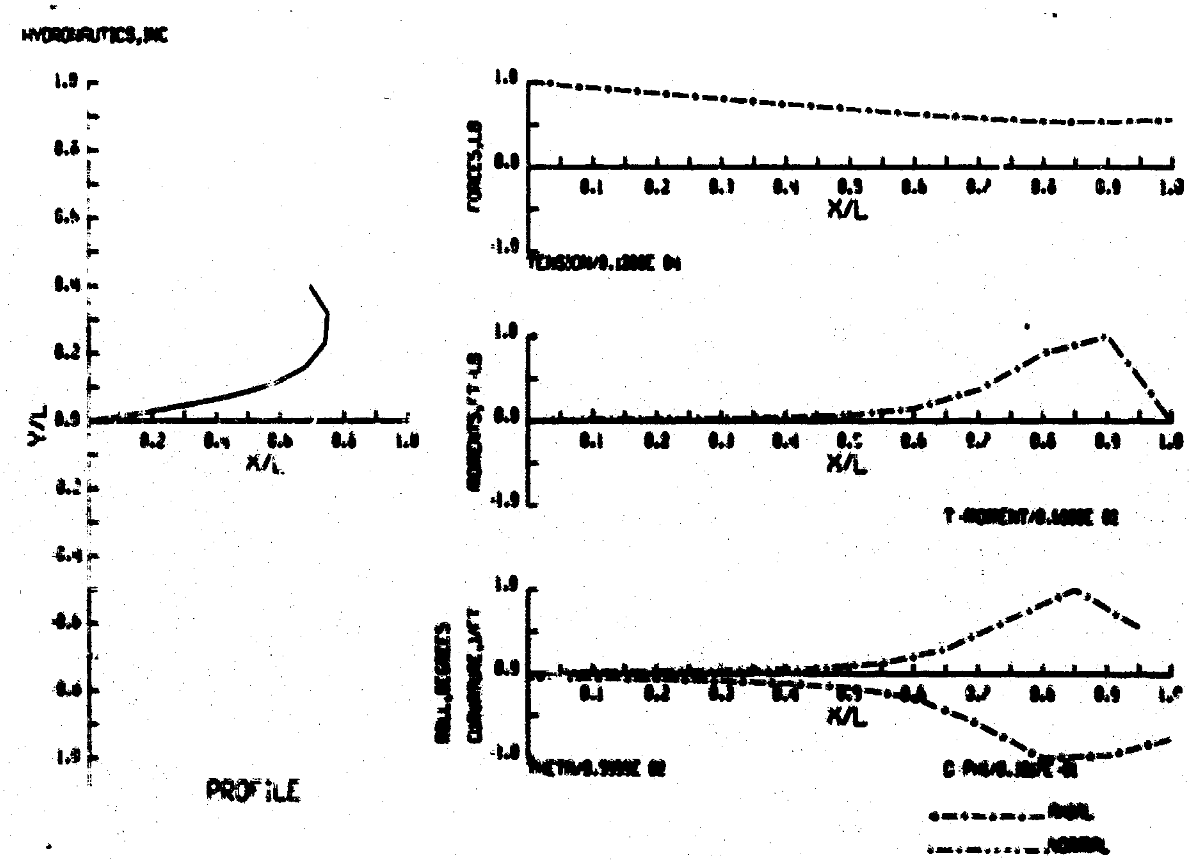

TEST NO. XI - 22 - 2 - 30

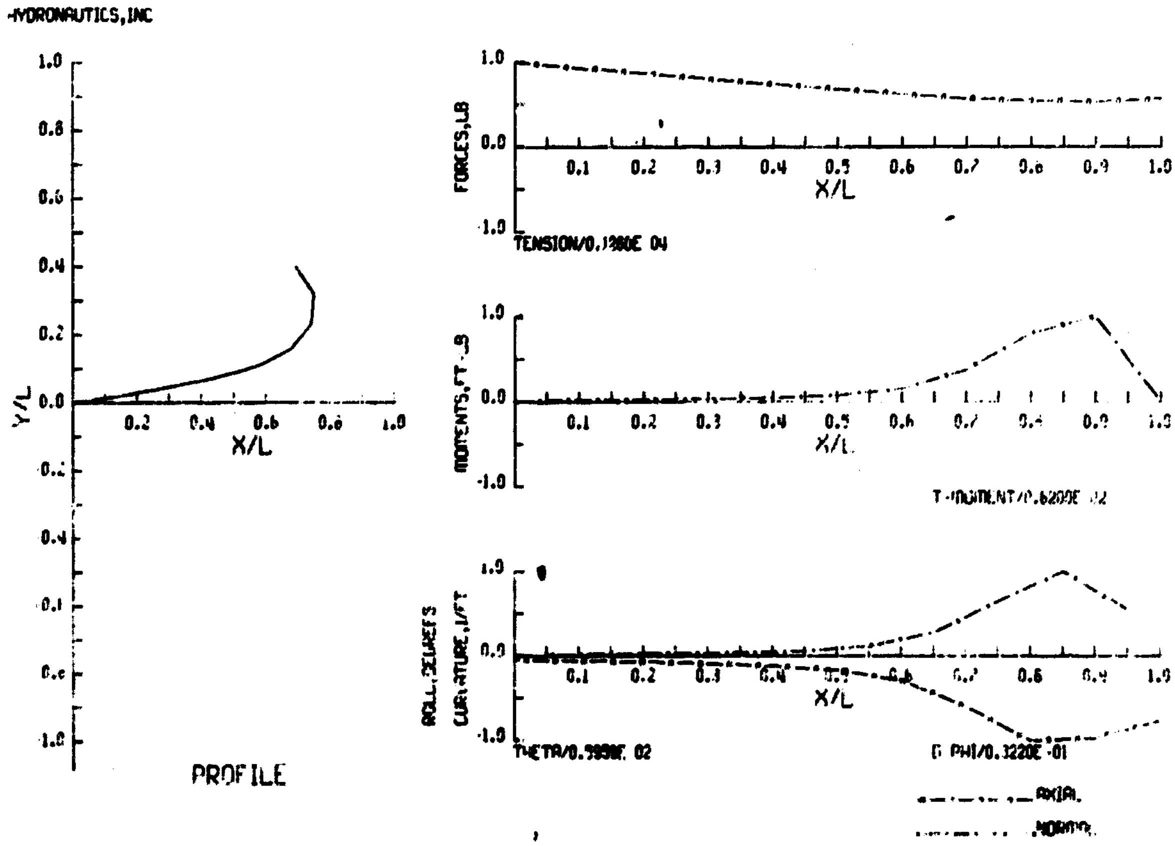

TEST NO. XI - 26 - 3 - 30

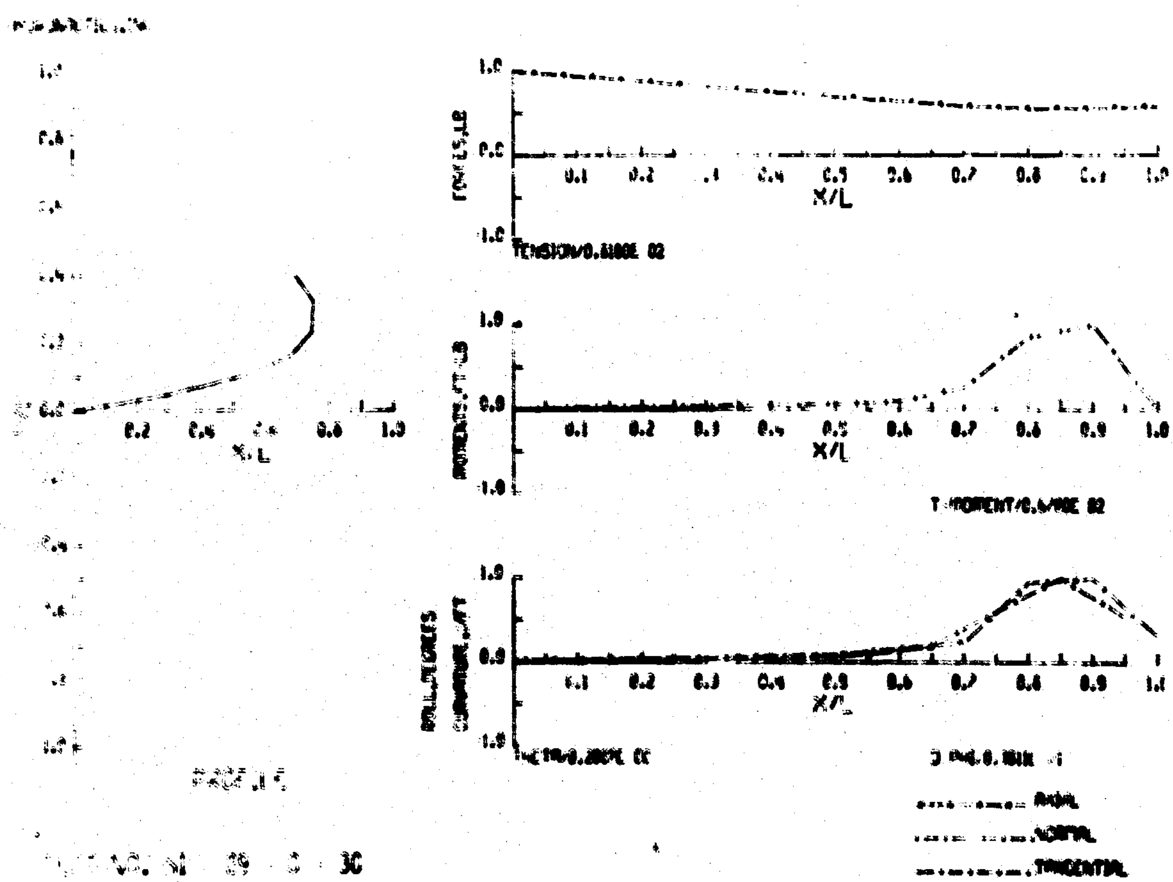

TEST NO. XI - 29 - 3 - 30

HYDRONAUTICS,INC

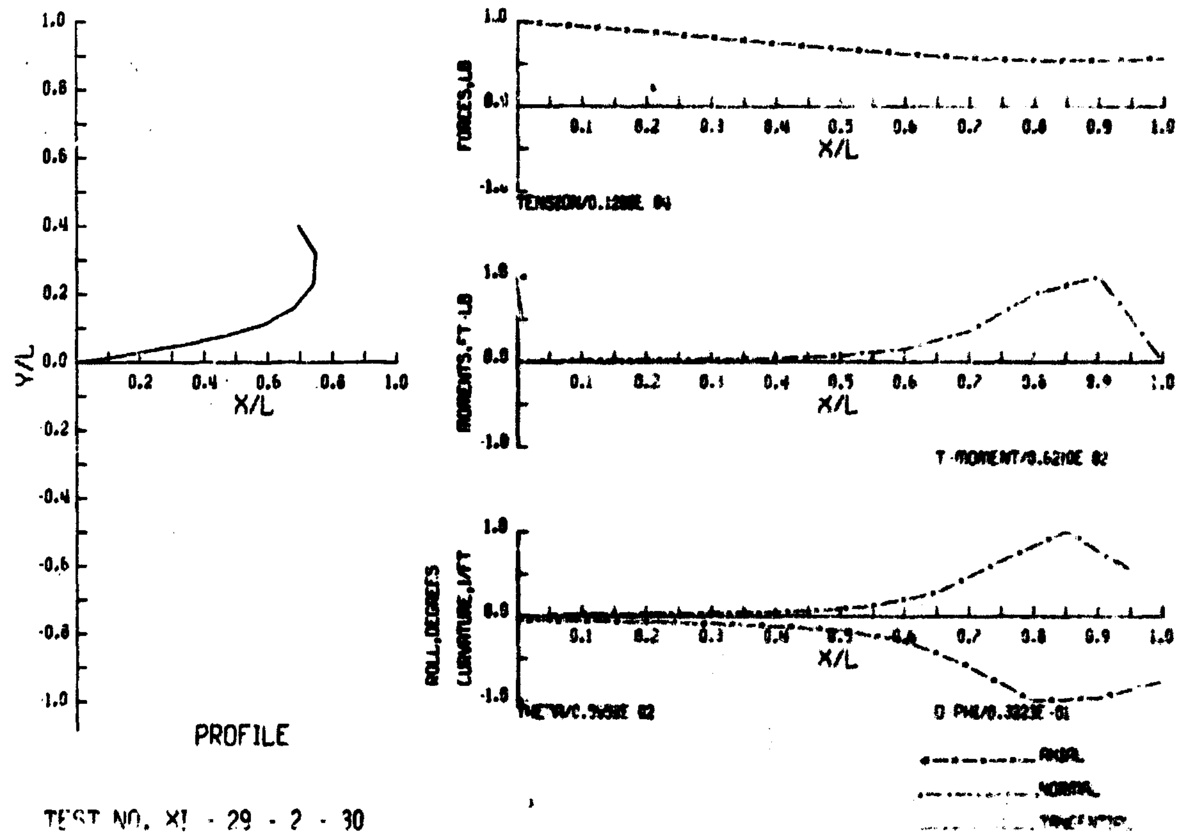

TEST NO. XI - 29 - 2 - 30

HYDRONAUTICS,INC

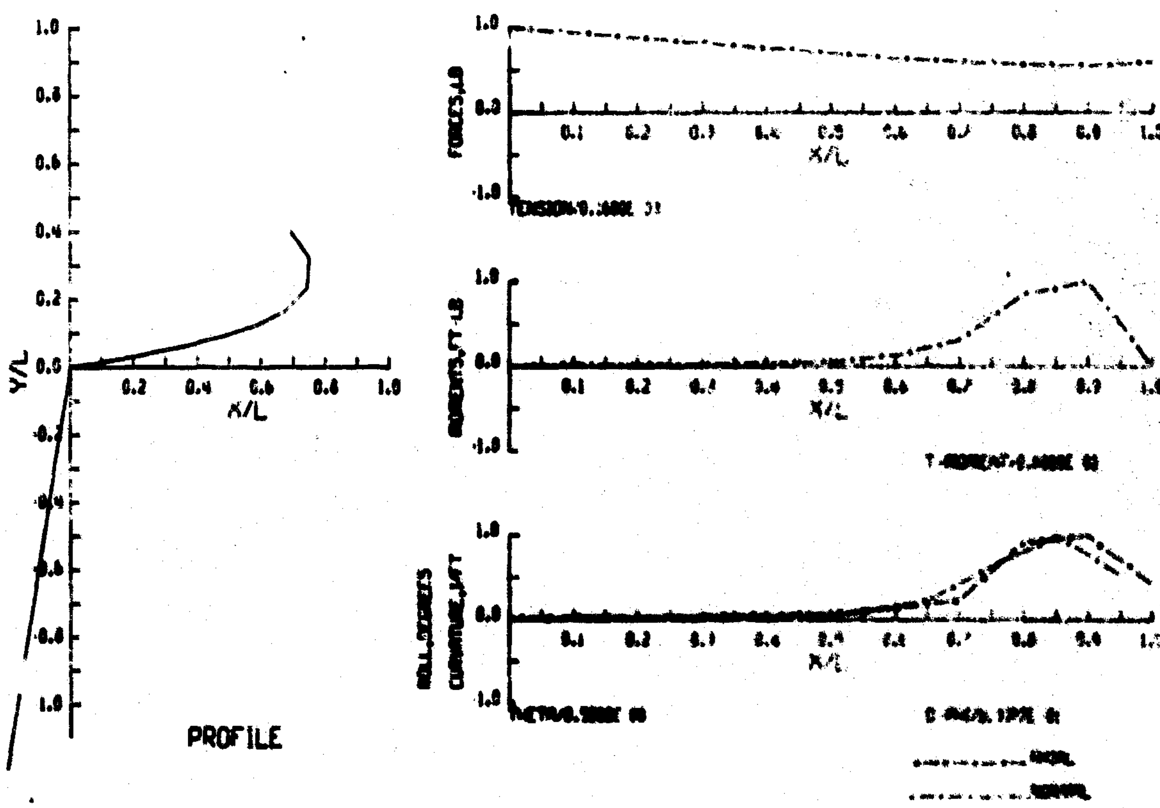

TEST NO. XI - 40 - G - 30

HYDRONAUTICS, INC

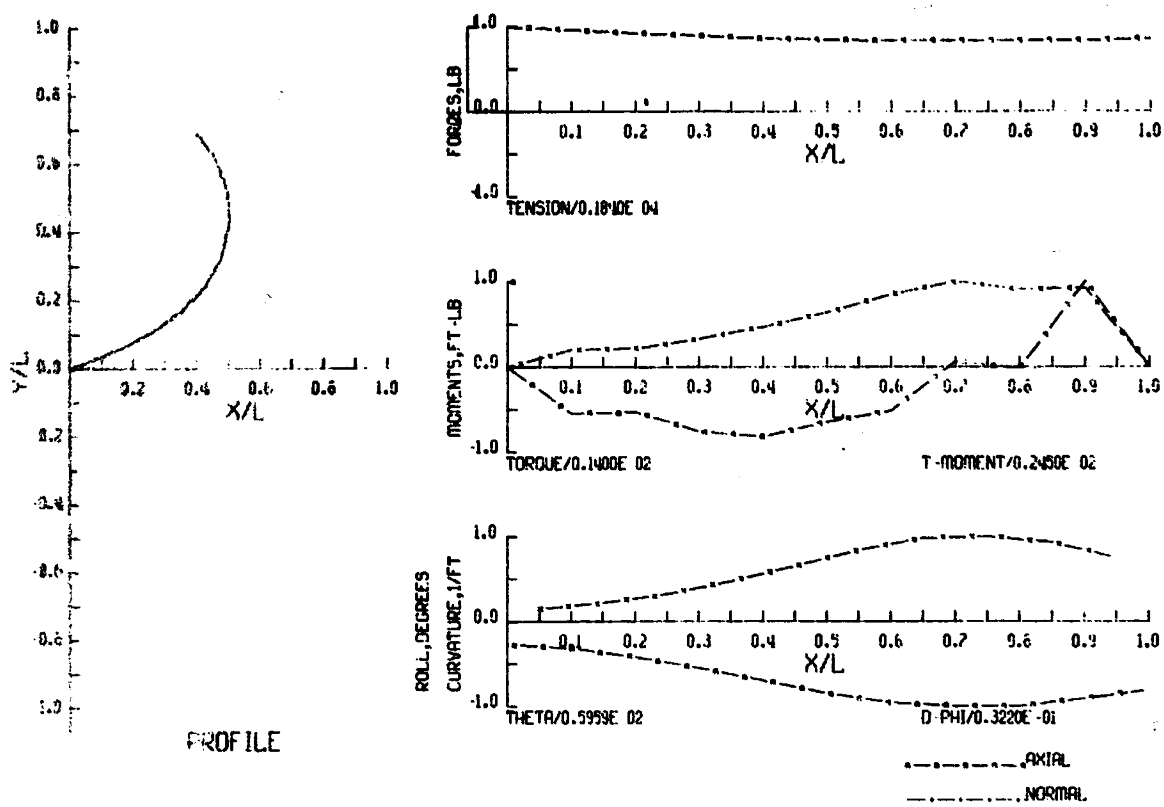

TEST NO. XI - 0 - 2 - 60

HYDRONAUTICS, INC

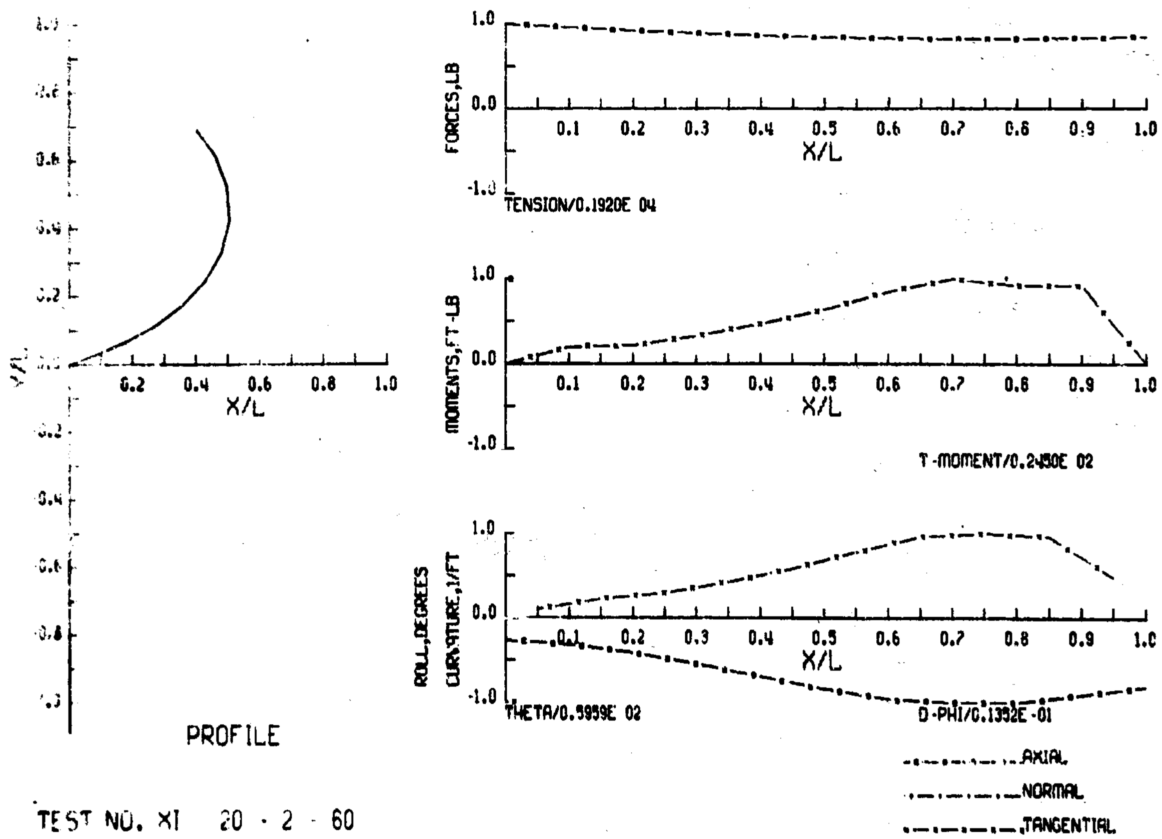

TEST NO. XI 20 - 2 - 60

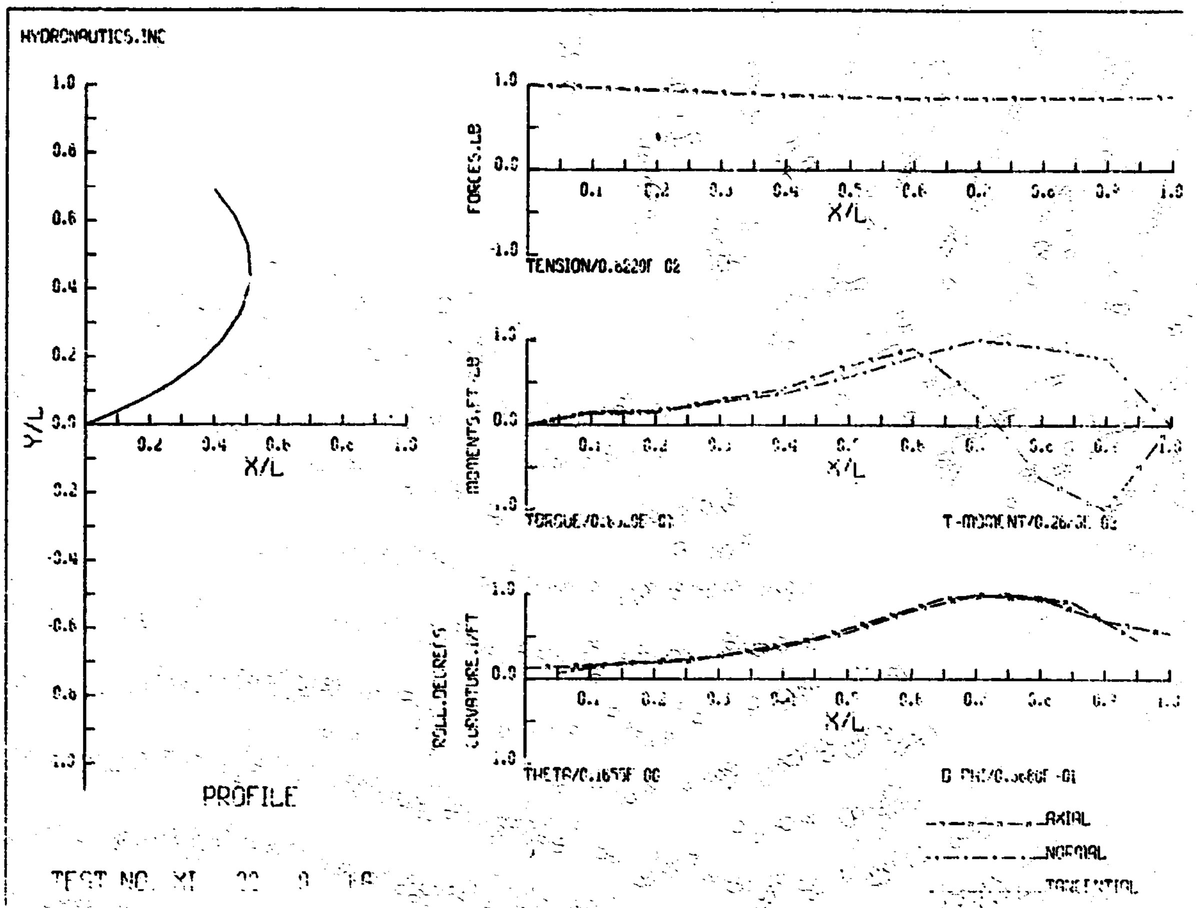

HYDRONAUTICS, INC
Y/L
X/L
PROFILE
FORCES, LB
TENSION/0.6220E 02
MOMENTS, FT-LB
ROLL, DEGREES
CURVATURE, 1/FT
AXIAL
NORMAL

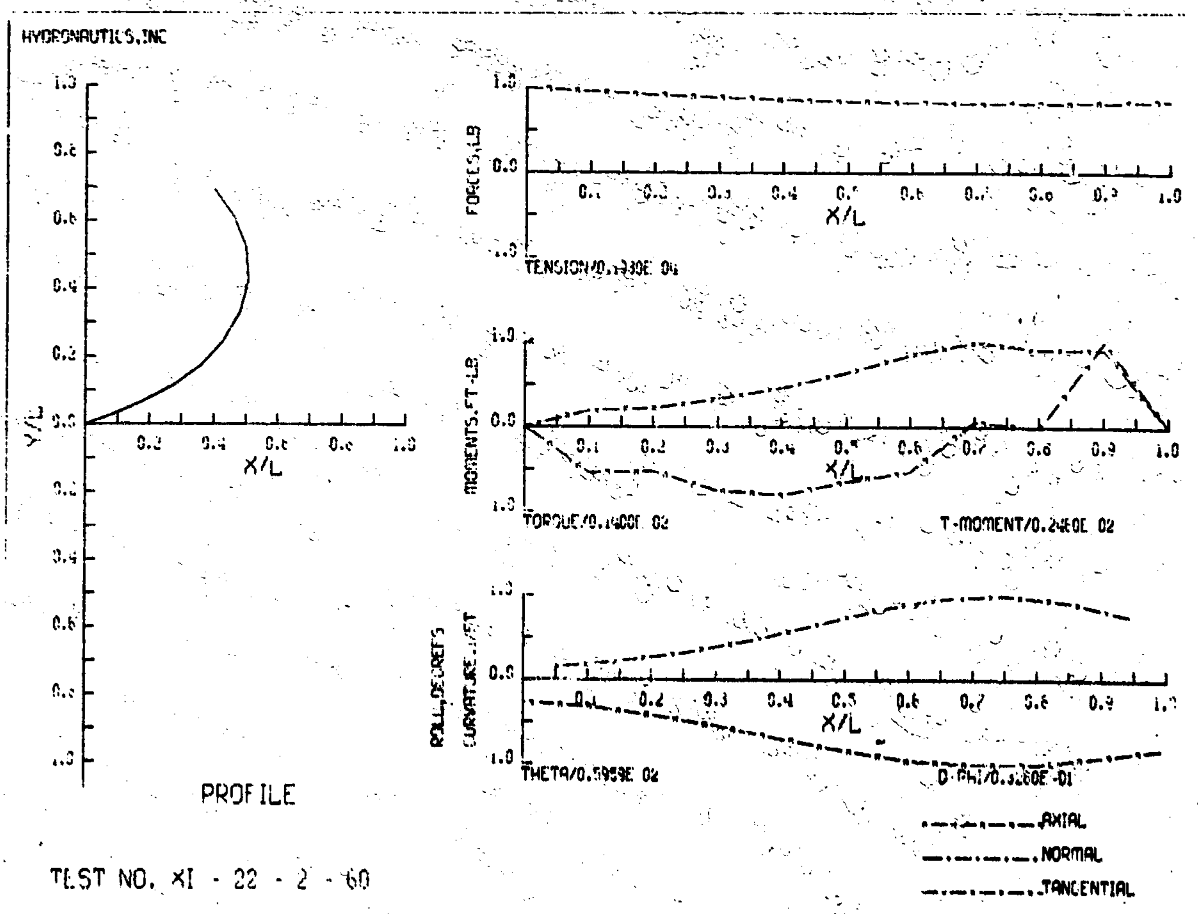

HYDRONAUTICS, INC
Y/L
X/L
PROFILE
FORCES, LB
MOMENTS, FT-LB
TORQUE/0.1400E 02
T-MOMENT/0.2460E 02
ROLL, DEGREES
CURVATURE, 1/FT
THETA/0.5959E 02
AXIAL
NORMAL
TANGENTIAL
TEST NO. XI - 22 - 2 - 60

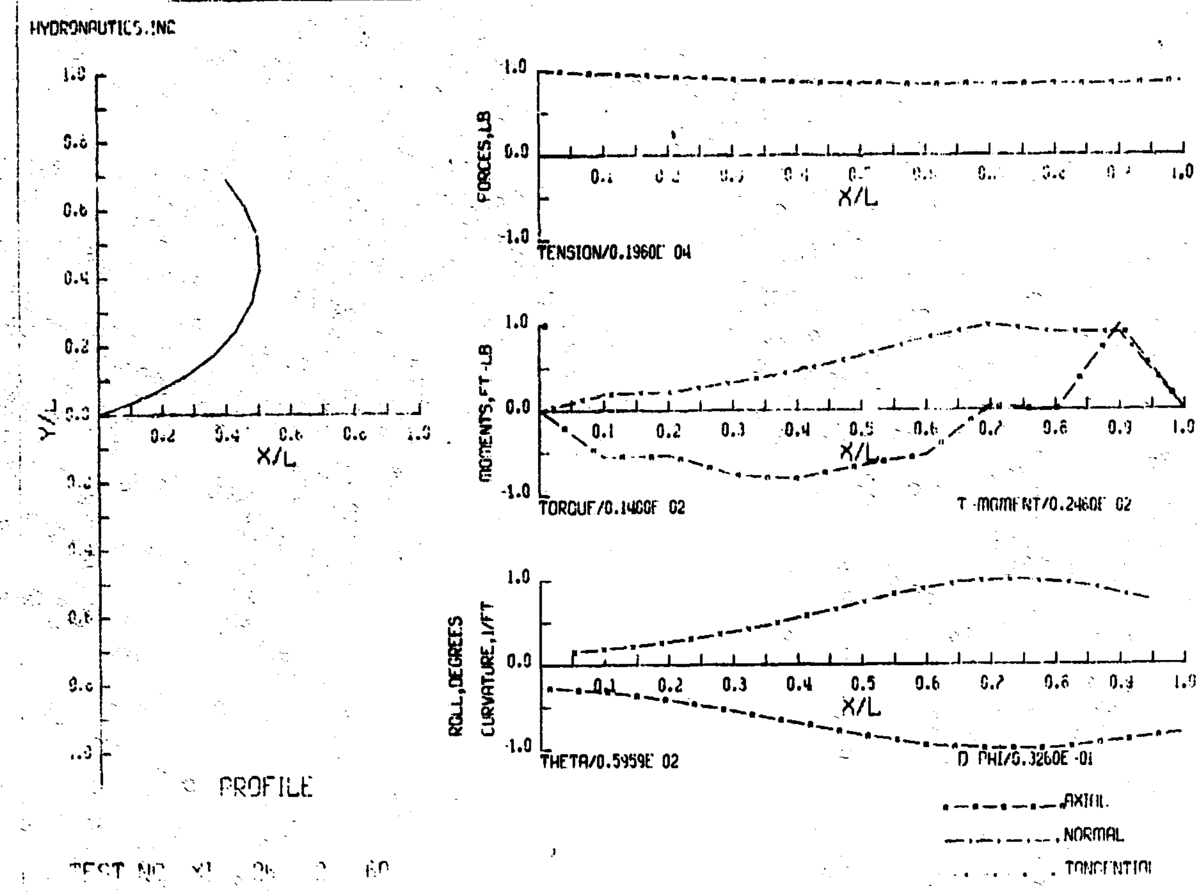

TEST NO. XI - [illegible] - 60

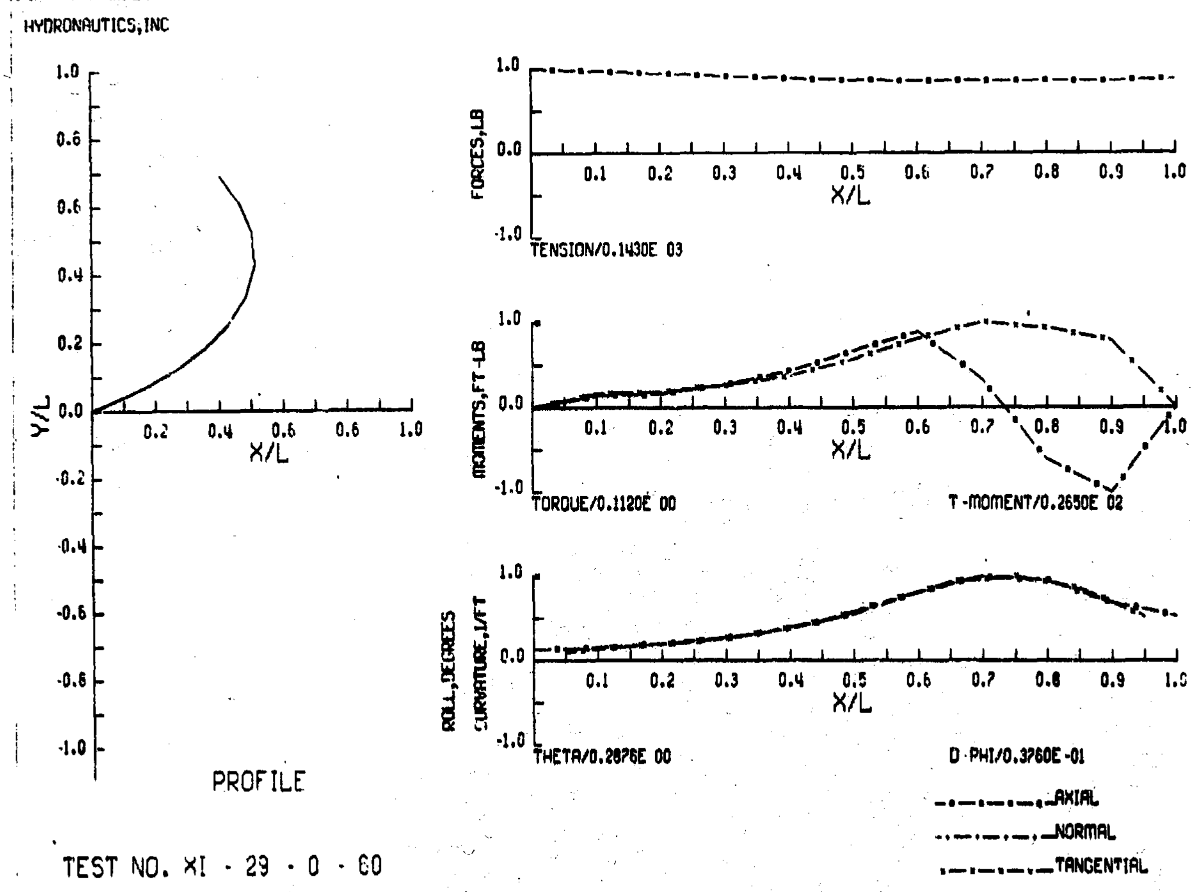

TEST NO. XI - 29 - 0 - 60

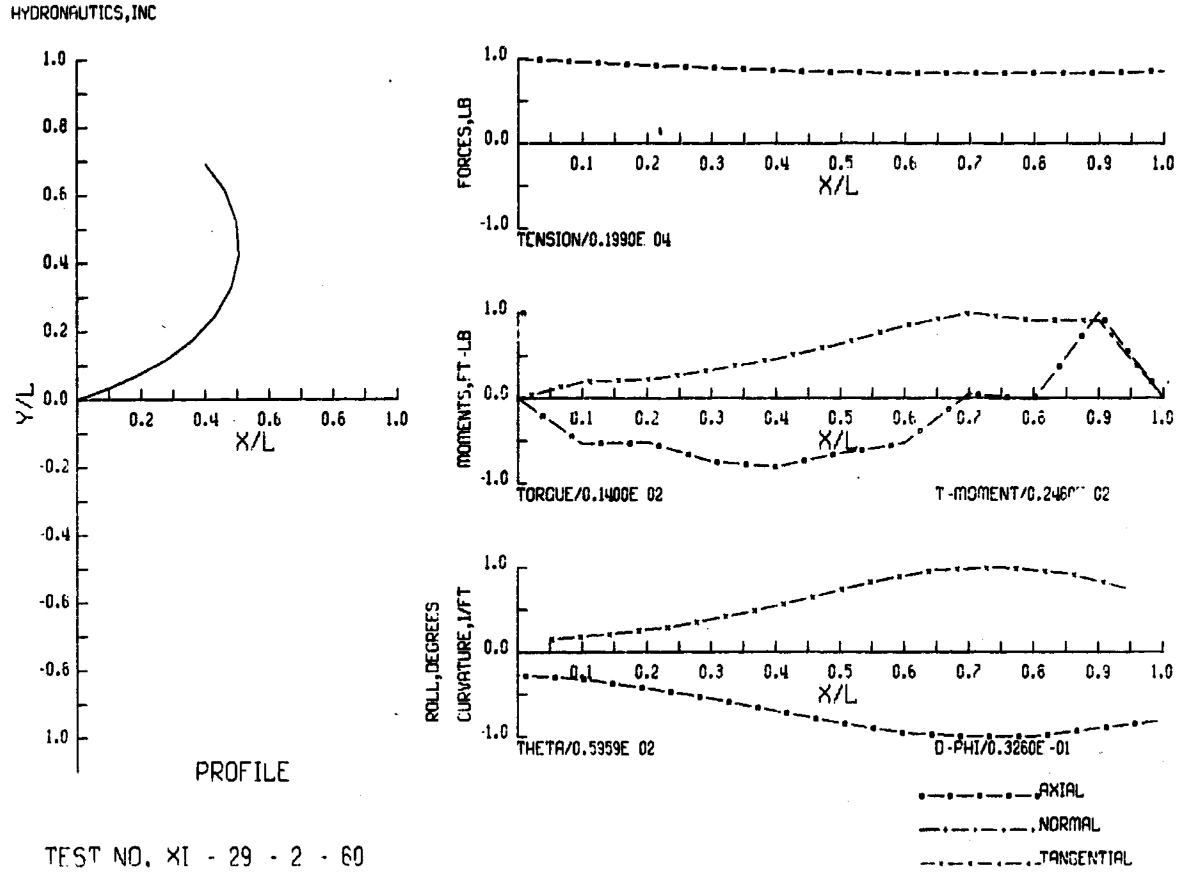

TEST NO. XI - 29 - 2 - 60

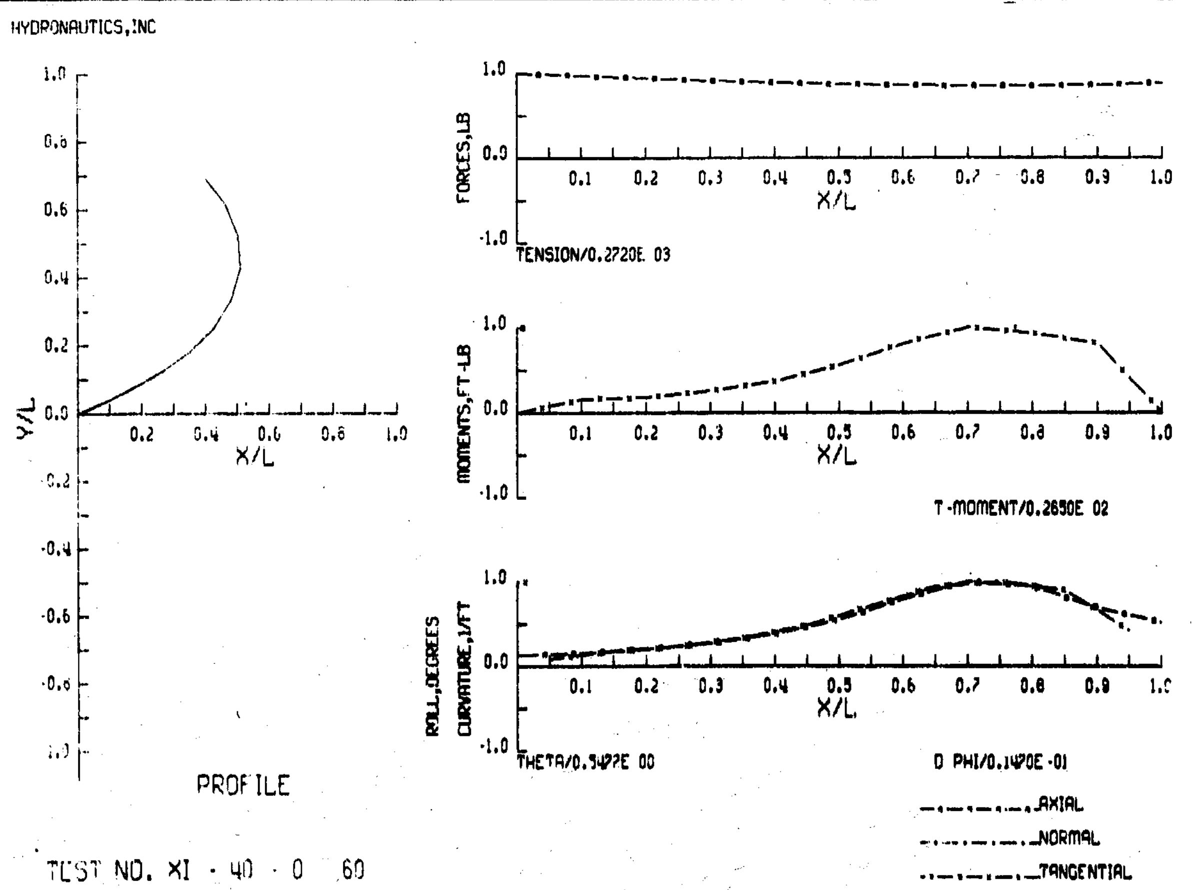

TEST NO. XI - 40 - 0 60

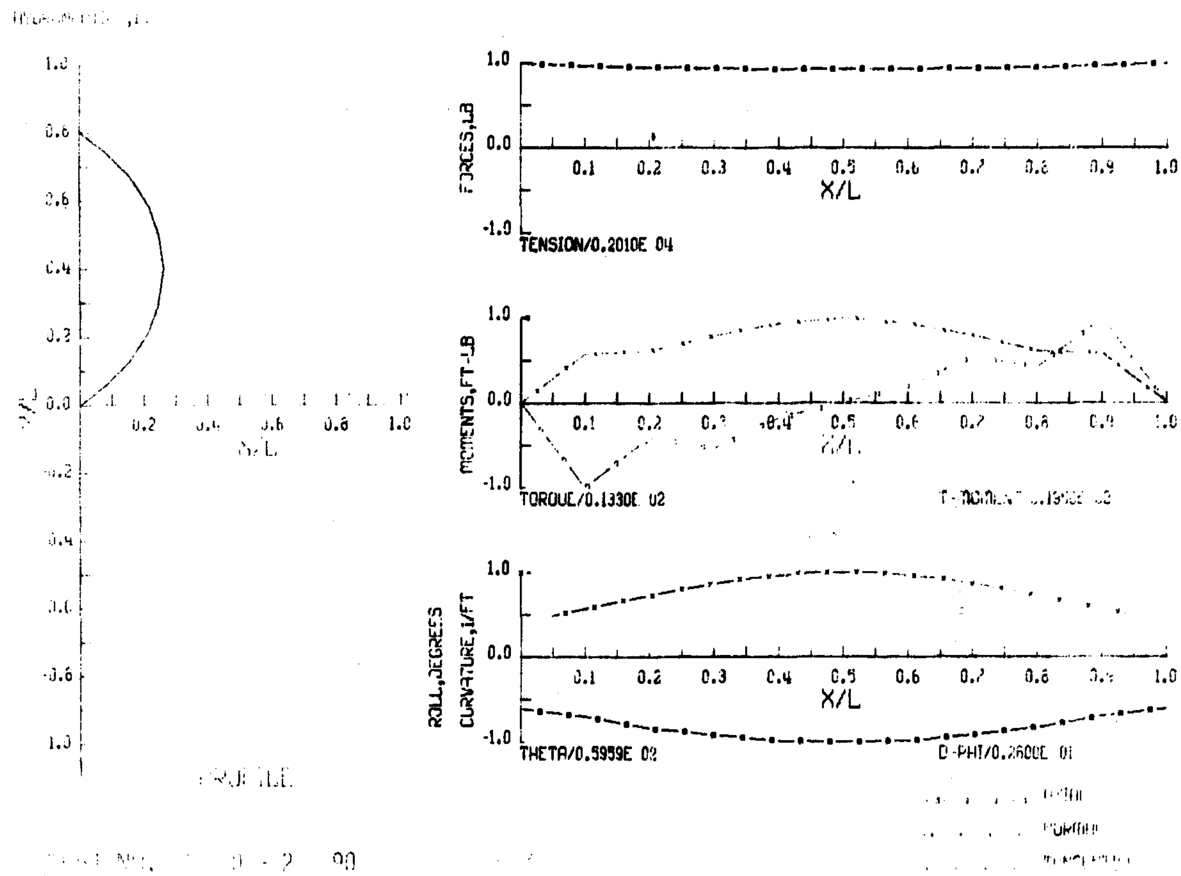
FORCES,LB
X/L
TENSION/0.2010E 04
MOMENTS,FT-LB
TORQUE/0.1330E 02
ROLL,DEGREES
CURVATURE,1/FT
THETA/0.5959E 02
D-PHI/0.2600E 01
PROFILE

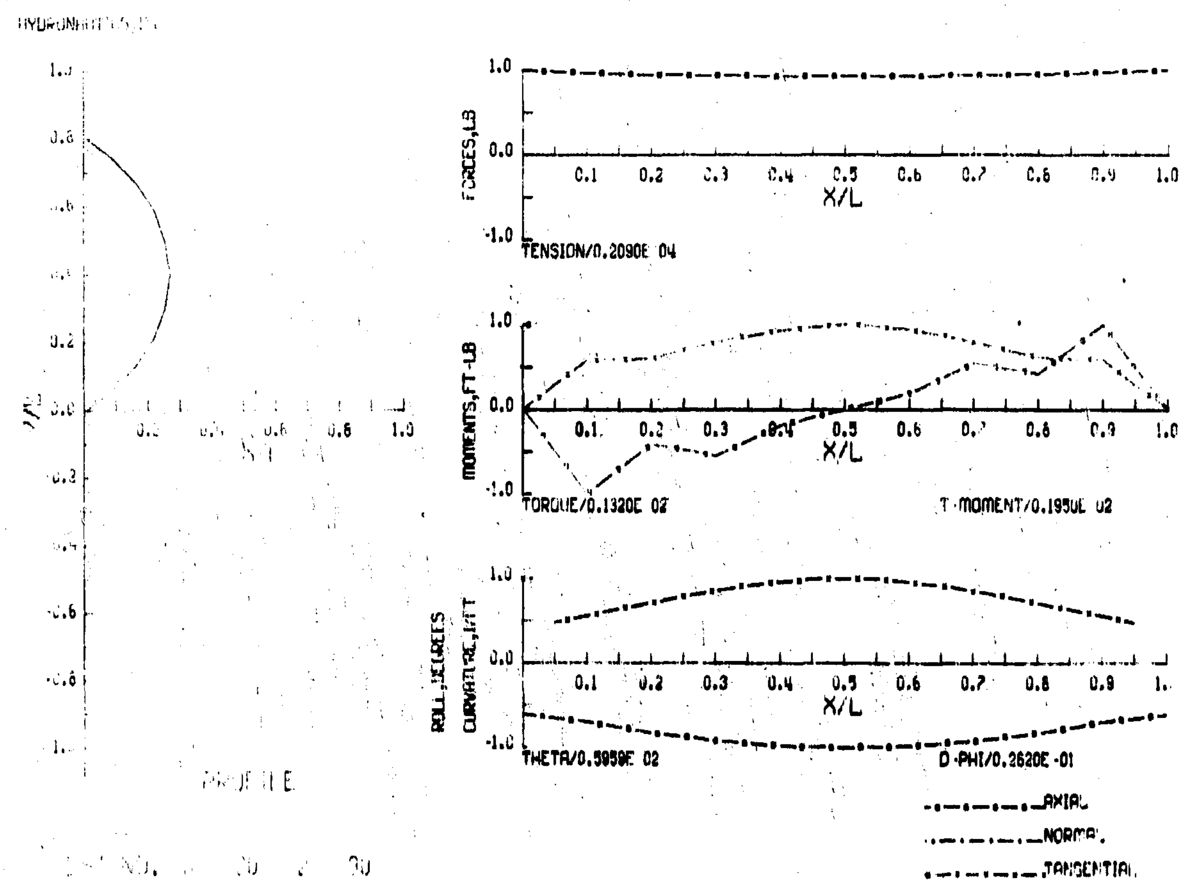
HYDRONAUTICS,INC.
FORCES,LB
X/L
TENSION/0.2090E 04
MOMENTS,FT-LB
TORQUE/0.1320E 02
T-MOMENT/0.1950E 02
ROLL,DEGREES
CURVATURE,1/FT
THETA/0.5959E 02
D-PHI/0.2620E -01
AXIAL
NORMAL
TANGENTIAL
PROFILE

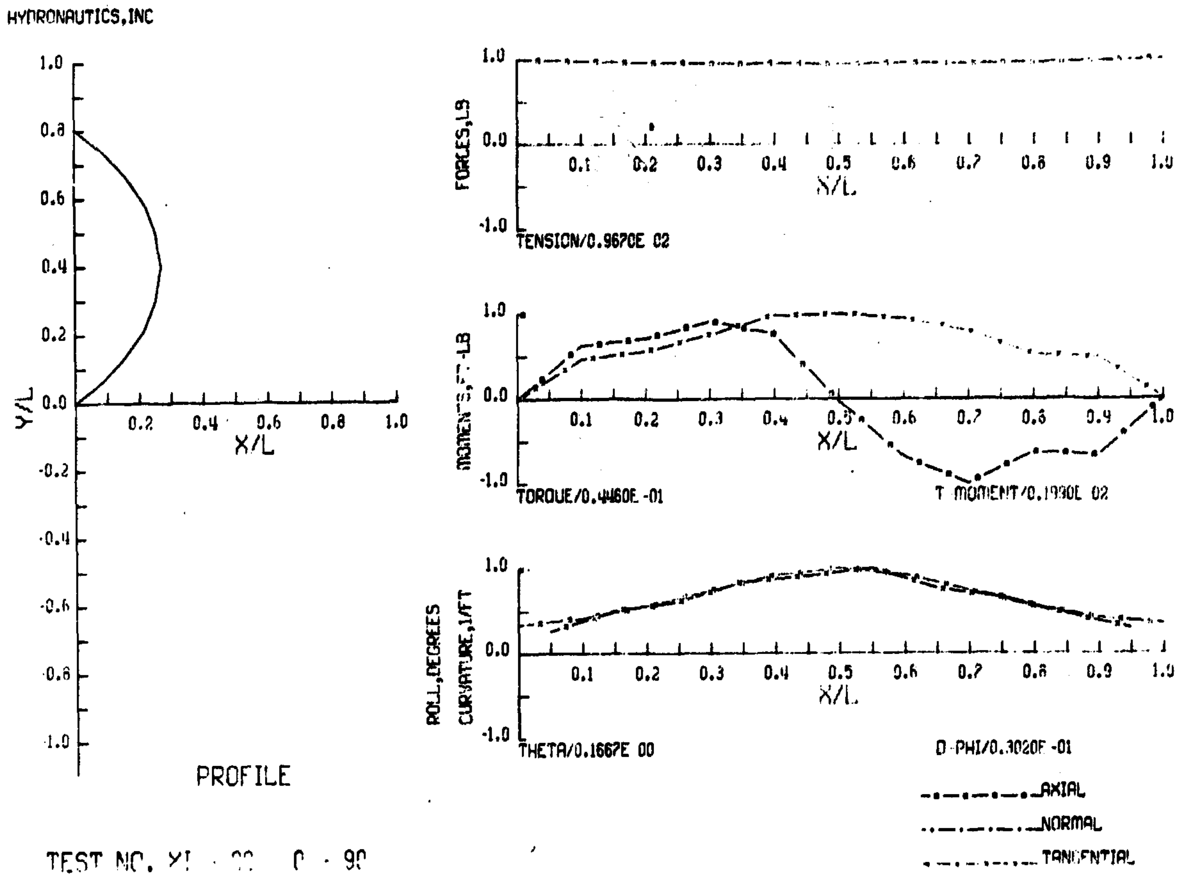
HYDRONAUTICS,INC
Y/L
X/L
PROFILE
FORCES,LB
TENSION/0.9670E 02
MOMENTS,FT-LB
TORQUE/0.4460E -01
T MOMENT/0.1990E 02
ROLL,DEGREES
CURVATURE,1/FT
THETA/0.1667E 00
D-PHI/0.3020E -01
AXIAL
NORMAL
TANGENTIAL

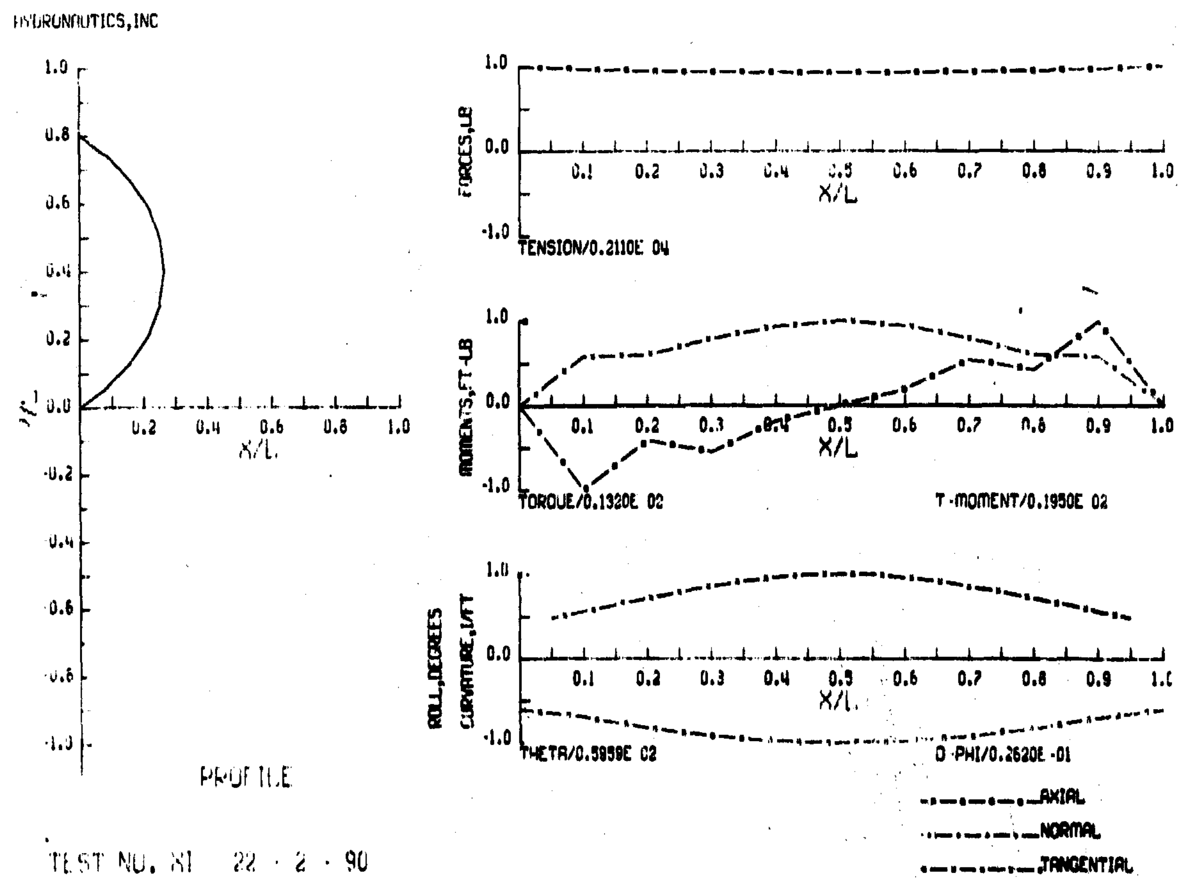
HYDRONAUTICS,INC
X/L
PROFILE
FORCES,LB
TENSION/0.2110E 04
MOMENTS,FT-LB
TORQUE/0.1320E 02
T-MOMENT/0.1950E 02
ROLL,DEGREES
CURVATURE,1/FT
THETA/0.5959E 02
D-PHI/0.2620E -01
AXIAL
NORMAL
TANGENTIAL
TEST NO. 81 22 - 2 - 90

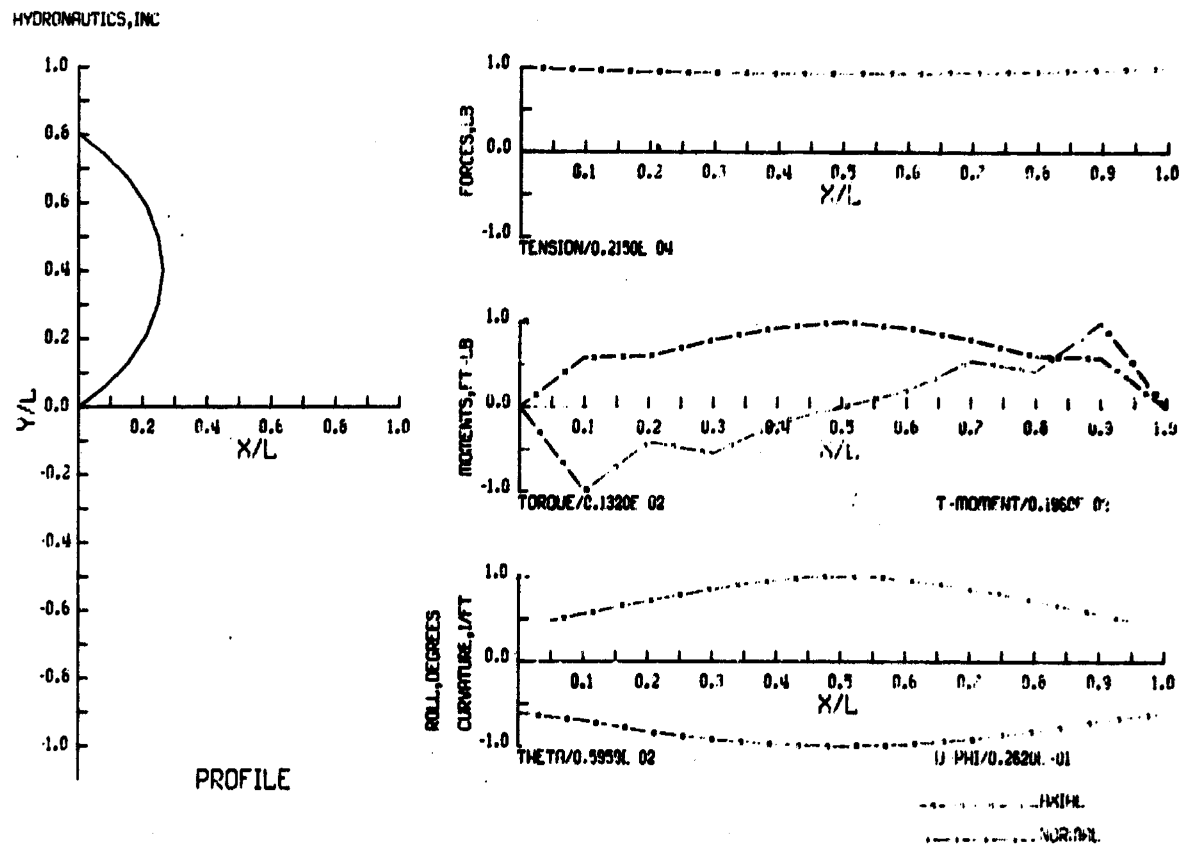

TEST NO. XI - 26 - 2 - 90

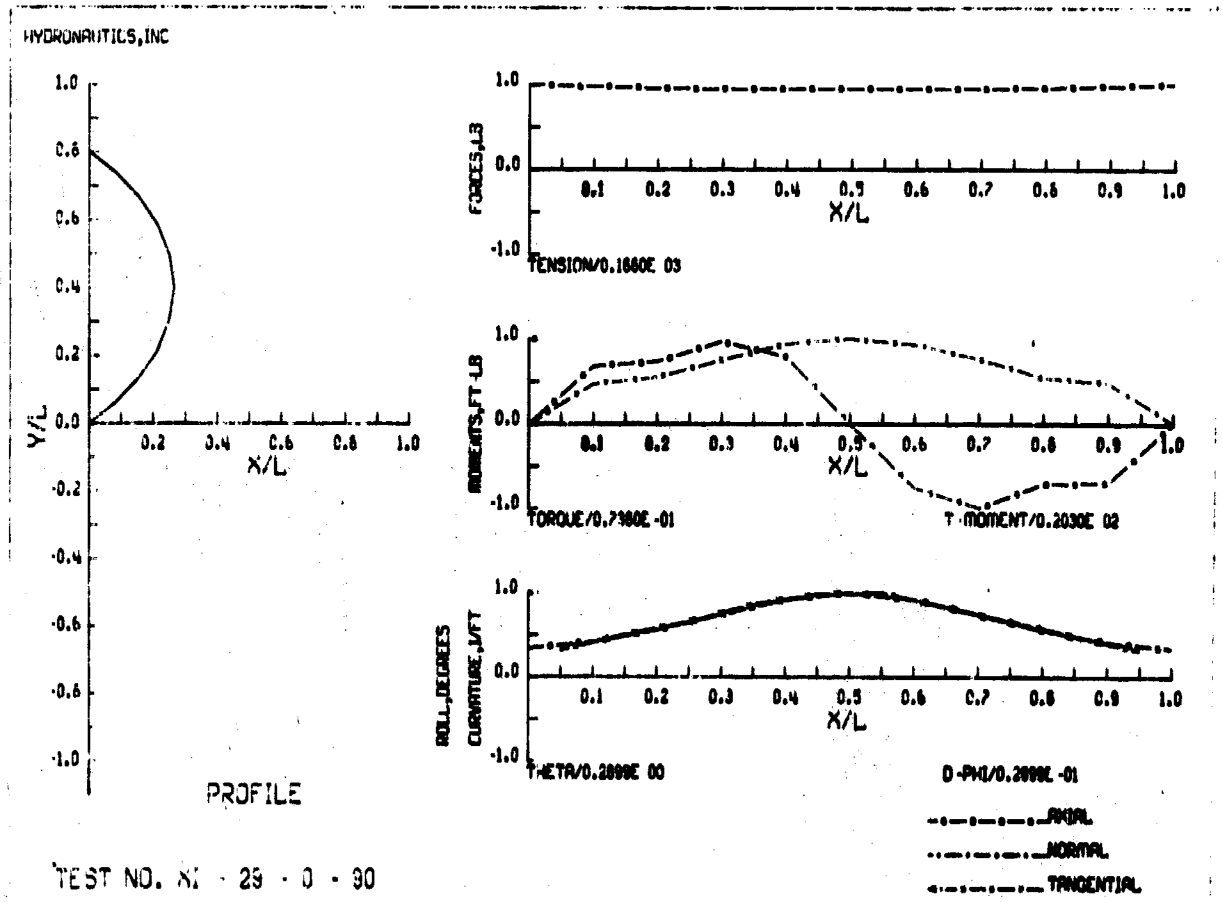

TEST NO. XI - 29 - 0 - 90

HYDRONAUTICS,INC

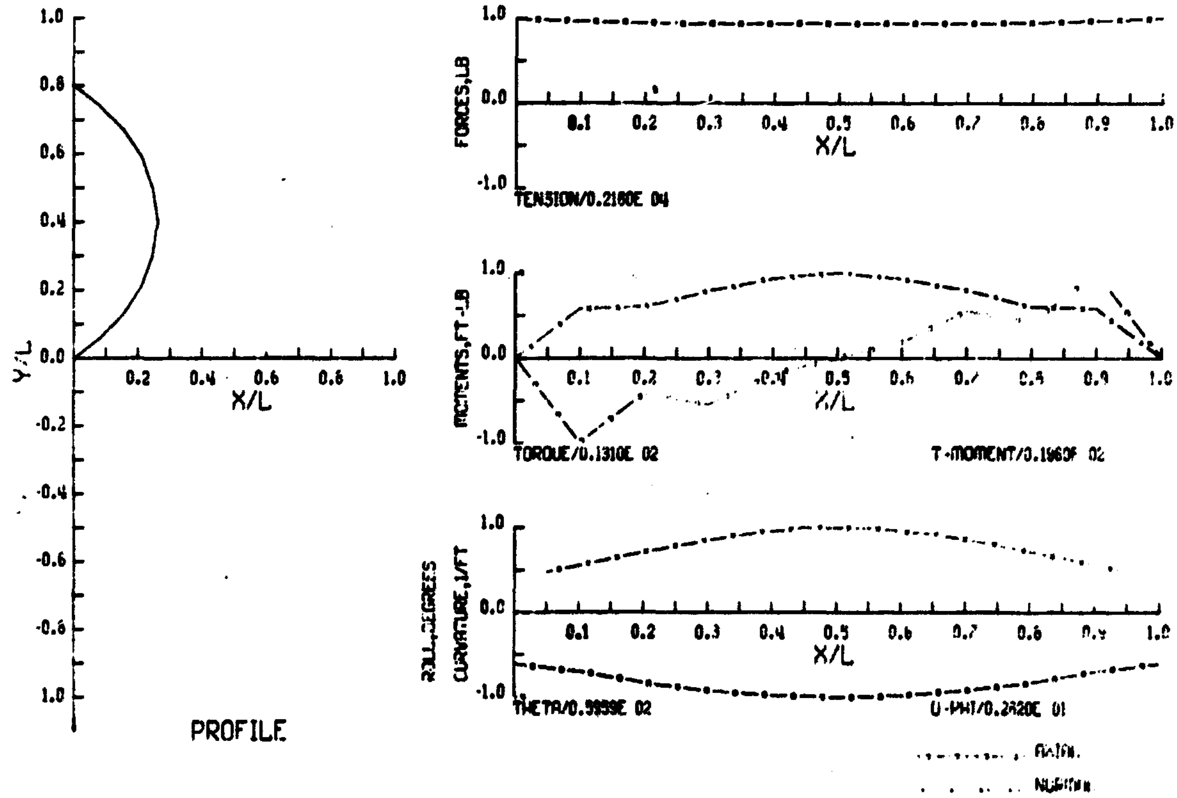

TEST NO. XI - 39 - 0 - 90

HYDRONAUTICS,INC

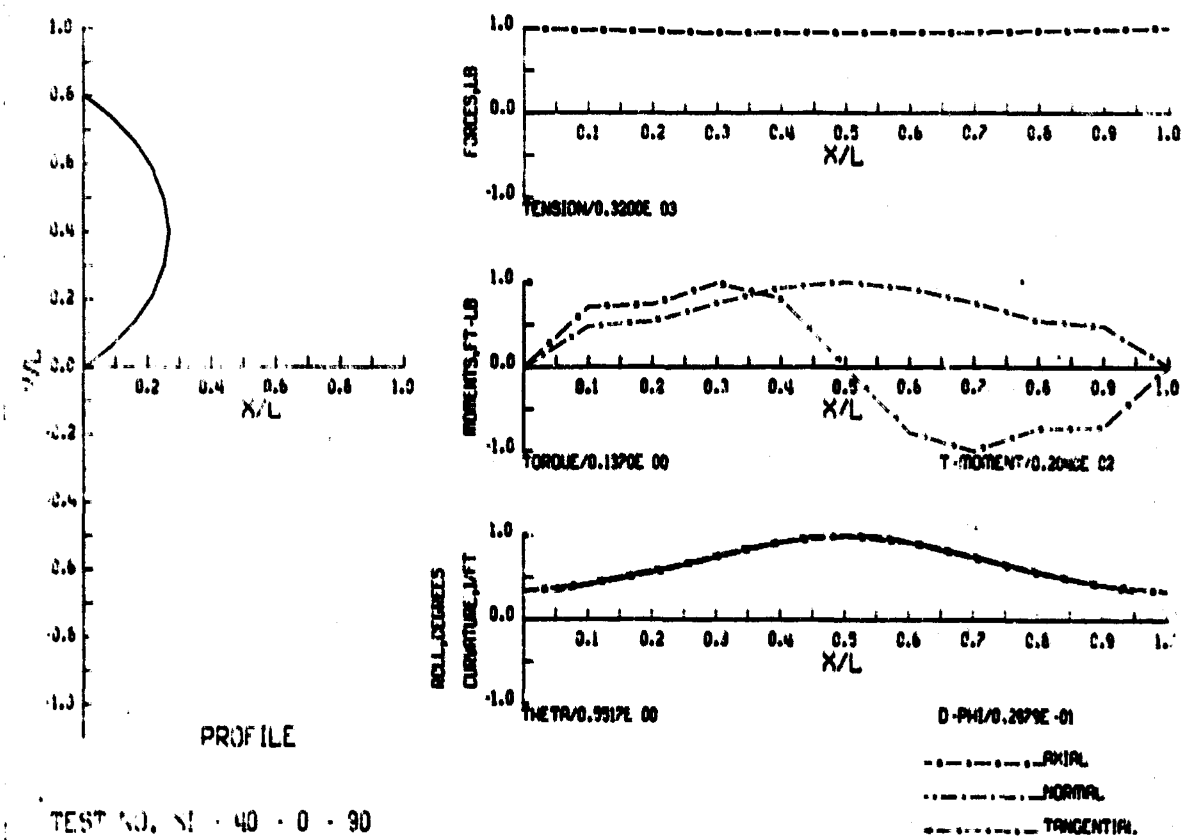

TEST NO. XI - 40 - 0 - 90

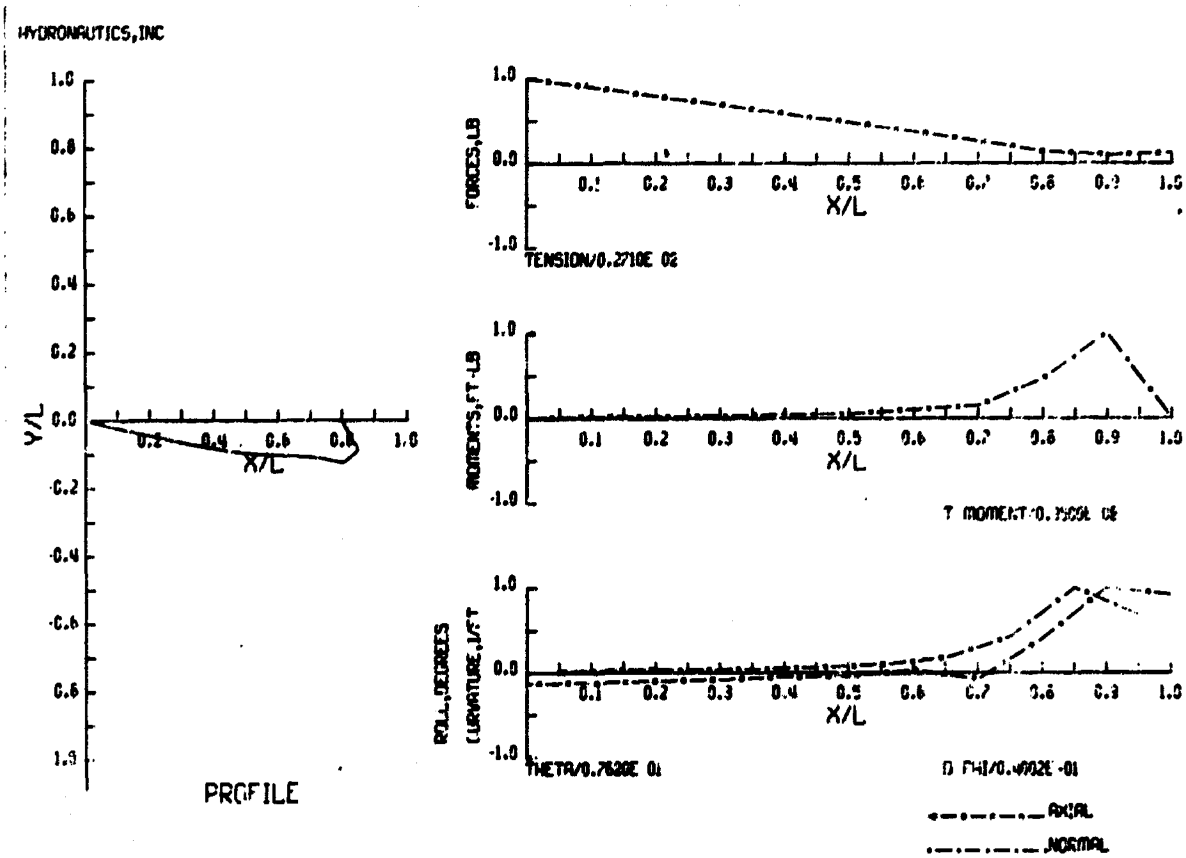

TEST NO. XII - 22 - 0 - 0

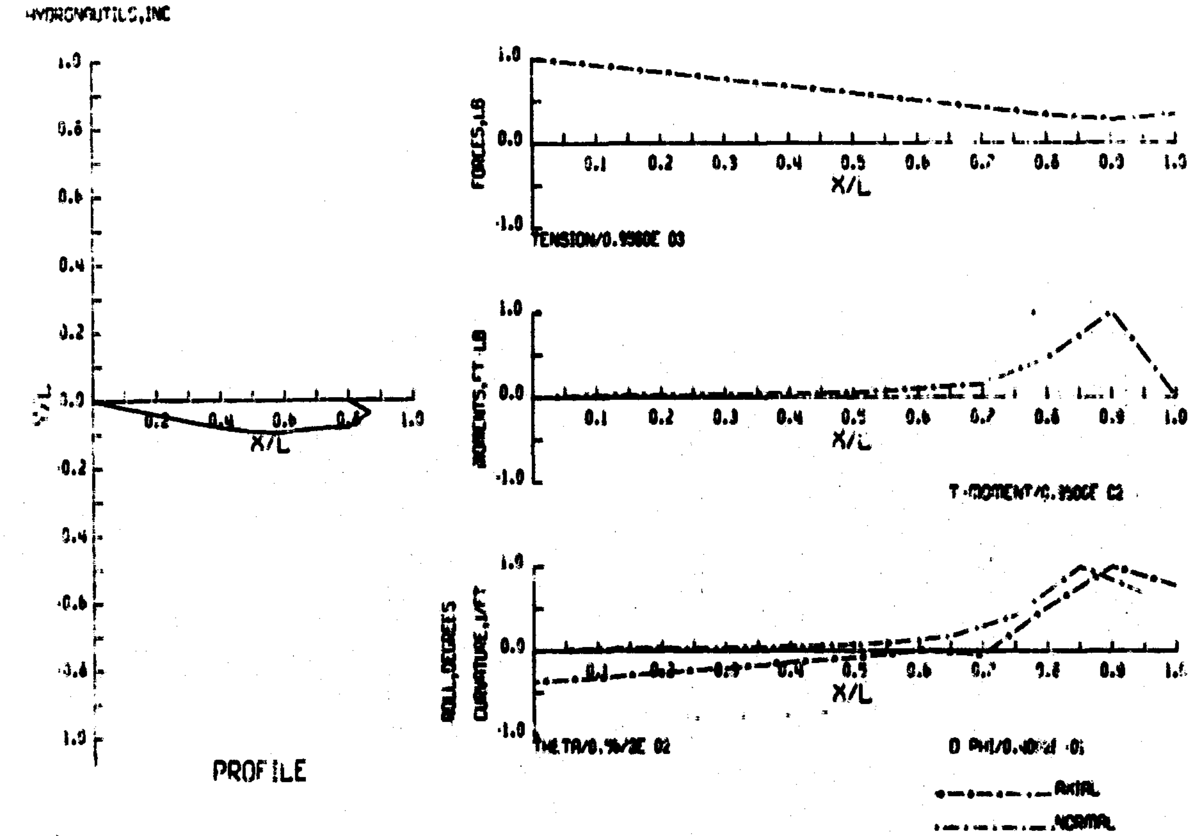

TEST NO. XII - 22 - 2 - 0

HYDRONAUTICS, INC

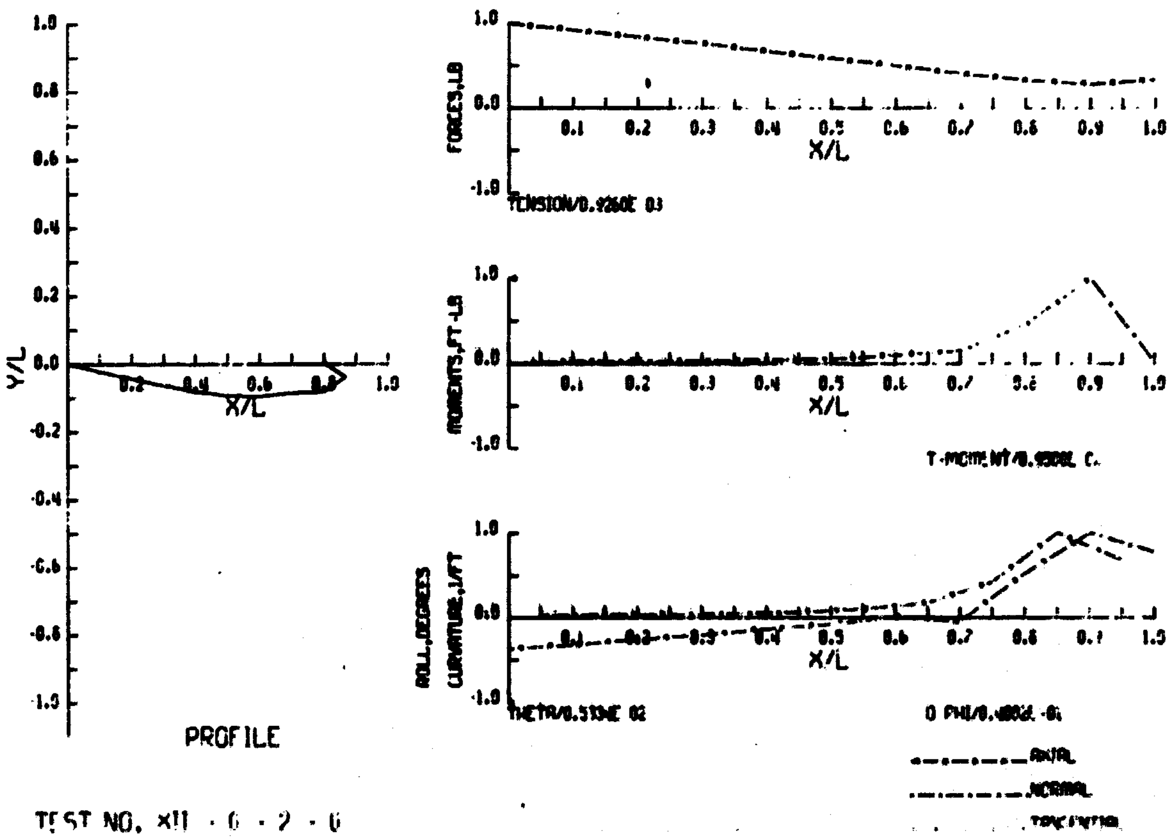

TEST NO. XII - 6 - 2 - 0

HYDRONAUTICS, INC

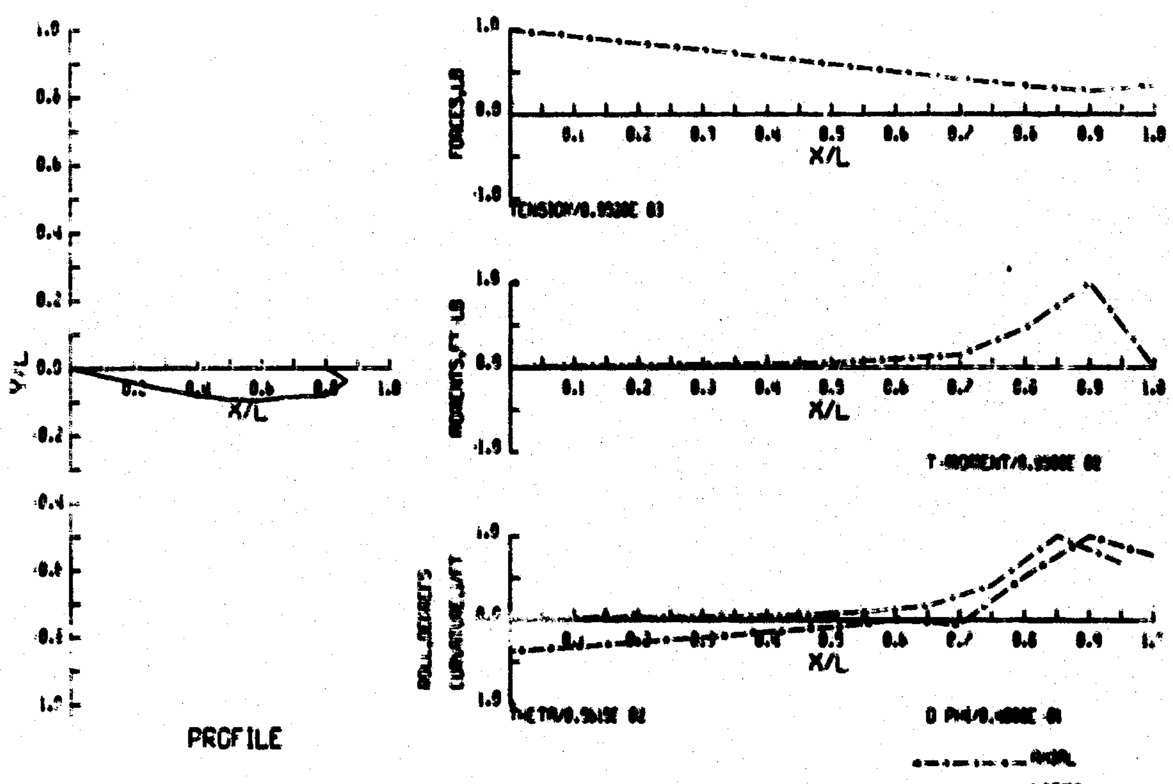

TEST NO. XII - 20 - 2 - 0

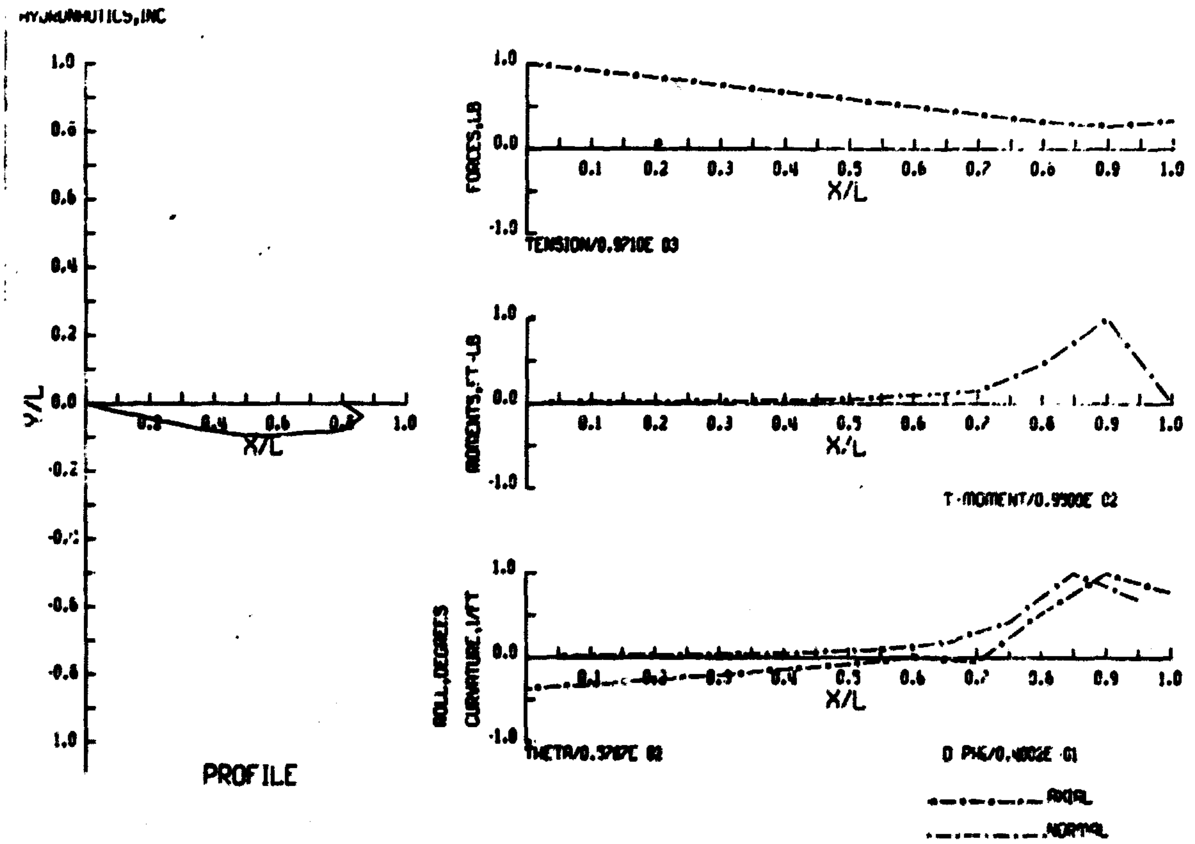

TEST NO. XII · 26 · 2 · 0

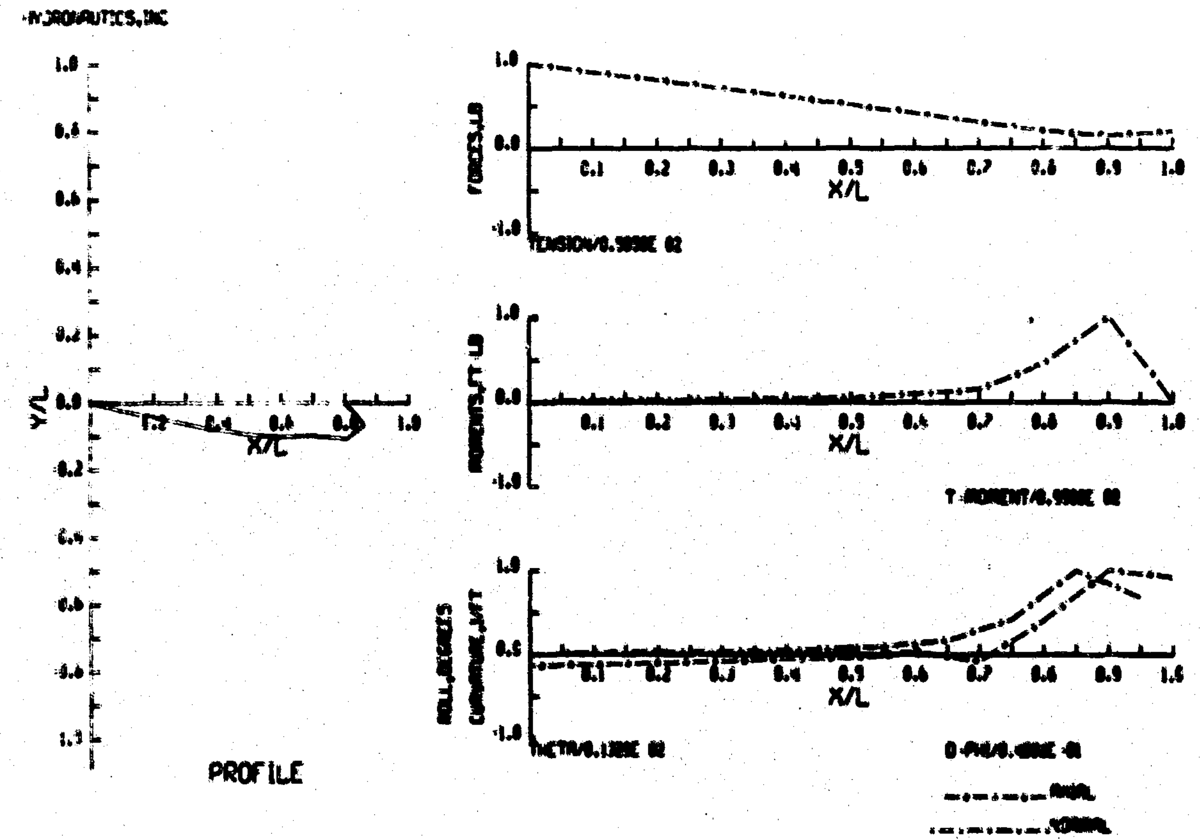

TEST NO. XII · 29 · 0 · 0

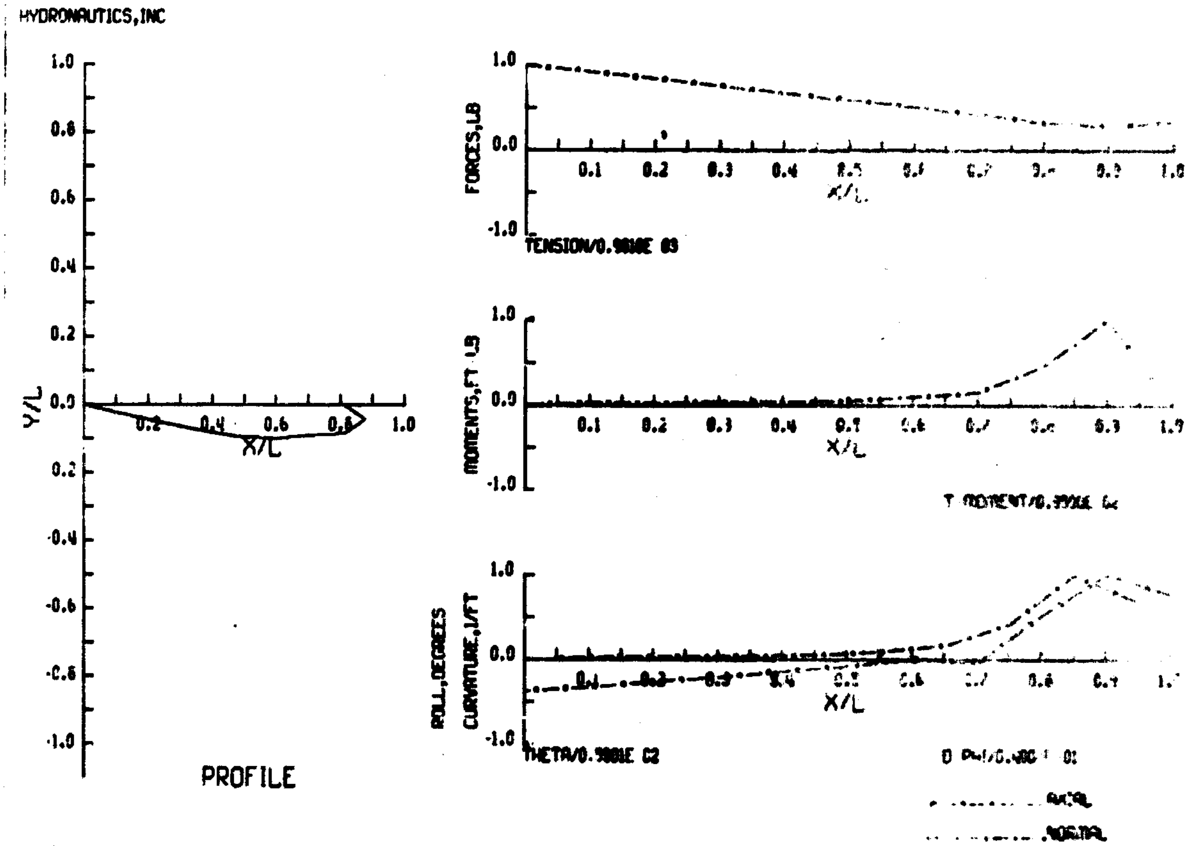

TEST NO. XII - 29 - 2 - 0

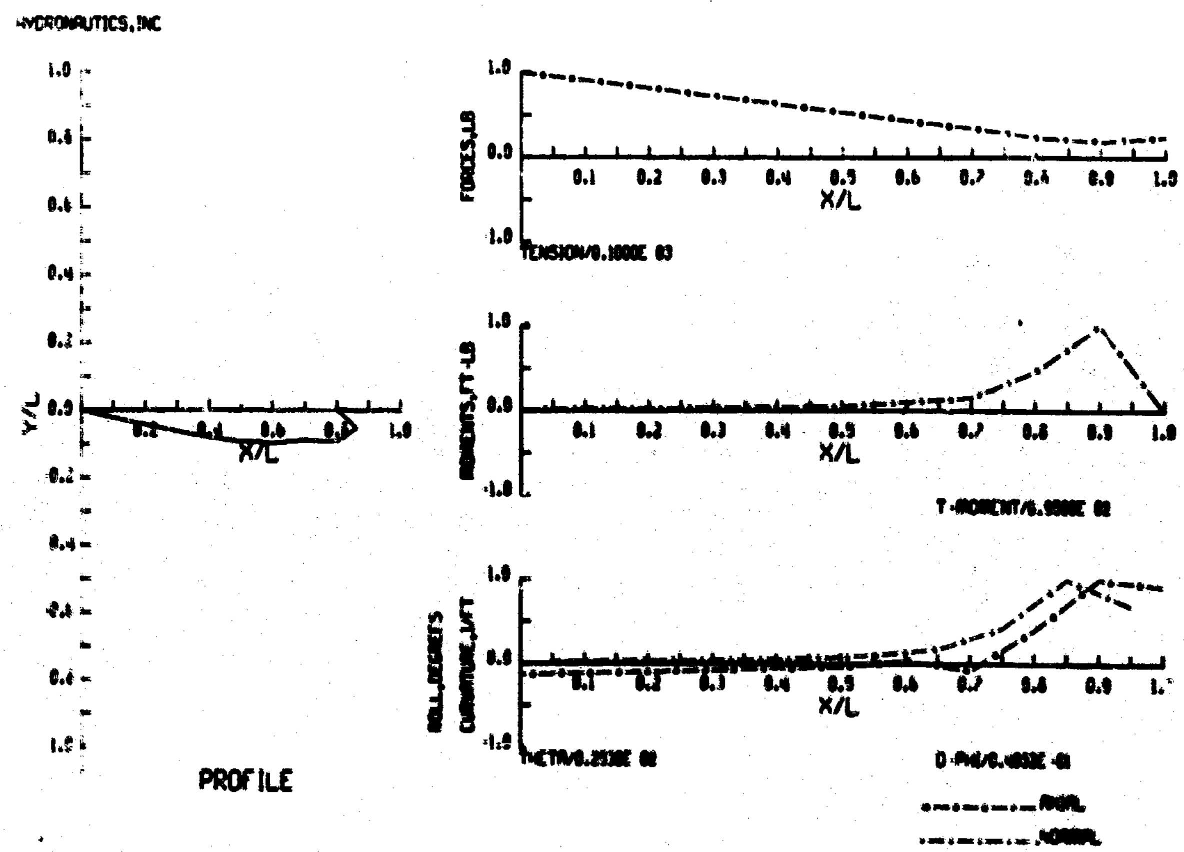

TEST NO. XII - 40 - 0 - 0

HYDRONAUTICS,INC

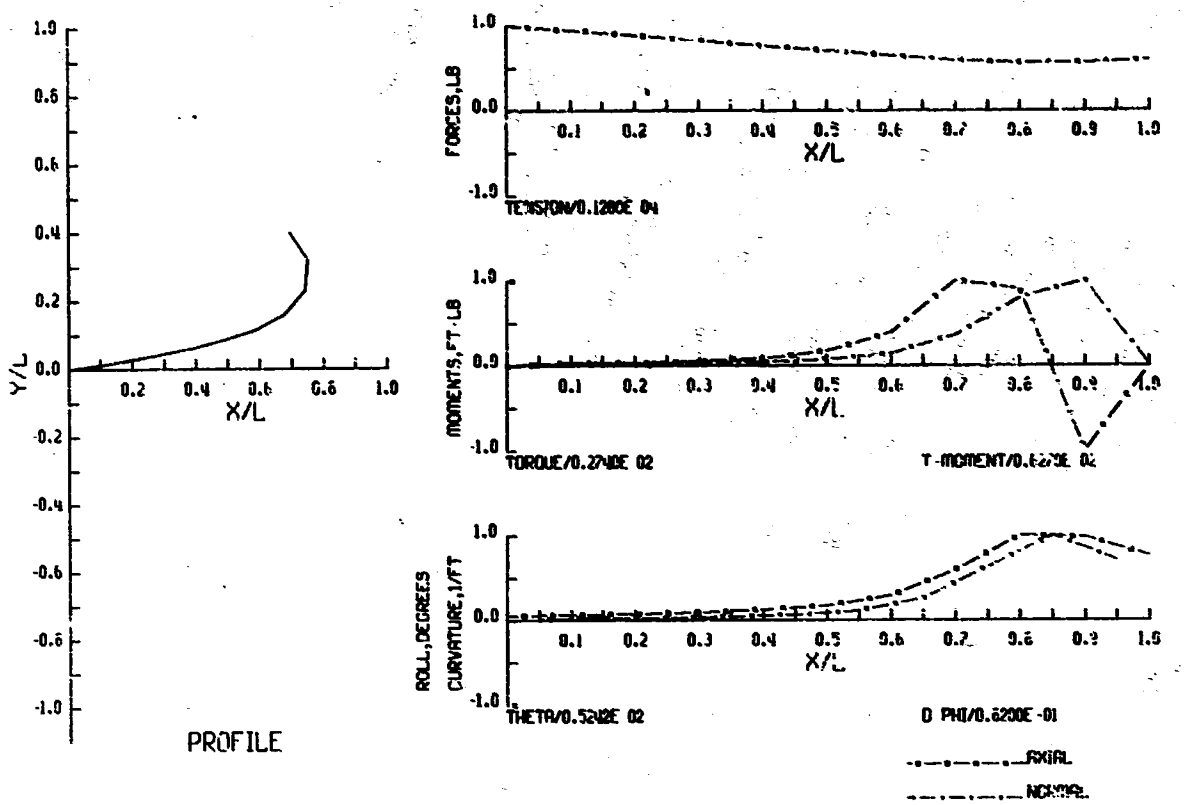

TEST NO. XII - 0 - 2 - 30

HYDRONAUTICS,INC

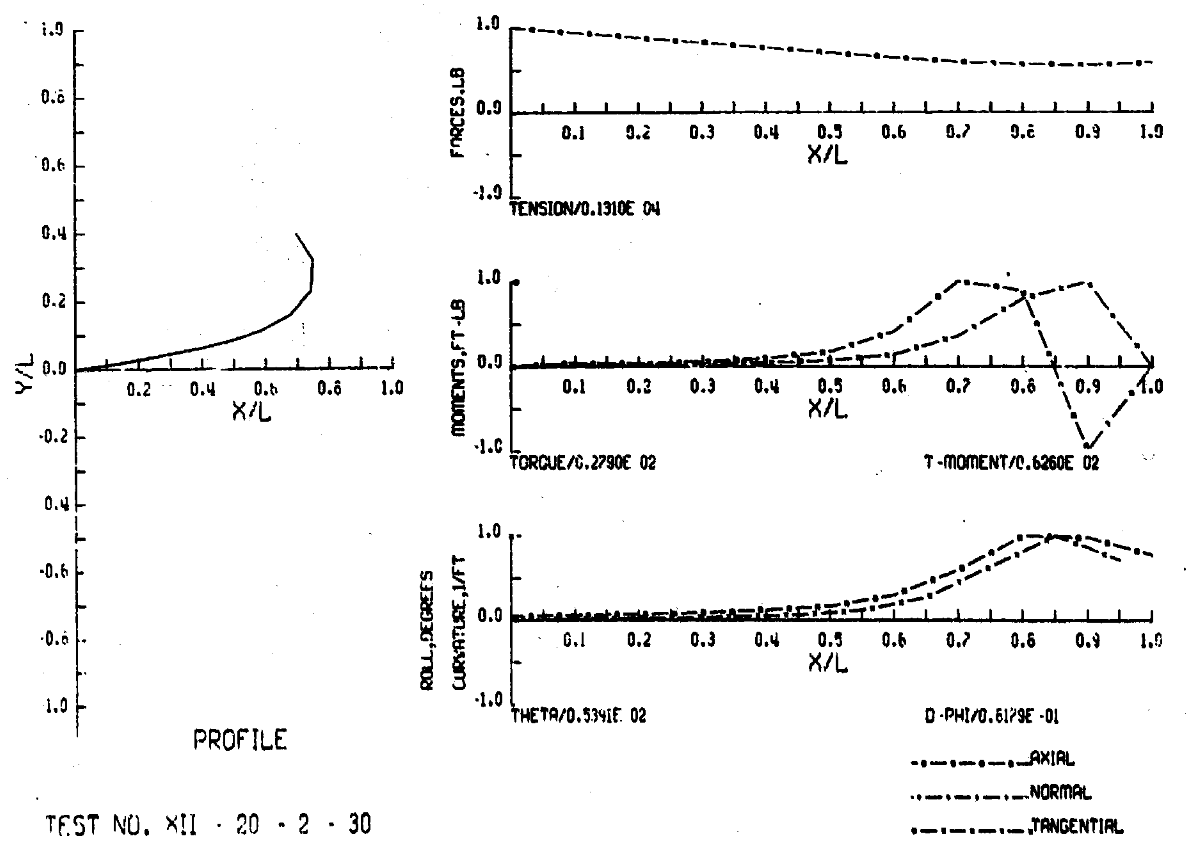

TEST NO. XII - 20 - 2 - 30

HYDRONAUTICS, INC

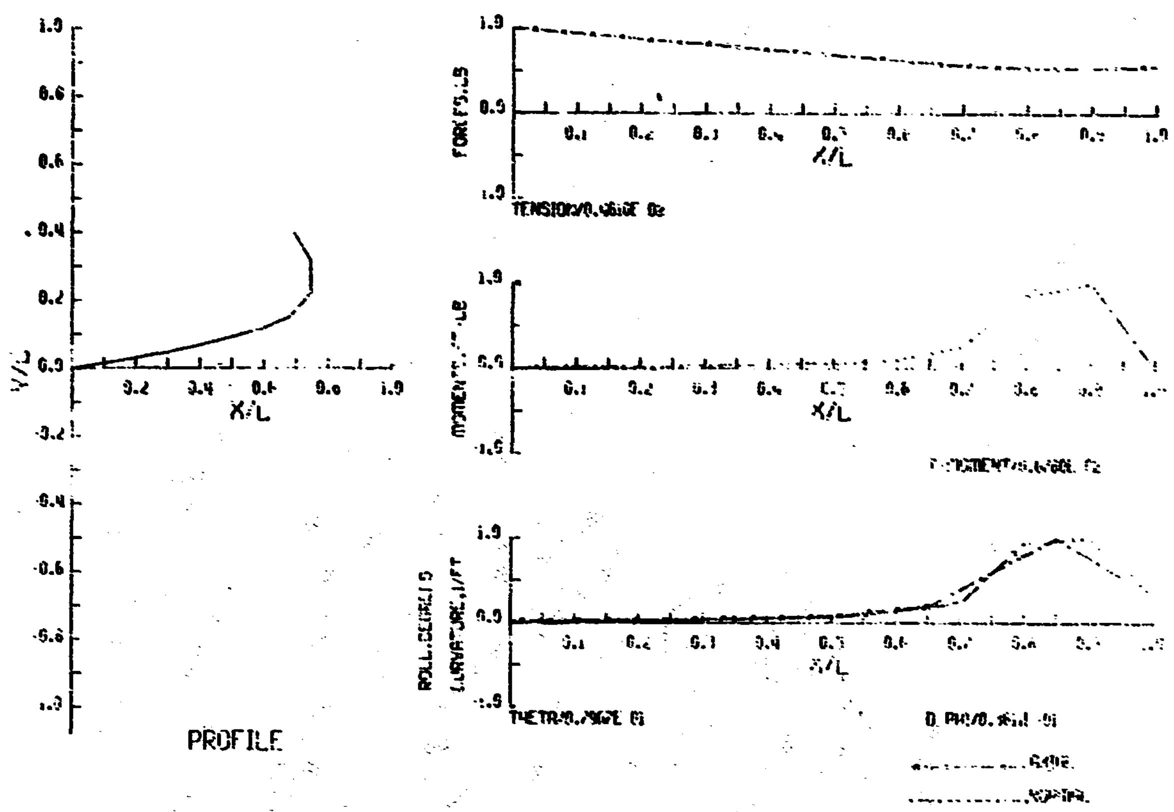

TEST NO. XII

HYDRONAUTICS, INC

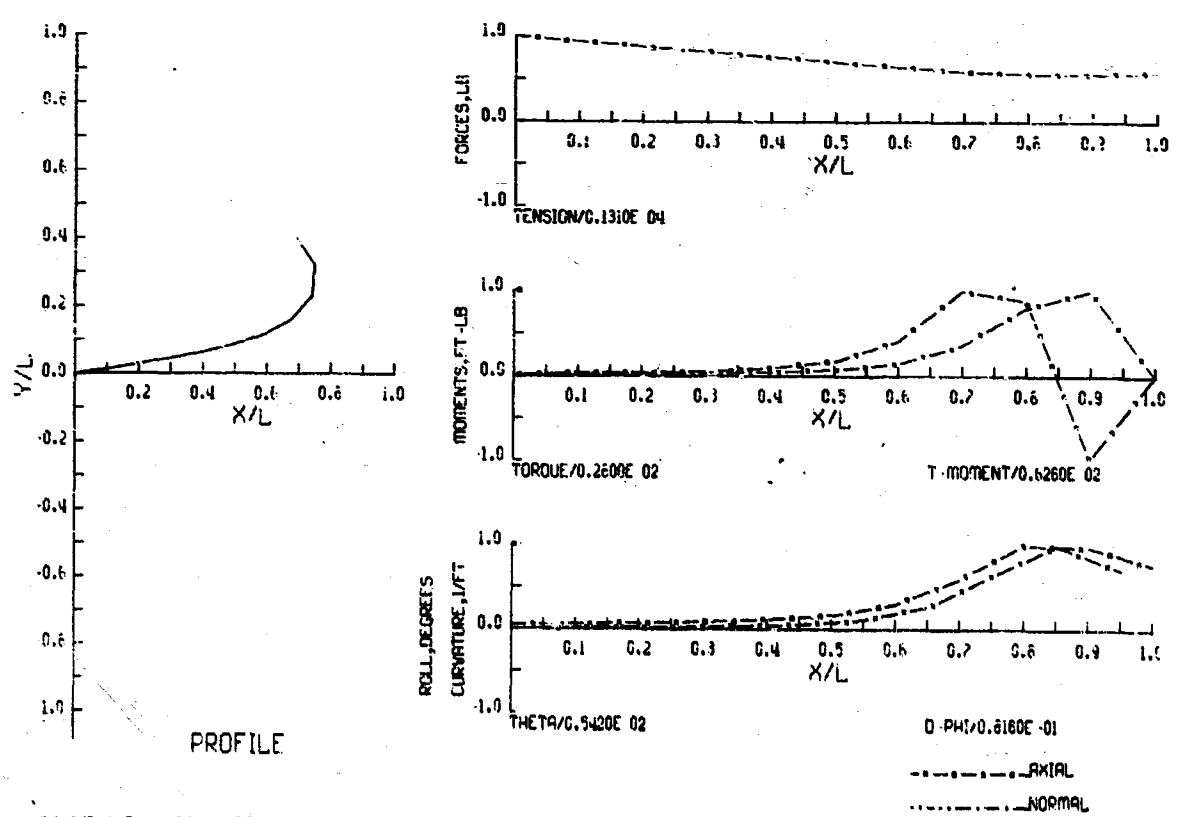

TEST NO. XII - 22 - 2 - 30

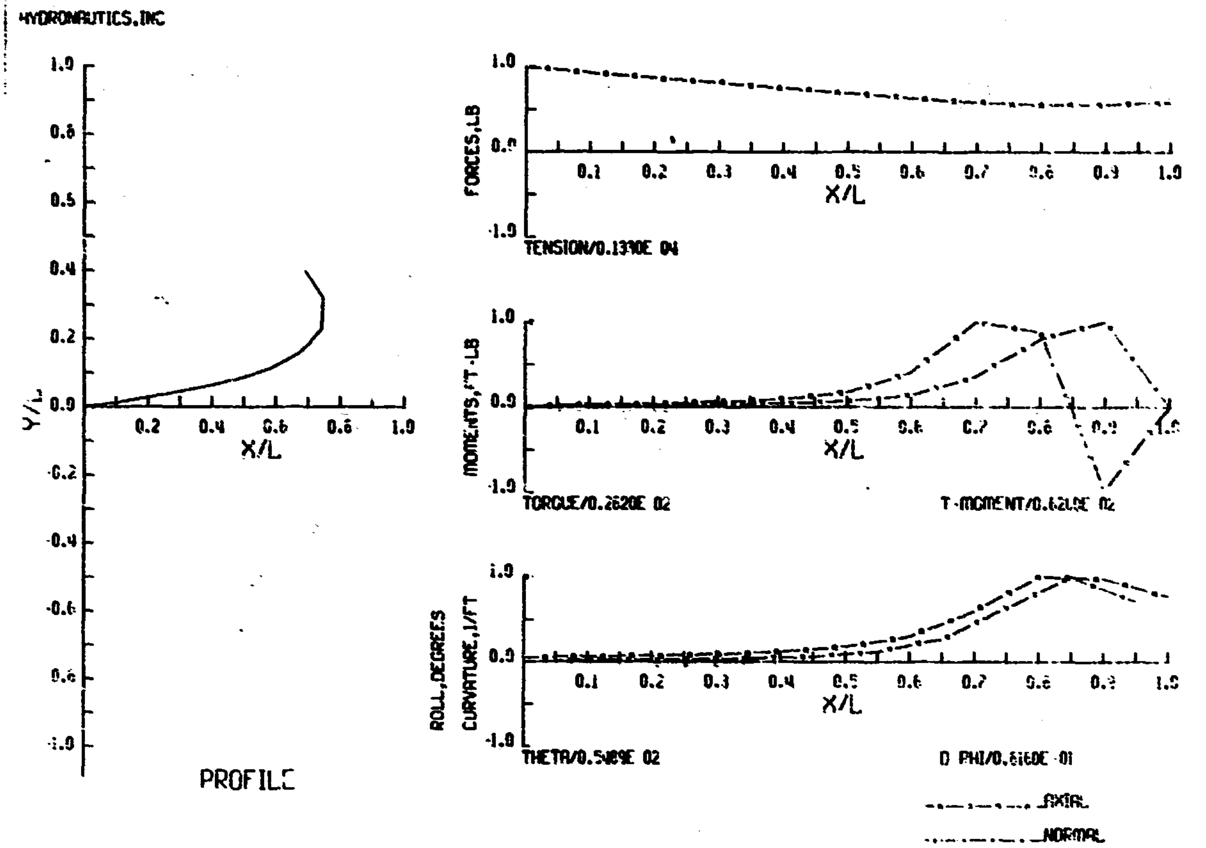

TEST NO. XII - 29 - 2 - 30

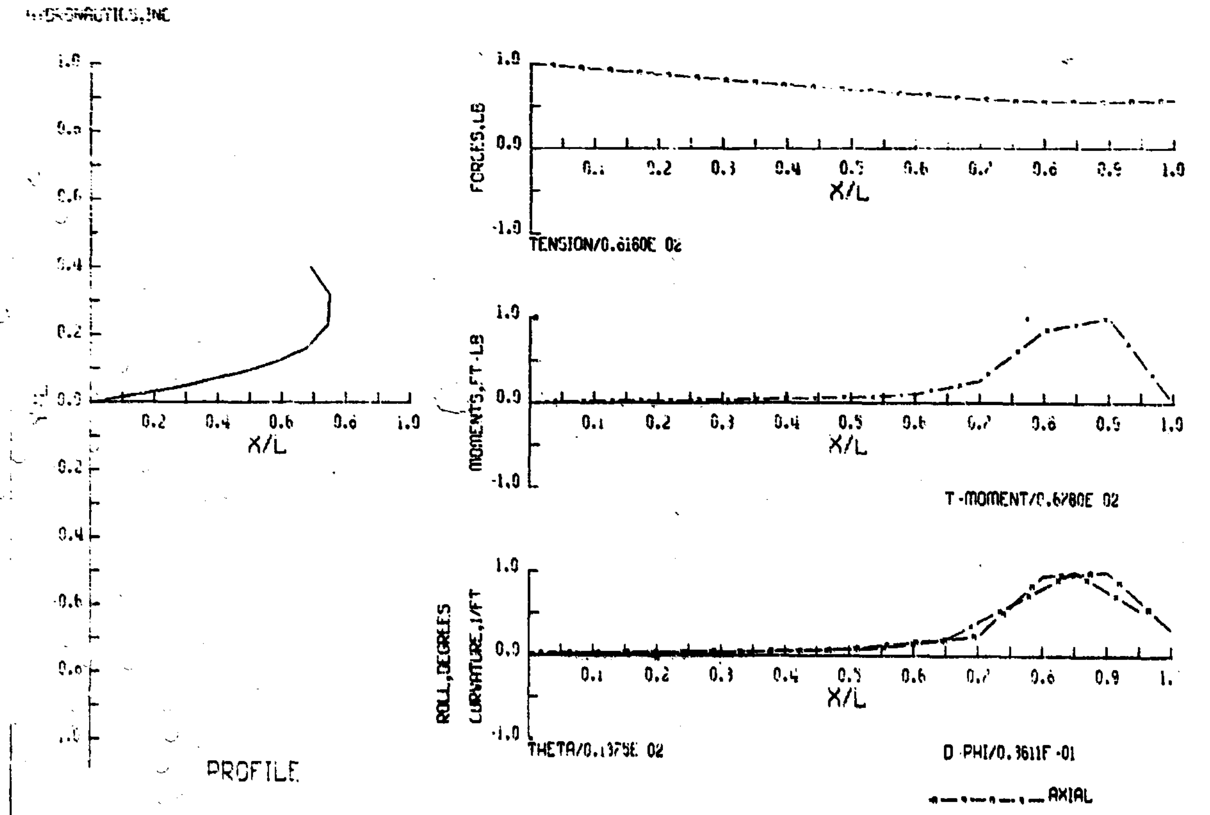

TEST NO. XII - 29 - 0 - 30

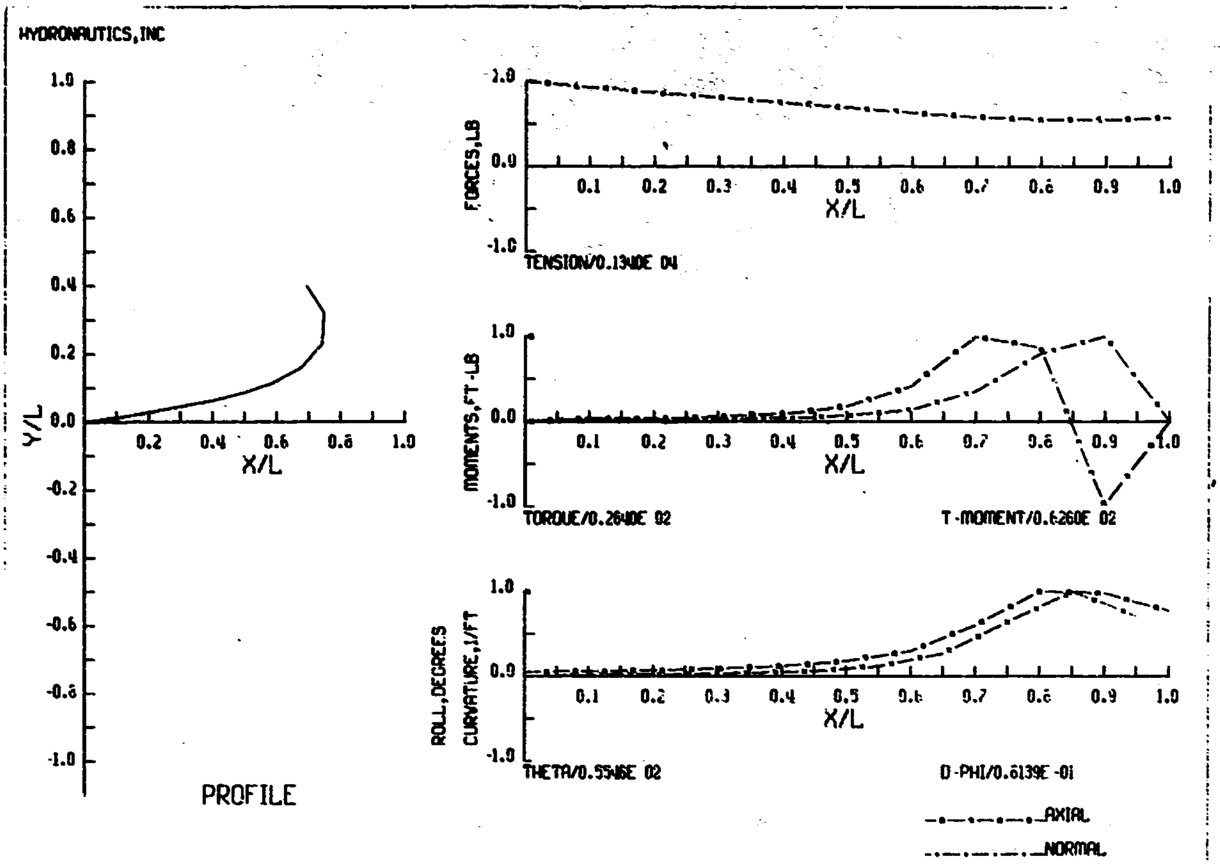

TEST NO. XII - 29 - 2 - 30

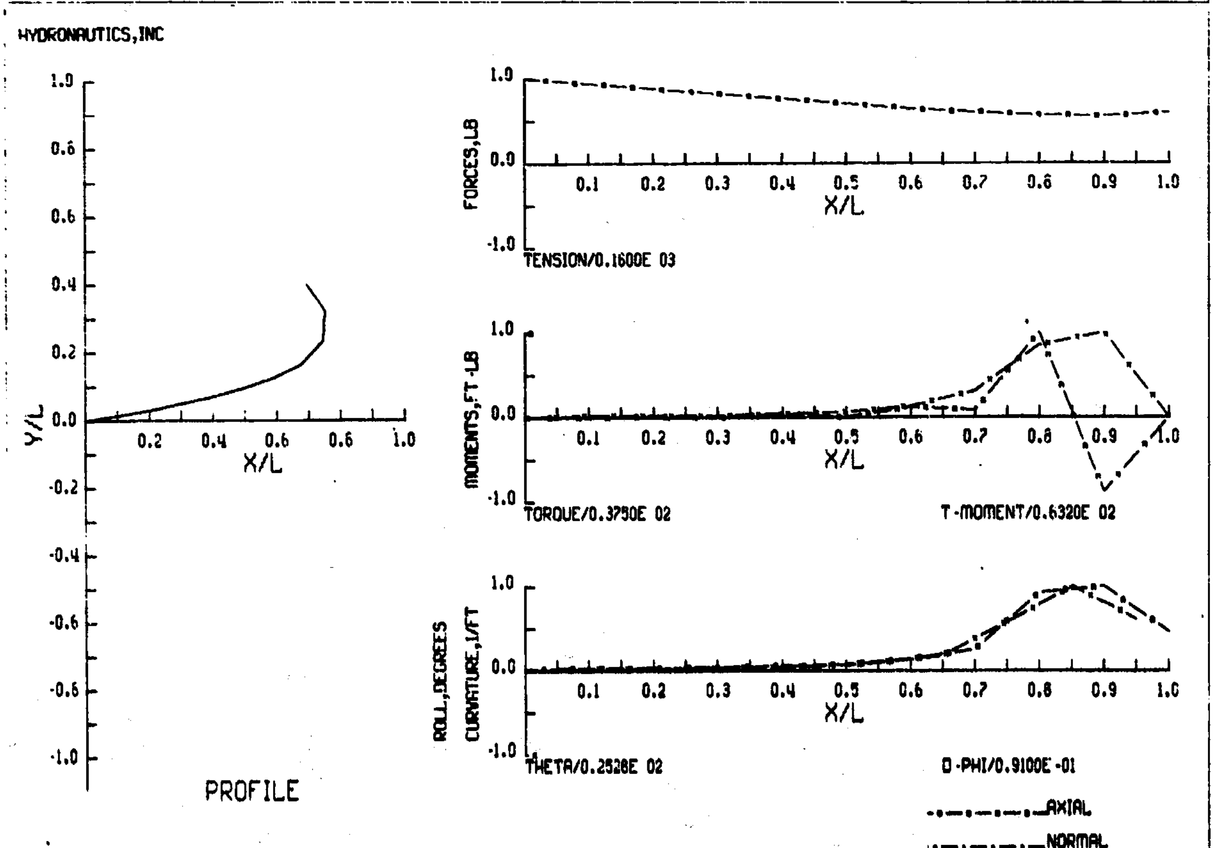

TEST NO. XII - 40 - 0 - 30

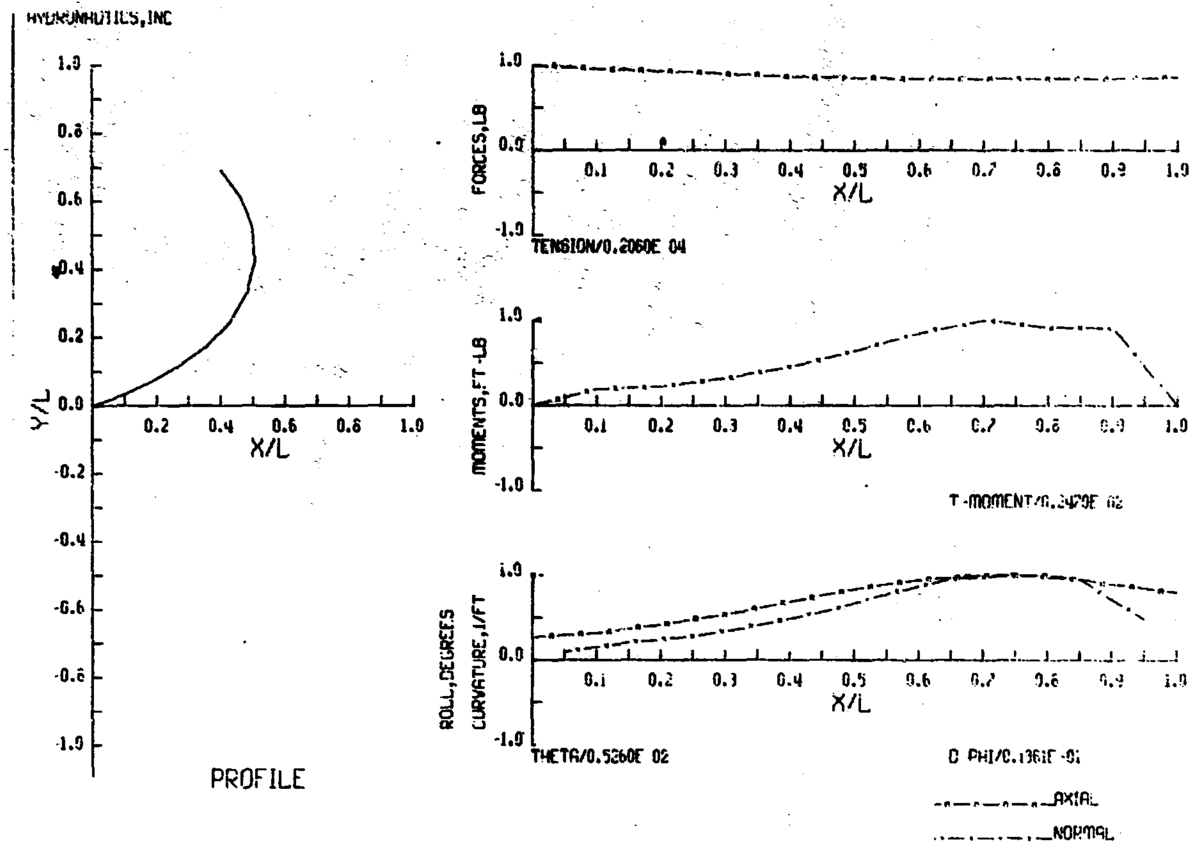

TEST NO. XII - 0 - 2 - 60

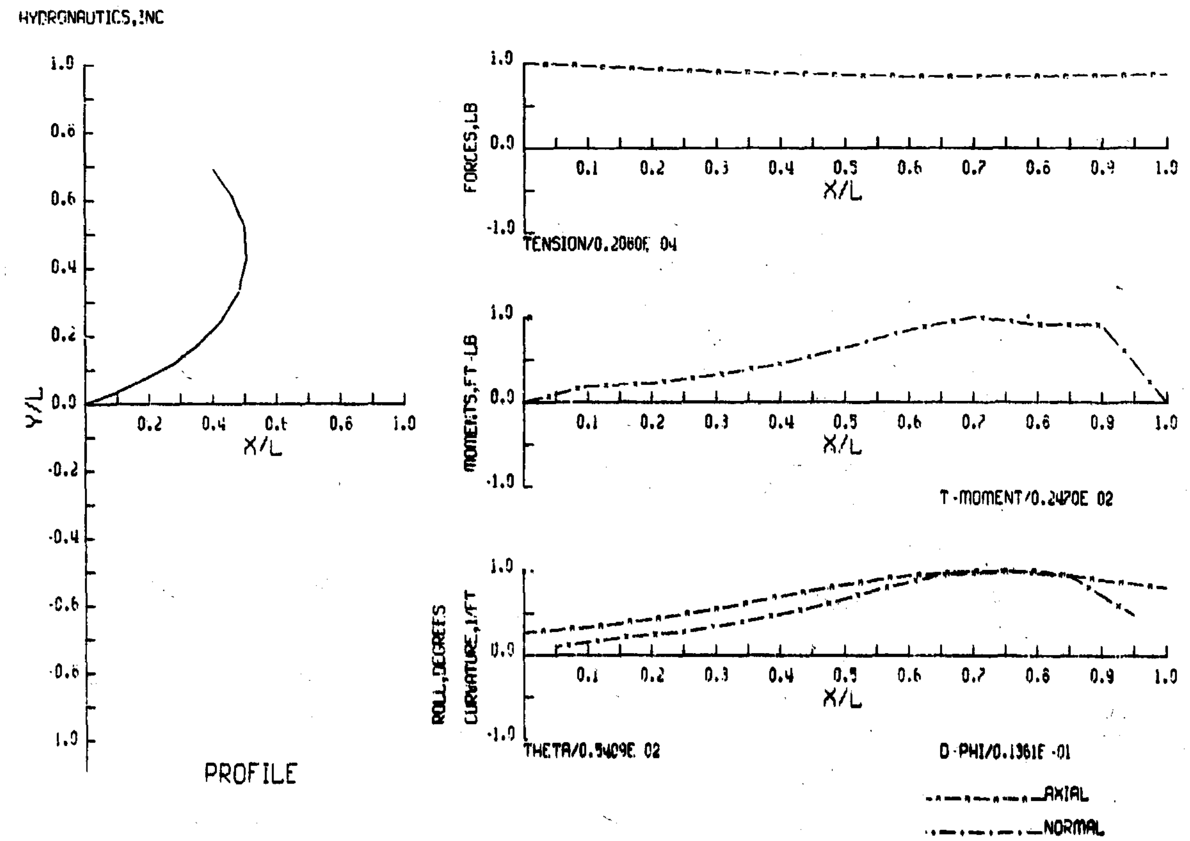

TEST NO. XII - 20 - 2 - 60

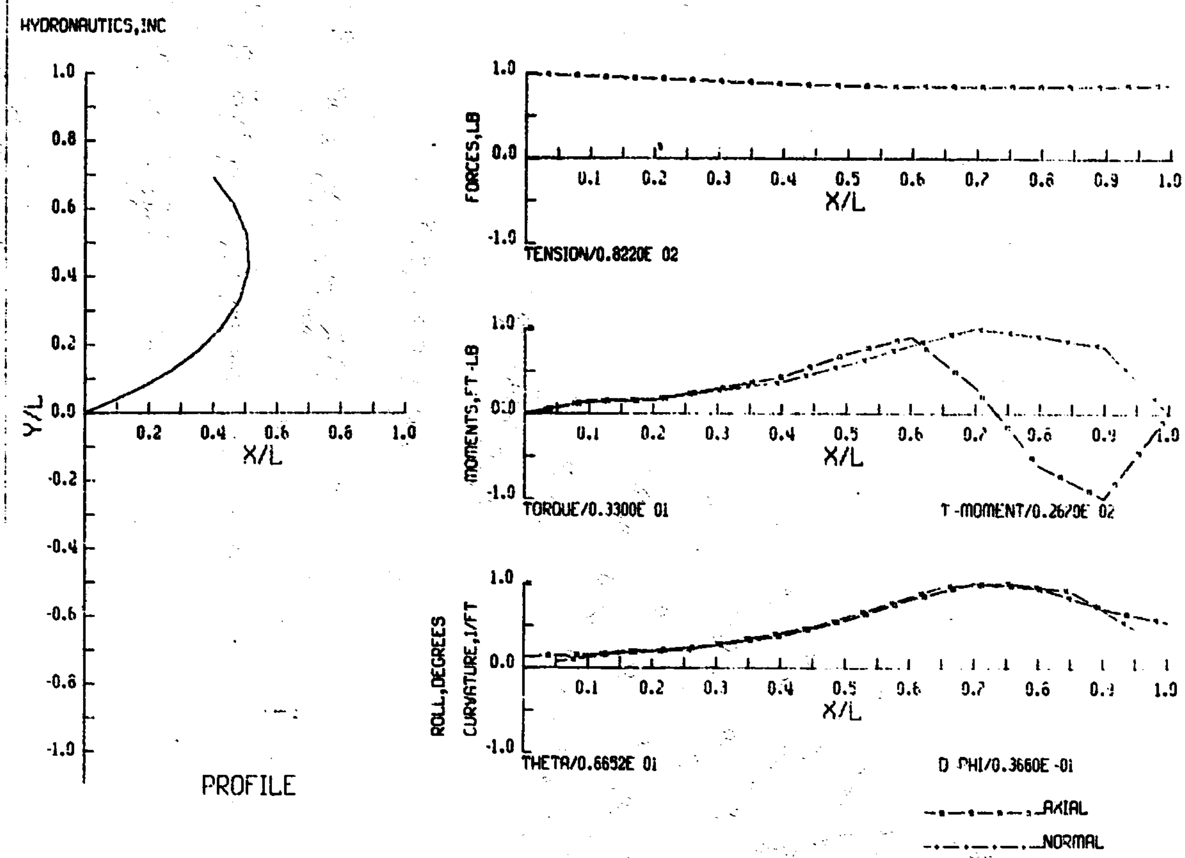

TEST NO. XII - 22 - 0 - 60

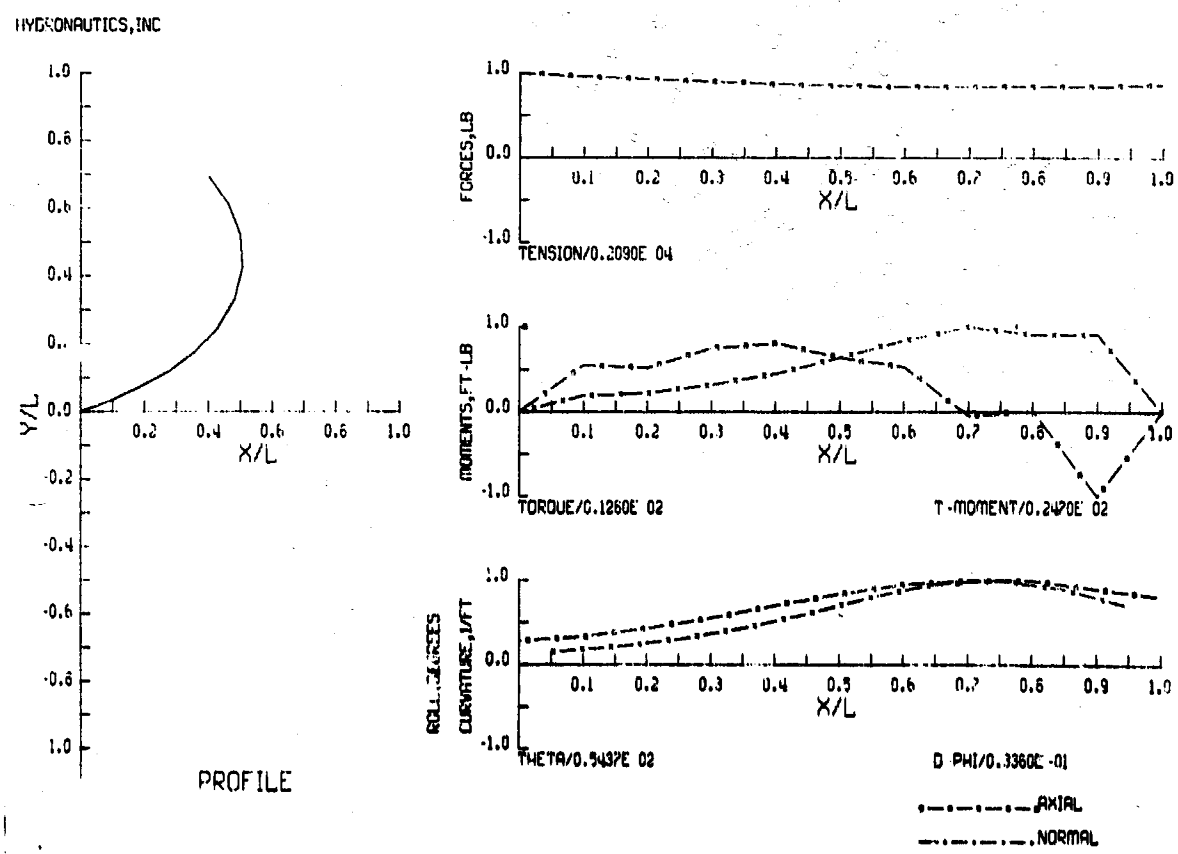

TEST NO. XII - 22 - 2 - 60

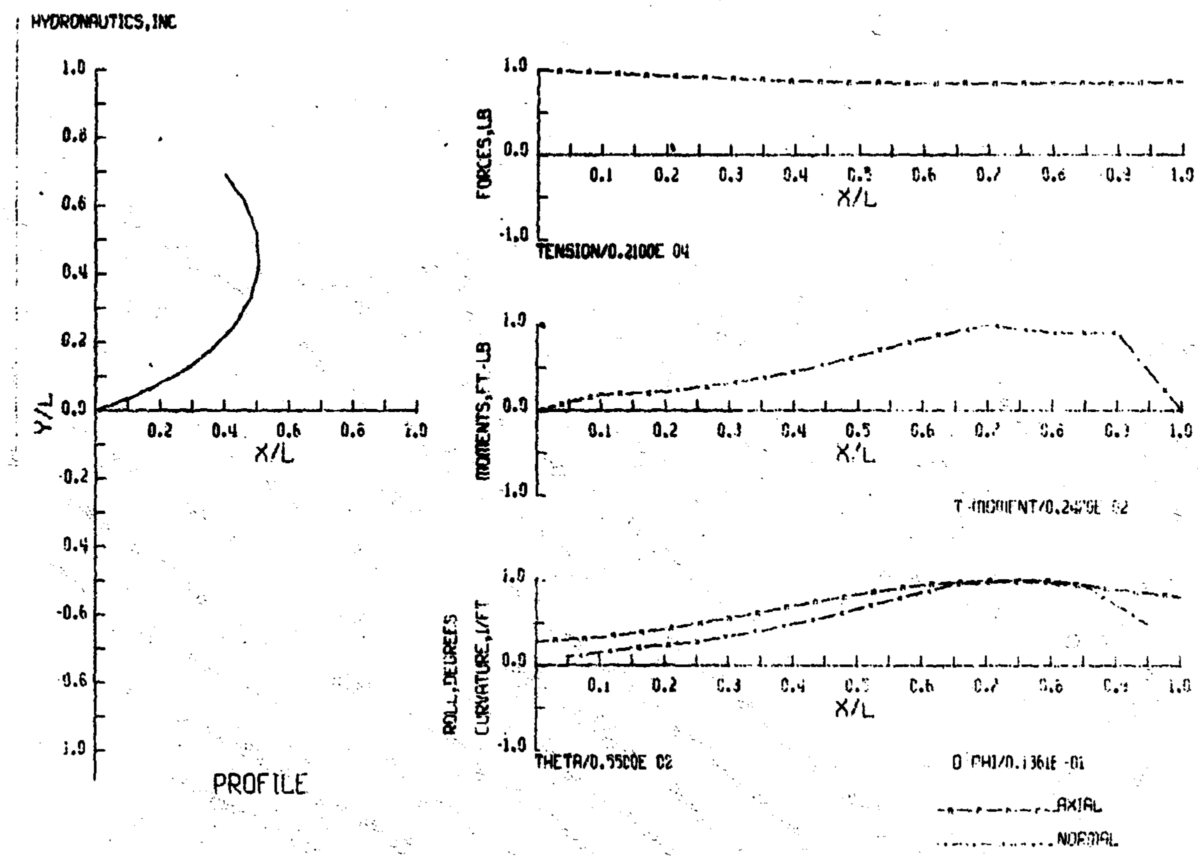

TEST NO. XII - 26 - 2 - 60

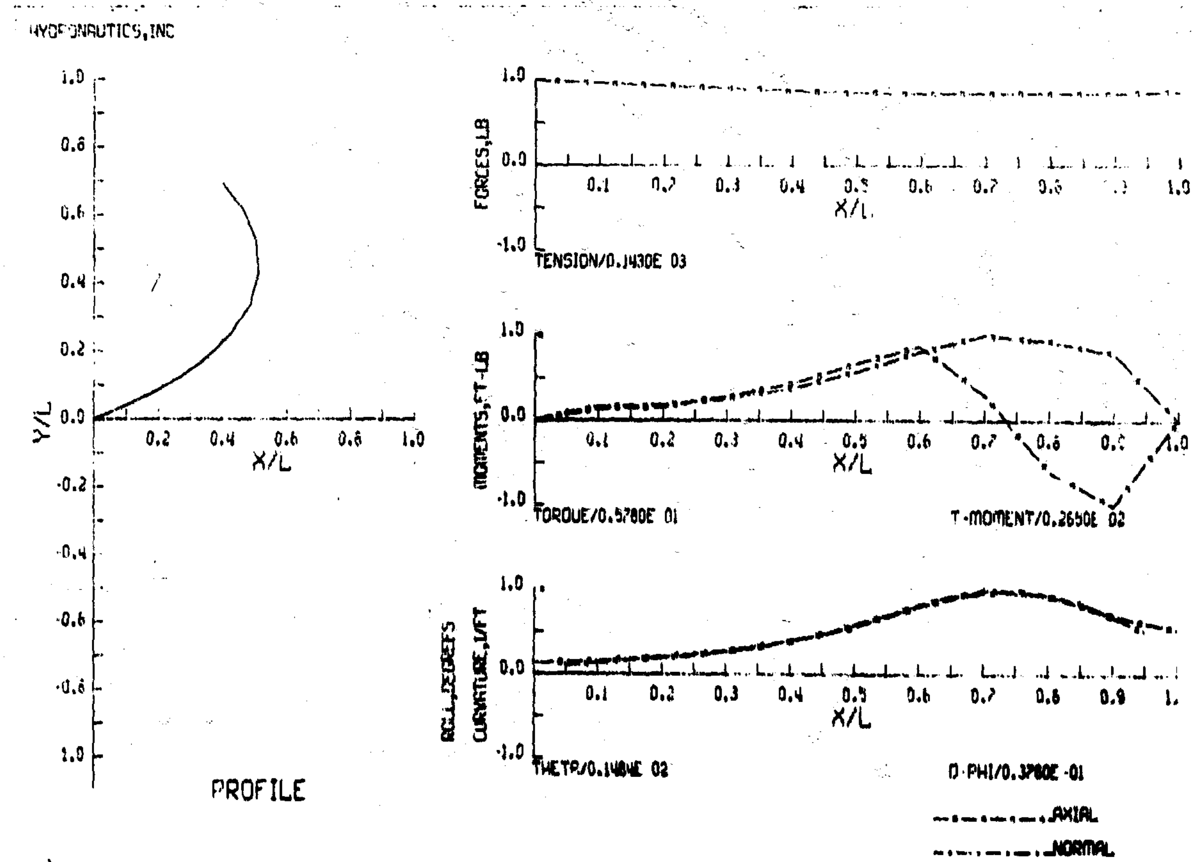

TEST NO. XII - 29 - 0 - 60

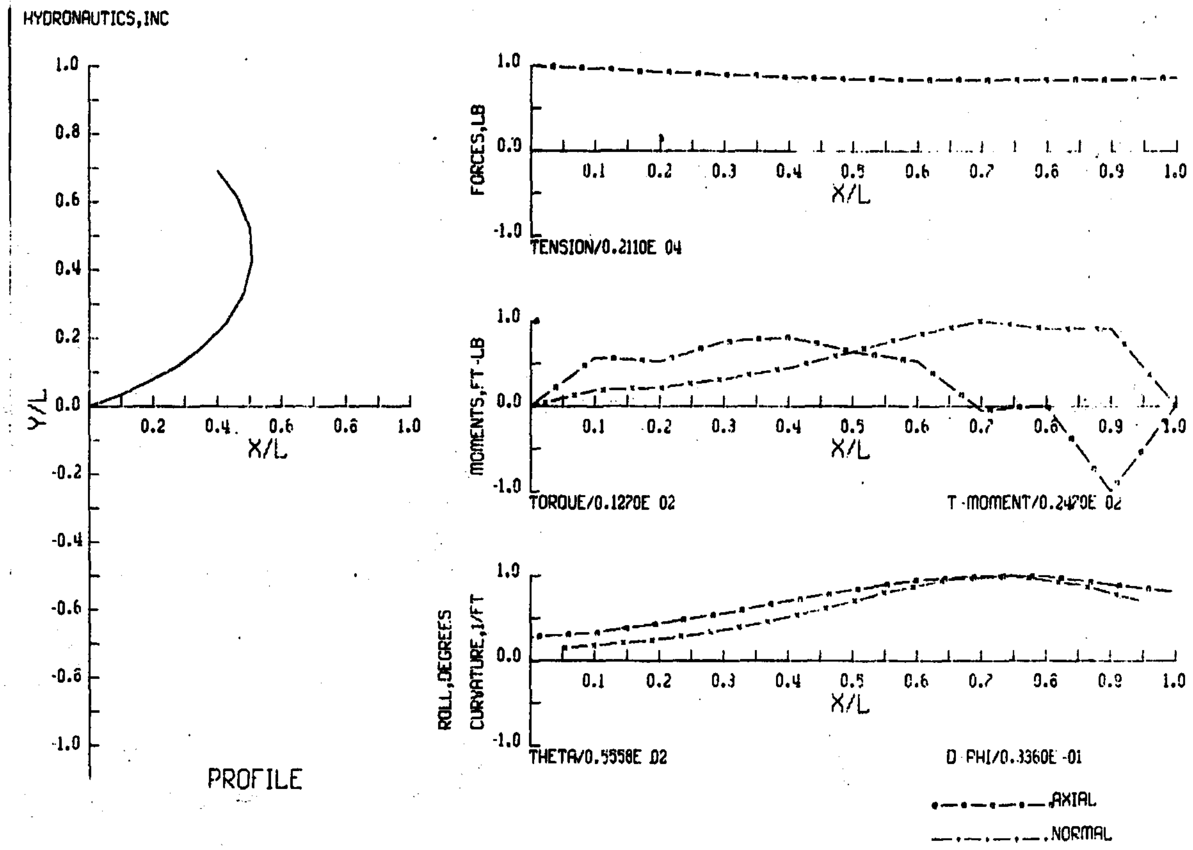

TEST NO. XII 20 - 2 - 60

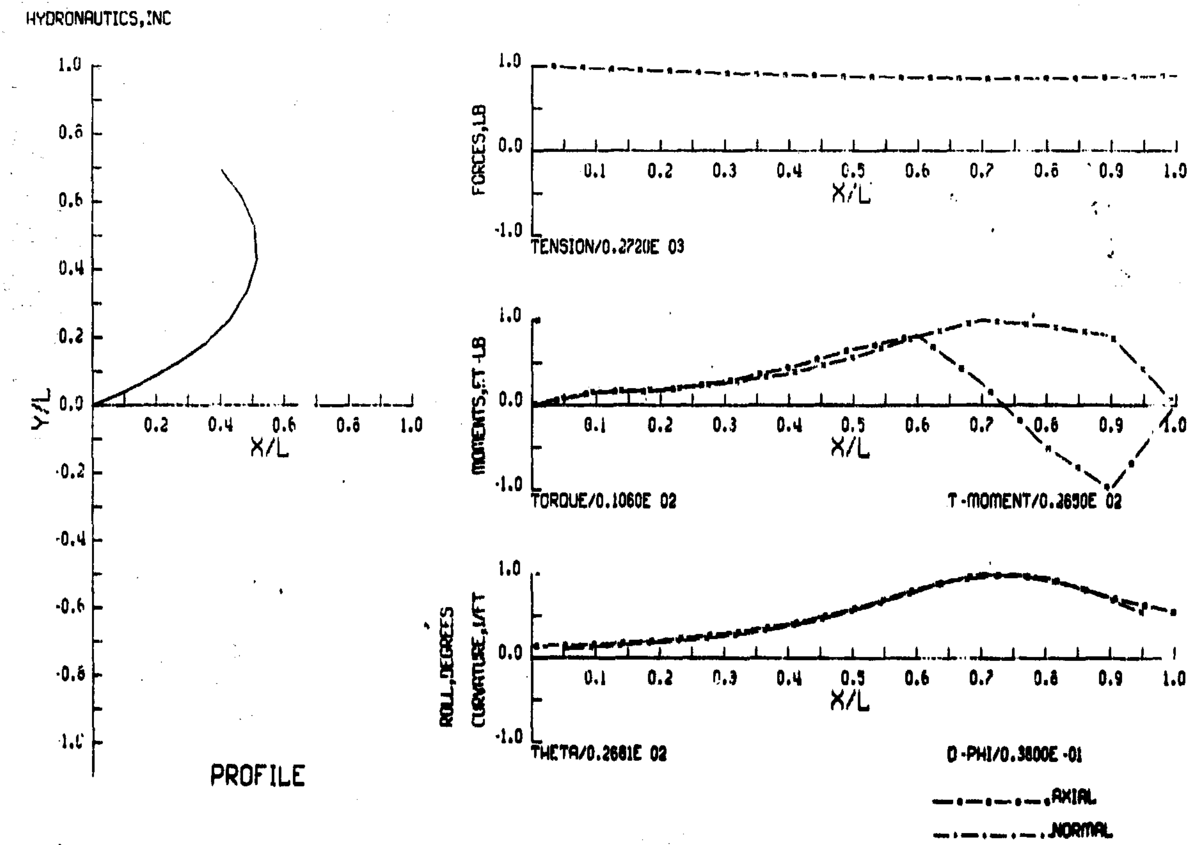

TEST NO. XII - 40 - 0 - 60

HYDRONAUTICS, INC

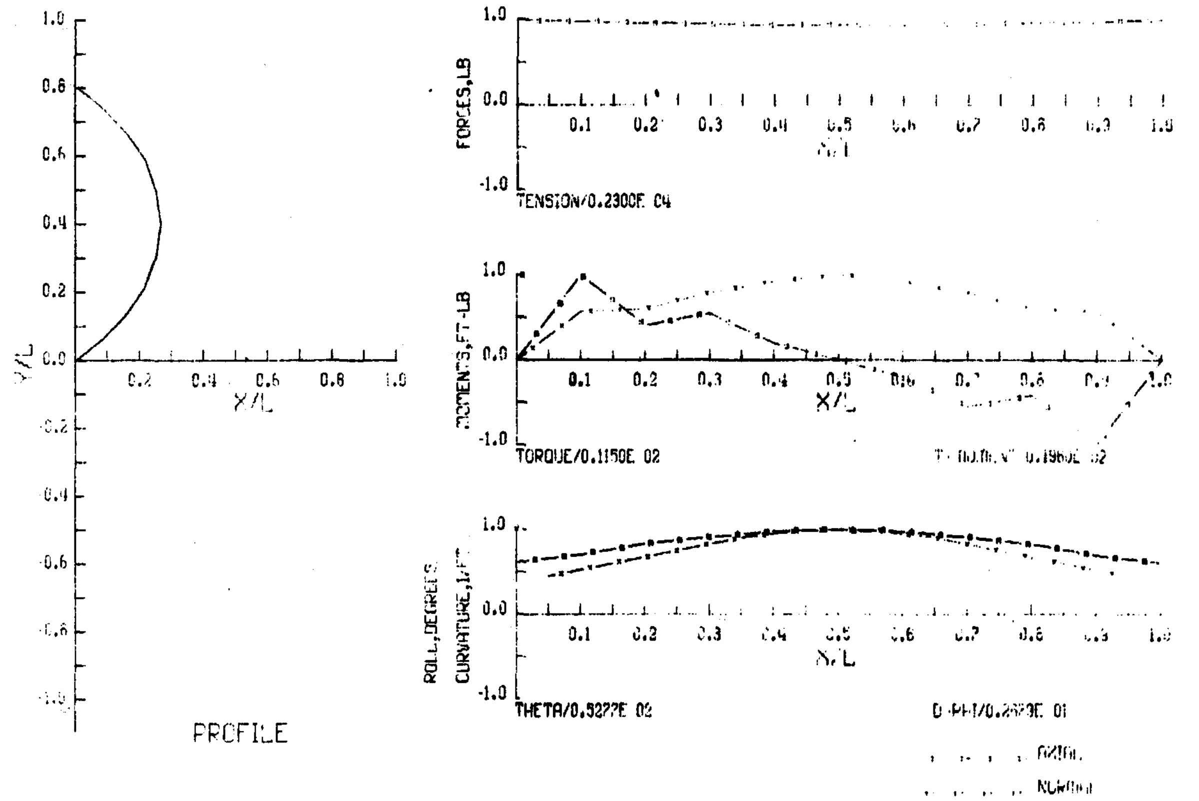

TEST NO. XII - 0 - 3 - 90

HYDRONAUTICS, INC

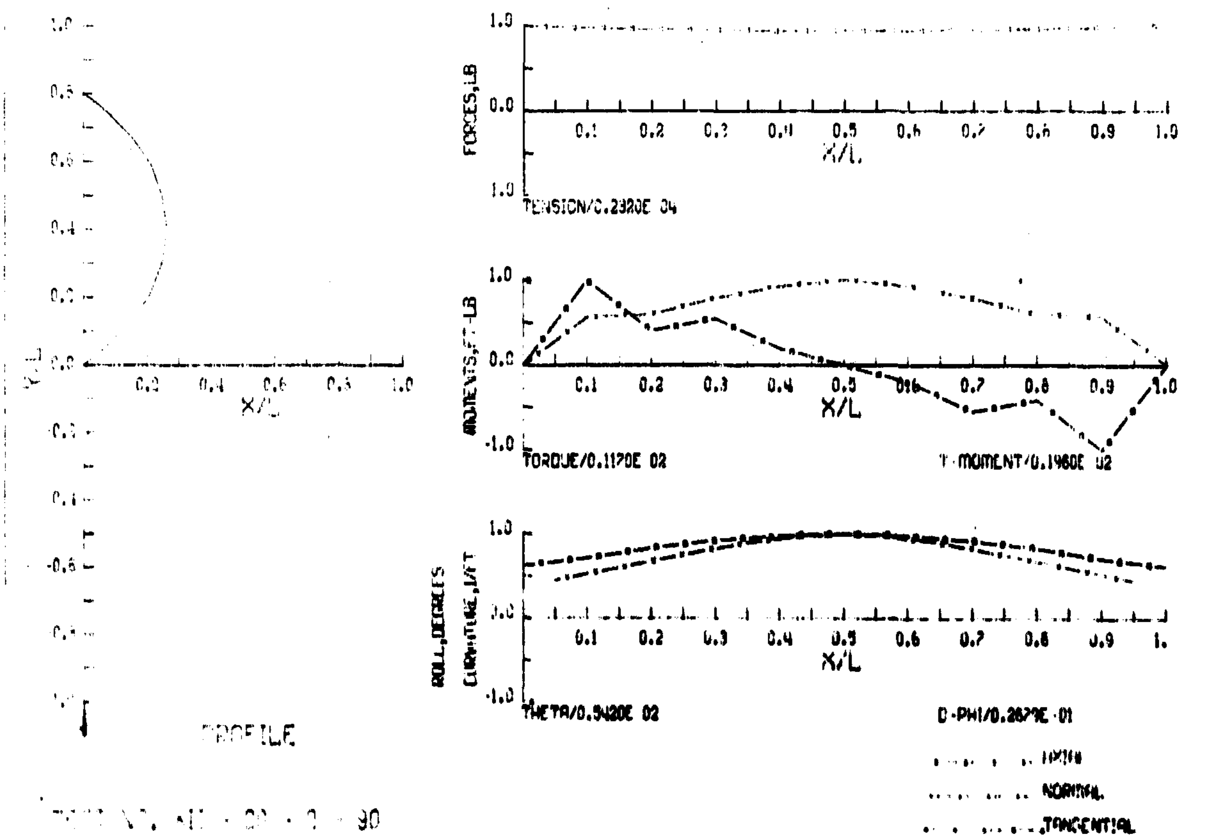

TEST NO. XII - 0? - 3 - 90

HYDRONAUTICS,INC

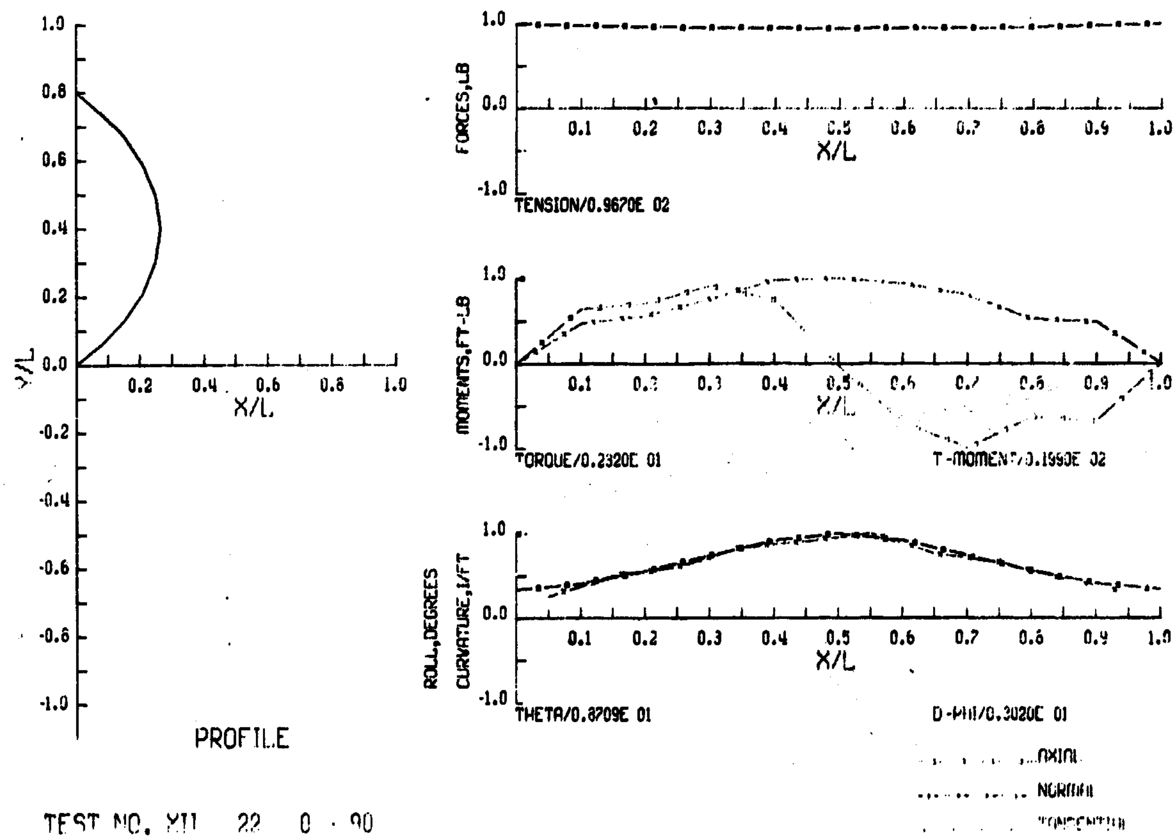

TEST NO. XII 22 0 90

HYDRONAUTICS,INC

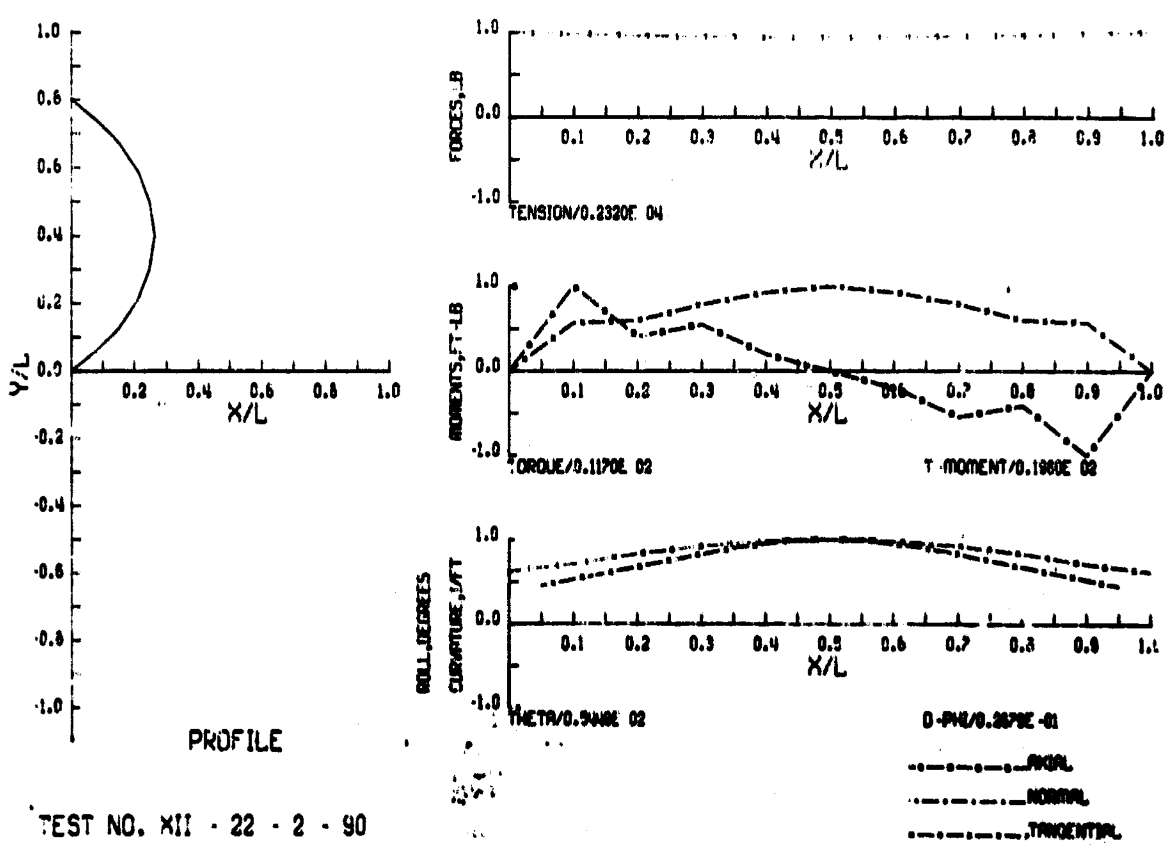

TEST NO. XII - 22 - 2 - 90

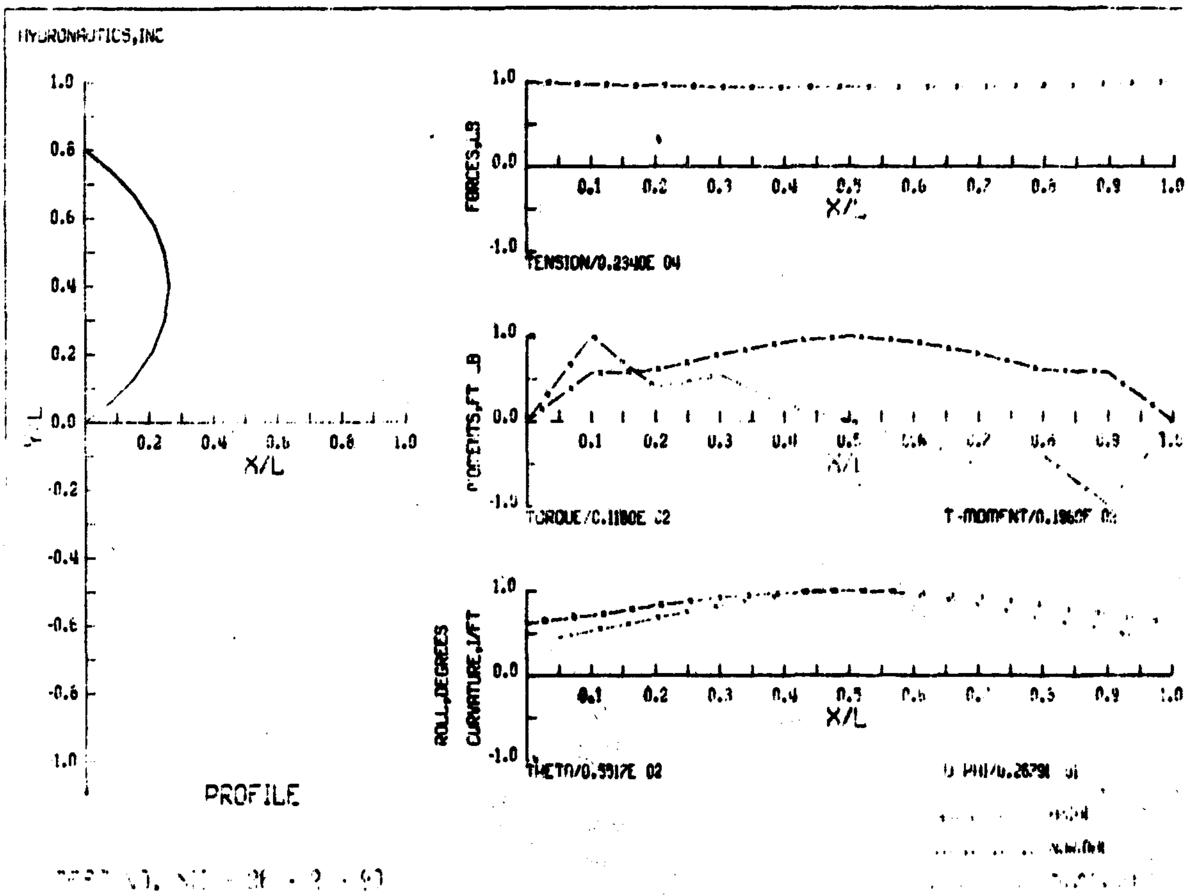
HYDRONAUTICS,INC
PROFILE
X/L
Y/L
FORCES,LB
TENSION/0.2340E 04
MOMENTS,FT-LB
TORQUE/0.1180E 02
T-MOMENT/0.1960E 02
ROLL,DEGREES
CURVATURE,1/FT
THETA/0.5317E 02
D-PHI/0.2679E 01

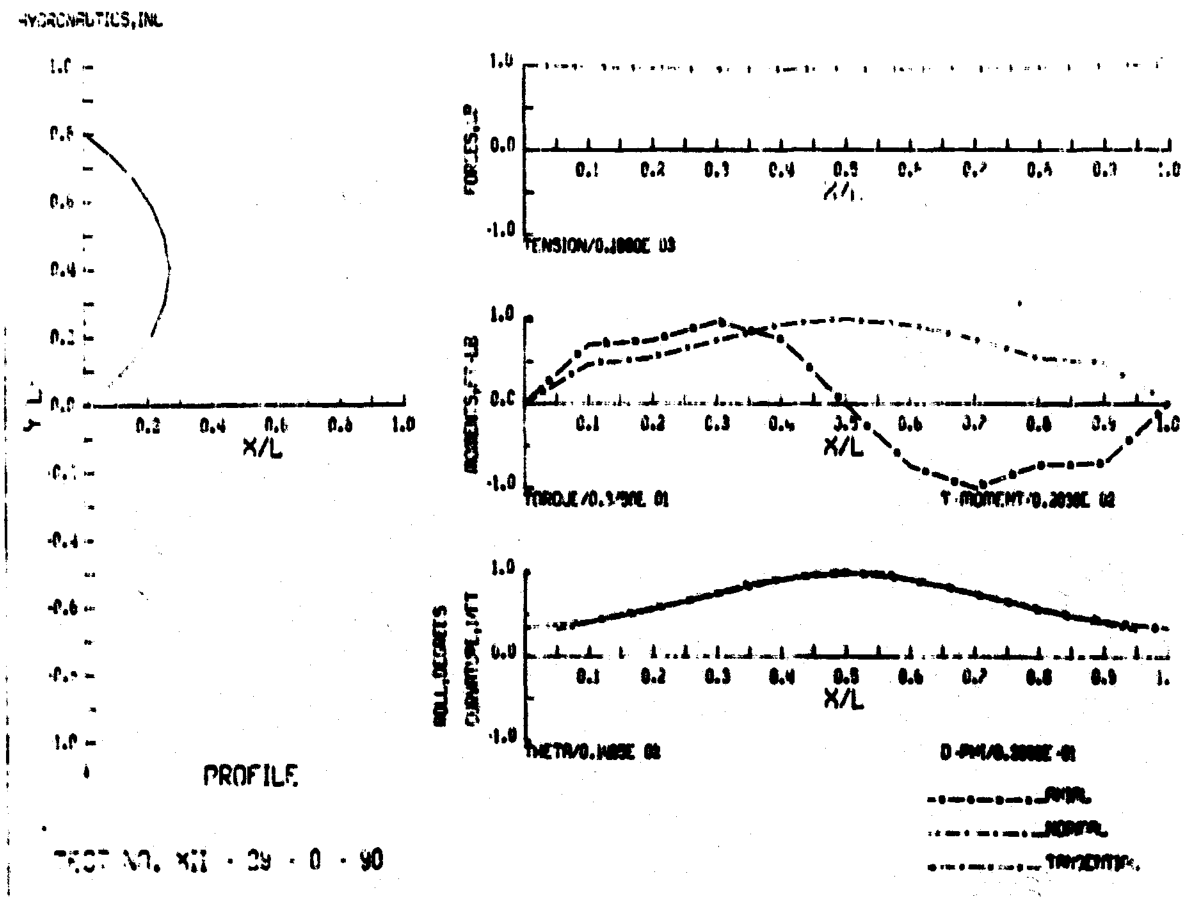
HYDRONAUTICS,INC
PROFILE
TEST NO. XII - 29 - 0 - 90
X/L
Y/L
FORCES,LB
TENSION/0.1880E 03
MOMENTS,FT-LB
T-MOMENT/0.2030E 02
ROLL,DEGREES
CURVATURE,1/FT
THETA/0.1405E 03
D-PHI/0.3000E 01
AXIAL
NORMAL

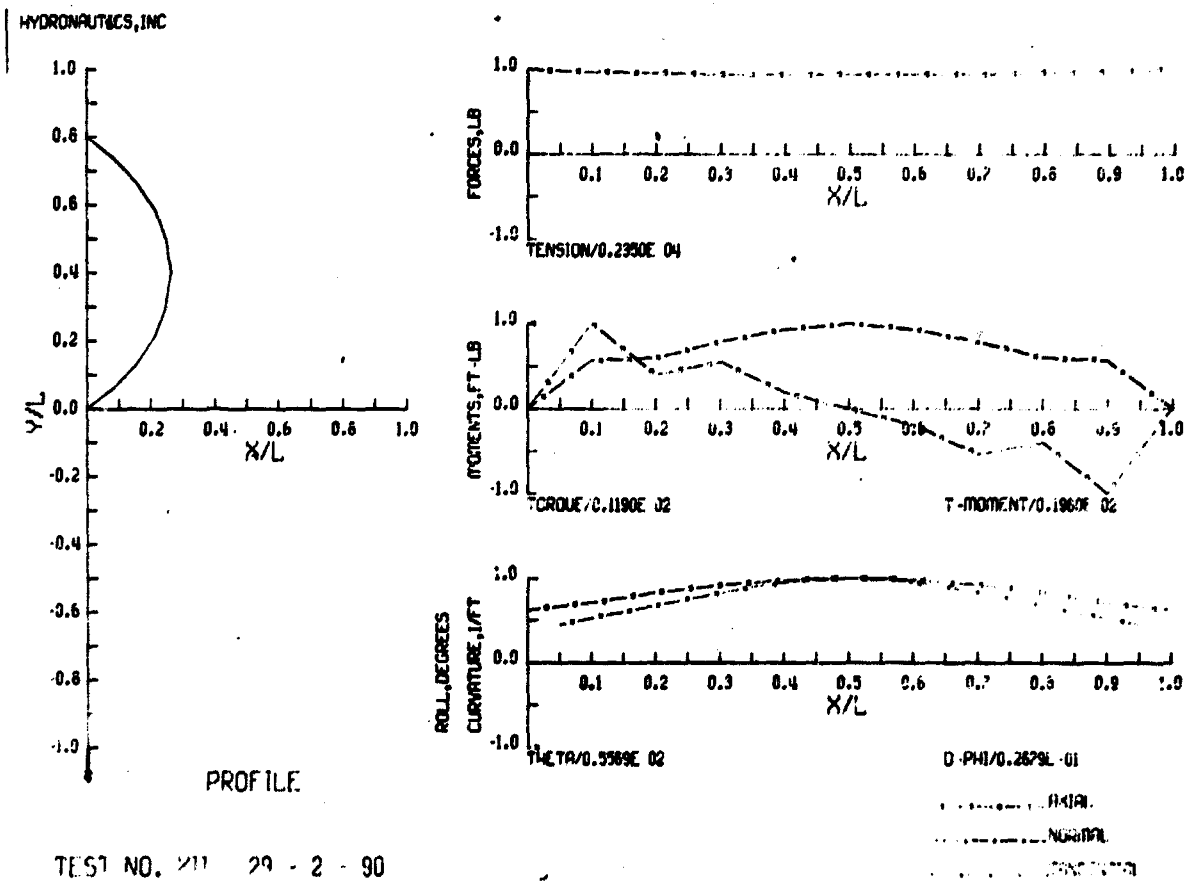

TEST NO. XII 29 - 2 - 90

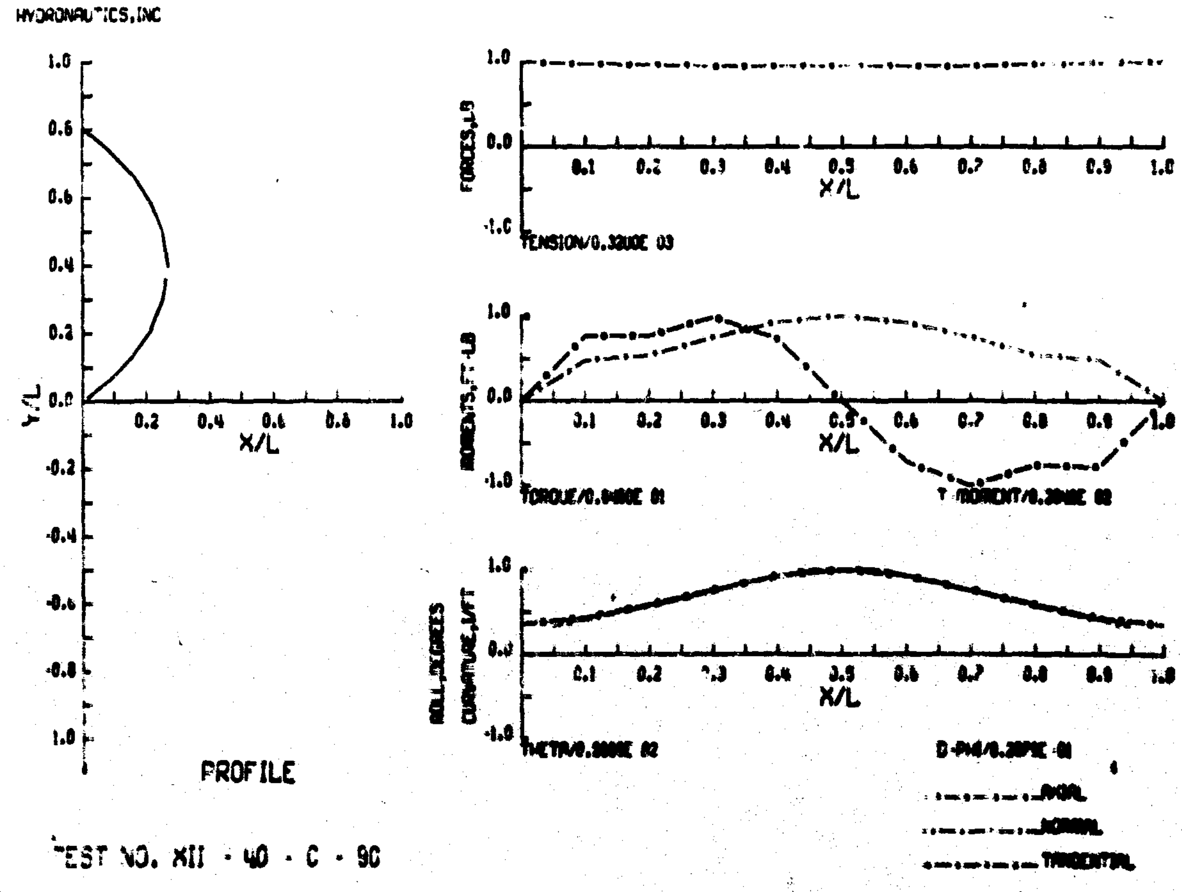

TEST NO. XII - 40 - C - 90

END